Durham University

Durham E-Theses

The response of alluvial fans and debris cones to changes in sediment supply, upland Britain.

Helen Mary Dunsford

How to cite:

Dunsford, Helen Mary (1999) The response of alluvial fans and debris cones to changes in sediment supply, upland Britain. Doctoral thesis, Durham University.

Use policy

The full-text may be used and/or reproduced, and given to third parties in any format or medium, without prior permission or charge, for personal research or study, educational, or not-for-profit purposes provided that:

- a full bibliographic reference is made to the original source
- a https://etheses.durham.ac.uk/id/eprint/1468/ is made to the metadata record in Durham E-Theses
- the full-text is not changed in any way

The full-text must not be sold in any format or medium without the formal permission of the copyright holders.

Please consult the full Durham E-Theses policy for further details.

Academic Support Office, The Palatine Centre, Durham University, Stockton Road, Durham, DH1 3LE
e-mail: e-theses.admin@durham.ac.uk Tel: +44 0191 334 6107
https://etheses.durham.ac.uk

The response of alluvial fans and debris cones to changes in sediment supply, upland Britain

Helen Mary Dunsford

Doctor of Philosophy

The copyright of this thesis rests with the author. No quotation from it should be published without the written consent of the author an information derived from it should be acknowledged.



17 JAN 2000

University of Durham

Department of Geography

The response of alluvial fans and debris cones to changes in sediment supply, upland Britain

Abstract

Alluvial fans and debris cones are characteristic features of the British uplands. They are depositional landforms which are frequently assumed to represent the reworking of glacial and periglacial sediments subsequent to deglaciation. Several studies have attempted to infer the chronological sequence of fan deposition stabilisation and incision in relation to reconstructions of environmental change or evidence for human impact. In most of these studies the importance of an availability of sediments in the supplying catchment has been considered implicitly. In this thesis the central aim is to examine explicitly the extent to which sediment supply control has moderated the geomorphological response of alluvial fans and debris cones in British uplands. The study is based around four field sites in contrasting upland environments of northern Britain (Glen Etive, Highland Region; Moffat Water and Yarrow Water, Dumfries and Galloway / Borders; Langdale and Bowderdale, the Howgill fells, Cumbria; and Langden Beck, the northern Pennines, County Durham). The contrasting glacial history, geological and geomorphological setting of the four sites provides an opportunity to examine the local and regional scale constraints of sediment supply on the history of fan and cone development. The analysis is based in three main parts. First, the detailed stratigraphy of the fan and cone deposits are examined and a number of ^{14}C dates used to constrain the chronology. Second, examination of the fabric characteristics is used to infer the nature of sediment transfer from the catchment to the fan or cone sequence. Third, a fingerprinting methodology, based largely on magnetic parameters is developed in order to assign source areas to the sediments preserved within individual sequences. Interpretation of sediment sources is aided by a combination of factor analysis and the use of unmixing models. Field evidence suggests that the nature of fan and cone development is intricate and variable. General models of increasing importance of fluvially transported sediment over debris flow transport and of a transition from glacial-dominated to solifluction-dominated sediment supplies are not easily supported. Changes in sediment transport mode and sediment source are often observed within individual cycles of fan or cone activity. Evidence for broadly contemporaneous activity on upland British fans and cones at around 1000 BP is supported by the present study.

I confirm that no part of the material presented in this thesis has previously been submitted by me or any other person for a degree in this or any other university. In all cases, where it is relevant, material from the work of others has been acknowledged.

The copyright of this thesis rests with the author. No quotation from it should be published without the prior written consent and information derived from it should be acknowledged.

Signed: HDunsford

Helen Mary Dunsford

Date: 22/7/99

TABLE OF CONTENTS

Abstract			ii
Table of Contents			iv
List of Tables			viii
List of Figures			ix
List of Plates			xiv
Acknowledgements			xv
Chapter One		**Introduction**	
1.1		Background	1
1.2		Research aims	2
1.3		Alluvial fan and debris cone erosion-deposition system	3
1.4		Structure of the thesis	4
Chapter Two		**Sediment transfer**	
2.1		Introduction	6
2.2		Sediment supply: catchment system behaviour	7
	2.2.1	Catchment process-response system	7
	2.2.2	Sediment supply: catchment system response	13
	2.2.3	The dominance of sediment supply in sediment limited environments	14
2.3		Sediment supply: deglaciated mountain environments	15
	2.3.1	The definition of sedimentological terminology in deglaciated mountain environments	15
	2.3.2	Characterisation of sediment supplies in upland environments of Great Britain	15
	2.3.3	Temporal fluctuations in sediment availability since deglaciation	17
	2.3.4	Sediment exhaustion	20
2.4		Sediment supply: a control of fan and cone response	21
2.5		Indicators of sediment supply control	24
	2.5.1	Indicator feasibility	26
	2.5.2	Indicator preservation	27
2.6		Summary	28

Chapter Three		**Approach and site description**	
3.1		Introduction	29
3.2		Temporal indicators of controls on sediment supply	29
	3.2.1	Methods of reconstructing mode of sediment transport	29
	3.2.2	Methods of ascribing changes in sediment source	32
	3.2.3	Chronological framework	34
3.3		Rationale of site selection	35
	3.3.1	Glen Etive	39
	3.3.2	Moffat	45
	3.3.3	The Howgill Fells	49
	3.3.4	Northern Pennines - Langden Beck	53
3.4		Inter- and intra-regional site integration	58
Chapter Four		**Fan and cone development framework**	
4.1		Introduction	62
4.2		Descriptive, sampling and laboratory methods	62
	4.2.1	Section location and environmental context	62
	4.2.2	Facies classification and sampling	63
	4.2.3	Laboratory methods	66
4.3		Glen Etive	69
	4.3.1	Coire Dionachd	69
	4.3.2	Causal development	78
4.4		Moffat - Yarrow Water	80
	4.4.1	Dry Cleuch	80
	4.4.2	Hermanlaw Burn	87
	4.4.3	Causal development	92
4.5		Howgill Fells	93
	4.5.1	Burnt Gill - Langdale Valley	93
	4.5.2	Nevy Gill - Langdale Valley	99
	4.5.3	Thickcombs Gill - Bowderdale Valley	102
	4.5.4	Leath Gill - Bowderdale Valley	108
	4.5.5	Gully Fan - Bowderdale Valley	111
	4.5.6	Causal development	112
4.6		Northern Pennines - Langden Beck	115
	4.6.1	Harthope Beck	115
	4.6.2	West Beck	120
	4.6.3	Causal development	124
4.7		Summary	125
Chapter Five		**Sediment transport mechanism recognition and sediment exhaustion**	
5.1		Introduction	128
5.2		Diagnostic properties of transport mechanism deposits	128
	5.2.1	Diagnostic properties of individual flow types	129
	5.2.2	Preservation potential of flow deposits	137
	5.2.3	Recognition	140
5.3		Methods used in transport mechanism discrimination	142
	5.3.1	Facies model: a descriptive measure of structure	142

	5.3.2	A measure of sorting as a tool for discrimination	144
5.4		Derivation of a sequential change in transporting mechanism	152
	5.4.1	The segregation of separately transported sediments	152
	5.4.2	$P_{90}M$: as a measure of sorting	155
	5.4.3	Unit assignment of transport mechanism	163
	5.4.4	Sensitivity of unit assignment	164
	5.4.5	The recognition of stratigraphic sediment exhaustion	169
5.5		Glen Etive - Coire Dionachd	171
	5.5.1	Chronology of fan aggradation	171
	5.5.2	Coire Dionachd development : evidence of sediment exhaustion	175
5.6		Moffat	176
	5.6.1	Dry Cleuch	176
	5.6.2	Hermanlaw Burn	178
5.7		Howgill Fells	180
	5.7.1	Burnt Gill	180
	5.7.2	Nevy Gill	184
	5.7.3	Thickcombs Gill	186
	5.7.4	Leath Gill	188
5.8		Northern Pennines - Langden Beck	188
	5.8.1	Harthope Beck	188
	5.8.2	West Beck	191
5.9		Evidence for sediment exhaustion	193
5.10		Summary	196
Chapter Six		**Sediment source supply and sediment exhaustion**	
6.1		Introduction	198
6.2		Principle and procedure of magnetic provenancing	198
	6.2.1	Measurement of magnetism and its discrimination	198
	6.2.2	Source material sampling	201
	6.2.3	Sample preparation and laboratory measurement	201
	6.2.4	Discriminating power of magnetic parameters	204
6.3		Source material characterisation and discrimination	207
	6.3.1	Methodology of source discrimination	207
	6.3.2	Glen Etive - Coire Dionachd	210
	6.3.3	Moffat - Dry Cleuch and Hermanlaw Burn	217
	6.3.4	Howgill Fells - Burnt Gill, Nevy Gill, Thickcombs Gill and Leath Gill	222
	6.3.5	Northern Pennines - Langden Beck - Harthope Beck	233
	6.3.6	Source discrimination: separation of source groups	239
6.4		Source assignment to samples from fan and cone sediments	240
	6.4.1	Sample screening	240
	6.4.2	Provenance: semi-quantitative and quantitative source assignment	242
	6.4.3	Fan and cone sediment source assignment	245
	6.4.4	Glen Etive - Coire Dionachd	250
	6.4.5	Moffat - Dry Cleuch and Hermanlaw Burn	251
	6.4.6	Howgill Fells - Burnt Gill, Nevy Gill, Thickcombs Gill and Leath Gill	256
	6.4.7	Northern Pennines - Langden Beck - Harthope Burn	267

6.5	Derivation of temporal changes in sediment source	268
6.6	Summary	271
Chapter Seven	**Sediment supply control: discussion and conclusion**	
7.1	Introduction	273
7.2	The signature of sediment exhaustion	272
7.2.1	Sediment exhaustion signatures and local controls	274
7.2.2	A regional comparison of sediment exhaustion signatures	278
7.3	Intra-regional extrapolation of sediment exhaustion	282
7.4	Original contribution and extension of previous studies	286
7.5	Recommendations for further research	289
Appendices		
Appendix I		293
Appendix 2		335
Appendix 3		351
Bibliography		360

LIST OF TABLES

		Page
2.1	Studies of alluvial fans and debris cones under contrasting environmental settings: a general presentation of resulting differences in their form and sedimentology	11
2.2	Examples of inductive approaches used to investigate controls upon fan and cone form and sedimentology	12
3.1	Basic geometric classifications of features	60
4.1	Facies code	65
4.2	Radiocarbon and AMS dates: a summary of stratigraphic context and information provided	68
5.1	Summary of the major physical properties of fluvial flow, hyperconcentrated flow and debris flow	130
5.2	Summary of the sedimentary structure and characteristics of dry grain, debris, hyperconcentrated and fluvial flows	141
5.3	Differences between pairs of deposits	143
5.4	A summary of commonly recognised measures of sorting	146
5.5	Sorting data for the index samples	158
6.1	Commonly occurring iron bearing minerals in natural sediments and soils	199
6.2	Magnetic parameters, ratios, graphical combinations and their interpretation	205
6.3	Summary of source group classification and region specific characteristics	208
6.4	Results of factor Analysis for catchment samples of Glen Etive: eigenvalues, eigenvectors and degree of variance	216
6.5	Results of factor Analysis for catchment samples of Moffat: eigenvalues, eigenvectors and degree of variance	224
6.6	Results of factor Analysis for catchment samples of the Howgill Fells: eigenvalues, eigenvectors and degree of variance	230
6.7	Results of factor Analysis for catchment samples of the Langden Beck: eigenvalues, eigenvectors and degree of variance	238
6.8	Summary of the magnetic properties of the palaeosols within the sections investigated	241
6.9	Magnetic data for glacial, solifluction and storage material source groups	255

LIST OF FIGURES

		Page
2.1	A schematic illustration of the relationship between a fan and cone with its supplying catchment	8
2.2	Controls upon response within the fan and cone environment	9
2.3	A schematic illustration of long and short term scales of sediment exhaustion	23
2.4	Classification of mass movement on steep slopes as a function of solid fraction and material type	25
3.1	The location of the study sites	36
3.2	The position of study sites relative to Loch Lomond ice cap or localised valley glacier limits	37
3.3	Geomorphological map of Glen Etive	40
3.4	Geomorphological map of upper Moffat Water and Yarrow Water	46
3.5	Geomorphological map of Langdale and Bowderdale, the Howgill Fells	50
3.6	Geomorphological map of Langden Beck	55
3.7	The location of the catchments studied at Glen Etive, Yarrow Water near Moffat, the Howgill Fells and Langden Beck	59
4.1	The surface features of Coire Dionachd fan, Glen Etive	70
4.2	Stratigraphic log, facies code, percentage loss on ignition, grain size and the chronological framework for CDS1, Glen Etive	72
4.3	Radiocarbon date, stratigraphic log, facies code, percentage loss on ignition, grain size and the chronological framework for CDS2, Glen Etive	73
4.4	Radiocarbon date, stratigraphic log, facies code, percentage loss on ignition, grain size and the chronological framework for CDS3, Glen Etive	75
4.5	A schematic illustration of the generalised sediment stratigraphy of the exposure within which CDS2 and CDS3 have been excavated	76
4.6	Visual correlation of the timing of cone aggradation at Coire Dionachd with local and regional patterns of change in climate and in human activity	79
4.7	The surface features of Dry Cleuch debris cone, near Moffat	81
4.8	Radiocarbon date, stratigraphic log, facies code, percentage loss on ignition, grain size and the chronological framework for DCS1, Moffat	82
4.9	Radiocarbon date, stratigraphic log, facies code, percentage loss on ignition, grain size and the chronological framework for DCS2, Moffat	84
4.10	The surface features of Hermanlaw Burn fan, near Moffat	88
4.11	Stratigraphic log, facies code, percentage loss on ignition,	90

	grain size and the chronological framework for HBS1, Moffat.	
4.12	Visual correlation of the timing of cone aggradation at Dry Cleuch with local and regional patterns of change in climate and human activity	91
4.13	The surface features of Burnt Gill debris cone, the Howgill Fells	94
4.14	Stratigraphic log, facies code, percentage loss on ignition, grain size and the chronological framework for BGS1, the Howgill Fells	96
4.15	Stratigraphic log, facies code, percentage loss on ignition, grain size and the chronological framework for BGS2, the Howgill Fells	97
4.16	The surface features of Nevy Gill fan, the Howgill Fells	100
4.17	Stratigraphic log, facies code, percentage loss on ignition, grain size and the chronological framework for NGS1, the Howgill Fells	101
4.18	The surface features of Thickcombs Gill debris cone, the Howgill Fells	103
4.19	Radiocarbon date, stratigraphic log, facies code, percentage loss on ignition, grain size and the chronological framework for TGS1, the Howgill Fells	105
4.20	Radiocarbon date, stratigraphic log, facies code, percentage loss on ignition, grain size and the chronological framework for TGS2, the Howgill Fells	106
4.21	The surface features of Leath Gill fan, the Howgill Fells	109
4.22	Stratigraphic log, facies code, percentage loss on ignition, grain size and the chronological framework for LGS1, the Howgill Fells	110
4.23	Radiocarbon date, stratigraphic log, facies code, percentage loss on ignition, grain size and the chronological framework for GFS1, the Howgill Fells	110
4.24	Visual correlation of the timing of cone aggradation at Burnt Gill, Thickcombs Gill and Gully Fan with local and regional patterns of change in climate and human activity	113
4.25	The surface features of Harthope Beck fan, Langden Beck	116
4.26	Stratigraphic log, facies code, percentage loss on ignition, grain size and the chronological framework for HHS1, the Howgill Fells	117
4.27	Radiocarbon date, stratigraphic log, facies code, percentage loss on ignition, grain size and the chronological framework for HHS2, the Howgill Fells	118
4.28	Stratigraphic log, facies code, percentage loss on ignition, grain size and the chronological framework for HHS3, the Howgill Fells	118
4.29	A planform schematic of the surface features of Westbesck fan, Langden Beck	121
4.30	Stratigraphic log, facies code, percentage loss on ignition, grain size and the chronological framework for WBS1, the Howgill Fells	122
4.31	Stratigraphic log, facies code, percentage loss on ignition, grain size and the chronological framework for WBS2, the	122

	Howgill Fells	
4.32	Comparison of timing of fan and cone activity between Glen Etive, Moffat and the Howgill Fells	126
5.1	A schematic illustration of the mechanism of large boulder support within a debris flow	133
5.2	Spatial variations of the sediment properties within debris flow deposits	134
5.3	A schematic illustration of the nature of flow transition from one phase flow to two phase flow	138
5.4	Particle support mechanisms of fluvial flow, debris flow and hyperconcentrated flow and their interrelationship	138
5.5	An illustration of the range of percentiles used to measure sorting	148
5.6	Bull's (1962b) discrimination of mudflow, stream-channel and intermittent flow deposits using CM patterns	149
5.7	A schematic illustration of P_nM values plotted on the particle size distribution of four contrasting samples	151
5.8	An example of unit boundary identification using $P_{90}M$ values and the characteristics of their spacing	154
5.9	A comparison of the $P_{90}M$ index with plots of other calculated measures of sorting	157
5.10	Differentiation between fluvial flow, debris flow and hyperconcentrated flow	160
5.11	An illustration of the relationship of $P_{90}M$ with size	161
5.12	The relationship of $P_{90}M$ values with coarse sand, medium sand, fine sand, silt and clay size fractions	162
5.13	An example of unit assignment using TGS2 from the Howgill Fells	165
5.14	Presentation of data for units assigned with a hyperconcentrated flow mechanism	166
5.15	The sensitivity of $P_{90}M$ in assigning transport mechanism (double page)	167
5.16	A schematic illustration of how scales of sediment exhaustion can be identified within a stratigraphic profile	170
5.17	The identification of separate flow units and the assignment of flow mechanism for CDS1, CDS2 and CDS3, Glen Etive (double page)	172
5.18	An illustration of the relationship between CDS2 and CDS3, Glen Etive	174
5.19	The identification of separate flow units and the assignment of flow mechanism for DCS1 and DCS2, Moffat (double page)	177
5.20	The identification of separate flow units and the assignment of flow mechanism for HBS1, Moffat	179
5.21	The identification of separate flow units and the assignment of flow mechanism for BGS1, the Howgill Fells	181
5.22	The identification of separate flow units and the assignment of flow mechanism for BGS2, the Howgill Fells	182
5.23	The identification of separate flow units and the assignment of flow mechanism for NGS1, the Howgill Fells	185
5.24	The identification of separate flow units and the assignment	187

	of flow mechanism for TGS1 and TGS2, the Howgill Fells (double page)	
5.25	The identification of separate flow units and the assignment of flow mechanism for LGS1, the Howgill Fells	189
5.26	The identification of separate flow units and the assignment of flow mechanism for HHS1, HHS2 and HHS3, Langden Beck (double page)	190
5.27	The identification of separate flow units and the assignment of flow mechanism for WBS1 and WBS2, Langden Beck	192
5.28	Plot of flow mechanisms for each feature against catchment size	195
6.1	Demagnetisation and magnetisation of six pilot samples through a range of field strengths to determine variability in the magnetic properties of the sediments	203
6.2	A summary of magnetic parameter biplot combinations and their interpretation	206
6.3	Location of catchment sample points, Glen Etive	211
6.4	Biplots of magnetic parameters showing the variation in magnetic concentration and magnetic remanence acquisition of the catchment source sediments of Glen Etive	213
6.5	Plot of loadings on Factor 1 and factor 2 obtained for Glen Etive catchment samples based upon the eight magnetic parameters used in the biplot analysis	214
6.6	Plot of loadings on factor 1 and Factor 2 for Glen Etive catchment samples using the maximum combination of measured magnetic variables and their ratios	215
6.7	Loadings of the magnetic variables on the first two factors of Glen Etive catchment source samples	216
6.8	A summary of the differentiation observed between the measured magnetic properties of the source groups at Glen Etive using factor analysis	218
6.9	Location of catchment sample points, Yarrow Water	220
6.10	Biplots of magnetic parameters showing the variation in magnetic concentration and magnetic remanence acquisition of the catchment source sediments of Moffat	221
6.11	Plot of loadings on Factor 1 and factor 2 obtained for Moffat catchment samples based upon the eight magnetic parameters used in the biplot analysis	223
6.12	Factor loadings of the eight magnetic parameters used in R- and Q- mode factor analysis at Moffat	224
6.13	Plot of ARM40-mT/SARM against Factor 1 shows the importance of this single magnetic parameter in differentiating between the three major source groups at Moffat	225
6.14	Location of catchment sample points, the Howgill Fells	226
6.15	Biplots of magnetic parameters showing the variation in magnetic concentration and magnetic remanence acquisition of the catchment source sediments of the Howgill Fells	228
6.16	Plot of loadings on Factor 1 and factor 2 obtained for Howgill Fells catchment source samples based upon the	229

	eight magnetic parameters used in the biplot analysis	
6.17	Loadings of the magnetic variables on the first two factors of the Howgill Fells catchment source samples	230
6.18	An illustration of the within and between catchment variability of the magnetic properties of source samples	231
6.19	Location of catchment sample points, Langden Beck	234
6.20	Biplots of magnetic parameters showing the variation in magnetic concentration and magnetic remanence acquisition of the catchment source sediments of Langden beck	235
6.21	Plot of loadings on Factor 1 and factor 2 obtained for Langden Beck catchment source samples based upon fourteen magnetic parameters used in the biplot analysis	237
6.22	Loadings of the fourteen magnetic parameters used in R- and Q- mode Factor Analysis at Langden Beck	238
6.23	Plot of section samples illustrating their position relative to source groupings identified for each of the four sites	243
6.24	A schematic representation of the interpretation and assignment of source to the convex hulls of individual flow units	247
6.25	Assignment of source for individual flow units identified in CDS1, Glen Etive	248
6.26	Assignment of source for individual flow units identified in CDS2 and CDS3, Glen Etive	249
6.27	Assignment of source for the individual flow units identified in DCS1 and DCS2, Moffat.	252
6.28	Assignment of source for individual flow units identified in HBS1, Moffat	254
6.29	Results of the unmixing model for CDS1 and CDS2, Moffat	257
6.30	Results of the unmixing model for HBS1, Moffat	258
6.31	Assignment of the source for individual flow units identified in BGS1 and BGS2, the Howgill Fells	259
6.32	Assignment of the source for individual flow units identified in TGS1 and TGS2, the Howgill Fells	262
6.33	Assignment of the source for individual flow units identified in NGS1, the Howgill Fells	264
6.34	Assignment of the source for individual flow units identified in LGS1, the Howgill Fells	265
6.35	Assignment of the source for individual flow units identified in HHS1, HHS2 and HHS3, Langden Beck	267
6.36	Assignment of the source for individual flow units identified in WBS1 and WBS2, Langden Beck	269
7.1	A schematic illustration of the interrelationship of supply and availability with sediment exhaustion and the resulting response with the fan and cone	280
7.2	Plot of catchment area against fan area for features found within the study reaches of the Howgill Fells, Moffat and Glen Etive	284

LIST OF PLATES

		Page
3.1	The main valley of Glen Etive	41
3.2	The valley of Yarrow Water, near Moffat	47
3.3	The headwaters of Langdale valley, the Howgill Fells	51
3.4	Langden Beck valley	56

ACKNOWLEDGEMENTS

I wish to thank to the University of Durham for providing me with funding through a University Scholarship and the Department of Geography for its support. I would like to thank my supervisors Dr David Higgitt and Dr Robert Allison for their continued support, guidance and patience throughout my time of study, and in particular for their frenzied efforts in ensuring the thesis was completed to schedule.

The help of the following is much appreciated whilst on fieldwork; Drs. Ben Horton, Robin Edwards, Neil Coe, Lu XiXi, despite frequent football commitments; John Thomson, Owen Kimber and Richard Bromley despite the cold conditions. I would like to thank Sam Cockings, torrential rain, Huw Gill, frogs and all things beyond my control.

My thanks goes to Yorkshire, Cumbrian and Scottish farmers for letting me on their land and providing warm cups of tea.

I would like to thank Chris Mullaney for allowing me to use his computer in my time of need, all the technical staff in the Quaternary Lab. (Derek, Frank, Brian, Ed), and Stella Henderson for helping with binding and photocopying. Dr. Nick Cox always had five minutes, going on one hour, to spare for those niggling stata questions - thanks. My appreciation goes to Dr. Roy Thompson for enabling me to use his magnetic equipment *cart blanche* for three weeks, accompanied by his help and valued advice.

The new insight and hearty meals provided by Drs Jeff and Christine Warburton continually spurred me on my way, interlaced with breaks provided by Fly Warburton. Bed and board was also provided by Dr. Emma Mawdsley - many thanks. I would like to thank Dr John Evans and Laura Evans for their continued support and Michele Johnson for numerous food/lunch runs and lunchtime de-stressing.

Special thanks during the final stages of writing up (which appeared to be endless) for help with finishing touches, doing appendices and generally keeping me sane go to Dr Alistair Kirk (references), Gaynor Cummins, John and Laura Evans.

Finally, I wish to thank my Mum, Dad and Aunty Margaret for their emotional and financial support.

I dedicate this thesis to Nan and Lavender

Chapter One

Introduction

1.1 Background

Processes currently operating within previously glaciated environments, transfer and rework a legacy of glacially and periglacially derived sediments. The continued domination of these sediments is a direct result of the imbalance of a large sediment volume in excess of postglacial erosion and transportation. The inability of the postglacial climate to maintain sediment supplies on the same scale, exacerbates the dominance of glacial sediment reserves. Slope and fluvial landforms have been shaped from the sediments, by a combination of processes that have been in operation since the retreat of glacial ice. In historically based studies, attention is primarily focused upon deriving the rate and nature of landform development in response to changes in causal controls. Climate change and the increasing influence of human activity from the mid- to late-Holocene are considered to be the two major controls that affect landform development. Acting either individually or together, the two controls regulate sediment transfer and its remobilisation following deposition.

In upland environments of Great Britain, heightened valley-floor alluviation and river terrace development within the late-Holocene has been attributed to secular climate change (Macklin *et al.* 1992; Rumsby, 1991; Macklin and Lewin, 1993; Tipping, 1994) and human activity (Tipping, 1995). Alluvial fans and debris cones assumed to have formed and stabilised during early deglaciation, show evidence of

late Holocene aggradation and incision, particularly within the last 300 years (Brazier *et al.* 1988; Brazier and Ballantyne, 1989; Innes, 1983; Tipping and Halliday, 1994). Attention is primarily focused upon addressing the coincidence of timing between causal factors such as climatic deterioration and human agricultural practices with the effect or response.

The changing behaviour of fans and cones influences the connectivity between slope sediment reserves and the main river system. The landforms represent a large volume of stored sediment. The remobilisation of predominantly coarse sediment from storage by incision and an increase in throughput of sediment directly from catchment sources, will alter the flood regime of the main river system (Harvey, 1996). The depletion of sediment reserves within catchments will enhance connectivity.

1.2 Research aims

This thesis represents the first study explicitly focusing upon the importance of sediment supply, acting as a major control on the development of alluvial fans and debris cones in upland environments of Great Britain. In understanding the importance of restricting sediment supplies in controlling fan and cone development, it is hoped that their response to scenarios of future climatic change and enhanced human activity can be predicted. This study aims to provide a general understanding of the effects of sediment exhaustion within an environment which experiences a wide variety in the relative amounts of sediment produced by a chequered glacial and varied cold climate history.

The aim of this thesis therefore, is to assess the importance of depleting sediment supplies within the fan and cone erosion-deposition system. To meet this aim a number of objectives have to be addressed.

1) Develop a methodology that can identify the manifestation of fluctuating sediment supplies in fan and cone form and sedimentology.
2) Investigate the degree of control exerted by sediment supplies on the response of fans and cones to human and climate controls.

3) Assess the findings in the light of regional and local variations in relative amounts of sediment and fluctuations in its transport availability.

4) Examine a variety of sites within UK upland environments, in an attempt to establish broad patterns of fan and cone evolution.

5) Through the use of radiocarbon dating, establish an activity pattern which can be related to sediment supply constraints.

1.3 Alluvial fan and debris cone erosion-deposition system

Alluvial fan and debris cone systems are separate and distinguishable from other sedimentary environments on the basis of their form and sedimentology (Blair and McPherson, 1994). The definition of an alluvial fan and a debris cone as adopted in this thesis are as follows.

"An alluvial fan is a low cone of gravels, sand and finer sediments that resembles an unfolded fan in outline..." (Patton et al., 1970 p112) "...that radiates down-slope from the point where the stream leaves the source area." (Bull, 1977 p 222).

"Debris cones are fan-shaped accumulations of poorly-sorted debris deposited... at the foot of steep gullies or tributary valleys." (Ballantyne, 1991a p 83).

Debris cones are similar to alluvial fans in planform but are generally steeper and supplied by comparatively smaller catchment areas. Both features are considered as part of an erosion-deposition system (Bull, 1977; Engelen and Venneker, 1988). Sediment eroded from the catchment is deposited at the zone of decreased confinement of flow. Deposited sediment can be reworked by runoff generated within the catchment.

The form and sedimentology of fans and cones record the rate and nature of sediment supply from the supplying catchment. Prolonged periods of stability are also recognisable, for example through palaeosol formation. Phases of incision are represented by erosional hiatuses. Depleting sediment supplies precondition the response to climate and human controls, leaving a traceable record within fan and cone form and sedimentology.

1.4 Structure of the thesis

This thesis is based upon the identification of traceable signatures in changing sediment supply, their fluctuation and depletion. In order to achieve the aim and objectives noted above, a range of techniques and methods of analysis have been employed. Field sites have been identified and detailed geomorphological maps constructed to establish characteristics of both sediment supply and deposition zones. By selecting four contrasting locations in upland Britain, fan and cone characteristics can be analysed within and between regions to establish a broad framework of development. An emerging picture of fan and cone chronology is established through the detailed investigation of sections in each of the field study locations. Stratigraphic analysis in the field is complimented by interpretation of changes in sediment transport mechanisms and sediment source characteristics using diagnostic methods previously used elsewhere but adapted for application in the context of fan and cone environments for the first time.

Chapter two reviews the role of sediment supply within fan and cone erosion-deposition systems. In reviewing the literature relating to fans within arid as well as humid temperate environments it is apparent that the role of sediment supply is important but rarely considered explicitly as part of any study. A range of methods can be identified which permit further consideration of sediment supply controls. The methods and techniques are described in chapter three, where rationale behind site selection is also presented. The four study locations, Glen Etive and Moffat in Scotland, the Howgill Fells and upper Teesdale in northern England, provide a range of upland environments where the objectives of the thesis can be addressed. In particular, their contrasting post-glacial histories have implications for the supply of sediments to alluvial fans and debris cones.

Chapters four, five and six contain the results from investigating fan and cone sedimentology. Chapter four is concerned with establishing the stratigraphy of each of the field sites by describing and classifying facies characteristics in appropriate fan and cone sections. Radiocarbon dating of organic inclusions provides a chronology for some of the sections. Chapter five presents diagnostic methods for identifying the mode of transport of the sediments preserved within fan and cone sequences. The facies classification presented in chapter four is developed further to consider

the properties of individual flow types, the implications of preservation potential and the application of sorting measurements as a means of discriminating between events. Chapter six introduces a method to determine the origin of sediment within fan and cone sequences, based upon mineral magnetic characteristics. A variety of magnetic parameters can be applied to infer the provenance of fan sediments. Hypotheses concerning the transition from glacially dominated to solifluction dominated sediment supply can be tested. Throughout chapters four, five and six, evidence from the individual study locations is considered in turn. The consequence is that interpretations become increasingly refined throughout the thesis.

The final chapter establishes, using the combined data from all sites, the extent to which a broad pattern of development can be determined for fans and cones in British upland environments. The original contribution of the thesis and additions to previous work are reviewed before suggesting areas of further study.

Chapter Two

Sediment transfer

2.1 Introduction

Sediment and its supply is essential for the development of fans and cones which, are in essence depositional landforms. The aim of this chapter is to identify suitable indicators within fan and cone form and sedimentology that are representative of changes in sediment supply operating within the catchment. To achieve this aim the pathways of sediment within the catchment system are reviewed focusing on the role of sediment supply in general catchment system behaviour. The characteristics specific to sediment supplies within upland environments of Great Britain are also considered. Attention is paid to variations in the relative amounts of sediment and changes in the rate at which material is made available for transport.

By combining this information the process-form relationships that result from fluctuating and depleting sediment supplies can be established. The process-form relationships can be used to reconstruct process from form. Equally important is an understanding of the sensitivity of fans and cones in recording these indicators because a methodology can be developed to ascertain the relative importance of sediment supply as a control upon the response and development of fans and cones.

2.2 Sediment supply: catchment system behaviour

The relationship of a fan and cone with its supplying catchment is summarised in Figure 2.1. The erosional and depositional systems are linked by the generation of runoff and the transport of sediment from within the catchment. The generation of runoff and the amount and nature of sediment transfer are regulated by processes operating internally and externally to the catchment. Sediment supplies are generally considered as a catchment component which responds to change as opposed to changing the response. This consideration can be partly attributed to the initial characterisation of fan system behaviour in arid or semi-arid environments where sediment supplies are unlimited (Bull, 1962a; Beaty, 1963; Denny, 1965; Hooke, 1968; Melton, 1965; Wasson, 1979).

2.2.1 Catchment process-response system

The key elements of the catchment process-response system and their inter-relationship are summarised in Figure 2.2. The two primary outputs from the system are transported sediment and runoff. The mode of sediment transport can vary from landslides to trunk stream entrainment. The capacity of runoff to transport sediment and rework deposited material within the fan and cone environment varies. The nature and magnitude of both runoff and sediment outputs are constrained by the balance operating between forcing conditions and resistance to applied force. The transport of sediment and sediment erosion within the fan or cone signifies that a critical value, condition or threshold has been exceeded (Schumm, 1979). In turn, the rate and nature of both force and resistance are governed by factors that operate externally to and internally within the catchment system (Brunsden and Thornes, 1979). Any change in external and internal factors will increase force or enhance resistance. Change can be through a direct response such as a debris flow. The rate of sediment build up within the trunk stream or on catchment slopes can be indirectly increased. Internal changes such as slope angle are less readily manifested.

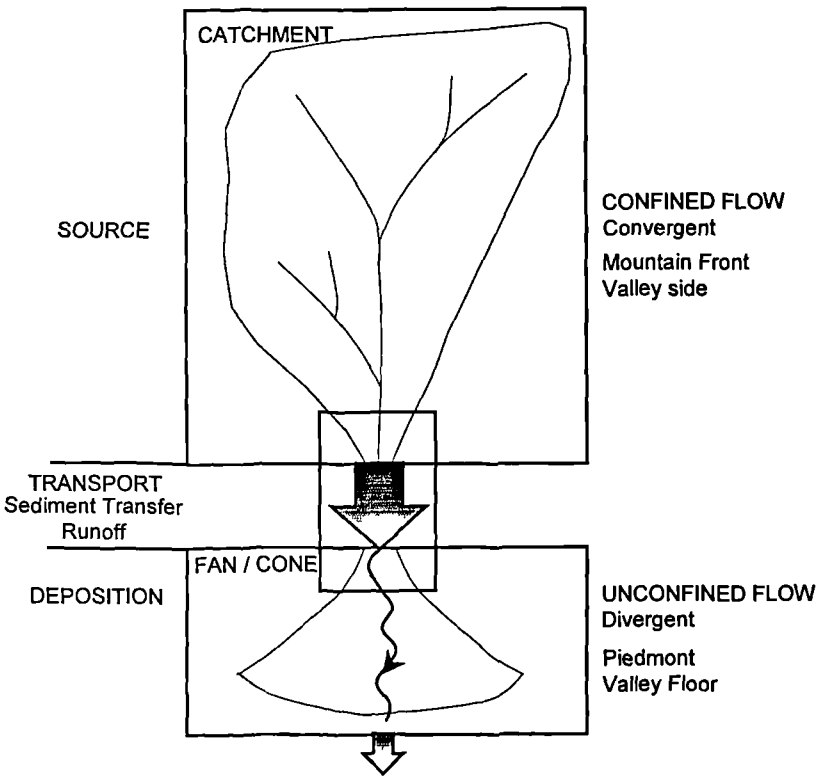


Figure 2.1. A schematic illustration of the relationship between a fan and cone with its supplying catchment. After Schumm (1977)

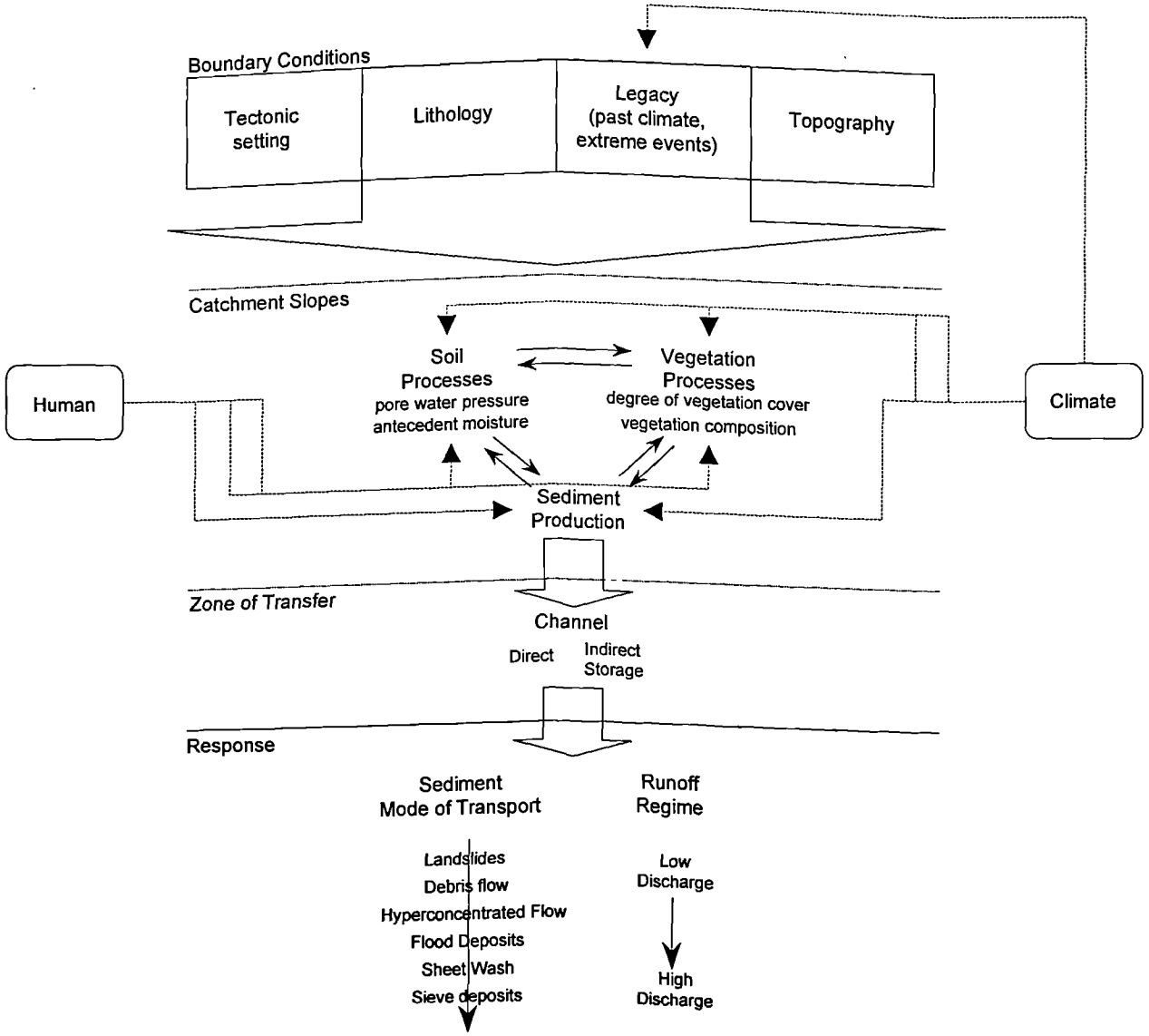


Figure 2.2. Controls upon response within the fan and cone environment. Both lithology and topography may regarded as intrinsic controls at Holocene timescales

Fan form and sedimentology record formative events (Brunsden, 1990) and are dominated by extremes such as aggradation by debris flow and the incision of deposits by runoff. The modifying actions of more frequent events have a limited role in creating landforms which persist for long periods (Brunsden, 1990). Following a path of inference, fan and cone sedimentology record the type and frequency of aggradation and the occurrence of sediment incision is represented by erosional hiatuses. Thus their presence is representative of the conditions associated with initiation, such as changes in climate or the stripping of vegetation cover by agriculture. Such changes are also indicative of the availability of sediment at the time of the forcing event.

The ability to compare fan and cone development between environments is based upon the assumption that process interactions conform to the same physical rules (Bull, 1977). The form and sedimentology of fans and cones, their size and rate of development, contrast under different climates such as semi-arid, humid-temperate, deglaciated mountain environments and arctic environments. This is due to the dominance of specific catchment components under any given climate regime including any additional geological and tectonic controls. Examples of the relationship of a dominant catchment component with fan and cone form are presented in Table 2.1. In identifying the differences in form and sedimentology of fans that result from spatial variation in climate, geology and tectonics, the importance of component dominance is highlighted. Similarly, if a change in the dominant component occurs this will be reflected in process interactions and ultimately in the temporal development of fans and cones.

The reconstruction of changes in dominant environmental controls operating in fan and cone catchments is based upon the analysis of sedimentary deposits. Studies are assisted by dating techniques and the construction of proxy records of past environmental conditions (Table 2.2). Past studies are primarily concerned with detecting alterations imposed on the landforms from outside the system. Studies are commonly focused upon linking fan and cone development to human and climate changes operating within the catchment at the time of the activity. In increasing the understanding of past response it is therefore possible to predict future change in the light of increased human interference and climate change. A review of past studies

Table 2.1. Studies of alluvial fans and debris cones under contrasting environmental settings, a general presentation of resulting differences in their form and sedimentology

Climatic Environment	Reference : Location	General Form and Sedimentology
Semi - Arid	Bull (1962) : California Beaty (1963) : California & Nevada Blissenbach (1954) Hooke (1967) Harvey (1988) : Spain Harvey (1989) Matthewson *et al.* (1990) : Utah Leece (1991) Whol & Pearthree (1991) : Arizona French *et al.* (1993) : Parker (1995) Viseras & Fernandez (1995) : Spain Guzzetti *et al.*, (1997) : Italy Siame (1997) : Argentina White & Walden (1997) :	⇨ lack of vegetation ⇨ migratory, multiple trunk channels ⇨ cut and fill sequences ⇨ debris flow and fluvatile deposits ⇨ active cyclic trunk stream, entrenchment and backfilling ⇨ tectonics influence sediment supply and its availability, commonly associated with fault scarp sequences ⇨ large range in size, Km's to m's ⇨activity governed by precipitation patterns
Deglaciated Mountain Environment		
Quaternary / Holocene deglaciation	Carryer (1966) : New Zealand Ryder (1971a) : British Columbia Ryder (1971b) : British Columbia Church and Ryder (1972) : British Columbia Roed and Wasylyk (1973) : British Columbia Cundill (1976) Allen (1981) Innes (1983) : Scotland Kostaschuck *et al* (1986) : Alberta Brazier *et al.* (1988) : Scotland Jenkins *et al.* (1988) : Scotland Brazier and Ballantyne (1989) : Scotland Derbyshire and Owen (1991) : Pakistan Gottesfeld *et al.* (1991) : British Columbia Owen (1991) Beaudoin & King (1994) Tipping and Halliday (1994) : Scotland Marchi & Tecca (1995) : Italy	⇨ Experience long periods of inactivity separated by periods of intense activity ⇨ surfaces commonly vegetated ⇨ trunk stream entrenched forming a sequence of fan terraces ⇨ snow melt an important trigger for the transport of sediment ⇨ steep channel gradients ⇨ commonly dominated by coarse sediment supplies linked to period of glaciation
Recently Deglaciated	Rickenmann (1990) : Switzerland Whitehouse & McSaveney (1990) : New Zealand Costa (1991) : Italy Dejong (1992) : West Greenland Ballantyne and Benn (1994) : Scotland Bertran & Texier (1994) : French Alps Ballantyne (1995)	⇨ steep slopes, large volumes of unconsolidated material ⇨ deposits comprised of debris flows, subsequently reworked ⇨ dominant trigger mechanism, rainfall events, oversteppend slopes and snow melt
Arctic Environments	Anderson & Hussey (1962) : Alaska Hoppe & Eckman (1964) : Sweden Leggett *et al.* (1966) : Alaska Catto (1993) : Northern Canada Harris & Gustafson (1993) : Yukon - Territory Fitzimons (1996) : Antarctica	⇨ activity restricted by the occurrence of rainfall ⇨ dominant mechanism of sediment transport is mass movement, reflected in feature sedimentology ⇨ presence of moisture linked with seasonal glacier and snow melt

Table 2.2. Examples of inductive approaches used to investigate controls upon fan and cone form and sedimentology

Author : Location	Main Aim of Study	Methodology
Tipping and Halliday (1994) Hopecarton Fan, Tweed Valley, Scotland	Deriving a human and / or a climatic causal control upon timing of fan aggradation	Radiocarbon dating, geomorphological and sedimentological investigations combined with comparison of findings with proxy records based upon palynological and archaeological data.
Brazier *et al.* (1988) Dalness chasm cone, Glen Etive, Scotland	Reconstructing the history of cone aggradation	A combination of stratigraphic investigation, pollen analysis and radiocarbon dating comparing findings with local proxy record of climate change
White *et al.* (1996) Cued Es Seffaia fan, southern Tunisia	Constraining the timing of fan aggradation with Late Quaternary climatic changes	The application of chronometic dating techniques combining AMS radiocarbon dating with optical dating techniques, dating identified stratigraphic horizons
Porat *et al* (1997) Nahal Sheharet fan, Israel	Determining the influence of tectonic activity on fan sedimentation rates	Using recognised horizons, sediments have been dated using infrared stimulated luminescence dating technique
White and Walden (1997) Tunisian southern Atlas Mountains	Provide dates for the onset and length of soils developed upon fan surfaces providing chronology of their succession	Measurement of Iron oxide enrichment within soils using mineral magnetics
Kostachuck *et al* (1986) Banff, Alberta, Canada	Determining controls upon the domination of debris flow and fluvial flow deposits upon fans that have experience similar environmental process history	Application of statistical analysis of fan area - basin relationships
Leece (1992) Western White Mountains, California and Nevada	To establish the control of differences of lithologic erodibility an sediment storage upon the form of alluvial fans	Application of statistical analysis of fan area - basin relationships
Marchi and Tecca (1995) Po valley, Italy	Determine geological and topographical controls upon fan development	Application of statistical analysis of fan area - basin relationships

indicates that a disproportionate attention is focused upon the development of alluvial fans. There is little comparable research on debris cone development.

2.2.2 Sediment supply : catchment system response

Fans and cones are depositional landforms. Understanding the cause of their dissection has been the focus of much work. The onset of aggradation and incision is used as an inference link to cause. The type of fan activity, be it aggradational or erosional, alters in response to three possible sets of controls: changes in water and / or sediment supply to the fan environment; intrinsic causes such as thresholds operating within the depositional environment; age-related causes (Schumm *et al.*, 1987).

Periods of fan aggradation reflect periods of excess sediment generation and delivery, whereas reduced sediment supply or increased transport capacity results in a reduction of the rate of fan sedimentation or even in fan dissection. If no sediment is available for transport at the time of a rainfall event fan deposits will be reworked. Phases of aggradation and incision alter in response to changes in environmental conditions that influence runoff and sediment supply to the fan. A change in the regime from deposition to erosion is indicative of changes to sediment availability, which are controlled by climate and human activity (Harvey, 1984a).

Empirical evidence of the cyclic behaviour of fans in response to internal thresholds was first identified from the experimental modelling of alluvial fans by Schumm *et al.* (1987). In their experimental studies of fan growth, precipitation was delivered to a sediment source area at a constant rate. Runoff and sediment were moved out of the miniature drainage basin to a piedmont area, where a fluvial fan formed. During fan growth a number of cycles of trenching and subsequent backfilling were observed within the channel of the fan's trunk stream. The lowering of the channel gradient by its erosion resulted in a switch to deposition and channel infilling. Following a period of infill the subsequent oversteepening of the channel gradient resulted in the renewal of channel trenching. The cyclical change from erosion to deposition was attributable to the sediment transport capacity of the trunk stream, a threshold ultimately controlled by continuous changes in channel gradient. The cyclic behaviour occurred under tightly controlled conditions and was not a result

of change in experimental procedure or to change in the intensity or duration of precipitation. Trenching was caused by exceeding an intrinsic geomorphic threshold (Schumm *et al.*, 1987).

Experimental evidence of cyclic fan behaviour has been corroborated by a field study carried out by Scott and Erskine (1994) on the development of 12 fans in Australia. They analysed the development of number of fans in response to a large storm using survey profiles. Despite the close proximity of fans, similar climate and human environmental controls, the response of fans differed markedly. The response was attributed to their threshold condition at the time of the storm. Eckis (1928) in his study of the Cucamonga fan at the base of San Gabriel mountains, Southern California, recognised that the general diminution of channel gradients and sediment yield through geologic time affects the evolution of fans. He suggested that as sediment yields decrease, alluvial fans should become deeply entrenched. Harvey (1984b, 1990) cites the ageing process as an explanation of the change from aggradational to incisional regime in fans in south-east Spain, arguing sediment cessation as a response to a Quaternary tectonic control.

2.2.3 The dominance of sediment supply in sediment limited environments.

The three controls on fan aggradation and incision described above all represent a valid causal explanation for the switch from aggradational to incisional regime. Of all environments in which fans and cones develop, deglaciated mountain environments have the most obviously restricted sediment supplies. The supply of sediment is inherited from the previous glaciation and a period of periglacial activity. The post-glacial climate is insufficient to regenerate sediment that has been transferred from slope storage. In comparison to Eckis's (1928) geological and Harvey's (1990) Quaternary timescale, 'ageing' in deglaciated mountain environments is constrained to the onset of deglaciation. The control of changes in sediment supply are more readily evident over much shorter timescales of fan and cone development. Following deglaciation, climate change and human control, the availability of sediment for transport depends on sediment supply which will have a finite volume.

The main argument of this thesis is that changes in sediment supply represent an important control on fan and cone development in sediment-limited environments.

Sediment-limited environments are characterised by low rates of sediment production and high rates of sediment transfer. Slope sediment reserves of unconsolidated glacial sediments once removed cannot be replenished by Interstadial rates of chemical and physical weathering. Sediment supply can be recast as the dominant catchment component control on landform development, as opposed to climate and human controls. The dominance is reflected in the temporal development of fans and cones. Instead of responding to changes in external controls, the internal depletion of sediment supplies controls the response. Using an inductive approach, in association with recognisable indicators of sediment supply acting as a control, it is possible to reconstruct temporal controls exerted by depleting sediment supplies on fan and cone development.

2.3 Sediment supply: deglaciated mountain environments

2.3.1 The definition of sedimentological terminology in deglaciated mountain environments

Prior to characterising the sediment system in context with deglaciated mountain environment controls, the terminology used for its description requires clarification. The terms sediment supply and sediment availability are often used interchangeably. Both can be taken to delimit relative amounts of sediment and to describe the provision of sediment for transport. In this thesis sediment supply is taken to represent the total amount of sediment present within a catchment. Any change or fluctuation in sediment supply will represent either addition to or depletion of sediment reserves. The availability of sediment equates to the capability of sediment transport, subject to the degree of force applied and boundary conditions or resistance to that force at any given point in time. Sediment supply and availability are inherently linked in that there must be a sediment supply for it to available for transport. Sediment exhaustion is a characteristic of sediment availability and supply. Sediment supply can be exhausted if sediment transport outpaces sediment production. Further transport would occur only as a result of a change in resistance or forcing conditions which operate at different spatial and temporal scales.

2.3.2 Characterisation of sediment supplies in upland environments of Great Britain

Climate has been the dominant factor in producing sediment supplies within upland environments of Great Britain. Variations in geology have either restricted or aided

the production of sediment in response to weathering processes, the characteristics of which are specific to outcrop location. The influence of tectonics, which plays a dominant role in semi-arid environments, is restricted to local changes in base-level.

Within the limits of the Devensian glaciation, which encompasses most upland environments in northern Britain, sediment supplies are a legacy of the Devensian and the associated period of intense cold following deglaciation. The onset of deglaciation and exposure to cold conditions varies from 18 Ka BP at maximum limits of Devensian ice (Penny *et al.*, 1969; Wintle and Catt, 1985) to between 16 Ka BP and 14 Ka BP in Scotland (Sutherland, 1991) and the Lake District (Bowen *et al.*, 1986). The period of cold persisted until approximately 13 Ka BP (Ruddiman and McIntyre, 1981). Devensian sediment supplies have been modified during the Loch Lomond Stadial conventionally assigned to the period 11-10 Ka BP. Where the less extensive Loch Lomond Glaciers formed, it is assumed that Devensian sediment supplies have been obliterated and replaced by sediment derived by Loch Lomond glacier ice (Ballantyne and Harris, 1994). Outside Loch Lomond glacial limits periglacial processes have modified and or added to Devensian sediment supplies through weathering and solifluction, although temperatures were not as severe as those experienced during Devensian glaciation (Briffa and Atkinson, 1997).

During interstadials, weathering processes operating under a warmer climatic regime, soil formation and the chemical and mechanical weathering of exposed bedrock are of insufficient strength to produce sediment supplies on the same scale. Following deglaciation and climatic amelioration, glacial and periglacial sediments which constitute the bulk of slope sediment supplies, once transferred from slopes, are irreplaceable. Relative amounts and the characteristics of slope sediments vary spatially according to glacial and periglacial history experienced following Devensian or Loch Lomond deglaciation. Relative amounts of sediment are influenced by underlying lithology and location in accordance with glacial limits. This results in marked local variations in sediment supply and composition, coarse gravels and presence or absence of fines, on valley slopes.

2.3.3 Temporal fluctuations in sediment availability since deglaciation

The rate at which sediment supplies are depleted is dependent upon the occurrence of conditions at which applied force can overcome resistance. Sediment availability fluctuates in accordance with changes in climate and in response to the influence of human activity. Sediment availability has thus changed over time as well as differing spatially. This is reflected in the amount of sediment remaining in the catchment and also in fan and cone development history. Sediment availability can also change under given force and resistance thresholds. At any given point in time only a certain amount of sediment is capable of being transported. Sediment availability can be characterised over both the long and short term.

Slope sediment reserves are subject to changes in force and resistance following exposure during deglaciation. The time period over which changes operate depends upon location within or outside Loch Lomond Glacial limits. Depending upon location, sediment supplies have undergone a series of climatically induced and internally regulated changes in sediment availability. Three long-term changes in sediment availability have been identified: the period of paraglaciation following deglaciation, cold conditions during the Loch Lomond Stadial and the long-term build up of material as storage within the catchment transport system.

The term paraglacial was originally used to refer to non-glacial processes directly conditioned by glaciation (Church and Ryder, 1972). The definition includes the reworking of readily entrainable or potentially unstable glacial deposits after the withdrawal of glacier ice. Unstable, unconsolidated glacial deposits, in combination with low vegetation cover and high precipitation as climate rapidly ameliorates, results in a high sediment availability and increased rates of sediment transfer. The paraglacial period resulted in the formation of distinctive landforms including alluvial fans and debris cones in Great Britain and other previously glaciated environments such as; British Columbia (Ryder, 1971a; Ryder, 1971b; Beaudoin and King, 1994), the Karakorum mountains (Derbyshire and Owen, 1990; Owen, 1991), Norway (Ballantyne and Benn, 1994; Ballantyne, 1995) and the Central Himalayas (Sharma and Owen, 1996). The time period of paraglacial activity varies between environments. It can be constrained to the time period between deglaciation and the establishment of vegetation cover and thus stabilisation of unconsolidated sediment.

Reduced activity is linked with the establishment of a vegetation cover and decreasing peak discharges with a resulting decrease in the capacity to entrain sediment within the supplying catchment (Ryder, 1971a; Church and Ryder, 1972; Johnson, 1984). Sediment transfer is restrained by the presence or absence of moisture. In the Vestfold hills, Antarctica paraglacial sediment is currently readily available for transport but due to limited precipitation, sediment transfer is restricted to gravity controlled mass movement (Fitzsimons, 1996). Evidence of climate conditions during the Devensian deglaciation are restricted to temperatures derived from beetle remains (Atkinson *et al.*, 1987). Evidence indicates that deglaciation took place under sustained cold continental conditions, characteristic of extremes in seasonal temperatures and lack of moisture. However, the glacial / interglacial transition was marked by extreme variability in temperatures and precipitation (Briffa and Atkinson, 1997).

The Loch Lomond deglaciation was short lived and characterised by retreating but still active glaciers (Benn, 1990). The diminution of snowfall under cold conditions is attributed as the cause of deglaciation (Benn *et al.*, 1992). Within close proximity to glaciers during their formation and retreat, permafrost and periglacial conditions returned for the duration of the Holocene (Ballantyne and Harris, 1994). Climate conditions during the Loch Lomond Stadial were not as severe as that experienced during the Devensian. In comparison to the current climatic regime, climate exhibited enhanced continentality and much colder winters. Precipitation was supplied by Atlantic depressions originating from the south-west and was subject to orographic controls. Enhanced periods of snow melt have been shown as an important trigger for sediment transfer, as debris flows or as stream transported sediment. According to contemporary studies snow melt is an important influence on paraglacial debris cone and fan formation (Ballantyne and Benn, 1994). It is reasonable to assume similar trigger mechanisms for Loch Lomond paraglacial debris cones (Brazier *et al.*, 1988). Despite the combination of low thresholds with high magnitude trigger mechanisms during the Loch Lomond Stadial no study has yet found evidence of fan and cone initiation outside Loch Lomond glacial limits or for the reactivation of Devensian features.

During the Late Devensian Interstadial and throughout the Holocene, apart from periods of transition, climate has experienced minor oscillations in temperature.

Significant changes in climate have seen periods of increased wetness which are usually accompanied by an increase in storminess (Briffa and Atkinson, 1997). Palaeoclimatic and palaeoenvironmental indicators of fluctuations in temperature and precipitation include, glacial limits, beetle remains, diatoms, pollen and foraminifera : reconstruction of the Holocene climate was based primarily on tree-ring and tree-line data. Data are collated from different time periods and different localities thus representing snapshots which are integrated to give general change. Under the Holocene climatic regime sediment transfer is restricted to the removal of material that built up within trunk streams or gullies and the direct erosion of slope sediment reserves by intense storms.

Sediment is introduced to trunk streams or side gullies from slope storage. Within debris cone systems with steeper catchment gradients, sediments that have been built up become increasingly unstable and subject to gravity. Removal of this sediment requires rainfall events of lower magnitudes as accumulated sediment approaches the angle of internal friction. The periodicity of sediment build up and subsequent removal is reliant upon configurational controls and the occurrence of a trigger mechanism of sufficient strength. Evidence of cyclicity in sediment supply is recognised in the response of relict fans to a recent storm event in the Howgill Fells (Wells and Harvey, 1987).

The removal of storage within low lying catchments of alluvial fans requires an event of a high magnitude in order to reach critical shear stress for sediment entrainment (Vandale *et al.*, 1996). High magnitude events also erode fresh slope sediments or reactivate old gully systems. It is argued that the resistance to a trigger mechanism, be it rainfall or snow melt, is influenced by the increasing activity of man from the Holocene to the present day. Extreme events are also linked to the initiation of debris cones and the reactivation of relict features. The inference is primarily based upon analogues with contemporary cone and gully reactivation by storm events (Carling, 1986a; Wells and Harvey, 1987). However, the role of extreme events in the reactivation of relict features is still uncertain (Ballantyne, 1991a).

At any given point in time under uniform boundary and forcing conditions, readily accessible sediment will be eroded. Forcing events of increasing magnitude are

required to erode sediment as sediment availability decreases exponentially. Subsequent sediment transfer will require a change in external and internal controls providing sediment which under previous conditions was unavailable for transport. Sediment availability changes according to the nature of the change in force and resistance. Short-term enhancement in sediment availability can also be attributed to an extreme storm with a long return period. The activated area can be constrained spatially to specific locations within the supplying catchment. Lowered thresholds within this area results in sediment transfer in response to events of lower magnitude and frequency in comparison with initial extreme event. The rate of sediment transfer decreases as the active area becomes stabilised if a sufficient period of time separates rainfall events (Brazier and Ballantyne, 1989).

Sediment availability can also be limited on a single event scale as sediment that has been made accessible has been removed. As the triggering storm or snow melt continues, the lack of available sediment for transport results in overland flow. If runoff is of sufficient capacity the initially eroded and deposited sediment can be re-worked. This has been shown in studies of contemporary debris flows to occur immediately following their deposition (Costa, 1988; Coussot and Meunier, 1996).

2.3.4 Sediment exhaustion

The condition of sediment exhaustion can operate over a number of scales: during a single storm event, in the recovery of an activated area, cyclically in association with the build up and removal of sediment, under given threshold conditions, and in the complete transfer of sediment from within the catchment. As sediment supplies diminish sediment availability decreases. Changes in sediment availability are reflected in the rate and timing of fan and cone development. Sediment exhaustion is an inherent part of fan and cone development. The removal and subsequent exhaustion of glacial sediment will significantly influence the development of fans and cones. As sediment supplies decrease, sediment becomes increasingly harder to erode replacing a predominantly aggradational regime with fan and cone incision.

2.4 Sediment supply: a control of fan and cone response

It is arguable that sediment supplies, combined with the limitation of sediment regulated by changes in its availability, control the nature of sediment transfer and the effectiveness of runoff from the catchment. Incision commonly follows the temporary depletion of sediment within the supplying catchment. The process can be extrapolated to scales of sediment exhaustion over the short- and long-term. The result of long-term depletion will result in a switch from a predominantly aggradational to predominantly incision regime. In a sediment limited environment, the switch will occur irrespective of the occurrence of conditions conducive to sediment availability.

Brazier and Ballantyne (1989) in comparing the nature of recent activity of two debris cones, Dalness Chasm at Glen Etive in the western Highlands and the Glen Feshie debris cones in the western Cairngorms, recognise the fundamental importance of an inherited sediment supply. At Glen Etive the debris cone has recently undergone fluvial reworking of previous cone deposits. In Glen Feshie two recent phases of cone aggradation have been identified. The contrasting response is attributed to the abundance of glacigenic and Late glacial scree deposits at Glen Feshie and their lack at Glen Etive. Inherited sediment supplies are therefore an important control on the continuation or cessation of debris cone accumulation. The control of long-term exhaustion of sediment reserves is clear from this particular example. However, the control of sediment supply in fan and cone development in response to other scales of sediment exhaustion is not as obvious from form alone. As most studies of fan and cone development have focused upon deriving the cause of changes in sediment availability, cursory attention has been paid to the nature of fan and cone activity following the initial onset of activity.

The cause of recent reactivation and aggradation in fans and cones have been attributed to secular climate change, the effect of human agricultural practices on resistance thresholds, extreme storms of long return period, and local controls (Ballantyne, 1991a). Climate and human activity are inherently linked by the need for storm events to provide a trigger mechanism for activity. The emphasis of most studies is upon reconciling the influence and control of these two factors. Tipping and Halliday (1994) argue the need for more studies to determine synchronicity of

data to support a single causal factor. Modern analogues of the response of relict features to contemporary storm events supports the importance of extreme events in past fan and cone development. Although credence is given to the role of extreme events in the reactivation of fan and cone activity, it is difficult to obtain direct evidence in fan and cone deposits.

In deriving the cause of two periods of cone aggradation at Glen Feshie, Brazier and Ballantyne (1989) provide three equally valid explanations. These are the occurrence of extreme storms of long-return period, secular climate change and the episodic migration of the River Feshie. Following the extreme event which initially increased sediment availability by lowering thresholds, sediment exhaustion is recognised as potentially stabilising the period of aggradation. Sediment is exhausted either by a decrease in sediment availability, by the recovery of vegetation following a storm-free period or by the removal of all accessible sediment. An equally valid explanation of cessation of aggradation is the direct transport of subsequent debris flows into the River Feshie. During apparent periods of stability the river has been shown to be located below the cone, thus allowing the direct throughput of a continuous supply of aggraded material. To reconcile the two explanations a means of identifying progressive exhaustion of sediment within available sediments is required. Progressive exhaustion is represented by a change in the character of sediment transported in response to decreasing availability and ultimately by a change to incision as available sediment is depleted or is made unavailable in the source area. Progressive exhaustion would also be validated if it were possible to determine a single point source origin for the sediment.

The response to a change in sediment availability, an extreme event or the long-term cyclic build-up of material, is partly controlled by the magnitude of the event but more importantly by the presence of accessible sediment. If no sediment is available the trigger mechanism generates runoff which, if of sufficient capacity, can incise fan or cone. If sediment is available it can be aggraded within the fan and cone. The response depends upon the timing of the event in the exhaustion cycle. The control exerted by sediment supply and availability is the same over all scales of sediment exhaustion (Figure 2.3).

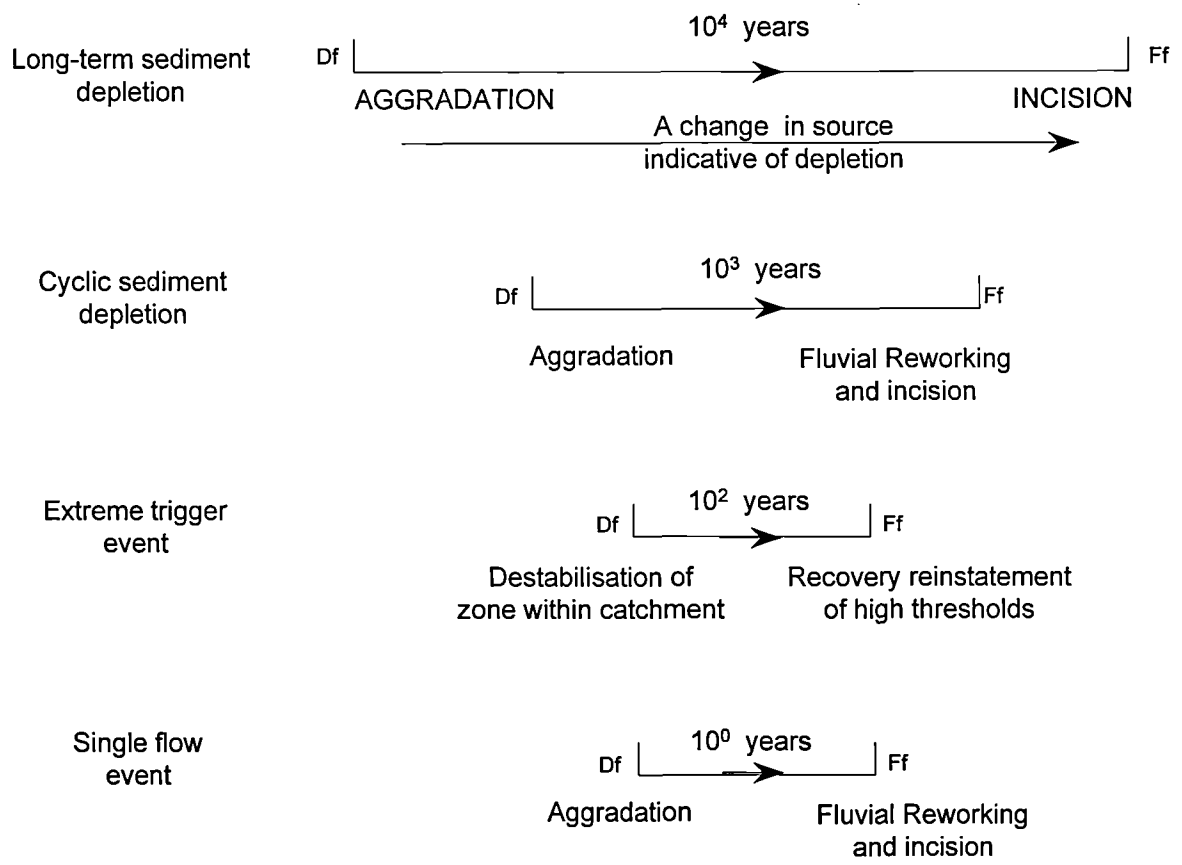


Figure 2.3. A schematic illustration of long and short term scales of sediment exhaustion

Changes in sediment supply are therefore important in the control of fans and cone development. This can be said of all fans and cones since their initiation immediately following deglaciation, during the Holocene and in recent phases of activity. As a result the controls of sediment supply should be detectable in their form and sedimentology.

2.5 Indicators of sediment supply control

Suitable indicators of controls on sediment supply need to be measurable over the different scales at which sediment exhaustion occurs. In addition the indicators must be independent of other process controls. Two such indicators can be identified. Their recognition is based upon limited sediment supplies in upland environments of Great Britain and of system dynamics which regulate the transport of sediment from catchment sources.

The first indicator is a change in the source of sediment supplied to the fan and cone over time, which is an inevitable response of exhausting sediment supplies. A sequential change in source evident in fan and cone stratigraphy is dependent upon the characterisation of distinct source types within the catchment. The actual signature of change in source will vary in accordance with regional and local variations in the characteristics of sediment supplies. Different source types include glacial material, scree, solifluction deposits and trunk stream and gully storage. As glacial sediment supplies are depleted alternative sources are tapped. The characterisation of aggraded sediment sources will help to distinguish point source origin of sediment and the cyclic aggradation of stored material. The recognition of multiple sources within fan and cone deposits is heavily dependent upon the use of a technique of sufficient resolution and investigation of deposits chronologically.

The second indicator is the method or mode of sediment transport, which is inherently linked to sediment supply. Coussot and Meunier (1996) considered the spectrum of different modes of sediment transport as a function of their solid fraction, material type and water concentration (Figure 2.4). A continuum exists between different flow types. The transition between each is controlled by changing water and sediment concentrations (Costa, 1988; Coussot and Meunier, 1996). It is the transition and reliance of flow type on sediment supply that provides the basis for its

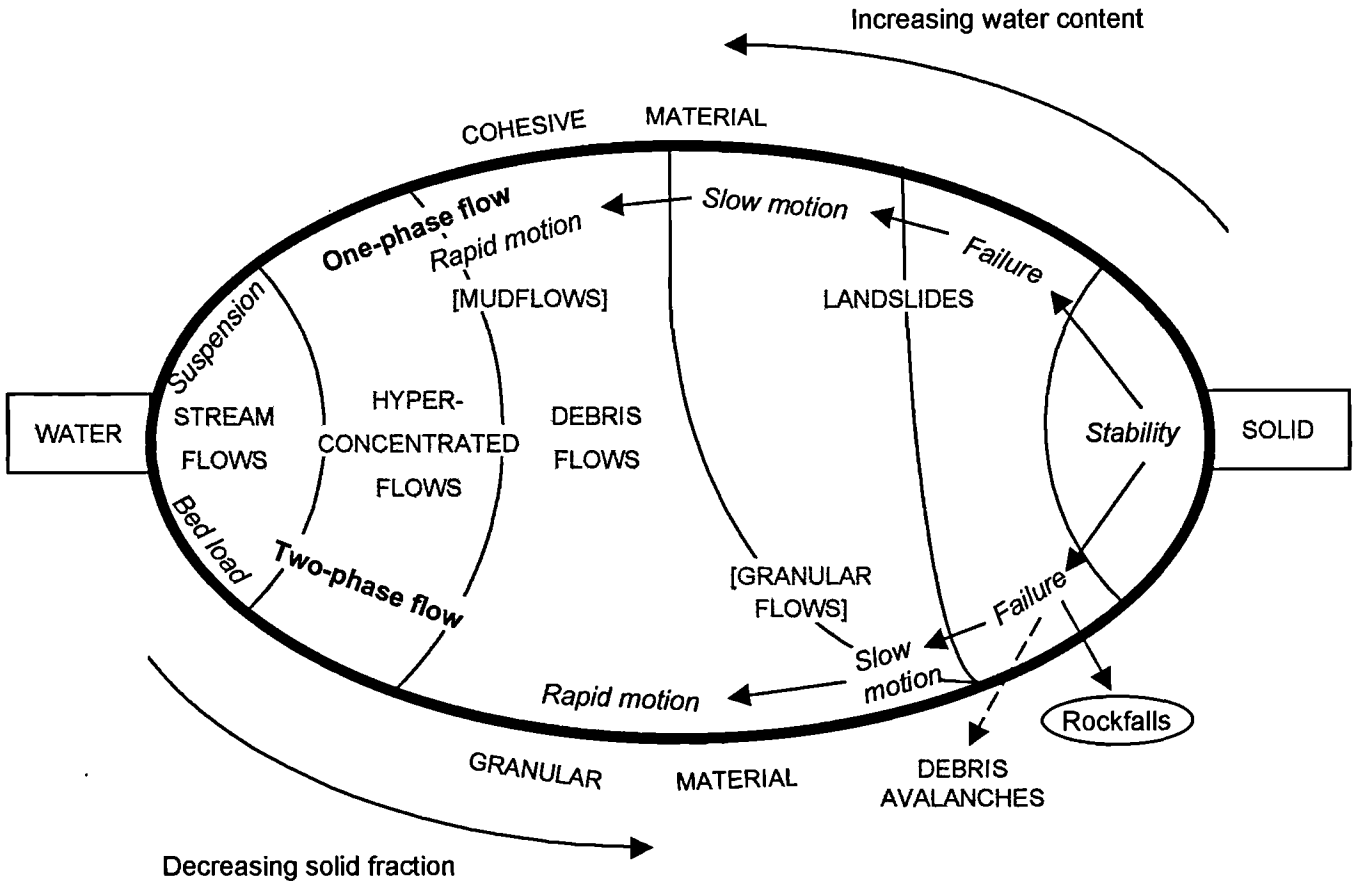


Figure 2.4. Classification of mass movement on steep slopes as a function of solid fraction and material type, from Coussot and Meunier (1996, p 214)

use as an indicator of sediment availability and thus exhaustion. Harvey (1984b) recognised a progressive change from debris flows to fluviatile deposition in fan sequences in southeast Spain in association with a long-term decrease in sediment availability due to climate change. A similar trend may be recorded in much smaller fans and cones in upland environments of Great Britain. A progressive change in transport mechanism would be evident over the fan and cone development sequence. Changes in response to cyclic sediment availability and in response to a recovery period following an extreme event would be superimposed on the long-term trend.

If the two indicators are successful in identifying the effects of sediment exhaustion within fan and cone stratigraphy, their sensitivity to future changes in sediment availability can be assessed. The usefulness of these indicators in fan and cone stratigraphy rests on their feasibility, preservation within deposits and the ability to measure them.

2.5.1 Indicator feasibility

A time-progressive change in sediment source can only be taken to represent a depletion of sediment supply. The identification of a sequential change in source from glacial through to solifluction in fan and cone deposits cannot be reproduced by other unrelated processes. Similarly, a change in sediment transport is inherently restricted by sediment availability. It is changes in sediment availability that can be produced by the independent action of different processes controls.

The presence of these indicators within individual features is conditioned by long-term and short-term changes in sediment availability. Regional and local factors need to be considered when interpreting the data, to account for individual catchment controls upon fan and cone development. A change in the mode of sediment transport is essentially independent of changes in source and can be more readily associated with short-term changes in sediment availability. Material properties can effect the character of different transport mechanisms but do not affect the progressive change in transport mechanism as sediment supplies become exhausted. Catchment size can precondition the dominance of particular modes of transport. Debris flows are more frequent in smaller steeper catchments (Wells and

Harvey, 1987; Harvey, 1996). This will influence the frequency of deposits recorded in features of different size but not the progression of the transport mechanism associated with sediment exhaustion. Catchment size effects must be reconciled in the interpretation of sequential change of flow types.

2.5.2 Indicator preservation

The preservation of an unbroken record of sediment transfer from a catchment is affected directly by extended periods of incision of fan and cone deposits, cyclic internal thresholds and by catchment size. Extended periods of incision associated with periods of low sediment availability can remove sedimentological evidence of previous phases. These can be recognised as erosional hiatuses. Threshold-controlled incision by fan entrenchment can also affect the sediment record (Schumm, 1977). The destruction of fan and cone deposits is exacerbated by the direct loss of sediment from the system as a result of the cycle of internal thresholds operating in the fan and cone system. Sediment preservation is commonly associated with backfilling of the trunk channel whilst sediment is lost if the trunk stream is undergoing entrenchment. The operation of cyclic thresholds can result in features formed under identical environmental conditions responding differently to the same forcing event (Scott and Erskine, 1994). As a result, the sequence stratigraphy is broken and changes in sediment supply operating in the catchment are not fully represented. It is difficult to identify this type of break in the sediment record. Cyclicity can only affect the record of change in transport mechanism, changes in sediment source are still recognisable.

The sequential change from fan entrenchment to fan aggradation is associated with feature size. Larger features are more likely to experience internal cyclicity as on smaller debris cones events commonly inundate the whole cone (Vandale, 1996). Increasing catchment size and an associated increase in feature size and effects of internal thresholds also restricts the preservation of deposits spatially.

Fan and cone incision, cyclicity and catchment size affect the sediment record available for investigation. Signatures of short-term changes in sediment availability are the most likely to be adversely affected, while long-term sequential changes are still identifiable. Where the sequence of changes in sediment transport is

ambiguous, the change in sediment supply can help in the interpretation of sediment exhaustion control.

2.6 Summary

The nature of sediment limitation found in upland environments of Great Britain provides an opportunity for establishing the importance of ageing or exhaustive sediment supplies in the development of fans and cones. Changes in sediment availability specific to upland environments of Great Britain have been shown to operate over a number of different scales. The effects of exhaustion in controlling fan and cone response are potentially traceable over all scales of operation using two of the indicators identified. This is constrained by the preservation of formative events in fan and cone stratigraphy.

The success of the two signatures of sediment supply and availability control on fan and cone response is governed by the resolution achieved by the methods and techniques adopted to measure their presence in the stratigraphic record. The investigation of the control of changes in sediment availability and supply must account for regional and local differences of relative sediment reserves to establish the generality of findings. The data can then be used as the basis for predicting the response of fans and cones to future changes in climate and human interference.

Chapter Three

Approach and site description

3.1 Introduction

The approach adopted in this thesis is in three parts. Initially the chronological framework and sediment sequencing is derived for a number of fans and cones. This is achieved by dating palaeosols and by an interpretation of the context of deposition and the feature surface form. The chronological framework is further constrained by the identification of individual flows, using a combination of facies description and measurement of sorting. The source material comprising each flow is discriminated by applying mineral magnetics. In deriving the number of distinct phases of aggradation, examining the inter-relationship of their constituent flows and determining the pattern of source change between and within separate phases, insight into the development of fans and cones in response to changes in sediment availability and supply can be obtained. The rate and nature of changes in sediment availability can also be derived.

3.2 Temporal indicators of controls on sediment supply

3.2.1 Methods of reconstructing mode of sediment transport

In upland environments of Great Britain, the major sediment transport processes relevant to fan and cone deposits include dry cohesionless flows (Innes, 1983), debris flows (Innes, 1983; Brazier and Ballantyne, 1989; Carling, 1986a; Wells and Harvey, 1987), hyperconcentrated flows (Wells and Harvey, 1987) and fluviatile flood

and reworked deposits (Brazier *et al.*, 1988; Wells and Harvey, 1987). The ability to differentiate between relict deposits and to recognise a hierarchy of bounding surfaces is essential in deriving signatures of sediment exhaustion. A methodology was required for this thesis to provide a framework for understanding associations among depositional forms and the transport processes responsible for them (Brierley *et al.*, 1993). In achieving this, sediment exhaustion can be recognised in association with a single storm, cyclically and throughout the whole sedimentary sequence.

Differentiation between different flow types is commonly based upon facies description, as flow deposits have been shown to exhibit diagnostic sedimentary structures. Diagnostic properties have been compiled for this research from the direct observation of contemporary flow sedimentology and morphology (Costa, 1984), from laboratory experimentation (Van Steijn and Coutard, 1989; Phillips and Davies, 1991), and from an understanding of flow rheology (Johnson and Rodine, 1974; Costa, 1988; Coussot and Meunier, 1996; Bertran *et al.*, 1997). The more detailed the facies description, the greater the resolution. High resolution detail was best achieved by the application of a facies model, which can differentiate between the deposits of different flow types (Hooke, 1967, Miall, 1977; Friend, 1983; Eyles *et al.*, 1988; Evans, 1991; Brierley *et al.*, 1993; Viseras and Fernàndez, 1994).

A facies model provides formally defined codes that encompass virtually all the variability present within sedimentary deposits, their sedimentary structures, contact boundaries, bedding planes, grain size and the identification of hiatuses. A number of facies models have been developed for the description of sediments in contrasting depositional environments including alluvial fans (Hooke, 1967; Miall, 1977). Eyles *et al.* (1983) proposed a facies model, subsequently refined (Miall, 1985; Miall, 1988), which makes use of the original fluvial dominated model and incorporates diamict coding. Regardless of depositional environment, a diamict is taken to refer to any poorly sorted clast-sand-mud admixture (Eyles *et al.*, 1983). It is the Eyles *et al.* (1983) facies model that has been applied to characterise and differentiate sediment structures which range from poorly-sorted, sub-angular debris flow deposits exhibiting little internal structure to stratified, laminated and re-worked fluvial sediments (Eyles *et al.*, 1988; Brierley *et al.*, 1993). The facies model is comprised

of 40 codes and is flexible enough to account for depositional and local environmental complexity (Eyles *et al*, 1983).

Despite a detailed description of sediment sequences, hyperconcentrated flow deposits can readily be mistaken as debris flow deposits as their sediments and structural characteristics are poorly understood (Costa, 1988). Both debris flows and hyperconcentrated flows can result in a wide range of sedimentary facies which reflect environment and process diversity. Variations are introduced by changing boundary conditions, the intensity of the trigger mechanism and specific material properties (Van Steijn, 1995). In accounting for the different characteristics in the context of this study, the interpretation of the deposit structures is open to a degree of subjectivity. Subjectivity is not constrained to the interpretation of deposits and of an individual flow but can be extended to a whole depositional sequence. A classic example of two contrasting interpretations of the same sequence of sediments involves the Trollheim fan sequence, Deep Springs Valley, California. Hooke (1967) found the sequence to be dominated by debris flow, sieve lobe, sheetflood and channel facies. Blair and McPherson (1993) argue that the fan was built exclusively by clayey and gravelly, matrix-supported debris flow deposits. What was originally interpreted as sheetflood deposits was therefore reinterpreted as debris flow deposits. Blair and McPherson (1993) argue that the debris flow deposits were winnowed by surface water, resulting in characteristics that have been mis-interpreted as sieve and sheetflood deposits.

In carrying out field descriptions of flows investigated as part of this research, individual units are not always readily discernible to the eye. To support the identification of the upper and lower boundaries of deposits and to increase the objectivity of the differentiation between flow types, the facies descriptions were supplemented by laboratory-derived physical characteristics. The rheological properties of flow types exhibit a scalar variation in the degree of sorting, which is symptomatic of their mechanisms of flow and the close relationship within a sediment : water flow continuum. Sorting indices have also been shown to be sensitive in the recognition of intermediary mudflow or hyperconcentrated flow deposits (Bull, 1962b; Hubert and Filipov, 1989). Differentiation was achieved here by using basic summary statistics and applying sorting indices. The interpretation of basic summary statistics can be affected by the wide range of grain size and

rheological characteristics exhibited by different flow processes (Woolfe, 1996). The sorting index was originally developed to differentiate between sediments deposited in major process environments (Passega, 1957). A wide range of sorting measures are available. They vary principally on the percentiles used to determine variability around the mean value in the overall particle size distribution. There was scope in this thesis for identifying a measure of sorting that is specifically attuned to the alluvial fan and debris cone process environment and the different sorting characteristics introduced by the varying rheological properties of debris flows, hyperconcentrated flows and fluvatile deposits. In applying both a facies model and a measure of sorting to differentiate between the relict deposits of major flow types, a degree of objectivity was achieved whilst still accounting for facies variability.

3.2.2 Methods of ascribing changes in sediment source

In determining a sequential change in the source of sediments within a stratigraphic profile the source of individual flows can be identified. The separation between different flows is confirmed whilst information is provided upon spatial differences in the supply of sediment between flows and their temporal sequence of change. The ability to achieve this degree of resolution is reliant upon there being a recognisable difference in the various source materials within the boundary of the supplying catchment.

The range of source materials which make up sediment supplies within the catchments of fans and cones in upland environments of Great Britain include glacial material, solifluction deposits, loose scree, soil horizons and mixtures of the deposits maintained as storage within the transport system. Blanket peat also represents a source of organic material that can be supplied to the fan or cone but is readily distinguishable from the different sediment sources listed. The terms used to describe the different sediment sources in this work are based upon the mechanisms that formed them, which in turn represent differing intensities of weathering experienced. The different sources were primarily derived from the post-deglaciation weathering of glacial material. On a much smaller scale material was also derived directly from the bedrock underlying the catchment. The variation introduced by two substrates and the subsequent weathering regime was sufficient to produce a measurable difference between sources, in order to fingerprint each source type.

A number of techniques were available to fingerprint sediment sources, including geochemistry (Collins *et al.*, 1998), scanning electron microscopy (DeBoer and Crosby, 1995), X-ray diffraction (Woodward *et al.*, 1992; Souch, 1994), radiometric measurements using Cs-137 and Pb-210 (Hutchinson, 1995) and mineral magnetics (Walden *et al.*, 1997). In a review of studies that have applied sediment tracing it was found that no investigation has been carried out in the alluvial fan and debris cone environment using this range of methods. The choice of which technique to adopt was based upon a consideration of, successful application in contrasting environmental settings, applicability within fan and cone environments, sampling procedure and treatment, ease of measurement and cost.

Mineral magnetics has been successfully applied in a number of contrasting environmental settings, primarily to assess erosion within catchments. The technique has been applied in river based studies (Oldfield *et al.*, 1979, Walling *et al.*, 1979; Oldfield *et al.*, 1985, Yu and Oldfield, 1989; Caitcheon, 1993; Caitcheon, 1998), lake studies (Flower *et al.*, 1984; Dearing, 1992) and reservoir studies (Stott, 1986; Yu and Oldfield, 1993, Hutchinson, 1995). All of these catchment studies represent markedly contrasting environments of transport or deposition. The technique is also rapid and non-destructive, allowing leeway with the number of samples that can be taken to fully characterise catchment sources. The principle is based upon the measurement of the strength of the magnetic signal of naturally occurring iron-bearing mineral compounds (Thompson and Oldfield, 1986). More detailed information upon mineralogical composition was obtained by measuring the reaction of a given sample to the artificial inducement and application of a magnetic signal. It is the liberation and removal or dissolution of iron compounds by weathering which introduces variation in the concentration and mineralogy of iron compounds present within natural sediments.

The only constraints recognised in the application of a sediment source provenancing technique within the fan and cone environment is the effect of catchment size and the timing of initiation. The shorter and longer transport distances from source to sink associated with debris cone and alluvial fan systems respectively, will affect the degree of mixing and thus the strength of the signature of a change in source. Within smaller catchment systems the variability of sources is

likely to be restricted. The post-depositional alteration of sediments by soil formation can also follow a break in fan and cone aggradation. In identifying changes in the source supplied to the fan and cone over time the features must have been initiated following the development of distinct sediment sources from the glacial material. The timing of initiation can be addressed in part by determining the source of sediment at the base of the sediment sequence under investigation. A more direct time period for the aggradation of the sediments can be obtained by dating available organic material preserved within the sediment profile.

3.2.3 Chronological framework

Establishing a chronological framework is essential for determining the sequential order of fan and cone sediments. Data upon changes in the mode of sediment transport and source can consequently be interpreted in the correct sequential order. An interpretation of the form of a feature can be used to identify the successive phases of aggradation or incision. Debris cones often comprise inset cone segments, whilst fans can exhibit a series of progressively lower terraces, isolating higher terraces as sites of deposition. Deposition can also be channelled to inset distal fans. Direct dates were obtained by the radiocarbon dating of organic material preserved within sediment exposures. The preservation of organic material is limited to its incorporation *in situ* by pedogenesis or transport as organic debris. The dating of the upper and lower horizons of preserved palaeosols was carried out to derive the age range of the soils formation which coincide with the onset and cessation of soil formation. The onset of soil formation corresponds to a period of stability or low sediment availability within the catchment and its cessation with catchment reactivation or high sediment availability. Dating a sequence of palaeosols allowed the correlation of the timing of activity with coincident changes in sediment availability. Where palaeosols were found and dated, the timing of activity was correlated with local proxy records of climate and human activity. The information obtained therefore adds to the current debate of climate and / or human causes of increased sediment availability (Ballantyne, 1991a; Tipping and Halliday, 1994). The nature of the response has been interpreted with regard to sediment supply control based upon the nature of the signature obtained from the two indicators.

The chronological framework established from phase sequencing and radiocarbon dates were further constrained by measuring two signatures of sediment supply control. The recognition of the source and mode of transport of the deposits of separate flows allows the identification of sediment exhaustion in response to single flow and extreme events (section 2.3.4.). It is therefore possible to identify separate phases of fan activity within fan and cone sediments aggraded between palaeosol indicators of stability. The signature characteristics of the sediments separated by the break in activity can be used to determine the nature of their separation, an erosional hiatus or a period of stability. If an immature palaeosol is distinguishable within the upper sediments of the lower flow deposit the time-period of stability can be assessed. Ultimately, in determining the sequential relationship of the deposits of separate flows, the rate of aggradation in separate phases may be inferred.

3.3 Rationale of site selection

The major selection criterion for this study was the identification of sites where the relative amounts of the glacigenic sediment legacy differ significantly. Given that a major aim of the work is to study the response of fans and cones to changes in the availability of glacial sediment reserves, sites that have experienced differing rates of sediment transfer in response to regional and local trigger mechanisms were also required. Four sites were chosen: Glen Etive, in the Western Grampians of Scotland; the headwaters of Yarrow and Moffat water, near Moffat in the Southern Uplands of Scotland; Langdale and Bowderdale Valleys in the Howgill Fells; and Langden Beck in the headwaters of the River Tees, the Northern Pennines (Figure 3.1). In the rest of this thesis, these sites will be referred to as Glen Etive, Moffat, the Howgill Fells and Langden Beck.

The differences in sediment supply between the four regions are a product of their different glacial histories, controlled by their locations relative to the Loch Lomond ice cap or localised valley glacier limits (Figure 3.2). Glen Etive is located well within the limits of the Western Grampian Loch Lomond Ice sheet. Devensian sediment reserves will have survived only in limited areas located above the maximum height reached by valley glacier ice. Sediments within the main valley were formed directly by a limited period of glaciation. As a result the relative

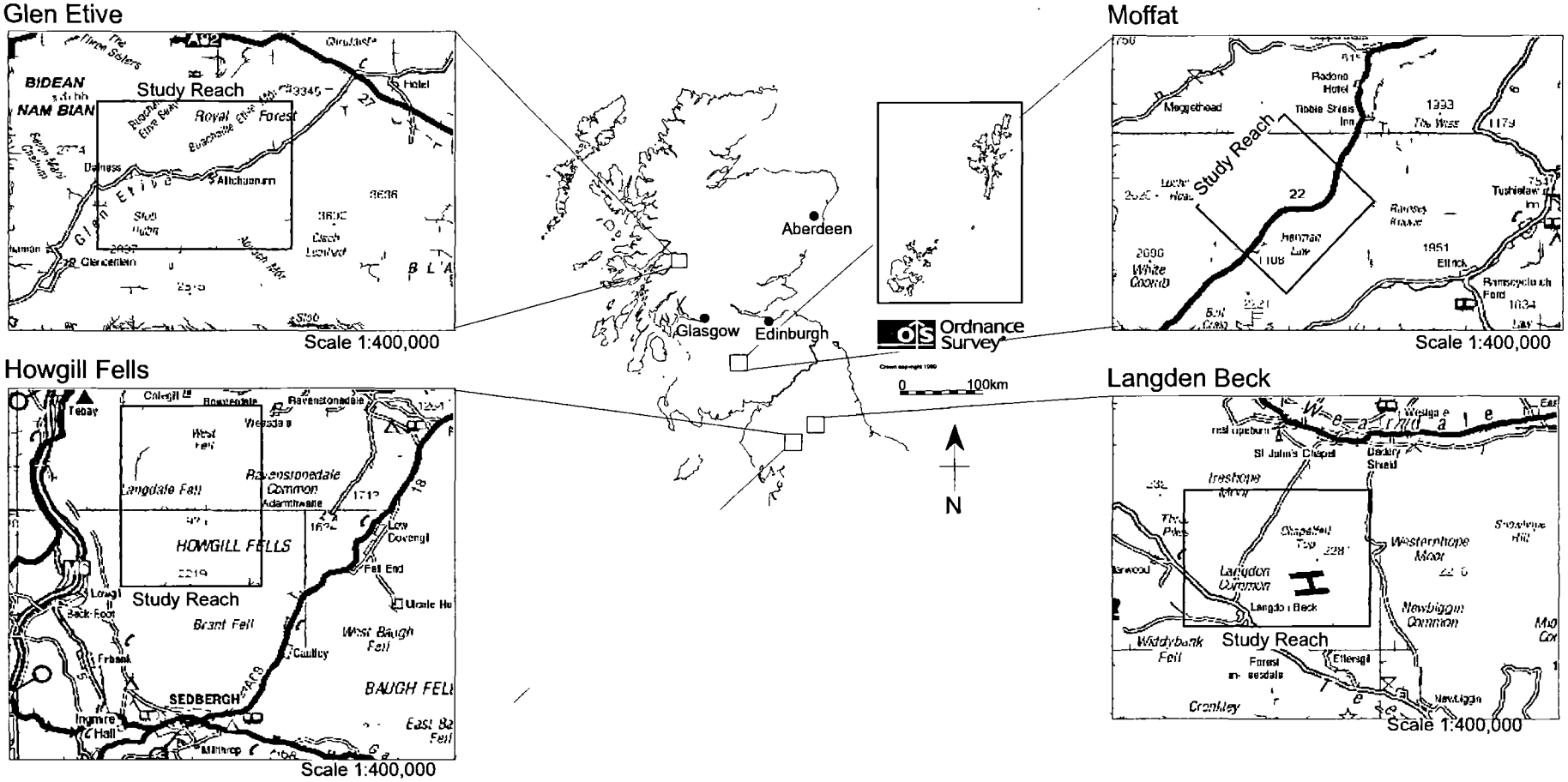


Figure 3.1 The Location of the study sites (source: www.ordgov.co.uk)

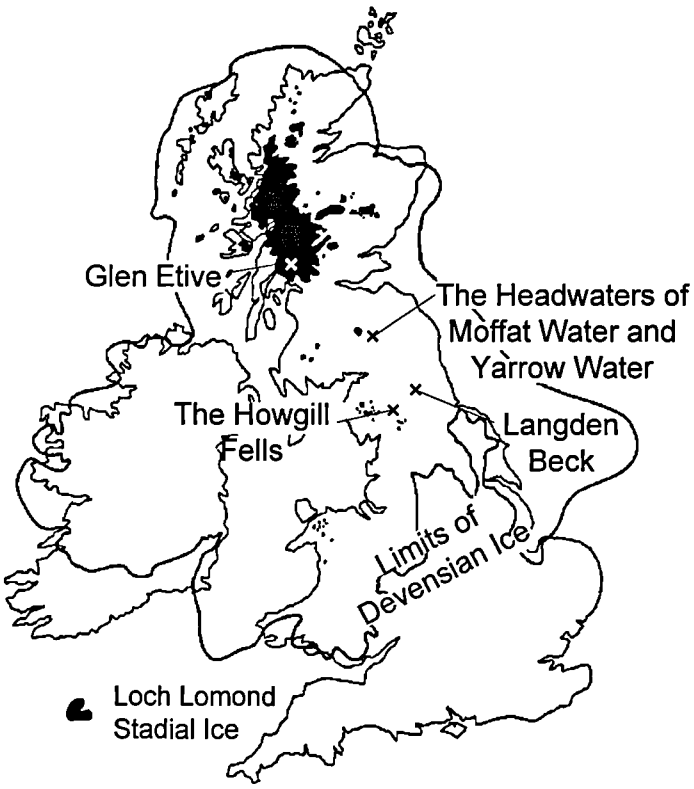


Figure 3.2. The position of study sites relative to Loch Lomond ice cap or localised valley glacier limits

After Ballantyne and Harris (1994)

amount, character and time period of availability of sediment supplies differ in comparison to areas outside Loch Lomond limits. Outside the Loch Lomond limits, relatively substantial Devensian sediment reserves are either altered and / or added to by the Loch Lomond Stadial climate. The degree of change rapidly decreases with increasing distance from Loch Lomond ice sheet boundaries or from the limits of localised valley glaciers (Ballantyne and Harris, 1994). The reaches studied at Moffat are immediately adjacent to former limits of local valley glaciers. The relative amounts of sediment and their characteristics should reflect the intensity of permafrost and freeze thaw weathering associated with the close proximity of local glacier ice. The remaining two sites lie well within Devensian glacial limits but do not lie in close proximity to glacier ice formed locally during the Loch Lomond Stadial.

The time period of slope sediment transfer at Glen Etive is restricted to the Holocene. For the other three sites the time period extends to the onset of the Devensian deglaciation. As a result of this variation, fan and cone initiation between the four sites can be paraglacial, immediately following deglaciation, could have occurred during the Windermere Interstadial or during the Holocene. The timing of initiation and subsequent reactivation is commonly associated with the occurrence of broad patterns of climate change such as deglaciation and enhanced periods of storminess during the Holocene. Initiation and enhanced sediment availability has been linked to identified waves of human settlement and the introduction of associated landuse practices (Harvey *et al.*, 1981; Harvey and Renwick, 1987). At each site the timing of previous human activity is specific to each region. Taken in concert with Holocene changes in climate, the rate of sediment transfer and thus the rate of sediment exhaustion could potentially vary considerably between sites. The depletion of slope sediment reserves at different rates will affect the stage at which features are in the sediment exhaustion cycle and the scale at which sediment exhaustion operates. At Langden Beck the link between human control and the resulting response is more direct. 19th Century localised mining activity drastically altered the hydrological regime and introduced large volumes of sediment into the system. The response within the fan and cone to artificially induced, dramatic changes in sediment availability and its exhaustion is clear. The nature of sediment supply control upon response, although at extremes, could be used to draw parallels in data found at the other sites.

For each region reaches within the main catchments were chosen for detailed study. Their boundaries were in part restricted by the location of exposures of fan and cone sediments. The reach must also be of sufficient area to enable characterisation of local sediment supplies and environmental parameters controlling sediment availability. Within each of the reaches changes in local geology and the location and thickness of lateral moraines affect sediment supply on a more localised scale. The height and thickness of glacial slope sediment reserves vary markedly within relatively short distances. Sediment availability also varies spatially within a catchment in response to drainage, topography and altitude. The principal geomorphic features within each reach were geomorphologically mapped using a combination of aerial photography and field investigation.

Each site exhibits regional patterns in the timing and nature of vegetation changes in response to broad climate change. The location and timing of human activity also corresponds to regional patterns of settlement expansion and withdrawal, although apart from Glen Etive there in no direct evidence of previous human settlement within studied reaches. Derivation of the timing of human and climate change relies upon proxy data obtained from locally derived archaeological and palynological evidence.

3.3.1 Glen Etive

Upper Glen Etive Valley was filled by glacial ice up to a height of *c.* 650m during the Loch Lomond Stadial, with ice moving westwards from the ice shed on Rannoch Moor (Thorp, 1981). A Loch Lomond Stadial age, 10,800 to 10,300 years BP, for the ice field has been provided by radiocarbon dates at Rannoch Moor (Walker and Lowe, 1977) and from marine shells at Loch Creran (Sutherland, 1984). The eskers, kettles, and kame terraces present in areas topographically suitable for the development of downwasting masses indicated that Loch Lomond glaciers, including Glen Etive, retreated actively and did not undergo stagnation and downwasting (Thorp, 1981). The time transgressive retreat exposed Loch Lomond glacial sediments to periglacial processes for decreasing time periods as it retreated up valley (Benn *et al.*, 1992).

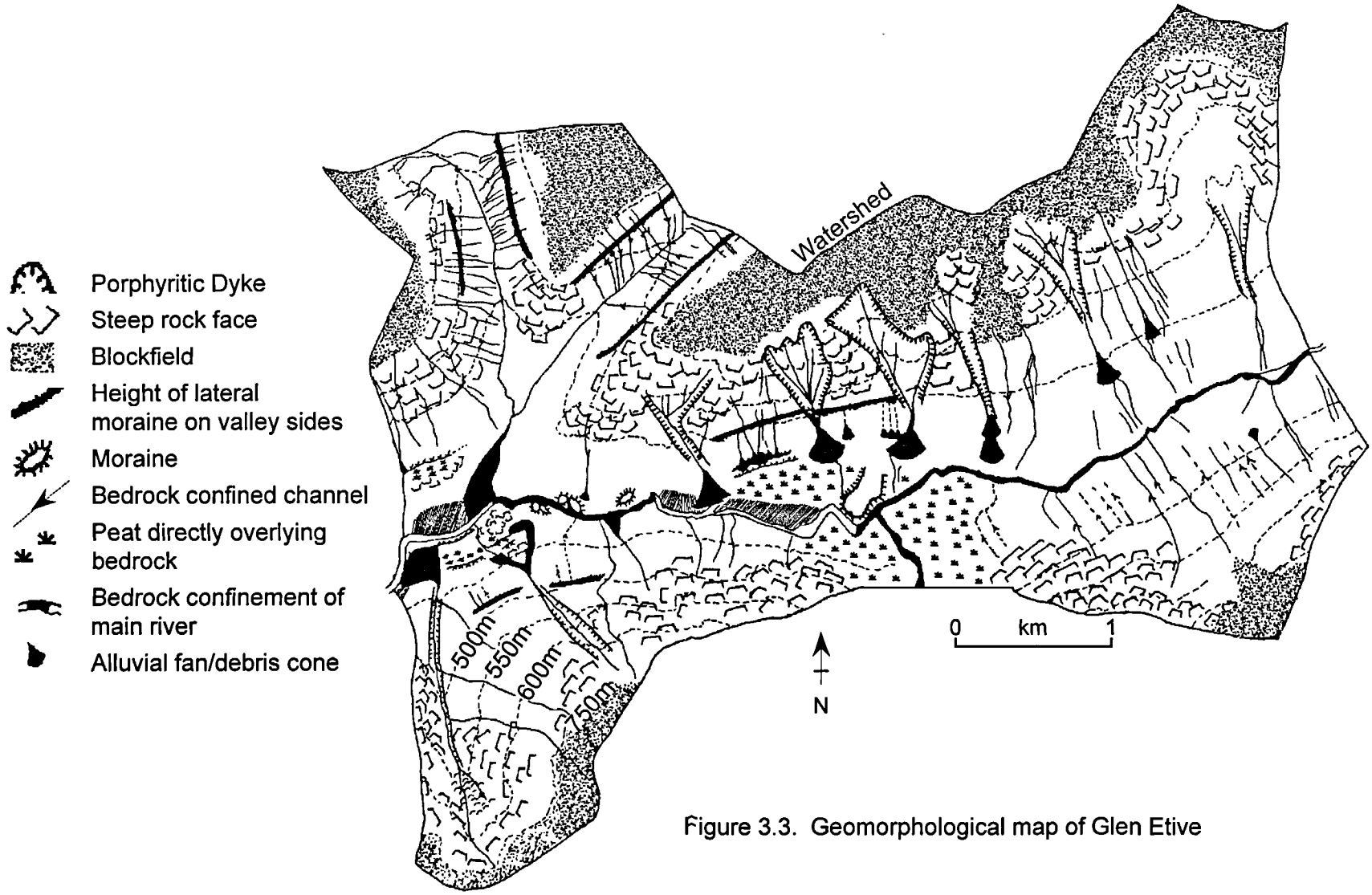


Figure 3.3. Geomorphological map of Glen Etive



Plate 3.1. The main valley of Glen Etive. The photograph highlights the distinctive character of the preferentially eroded porphyritic dykes of the debris-cones-supplying gully systems.

Within the study reach (Figure 3.3), slope sediment supplies consist of lateral moraine and frost weathered detritus (Plate 3.1). The thickness of lateral moraines is not uniform, being noticeably thicker on cols whilst main valley slopes are covered by a thin veneer of sediment. The upper limit of lateral moraines on valley sides is fairly uniform as is the upper trimline of the valley glacier. Areas exposed above glacier ice during the Loch Lomond Stadial were subject to intense frost action, the formation of permafrost and cold climate weathering processes. Frost-shattered detritus formed on valley interfluves and side slopes during the Devensian deglaciation was subsequently added to or modified (Ballantyne, 1991b). Exposed areas include unoccupied cirques and main valley gully heads found above the level of glacier ice, although corrie glaciers existed contemporaneously with valley glaciers (Thorp, 1991). Within the gullies localised erosion resulted in limited build up of scree within trunk gully systems.

Deeply incised gullies within main valley slopes owe their presence to porphyritic dykes, which are more readily susceptible to weathering than the surrounding granite. The solid geology of Glen Etive is characterised by granite, capped by rhyolite lavas which are exposed high in the valley sides. It is this geology which is punctured by porphyritic dykes of varying thickness, striking in a predominantly north, north east direction. The preferential erosion of the dykes to form deeply incised gullies has resulted in a stark contrast in sediment supply between the features and the main valley sides. This is reflected in the size of cones formed on main valley sides, through the incision of lateral moraine deposits and those formed in association with the larger gully systems. The solid geology underlying the catchment represents an important control on slope sediment supply and spatial variability.

Debris cones within the reach are isolated from the main river. Continuity between slopes and the main river is restricted to the width of the valley floor and where narrow, its confinement within a bedrock gorge. The valley floor is characterised by wide flat terraced floodplains which are separated by rock constrictions. Overall, the valley gradient is steep but the change in gradient follows a step like progression. Apart from the large volumes of reworked sediment within terrace sequences, the remainder of the valley floor is buried in a thin veneer of sediment with intermittent and isolated hummocky moraine. In some parts peat has

developed onto ice scoured granite. The current climate favours the formation of peat. The annual rainfall received at Glen Etive varies between *c.* 1,500 and 4,000 mm y^{-1} with areas of high ground receiving greater than 2,500 mm y^{-1} (Thorp, 1991). Currently, water-logged peat dominates the valley floor. On valley slopes as drainage improves peat decreases in thickness and is replaced by grass and sedges growing within lateral moraine. A large number of fossil tree stumps have been preserved within valley floor peat and slope sediments, remnants of a previous extensive forest cover.

Changes in climate following deglaciation resulted in a series of marked changes in vegetation colonisation and composition. A peat profile preserved in a kettlehole at the head of Glen Etive displays a relatively unbroken record of vegetational changes since the Loch Lomond deglaciation (Walker and Lowe, 1977). The timing of changes can be extrapolated to include the onset of change within Glen Etive valley. However, as Glen Etive is relatively sheltered in comparison to Rannoch Moor, the pattern of change and species composition will differ. Nonetheless the general vegetation changes and their timing will be comparable. Walker and Lowe (1977) have shown the time period between Loch Lomond deglaciation and the recolonisation by vegetation can be measured in decades. The earliest records within the sequence indicate the presence of pollen from pioneer vegetation such as Heath and Juniper scrub is accompanied by an abrupt change from minerogenic to organic accumulation within the Kettlehole sequence. In comparison, recently exposed, unconsolidated and readily available slope sediments are only available for transport for a relatively short period of time. The time period within which periglacial processes such as solifluction could act to modify sediments is limited when compared to the ~ 3,000 years of periglacial conditions experienced during the Devensian deglaciation. By *c.* 9,000 years BP, Birch copses, heath and moorland were followed by the arrival of Hazel. Juniper scrub was out competed and restricted to upland slopes. The arrival of pine and birch by 7,000 years BP occurred in response to the onset of wetter conditions (Walker and Lowe, 1981). A mixed tree forest, dominated by pine on Rannoch Moor began to decline at around 4,500 years BP (Birks, 1975, Pennington, 1974; Walker and Lowe, 1981, Bridge *et al.*, 1990). Within Glen Etive fossil stumps are found rooted within valley side sediments right to the base of exposed bedrock. The loss of trees therefore had important implications for the increase in slope sediment availability at this time, although it is argued that

the decline began 6,000 years BP and was sustained over a 2,000 year period (Walker and Lowe, 1977). Their death is attributed to climate deterioration and an associated increase in climatic wetness occurring concomitantly with the with growth and extension of acidic blanket peat on catchment slopes. Walker and Lowe (1977) argue that the decline was unlikely to have resulted from the influence of Neolithic man due the remoteness of Rannoch Moor. Blanket peat on slopes was replaced by a heather moorland as the climate became drier.

Studies dealing with human settlement within the region are limited. Within Glen Etive there is tangible evidence of previous occupation and agriculture in the form of hut circles and the presence of lazy beds. The remains of former settlement have been linked to a period of fluvial incision which resulted in the formation of an inset fan within the debris cone formed at the base of Dalness chasm (Brazier et al., 1988). The timing of activity is dated at 550 ± 50 years BP from a buried palaeosol. An analysis of pollen before and following the burial of the former soil indicates an increase in the concentration of agricultural weeds associated with the inclusion of charcoal. Fire and agriculture and their destruction of the natural vegetation cover is cited as the trigger of fluvial incision of debris cone surficial sediments to form a fan of reworked sediment. As Dalness chasm is located within the study reach the link between fluvial incision and the influence of relatively recent human activity can be extrapolated to other cones within close proximity.

A maximum age for the cessation of accumulation on the debris cone at Dalness chasm is given at 4480 ± 300 years BP. The cause of cessation is linked to the depletion of sediment supplies within its deeply incised supplying gully (Brazier *et al.*, 1988). The ultimate long-term exhaustion of sediment supply within this feature is clear, as is the nature of the response within the fan and cone environment. Human activity disturbed vegetation in the cone surface and a subsequent storm event incised the cone surface in response to lowered thresholds. Approximately 170 000 m^3 of sediment have accumulated within the debris cone over a period of 6,000 years (Brazier *et al.*, 1988). The rate of its development within this time period is questionable. Two periods of enhanced sediment availability have been identified, the short lived period of deglaciation and the period of tree decline on slopes. The cone could also have undergone sustained aggradation over the 6,000 year period. The importance of sediment availability upon cone development is unclear.

3.3.2 Moffat

The headwaters of Moffatdale and Yarrow Water in the Southern Uplands of Scotland were completely covered in ice locally developed from Tweedsmuir during the Late Devensian Maximum. Ice accumulating at St Mary's Loch flowed towards the town of Moffat, excavating a major fault line. The fault line is part of a series of faults that have developed as a result of large scale folding of the sequence of Ordovician Mudstones, Greywackes and Silurian rocks, fine grained shales, Mudstones and Greywackes overlying an unconformity (Weir, 1979).

Deglaciation began earlier in the Southern Uplands and was complete at 13,500 BP with no evidence of a still stand or a readvance (Sissons, 1976; Sutherland, 1984). Slope deposits and mountain plateaux were subjected to an extended period of periglacial activity, modifying glacial sediments and increasing sediment reserves. During the Loch Lomond Stadial a series of valley glaciers developed locally. The largest glacier developed was at Loch Skeen and ice penetrated the head waters of both Moffat Water and Yarrow Water (May, 1981) (Figure 3.4). Areas proximal to the ice experienced harsher periglacial conditions throughout the Loch Lomond Stadial, and Late Devensian sediment reserves were subject to approximately a thousand years of modification and addition.

Sediment supplies are comprised predominantly of extensive and thick solifluction deposits, which dominate slope sediment supplies within the region. Solifluction deposits, overlying lateral moraine from which they were derived, extend from hill tops to the valley floor terminating in solifluction benches (Plate 3.2). Solifluction deposits predominantly formed within lateral moraine deposits to the depth of the active layer, formed within permafrost to an estimated depth of 1m (Tivy, 1962). The height reached by lateral moraine is readily evident on valley sides. May (1981) has constrained a maximum moraine height at 275m. On hill tops extensive former blockfields are overlain by blanket peat, which disappears at the convex break of slope.

The topography within the studied reach is characterised by smooth rounded hills, interconnecting ridges and rectilinear slopes. Smooth slopes are attributed to a

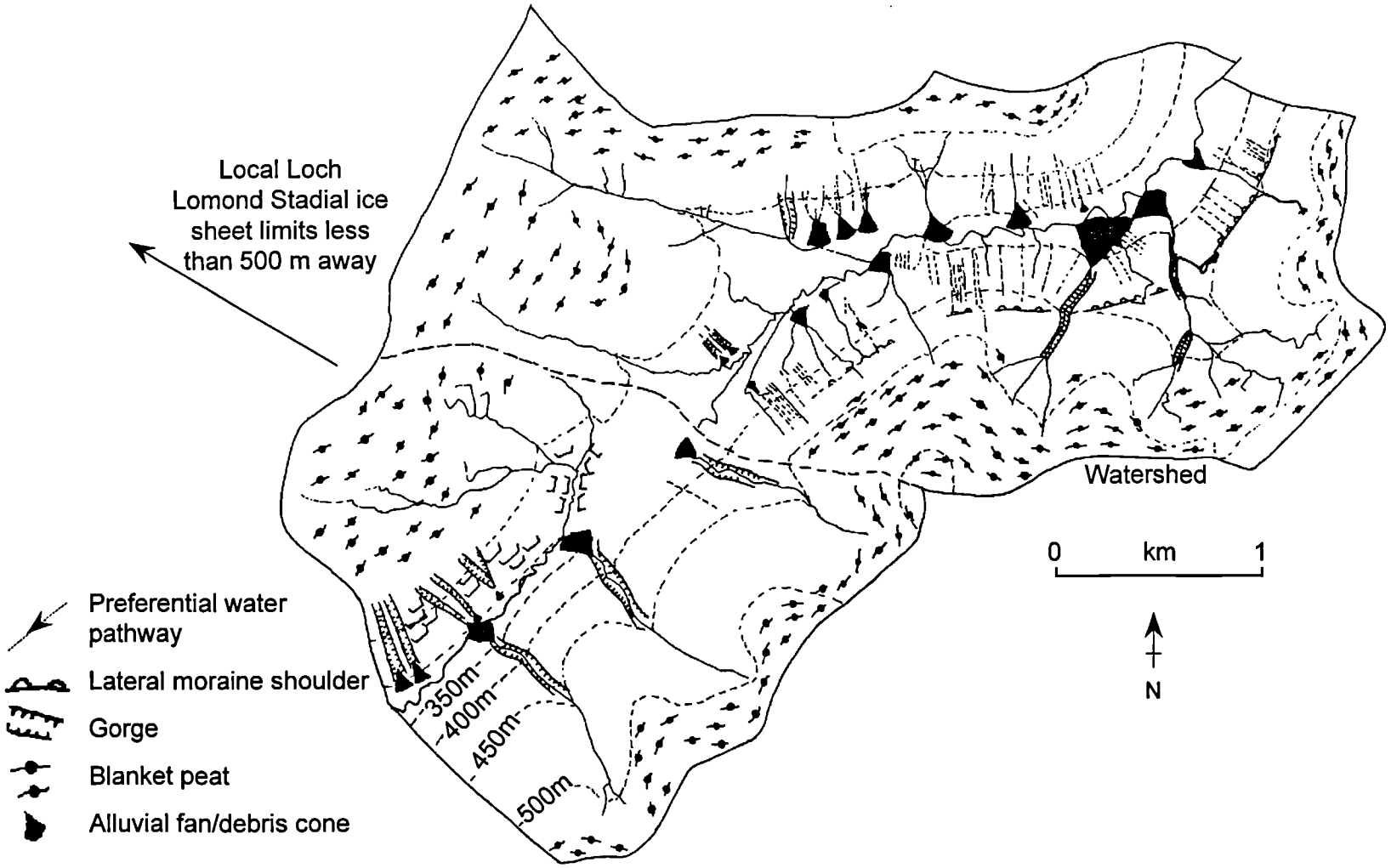


Figure 3.4. Geomorphological map of upper Moffat Water and Yarrow Water, Moffat

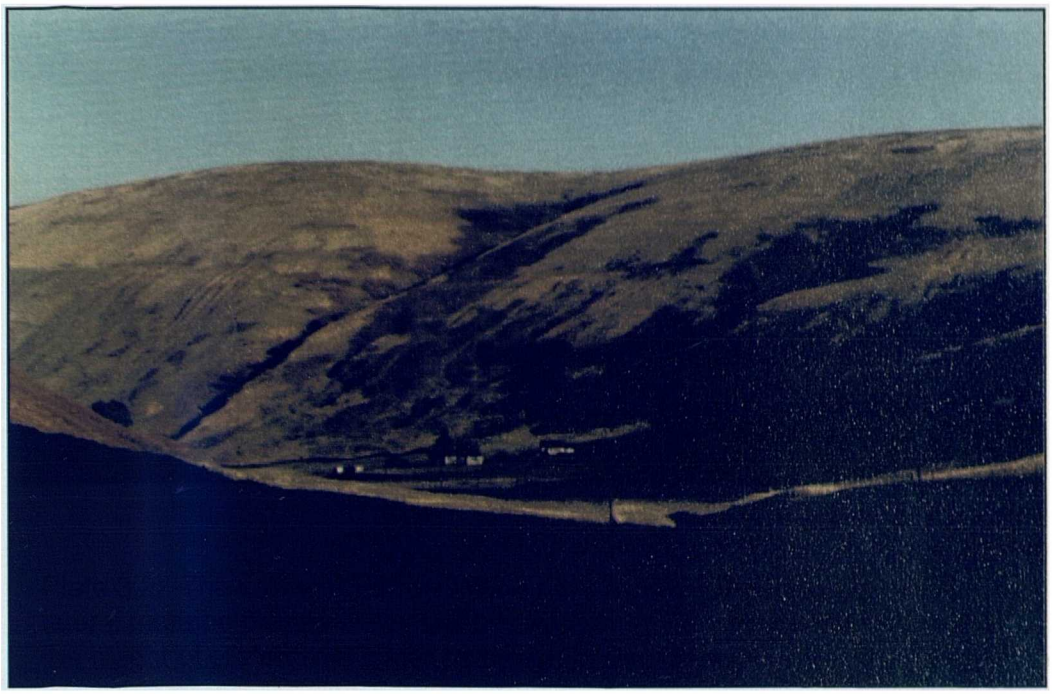


Plate 3.2. The valley of Yarrow Water near Moffat. The height at which lateral moraine drapes valley sides is apparent. The direct association with the height of preferential water pathways is also clear.

steeply dipping solid geology, rapid changes in lithology and the comparable resistance to erosion within each lithology. Outcrops of bedrock are restricted to the base of linear gully systems, which dissect main valley slopes and trunk streams of alluvial fans. Within the reach the width of the valley floor varies considerably. Continuity between cones and the main river is high where the valley floor narrows. Debris cones are isolated from the main river where the valley floor widens, although the distal regions of alluvial fans abut with the main river. Parallel with the linear gullies on the main valley side are a series of linear preferential water pathways. The pathways originate at a uniform height on the valley side, concomitant with the maximum height reached by lateral moraine. Where the upper limit of the lateral moraine is visible, a direct association with the origin of preferential water pathways is clear. The top of the lateral moraine can be taken to represent a permeability unconformity, which can increase instability within slope deposits where the pathways are located. During snow melt and during storm events of high rainfall intensity large volumes of water draining off blanket peat may by channelled by the pathways. Prior channelization within macro and micro pores of the blanket peat may also compound the concentration of flow.

Blanket peat was formed on valley tops in association with broad climatic increase in wetness, although locally peat has been shown to have developed earlier at higher altitudes. The local history of climate change, vegetation change, the degree and pattern of human activity and settlement has been compiled by Tipping (in press) from a number of archaeological and palynological studies carried out in and around Annandale and Eskdale. The study reach used in this research is located well within the region studied by Tipping. The timing and nature of change can be extrapolated from data compiled by local studies.

A series of climate and vegetation changes have been identified. The influence of human settlement also plays an important role in affecting local vegetation, through forest removal, regeneration and an increase in pastoral landuse practices. The timing of fan and cone initiation within the reach, and subsequent phases of activity, can be linked to climate and human-induced changes in sediment availability. Topographically induced instability, in the presence of preferential pathways, may also play an important role on the development of debris cones within the reach.

3.3.3 The Howgill Fells

Two main catchments within the Howgill Fells, Bowderdale (6.75 km^2) and Langdale (8 km^2), were selected for investigation (Figure 3.5). The valleys were shaped by local ice which was centred over the Calf, the highest point in the Howgill Fells at 676m, during the Late Devensian Stadial. Ice from both valleys joined ice flowing from the Lake District eastwards across to Stainmore (Marr and Fearnsides, 1909). As the Howgill Fells is in the rain shadow of the Lake District, the area probably underwent early deglaciation which was complete in the Lake District by 14,500 BP. During the Loch Lomond Stadial the formation of local ice is severely limited to a few areas of small cirque glaciers. Mitchell (1991) mapped a small 0.24 km^2 glacier at Cautley Crags on the south-eastern edge of the Howgills. The rest of the Howgill Fells remained under long lying snow patches, experienced snow melt and limited periglacial modification of slopes (Mitchell, 1996).

A thick mantle of solifluction deposits extends from hill top to valley floor. Two clearly separate layers of soliflucted material can be identified within slope deposits. It is likely that the shallower upper layer formed within Late Devensian solifluction deposits during the Loch Lomond Stadial. The valley interfluves comprise former blockfields, which are buried by extensive blanket peat although the current peat cover is punctured by numerous deflation surfaces that have exposed highly weathered, frost shattered detritus. The main valley slopes are also characterised by linear preferential water pathways, although moraine heights within Bowderdale and Langdale have not been documented and are not immediately obvious. The underlying geology consists almost entirely of relatively impermeable, massively jointed Silurian Grits, Shales and Flagstones with small inliers of Ordovician rocks. The Silurian is openly folded in a dominantly east-west direction. The rounded topography is attributable to breakdown of the impermeable Silurian lithology (Ingham, 1966). Bedrock exposures are limited to the trunk streams of linear gullies dissecting steep slopes.

The extensive migration of the main river in both valleys has removed and reworked large amounts of glacial deposits on the valley floor. Remnants have been preserved at intervals along the length of both valleys. A substantial phase of down-

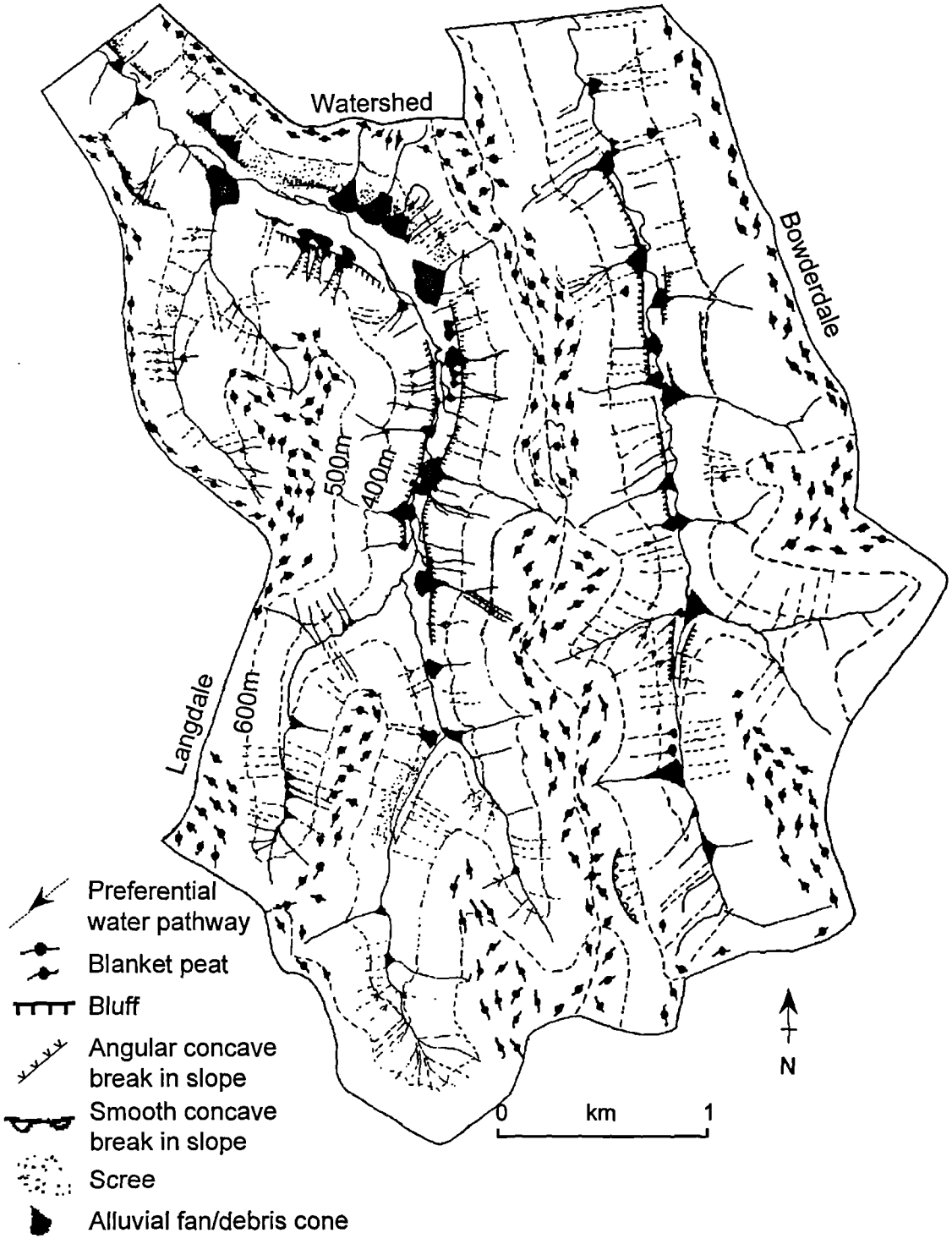


Figure 3.5. Geomorphological map of Langdale and Bowderdale, the Howgill Fells



Plate 3.3. The headwaters of Langdale Valley, the Howgill Fells. The valley side bluff and the presence of preferential water pathways are clear from this photograph as is the migratory nature of the main river.

cutting has resulted in the formation of a high bluff on valley sides where exposed glacial till is shown to be overlain by solifluction deposits (Plate 3.3). In addition, two separate generations of cone formation are separated by this period of downcutting, a characteristic of debris cone development in both valleys. Cone deposits found on the bluff may have formed during the Interstadial and have been preserved by the subsequent lowering of valley floor. Where the main valley is narrow later phases of cone aggradation have been deposited directly onto the contemporary floodplain. Cones and fans grade into the remnants of a former terrace and the modern floodplain where valley width has permitted river terrace preservation. Some cones have undergone incision as the main river has changed its position, in some cases more than once. The abutting deposits of sequential phases of aggradation have systematically been incised by the main river following their deposition.

The formation of a large number of cone segments within features is testament to previous high rates of activity within gully systems. Some systems have been recently reactivated in response to an intense storm in June, 1982 (Harvey, 1986). Debris cones showed varied response to the storm event. Some underwent aggradation, others showed no response. The varied response is linked to the periodic build-up of sediment within gully systems (Wells and Harvey, 1987). In the headwaters of Langdale, smaller gully systems are currently actively supplying sediment to the main river (Harvey, 1987). The current high intensity of erosion within the Howgills, under an annual rainfall of 1,075 mm $yr.^{-1}$ is attributed to the high intensity of sheep grazing, maintained and increased historically from the Medieval period (Cundill, 1976; Rickson and Morgan, 1988). Testament to high grazing pressure, terracettes are common on steep slopes and extend into loose scree that has built up within gullies.

Sheep grazing in association with Viking settlement has been cited as the cause of historical cone aggradation dated at *c.* 1,010 ± 95 years BP by Harvey *et al.* (1981). The onset of cone aggradation and the subsequent burial of a former terrace is linked to human-induced changes in local vegetation, identified in the pollen record of the terrace soil and within the overlying sediments. A partially forested landscape of Oak and Elm was replaced by plants which are indicators of disturbed ground or pasture. A more extensive pollen recorded at Archer Moss, on the western limits of the Howgill Fells, provides a relatively unbroken record of

vegetation change from 3,500 years BP (Cundill, 1976). Cundill identified four prominent woodland declines at 3,480 ± 100 years BP, 2,390 ± 80 years BP, with two subsequent phases which have no date attached. Each phase can be linked with agricultural activities of man. He argues the removal of woodland cover led to soil erosion as slope sediment exposed to heavy rainfall results in the formation of rills and gullies. Below Archer Moss within Carlingill a sequence of organic peat dated at 2,290 ± 80 years BP is overlain by alluvial fan deposits. The onset of inorganic sediment accumulation was immediately preceded by a period of woodland clearance. There is no direct link between human interference and woodland clearance due to the lack of archaeological evidence. The timing of woodland clearance can be correlated with the documented expansion and agricultural development associated with the Bronze Age, Iron Age, Dark Age, Norse and Roman settlement patterns (Atherden, 1992). The timing of woodland clearances also coincided with periods of climate change although Cundill (1976) argues that the pattern of woodland clearance was too abrupt for a climatic cause.

Harvey, *et al.* (1981) constrained the timing of cone initiation in Middle Langdale at approximately *c.* 1,010 ± 95 years BP. However, it has been demonstrated that an earlier phase of activity is preserved on the high bluffs within both Bowderdale and Langdale. The bluff absent in Middle Langdale returns up and down stream. The timing of the earlier phase of activity is unknown. The lack of the bluff at Middle Langdale may indicate its previous removal, eroded by the main river. If this is the case, evidence of the earlier phase of activity at this site has been lost.

3.3.4 Northern Pennines - Langden Beck

Langden Beck is located near to terrain that was occupied by the Northern Pennine ice cap centred on Cross Fell, with ice flowing east and down into the Tees Valley (Beaumont, 1968). Slopes are mantled by glacial till within which periglacial landforms have developed. Blockfields, frost shattered rock, patterned ground and geliflucted till solifluction deposits are characteristic periglacial phenomenon of the period following Devensian deglaciation and the Loch Lomond Stadial (Boardman, 1985). Within the western Pennines the onset of the Devensian deglaciation has been dated at approximately 14,500 years BP (Gascoyne *et al.*, 1983).

The underlying geology of Carboniferous middle and upper Limestone groups comprises interbedded sandy shales, jointed limestones and sandstones (Johnson and Hickling, 1970). The interbedding of lithologies of varying resistance to erosion is a major control upon valley topography (Plate 3.4). A series of stepped benches have formed in association with alternating bands of resistant sandstone and limestone with readily eroded shales. Slope sediment supplies comprise a fine clay glacial till overlain by solifluction deposits with incorporated sandstone fragments (Carling, 1986b). The underlying geology represents a source of sediment with undercut, readily eroded shales destabilising overlying sandstone and limestone. Glacial and periglacial deposits are buried by an extensive cover of blanket peat. The thickness of the peat generally varies between 1-2m depth and extends to the valley bottom, although peat thickness is less on steeper gradients. Within Langden Beck, the gently sloping topography has limited the formation of debris cones. Alluvial fans are comparatively rare features in north Pennine valleys (Warburton and Higgitt, 1998). The two alluvial fans, West Beck and Harthope Beck, within Langden Beck are associated with tributaries adjoining the main river.

Sediment supplies are not strictly exhaustible in the long term but they have experienced changes in availability. The most dramatic change was associated with mining activity, which began in Roman times and continued up to the 17th Century. Mining activity within the local region left an enormous impact on the local landscape (Warburton, 1998). There is a direct link between the response of the features to the changes to the hydrological regime and the dramatic input of sediment. The spatial concentration of mining activity within the catchment is illustrated in Figure 3.6. West Beck has undergone the greatest change, with mining activity directly interacting with the surface of the fan. Activity within Harthope Beck is restricted to mining operations within the trunk and tributary stream system. The effect of mining activity upon fan development is small in comparison to the overall size of both features. Both fans have clearly undergone substantial phases of aggradation following their initiation. Due to the size of their supplying catchments, regardless of mining activity, it appears that their development immediately followed the Devensian deglaciation.

Locally, vegetation recolonisation has been shown to be concomitant with deglaciation (Gascoyne *et al*, 1983). By 7000 years ago an extensive mixed deciduous forest cover, including pine was well established on valley floors and

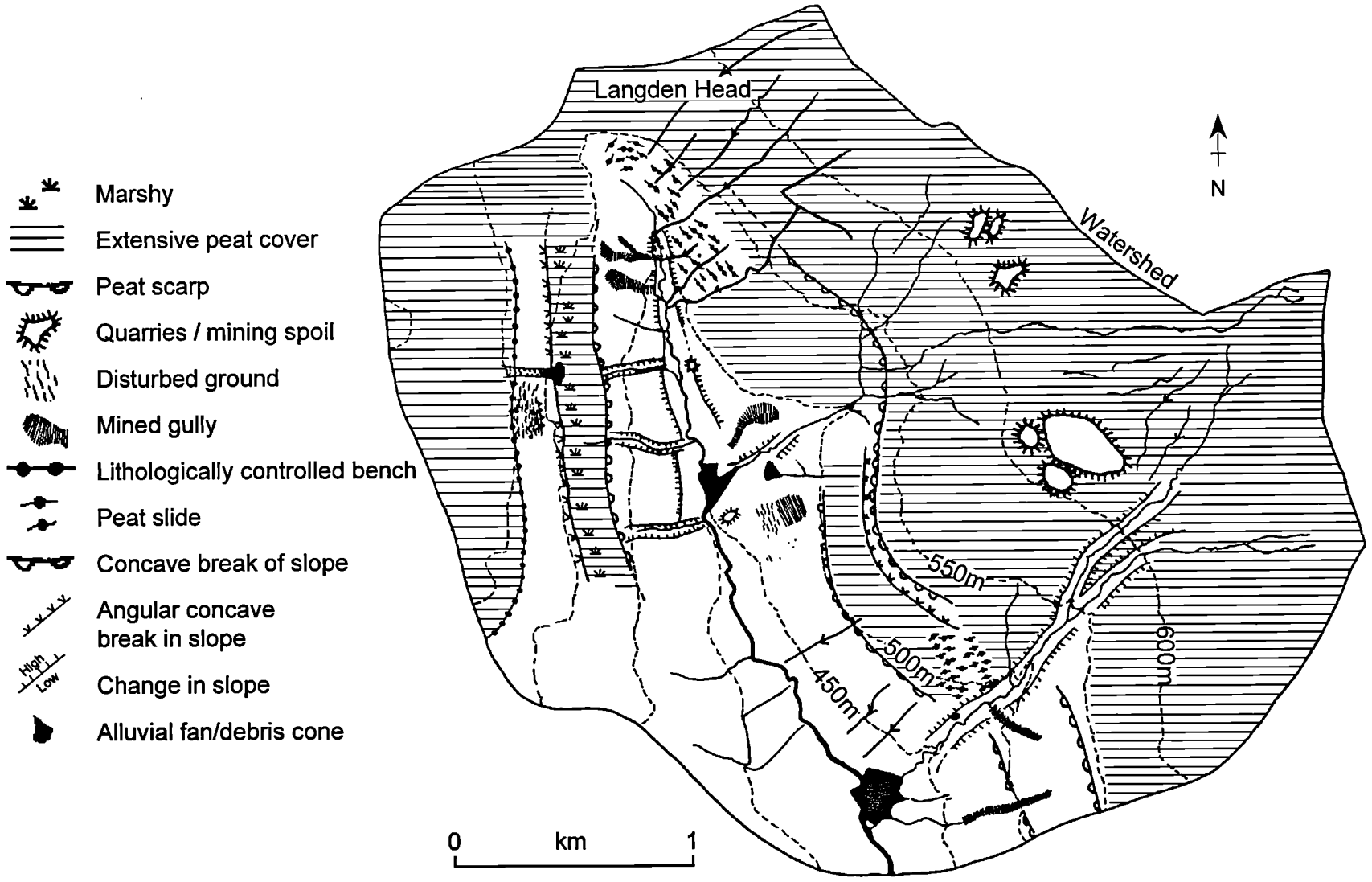


Figure 3.6. Geomorphological map of Langden Beck

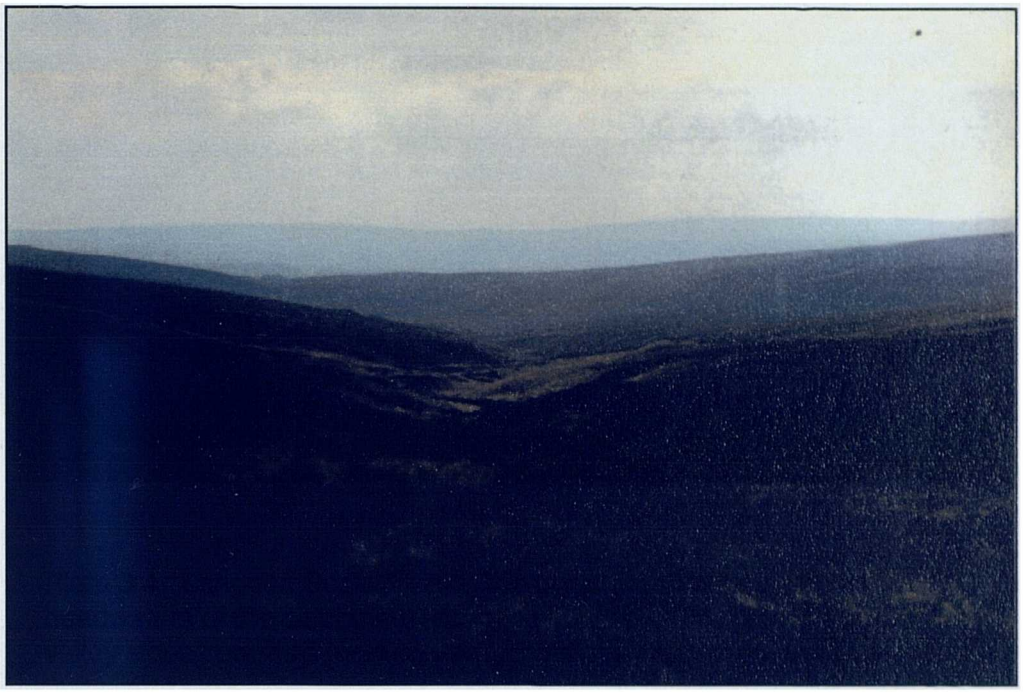


Plate 3.4. Langden Beck Valley. The photograph is taken from the headwaters of the catchment facing downvalley. The gentle slope of the valley sides contrasts markedly with the slope characteristics of the other three sites.

extended up to all but the highest summits. Forest development was associated with a reduction of sediment availability. Human activity at this time was restricted to highly localised clearing of woodland and limited agriculture (Squires, 1978). A forested landscape was replaced by peat at around 4000 years BP, although peat formation began earlier at higher altitudes (Turner, 1979). There is no direct evidence of previous human occupation within Langden Beck but an increase in human activity has been dated at around 3,000 years BP (Squires, 1978). Phases of forest clearance and regeneration have been associated with the expansion and retreat of agriculture into upland areas (Squires, 1978). The current landscape is characterised by peaty moorlands, with higher slopes subject to common grazing by sheep. Within the broad expanse of peat artificial open moor drains have been excavated.

Peat slides currently characterise activity within Langden Beck. Within the headwaters of Langden Beck at Noon Hill, an extensive composite peat slide occurred during a convective summer thunderstorm on 17th of July 1983 (Carling, 1986b). The slide had a substantial effect on the local river regime. Some 30 000 tonnes of peat were transported along the main river system to the mouth of the catchment. Large amounts of main river sediment were also reworked in response to high discharges. On a larger scale, a peat slide within Harthope beck resulted in the removal of substantial amounts of peat and the erosion of the underlying bedrock within the side gully, fed by the peat slide. The peat and eroded material was shunted along the trunk stream system at Harthope Beck, modifying the position of the channel. The slide occurred in association with the rapid thaw of snow cover. Both peat slides are associated with the rapid supply of large volumes of water, an underlying impervious clay layer of solifluction deposits and the resulting high pressure placed upon the macropipe system within the peat. This contemporary evidence of the conditions which lead to peat slides and their magnitude can be extrapolated to the previous occurrence of high magnitude storm events within the catchment since the establishment of peat cover.

3.4 Inter- and intra-regional site integration

In all four regions investigated in the thesis, the study of the sediment sequence of more than one feature offers the prospect of identifying spatial variations in a region that has experienced a specific set of environment controls (Figure 3.7 and Table 3.1). At Glen Etive the investigation is focused upon understanding the rate and nature of the development of the debris cone issuing from Coire Dionachd. Two exposures within the debris cone offer the opportunity to examine the control of changes in sediment availability upon phases of cone aggradation separated in time and space. The feature is comparable in form to the cone studied by Brazier *et al.* (1988). The cone is supplied by a trunk stream which opens out to a cirque in the headwaters of the catchment.

Two features within Yarrow Water at the Moffat site have exposures of their internal sediments. A small debris cone is deposited at the base of Dry Cleuch, a single linear gully which opens out into a shallow headbowl at the convex break of slope. Dry Cleuch catchment's area is much smaller in comparison to that of Hermanlaw Burn. The trunk stream of Hermanlaw is confined within a bedrock gorge along most of its length but opens out in the headwater regions. A large alluvial fan has formed at the mouth of Hermanlaw Burn and sediments have been exposed that relate to its earliest phase of aggradation. The two features have similar characteristics in their sediment supplies and a comparison will therefore highlight what effect catchment size has upon the rate and nature of sediment supplies and availability.

Within Langdale and Bowderdale, the large number of fans and cones located within a relatively small area has resulted in a number of features having sediment exposures available for investigation. Five features have been investigated in detail within the catchment (Table 3.1). The range in the size of features and their associated catchment areas have again afforded the opportunity to derive the influence catchment size has upon sediment supply and availability. The similarities observed in the catchment size of Burnt Gill and Thickcombs Gill and their close proximity gives the opportunity to compare the nature of their development under similar environmental conditions.

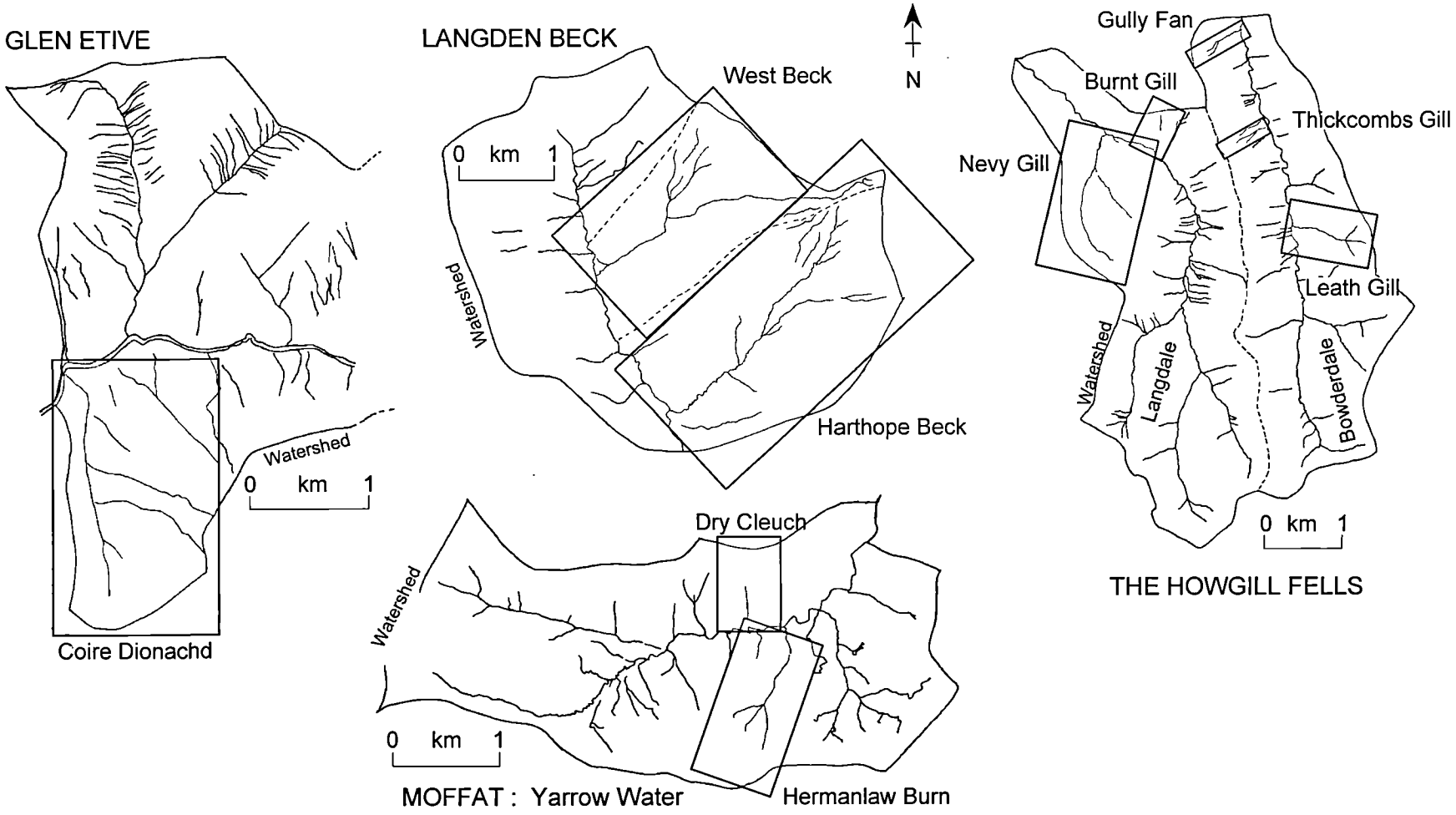


Figure 3.7. The Location of catchments studied at Glen Etive,Yarrow Water near Moffat, Langden Beck and the Howgill Fells

Table 3.1. Basic geometric characteristics of features

Name	Description	Grid Reference (10m)	Catchment area	Feature area	Relative Relief	Transport Distance	Gradient
Coire Dionachd	Composite cone and fan	NN 1675:5065	1.6 km^2	0.055 km^2	778 m	1.9 km	0.4095
Dry Cleuch	Debris cone	NY 2184:1702	0.085 km^2	0.012 km^2	245 m	674 m	0.3635
Hermanlaw Burn	Tributary alluvial fan	NY 2219:1695	0.523 km^2	0.052 km^2	314 m	1.3 km	0.2415
Burnt Gill	Debris cone	NY 6623:0160	0.052 km^2	0.022 km^2	160 m	275 m	0.5818
Nevy Gill	Tributary alluvial fan	NY 6570:0150	1 km^2	0.071 km^2	297 m	1.7 km	0.1747
Thickcombs Gill	Debris cone	NY 6778:0135	0.120 km^2	0.016 km^2	232 m	525 m	0.4419
Leath Gill	Tributary debris fan	NY 6780:0108	0.369 km^2	0.031 km^2	260 m	850 m	0.3058
Gully Fan	Gully fan	NY 6740:0210	0.034 km^2	0.005 km^2	230 m	325 m	0.7077
Harthorpe Beck	Tributary alluvial fan	NY 8556:3229	2.5 km^2	0.056 km^2	263 m	2.7 km	0.0971
West Beck	Tributary alluvial fan	NY 8691:3370	1.9 km^2	0.055 km^2	233 m	2.4 km	0.0971

The two fans at Harthope Beck and West Beck within the Langden Beck catchment have both experienced differing intensities of mining activity. West Beck has had a dramatic influx of sediment and marked change on the fan's hydrological regime. At Harthope the major change has been dominated by changes in the catchment hydrological regime.

The findings obtained for the development of fans and cones at each site can be extrapolated to include features of comparable form and size within each study reach. The ability to extrapolate information is based upon the long-established principle that the form of a fan is in direct association with a combination of catchment lithology and climate history controls operating within the supplying catchment (Bull, 1962a; Kostaschuk, 1986; Silva *et al.*, 1992; Oguchi and Tokyo, 1994). Fans similar in form within a given region have developed under the same processes within the supplying catchment. The spatial variation in the form of features is taken to be indicative of a difference in controls operating within the supplying catchment. Large fans are associated with a less resistant catchment lithology (Leece, 1991) for example. By carrying out a morphometric systematic investigation of the form of features found within each study reach, the question of similar timing of features can be addressed. The controls upon fan and cone development established for an individual feature can be extrapolated to comparable forms.

The study reach in the Howgill Fells shares a number of geomorphological characteristics with the site at Moffat including the physical topography, sediment supply, blanket peat on catchment interfluves and the presence of preferential pathways within sediment supplies on the main valley slopes. The stark contrast in sediment supply between the two sites and Glen Etive may be reflected by contrasting rates and timing of sediment transfer and exhaustion. It is likely that parallels can be drawn with the findings at Langden Beck and data observed in fan and cone sequences at the other three sites. In comparing the development of features investigated at different sites it is hoped that general characteristics are observed in the nature of sediment supply control, despite the contrast in the rate of sediment transfer and the relative amounts of sediment available, can be established.

Chapter Four

Fan and cone development framework

4.1 Introduction

An important part of this thesis is to establish appropriate methods and define criteria to provide a standard framework for the description and interpretation of fan and cone development history. An appropriate framework will allow the comparison of sections, within and between features, that have developed in contrasting regions. Periods of stability and the timing of phases of fan and cone activity are based upon consideration of the environmental context, the form of the feature and investigation or characterisation of stratigraphical changes that represent periods of stability and rapid change. The identification and interpretation of changes in sediment emplacement mechanisms and source of materials supplied to the fan or cone can thus be placed within a temporal and contextual framework.

4.2 Descriptive, sampling and laboratory methods

4.2.1 Section location and environmental context

For the current research, stratigraphical analysis is restricted to a vertical two dimensional analysis due to the nature of the fan and cone exposures. To compensate for limited lateral investigation, within-feature variation was achieved by analysing two or more sections from the same feature. Internal variation within a fan or cone results from changes in the position of the main axis of deposition. Changes in axis position can occur during and between phases of activity. Fan and cone

deposits can also be reworked and sedimentological evidence of previous events can be completely removed resulting in hiatuses in the sediment record. Internal variation in the preservation of the deposits of a particular event can thus occur horizontally. The thickness of the deposits preserved and the vertical sequence can vary laterally. Sections located within the same phase of development will also identify lateral variations. A change in the focus of deposition can result in the lateral isolation of deposits within fan terraces. The analysis of within-fan terraces provides information upon the temporal development of fans or cones. Care must be taken in the interpretation of sediments within fan terraces as material from previous phases are reworked as part of their development.

The number and location of sections used to investigate fan and cone sedimentology is controlled by the form of the fan or cone. Sediments can be exposed by incision by the main river or by the trunk stream of the feature itself. Establishing the environmental context of the section under investigation and its location with respect to the fan or cone apex has important implications for the interpretation of results. A vertical section only gives a slice of sediments at a given point, which may not record all of the events that have occurred on the feature. An event could have occurred with extensive thick lateral deposits at the axis of deposition but with the section investigated located away from the axis for example. The deposits are interpreted without knowledge of the larger event. Investigation of the horizontal continuity of palaeosols is also restricted by a vertical section. At all sites where palaeosols were found, extensive slumping of material restricted the lateral investigation of soil profiles.

When interpreting results from a vertical section consideration of the lateral development of features as well as the potential reworking of deposits is essential. The preferential preservation of deposits is also controlled by the type of feature, the nature of the supplying drainage basin and its interaction with the main valley floor.

4.2.2 Facies classification and sampling

The description of field sections is based primarily upon clast and matrix ratios, obvious changes in the nature of sorting and texture. A facies scheme was developed using field descriptions and photographs in an attempt to establish a basis

for correlation of visual changes in fan and cone sedimentology. The facies code applied is an adaptation of the lithofacies model developed by Eyles *et al.* (1983). To provide a complete description of the fan and cone sections, codes were added to the model detailing the organic content. Organic matter is incorporated into a section *in situ* as a palaeosol or transported in as debris. Soil profile descriptions of the palaeosols sampled are given in appendix 1.1. The facies scheme is relatively simple, yet provides sufficient detail for the interpretation of depositional change and the identification of process changes within the stratigraphic section. Table 4.1 provides a key to the principal codes used. The logs are plotted on a vertical scale of 1:1 (cm) and extend from zero depth to stream level. Information concerning contact boundaries, the internal structure of the sediments and the nature of the sediment packing are presented. Codes in the Eyles *et al.* (1983) lithofacies model give information upon the range of particles sizes, not the actual sizes and proportions. The dominant size of the matrix material is added to the main code for subsequent use in the reconstruction of flow events (Chapter Five).

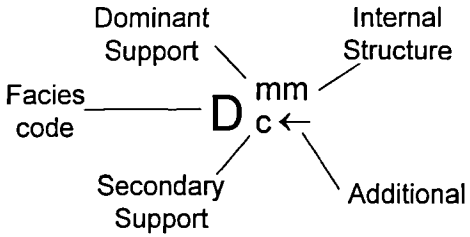
A section sampling scheme was developed on the basis of field classification and the identification of individual layers for a given section. Bulk samples were taken sequentially from each layer working from the bottom to the top of the section to avoid contamination and sealed in plastic bags. On return to the laboratory all samples were stored in a refrigerator before analysis to prevent alteration of the material by bacterial and fungal activity. The bulk samples were then air dried and sieved for the < 2 mm fraction. Representative sub-samples were split for measurement of organic content and particle size using a sample splitter.

Samples of organic material were taken from all occurrences of organic debris and palaeosols present within sections. By sampling material from the top of the palaeosol the onset alluvial fan or debris cone aggradation can be dated. Samples of organic material from the base of the organic horizon can provide a date for the oldest organic carbon incorporated during initial soil formation. A mature palaeosol located in a fan section represents a marked phase of stability in fan and cone history. Dates obtained from an *in situ* soil horizon can be affected by the inclusion of rootlets and residence times or translocation rates of organic carbon. Care was taken to avoid sampling of palaeosol material that could have potentially been contaminated by younger organic material through natural penetration by plant

Table 4.1. Facies Code. After Eyles *et al.* (1983)

Facies Code	Support	Internal Structure	Additional
D - diamict	m - matrix supported c - clast supported	m - massive ps - poorly sorted s - stratified → - graded bottom to top ← - inversely graded : top to bottom Affix: s - size change *No* - change in number *inNo* - increase in number of clasts *deNo* - decrease in number of clasts	*un* - uniform size *int* - intermittent clasts *imb* - imbricated *mg* - manganese nodules *dm* - dominant matrix material Affix: *(gr)* gravel *(sd)* sand *(st)* silt *(cl)* clay *:* - mixture
S - Sand	h - horizontal lamination t - trough cross-bedded		
0 - Organic content	fp - fibrous peat or - organic rich od - organic debris		
P - Palaeosol	r - rootlets i - iron staining		Soil colour: *(pg)* - pale grey *(g)* - grey *(bg)* - blue grey *(dg)* - dark grey





roots. Samples were taken just below a contact to minimise soil residence time effects (Harvey *et al.*, 1981). Although dating of organic debris within fan and cone deposits can produce results significantly older than the actual timing of the transporting event itself, it provides a useful means of clarifying the internal consistently and gives a broad time range for the sediment deposition.

4.2.3 Laboratory methods

An assessment of the organic material content was obtained using Loss On Ignition (LOI). The presence of immature palaeosols or an event that has incorporated organic material can be discerned using LOI, which gives the percentage of organic material within a given sample. The method used to estimate organic content follows that used by Ball (1964). The representative sub-sample was added to a crucible of known weight, oven dried at 100°C overnight and weighed. The sample was then placed in a furnace at 550°C for four hours. Heating at this temperature removed all of the organic matter. The percentage of organic material per sample was calculated using the standard equation (Eq. 4.1) (see Appendix 1.2).

$$\%\text{L.O.I.} = \left[\frac{\left[\begin{array}{c}\text{Dry weight and crucible} - \\ \text{weight of crucible}\end{array}\right] - \left[\begin{array}{c}\text{Ignited weight and crucible} - \\ \text{weight of crucible}\end{array}\right]}{\left[\begin{array}{c}\text{Dry weight and crucible} - \\ \text{weight of crucible}\end{array}\right]} \times 100 \right] \qquad \text{Eq. (4.1)}$$

Not all soils have high percentages of organic material, the bulk of which is often restricted to the uppermost layers of a developing soil. Within alluvial fan and debris cone environments the upper surface of the fan can be stripped by the occurrence of debris flow or sheet flow. Consequently, the upper organic layer is removed leaving only the B and C horizons of the soil, which have much more limited amounts of organic material within them. Organic material can also be reduced and incorporated into the soil to become part of the clay aggregate complex. Anaerobic conditions common in gleyed soils are associated with the break down of organic material.

To measure particle size the sample was first treated to remove organic material. After treatment, 5 ml of Sodium Hexametaphosphate was added to disaggregate the sediment. Measurements were carried out using a Laser Coulter® Counter, Model

LS230. The equipment measures a particle size range of 0.04 μm to 2 mm. Samples are added via a fluid module. The size distribution of a sample is measured using two lasers. The 2000μm to 1μm size range is measured using standard laser refraction techniques. The smaller < 0.04μm fraction is measured using Polarisation Intensity Differential Scatter. The light scatter intensity at two optical polarisation angles for three wavelengths and polarisations is measured. The data from the two methods are combined to produce a size distribution, reproduced to the operators specifications.

A pilot run was carried out to determine the internal accuracy of the machine and the repeatability of sample runs. The results indicate that the greatest variation occurs at the two extremes of the particle size measurements but that the degree of variation is acceptable. Particle size data are presented as size fractions using the Udden-Wentworth grain size scale (see Appendix 1.2).

Dating of organic material is the most commonly applied method used to constrain the time-scale of fan and cone development. The usefulness of radiocarbon and AMS dating is restricted by the availability of organic material and characteristics of its formation and its environmental context. Twenty samples were collected for dating from palaeosols and organic debris identified in the sections. The samples were dated by NERC using radiocarbon and AMS techniques. AMS techniques were applied when organic material was present in insufficient quantities for radiometric radiocarbon dating. Reported ages are calculated as conventional radiocarbon years B.P (AD 1950) and given at the $\pm 1\sigma$ level for overall analytical confidence.

The specific details for each date, the methodology used, the type and stratigraphic location of the organic material are noted in Table 4.2. Some of the dates are not internally consistent. The stratigraphic and environmental context of organic material dated is provided in the following sections and is used to assess the reliability of the dates obtained. The age obtained from organic material, transported or developed *in situ*, preserved within a sediment profile can be affected by a number of factors pre- and post- burial: Martin and Johnson (1995) provide a useful summary. Errors can be introduced in the initial formation of a soil. Organic carbon incorporated into plant material, which is subsequently incorporated into the

Table 4.2. Radiocarbon and AMS dates,a summary of stratigraphic context and informtation provided

Site/section	Depth (cm)	Context	Information	Method/Date ±1σ	NERC Code
GE CDS1	128	Transported organic material, fibrous characteristics comparable to peat. Layers discontinuous apart from the uppermost layer	Maximal age for fan aggradation	RC 3,580 ± 70	SRR - 6014
	152			RC 4,370 ± 45	SRR - 6015
	177			RC 3,310 ± 50	SRR - 6016
	187			RC 4,485 ± 50	SRR - 6017
GE CDS2	145			RC 4,295 ± 50	SRR - 6018
M DCS1	240	Palaeosol : Developed within fan and cone sediments	Onset of soil formation and phase of cone aggradation	RC 895 ± 45	SRR - 6019
	267			RC 975 ± 40	SRR - 6020
	320	Transported branch within fan and cone sediments	Maximal age for fan aggradation	RC 1,490 ± 45	SRR - 6021
	356	Transported peat	Maximal age for fan aggradation	RC 3,565 ± 45	SRR - 6022
	391			RC 3,220 ± 45	SRR - 6023
M DCS2	185	Palaeosol : Hydromorphic soil	Onset of soil formation and phase of cone aggradation	AMS 610 ± 40	CAMS - 41323
	227			RC 870 ± 45	SRR - 6024
HF TCS1	120	Palaeosol : Hydromorphic soil	Onset of soil formation and phase of cone aggradation	RC 790 ± 45	SRR - 6025
	155			RC 855 ± 45	SRR - 6026
HF TCS2	138	Palaeosol : Hydromorphic soil	Onset of soil formation and phase of cone aggradation	AMS 930 ± 40	AA - 24205
	161			AMS 900 ±40	AA - 24204
HF GFS1	28	Samples taken from top of peat developed *in situ*	Onset of peat formation and fan aggradation	RC 195 ± 45	SRR - 6027
	53			RC 300 ± 45	SRR - 6027
LB HBS2	68	Palaeosol : Hydromorphic	Onset of soil formation and phase of cone aggradation	AMS 19,235 ± 130	AA - 24207
	108			AMS 18,730 ± 125	AA - 24206

developing soil, can have sources of old carbon. Carbonates from underlying limestone lithology are one example. The reliability of dates from organic material developed *in situ* also depends upon the nature of the soil-forming event. A palaeosol can be affected by a post-burial input of organic material. Translocation of organic material to the base of the soil can alter the time profile usually found within a soil. The uppermost layer of a soil can be stripped by an erosive event. The most recently incorporated organic material is thus lost, resulting in an anomalously older age for the cessation of soil formation and the onset of fan or cone aggradation. The interpretation of organic debris must be done with care, taking into account the environment from which the sample is taken and the type of organic material. Organic debris within transported deposits can be significantly older than the actual timing of the transporting event.

4.3 Glen Etive

4.3.1 Coire Dionachd

The successive phases of activity that have resulted in the current form of the tributary fan of Coire Dionachd are illustrated in Figure 4.1. The majority of the fan's surface is vegetated but on its western side the entrenched trunk stream is characterised by a wide splay of fresh coarse debris and boulders. From the surface morphology of the fan, three earlier phases of activity can be recognised. The following interpretation is aided by the presence of lazy beds, a Medieval farming practice, located upon the surface of the cone.

Initially, a substantial phase of aggradation deposited sediments onto a high terrace, the remnants of which are preserved on the eastern side of the fan (Phase A, Figure 4.1). This was then partially buried by sediments transported from the catchment (Phase B, Figure 4.1). The second aggradational phase must have occurred after the emplacement of the lazy beds, as the latter are buried by the former. The deposits of these two aggradational phases have subsequently been incised, forming a series of channels on the fan's surface of varying depth (Phase C and Phase D, Figure 4.1). The channels have since been abandoned by formation of the current, deeply entrenched, trunk stream system (Phase E, Figure 4.1).

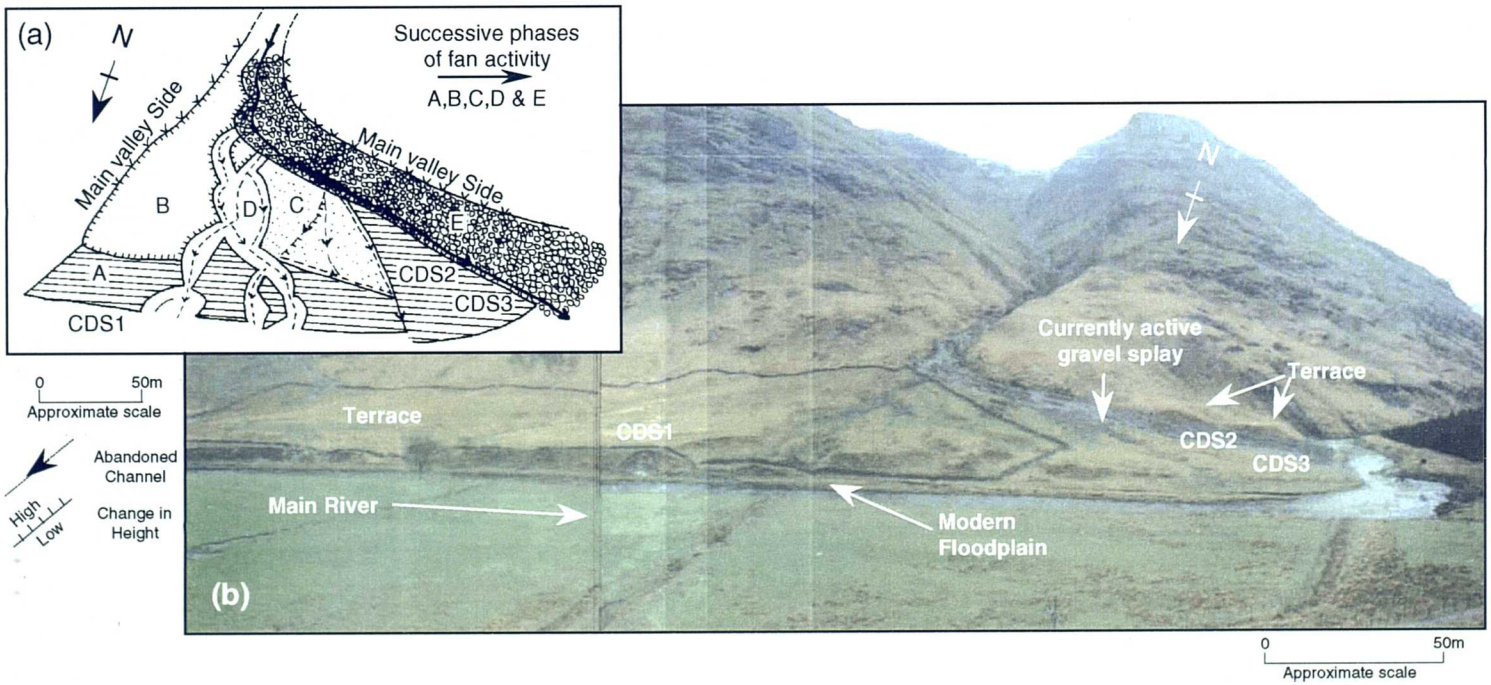


Figure 4.1. The surface features of Coire Dionachd fan, Glen Etive. (a) A planform schematic of surface features.

The previous and current incision of fan sediments has focused upon the western side of the fan. The erosion of the distal outside edge of the fan indicates that the slope of the first phase dips from east to west. The focus of incision on the western side of the convex profile can be attributed to the removal of previous fan sediments, including the high terrace upon which fan sediments were initially deposited. Subsequent flows have buried earlier channels, resulting in the relatively uniform surface which has since been incised and within which lazy beds have been emplaced. Any sediments pertaining to previous phases of activity on the western side of the feature have been effectively removed by the concentration of fan incision in this region. The trunk stream of the fan has recently incised into the distal deposits of sediments relating to the first phase of fan aggradation. Two sections, 15m apart, have been logged within the same exposure. CDS2 is located higher up the section and closer to the fan apex than CDS3. Section CDS1 has been taken from a small exposure of sediments of the first phase of fan activity on the eastern part of the fan. All three sections are located within the deposits of Phase A (Figure 4.1). CDS1 is separated from CDS2 and CDS3 by over 100 m. The internal chronology of sediments preserved between the two localities may as a result differ.

Organic material, formed *in situ* or incorporated as debris, is not visible within the 205 cm of excavated sediments from CDS1. The loss on ignition profile indicates a sharp increase in organic content within the top 44 cm (Figure 4.2c). At 44 cm depth loss on ignition increases from 4 % to 11 % within a vertical interval of 8 cm. The high values are maintained and increase sequentially towards the uppermost sample. As the increase occurs within upper most samples, its presence can be associated with the modern soil horizon. The depth at which the marked increase in loss on ignition occurs also corresponds with a marked change in the visual properties of the sediment (Figure 4.2a & b). The coarse particle size contribution of the matrix sediment also starts to decrease at this depth. The high organic content may have been incorporated into the uppermost layer during its transport. The identification of separately transported layers of sediment will be investigated in Chapter Five to determine the association of high organic material with a distinct sediment flow.

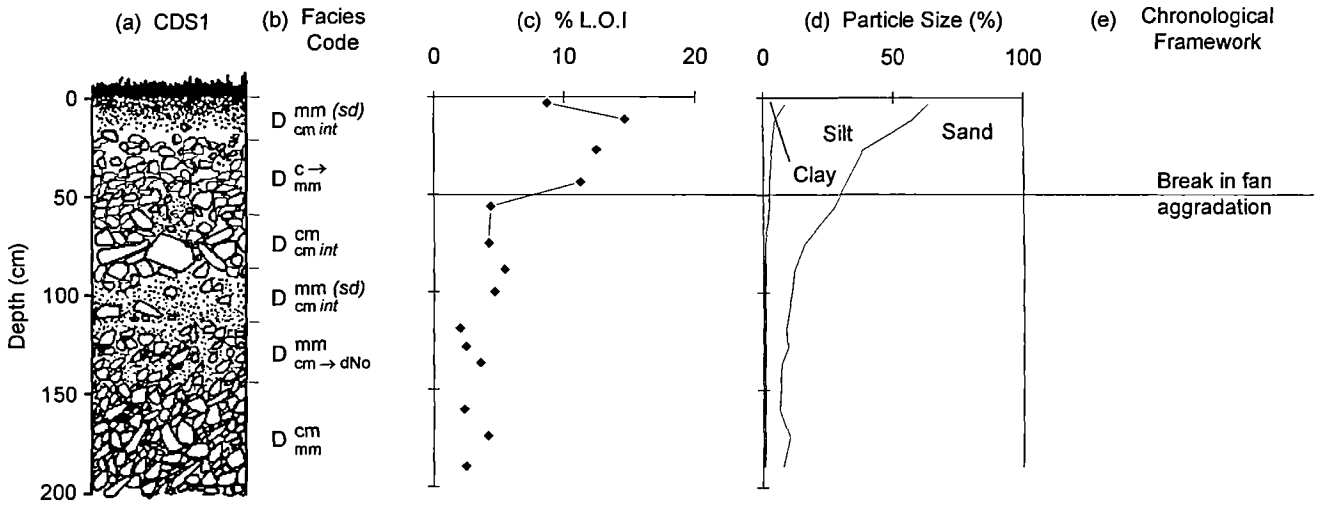


Figure 4.2. Stratigraphic log, facies code, percentage loss on ignition, grain size and the chronological framework for CDS1, Glen Etive. The key for the facies code is given in Table 4.1.

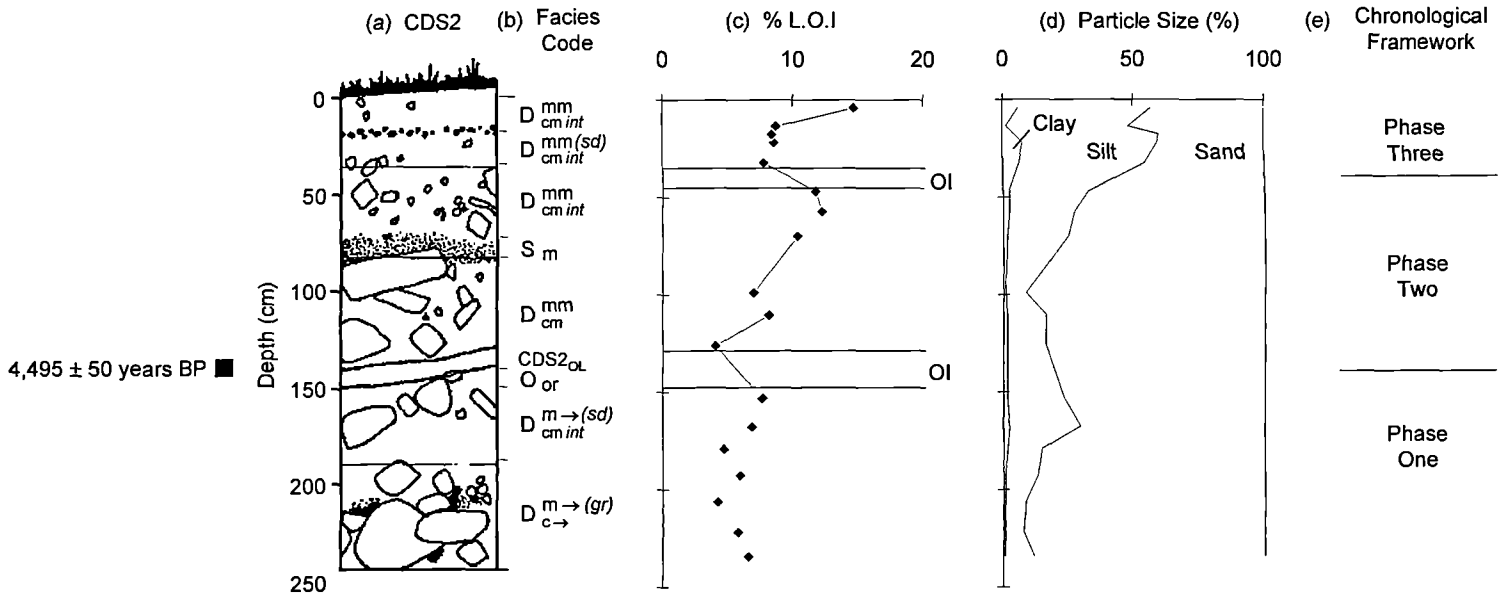


Figure 4.3. Radiocarbon date, stratigraphic log, facies code, percentage loss on ignition, grain size and the chronological framework for CDS2, Glen Etive. The key for the facies code is given in Table 4.1, OI : Organic Inversion.

At 145 cm depth in CDS2, a 2 cm thick dark organic layer, preserved within a sandy matrix, divides the fan sediments (Figure 4.3). The organic layer $CDS2_{OL}$ is preserved laterally but is broken over a distance of 2 m downstream of the section. Roots within the layer do not show vertical growth within the horizon, their chaotic nature suggests that they were not grown *in situ.* The organic layer has been transported. The fibrous nature of the organic material and the high density of roots and organic matter preserved suggests a peat source of the transported material. A sequential but sustained increase in loss on ignition from the base of CDS2 is truncated at approximately 140 cm and replaced by a significantly lower organic content. A similar inversion in organic content is repeated at 34 cm. The depth at which the organic decline occurs corresponds to changes in the sediment properties in the section and changes in the particle size characteristics of the matrix sediment (Figure 4.3a, b & c). The lower organic inversion corresponds to the upper sediments of the sandy horizon within which the organic layer is preserved. Loss on ignition has decreased by 5%. The second inversion occurs when massively stratified gravels with large boulders are capped by a visually distinct layer of sediment in sharp contact. Loss on ignition decreases from 11% to 7%. Although the differences appear to be small they are large relative to the loss on ignition values in the section overall. The two organic inversions split the sediments within the section into three distinct zones.

The sediment layering logged in section CDS3 is different to that observed in CDS2. Organic material similar in character to that found in $CDS2_{OL}$ is incorporated into 69 cm of sediment between 124 cm and 193 cm depth. Organic material at four sequentially separate levels can be identified, $CDS3_{OL1}$ $CDS3_{OL2}$ $CDS3_{OL3}$ and $CDS3_{OL4}$ (Figure 4.4b) Only the uppermost layer $CDS3_{OL1}$ at 124 cm is continuous within the section. Its lateral extent within the exposure is limited and it peters out to the left of the section. To the right the sediment sequence is obscured. As in CDS2, two organic inversions can be seen within the loss on ignition values. Both inversions are coincident with visual changes in the sediment sequence.

A schematic representation of the lateral deposits, where visible, of the 30m exposure is presented in Figure 4.5. The difference and similarities in the sedimentary layering between the two sections is highlighted. The sedimentary environments within which the organic layers are preserved are comparable

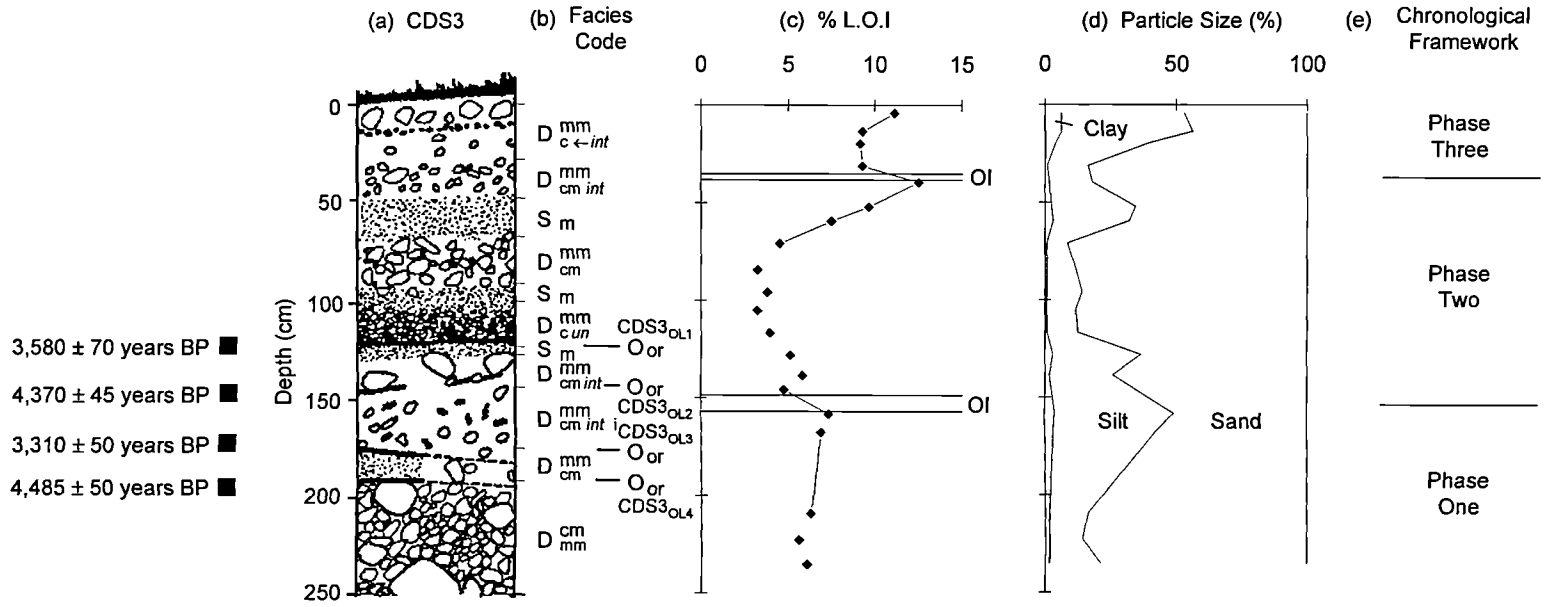


Figure 4.4. Radiocarbon dates, stratigraphic log, facies code, percentage loss on ignition, grain size and the chronological framework for CDS3, Glen Etive. The key for the facies code is given in Table 4.1, OI : Organic Inversion.

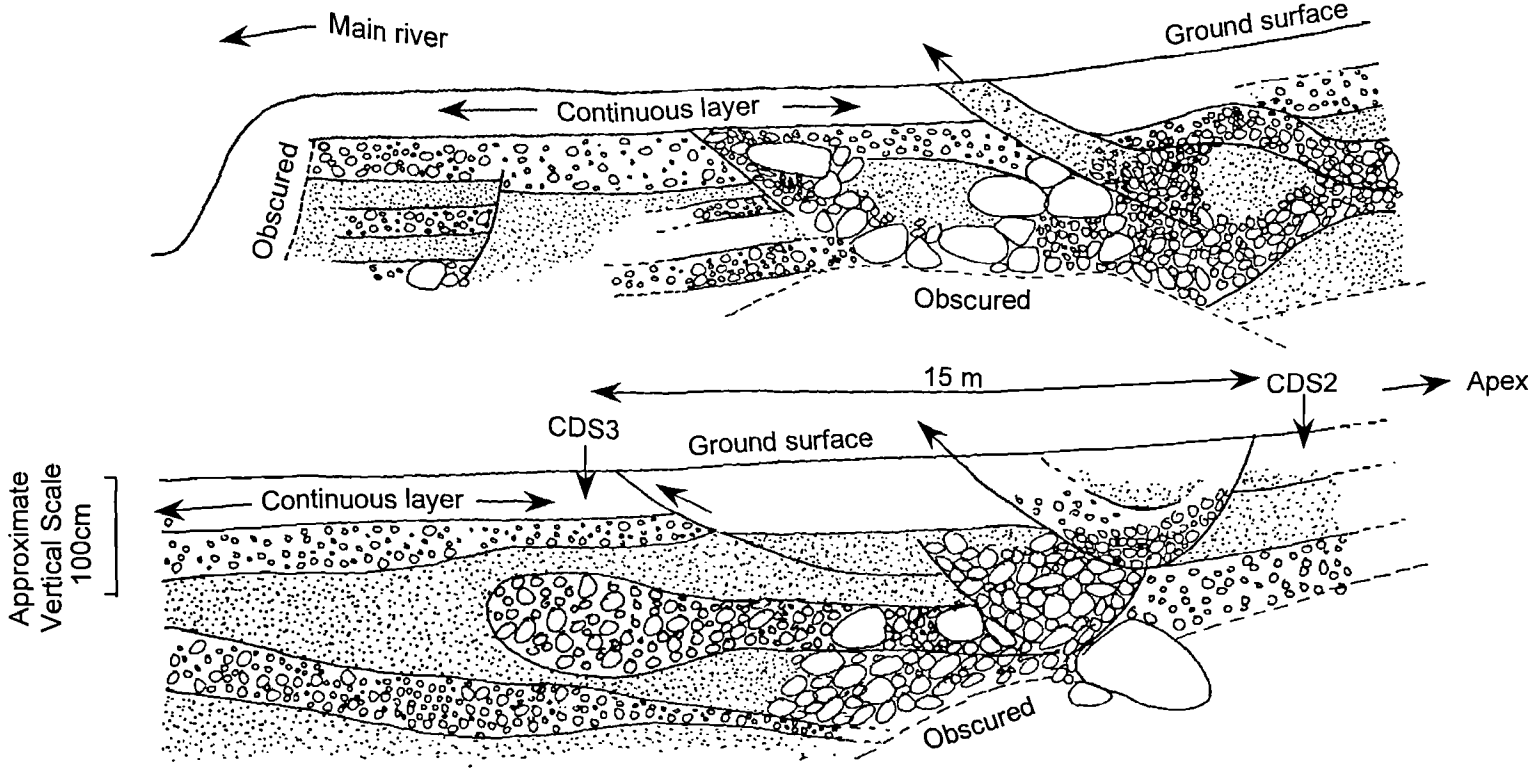


Figure 4.5. A schematic illustration of the generalised sediment stratigraphy of the exposure within which CDS2 and CDS3 have been excavated.

between the two sections. The depth of the organic layers from the surface of both sections are similar. Layered organic material is preserved within a sandy matrix, capped by a layer with a poor admixture of clasts that have a large range of clast sizes. The thickness of the organic horizons and the characteristics of organic matter preserved is consistent in both sections. The similarities observed in the organic horizons found in both sections suggests a similar mechanism of transportation. The relative timing of the date obtained for $CDS2_{OL}$ is of a comparable age with $CDS3_{OL2}$ and $CDS3_{OL4}$ (Figure 4.3 and Figure 4.4). The nature of the layering of organic horizons in CDS3, and the internal inconsistency of their statistically distinct dates can only be interpreted by establishing the transport mechanism of sediments surrounding and incorporating the organic matter. This will be addressed in Chapter Five.

CDS1, CDS2 and CDS3 are, based primarily upon a visual interpretation of fan development, located in the same aggradational phase. A change in the loss on ignition within the top sediments, which coincides with changes in the sedimentary properties, is the only comparable characteristic observed in the uppermost sediments of each section. The layers could have been deposited during one event which buried the whole surface of the fan. The contrast in the remaining sediments of CDS1 with CDS2 and CDS3, indicate a spatial separation in activity between the two localities. Despite the close proximity of CDS2 and CDS3 in the same exposure, marked contrasts in sediment stratigraphy is evident. A change in the environment of deposition experienced between the two sections, 15 m apart with a height differences of approximately 1.5 m, may help to explain the differences between the two sections. CDS3 is much lower and closer to the main river than CDS2. At the time of deposition the level of the main river could have been higher. Sediments deposited by the river and by the fan could have intercalated, whereas CDS2 is much higher in position and 15 m further away from the main river. The hypothesis would explain the sediment layering characteristics observed within CDS3 and in the lower part of the exposure. It would also explain the lack of similar layering being found in CDS2. The hypothesis will be tested in Chapter Five in the investigation of the transporting mechanisms.

4.3.2 Causal development

A detailed investigation into the temporal development of Dalness chasm cone in Glen Etive, 7 km upstream from Coire Dionachd, provides valuable information upon the composition of vegetation prior to and after a recent phase of fluvial incision (Brazier *et al.*, 1988). The only other information on local changes in vegetation during the Holocene is provided by the study of kettlehole deposits by Walker and Lowe (1977) at the head of Glen Etive on the edge of Rannoch Moor. Archaeological studies within the region are limited. Brazier *et al.* (1988) do link evidence of local medieval farming with a phase of fluvial reworking of Dalness Cone sediments. The relationship between the timing of regional changes in climate, vegetation and activity in Dalness chasm cone and the radiocarbon dates obtained for Coire Dionachd are presented in Figure 4.6.

The dates of transported material for Coire Dionachd correspond to the time period of a climatically induced change from a forested landscape to an acid blanket peat cover. Peat at that time extended up valley side slopes and it is possible that peat was present within the lower part of the supplying catchment at Coire Dionachd and may have provided the source of the organic matter preserved in CDS2 and CDS3.

Brazier *et al.* (1988) has linked the timing of alluvial reworking of cone sediments with a phase of medieval agriculture within the valley reach where the cone is located. At Coire Dionachd, evidence of agricultural activity is comparable to that detailed at Dalness. The whole of the upper surface of the Coire Dionachd fan is covered in Lazy beds. The fan's surface and the Lazy beds have been dissected by numerous channels of varying width. The pattern of Lazy beds are continuous either side of the channels, which suggests that incision of the fan occurred after its upper surface was cultivated. Within the top sediments of both CDS2 and CDS3 a similar layer is found at the same depth. Charcoal has been found associated with the layer which consists of heather roots that appear to have been burnt. The human interference that resulted in fluvial activity at Dalness can be extrapolated to account for the phase of fluvial incision observed at Coire Dionachd dated at 550 ± 95 years BP (Brazier *et al.*, 1988). Activity on Coire Dionachd was not restricted to the incision of the fan's surface. The Lazy beds were buried by the deposits of the

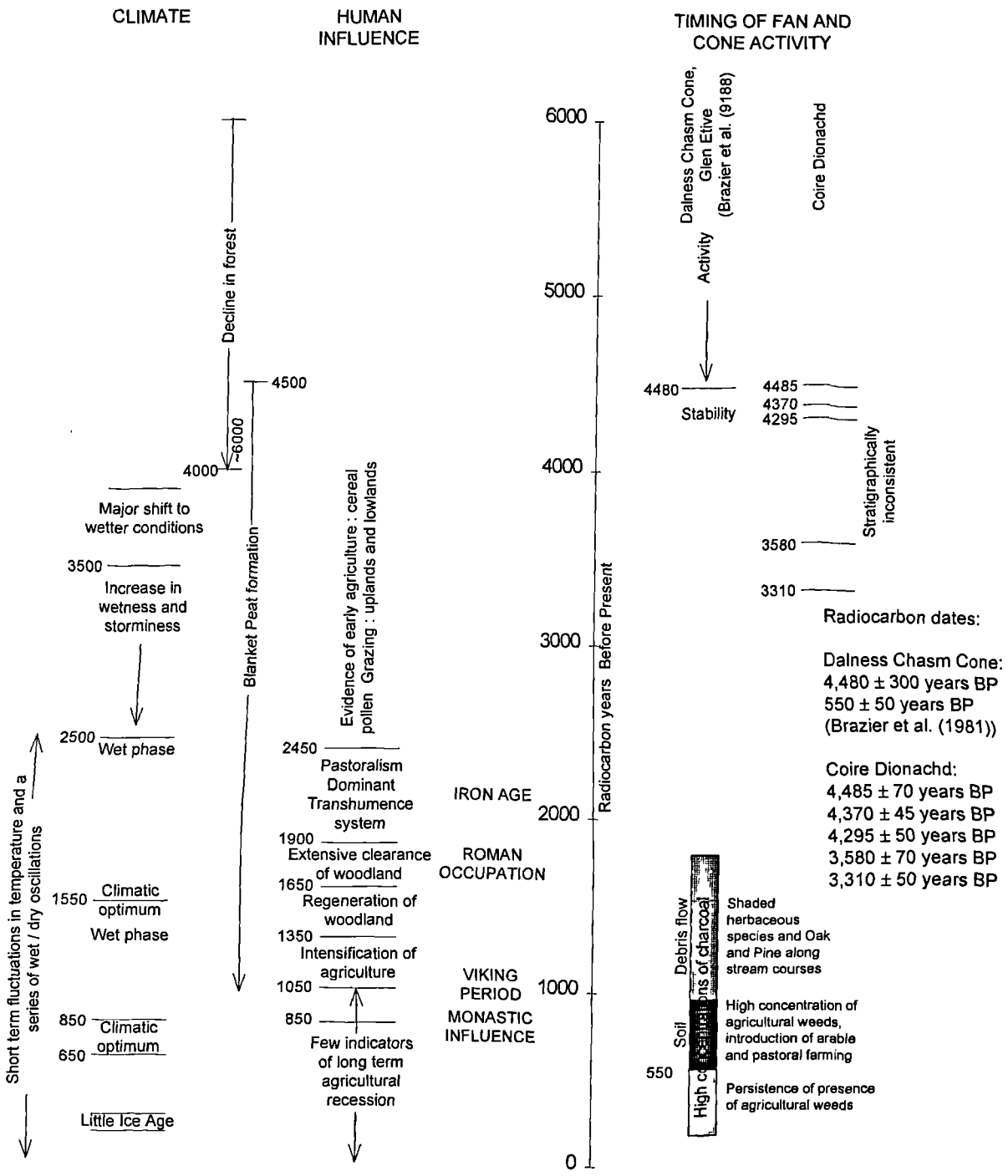


Figure 4.6. Visual correlation of the timing of cone aggradation at Coire Dionachd, with local and regional patterns of change in climate and in human activity.

second phase of activity observed within the fan. In addition to fluvial incision the period of instability at Coire Dionachd can also be linked with an aggradational phase. In contrast with Dalness Chasm sediments stores at Coire Dionachd had not been exhausted. The inter-relationship between the two different responses is difficult to establish. It is highly likely that the burning of woodland cover within the supplying catchment destabilised slopes, resulting in the second aggradational phase. Readily available sediment supplies within the trunk stream were exhausted, resulting in the subsequent incision of first and second phase sediments.

4.4 Moffat - Yarrow Water

4.4.1 Dry Cleuch

The uniform surface of the debris cone that issues from the gully Dry Cleuch is illustrated in Figure 4.7. The excavation of a road through cone sediments near the apex has hidden some of the cone surface features. There is no evidence of distinctly separate phases of activity on the cone surface. Above the road cutting topographic features point towards an older phase of activity, over which the bulk of the cone deposits now lie. The ephemeral nature of the flow issuing from Dry Cleuch does not warrant the presence of a stream channel on the debris cone, although a vegetated shallow channel is present near the cone apex. The channel either relates to the last event that covered the surface of the cone or is evidence of a previous phase of cone incision.

Dry Cleuch is located in a narrow section of the Yarrow Water valley. The valley floor at this point is only 15m wide. The containment of the main river, combined with phases of down-cutting, has resulted in the formation of valley side bluffs which are present on both sides of the debris cone. It is evident that the cone post-dates the formation of the bluffs and debouches directly onto the valley floor. Extrapolation of the surface of the cone indicates that it once extended over half of the valley floor width. Interaction between cone deposits and the sequential development of river terraces is possible. The nature of the relationship is unclear but remnants of previous floodplains could be preserved within the debris cone. The eastern side of the cone has been deeply incised by the lateral movement of the main river. Most of the exposure has been buried by slumped and weathered material. Two sections have been studied from the exposure. DCS1 is in close proximity to the cone apex.

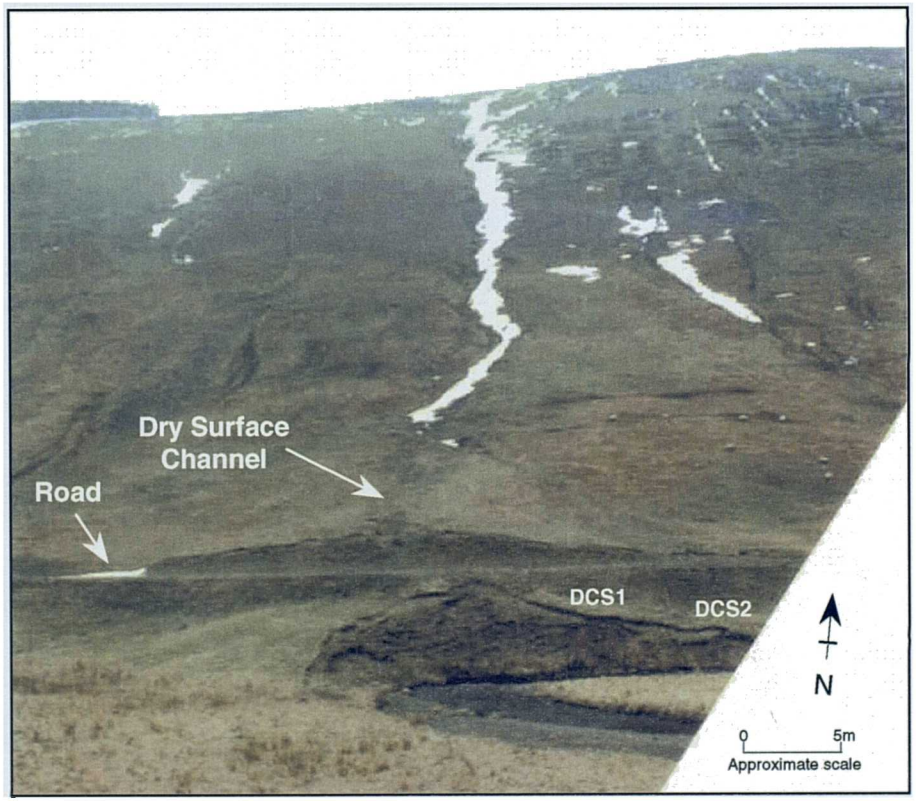


Figure 4.7. The surface features of Dry Cleuch debris cone, Yarrow Water near Moffat

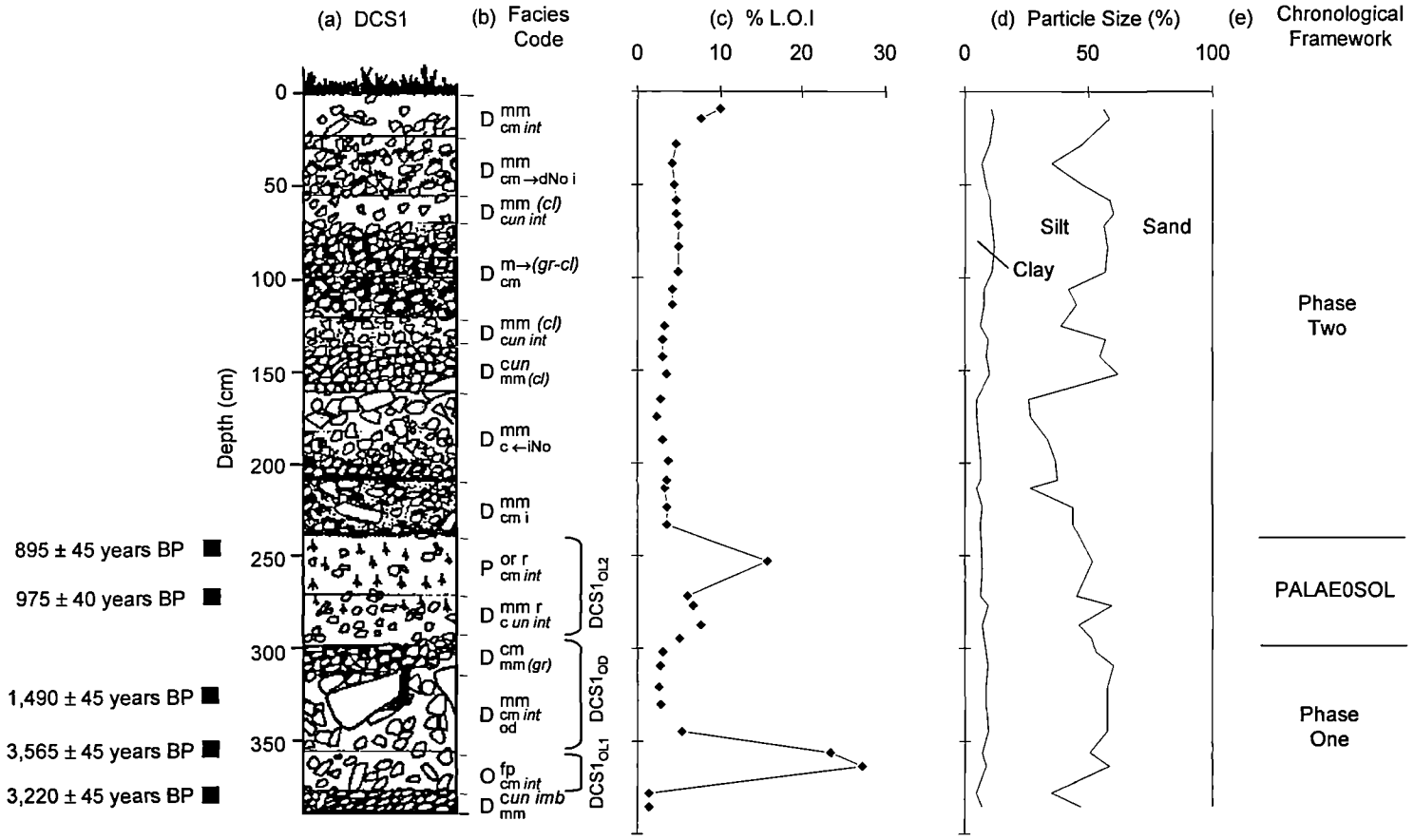


Figure 4.8. Radiocarbon dates, stratigraphic log, facies code, percentage loss on ignition, grain size and the chronological framework for DCS1, Moffat. The key for the facies code is given in Table 4.1.

DSC2 is in lateral deposits and is located further away from the cone apex than DCS1.

Within DCS1 two organic layers of contrasting characteristics have been identified (Figure 4.8). The first, $DCS1_{OL1}$, is located near to stream level between 377 cm and 356 cm depth. The layer has a sharp contact with sediments above and below. Organic material within the layer is fibrous in nature: high losses on ignition of between 27 % to 23 % reflects the presence of peat. Intermittent clasts are also incorporated within the 19 cm thick layer. The presence of the clasts and the substantial contribution of minerogenic material over 63 μm indicates that the organic horizon did not develop *in situ* (Faegri and Iverson, 1975). The layer has been transported from within the supplying catchment. Slope angle and climate have restricted peat to catchment interfluves. The second organic layer, $DCS1_{OL2}$, is between 239 cm and 299 cm depth. It represents the boundaries of a soil horizon, a palaeosol representing a break in cone sedimentation. The organic content of the palaeosol is markedly less than that for $DCS1_{OL1}$, varying between 6% and 16%, increasing to the top of the palaeosol. The properties of the palaeosol are indicative of a brown earth soil that has developed within a free draining environment (Figure 4.8).

Two visually distinct layers of sediment separate the two organic layers. Organic debris is present within the layer which directly overlies $DCS1_{OL1}$. The debris is incorporated within the whole of the layer $DCS1_{OD}$ and indicates no preferential sorting. As organic material is commonly lost if sediments have been transported by fluvial activity, the evidence points towards transportation by debris flow (Costa, 1984). As a result $DCS1_{OL2}$ has formed within debris cone deposits and represents a period break in cone activity. $DCS1_{OL2}$ is in sharp contact with 239 cm of cone sediments. Within the sediments low loss on ignition values show little variation although the sediments do undergo marked changes in their visual properties.

In DCS2 a palaeosol has been preserved 99 cm above stream level (Figure 4.9). The soil extends to the base of the exposed section. Samples taken from the exposure within which the palaeosol has formed exhibit particle size properties that differ from the rest of the sediments within the section. Fine material below 63μm is absent. Its stratigraphic depth and the preferential removal of fines suggest that the

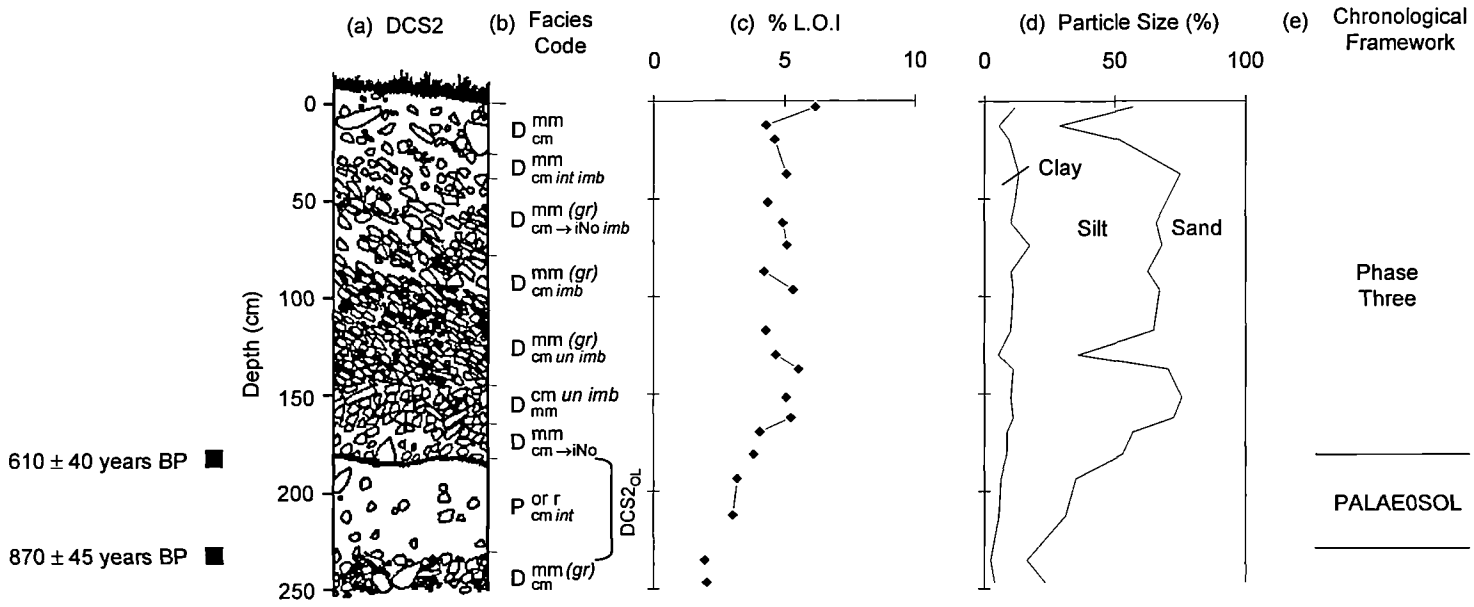


Figure 4.9. Radiocarbon dates, stratigraphic log, facies code, percentage loss on ignition, grain size and the chronological framework for DCS2, Moffat. The key for the facies code is given in Table 4.1.

soil was formed in river terrace sediments. The palaeosol $DCS2_{OL}$ is markedly distinct from the surrounding sediments because of the stark contrast in the colour of the material. The sediments are blue / grey in colour and mottled with iron stains formed around rootlets within the palaeosol. The properties are characteristic of a hydromorphic soil that formed in a gleyed or waterlogged environment (Wright, 1992). Low loss on ignition values, fluctuating at around 3 %, do not reflect the presence of the soil horizon. The low values can be attributed to the redox environment active during soil formation. Organic material has been broken down or reduced and incorporated into the soil clay complex. Organic material within the environment can be mobile within the profile and may affect the radiocarbon dates taken from this horizon.

Debris cone sediments are in sharp contact with the palaeosol. The nature of the contact suggests that it is erosive in nature. It is possible that the upper sediments of the palaeosol could have been stripped as the overlying sediments were deposited. The soil does not have an obvious A1 organic horizon. The rate of pedogenesis could have been greater than the deposition of organic material, preventing A1 horizon formation. If the upper organic layer is removed the radiocarbon date taken from the upper level of the preserved palaeosol may be older than the actual timing of the cessation of soil development. The contacts between the debris cone sediments have a distinctive slant which is attributable to the section location in the distal part of the debris cone. There is no increase in the organic content until the uppermost 10 cm of the section, the modern soil layer. The depth of the modern soil in the section is much shallower than that found for DCS1. The organic content also differs, with DCS1 reaching 10% in comparison to the 6% of DCS2. The difference is minimal but it is suggestive of a longer time period for the formation of the modern soil horizon in DCS1.

Dry Cleuch radiocarbon dates have been obtained from organic layers preserved within both sections. Dates obtained for the *in situ* palaeosol $DCS1_{OL2}$ are the most reliable in this section. The uppermost date of the palaeosol indicates a period of cone aggradation that began at 895 ± 45 years BP. The dates from the two transported organic layers below are constrained by the date obtained for the palaeosol, the organic material must have been transported before 975 ± 40 years BP. The dates for the transported material are internally consistent. There is no way

of firmly establishing the timing of their deposition due to their transported nature. Based upon the stratigraphic relationship of the transported layers two scenarios are possible. The two layers were transported either as a result of two separate phases of activity or as part of the same event. In both cases it is clear that the sediments were deposited prior to the period of soil formation.

The date for the peat layer $DCS1_{OL1}$ is coincident with the formation of peat in the area during the late Holocene. This suggests that the date of the peat layer may represent its *in situ* period of formation within the supplying catchment. The dates therefore are unlikely to represent the timing of its deposition, which could have occurred much later but prior to 975 ± 40 years BP. The timing of its deposition is further constrained by the date of organic debris taken from the $DCS1_{OD}$ directly capping the transported peat horizon. A remnant branch was dated at 1490 ± 45 years BP. The radiocarbon date represents the time period of its growth. The date can be interpreted in two ways depending upon its state prior to transportation. If the branch was part of a live tree prior to its inclusion within the transporting event the date would provide the relative timing of its transportation. If it had been deadfall and subsequently incorporated into the transported sediments the date would be older that the actual timing of the sediment flow. The relationship between the timing of deposition is still in question. The peat layer does not contain tree branches or twigs, as does the layer above. Their absence suggests the transportation of the peat layer at a time period when trees were not present within the supplying catchment, through clearance or in response to a deteriorating climate. The contact between the two layers is sharp and distinct, suggesting an erosive contact, which points towards a period of time separating the two layers. It is possible that an erosive event may have stripped the peat from within the catchment, depositing it within the debris cone, followed by the erosion of the disturbed and exposed sediments. The deposition occurred either immediately following the removal of the peat or during the period of recovery, when threshold levels were lowered. If the deposition of $DCS1_{OD}$ occurred during the same event some degree of mixing would be in evidence. It is possible that this was removed by erosive nature of the contact evident between the two layers. What is clear is that the erosive contact and lack of tree debris points towards a hiatus between the deposition of the two layers. What is not clear is what period of time the hiatus represents.

The contact of $DCS2_{OL}$ with the layer above is sharp and erosive. The uppermost date, indicative of the onset of a phase of cone aggradation, may be older than it should be. It does point towards a later phase of cone aggradation at 610 ± 40 years BP within this part of the debris cone. Dates for the onset of activity in DCS1 at 895 ± 45 years BP and DCS2 at 610 ± 40 years BP represent two successively younger phases of aggradation in the cone. As $DCS2_{OL}$ is potentially formed within terrace sediments the separation of the deposits burying the palaeosol into an aggradational phase separate from sediments in DCS1 is supported. Although the visual properties of sediments in DCS2 and the sediments which bury $DCS1_{OL2}$ show no similarities, the exact interrelationship of the sediments is still to be examined. It is possible that the uppermost sediments within phase 2 and phase 3 could have been formed by the same event. The chance of interrelationship between the two phases increases within the uppermost sediments.

Taking all into factors into account the sequence of events illustrated in Figure 4.8e and Figure 4.9e can be used to explain the temporal development of the Dry Cleuch debris cone.

4.4.2 Hermanlaw Burn

Hermanlaw Burn catchment area has a large tributary fan which debouches onto the main valley floor as the trunk stream emerges from a bedrock constrained gorge system. The surface of the feature is fairly uniform and there is no visual distinction in the phases of activity that have formed the fan (Figure 4.10). The trunk stream has a perennial flow and is located on the western edge of the feature. The lateral migration of the trunk stream has resulted in the formation of a fan terrace sequence, in total four terraces are visually apparent. Current activity on the fan is limited to the entrenched trunk stream system. Where the trunk stream meets the main river there is evidence of previous events that have resulted in the formation of small fans (Figure 4.10).

The outward development of the fan has not been impeded as the valley floor is wide at this point. It is not clear whether the fan has been deposited upon former terraces. On the western side of the fan the main river has removed any evidence pertaining to a former river terrace. The opposite edge of the fan abuts with another

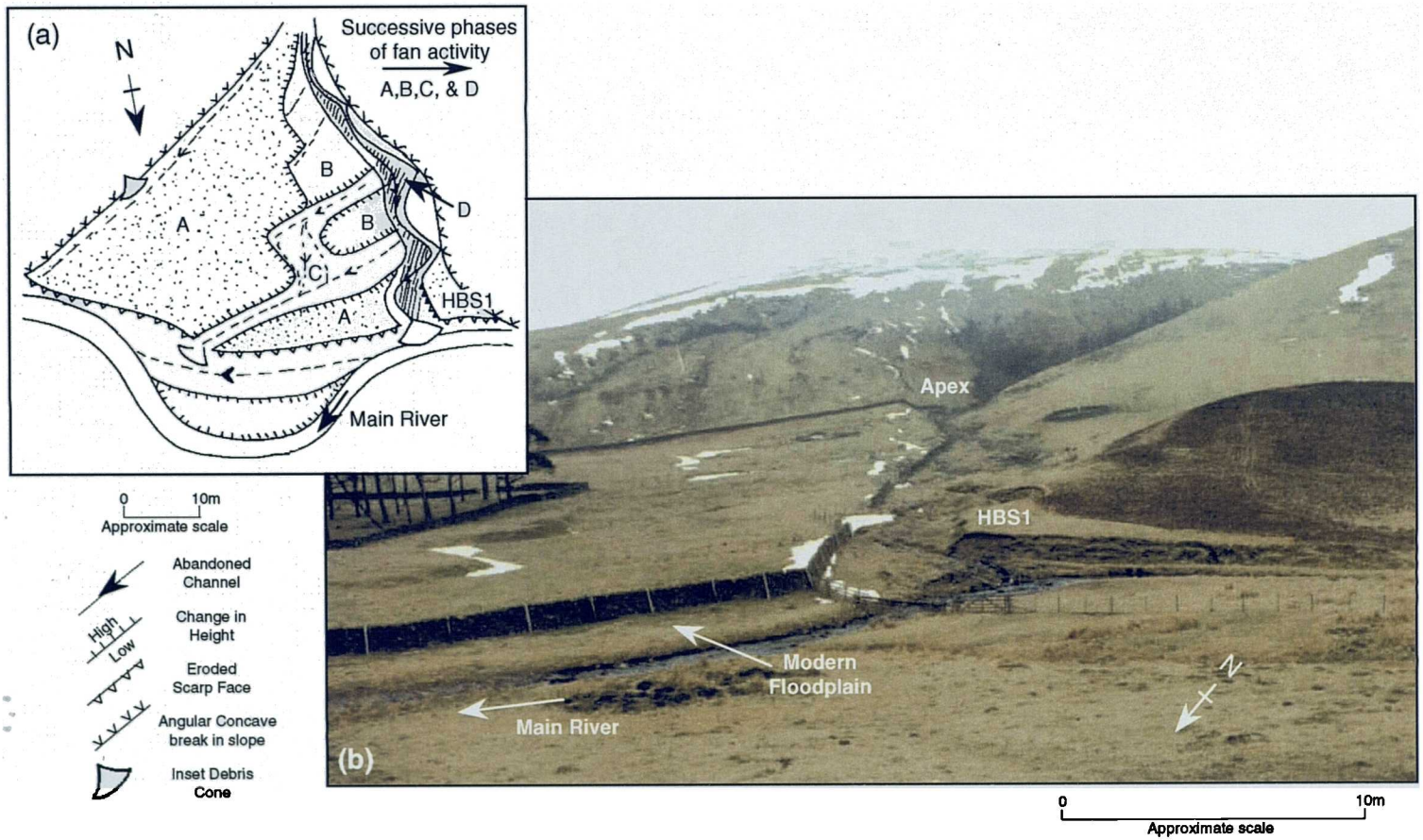


Figure 4.10. The surface features of Hermanlaw Burn fan, Yarrow Water near Moffat. (a) A planform schematic of surface features.

tributary fan. The fan has acted to constrain the location of the main river to its position on the opposite side of the valley floor. There is no evidence of fan deposits on the opposite bank of the river. The main river and its migration has cut into alluvial fan deposits, forming a bluff along most of the fan's outside edge. This has since been abandoned and a modern floodplain has formed at the base of the fan bluff. The bluff of fan sediments is heavily vegetated and exposures of fan sediments on the feature as a whole are limited. The erosive nature of the fan's trunk stream has exposed internal fan sediments where the trunk stream joins the main river. The sediments that have been exposed relate to the highest terrace, the oldest fan sediments. The section HBS1 is located well above the stream level of the main river, 1.5 m, and the trunk stream of the fan, 0.5 m. The bottom-most sediments were difficult to clear at a greater depth.

There are no obvious organic layers exposed within HBS1. The sediments do exhibit visually distinct differences in their sediment properties. The organic content of sediment samples taken from the profile also indicates variation with depth. At 67 cm a gradual increase in the organic content of the samples of 3% is replaced by an obvious sharp decrease. The organic content above the unconformity remains at a similar level, fluctuating within 0.5% until it increases by 2% in the uppermost sample. Although the change in the percentage organic content is only slight, it is backed up by a coincident change in the nature of the section sediments at the same depth. The difference is also exhibited by the change in particle size characteristics. The nature of the contact between the two layers suggests a sharp, erosive contact. The small increase in organic content and the lack of characteristics indicative of a well developed soil suggests that the increase is potentially caused by the initial stages of soil development. An immature soil has been capped by the later phase of development, rather than the removal of the upper layers of a well developed soil by the erosive contact with the upper layer.

As there was no organic material available for dating within HBS1, the timing of activity is unknown. Only the sequential development of the feature can be established from its form. It is evident that sediments within HBS1 relate to the first and uppermost aggradational phase of development, which can be split into two separate phases. The phase of fan incision which produced the entrenched sequence of fan terraces has subsequently taken place. Within the section taken

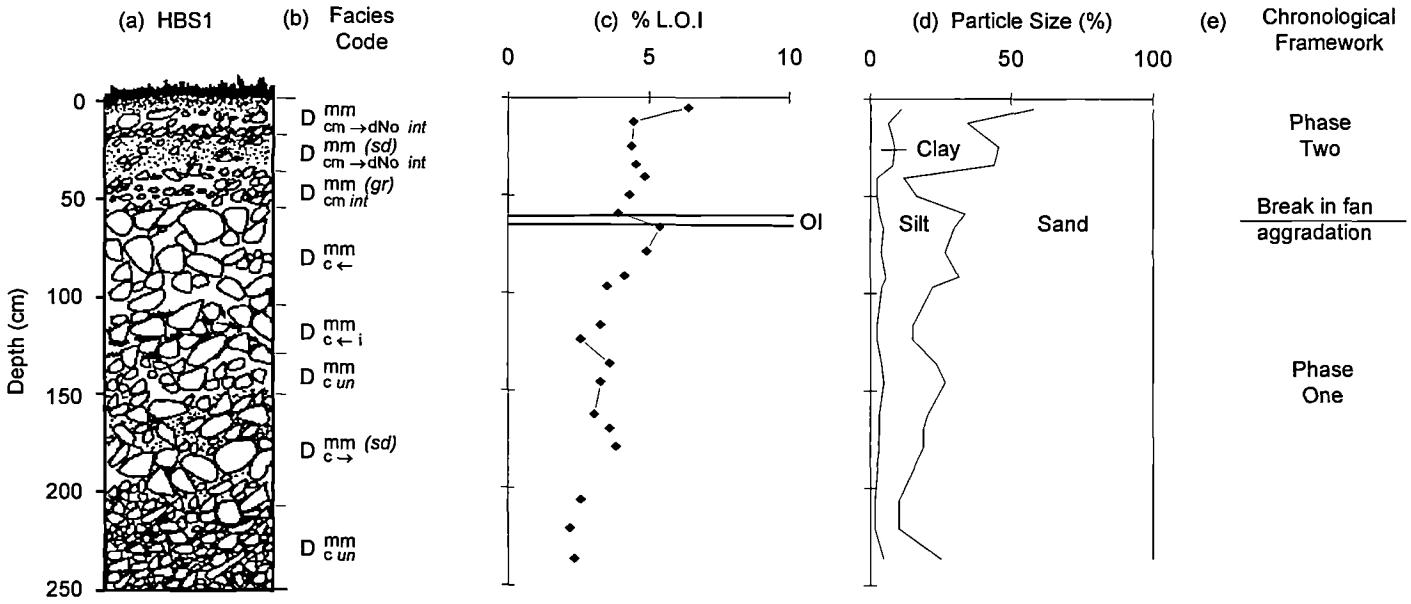


Figure 4.11. Stratigraphic log, facies code, percentage loss on ignition, grain size and the chronological framework for HBS1, Moffat. The key for the facies code is given in Table 4.1. OI : Organic inversion

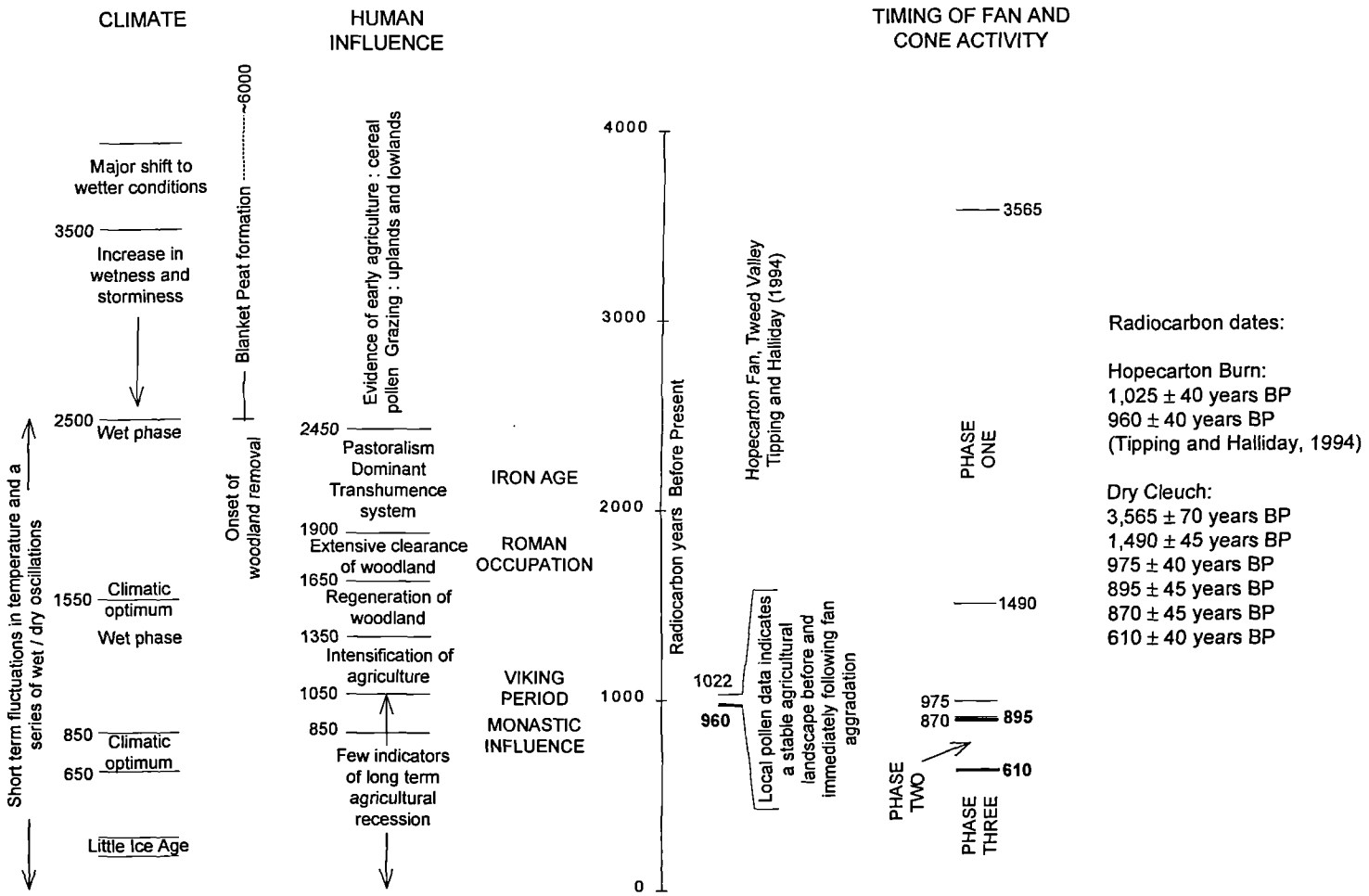


Figure 4.12. Visual correlation of the timing of cone aggradation at Dry Cleuch with local and regional patterns of change in climate and in human activity

from the Hermanlaw tributary fan, two different phases of activity have been identified (Figure 4.11e).

4.4.3 Causal development

The relationship between the timing of regional changes in climate and local human activity with the timing of phases of activity that occurred in Dry Cleuch are illustrated in Figure 4.12. Additionally, the timing of activity on a fan studied in the Tweed valley within the area is also included. Pollen data from this study directly links the timing of the event with the vegetation composition prior to and after the phase of deposition in the Hopecarton fan.

The first phase of the cone aggradation occurred at some time during the period when the landscape was undergoing a phase of woodland regeneration after Roman occupation. The area was previously an Iron Age agricultural landscape, where both arable agriculture and pastoralism have been documented. The phase of woodland regeneration is more likely to have occurred on abandoned land but some areas would have remained agriculturally active. The phase of activity also corresponds to a climatic optimum, which would have resulted in agricultural expansion in marginal areas. The second aggradational phase occurred approximately 100 years after the 10th century period of Viking settlement, which has been linked to widespread man-induced woodland clearance and intense grazing pressure (Harvey *et al.*, 1981; Harvey and Renwick, 1987). The phase also occurred just after fan aggradation in Hopecarton Fan in the Tweed Valley (Tipping and Halliday, 1994), where the pollen indicates a stable agricultural landscape both prior to and after fan incision. There is no evidence of a stark human change in vegetation composition. The third and final stage of aggradation occurred just after the climatic optimum that resulted in an agricultural expansion in marginal regions during the medieval period. Approximately 200 years previously the monastic influence of the region resulted in widespread grazing that was not restricted to lowland sites.

Each phase of cone activity can be tentatively linked to human changes and periods of increased intensity of landuse. However, as there is no direct link between the timing of activity within Dry Cleuch and site changes in vegetation,

interpretation is reliant upon comparison with the timing and character of regional changes.

4.5 Howgill Fells

4.5.1 Burnt Gill - Langdale Valley

The combined activity of two parallel gullies, similar in size and cutting into the main valley side, has formed a composite debris cone (Figure 4.13). Although the distal region of the debris cone has been incised by the main river it is obvious that the cone was deposited upon the highest river terrace and that its outward development was not impeded. The formation of the cone thus predates the development of the modern floodplain. Remnants of the terrace, which is currently being eroded by the lateral migration of the main river, are present on both sides of the cone.

The studied exposure, which extends to over 5m in height, is not fresh and the stratigraphy has been obscured by slumping and weathering. Two sections have been excavated from the exposure and reveal cone sediments in distal sediments at the furthest edges of the composite cone, BGS1 and BGS2 respectively. As a result of the close proximity of the two linear gullies, the surface form of the composite cone is complex but separate phases of activity can be identified. The most recent events have built up within the apex region of both cones and extend into each gully system (Figure 4.13). The form and size of the events suggests the periodic build up and removal of sediment from within the upper reaches of each gully. The current build up of coarse clasts stored within the downstream and upstream gully is similar in character to the sediment of the uppermost unvegetated phase of activity in both gullies.

A visual interpretation of the sequencing of events indicates that the scale and extent of each phase of activity has decreased as the cone has developed (Figure 4.13). The gully sources of the most recent and smaller scale phases can be readily assigned. However, the exact contribution from each gully to the formation of the larger and more extensive initial phases of activity is not as obvious. It is possible that sediments issuing from both gullies forming the first phase of cone aggradation could have mixed or intercalated with each other. As BGS1 is located on the far left of the debris cone, sediments within BGS1 are unlikely to have come

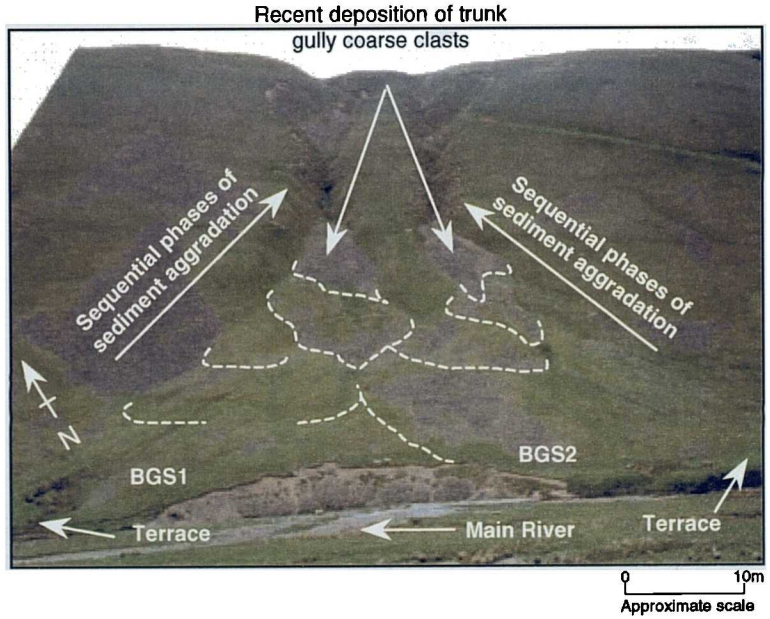


Figure 4.13. The surface features of Burnt Gill debris cone, the Howgill Fells

from the upstream gully. BGS2 is located just below the zone where events from both gullies are seen to overlap (Figure 4.13). It is possible that sediments within the section have originated in both gully systems.

The stratigraphy of the Burnt Gill cone has already been investigated by Harvey *et al.* (1981). Their investigation provides valuable information upon the timing of cone activity in association with vegetation changes that occurred at that time. BGS1 was taken as near as possible to the section location used by Harvey *et al.* (1981) in the downstream distal region of the cone. The stratigraphy closely correlates with that found by Harvey *et al.* (1981) but with some differences. The cone was resampled, including the additional section BGS2, to carry out further analysis. The palaeosol found by Harvey *et al.* (1981) is present within section BGS1 at between 178 cm and 213 cm, 137 cm above stream level (Figure 4.14). The soil horizon $BGS1_{OL}$, is deeply weathered, exhibiting characteristics typical of a podsol. A lower horizon of pale grey fine sediments is capped by a dark organic peaty layer, which in turn is capped by a grey clay layer of uniform thickness. (Figure 4.14). The loss on ignition increases from the base of the soil at 3 % to 17 % in the uppermost grey layer. The organic content for the rest of the section shows minimal fluctuation around a baseline value of 3% and thus does not provide an indicator of break in cone activity. Within the upper 8 cm the modern soil horizon, an anomalously high loss on ignition value of the 31% is obtained along with a low value of 3%. Visually the modern soil layer is very dark in colour which may be caused by a high organic content. The high value could also have resulted from the presence of modern roots incorporated within the sample.

Between 88 cm and 103 cm, the cone sediments exhibit markedly different characteristics in comparison with those above and below. The layer consists primarily of coarse clasts, uniform in size and with no matrix support. The upper and lower contacts of this layer are also sharp. The lower contact at 88 cm is abrupt, indicative of an erosive contact. The upper contact has been buried by two visually distinct cone deposits: the characteristics of both layers contrast with cone deposits found below the matrix-less layer. The erosive contact of the matrix-less layer and the visual contrast observed in the cone deposits above and below represent a break in cone sedimentation and indicate a change in sediment source.

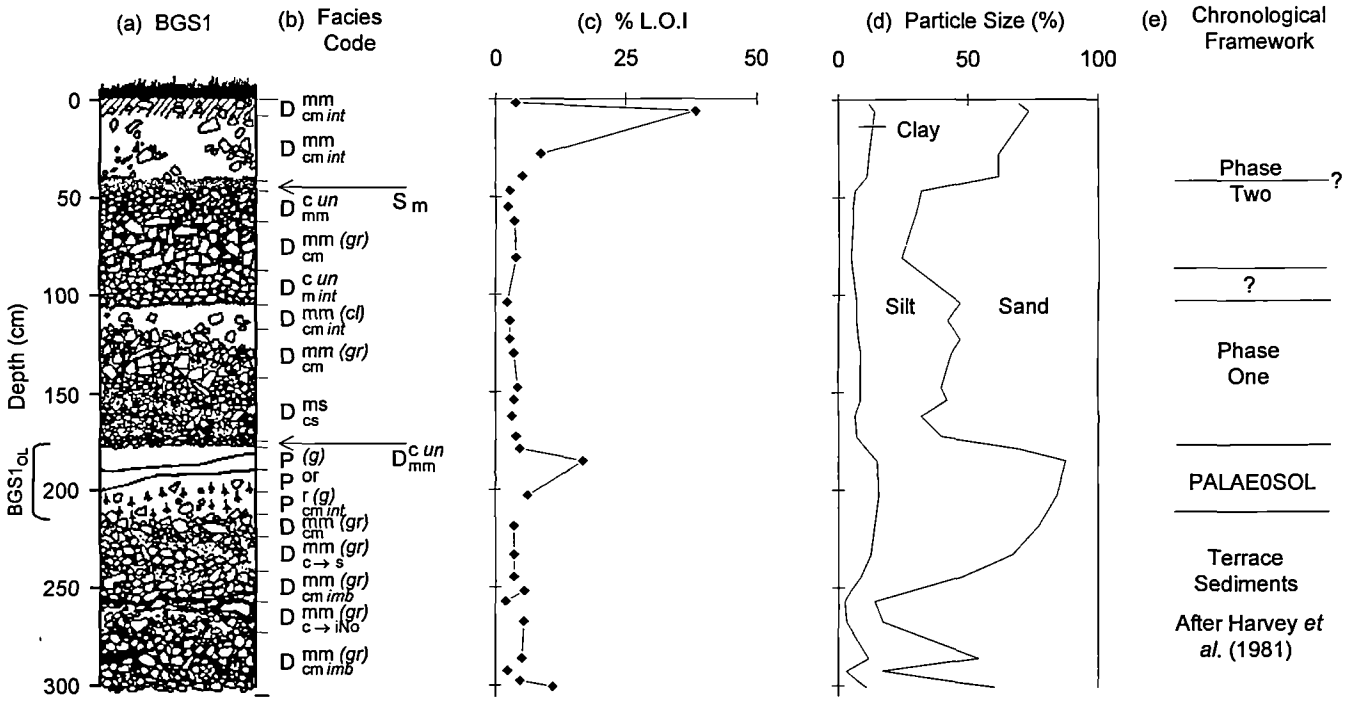


Figure 4.14. Stratigraphic log, facies code, percentage loss on ignition, grain size and the chronological framework for BGS1, the Howgill Fells. The key for the facies code is given in Table 4.1.

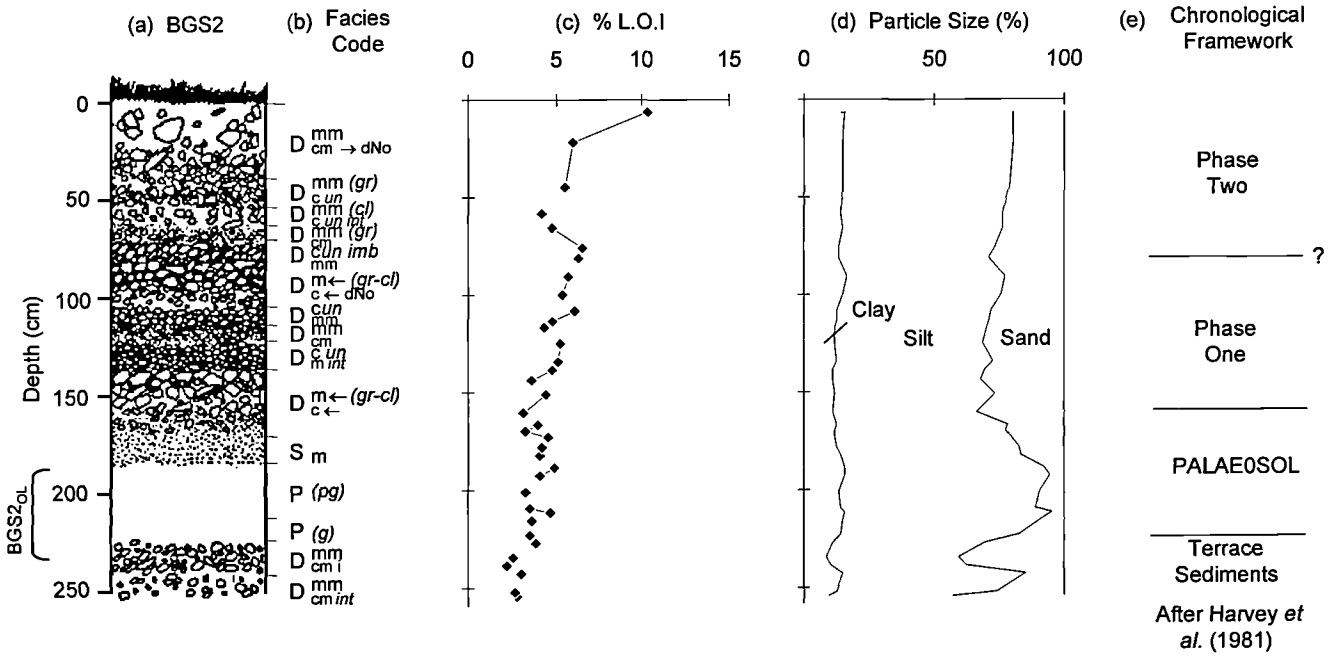


Figure 4.15. Stratigraphic log, facies code, percentage loss on ignition, grain size and the chronological framework for BGS2, the Howgill Fells. The key for the facies code is given in Table 4.1.

The palaeosol $BGS2_{OL}$ present in BGS2 between 185 cm and 223 cm, does not exhibit the same characteristics as $BGS1_{OL}$ (Figure 4.15). The dark peaty layer is absent and loss on ignition values for the soil are indistinguishable from the layers above and below. The low loss on ignition values and gleyed characteristics point towards formation in a waterlogged environment, with organic material being lost by solution. The lowest loss on ignition values are found in the sediments immediately below $BGS2_{OL}$. The sediments that cap the palaeosol indicate a fluctuating increase with the greatest increase occurring in the top 9 cm. One major fluctuation within the cone sediments at 70 cm, where loss on ignition values decrease by 2% and then continue to increase, corresponds with a marked change in the visual characteristics of the sediments. The change observed in loss on ignition at this depth is also mirrored in the particle size characteristics of the section. Even though loss on ignition values do not vary significantly within the diamict of both sections, the visual properties and particle size change with depth. The greatest difference is found in the comparison of the diamicts above and below both palaeosols. Harvey *et al.* (1981) have argued that cone deposits debouch directly onto a former river terrace but the observed properties and particle size are not distinguishable from above or below the palaeosol. If sediments below the palaeosol represent river terraces sediments, their origin will be reflected in the sorting characteristics of the sediment.

Harvey *et al.* (1981) dated organic material taken from the lower and upper parts of the palaeosol. The palaeosol was formed over approximately 1,800 years between *c.* 2580 ± 55 years BP (UB-2212) and *c.* 940 ± 95 years BP (UB-2213). The latter indicates the onset of cone aggradation for the downstream edge of the cone deposit. The characteristics of palaeosol formed within river terrace sediments does differ between the two sections. In section BGS2 the palaeosol varies in form, organic content, and height above stream level. The two sections are over thirty meters apart. It is possible that within that distance environmental conditions for soil development could have varied sufficiently to produce the different characteristics exhibited by the two palaeosols. It can be argued that even though the character of the soil profiles do vary between sections, the development history of the cone is the same. Soil formation ceased at around *c.* 940 ± 95σ 1 yr. BP (UB-2213) when it was buried by cone sediments. Within both sections the potential exists for two phases of activity in the accumulation of cone sediments above the palaeosol.

Unfortunately, the timing of the two phases of activity is not known and cannot be obtained using conventional dating methods.

4.5.2 Nevy Gill - Langdale Valley

A large tributary fan has formed as a result of the combined activity of Little Nevy Gill and Great Nevy Gill, adjoining tributary valleys. The Nevy Gill alluvial fan extends over most of the valley floor which is 30 to 40m wide at this point. The alluvial fan has two major fan terraces Figure 4.16). A few remnants of the upper terrace remain, mainly on the right hand side of the fan. The second terrace has the largest extent. A large number of former channels are evident on its surface. The trunk stream at this stage of its development migrated over most of the second terrace's surface. The second terrace was than abandoned and the trunk stream incised to its current entrenched position. The modern floodplain has formed within the confines of the entrenched channel. The main river has been blocked by the alluvial fan and is constrained in its current position (Figure 4.16). The main river is incising the outermost edge of the alluvial fan in its distal region and has exposed a 5 m long section of sediments of the oldest and highest fan terrace. It is from this exposure that a section has been taken, NGS1 (Figure 4.16). The remainder of the fan sediments are vegetated and inaccessible, even along the fan's entrenched trunk stream.

The most obvious characteristic of the fan is the lateral migration of its trunk stream system, both in the past and in the current development of the trunk stream's modern floodplain. Sediments within the alluvial fan have been reworked as the trunk stream has migrated. The fan debouches directly onto the valley floor. There is no evidence for the deposition of the fan upon former river terraces as at Burnt Gill. On the northern edge of the fan no river terraces are evident. At some point the southern edge of the fan has been incised by the main river when it previously occupied that position. The outward growth of fan downstream has been restricted by the valley side, which extends some distance along the northern outside edge. Where the fan does reach the valley floor it appears that fan sediments grade into a low river terrace.

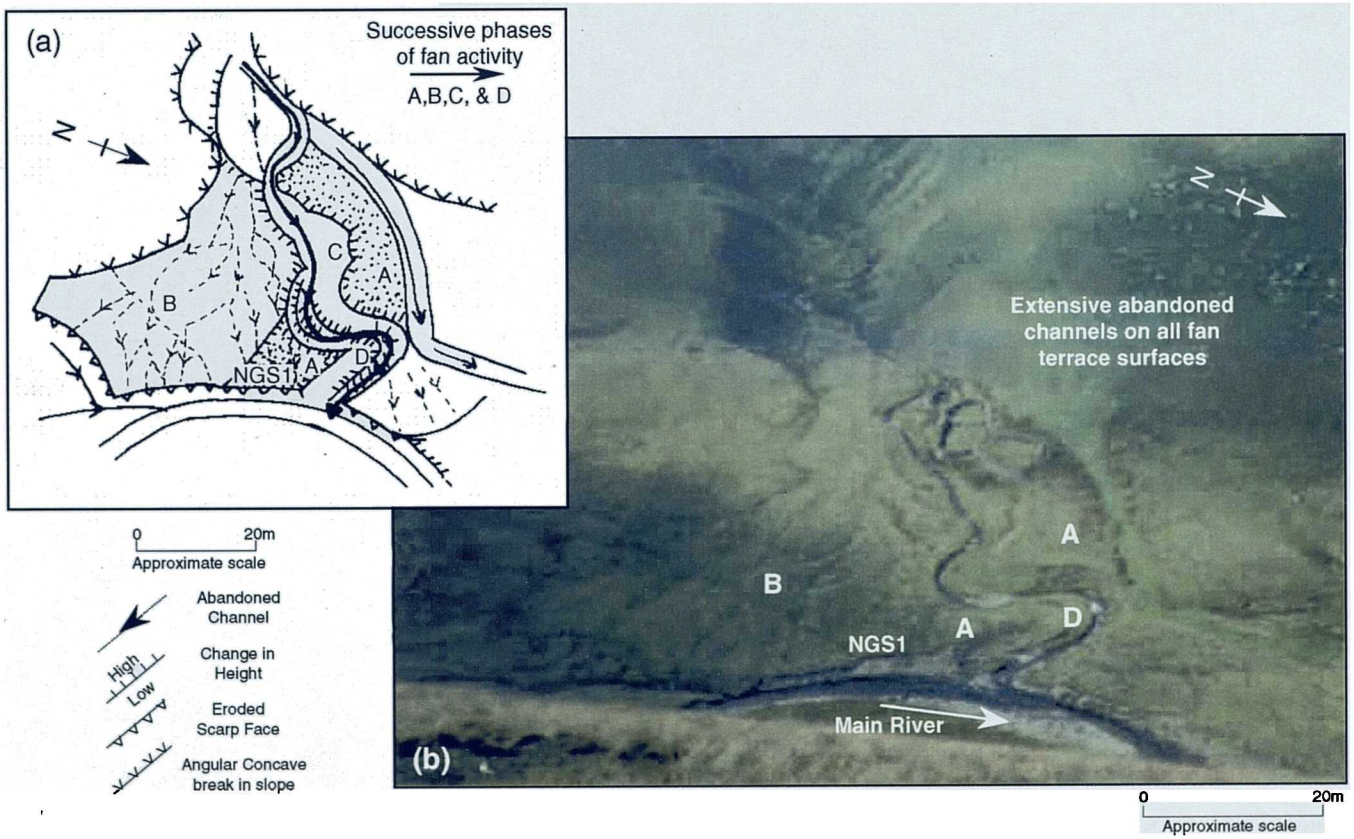


Figure 4.16. The surface features of Nevy Gill fan, the Howgill Fells. (a) A planform schematic of surface features.

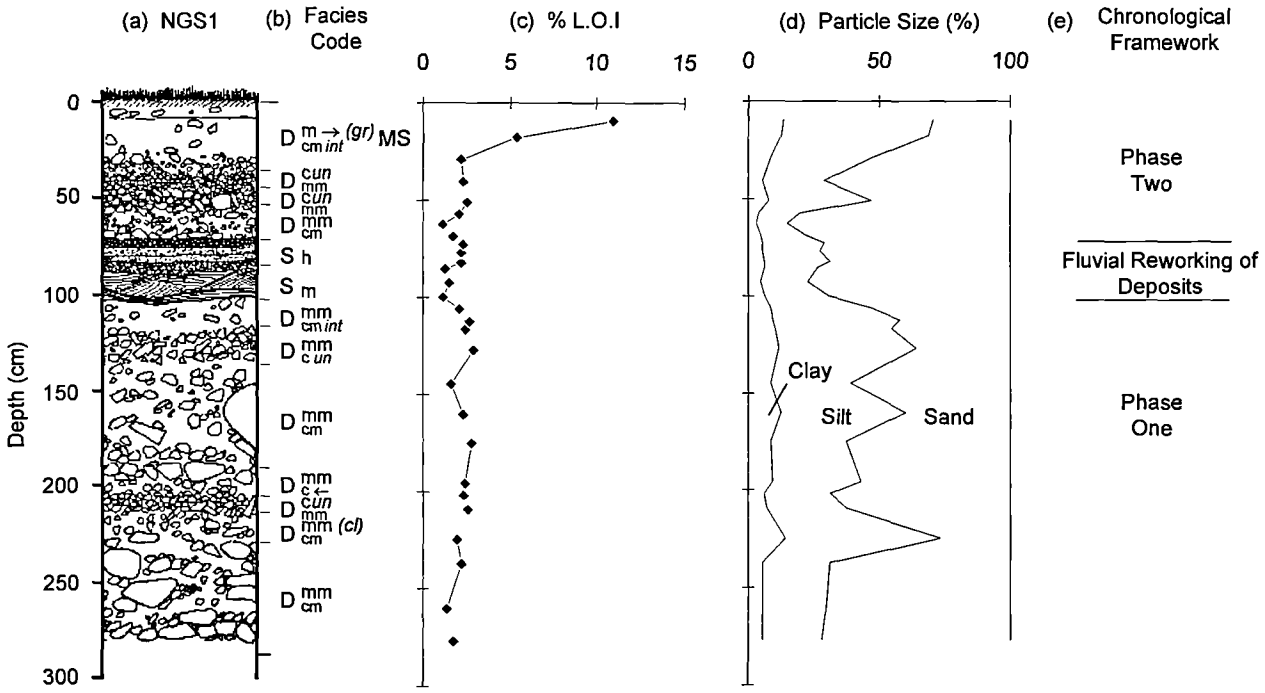


Figure 4.17. Stratigraphic log, facies code, percentage loss on ignition, grain size and the chronological framework for NGS1, the Howgill Fells. The key for the facies code is given in Table 4.1.

Within NGS1 there is no visual evidence of organic material that has developed *in situ* or transported within the fan sediments (Figure 4.17). As expected, loss on ignition increases within the top 20 cm as part of the modern soil horizon. For the rest of the section loss on ignition fluctuates around an average value of 4% to 5%. The section can be split into two based upon marked changes in the visual and particle size characteristics of the fan sediments. At 104 cm depth, sediments change from a poorly sorted admixture of clast and matrix sediments to clearly defined structured sediments that have been cross-bedded, stratified and layered. The processes that resulted in that type of sorting are associated with the lateral migration and reworking of a channel bed. The second change occurs at 74 cm. The stratified layers are capped by poorly sorted sediments, characteristic of the bottom-most sediments, suggesting a continuation of fan aggradation.

The sediments within NGS1 relate to the first phase of fan development, and the oldest fan deposits. From section analysis it is evident that the profile can be split into three separate phases. The first phase involved the aggradation of fan sediments. All contact between identified layers within this phase are diffuse and are not suggestive of erosive contacts. At some point the trunk stream migrated laterally, instigating the second phase of activity. As the stream migrated it potentially eroded the uppermost sediments of the previously aggraded sediments, reworking them and re-depositing them. The channel sediments were then capped by the continuation of fan aggradation. There was no organic material available for dating within NGS1 and the actual timing of activity is therefore unknown.

4.5.3 Thickcombs Gill - Bowderdale Valley

A combination of non-linear gullies have formed a debris cone with two separated periods of activity. The initial stages of the cone development have been stranded on a bluff after a marked period of incision by the main river. The remaining cone sediments have been deposited on the main valley floor. The cone sediments preserved on the valley side bluff have undergone incision and a series of channels dissect the cone's surface. The timing of incision appears to have occurred after its abandonment as the surface channel dissects into the valley side bluff (Figure 4.18). The sediments deposited directly onto the lowered main valley floor constitute the bulk of the cone. Most of the cone sediments have since been eroded by the lateral

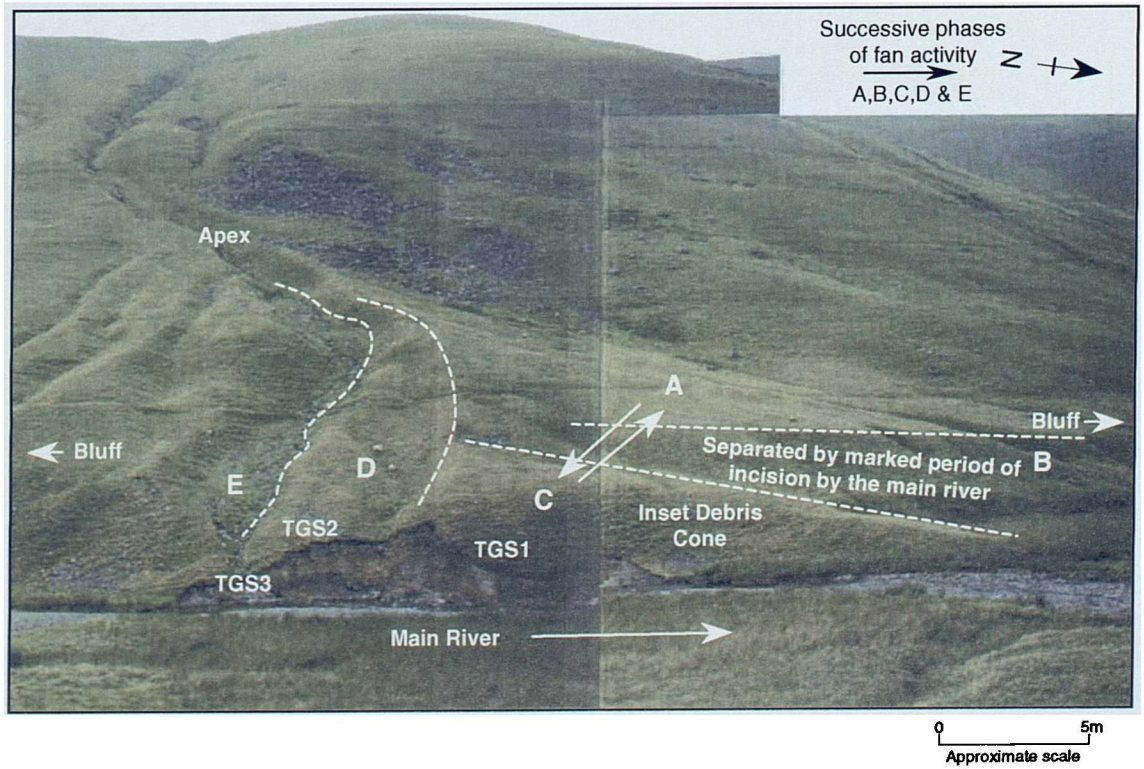


Figure 4.18. The surface features of Thickcombs Gill debris cone, the Howgill Fells

migration of the main river. There are no remnants of river terraces on either side of the feature. The separate phases that have resulted in the cones current form are illustrated in Figure 4.18. After the period of deposition on the main valley floor, a period of incision removed the cone sediments along its medial axis. The resulting channel was then infilled as the cone aggraded and the trunk stream incised to its current position.

At some point, erosion by the main river has removed most of the cone distal deposits. The exposure stabilised and became vegetated as the river migrated away to the opposite side of the valley. The cone sediments are currently undergoing a renewed phase of erosion and a large section of cone sediments have been exposed. Three sections have been investigated. TGS1 is directly below sediments that relate to the initial aggradation of the cone on the valley floor. TGS2 was excavated 6 m upstream within cone sediments that are inside the boundaries of the channel thought to have been subsequently infilled. Sediments relating to the current trunk stream TGS3, have also been exposed. The section is only 0.5 m in depth. The sediments relate to the last phase of activity within the cone but is possible that deposits of debris flows within the channel have been reworked and sorted by stream-flow in the trunk channel.

Diamict sediment in TGS1 is separated by a palaeosol 28 cm in thickness, 151 cm above stream level (Figure 4.19). The palaeosol $TGS1_{OL}$ is uniform in character, pale grey with iron-staining around rootlets. The characteristics are found in soils that have developed in waterlogged conditions. The loss on ignition values for the palaeosol are high, between 6% and 13%. Values for the palaeosol are much higher than the values for sediments above and below it. Cone sediments are in sharp contact with the top of the palaeosol. The origin of the deposits within which the palaeosol has developed is questionable. Loss on ignition does not differ in comparison to the sediments that cap the palaeosol. Particle size characteristics do. The matrix material of the lower sediments is predominantly made up of fines, with limited contribution from the > 212 μm fractions. Within the sediments above the palaeosol the total sand fraction is much higher. The characteristics of particle size fractionation for sediments above and below the palaeosol are similar, suggesting deposition by one type of process. At the moment there is nothing to suggest that the bottom-most sediments are river terrace and not cone deposits.

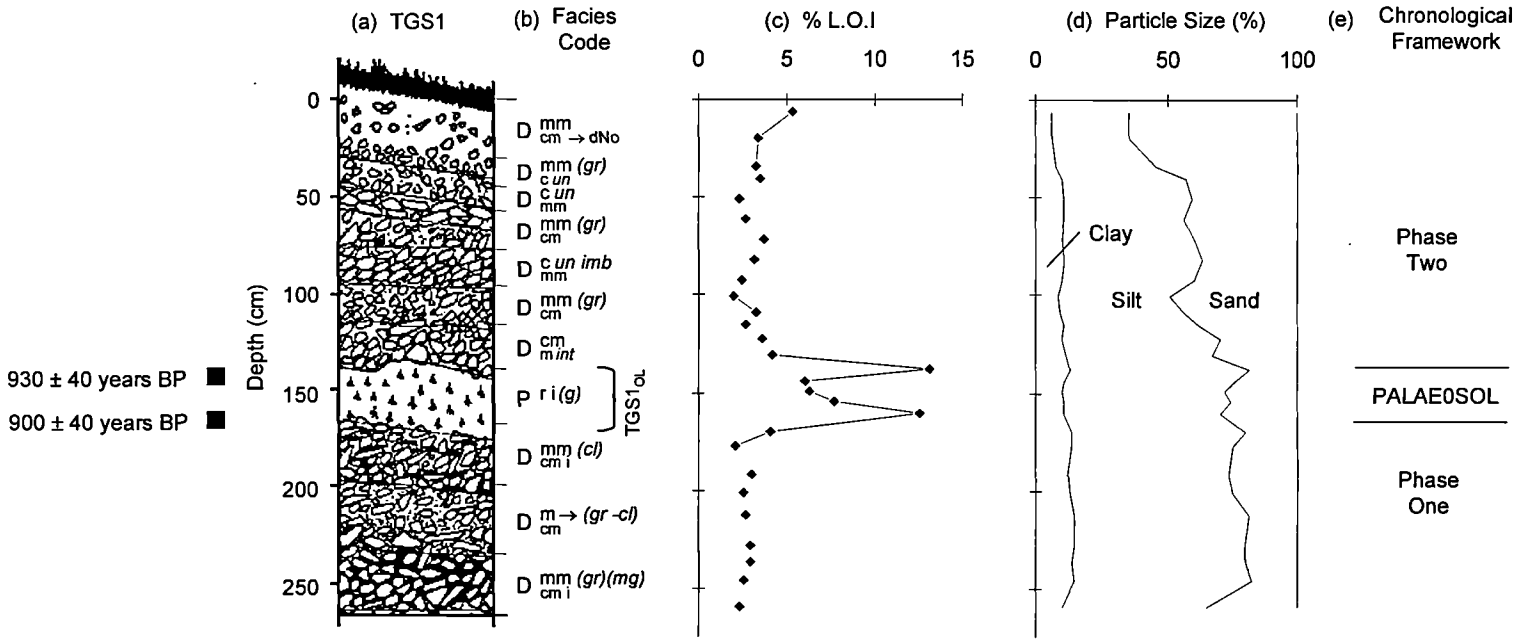


Figure 4.19. Radiocarbon dates, stratigraphic log, facies code, percentage loss on ignition, grain size and the chronological framework for TGS1, the Howgill Fells. The key for the facies code is given in Table 4.1.

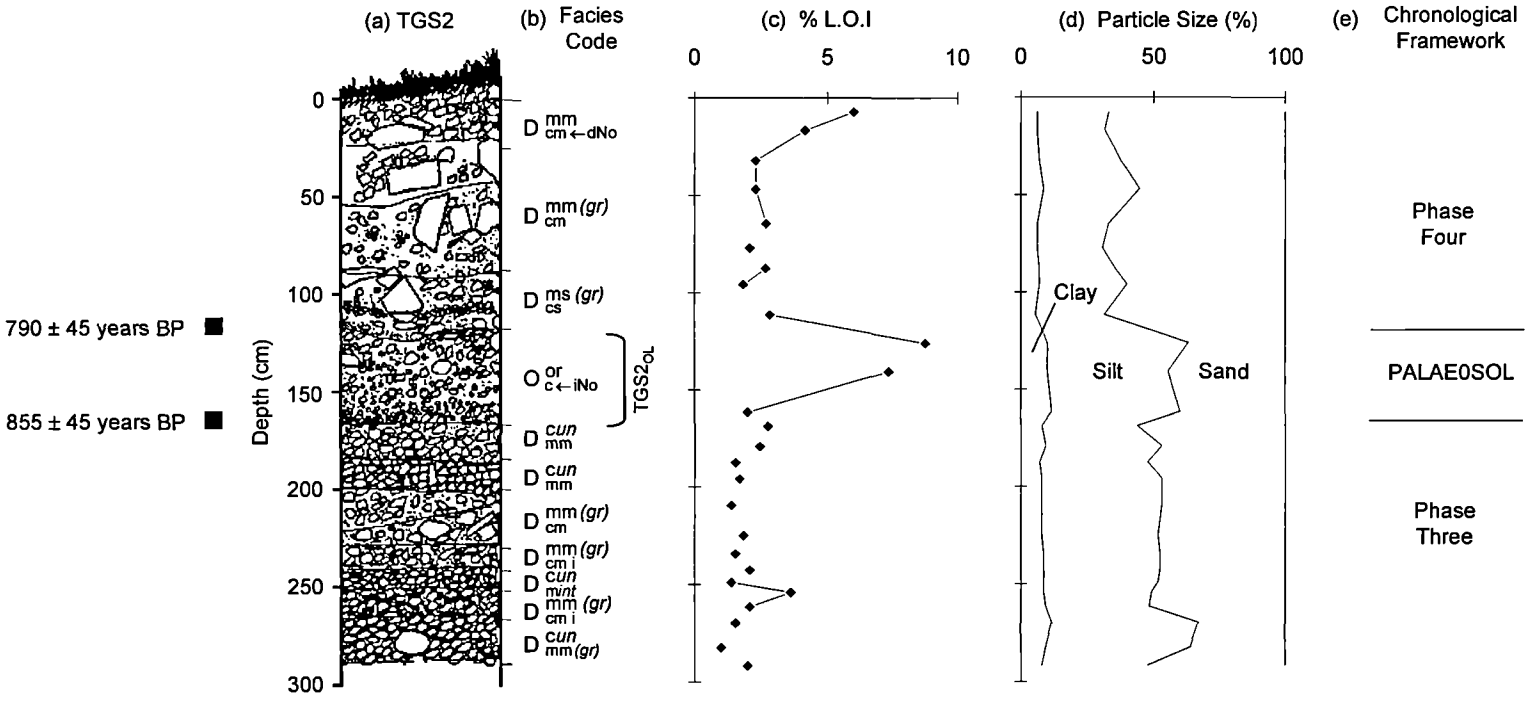


Figure 4.20. Radiocarbon dates, stratigraphic log, facies code, percentage loss on ignition, grain size and the chronological framework for TGS2, the Howgill Fells. The key for the facies code is given in Table 4.1.

A similar situation exists in TGS2. A palaeosol has developed mid-way in the section at between 117 cm and 166 cm (Figure 4.20). $TGS2_{OL}$ is 50 cm thick and has formed 230 cm above stream level. The characteristics of the palaeosol contrast with the palaeosol in TGS1. The organic content is lower, the palaeosol contains clasts and the characteristics are indicative of a soil that has developed within a free-draining environment. There is no evidence of transported organic debris within the palaeosol horizon. The organic content of the palaeosol is only 4% to 5% higher than the sediments above and below it and only slightly higher than the organic content of the modern soil layer at 25 cm. The sediments above and below the palaeosol differ visually. The sediments that cap the soil horizon have a higher sand content but the degree of fractionation is mirrored in the sediments below the palaeosol. The height of the palaeosol above stream level, the presence of clasts within the soil and the lack of organic debris implies that the soil formed within cone sediments. If this is the case, the palaeosol represents a break in the activity within the cone system.

TGS3 has a modern soil which is very shallow. Loss on ignition values and particle size characters are uniform within the 50 cm section

Radiocarbon dates have been obtained from both palaeosols. The dates obtained for $TGS1_{OL}$ are identical within 1 standard deviation. The date taken from the bottom of the palaeosol may have been contaminated by the translocation of younger carbon from above and the palaeosol does contain the remains of plant roots. The uppermost date, taken directly below the contact with the capping cone deposits at 930 ± 40 years BP, is statistically the same as the date of 940 ± 95 years BP obtained for the palaeosol at Burnt Gill (Harvey *et al.*, 1981). The date is reasonable, considering that Thickcombs Gill and Burnt Gill are directly opposite each other either side of the watershed boundary between Langdale and Bowderdale.

In TGS2 soil formation ceased at 790 ± 45 years BP. The soil profile characteristics of the soil indicate it is immature, the date of organic material sampled from the base of the soil is therefore unlikely to have been markedly

affected by the translocation of younger carbon from above. The formation of the soil is constrained between 855 ± 45 years BP and 790 ± 45 years BP.

The timing of the formation of sediments of the trunk stream in section TGS3 is not discernible but based upon a visual interpretation occurred after the accumulation of the uppermost sediments in TGS2.

The characteristics of the palaeosol in TGS1 and Burnt Gill (Harvey *et al.*, 1981) are comparable, suggesting similar environmental conditions experienced during their development. If the date for TGS1 is to be accepted, the timing of cone activity or accumulation began at 930 ± 40 years BP in this part of the cone. The parent material for the soil could be either river terrace or debris cone deposits. After the accumulation of cone gravels within section TGS1, sediments aggraded in TGS2 to form the lower part of the section prior to 855 ± 45 years BP (Figure 4.19e). If sediments in TGS2 had formed entirely separate to sediments in TGS1, which is suggested from a visual interpretation of the cone's form (Figure 4.18), the phase of aggradation must have occurred between 930 ± 40 and 855 ± 45 years BP. The uppermost sediments of TGS2 were then deposited at 790 ± 45 years BP (Figure 4.20e). The trunk stream then incised to its current position potentially reworking the sediments deposited at around 790 ± 45 years BP or earlier.

4.5.4 Leath Gill - Bowderdale Valley

The fan deposits of the gully tributary Leath Gill again indicate the distinctive isolated phases of activity separated by the lowering of the valley floor by main river incision (Figure 4.21). The first phase has been abandoned on the valley side bluff, whilst the next phase has been deposited directly on the current valley floor. It extends to cover most of the valley floor and has buried numerous palaeochannels. No terraces are evident on either side of the fan. Any remnants of former river terraces have been removed by the migration of the main river within the confines of the narrow valley floor. The fan deposits have forced the main river to maintain a narrow corridor on the opposite side of the valley floor. Following the deposition of the fan on the valley floor the trunk stream has since incised the fan and is currently entrenched on its northern edge. In the previously discussed 1982 storm, Wells and Harvey (1987) recorded the deposition of fresh deposits on the fan surface.

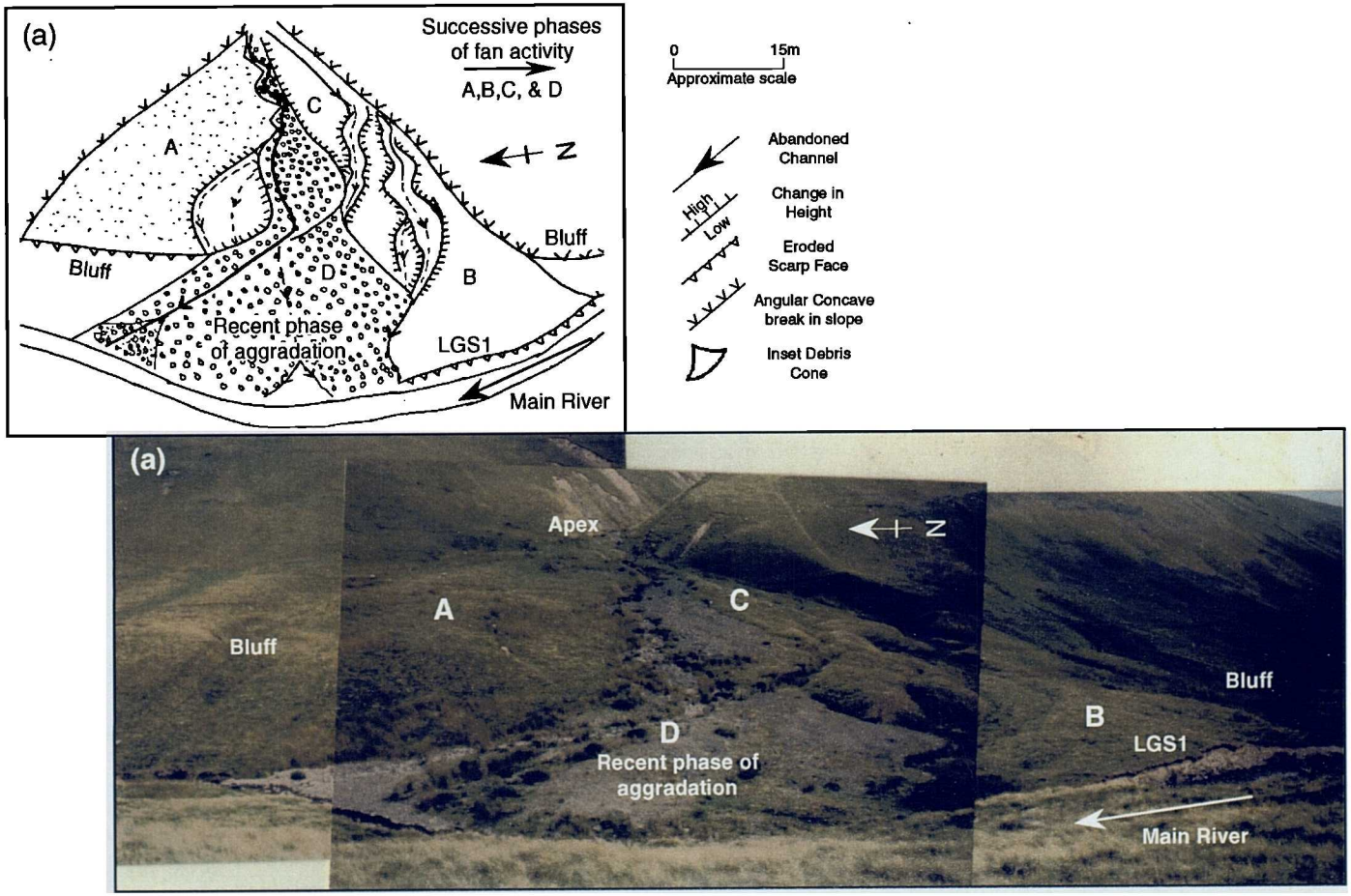


Figure 4.21. The surface features of Leath Gill fan, the Howgill Fells. (a) A planform schematic of surface features.

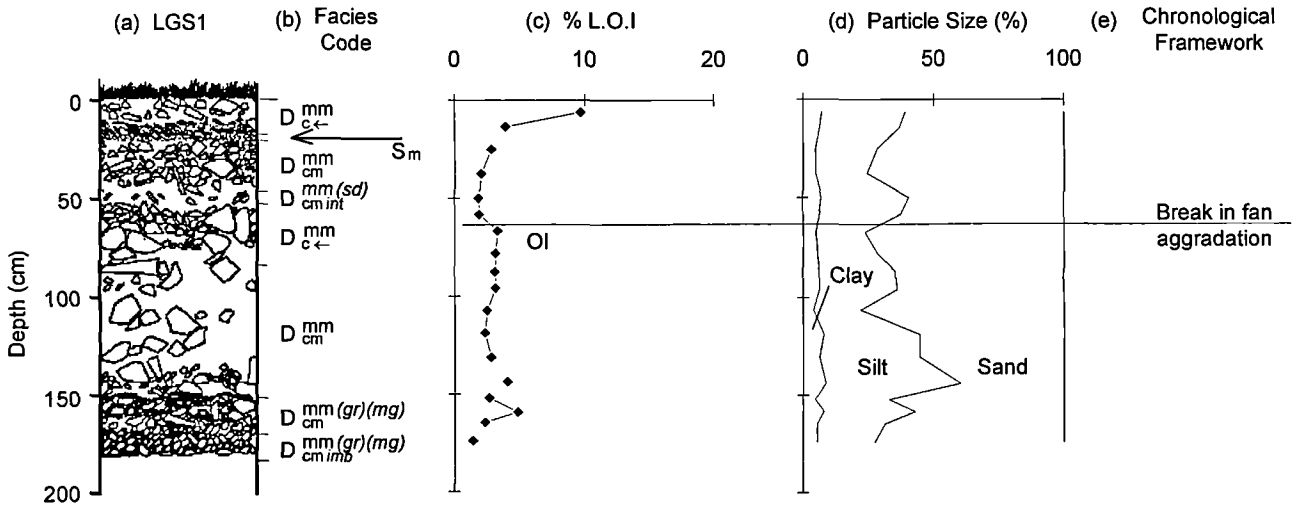


Figure 4.22. Stratigraphic log, facies code, percentage loss on ignition, grain size and the chronological framework for LGS1, the Howgill Fells. The key for the facies code is given in Table 4.1. OI : Organic inversion

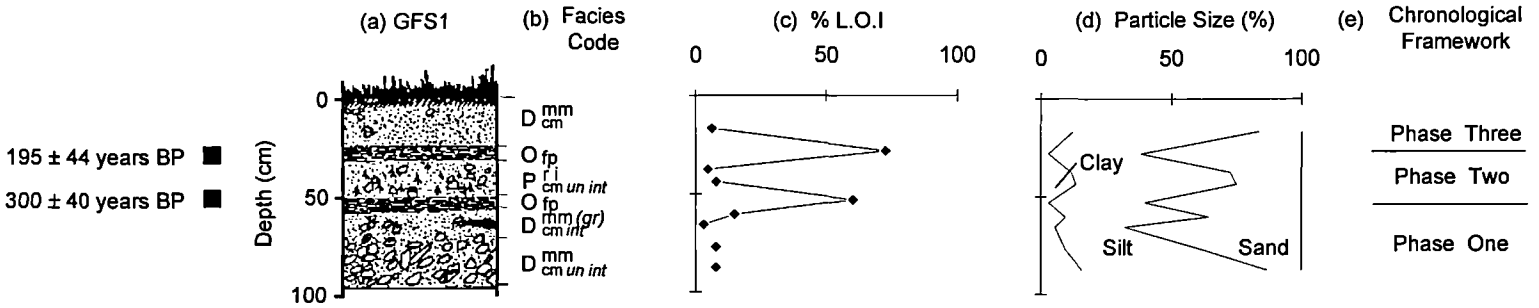


Figure 4.23. Radiocarbon dates, stratigraphic log, facies code, percentage loss on ignition, grain size and the chronological framework for GFS1, the Howgill Fells. The key for the facies code is given in Table 4.1.

Deposition was localised and sediments were shunted along the entrenched channel system. Only in the distal region of the fan, where the trunk stream joins the main river, has sediment been deposited on the vegetated surface of the fan. The main river is currently incising the southern distal region of the vegetated fan deposits (Figure 4.21).

The section LGS1, which extends to stream level, consists entirely of fan sediments with no obvious breaks in cone activity (Figure 4.22), although the visual properties of the section do change between 53 cm and 84 cm depth. At this vertical depth the clast content increases and becomes more uniform in size. The visual change is also coincident with a significant decrease in organic content. After a gradual increase in organic content, loss on ignition sharply decreases and then continues to increase up to the modern soil horizon, forming an organic inversion. It is possible that this represents a break in fan activity, where the initial stages of soil formation have been capped by a later phase of activity.

It is evident that sediments within LGS1 relate to the distal deposits of the second aggradational phase of development onto the main valley floor. As fan sediments have not been deposited directly onto a river terrace surface and no soils have developed *in situ*, the timing of activity is difficult to determine. Only the sequential development of the feature can be established from its form. Within the section taken from the Leath Gill fan two potentially different phases of activity have been identified (Figure 4.22e).

4.5.5 Gully Fan - Bowderdale Valley

The gully fan is very small in comparison to the other features investigated. Its supplying gully is shallow and bedrock is not visible within its channel. The fan debouches directly onto a river terrace, which is currently being eroded by the main river exposing fan sediments. The fan is uniform in shape and size and has a classic concave profile. There is no evidence of incision on the fan surface. Main river incision has caused the sediments to slump, exposing the uppermost part of the fan. The remaining sediments are obscured by the slumped material. One section has been taken within the fan sediments near the apex. The section is only 95 cm in depth but within this depth five distinct layers are evident (Figure 4.23). Two sharply

defined, peaty organic layers are separated by pale grey horizons. Both organic layers are of uniform thickness. It is possible that the material may have been deposited but peaty material is light and is often removed during transportation. Due to its uniform thickness and lateral extent in the exposure it is more likely to have developed *in situ*.

Radiocarbon dates have been taken from the uppermost part from each peat layer and are stratigraphically consistent. The two dates provide the timing of a phase of development of peat as well as providing the timing of fan activity. Peat formation was stopped at approximately 300 ± 40 years BP and 195 ± 40 years BP by deposition of two layers of fine material. As the upper contact is sharp it is possible that the upper levels of peat could have been stripped as each sediment layer was laid down. The two sediment layers sandwiched between the peat have no internal structure and their visual properties do not change. The contextual framework of development is illustrated in Figure 4.23e.

4.5.6 Causal development

The study by Harvey *et al.* (1981) provides a direct link between the timing of activity within Burnt Gill and local changes in vegetation composition (Figure 4.24). A partially forested landscape dominated by an Alder-Carr community changes to heath species and *Plantago* indicative of disturbed ground. The change occurs within the top few centimetres of the palaeosol preserved within the fan. Harvey *et al.* (1981) correlate the onset of cone aggradation and burial of the palaeosol with the introduction of Scandinavian sheep farming after 1050 yr. BP (Tenth Century).

Due to the close link in time between the initial formation of Burnt Gill and Thickcombs Gill and their close proximity either side of the watershed boundary, the two cones may have formed in response to the same storm event. It is also fair to assume that the change in vegetation that occurred at the time of soil formation is applicable to the development of Thickcombs Gill. In addition alluvial fans in the Hodder River system in the Bowland Fells were also active in this time period (Harvey and Renwick, 1987).

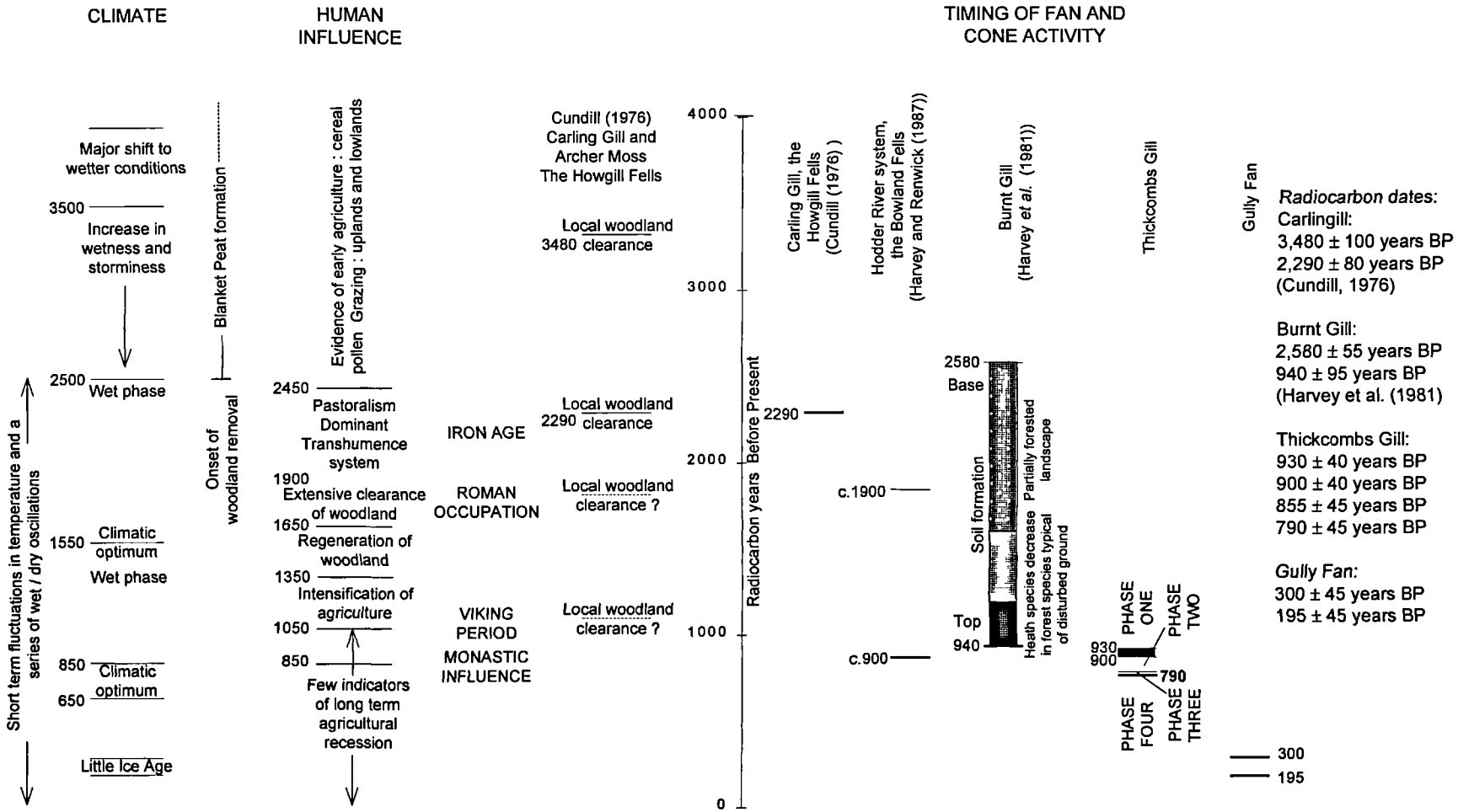


Figure 4.24. Visual correlation of the timing of cone aggradation at Burnt Gill, Thickcombs Gill and Gully Fan, with local and regional patterns of change in climate and in human activity

A second palaeosol preserved in Thickcombs Gill provides a date for the last aggradational phase in the cone. The timing of aggradation corresponds with the introduction of Monastic sheep farming practices in the Howgill Fells. The climate at that time was relatively warm, resulting in the increased use of marginal areas such as the inaccessible valleys of the Howgill Fells. Intensive sheep grazing at that time and since has constrained the vegetation composition to consist almost entirely of grasses and heather. Grazing pressure is indicted as the cause of the reactivation of a large number of relict gully systems in the Howgill Fells (Harvey, 1986).

Most of the large-scale fans and cones within the two valleys exhibit similar sequencing of development. After a marked period of river incision, which formed a number of terraces within the valley floor, a second and more extensive phase of activity capped river terraces, where the valley floor width allowed their preferential preservation. Where remnants of former river terraces have been removed, cone and fan sediments bury palaeochannels preserved within the modern floodplain. A tentative link can be made about the timing of their development. The correlation in size and surface characteristics and sequential development suggests similar conditions existed during their development.

The timing of two phases of activity evident within exposed sediments of the gully fan, a small scale feature, can be tentatively linked to the timing of the onset and cessation of the Little Ice Age (Figure 4.24). The Little Ice Age is characterised by worsening climatic conditions, temperatures decreased in association with a change in seasonality (Lamb, 1977; Bradley and Jones, 1993). Peat was formed at this time and was truncated by the intercalated deposition of minerogenic deposition of slope sediments triggered by a combination of climatic controls and a high intensity of sheep grazing. The Howgill Fells at this time was common ground and was predominantly used for sheep farming.

Although the study by Harvey *et al.* (1981) provides a direct link between cone aggradation and vegetation change, the causal link is based purely upon a correlation of the timing of activity with the onset of Scandinavian settlement expansion. The younger dated phase of cone aggradation in Thickcombs Gill can be tentatively associated with a marked increase in grazing pressure caused by the introduction of Monastic farming practices. The onset of cone aggradation has

strong indirect causal links with historical agricultural practices but, the importance of extreme storm events with a long return period needs to be considered.

4.6 Northern Pennines - Langden Beck

4.6.1 Harthope Beck

The alluvial fan that issues from Harthope Beck is extensive in form and is deposited where the valley width decreases. The fan extends over most of the valley floor width, especially where valley floor width narrows (Figure 4.25). Downstream fan deposits have constrained the main river to a narrow corridor along its distal extent. The main river is currently eroding into distal deposits of the eastern edge of the fan, exposing a sedimentary sequence to stream level. The upper surface of the fan is uniform but an extensive area in the medial region has been incised by the sequential entrenchment of the fan trunk stream. The modern floodplain of the trunk stream and two terraces have been formed within the entrenched system (Figure 4.25). At the apex of the fan, sediments up to the height of the first terrace have been exposed. Fan sediments relating to the second terrace have also been exposed by trunk stream incision.

The effects of a recent peat slide within the sub-catchment of are evident on the fan surface. A large amount of coarse sediment eroded from the side gullies and from within the main gully were transported along the trunk stream system. The material was shunted along the channel system, changing the former channel position. A gravel splay at the mouth of the trunk stream and blocks of peat are found all over the fan surface. There is no evidence that the fan has been deposited upon a former terrace. The distal upstream deposits of the fan have been previously eroded to form a bluff. The river has since changed its position and the exposure has become vegetated. A high river terrace is located down-stream. Deposits of the down-stream edge of the fan may bury this terrace and sediments appear to grade into the terrace surface. The sedimentary characteristics of the river terrace, exposed by main river incision, differ markedly from the sediments revealed in the section which exposes fan deposits. The river terrace may have therefore formed after the deposition of the fan.

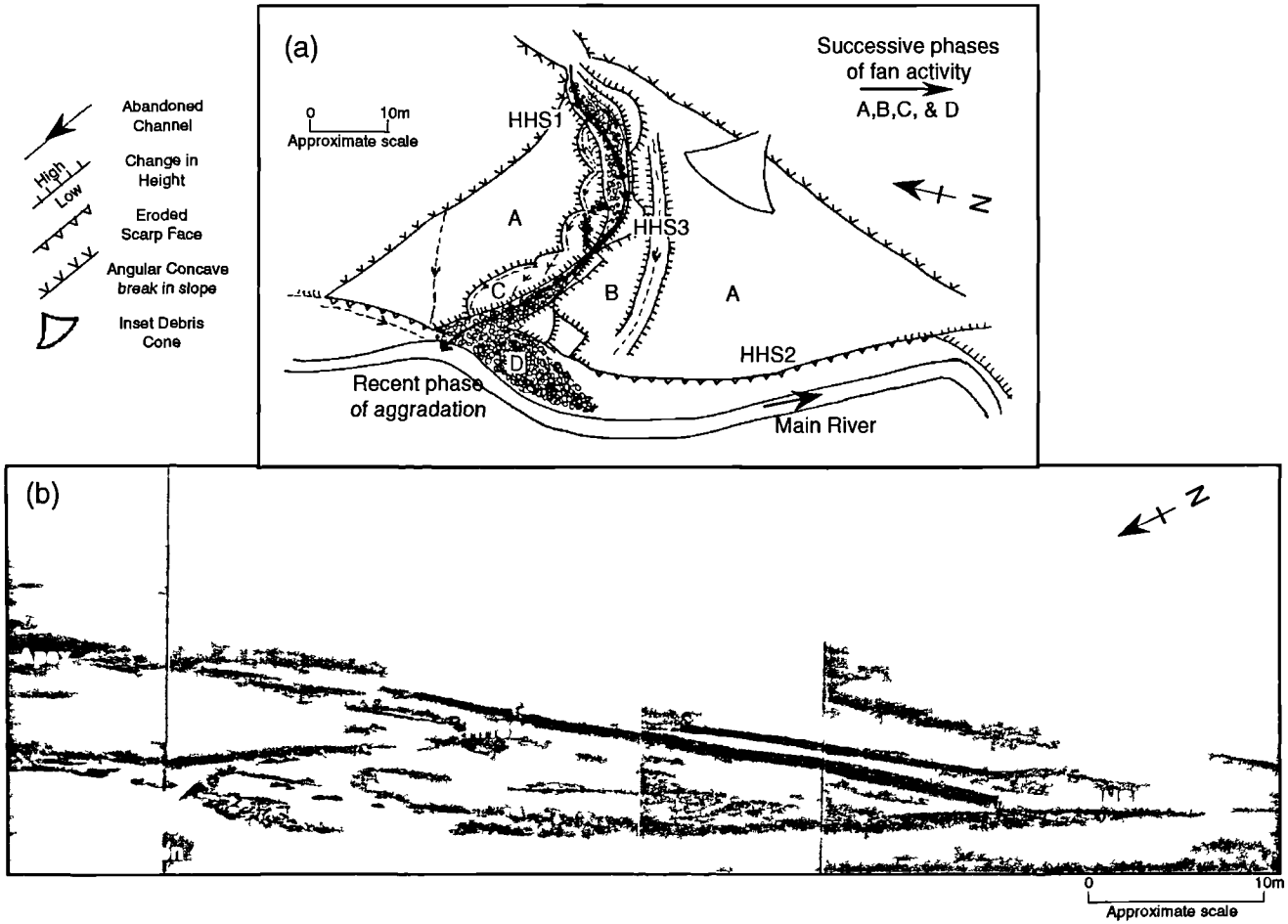


Figure 4.25. The surface features of Harthope Beck fan, Langden Beck. (a) A planform schematic of surface features.

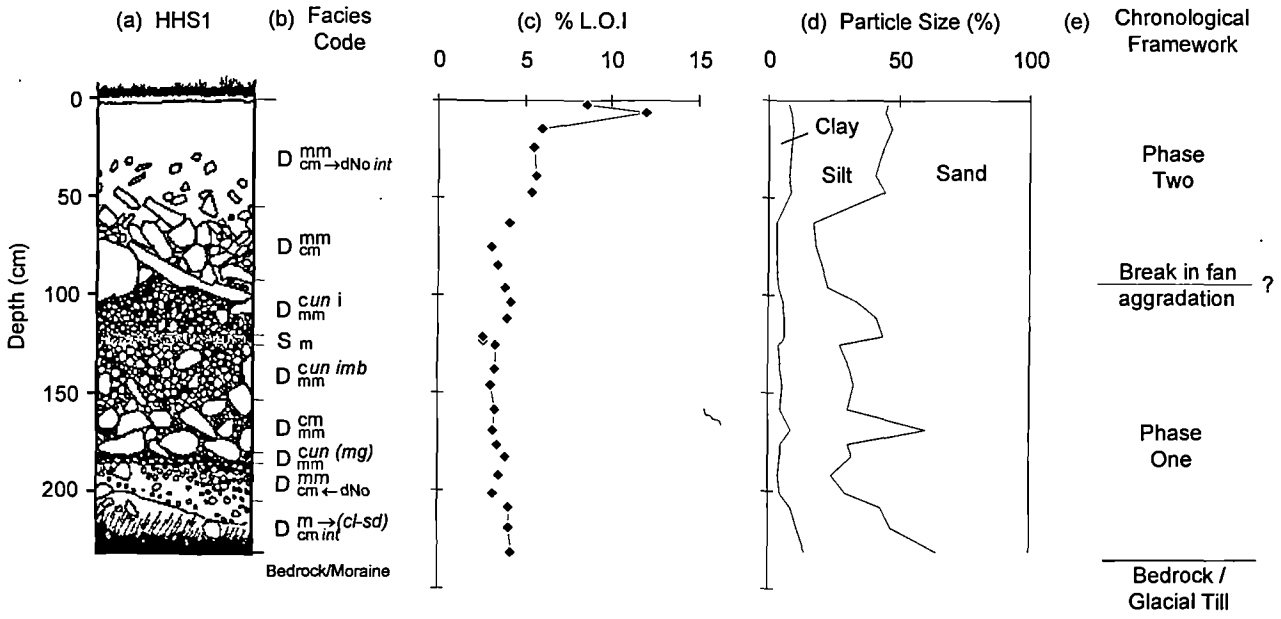


Figure 4.26. Stratigraphic log, facies code, percentage loss on ignition, grain size and the chronological framework for HHS1, Langden Beck. The key for the facies code is given in Table 4.1.

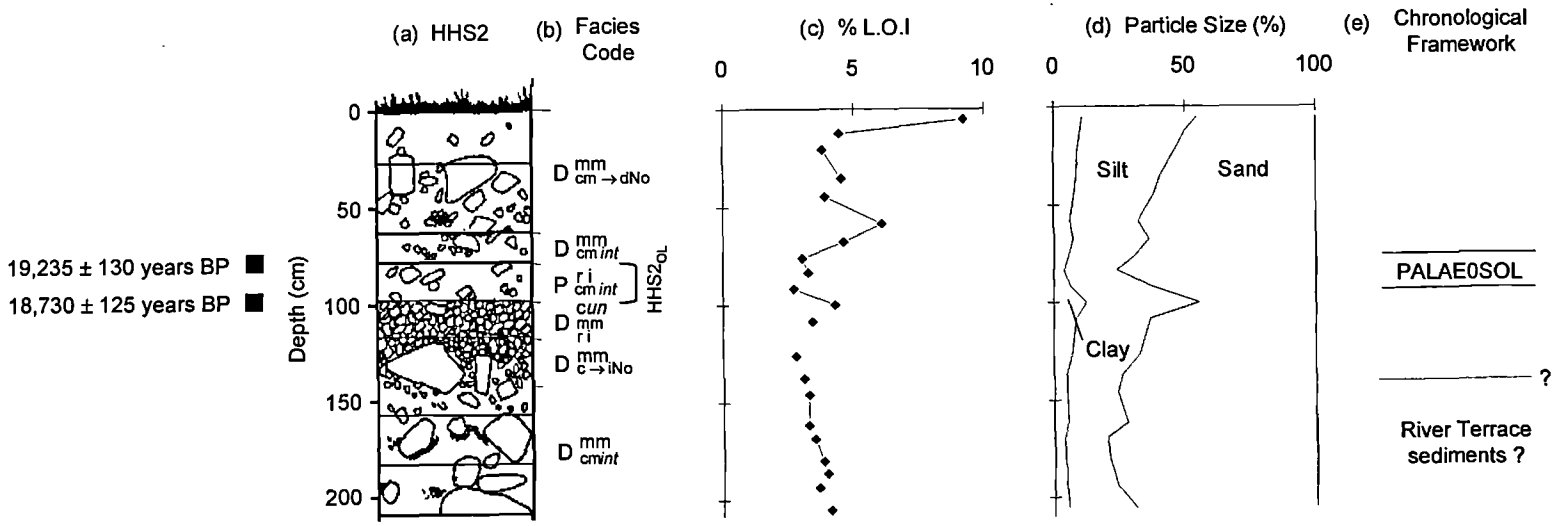


Figure 4.27. Radiocarbon dates, stratigraphic log, facies code, percentage loss on ignition, grain size and the chronological framework for HHS2, Langden Beck. The key for the facies code is given in Table 4.1.

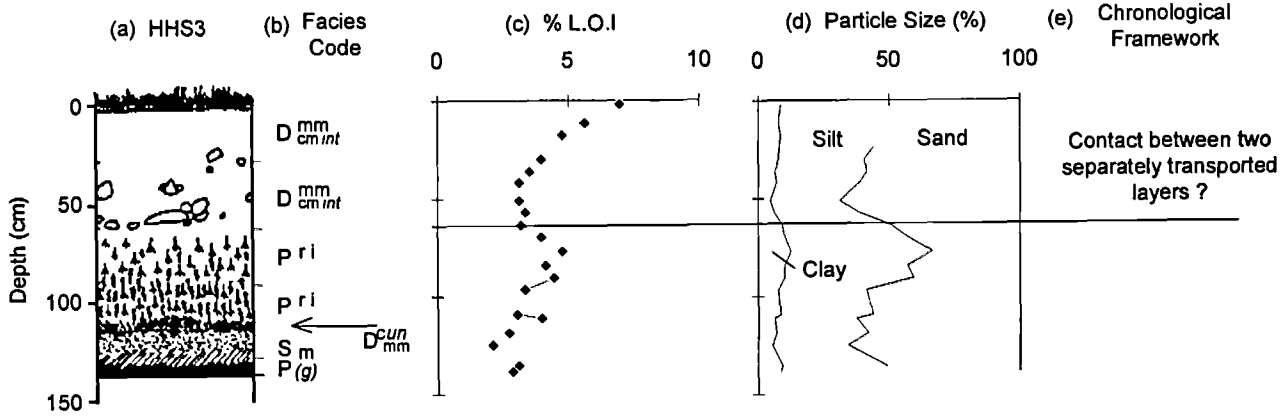


Figure 4.28. Stratigraphic log, facies code, percentage loss on ignition, grain size and the chronological framework for HHS3, Langden Beck. The key for the facies code is given in Table 4.1.

The location of the three sections that have been excavated for detailed analysis are shown in Figure 4.25. HHS1 (Figure 4.26) and HHS2 (Figure 4.27) have been taken from potentially the same deposit but exposed respectively near the fan apex and in distal deposits on the outward edge of the fan. HHS3 (Figure 4.28) has been taken from the exposure of sediments from the second fan terrace. There is no organic material, transported or formed *in situ*, evident within HHS1 other than that of the modern soil horizon which has the highest loss on ignition values in the section. Loss on ignition values rarely exceed 4%. A change in the visual properties of the sediment at 92 cm may represent a boundary between different phases of fan sedimentation. In HHS2, the distal deposits of the same uppermost fan surface, a palaeosol has formed between 62 cm and 97 cm, 146 cm above stream level. The palaeosol $HHS2_{OL}$ has formed around clasts but has a sharp upper contact with the sediment layer above. The soil is pale grey in colour. There is a lot of iron-staining around rootlets and clasts within the palaeosol. The characteristics exhibited by the palaeosol are indicative of formation in water-logged conditions. The organic content of the palaeosol is low and indistinguishable from the sediments above and below. The modern soil horizon is shallow and only extends to the top 12 cm of the section. The remainder of the sediments do not provide any evidence of a break in the sedimentation. Immediately below the soil, the clasts are tightly packed and rounded. It is possible that the sediments may be part of the river terrace. The height of the palaeosol is similar to the height of the river terrace downstream of the feature.

The sedimentary profile of HHS3 can be split into two layers exhibiting similar characteristics. At 61 cm a phase of fan aggradation is in sharp contact with the pale grey layer of sediments below. The visual properties, organic content and particle size characteristics confirm the differentiation (Figure 4.28b). As the section is located within the second terrace level within the entrenched system, there is a high chance that the sediments have been fluvially reworked and deposited.

Radiocarbon dates have been obtained for the upper and lower organic material of the palaeosol. The dates are stratigraphically inconsistent (Figure 4.28). The dates represent a physical impossibility as soil formation would have occurred underneath ice as the area was covered by the local Northern Pennines ice cap at this time (Beaumont, 1968). The dates can be explained by the incorporation of old

carbon from the limestone bedrock within the catchment. This is confirmed in part by the investigation of pollen from within the palaeosol. The pollen was severely degraded and weathered but from the limited remains the vegetation composition is indicative of species documented locally at *c.* 7,000 years BP (Innes, personal communication).

As a consequence the timing of the deposition of fan sediments on the palaeosol surface is unknown. The timing of activity in sections HHS1 and HHS3 has been tentatively linked with late- to the mid- Holocene. Sediments within section HHS1 and HHS3 were formed and deposited after the first period of aggradation by the trunk stream (Figure 4.26e and Figure 4.28e). The terrace has since been abandoned to form the current trunk stream's modern floodplain, where the bulk of activity has taken place. Although both HHS1 and HHS2 are taken from the upper-most sediments of the highest fan terrace, the sediments vary considerably due to their relative positions within the fan. The greatest value in logging the two sections is derived from a comparison between the transportation characteristics of the sediments in each section.

4.6.2 West Beck

An alluvial fan has formed at the base of West Beck. The fan surface form has been added to and altered by a period of intense mining activity within the supplying catchment area (Figure 4.29). It is difficult to determine the sequential development of the fan. It is evident the original fan has been added to by mining activity concentrated within a side gully that issues directly onto the original fan and past its apex. It is possible that activity originating in the West Beck catchment may mix and intercalate with the sediments issuing from the side gully. The trunk stream of West Beck fan is currently entrenched but its lateral development has been restricted and is not extensive. A second terrace has formed at West Beck. The upper sediments of the terrace have been exposed in the distal region of the fan. Section WBS1 (Figure 4.30) has been investigated from this exposure.

Mining activity has obscured how the fan interacts with its depositional environment. Upstream and especially downstream of the fan the remnants of a terrace have been preserved. The combined West Beck fan may deposit onto the

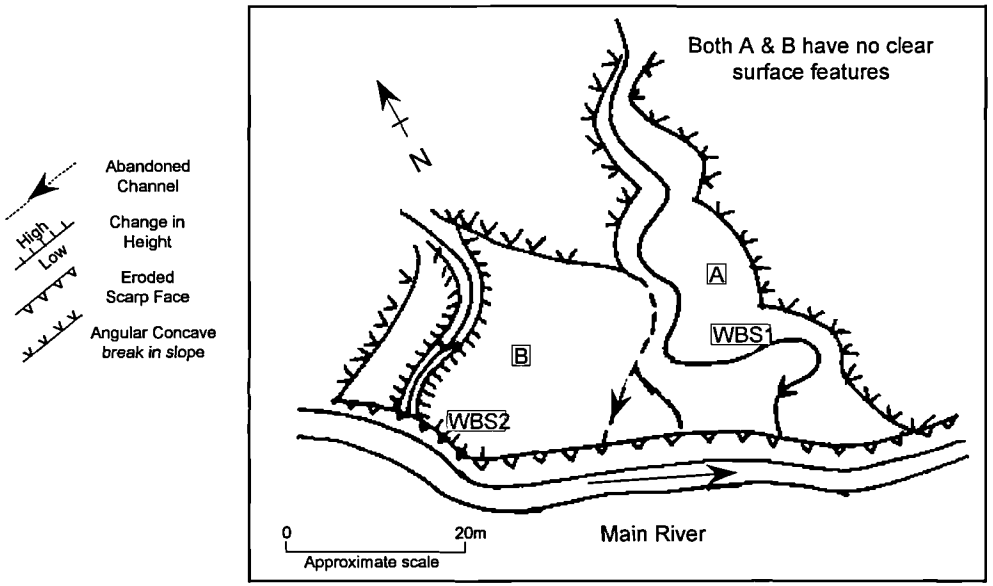


Figure 4.29. A planform schematic of the surface features of West Beck fan, Langden Beck.

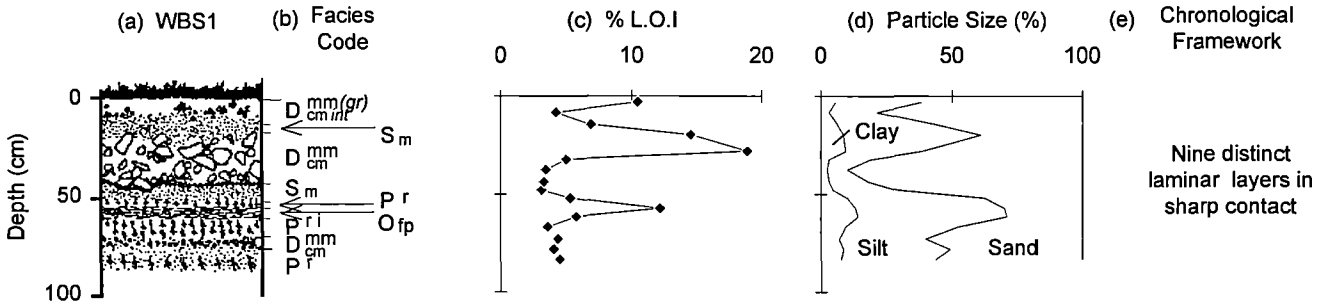


Figure 4.30. Stratigraphic log, facies code, percentage loss on ignition, grain size and the chronological framework for WBS1, Langden Beck. The key for the facies code is given in Table 4.1.

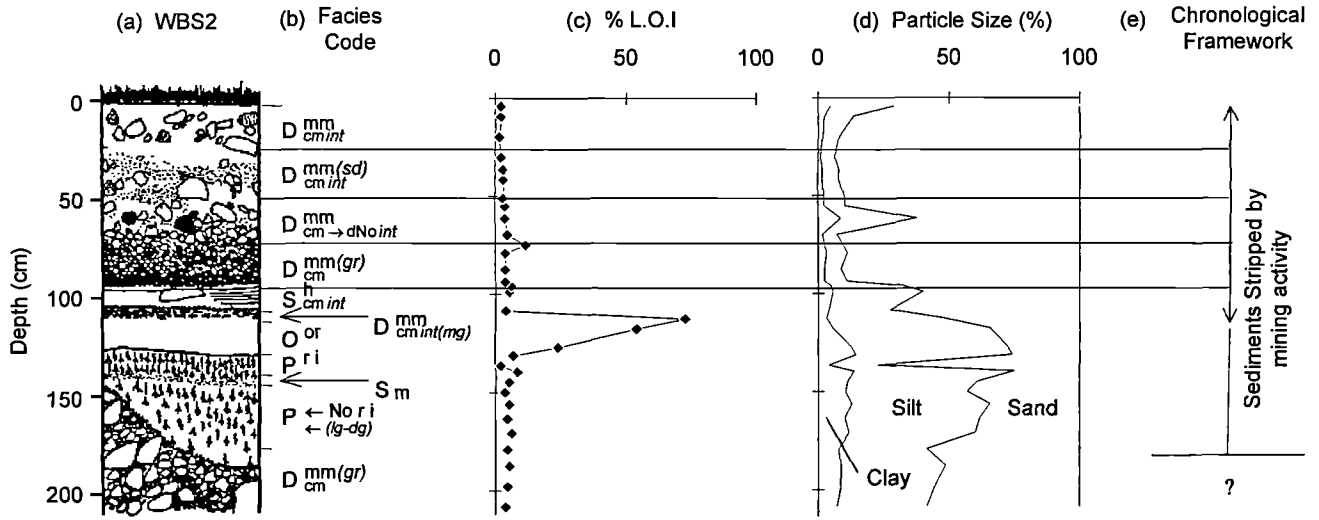


Figure 4.31. Stratigraphic log, facies code, percentage loss on ignition, grain size and the chronological framework for WBS2, Langden Beck. The key for the facies code is given in Table 4.1.

higher surface. The main river is currently incising into the western edge of the fan, predominantly formed by activity from the side gully. A section of sediments to stream level have been exposed. Section WBS2 (Figure 4.31) was cleared for investigation. Unfortunately, there is no exposure of sediments from the eastern deposits of the fan.

Within the small 75 cm section of sediments exposed in WBS1 nine distinct and separate changes in the sediment properties have been observed. The stratigraphy of the section is comparable to HHS3. The sedimentary profile of WBS1 can be split into two layers at 50 cm depth, both exhibiting similar characteristics. The bottom-most layer in WBS1 displays characteristics of soil formation. At 53 cm a 5 cm thick layer of peat has developed *in situ*. The peat is then capped by a fine layer of pale grey sediment which is in sharp contact with a sandy layer, which constitutes a change in the visual properties of the section.

The loss on ignition profile of the sediments indicates the presence of the layer of peat but another increase, not associated with modern soil development, is evident within the thickest layer of sediments at between 16 cm and 42 cm depth. This may potentially represent the previous surface of the section and an old soil horizon. The visual characteristics are not indicative of soil development. The organic content is more likely to have been incorporated within the section during transport. The characteristics of the layer, the uniform size of clasts and its distal location, suggest that the layer may represent the remnants of a large event that occurred within the supplying catchment. The layer may have been deposited by the effects of hushing, a mining process which strips the uppermost unconsolidated sediment, within the supplying catchment. The section itself is essentially made up of fine sediment with the exception of one layer. Each separate layer may have been deposited in response to the mining activity upstream within the catchment.

The sedimentary profile of WBS2 can be split into two layers. At between 110 cm and its greatest depth of 174 cm a pale grey layer of fine sediments separates the section. The layer is in sharp contact with sediments above and below and it is separated into distinct layers. The uppermost 17 cm consists of peat chaotically deposited. The high loss on ignition values of between 24% and 72% confirm the presence of the peat. The remaining sediments have low organic content including

the uppermost sediments. As loss on ignition does not increase within the top few centimetres it can be suggested that it has had insufficient time to develop. The sediments above the peat show a sequential change in their characteristics as depth decreases. Five layers can be identified. A sandy layer is capped by sediments characterised by a domination of clasts of uniform size and shape. This is capped by a layer which has incorporated lumps of peat. A fine sandy layer with intermittent clasts is deposited above that. The final layer has large lumps of shale within the layer which still maintains its structural characteristics.

The whole profile above the pale grey layer at 127 cm is indicative of the sequential removal and erosion of the uppermost unconsolidated sediment present within the supplying gully. What remains unclear is the origin of the bottom part of the section below 127 cm. A pale grey layer, between 127 cm and 174 cm, exhibits characteristics indicative of soil development. It is, however, in sharp contact with the layer below and is not laterally consistent (Figure 4.31a). The bottom-most material, below the grey sediments, could be the eroded remnants of river terrace deposits. A river terrace of similar height is present within close proximity upstream of the section.

4.6.3 Causal development

The timing of activity in WBS2 occurred when mining activity was initiated in the supplying side gully. There is no exact date for the onset of mining activity within the catchment as it was not part of the major companies that operated within the headwaters of Weardale and Teesdale. Due to the character of deposition within WBS1, the onset of fan incision and the deposition of sediments within the section occurred as a direct result of mining activity within the supplying catchment. The timing of aggradation of Harthope Beck is not as obvious. Pollen analysis of samples taken from the upper and lower contacts of the palaeosol in HHS3 constrains the timing of palaeosol formation. The pollen within the samples was badly damaged but the composition of the vegetation constrains palaeosol formation to a maximum approximate age of 7,000 years BP. The initial phases of aggradation thus occurred prior to the onset of mining activity which is located within side gullies and the main gully of the supplying catchment. The fan has since undergone a phase of incision to produce the fan terrace sequence. The cause of incision could

have been caused in response to a phase of down-cutting within the main valley, which produced a terrace sequence below the fan. It is more likely mining activity within the catchment increased water flow and mining lowered ground water levels. HHS3 shows similar characteristics but less layering to WBS1 from the second highest fan terrace. It is possible that the formation of the second terrace and the nature of its aggradation was caused by mining activity within the catchment.

4.7 Summary

The sequential development for each feature investigated has been established from its form and, where possible, confirmed by carbon dating. The resulting contextual framework constructed for each section provides the basis for determining changes in sediment transport mechanisms and their source over time. Dates obtained for the onset and cessation of fan and cone activity also add to the current database that links the timing of geomorphic activity with episodes of climatic deterioration and increased agricultural pressure within the Holocene time-scale.

The timing of fan and cone aggradation identified for all features investigated is summarised in Figure 4.32. A correlation exists in the timing of activity between regions at around 900 year BP. Due to the nature of carbon dating techniques, the interval could be as tightly constrained by a few decades or could span over 200 years. The time period immediately follows the major phase of Viking settlement of the Tenth Century. An increase in the intensity of land use or grazing pressure at that time is commonly cited as a cause for the onset of fan or cone aggradation including increased fluvial activity (Macklin and Needham, 1992) and peat gullying (Tallis, 1985). Harvey *et al.* (1981) provide a direct link between a change in vegetation composition and the onset of Burnt Gill cone aggradation in the Howgill Fells. Tipping and Halliday (1994) however, found that in the Southern Uplands aggradation in the Hopecarton Burn fan occurred in an environment with a stable agricultural landscape.

Dates obtained in this study from the Howgill Fells and the Southern Uplands confirm the general 900 year time period of initiation and / or reactivation of fan and cone activity at both sites. The causal link is weak. Inference of cause is heavily reliant upon data obtained from other sites, for example, vegetation changes

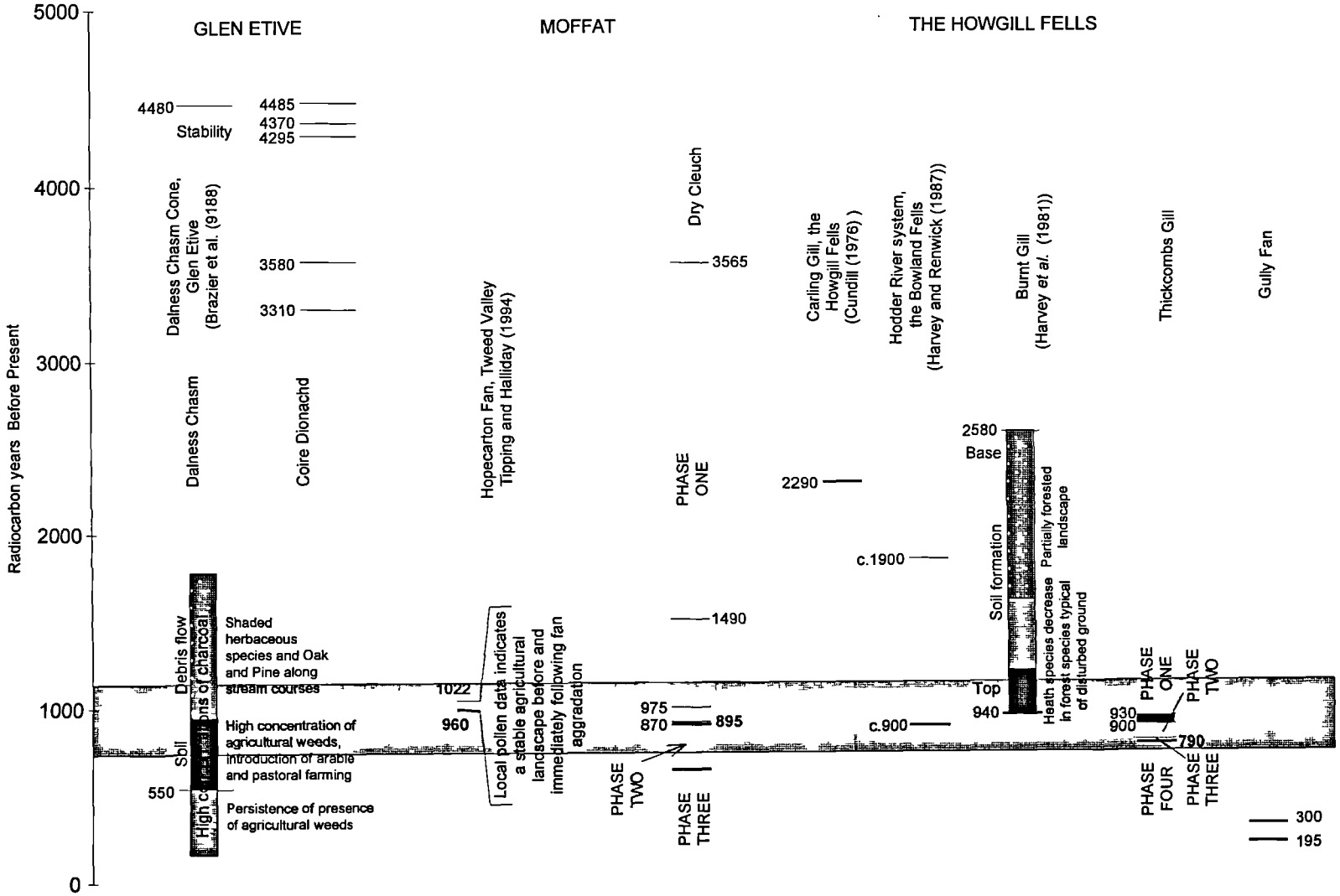


Figure 4.32. Comparison of timing of fan and cone activity between, Glen Etive, Moffat and the Howgill Fells

obtained from local stable environments. In order to establish contemporaneity between sites more detailed site information is required along with the means to reconcile difficulties in the correlation between different lines of evidence.

The two causal hypotheses provided by Tipping and Halliday (1994) and Harvey *et al.*, (1981) conflict with each other. In ascribing both a climatic and human causal hypothesis, the role of intrinsic characteristics and the inter-relationship between thresholds of resistance and the magnitude of the initiating force is underestimated due to difficulties in establishing the importance of one storm event. It is possible that the timing of erosional events may be linked to high magnitude storms of random occurrence, which do not relate to a climatic or human causal hypothesis (Ballantyne, 1991a).

Establishing the number of events that produced the sequence of fan sediments or the rate of aggradation will constrain the development history further. Derivation of the timing of aggradation is essential in determining rates of sediment accumulation but is restricted by the lack of datable organic material. By testing the hypothesis of a change in transport process as evidence of decreasing sediment reserves, information upon the importance of extreme events can also be obtained. Based upon physical transport mechanisms, similarities between the sequential and stratigraphical inter-relationship of sediment layers will point towards a common transport mechanism as well as establishing its change with depth.

Chapter Five

Sediment transport mechanism recognition and sediment exhaustion

5.1 Introduction

The principal aim of this chapter is to test the hypothesis that sediment exhaustion will result in a change in the dominant transport mechanism from debris flow through to fluvial flow as the fan or cone develops. To test the hypothesis, the ability to isolate and recognise sediments that have been transported by dry grain flow, debris flow, hyperconcentrated flow and fluvial flow is essential. The methodology to do this is based upon a review of the rheological properties of each process to establish individual diagnostic sedimentary properties, an evaluation of the techniques available to separate transport mechanisms itself and the design of a sampling framework. In establishing the number and type of slope process that contribute to the form of a given fan or cone their development history can be further constrained.

5.2 Diagnostic properties of transport mechanism deposits

Each type of flow, dry grain, debris, hyperconcentrated and fluvial, can result in a wide range of sedimentary facies which reflect environment and process diversity. Variations are introduced by changing boundary conditions, the magnitude and type of trigger mechanism applied and specific material properties (Van Steijn, 1995). The rheological properties and sedimentary structures of each flow type, established from studies of contemporary flows and laboratory investigations of their sediments taken from numerous environmental settings, have been described in many papers (Costa, 1984; Johnson and Rodine, 1984; Costa, 1988; Van Steijn, 1995; Bertran *et*

al., 1997). The following review will present the diagnostic properties that are applicable for the recognition of the relict deposits of each flow mechanism. The preservation potential of deposits of each flow type can then be considered in relation to the structural integrity of flows during transport and the effects of post-depositional alteration.

5.2.1 Diagnostic properties of individual flow types

The major physical properties of dry grain flow, hyperconcentrated flow, debris flow and fluvial flow are summarised in Table 5.1. Each flow type cannot be separated by a single value of sediment concentration as it fluctuates between surges and more fluid phases of flow (Costa, 1988). Examples are drawn from contemporary flows from a variety of different environments. Few examples of contemporary studies have been carried out in Great Britain. Carling's (1986a) study of a debris flow at West Grain, Northern Pennines has provided values concerning its physical properties. These values (Table 5.1) are comparable to those presented by Costa (1988). There are few examples of studies of debris flows within a UK setting (Innes, 1983; Prior *et al.*, 1970; Stratham, 1976; Carling, 1986a; Wells and Harvey, 1987). Their physical properties are diagnostic of flow process (Addison, 1987).

Although the following flow descriptions are primarily based upon descriptions of flow properties of flows outside the UK, the rheological properties of flows are comparable between environments. Differences in material properties and boundary conditions of flow, including catchment size will constrain flow characteristics, thickness and spread.

A grain flow is essentially the rapid movement of openwork clasts and can be defined as a 'sediment gravity flow in which a dispersion of cohesionless grains is maintained against gravity by grain dispersive pressure (Lowe 1976). Dispersive pressure is the term used to explain the effect of multiple particle collisions. Grain flows are commonly associated with areas of rock fragment build up, on scree slopes or within the trunk channel of gully systems. Over-steepening of the deposits by the build up of sediment and increased loading combined with the force of the impact of rocks falling from above can lead to the initiation of grain flows (Van Steijn, 1995).

After initiation, flow is maintained by dispersive pressure. The larger the grain area the greater the dispersive pressure. This effect influences the grain size

Table 5.1. Summary of the major physical properties of fluvial flow, hyperconcentrated flow and debris flow

Physical property	Water flood/fluvial flow	Hyperconcentrated flow	Debris flow	
Sediment Concentration	1% - 40% by wt. 0.4- 20% by vol.	40% - 70% by wt. 20 -47% by vol.	70% - 90% by wt. 47% – 77% by vol.	
			64% - 75% by wt.	Carling, (1986a)
Bulk Density (g/cm^3)	1.01 - 1.33	1.33 - 1.80	1.80 - 2.30	
			1.50 – 1.8	Carling, (1986a)
Shear Strength ($dyne/cm^3$)	0 - 100	100 - 400	> 400	
			249 – 289	Carling, (1986a)
Fluid Type	Newtonian	Non-Newtonian	Viscoplastic (?)	
Major sediment support mechanism	Eloctrostatic forces, turbulence	Buoyancy, dispersive stress, turbulence	Cohesion, buoyancy dispersive stress structural support	
Viscosity (poise)	0.01 - 20	20 > 200	>>200	
			$10^2 - 5\times10^4$	Carling, (1986a)
Fall Velocity (% of clear water)	100 - 33	33 - 0	0	
Sediment Concentration Profile	Nonuniform	Nonuniform to uniform	Uniform	
Predominant flow type	Turbulent	turbulent	laminar	

distribution within the flowing mass by forcing finer particles to the base of the flow and coarser clasts to the top (Bagnold, 1954). The resulting velocity profile of the flow, low at the base and increasing to the top of the flow, results in the deposition of fines upslope whilst coarser material continues on downslope (Lowe, 1976). The sieving process splits the grain flow into two distinct units over a relatively small transport distance. A matrix rich bed, with finer clasts and a coarser bed of openwork clasts, inversely graded can be found along the longitudinal profile of the flow with grain size increasing downslope (Van Steijn, 1995). This sediment structure is achieved in flows less than 200m in length. Downslope deposits maintain an inversely graded openwork clast structure due to the complete loss of fine material by infiltration upslope. The sliding of dry material is only found on relatively steep slopes because of the high friction values between clasts. The mobility of flows can be enhanced by a change in resistance to flow. If clasts are frost-coated, flows can develop at below the angle of internal friction for the same material under dry conditions (Van Steijn, 1995). It is difficult to differentiate between a frost-coated flow and a dry flow. Within frost-coated flows clasts show greater imbrication and individual clasts are coated in fine material as the migration of fines is inhibited by the frost coating. Fines are commonly removed by percolation of water immediately following the event. In subaerial deposits fines can migrate from above due to eluviation and illuviation confusing differentiation.

A debris flow is a form of rapid mass movement of a body of granular solids, water and air (Varnes, 1978). Flows originate when poorly sorted rock and soil debris are mobilised from hillslopes and channels by the addition of moisture (Costa, 1984). A debris flow is a water-debris mixture, a one-phase flow of a viscous fluid (Coussot and Meunier, 1996). Solid particles and water move together as a single visco-plastic body (Johnson, 1970). The possible particle size composition of debris flows is highly variable. Flows can contain predominantly clay and silt or can comprise cobbles and larger clasts (Johnson and Rodine, 1984). Consequently, the term debris flow can be broadly interpreted to include mudflows, granular flows, till flows and debris avalanches (Costa, 1984).

The movement of debris flows can be described by two rheological models, visco-plastic (Johnson, 1970; Johnson and Rodine, 1984) or flow (Takahashi, 1980). Most debris flows posses elements from both rheological models during motion (Meunier, 1994) resulting in the interaction of a number of particle support

mechanisms: cohesion, buoyancy, dispersive pressure, turbulence and structural support. As the physical properties of debris flow sediments vary so will the relative importance of the particle support mechanisms (Coussot and Meunier, 1996). A fine-grained matrix provides cohesion within a flow. Coarser clasts supply internal friction which originates from particles interlocking. The more poorly sorted the sediment the greater the dispersion of energy and the greater the shear strength of the flow. High concentrations of sediment increase the viscosity of a flow and also contribute to its overall shear strength.

A distinguishing characteristic of a debris flow is its ability to transport large boulders. The boulders are supported by the combined action of the particle support mechanisms (Figure 5.1). The particle support mechanisms also prevent the selective deposition of any but the coarsest clasts. Sediment entrainment within a debris flow is commonly irreversible. The process of particle dispersion occurs independent of particle size. Small differences in density that occur between boulders and the fluid matrix in response to buoyant forces, and dispersive pressures, can concentrate larger clasts or particles at the top of the flow (Fisher, 1971). The process of kinematic sieving results in finer material becoming concentrated at the base of the flow. Coarse particles within a flow move towards zones of low shear, commonly found at the front and outer extremities of a flow. Differences in the thickness of a debris flow can therefore occur both laterally and longitudinally. The magnitude and scale of the kinematic effect within a debris flow varies with the size and volume of the flow. The spatial differences in the deposits of a small scale debris flow are illustrated in Figure 5.2. Volume and strength of flow also controls the maximum extent of a debris flow. On a fan or cone, surface antecedent conditions such as slope angle and roughness play a minor role. Flow strength and thickness varies with water and sediment ratios. More fluid flows and less sediment content by volume can extend much further from the source area than a viscous flow, purely because of the difference in shear strength or resistance to flow between the two.

A debris flow will stop when internal shear stresses are exceeded by the shear strength of the flow. Pore fluids escape which promote an increase in internal friction. The magnitude of the increase is a function of the sorting and overall size range of particles included in the flow. When a debris flow stops, lateral spreading occurs. Spread is concurrent with a decrease in the thickness of flow sheets. Debris

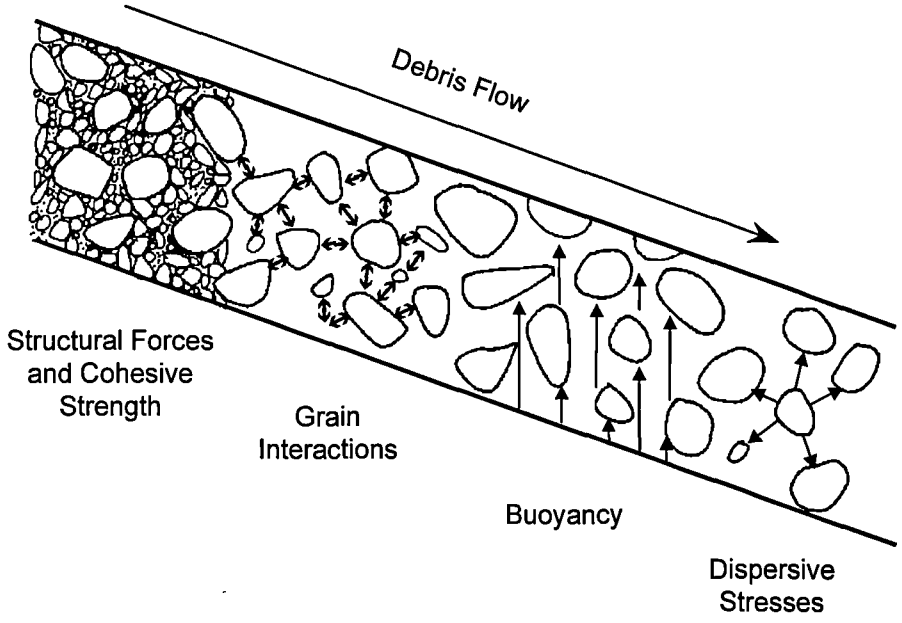


Figure 5.1. A schematic illustration of the mechanism of large boulder support within a debris flow.

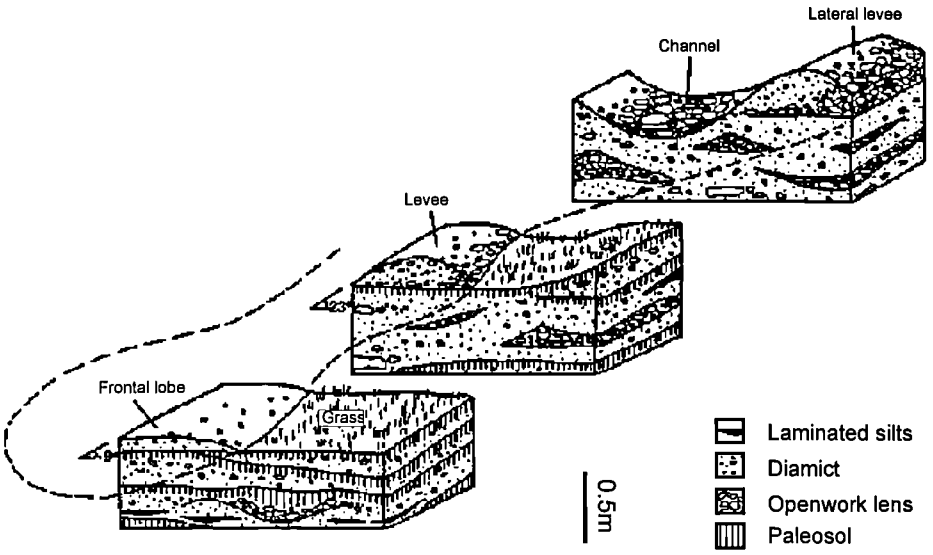


Figure 5.2. Spatial variations of the sediment properties within debris flow deposits, from Van Steijn *et al.* (1995, p 138).

flows have been shown to cover rather than erode the underlying material surface, resulting in a sharp contact between deposits stratigraphically (Costa, 1984). The depositional structure of a debris flow is composed of the whole mass and differs only slightly in form from the stopped flow even after settling and drainage. A debris flow deposit can be clast supported if the matrix drains or is washed away. However, removal of the matrix does not detract from the characteristically poorly sorted deposit structure (Costa, 1988). Debris flows can also contain light weight materials such as wood and bark fragments incorporated within the deposit. If fluvial flow or hyperconcentrated flow are involved, organic material would float upon the flow upper surface and be removed from the fan or cone system (Costa, 1988). Sedimentary structures, including stratification are virtually non-existent but characteristically contacts between different flows tend to be sharp and distinct. If any structures do exists they result from small differences in density that occur between boulders and the fluid matrix. Buoyant forces and dispersive pressures concentrate larger particles at the top of the deposit forming reverse grading (Fisher, 1971). The sedimentary properties of the flow can vary both laterally and longitudinally. Dissection of relict stratified deposits can reveal lateral levees, channel deposits and terminal lobes as well as mid-flow deposits. However, despite the concentration of larger particles, the overall structure will still be poorly sorted and thus recognisable within a vertical section (Johnson, 1970).

Fluvial flows essentially have no yield or shear strength and are unable to resist an applied shear stress without deformation. Sediment and water are two distinct and separate phases. The flow is two-phase. Sediment moves by suspension and saltation, driven by the transfer of energy from moving water to the sediment particles. Water flows can vary their sediment load by hydraulic sorting, deposition and erosion. Transported particles can also change size by abrasion. The significance of abrasion increases over greater transport distances (Kodama, 1994). Within the study, the maximum transport distances of most of the catchments under investigation are of insufficient length for abrasion to have any marked effect.

When sediment concentration is low in water flows, shear strength increases slowly with increasing sediment load approximating to a Newtonian flow. At a critical value of sediment load shear strength will increase concurrently. With increasing sediment concentrations water floods lose their Newtonian character and the shear strength of the flow must be exceeded before any deformation or flow occurs. Shear

strengths obtained in fluvial flows, by increasing sediment content by erosion, are much smaller in comparison to those exhibited by debris flows (Table 5.1). Due to the erosive nature of fluvial flows, debris flow deposits preserved within a sediment profile can be eroded, reworked and replaced by the deposits of the fluvial flow that eroded them. Fluvial deposits are sorted, imbricated, cross-bedded and stratified. In a fluvially aggrading environment deposits have massive gradational boundaries. On alluvial fans sieve deposits are a distinctive characteristic fluvial deposit. Sieve deposits do not form if fine material is present in large quantities, as it acts to plug underlying material. Sieve deposits contain no fines, no unusually large boulders, have gradational contacts and exhibit an approximate homogenous clast distribution (Costa, 1984). The duration of an event and its transport distance will act to control the time in which fluvially transported sediments undergo sorting. The magnitude of the event, the sediment entrained, eroded from the channel, fan or cone, will determine the particle size range at which sediments are selectively removed. Small transport distances may result in deposits that are not as sorted in comparison to deposits that have been transported further. Thus, it is likely that fluvial events compared between a debris cone with a single linear gully and a large dendritic supplying catchment of an alluvial fan will differ.

Hyperconcentrated flows and their characteristics are poorly understood. The characteristics of the flow lie somewhere between water flow and debris flow, retaining the characteristics of both (Costa, 1988). Hyperconcentrated flows are rare, transitional and also difficult to interpret. (Costa, 1988). The flows have less percentage volume of sediment and are coarser in nature, with distinctively less fines than debris flow deposits. Hyperconcentrated flows exhibit two phases. In comparison to fluvial flows hyperconcentrated flows are more poorly sorted than most water flood deposits of a similar median size. The deposits of hyperconcentrated flows have a generally massive or poorly developed horizontal stratification with thin gravel lenses. A clast supported, non-cohesive, open work structure and reverse graded units are also characteristics (Scott, 1985). A rare study of the transition of debris flow to hyperconcentrated flow (Starkel, 1972) provides valuable sedimentological field evidence. Starkel (1972) found two main sedimentological differences. Hyperconcentrated flows had smaller relative amounts of fine-graded sediments and the coarser clasts were imbricated. The greatest difference occurs in the sand fraction. Hyperconcentrated deposits are dominated by coarser size fraction. The two-phase hyperconcentrated flow deposits are

washed or sieved and the coarsest fines float away resulting in a tell-tale difference in the sand fractions, hyperconcentrated flow deposits having a higher percentage of sand relative to debris flow deposits (Coussot and Meunier, 1996). The amount of sand within a flow is limited by the amount present within the original source material.

5.2.2 Preservation potential of flow deposits

Each flow process is related by a sediment : water continuum. The addition of sediment or water can result in a change in flow type during transport. The transition in flows during transport is a function of a change in the particle support mechanisms, triggered by an increase in the water to sediment ratio. Transition between flow types during transport does not affect the structural integrity of the deposits of individual flow processes preserved within a stratigraphic profile.

A physical explanation of the mechanism of transition, based upon a comprehensive review of the current understanding of mass movement processes, is provided by Coussot and Meunier (1996). The main points are illustrated in Figure 5.3. They state that sediment threshold conditions exist for given flow conditions and sediment concentration characteristics. The conditions can affect the particle support mechanisms and hence the material strength of a flow (Figure 5.4). High concentrations of sediment provide an interactive network between the solid particles which gives rise to material strength. An increase in the sediment concentration, which increases the fluid density of the flow above the critical threshold of 1.5 g cm^{-3} to 1.8 g cm^{-3}, results in the change from two-phase to one-phase flow or debris flow. Beyond the fluid density threshold sedimentation is negligible due to irreversible sediment entrainment. If the sediment concentration falls below the critical value, a decrease in the material strength and a change in the particle support mechanisms occurs. The coarsest particles can no longer be supported and will fall out of the flow, further decreasing the material strength. A chain reaction is set up as a new grain size class begins to settle, resulting in the transition to a flow that has hyperconcentrated flow characteristics. The situation persists until fluid flow is reached (Figure 5.3). Fluctuation around the critical threshold value will result in a change in particle support mechanism of the flow and hence a rapid change in flow type.

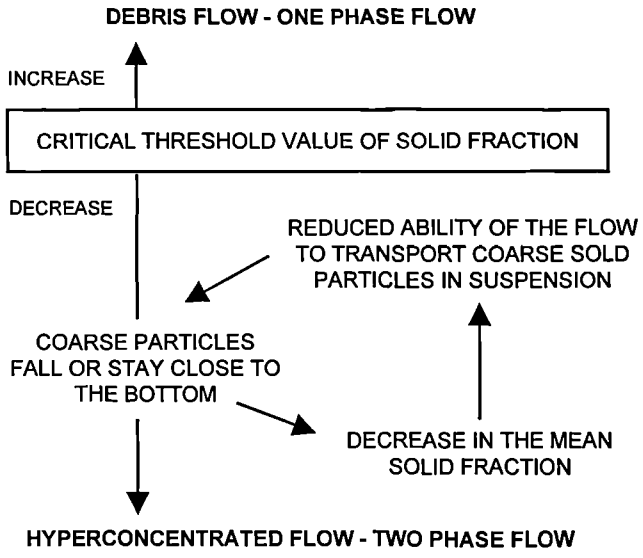


Figure 5.3. A schematic illustration of the nature of flow transition from one phase flow to two phase flow. After Coussot and Meunier, (1996)

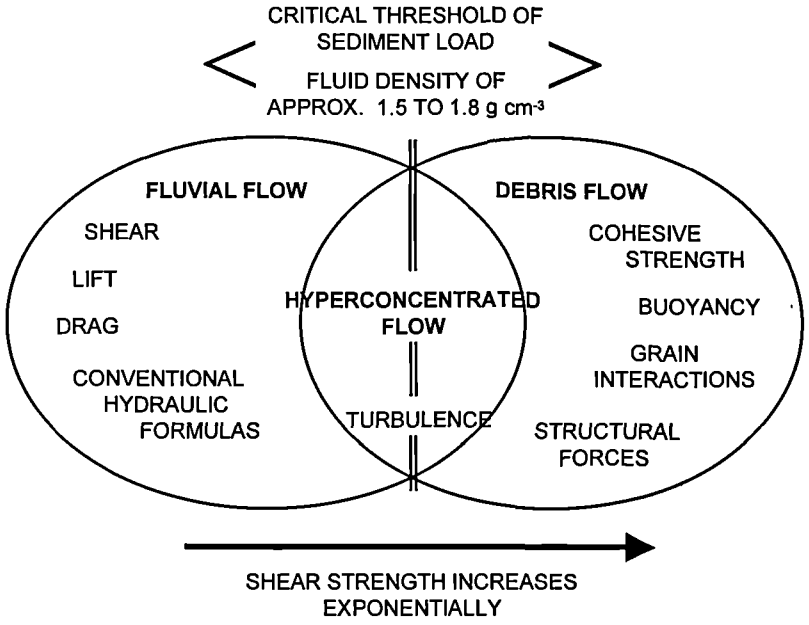


Figure 5.4. Particle support mechanisms of fluvial flow, debris flow and hyperconcentrated flow and their interrelationship. After Costa, (1988)

A change in the particle-size characteristics of the source material during a flow will result in a transition between flow types but only if the particle size characteristics result in a change in sediment concentration around the threshold value. If above the threshold value, the additional sediment added to a debris flow will be incorporated into the flow, mixed and dispersed by the particle support mechanisms. A change in the contributing particle size distribution does not affect the sorting properties of the sediment. Additional sediment only adds to or dilutes the particle size range of the sediment. If the transport distance after the addition of sediment is of insufficient length it can result in deposits with multi-modal sediment size distributions. If sediment is added to a fluvial flow and the resulting fluid density does not pass the threshold level, sediment will be selectively removed. The size fraction affected is dependent upon the magnitude of the fluvial flow and the range of particle sizes added.

It is the condition of irreversible sediment entrainment, that occurs at a critical value of sediment load, which separates debris flow from two-phase flows (Hooke, 1967). A debris flow cannot be converted into a fluvial flow by deposition. A decrease in velocity does not result in the settling of solids from fluids, the entire water / solid mass moves as a whole and stops in place when the internal friction is exceeded by shear strength. The transition from debris flow to hyperconcentrated flow and *vice versa* involves a huge change in sediment concentration. A change from debris flow to hyperconcentrated flow involves a change in sediment concentration from 70-80% to 30-35 % (Pierson, 1985). Under given material and flow conditions, no stable flow with an intermediate concentration of sediment can exist (Coussot and Meunier, 1996). As a flow of intermediate sediment concentration cannot exist, the transition from one type of flow to another requires strong or continuous changes of material or water concentrations. The rapid transition between flows during transport means that the deposits will retain the individual diagnostic characteristics of their flow type.

Degradation of the original structures and fabric of a deposited flow is possible after its burial but the degree of change is limited (Van Steijn, 1995). It is the reworking and erosion of material that can alter and remove evidence of single or multiple flow deposits that were previously laid down. Reworking can occur before the burial of flow material. After burial, subsequent fluvial flows can degrade deposits rich in fines, causing the eluviation and illuviation of fine material. If the flow

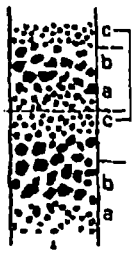
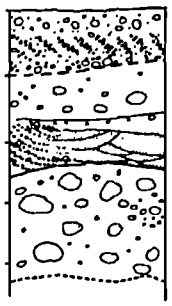
is sufficiently competent sediment can be stripped. The time period that hiatuses in a stratigraphic profile represent is difficult to determine unless a dating control can be applied. In wet, humid environments, there is more opportunity for deposits to be reworked, destroying the stratigraphic evidence of the original genesis of the deposits (Costa 1984). An increase in precipitation does not necessarily equate to a decrease in debris flow occurrence. The import of debris flows in fan and cone environments can be underestimated (Costa, 1988).

5.2.3 Recognition

The rheological properties of each flow type results in apparent differences in their respective sedimentary deposits (Costa, 1988). Thus each flow type has recognisable diagnostic features and depositional structures that can be used in their identification. Table 5.2 summarises the diagnostic properties of each flow type which can be used to distinguish between the transport mechanisms discussed in the above sections. The difference observed in the sorting characteristics between deposits, especially between debris, hyperconcentrated and fluvial flows provides the greatest means of differentiation. As long as water and sediment ratios persist for sediment supplies after flow initiation the sorting characteristics remain the same no matter what the source particle size characteristics were at the outset. Particle size characteristics of parent material may introduce differences in the character of the sedimentary deposits and to a certain extent may moderate the characteristics of a given flow type, but the sorting characteristics remain the same after initiation if water : sediment ratios remain constant.

The ability to retrodict the transport mechanism of relict deposits within a stratigraphic profile is reliant upon three assumptions. First, that prior to transport, the sediment source is poorly sorted and structureless. Secondly, that it is the rheological properties of the given transport mechanism itself that produce the associated diagnostic sediment properties (Costa, 1984, Van Steijn, 1995). Thirdly, that the deposits of each flow type are distinct separate stratigraphic units with a homogenous textural and compositional fingerprint.

Table 5.2. Summary of the sedimentary structures and characteristics of relict dry grain, debris, hyperconcentrated and fluvial flows

Flow type	Sedimentary characteristics	Example
Dry Grain Flow	⇨two distinct units (two directional) ⇨i) matrix rich bed of finer clasts ⇨ii) coarse bed of openwork clasts inversely graded ⇨grain size increases downslope successive plugs of material, ⇨cyclic sequence of sediments relating to the same flow event but showing a progressive decrease in size	 Tail of fine gravel Van Stejjn *et al.* (1994)
Debris Flow	⇨presence of large boulders ⇨sharp contact between deposits ⇨poorly sorted if matrix or clast supported: for all size ranges clay - silt and coarse sand -larger clasts / cobbles ⇨contain light weight materials, wood bark fragments ⇨structural differences ⇨larger clasts / particles can be concentrated at the top of a flow ⇨slight reverse grading ⇨normal grading if resistant to flow at contact surface	
Hyperconcentrated Flow	⇨clast supported non-cohesive open framework structure ⇨reverse sub units ⇨ massive ⇨poorly developed horizontal stratification with thin gravel lenses ⇨dewatering structures ⇨more poorly sorted than most fluvial deposits of similar median ⇨loss of sediment in sand fractions	
Fluvial Flow	⇨sorted ⇨imbricated, can be cross-bedded; ⇨stratified ⇨massive gradational boundaries ⇨weak to strong imbrication ⇨clast supported ⇨cut and fill sequences ⇨eroded basal contact Sieve deposits: ⇨open framework of coarse clasts ⇨no fines, no unusually large boulders ⇨gradational contacts ⇨approximate homogenous clast distribution	 Maizels and Aitken (1994)

Compiled from : Johnson and Rodine (1984), Harvey and Wells, (1986), Van Steijn *et al.*, (1995) Costa, (1988) Coussot and Meunier, 1996) Bertran *et al.*, (1997)

5.3 Methods used in transport mechanism discrimination

The differences found between the relict deposits of each flow type can be exploited for their identification (Table 5.3). Three techniques have been adopted to provide a measure of structural and textural properties. A facies model has been used to provide a systematic qualitative description of the structure of fan and cone sediments. Physical measures of particle size were used to provide a quantitative measure of sorting. Total sand content and the nature of its fractionation (see section 4.2.3) is used to aid the differentiation of hyperconcentrated flow deposits from both debris flow and fluvial flow sediments (Starkel, 1972). The combination of descriptive and physically measured techniques results in a discrimination between deposits which account for facies variability but also provides a degree of objectivity in transport mechanism assignment. Due to the nature of the down-section sampling framework any change in physically measured properties with depth can have a maximum and minimum range, a depth interval over which the change has occurred.

5.3.1 Facies model: a descriptive measure of structure

Application of a facies model (see section 4.2.2) provides valuable qualitative information on clast texture and depositional morphology and form. The assignment of facies codes also accounts for facies variability between the four study sites. In using the model, information concerning the depth at which visual contact boundaries occur is provided, identifying potential boundaries between distinct flow units. Information about the nature of the contact between units whether sharp or diffuse is also supplied. The description of all structures found within the sections aid the assignment of a transport mechanism. Clast grading helps to differentiate between fluvial and debris flow sediments. The model provides the only means of identifying dry cohesionless flow deposits and separating them from sieve deposits.

If used on its own to assign a transport mechanism, qualitative information supplied by the model is open to subjective interpretation. Using the model and the description of structure alone it is therefore difficult to determine whether deposits have been reworked. The upper sediments of what appears to be a discrete debris flow deposit may have been reworked (Blair and McPherson, 1993). The model does provide a valuable means of identifying sequential change in the characteristics of the transported sediment. A description of the clast to matrix ratio and the size

Table 5.3. Differences between pairs of deposits

DGf : Df / Hf / Ff	⇨ occurrence limited to steeper slopes > 34°
	⇨ better development of internal structure - two directional
	⇨ dominated by openwork clasts
Df : Ff	⇨ poorly sorted
	⇨ extreme particle size range
	⇨ lack of internal structure
	⇨ presence of large boulders throughout flow deposit, from the base to the upper sediments
	⇨ inclusion of light weight debris within the boundaries of the flow deposit
Hf : Df	⇨ particle size sorted
	⇨ preferential removal of sand fractions
	⇨ exhibition of internal structure
	⇨ normal grading and dewatering structures
Ff : Hf	⇨ better sorted with similar initial particle size distribution
	⇨ greatest loss in finer sand fractions
	⇨ clear structures both depositional and erosional flows

DGf : Dry grain flow, Df : Debris flow, Hf : Hyperconcentrated flow and Ff : Fluvial flow
After Van Steijn *et al.* (1995)

range of clasts will provide a qualitative measure of the characteristics of the sediment transported by a given flow.

Detailed fabric analysis of the larger clasts is often used in the investigation of relict fan and cone sediments to reconstruct flow directions and quantify clast size and sorting (Bull, 1962b; Hubert and Filipov, 1989; Blair and McPerson, 1993). A change in flow direction signifies a change in the axis of flow deposition, the degree of change observed is directly related to the size and surface morphology of the feature (Eyles and Kocsis, 1988). In the features investigated in this study the short distance observed between the site of deposition and the point source, at the base of the gully or supplying catchment, is unlikely to result in marked changes in flow direction. The sampling of coarse clasts is reliant upon the visual identification of the upper and lower boundaries of the deposits of distinct flows. Clasts are randomly sampled throughout the constrained deposit. Clast orientations are averaged to give a flow direction for the sampled layer and sorting is obtained using the distribution of the clast sizes measured. The deposits of separate flows are not always visually identifiable within a stratigraphic profile. The visually identified upper and lower boundaries may contain the deposits of more than one flow. The flow direction and degree of sorting obtained using the clasts sampled will as a result be meaningless.

The successful use of clast sorting in discriminating flow mechanisms is dependent upon identification of the contacts of successive flow deposits. Physical measurements based upon matrix material instead of clasts allows analysis of the section at a higher resolution, between visually identified layers. It has been demonstrated that the diagnostic properties of sorting encompass the total size range of the transported material, including the matrix material. The measurement of sorting has been obtained from a sampling framework of matrix sediments.

5.3.2 A measure of sorting as a tool for discrimination

A variety of methods for measuring sorting are available (Table 5.4). These measurements are descriptive in the manner in which a mass of particles are arranged within a specified size class on a specified scale. Measurements of sorting can be split into two categories. First, sorting measures which are basic descriptive statistics can be used on a numerical scale or can be plotted as bivariate scattergrams. From the scattergram graphical envelopes are identified within which deposits of a specific mechanism will lie. Second, graphical sorting indices are

independent of summary statistics but use a similar graphical approach in separating between depositional environments. The sorting indices were originally developed to discriminate between the deposits of major process environments. Both sorting indices have been shown to be sensitive to variations within individual process environments (Landim and Frankes, 1968; Royse, 1968; Vandenbergtie, 1975; Lewin *et al.* 1993, Hubert and Filipov, 1989). The fundamental difference between all of the techniques is the size of the percentiles used to summarise the spread of particle size distribution. The success of the discrimination relies upon using a sorting measure which exacerbates the differences in the specific deposits attempting to discriminate.

The size range used in the measures of sorting is not limited. The choice of the upper limit is restricted only by the need for the range to encompass the size differences that discriminate the deposits under investigation. Studies that have sampled deposits from fan and cone environments have an upper size ranging from 10 cm to 2 mm (Bull, 1962b; Huburt and Filipov; 1989). In this study sorting measurements have been based on matrix material < 2 mm (section 4.2.2). As discussed by Johnson (1970), the properties of debris flow are independent of scale over a large range of dimensions. Differences between debris flows and hyperconcentrated flows occur in the sand fraction. In fluvial deposits all particle sizes are preferentially sorted. Consequently, it is believed that the particle size distribution of the <2 mm fraction retains the sorting characteristics of each transport mechanism.

The choice of which sorting measure to use in the discrimination between debris, hyperconcentrated and fluvial flow deposits is based upon four criteria. A continuous scale of sorting is required in order to establish boundaries for the discrimination between the deposits of each flow type. The measure must provide a relative comparison of sorting between deposits with markedly different particle size distributions. Variation is introduced by spatial and temporal changes in the character of the parent material supplied for transportation. The capacity to recognise distinct transport units within a stratigraphic profile is required in order to readily establish changes in transport process with depth. The difference between fluvially sorted and debris-flow transported sediment is introduced by the preferential and selective loss of sediment by hydraulic sorting. The velocity of a given flow determines the particle size range at which sorting is concentrated but this is

Table 5.4. A summary of commonly recognised measures of sorting

	Measure of Sorting		Examples of application
Basic descriptive Techniques	Mean		Sahu (1964) Hubert and Filipov (1989)
	Standard Deviation	Graphic standard deviation v graphic mean	
	Skewness	Graphic skewness v graphic mean	
	Kurtosis		
	Particle size	Triangular plot of % gravel, silt and clay	
Graphical measures of sorting	Trask measure of sorting (1930)	√(75mm - 25mm)	Costa (1984), Costa (1988) Coussot and Meunier (1996)
	Trask sorting coefficient modified by Krumbein (1934)	√(Ø75 - Ø25)	
	Otto (1939) and Inman (1952)	(Ø84 - Ø16)/2	Stokes *et al.* (1989)
	Folk and Ward (1957)	(Ø84 - Ø16)/4 + (Ø95 - Ø5)/6.6	
	McCammon (1962)	(Ø70 + Ø80 + Ø90 + Ø97 - Ø3 - Ø10 - Ø20 - Ø30)/9.1	
Sorting indices	Buller and McManus (1972, 1973): Qda : Md Plot	Qda (Ø75 - Ø25) plotted against Md (Ø50)	Pe and Piper (1975)
	Passega (1957, 1964, 1977): CM plot	C (Ø99) plotted against M (Ø50)	Bull (1962b) Landim and Frakes, (1968) Royse (1968) Lewin *et al.* (1983) Magilligan (1992)
Multivariate Statistics	Using above measures in Principal Component Analysis and Factor analysis		East (1987)

commonly within the coarser sediments. A sorting measure which concentrates on measuring spread within the coarser half of the particle size distribution will highlight the difference in sorting of the transport mechanisms.

The percentiles used by each technique are summarised in Figure 5.5. From the diagram it is evident that only CM patterns developed by Passega (1957) concentrate upon the variation in the coarsest half of the sample. C is the size value at the 99th percentile which is given as the upper limit of competence (of samples analysed) of a depositional agent. M represents the middle value of a sample provided that a full range of sizes was available for transport. The parameters of C and M were originally selected by Passega (1957) because the agents of deposition are best characterised by parameters that give more information on the coarsest rather than the finest fractions. CM patterns were successfully used by Bull (1962b) to separate between his three-fold classification of alluvial fan sediments. The CM patterns were indicative of the different sedimentary processes : mudflows (debris flows) and water-laid deposits (fluvial flows), giving discrete groups overlapped by samples formed of intermediate flow deposits (Figure 5.6). Bull (1962b) stated that fluvial transportation in alluvial fan environments is typified by a small difference between C and M. In contrast, mudflows exhibit large differences between C and M as the process is characterised by limited sorting. Bull (1962b) also found evidence that CM patterns can distinguish between more fluid phases of mudflow. Smaller C and M values represent deposition between more fluid phases at a lower velocity than that at which the coarser material is deposited. The CM pattern is sensitive to variations in supplied particle size characteristics. Care must be taken in interpreting CM plots as marked changes in particle size supplied as well as degree of sorting will produce distinct graphical envelopes. As it is a graphical technique, variations with depth are difficult to interpret. The CM pattern plot can be modified to meet the specified criteria.

The modification of the CM plot must result in a sorting measure that can be used to provide a visual change with depth and give a relative value for the difference between the median and coarsest particle size which is indicative of the degree of sorting of the sample. A relative numerical measure, on a continuous scale is provided by the following equation

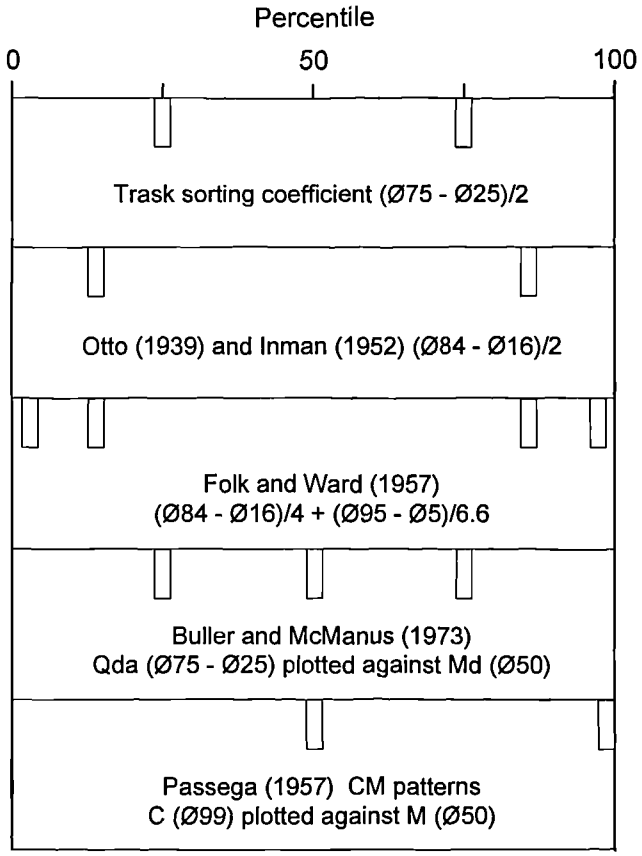


Figure 5.5. An illustration of the range of percentiles used to measure sorting.

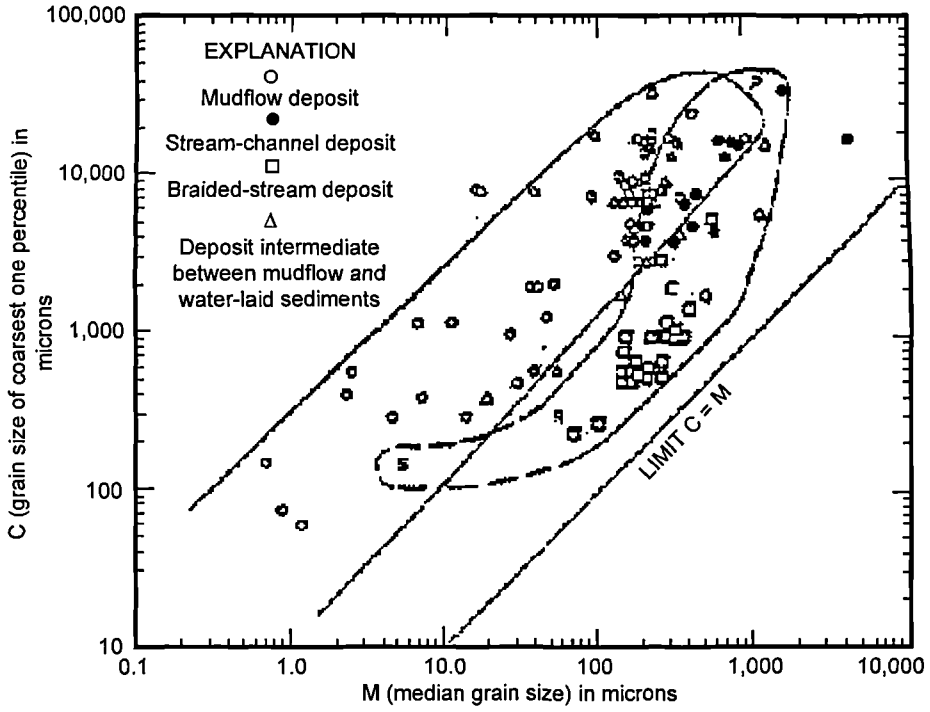


Figure 5.6. Bull's (1962, p214) discrimination of the mudflow, stream-channel and intermittent deposits using CM Patterns.

$$\text{CM difference} = \frac{C - M}{M} \qquad \text{(Eq. 5.1)}$$

The dimensionless index provides a relative measure of the gap between the median value and the 99th percentile, allowing comparison between particle sizes of difference size particle size distributions. The resulting dimensionless value will still be related to the median value. If the median is high, C-M is constrained so the CM difference must be small. If the median is low, CM differences will be proportionally higher. Despite the association the CM difference is still an effective measure of sorting as the differences observed are minimal.

The artificial cut-off of the matrix material sampled at 2 mm will produce an edge effect apparent in the particle size distribution. To account for the added bias influencing the gap between the median and the 99th percentile, the 90th percentile is taken as a measure of the coarsest particle size within the measured distribution. In all, three percentiles have been chosen to be included in the index, the % difference between M or median value and the 70th, 80th and 90th percentiles

$$P_nM \text{ difference} = \frac{P_n - M}{M} \qquad \text{(Eq. 5.2)}$$

where $P_n = n^{th}$ percentile.

The larger the P_nM value the less sorted the sample. The use of three equally spaced percentiles provides a useful summary of the coarsest half of a samples particle size distribution (see Appendix 1.2). Figure 5.7 illustrates how P_nM values can be used to show the characteristics of the upper regions of the particle size distribution relative to each other and how different particle size distributions can affect the spacing of percentile values.

Although the median value is mathematically cancelled out in the P_nM index, values of the index are associated with the median size. Low $P_{90}M$ values, indicative of a well sorted sediment, commonly have high median values. The negative association is linked to fluvial transport. The size range at which preferential loss occurs depends upon two factors, the particle size range of the parent material and the velocity of the event. The velocity of the transporting water determines which

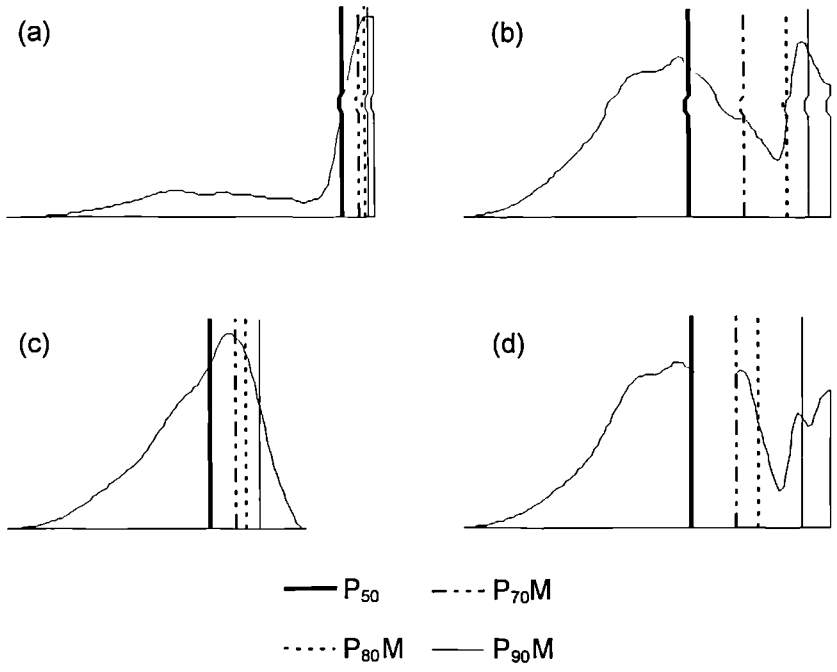


Figure 5.7. A schematic illustration of P_nM values plotted on the particle size distribution of four contrasting samples. (a) NGS1 $S_{no}15$. (b) BGS2 $S_{no}10$. (c) WGS1 $S_{no}1$. (d) TGS1 $S_{no}20$

particle size can be maintained within the moving water column. The coarsest particle sizes within the marginal entrainment velocity range will undergo preferential transport by saltation and traction at the channel boundary. The change in velocity required to lose particles from suspension is smaller for the coarsest particle sizes and greater for the fine material. The preferential removal of sediment from the sample will occur in the finest particle size fractions. Coarser sized clasts are concentrated in the sample resulting in a higher median value in the samples particle size distribution. A measure of the skewness of the particle size distribution will link together samples with a high median value and a low P_nM values. The P_nM difference for samples from fan sections provides a method for determining changes in the transport mode, sorting by fluvial action (low P_nM difference) or deposition by debris flow (high P_nM difference), with depth. To assign a mechanism of transport to separate layers the information supplied by P_nM values needs to be confirmed by the other two techniques. The index however provides an independent means of identifying samples that exhibit similar values and sorting characteristics. Individual units can be identified which were transported and deposited by the same flow.

5.4 Derivation of a sequential change in transporting mechanism

The identification of a sequential change in the mechanism of sediment delivery within a vertical section is achieved in two steps. Initially, the vertical section is segregated into separate units, each having distinctive structural and physically measured characteristics. The characteristics are then used to assign a transport mechanism in agreement with diagnostic properties. The successful assignment of a transporting mechanism is reliant upon the ability to clearly delineate boundaries between separately transported sediments.

5.4.1 The segregation of separately transported sediments

Working from the base of a section, the identification of separate layers has been achieved in this research by grouping together samples that exhibit similar properties. Unit segregation is primarily based upon the assumption that the deposited sediments of a given flow will exhibit comparative if not uniform properties throughout its preserved depth. The depth at which structural and measured properties change, represents a transition between flow deposits. The upper and lower boundaries of a distinct depositional unit can therefore be defined if the sampling framework used is of sufficient resolution. Reliance is also placed upon

samples retaining representative properties of the sedimentary deposit from which it was taken. The type of changes considered to signify a transition between flow deposits include a substantial increase or decrease in $P_{90}M$, a change in percentile spacing (figure 5.7), a stark decrease or increase in total sand content coincident with a change in sand fractionation, and any obvious visual change in sediment characteristics such as structure, fabric and texture.

The stratigraphic log and down-section plots of the measured physical properties for each section are presented by site. The unit segregation adopted within each section is also illustrated, including a code which summarises the character and type of change that resulted in the recognition of each transition. The data for each measured property are given in Appendix 2. An example of the unit identification is given in Figure 5.8, using section TGS2 from Thickcombs Gill, the Howgill Fells. In identifying unit boundaries it was found that their placement is commonly confirmed by a change in more than one property at the same depth interval between two relatively uniform layers. The majority of the units contain two samples or more which exhibit comparable properties. Units also have clearly defined upper and lower boundaries. The uniformity displayed by samples within a number of units attests to the sample representability. It can be assumed that fluctuations observed in samples within a unit result from the character of the transport mechanism rather than from sampling error.

There is a close correlation between the depth at which physically measured properties and visual characteristics change and where changes have been identified in the contextual framework. Not all transitions are visually apparent. In some instances a change in sorting properties alone serves to identify a transition between separately transported units. $P_{90}M$ values and percentile spacing provides a useful summary of the characteristics of the coarser half of a sample particle size distribution. Slight changes in spacing between percentiles can be readily seen. Thus, it is easier to observe samples which exhibit uniform sorting characteristics and to differentiate sequential changes.

A transition between units is not always associated with extreme change. A relative change in the percentile spacing of samples from even to left skewed can represent a transition between separately transported sediments. The uniformity of sorting properties within a unit suggests their transportation by a single mechanism.

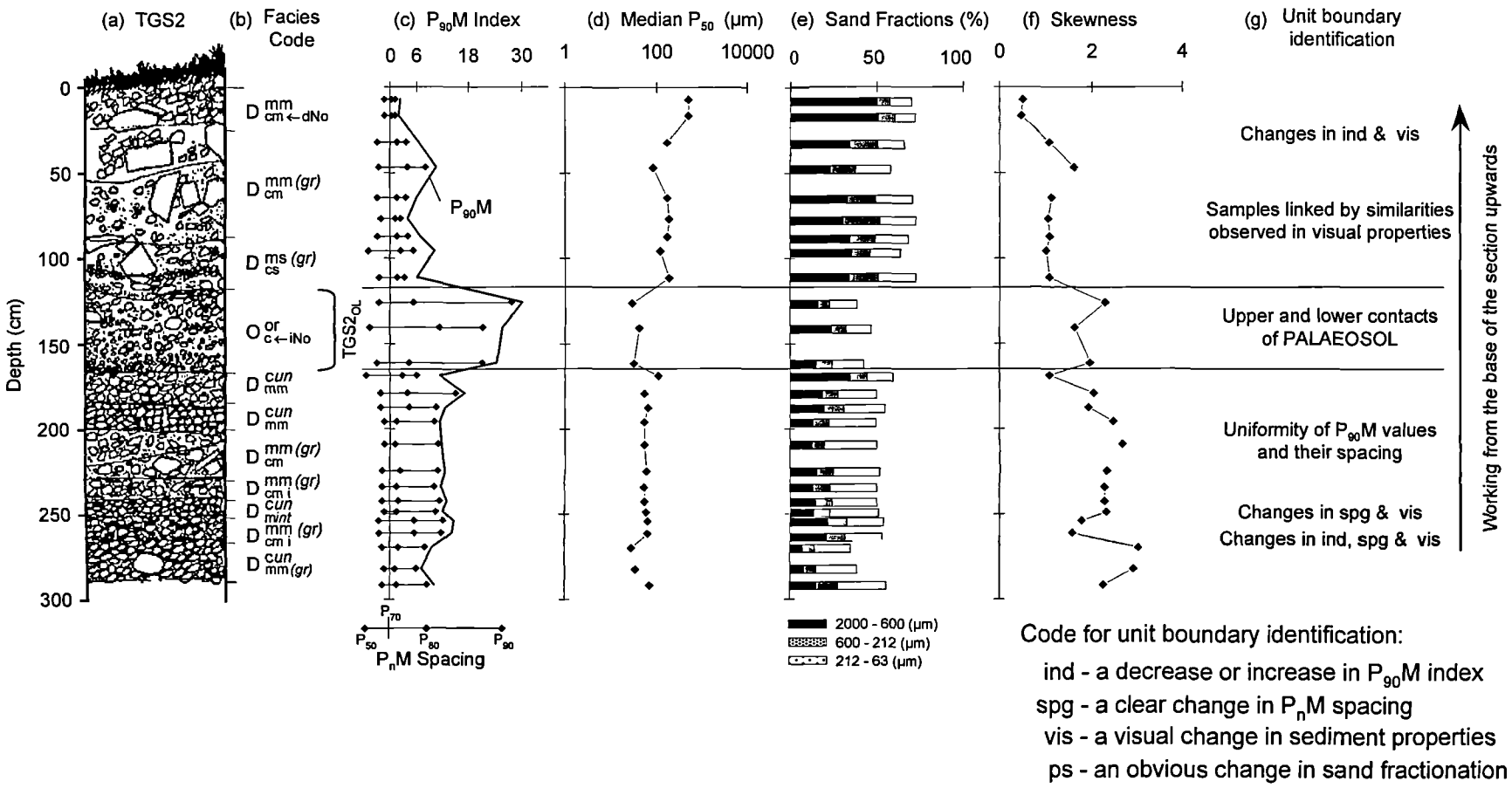


Figure 5.8. An example of unit boundary identification using: $P_{90}M$ and P_nM spacing; visual changes in sediment properties; and sand content and fractionation. TGS2 from the Howgill Fells is used as an example.

Relative transitions based upon small but sufficient changes in sorting properties highlight the sensitive nature of the technique in separating layers. The layers have been transported separately, but by a similar transport mechanism. Sorting properties in a small number of units do not have a discernible pattern between adjacent samples. Unit separation using sorting properties in layers which have uniformly low $P_{90}M$ values <3, is not as sensitive. Sorting properties cannot be used alone as a means of unit segregation. Sedimentary structures and differences observed in the overall particle size distribution have therefore been used where necessary. A combined approach is essential in identifying boundaries between separately transported sediments. Where change in only one property separates a unit, a degree of subjective interpretation is required.

The diagnostic difference in the sorting properties between the flow mechanisms provides the basis for the differentiation between relict deposits of each flow type. The capability of $P_{90}M$ as a measure of the degree of sorting of a sample must first be established before data from all measures combined can be used to assign a transport mechanism.

5.4.2 $P_{90}M$: as a measure of sorting

If $P_{90}M$ represents a continuous scale of sorting, $P_{90}M$ values of debris flow and fluvial flow deposits should be distinguishable. The difference in sorting properties of sediments of two- and one-phase flow, introduced by their rheological properties, is expected to result in a measurable difference. The difference is expressed by an apparent break or gap where sorting characteristics, and thus $P_{90}M$, significantly change in response to changing transport mechanisms. A log frequency plot of all $P_{90}M$ values is presented in Figure 5.9a. Their distribution is clearly bimodal. Samples known to have been transported by fluvial action and by debris flow were chosen as index samples to test the continuity of the $P_{90}M$ scale. An exposure of deposits near the apex of Wolflea Gill, Langdale in the Howgill Fells is composed almost entirely of deposits exhibiting all the classic characteristics of debris flow deposits. The 2 m sequence is composed of massive, structureless material within which large boulders are dispersed throughout. Samples were taken principally from this exposure to provide an index sample of debris flow which deposited 2 m of sediment in one flow. A summary of the characteristics of each index sample is presented in Table 5.5. The plotted position of index samples in the frequency distribution confirms the continuity of $P_{90}M$ values. Their position also indicates that

the two modes evident in the distribution represent a change in transport mechanism from fluvially sorted to debris flow deposits.

Comparison of the $P_{90}M$ plot with plots of other calculated measures of sorting emphasises its success (Figure 5.9). Although some of the frequency plots show bimodality, the position of the index samples (Table 5.5) indicate that the sorting measures do not represent a clear continuum transition between flow mechanisms. The index samples overlap in the frequency plot of the original Trask coefficient (Figure 5.9c). It is argued that the concentration of $P_{90}M$ upon the coarser half of the particle size distribution has resulted in the clear bimodality and continuity of the index values. The characteristics exhibited by $P_{90}M$ signify its usefulness as a tool for transport mechanism assignment. It is clear that transition between fluvial flow and debris flow occurs in the < 2 mm size range.

The size of the peaks in each modal distribution suggests that in all of the features investigated debris flows have been more frequent than fluvial flows. The range of values in each peak signifies that $P_{90}M$ values represent a wide range of sediment concentrations, essentially sediment concentrations increase with increasing $P_{90}M$. The overlap between the two populations represents a zone of transition within which the rheological properties and thus sorting characteristics change. The transitional zone contains extremes of fluvial and debris flow deposits and the whole of range of hyperconcentrated flow deposits. Boundary values of $P_{90}M$ that can be used to separate between fluvial flow, hyperconcentrated flow and debris flow deposits are equivalent to a range of $P_{90}M$ within which the two peaks overlap (Figure 5.10b). The values are specific to the characteristics of the deposits sampled in this study. Application of the technique elsewhere will have to account for wide-scale variety in the deposits sampled.

The spread and range of $P_{90}M$ within the fluvial peak is much smaller in comparison to the range exhibited by the debris flow peak, ranging between 0.4 and 3.4. The debris flow peak ranges from 5 up to values of 40 plus. If the assumption of a continuous $P_{90}M$ scale holds, $P_{90}M$ values of hyperconcentrated deposits will fall somewhere between > 2.5 and < 4. These two values are taken to represent an arbitrary upper limit of fluvial and lower of debris flow respectively. The marked difference in the range of $P_{90}M$ values between fluvial and debris flow deposits is controlled by flow rheology. The rheology of debris flow deposits is much more

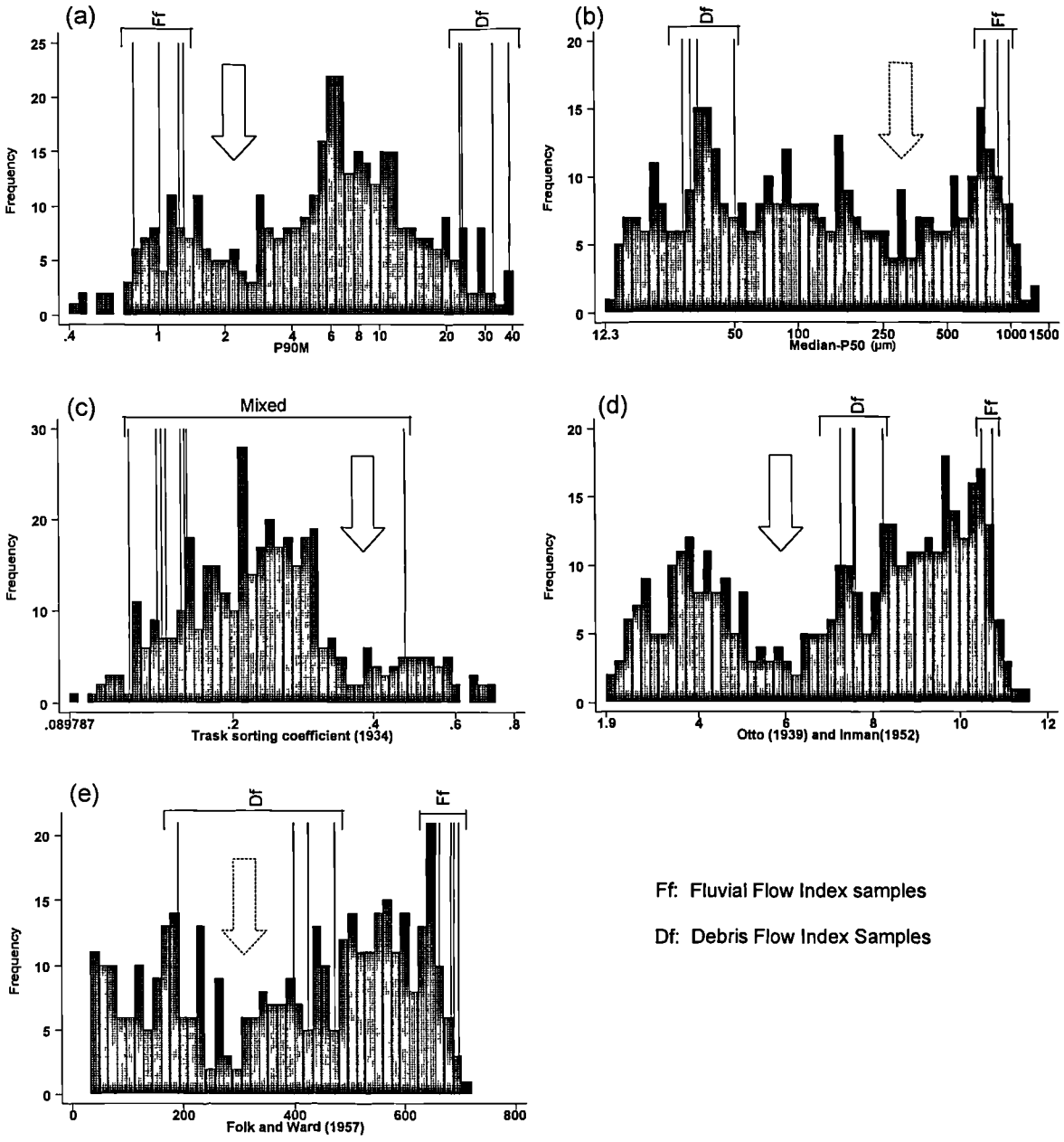


Figure 5.9. A comparison of the $P_{90}M$ index with plots of other calculated measures of sorting

Table 5.5. Sorting data for the index samples

Section	Sample Number	√(Ø75 - Ø25) Krumbein (1932)	(Ø84 - Ø16)/2 Otto (1939) and Inman (1952)	(Ø84 - Ø16)/4 + (Ø95 - Ø5)/6.6 Folk and Ward (1957)	Median Ø50	$P_{90}M$
NGS1	15	0.14	10.49	662.7	754.8	1.25
	16	0.47	10.75	684.0	9873	0.78
	17	0.16	10.77	689.19	874.3	1.02
	18	0.12	10.75	697.5	763	1.31
Maximum		0.72	11.48	712.7	0.310	40.09
Median		0.26	7.21	391.37	262.19	8.11
Minimum		0.09	1.95	33.21	12.3	0.41
WGS1	1	0.16	7.27	397.7	30.92	32.6
	2	0.14	7.61	423.5	28.47	38.6
WGS2	1	0.14	8.24	190.0	33.51	23.8
	2	0.16	7.57	472.4	50.37	23.3

variable and this is reflected in the wide range of values and variability found in the second debris flow peak. The wide range of $P_{90}M$ values are more likely to be governed by a number of factors including the character of the parent material supplied, the magnitude of the initiating force, boundary conditions, transport distance, and the overall volume of transported sediment. As the debris flow index points are taken from a 2 m section of sediments that were deposited by the same initiating force, the high $P_{90}M$ values may reflect the high magnitude of the event. It is possible that lower $P_{90}M$ values near or around the boundary identified may have undergone post-depositional alteration, reworking, illuviation or eluviation of fines. In the assignment of transport mechanism a signal of post-depositional alteration will be found at the upper and lower boundary values of identified debris flow units. Careful attention must be paid to the nature of contacts between debris flow and fluvial flow units to determine if upper parts of debris flow deposits have been reworked.

A plot of $P_{90}M$ versus the median, a measure of size, emphasises the differences observed in the characteristics of fluvial flow from the other flow types (Figure 5.11c). The plot reveals an association between size range, the degree of sorting and hence the transportation mechanism. The size range between 250 μm and 500 μm represents a threshold or preferential size at which change occurs between transport mechanisms. The association between debris flows and size is not strong. Increasing $P_{90}M$ values in the debris flow peak are not specifically associated with a change in a particular size range. In Figure 5.11c a huge range in the size of the median is apparent for any given $P_{90}M$ value, although variability decreases with increasing $P_{90}M$ values. Changing sediment source characteristics may account for the variation.

Fluvial deposits have tightly constrained median values which taken alone show a high negative correlation. Below a $P_{90}M$ value of 3 there is a -0.87 correlation with the median value. The strong negative correlation indicates that with decreasing size $P_{90}M$ values increase, highlighting the strong association between particle size and the preferential sorting action of water. With increasing velocity larger particle sizes are maintained within the sorting column and thus the median value of the remaining sample is high as a result. The association of $P_{90}M$ in the fluvial peak with size is made clear by plotting $P_{90}M$ against each particle size fraction (Figure 5.12). The greatest variability in fluvial deposits is seen in the plot against the medium sand

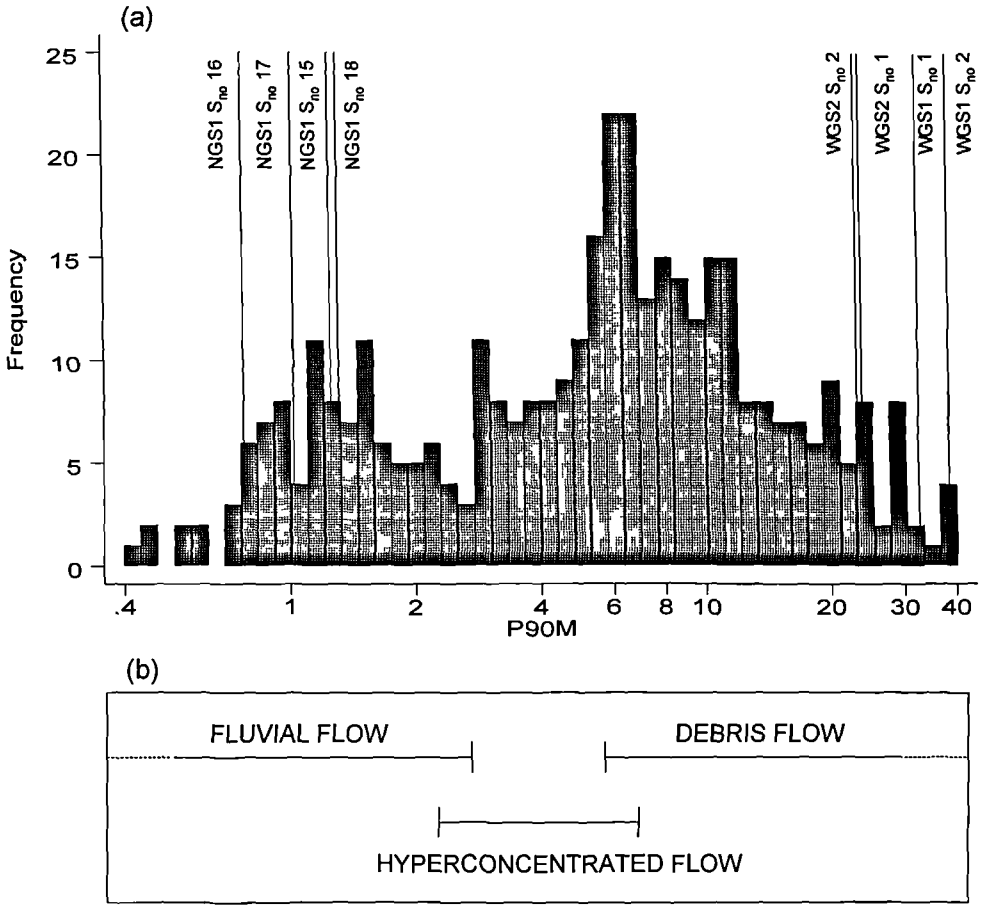


Figure 5.10. Differentiation between fluvial flow, debris flow and hyperconcentrated flow (a) a plot of $P_{90}M$ for all section samples results in a bimodal distribution (b) the identification of boundaries between each flow type

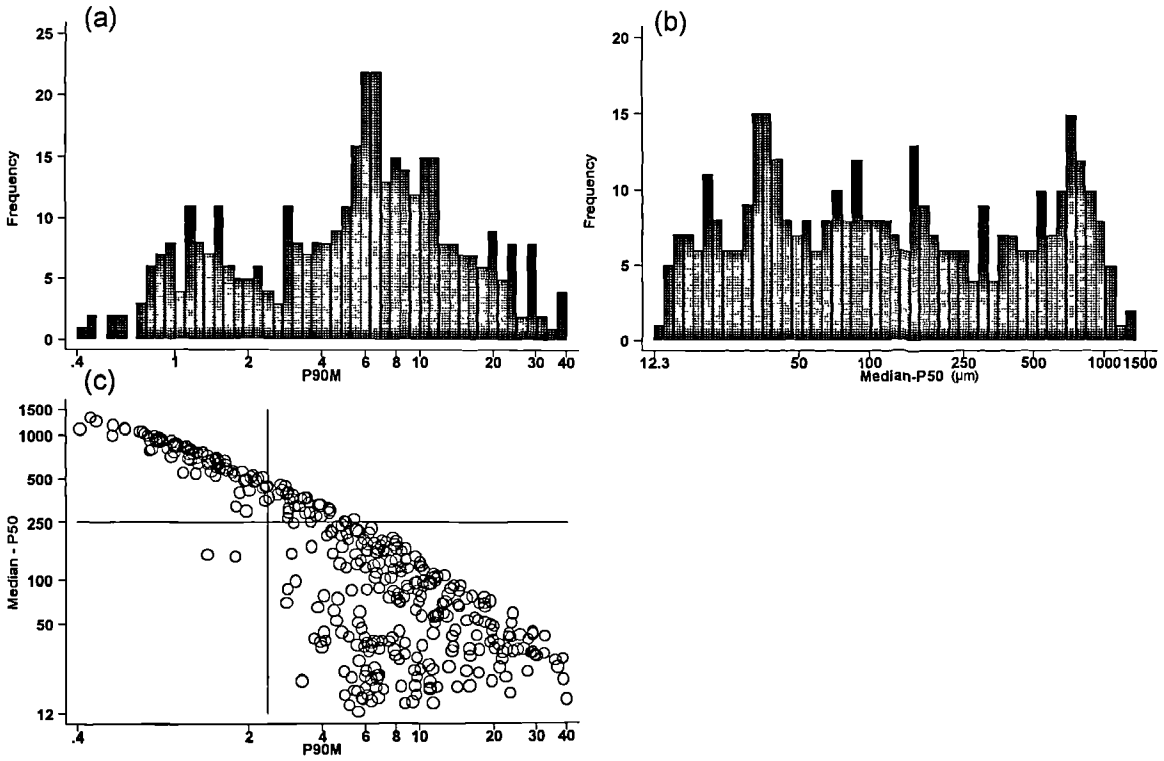


Figure 5.11. An illustration of the relationship of $P_{90}M$ with size. The plot of median for each sample (b) does not exhibit the same bimodality as $P_{90}M$.

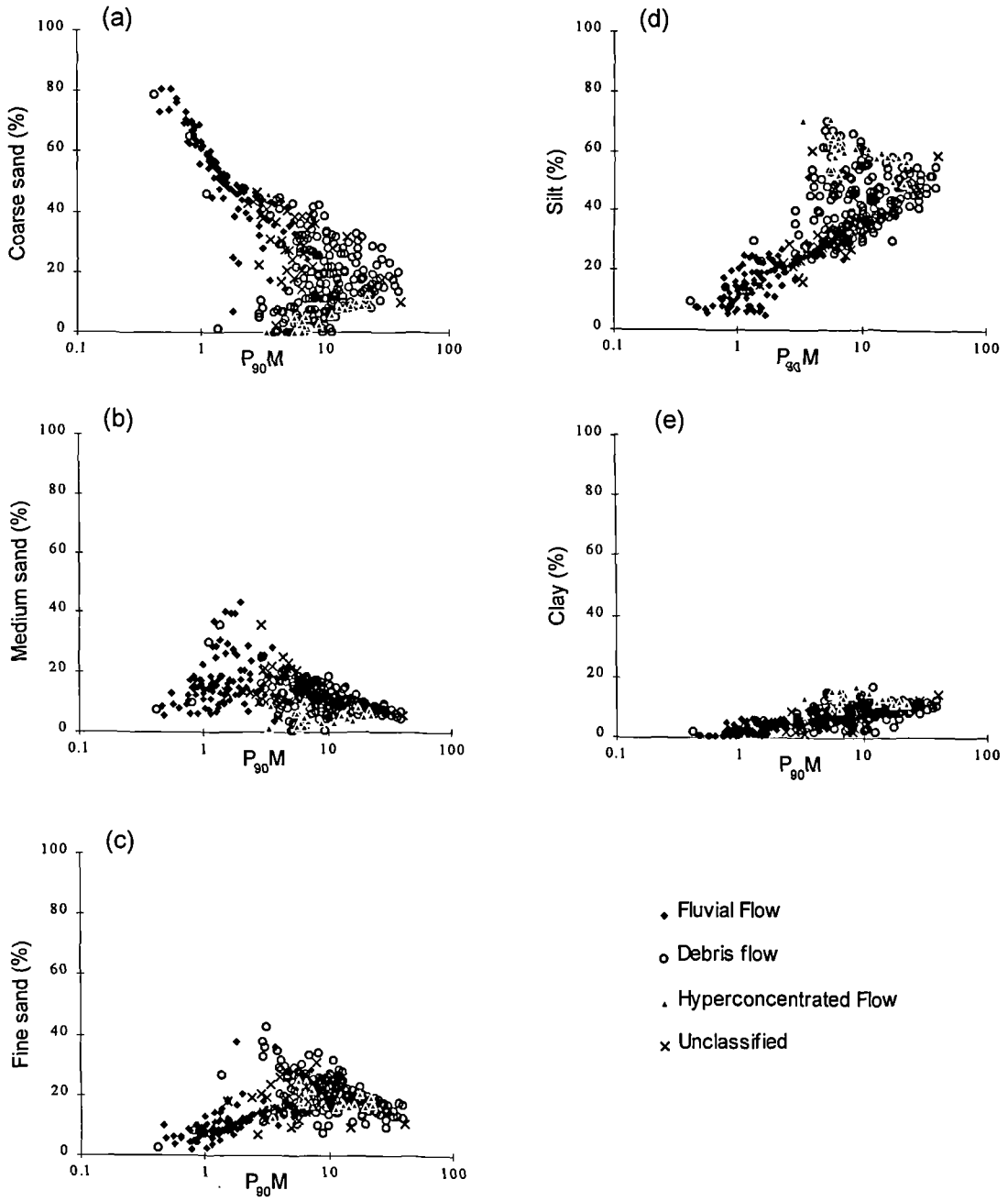


Figure 5.12. The relationship of *P90M* values with (a) coarse sand, (b) medium sand, (c) fine sand, (d) Silt and (e) clay size fractions

fraction (Figure 5.12b). As the median sand fraction increases, $P_{90}M$ increases. The relationship suggests an association between $P_{90}M$ values and increasing velocity or magnitude. A similar trait is found for the relationship between the $P_{90}M$ and the finer sand fraction (Figure 5.12c). A higher $P_{90}M$ in the fluvial range indicates a higher magnitude transporting event. Within and above the range, variation in particle size with increasing $P_{90}M$ represents a change in the magnitude of transporting flow. Variation in debris flow characteristics is maintained in all particle size fractions (Figure 5.12), as debris flows cannot preferentially remove a specific particle size. The association of fluvial $P_{90}M$ values with particle size and the wide range of $P_{90}M$ values found for debris flow deposits highlights the sensitivity of the $P_{90}M$ technique. The potential exists to differentiate between deposits that have been transported by the same transport mechanism but in response to different controlling factors.

In the assignment of a transport mechanism a degree of uncertainty is introduced for samples which have $P_{90}M$ values that fall within the range between the two bimodal distributions (Figure 5.10b). Other diagnostic properties have been used to supplement transport mechanism identification. An evaluation of the overall sand fractionation, position of the median and the overall clay content are used to differentiate between higher magnitude fluvial events and debris flow deposits. Fluvial flows have a higher median, a greater contribution from the coarse sand fraction, and low clay contents. The recognition of hyperconcentrated flows is difficult as the deposits are likely to exhibit sorting characteristics comparable to both high magnitude flow events and debris flows. The identification of hyperconcentrated flow within this range relies primarily upon an evaluation of the total sand content.

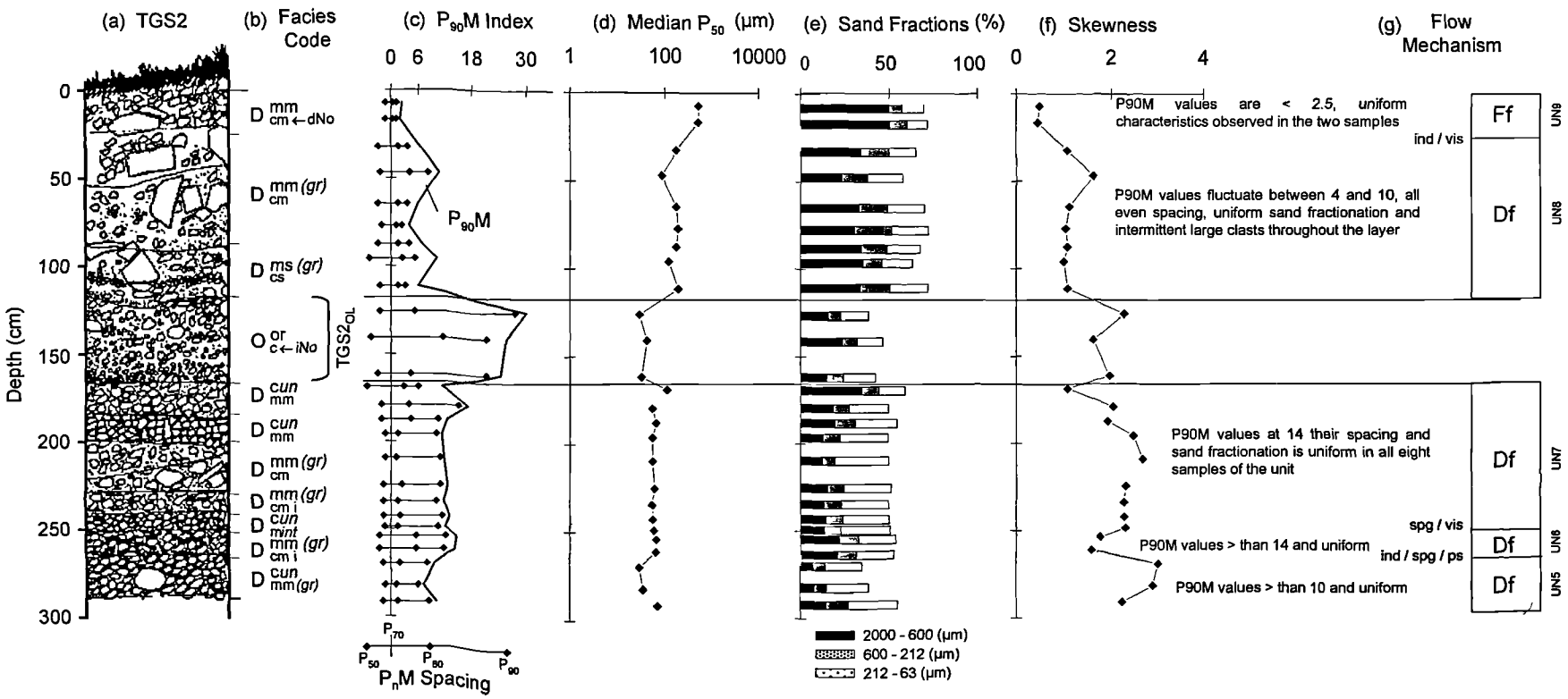
5.4.3 Unit assignment of transport mechanism

Using the characterisation of $P_{90}M$ values all measure were combined to assign a transport mechanism to each unit. A summary of the properties exhibited by each unit, used in the assignment of its transporting mechanism, can be found in Appendix 2. An example of how transport mechanism was assigned is illustrated in Figure 5.13. In each unit identified not all $P_{90}M$ values are uniform. It is the restriction imposed by upper and lower boundaries which confine samples to the same units. Despite the fluctuations, each individual unit exhibits a unique character which separates it from the layer immediately above and below.

In only two units is there a degree of uncertainty introduced in the assignment of a transport mechanism. Sorting properties fluctuate markedly in $NGS1_{UN2}$ and $WBS2_{UN2}$ (Appendix 2): their assignment is therefore based upon other diagnostic properties. In all other units P_nM values and spacing have identified upper and lower boundaries of separate flow deposits and has proved sensitive in the identification of the mechanism of transport. In a number of cases sorting characteristics have identified fluvial deposits that, without the aid of $P_{90}M$, would have been identified as debris flow deposits. The facies description of $HBS1_{UN1}$, $HBS1_{UN2}$ and $HBS1_{UN3}$ indicates poor sorting of the larger clasts throughout each unit, a characteristic associated with debris flow deposits. Low P90M values of < 2 however indicate that the sediments have undergone sorting. The presence of large clasts throughout the units can be associated with their deposition in chaotic flood conditions. Deposits have also been identified which have the greatest potential for having been transported by hyperconcentrated flow (Figure 5.14). The units have $P_{90}M$ values that are more comparable to debris flow than fluvial deposits. Hyperconcentrated flows have been found to have sorting characteristics more comparable to fluvial deposits. The potential hyperconcentrated flow units identified could represent debris flow deposits with a source material severely lacking in sand. The low total sand in the two units is more likely to be an indicator of the sand-deficient nature of the source lithologies. On this basis the units could therefore also have been transported by debris flow activity.

5.4.4 Sensitivity of unit assignment

Taking all properties into consideration each unit has a unique distinguishing characteristic, structural or measured. An obvious variation between fluvial units is based upon the characteristics of sedimentary structures. There is a clear difference between those assigned fluvial units with structure and those without. It is the change in their visual characteristics which indicate their association with different fluvial environments (Gregory and Maizels, 1991). Fluvial units within NGS1 present the full range of fluvial structures encountered in this study (Figure 5.15). Units $NGS1_{UN4}$, $NGS1_{UN5}$ and $NGS1_{UN6}$ all have similar measured characteristics. Their sediment structure indicates a sequential change in fluvial environment from deposits that are associated with the proximity of a channel through to chaotic flood deposits (Figure 5.15a). Units identified as chaotic flood deposits exhibit a range in $P_{90}M$ values. Flood deposits with higher $P_{90}M$ values and thus a larger contribution



Code for unit boundary identification:

ind - a decrease or increase in $P_{90}M$ index

spg - a clear change in P_nM spacing

vis - a visual change in sediment properties

ps - an obvious change in sand fractionation

Code for unit assignment:

Df - Debris flow

Ff - Fluvial flow

Hf - Hyperconcentrated flow

? - unclassified

Figure 5.13. An example of unit assignment using TGS2 from the Howgill Fells. An explanation of the facies codes is given in Table 4.1. The codes outlined on this diagram serve as a key for the following diagrams.

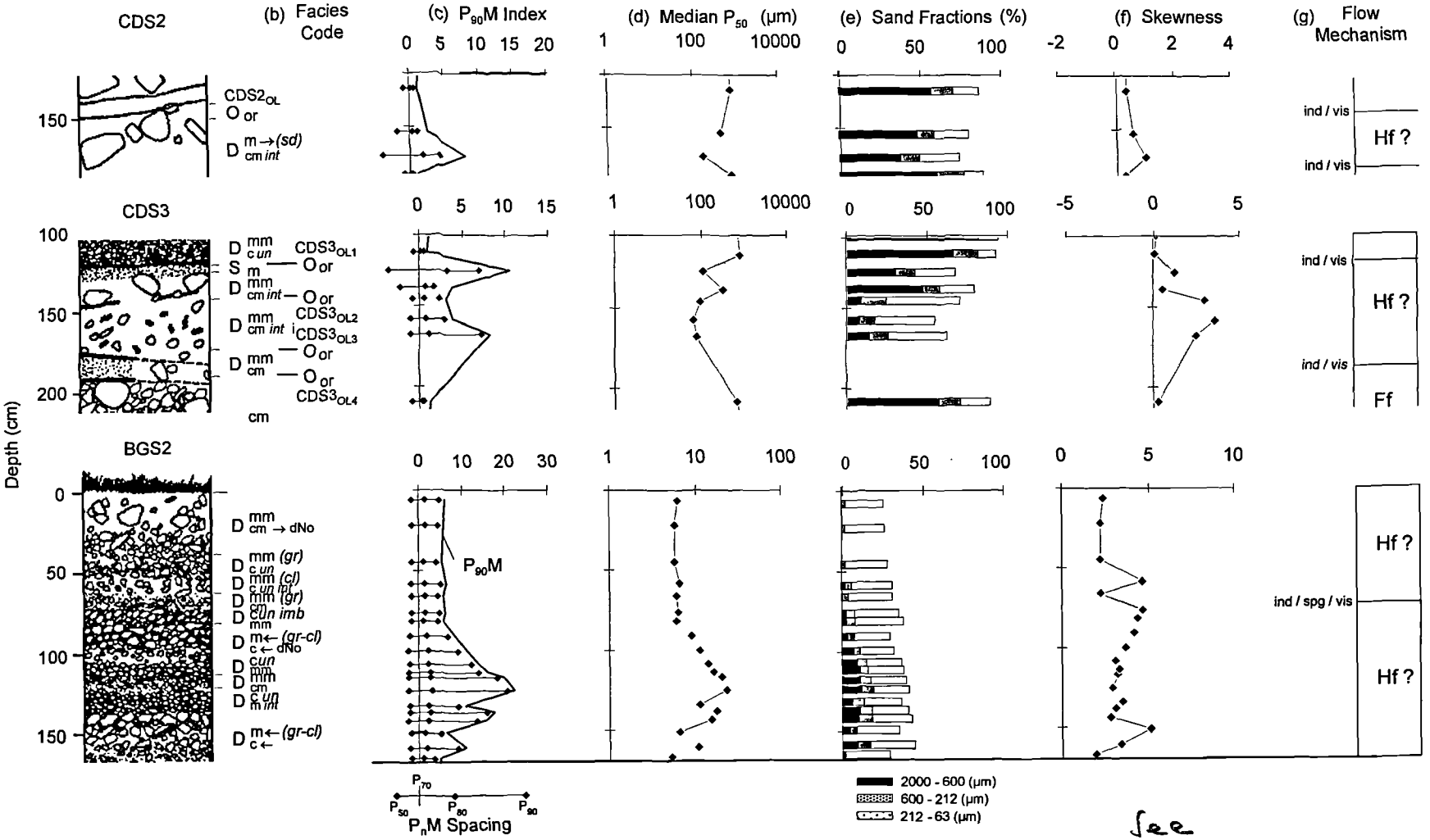


Figure 5.14. Presentation of data for units assigned with a hyperconcentrated flow mechanism. (See Figure 5.13 for key to flow mechanism assignment (g) and Table 4.1 for facies code explanation)

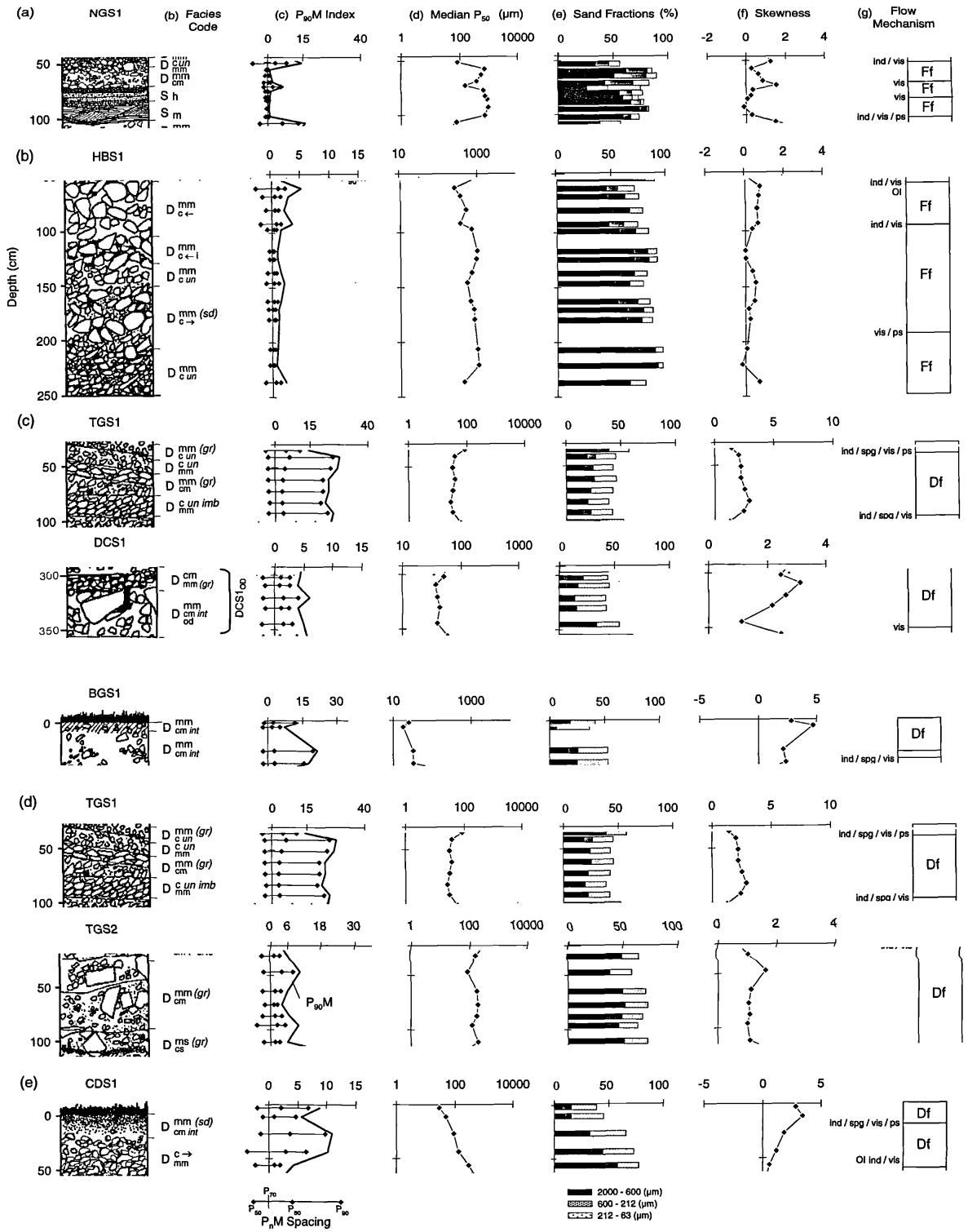


Figure 5.15. The sensitivity of the $P_{90}M$ Index and P_nM Spacing in assigning transport mechanism. Figure 5.13 for key to flow mechanism assignment (g) and Table 4.1 for facies code explanation)

from the finer sand fractions are taken to represent floods of high magnitude. An example of chaotic flood deposits of different magnitude are found in three units overlying each other in HBS1(Figure 5.15b). A difference in the size of large boulders preserved in each unit is evident. The overall size range in the larger clasts can be taken as an indicator of flow magnitude required to transport the largest boulder size. The largest boulder size can also be a reflection of the maximum particle size available for transport at the time of initiation of flow.

A combination of three factors introduces variations in the properties of the identified debris flow units. High $P_{90}M > 5$ either fluctuate or are uniform throughout the unit. Overall $P_{90}M$ values are variable between units, ranging from 5 through to 10 and 20. The visual size range of larger clasts incorporated within a flow can differ significantly (Figure 5.15c).

A change in the uniformity of $P_{90}M$ values indicates a difference in the dominance of particle support mechanisms between debris flows. Uniform properties are associated with thick viscous flows within which a rigid plug forms (Johnson and Rodine, 1984). Viscous debris flow deposits are characterised by uniform values of $P_{90}M$ and P_nM spacing that occur throughout the flows depth. The effect of longer transport distance may also result in uniform $P_{90}M$ properties. In more fluid flows turbulence is more dominant (Costa, 1988) resulting in non-uniform $P_{90}M$ properties. Turbulent debris flows are characterised by high but fluctuating values of $P_{90}M$. The character of the spacing between values of P_nM is repeated in all samples within the flow, it is the relative proportion of the gap between percentiles that fluctuates. Units $TGS2_{UN3}$ and $TGS2_{UN4}$ (Figure 5.15d) taken from Thickcombs Gill in the Howgill Fells, represent the two extremes. Both deposits are thick with over a 1 m of sediment deposited by a single flow. It is likely that the range of $P_{90}M$ values are associated with changes in the character of the supplying sediment, which is ultimately linked to regional site and catchment controls in sediment supply. Changes in the overall particle size supplied does not really affect the sorting characteristics, which remain poor. It does however affect the size of $P_{90}M$.

The character of the sediment within debris flows varies significantly. The greatest contrast is found in comparing two overlying and clearly separate debris flow units in GES1 (Figure 5.15e). In this instance it is clear that between the deposition of the two units there has been a change in sediment source. The

difference observed is not attributable to pedogenesis, the modern soil formed in the uppermost debris flow is too shallow (section 4.3.1.). Other more subtle differences in the character of sediment supply are evident in comparison between other debris flow deposits. Both spatial differences and temporal changes in the available sediment within the supplying catchment may account for a sequential change in the sediment characteristics of debris flow units. The nature of the change will be governed by regional and catchment controls.

The available structural data and measured characteristics of debris flow units cannot be readily associated with the magnitude of the debris flow. The link is not as obvious for debris flow deposits as it is for fluvial deposits, due to the difference in rheological properties between the two flow types. The detailed fabric analysis of sediments within the quantitative boundary limits of the flow deposits will however provide more reliable transported clasts sizes and flow directions. Reconstructed flow directions of the identified units in sections at Coire Dionachd and Dry Cleuch did not help in the differentiation of deposits (section 5.3.1). Reconstruction of lateral deposits of the same flow will however provide valuable information upon internal flow dynamics of the relict deposit. The use of $P_{90}M$ index will facilitate cross section and lateral correlation of an individual debris flow unit. A large magnitude debris flow on a debris cone is likely to inundate the whole surface. An idea of the lateral changes in flow thickness, direction, clast size and sorting of the same debris flow unit will provide a greater idea of the magnitude of the flow event. The combined analysis of matrix and clast material can be used to further the potential reconstruction of the rheological properties of relict flow deposits.

5.4.5 The recognition of stratigraphic sediment exhaustion

The information provided by the assignment of transport mechanism can be used to provide a comprehensive interpretation of the sequential change of transport mechanisms. The following sequential information can be obtained from available data.

1 Units that were laid down in response to the same event, provide evidence of short term sediment exhaustion.
2 Individual flows that have been reworked and those that have not; thus the time period that separates flow may be inferred.

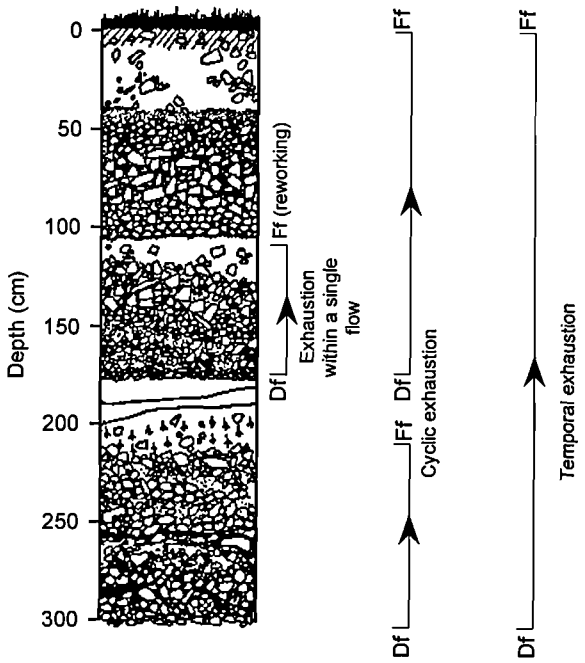


Figure 5.16. A schematic illustration of how scales of sediment exhaustion can be identified within a stratigraphic profile

3. Temporal change in transport mechanism depositing sediment in fan or cone providing evidence of long-term sediment exhaustion.
4. Change in the character of the sediment supplied to discrete transported units over time.
5. Change in sediment material properties relate to change in the spatial source of sediment from within the supplying catchment.

A schematic representation of how both scales of sediment exhaustion are identified within a stratigraphic profile is shown in Figure 5.16. The interpretation of the sequential change in transport mechanisms will be presented initially for each individual catchment grouped by site. In establishing the frequency of occurrence of each flow type and interpreting its position stratigraphically the contextual framework presented in (Chapter Four) can be appropriately modified. The comparison of data between features within and between sites can be used to determine the effect of catchment size upon the frequency of flow types that dominate in fan and cone sections.

5.5 Glen Etive - Coire Dionachd

5.5.1 Chronology of fan aggradation

The stratigraphic log and downsection plots of the measured physical properties for CDS1, CDS2 and CDS3, including an interpretation of the sequential change in transport mechanism are presented in Figure 5.17. The bulk of the oldest sediments exposed in CDS1, taken to represent the first phase of fan aggradation, were laid down by one flood event. The deposits were subsequently buried by shallow deposits of a later flood event. The size of the largest clasts increases significantly between the two deposits suggesting a higher magnitude for the later flood event. A change in sediment source characteristics can also account for the change. The fluvial deposits are sharply overlain by a clast supported shallow debris flow deposit. The clasts are uniform in size which is rare in a debris flow deposit. Its $P_{90}M$ values confirm its debris flow assignment. The presence of uniform clasts sizes within the debris flow deposit suggests prior sorting of the clasts. It is possible that channel storage was incorporated into the flow. The overlying debris flow, the last phase of aggradation within the section, contrast markedly with the debris flow it buries. The lack of clasts in the upper debris flow unit suggests a change in the character of supplying sediment between the two debris flows. In the later flow either all clasts

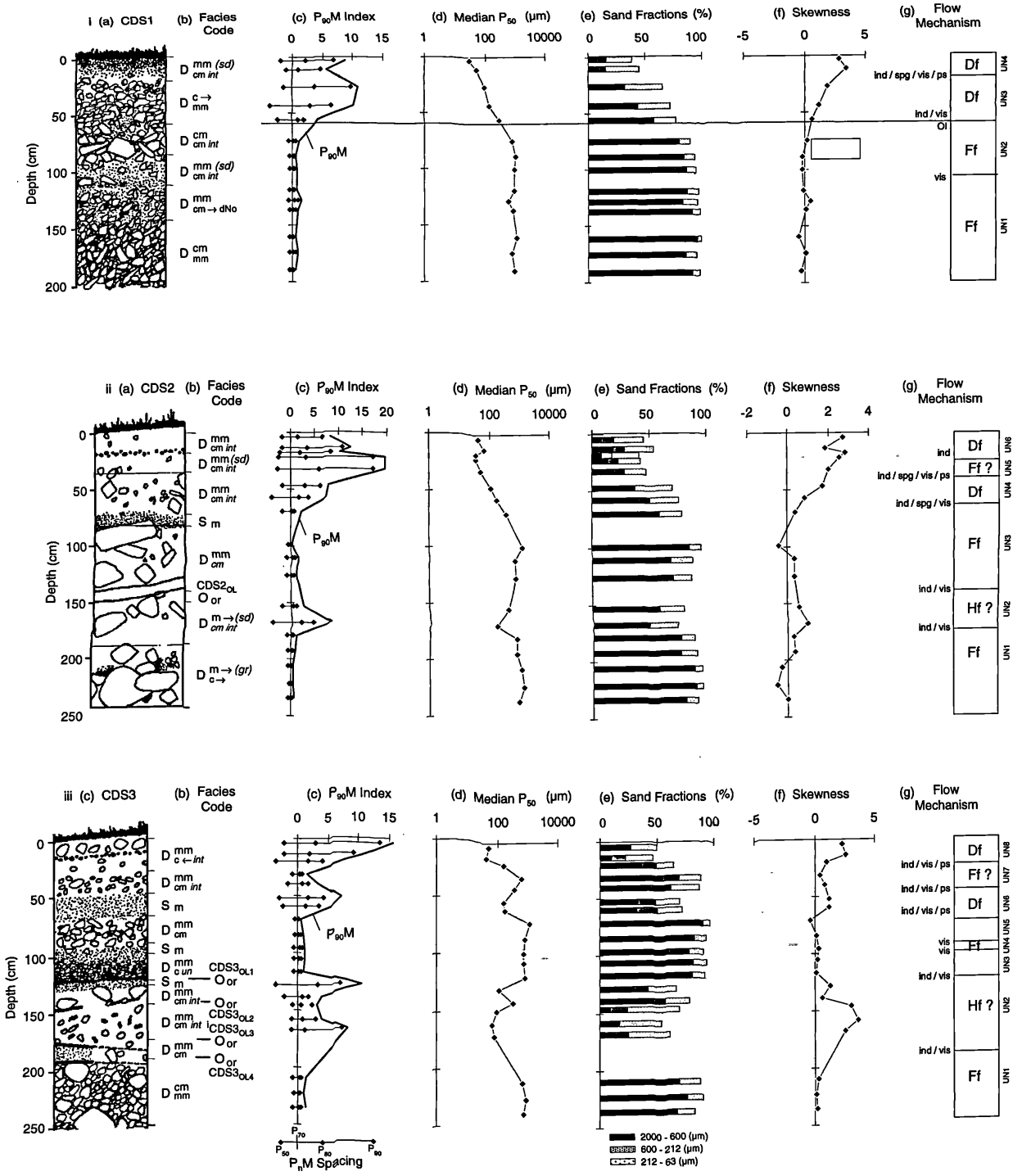


Figure 5.17. The identification of separate flow units and the assignment of flow mechanism for (i) CDS1, (ii) CDS2 and (iii) CDS3, Glen Etive (see Figure 5.13 for key to flow mechanism assignment (g) and Table 4.1 for facies code explanation)

have been removed from the channel or, due to the dominance of fines, the debris flow originated elsewhere. Within the catchment there is an obvious spatial difference in the character of the sediment available for transportation. The contrast between the only source of fines found on the east facing slopes and the clastic scree on the western side of the catchment would account for the differences observed between the debris flow units. The two units show a relationship as both have high and similar organic contents. This can be attributed to soil development as the percentage of organic material is comparable in value to that found for the soils in CDS2 and CDS3.

In CDS2 the sequential change in the transporting mechanisms is closely mirrored in CDS3. The bulk of the sediments in both sections were aggraded during the first phase of activity. The period of stability, detected at a comparable depth, was broken by the same debris flow event. It is within the first phase of fan aggradation that recognisable differences between the sections are encountered. The relationship between the deposits in the two sections is illustrated in Figure 5.18. The properties of the sediments in the two lowest units in both sections indicate that the deposits are attributable to the same two flow episodes. At the base of both sections, chaotic flood deposits are overlain by a layer which contains thin organic horizons. This layer has been recognised as the only unit in the study to have the required combination of characteristics which are suggestive of hyperconcentrated flow (Appendix 2). The preservation of organic material within hyperconcentrated flow deposits helps to explain the chaotic age sequence of the sequentially sampled radiocarbon dates obtained from CDS3 (Section 4.3). Organic material transported by hyperconcentrated flows float on its upper surface. The parallel laminar nature of the organic material observed can be explained by the sequential burial of the upper surface by consecutive pulses of the same flow. The internal inconsistency of the dates in CDS3 can be attributed to a peat block source. When peat is formed, successively younger material is incorporated producing a chronological sequence of organic material. In peat slides, peat can be transported as blocks (Warburton and Higgitt, 1998). The age sequence of the peat as a result can become mixed resulting in internally inconsistent dates.

The characteristics of the units which bury the hyperconcentrated flow show the greatest contrast between the sections. In CDS2 the unit burying the hyperconcentrated flow exhibits characteristics of a normally graded chaotic flood

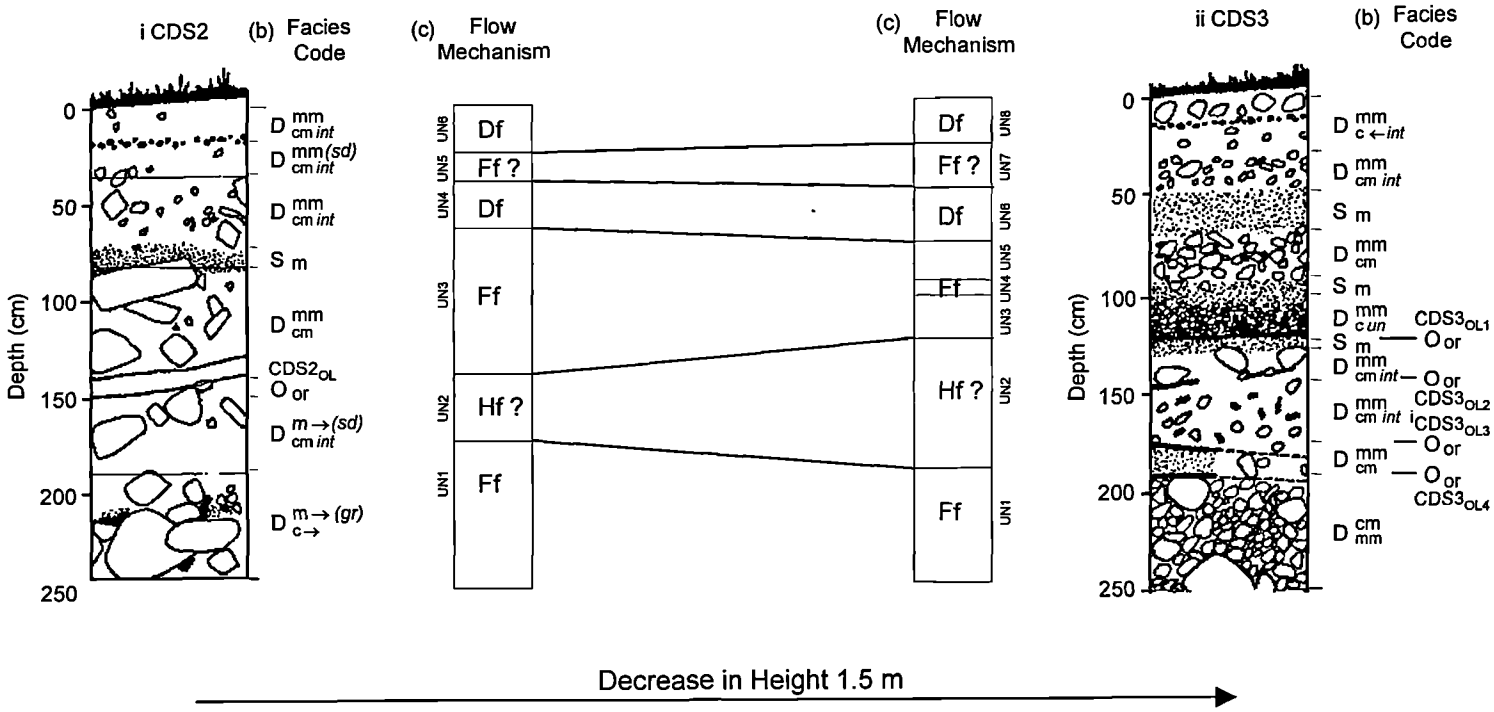


Figure 5.18. An illustration of the relationship between CDS2 and CDS3, Glen Etive. (see Figure 5.13 for key to flow mechanism assignment (g) and Table 4.1 for facies code explanation)

deposit. The flood deposit is overlain by a thick debris flow. Both units contain large boulder clasts over 20 cm in length. The equivalent deposits in CDS3 are made up of five sharply contacting and visually distinct layers. Their character, illustrated in Figure 5.17ii(a), is suggestive of separate transportation and thus deposition. The distance separating CDS3 from CDS2 is not sufficient to have produced the huge contrast observed in the clast sizes of the deposits. It is possible that fan sediments have undergone reworking but the stark contrasts observed in their character signifies an alternate source of sediment for units $CDS3_{UN3}$, $CDS3_{UN4}$ and $CDS3_{UN5}$. The close proximity of CDS3 to the main river both in height and distance suggests that the five units may represent intercalating main river and fan deposits (Figure 5.18). The immature soil has developed in contrasting sediments in the two sections. The formation of the soil represents a period of stability in both the main river and within the supplying catchment. As the debris flow deposits which cap the immature soil in both sections relate to the same flow, the source of the sediment is thus restricted to the supplying catchment.

5.5.2 Coire Dionachd development : evidence of sediment exhaustion

The first phase of fan aggradation was deposited without being influenced by activity operating within the main river. Either the river was not close enough to have interacted with fan deposits or the effects of the trigger mechanisms were restricted to a short spatial zone affecting the close surrounds of the supplying catchment. The subsequent intercalation of main river deposits with fan deposits implies the close proximity of the main river achieved by its lateral migration. The evidence signifies that activity in the main river and the supplying catchment is concurrent. The trigger mechanism must have been of a significant magnitude to have caused flooding. A general causal climatic control could have caused the intercalation of fan and main river sediments. The main river subsequently migrated to its current position as the last phase of activity preserved within CDS2 and CDS3 is a debris flow event which was generated from within the supplying catchment.

In all three sections, a debris flow is the last type of flow to be preserved before the onset of a period of stability. In CDS1, differences in the character of the sediment transported by separate but overlying debris flows indicate a spatial change in source. In CDS2 and CDS3 all of the units have a high matrix to clast ratio. The second phase of fan building continued to erode substantial drift deposits found on the eastern slopes of the catchment and within the base of the corrie in the

headwaters. The character of the sediments in the first and second phase of fan aggradation contrast markedly with the deposits of recent phases of activity which is dominated by large clasts and boulders.

5.6 Moffat

5.6.1 Dry Cleuch

In assigning transport mechanisms to the sediments of both DCS1 and DCS2 the contextual sequence of cone aggradation (section 4.4.1) is confirmed. The palaeosol in DCS2 has been formed within fluvially-transported river terrace sediments. Transport units at the top of both sections show no relationship and the three phases of aggradation are discrete. To ease interpretation of layer sequencing within the cone, the two down-section plots have been separated according to the phase order outlined in the chronological framework, with phase one at the base (Figure 5.19).

Three debris flow units constitute the first phase of cone aggradation. Their debris flow assignment confirms that the organic material dated from unit $DCS1_{UN2}$ and $DCS1_{UN3}$ was transported. The stratigraphic relationship of the three units indicates that the layers were deposited separately. The sequence of debris flow units can be interpreted as representing the complex interplay of environmental changes within the supplying catchment. Unit $DCS1_{UN1}$, due to the lack of organic material, was deposited prior to the onset of peat formation. The second unit represents the stripping of peat which has subsequently formed. The overlying debris flow originated from the exposed area and also contains debris suggestive of a wooded environment at the time of the flow. In the second phase of aggradation the palaeosol has been buried by seven separate debris flow events, aggrading over two meters of sediment. The separation of the sediments into seven discrete units is based upon relative changes in $P_{90}M$, changes in clast abundance and differences observed in the overall particle size fractionation characteristics (Appendix 2). The only evidence of fluvial activity out of all cone sediments is associated with the thickest debris flow unit in this phase. The upper sediments of the debris flow of $DCS1_{UN5}$ were reworked following its deposition to give $DCS1_{UN6}$.

Two shallow debris flows represent the onset of erosion in the third aggradational phase. They are followed by the deposition of the bulk of the sediments by one flow.

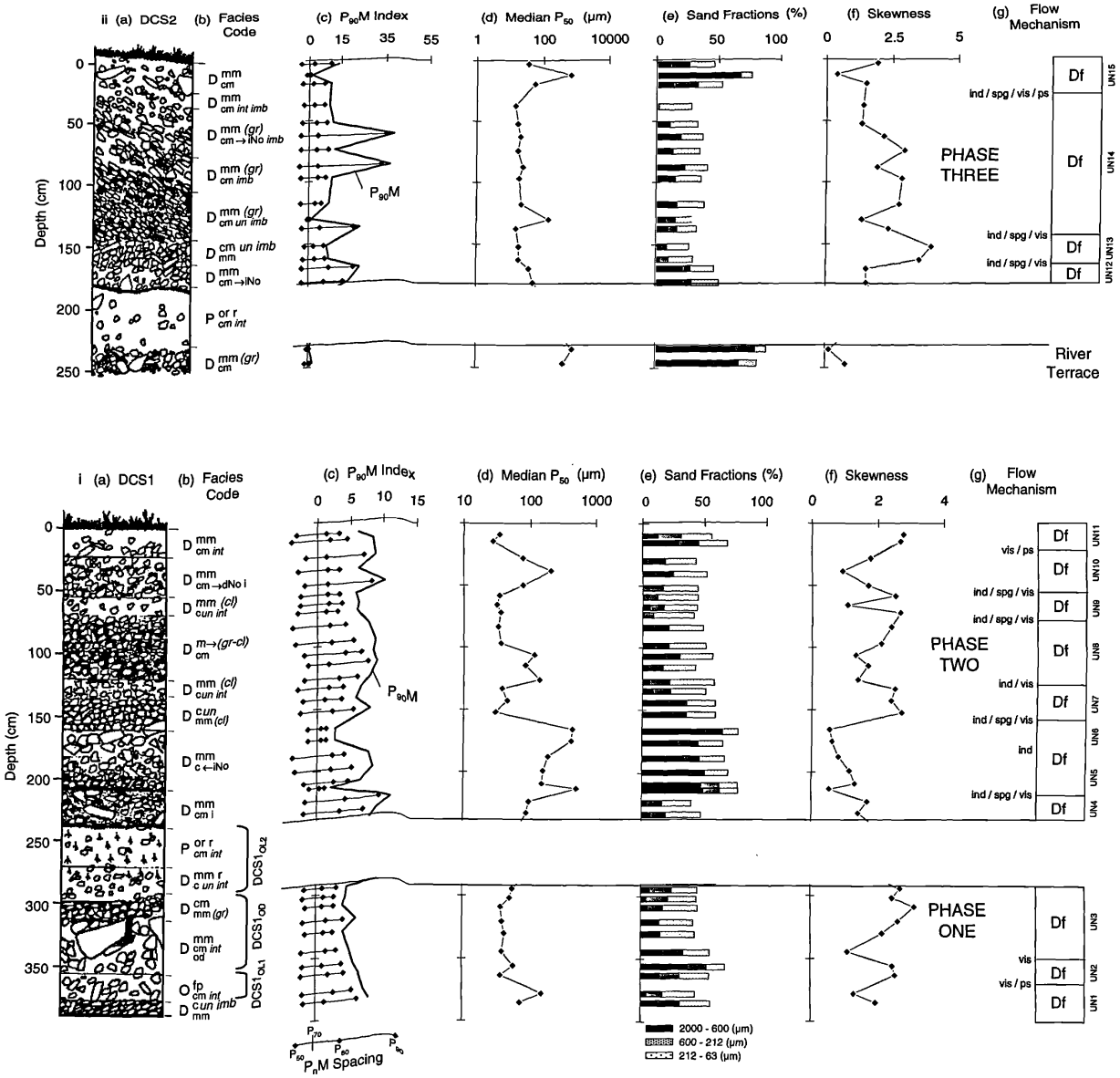


Figure 5.19. The identification of separate flow units and the assignment of flow mechanism for (i) DCS1 and (ii) DCS2, Moffat (see Figure 5.13 for key to flow mechanism assignment (g) and Table 4.1 for facies code explanation)

Activity in the cone ends with a shallow debris flow deposit. The number of debris flows aggrading a similar thickness of deposits contrasts between phase two and phase three, suggesting a difference in the rate of sediment aggradation. Phase three was deposited more rapidly that phase two. A temporal difference in the environmental conditions operating within the supplying catchment at the time of each phase of aggradation would explain the difference. The change can be attributed to an increase in the frequency of rainfall events or to human or climate induced lowering of resistance thresholds.

In phase two, two different lines of evidence of sediment exhaustion have been recognised. The overall particle size characteristics of the reworked debris flow ($DCS1_{UN5}$ and $DCS1_{UN6}$) contrast with that of the debris flows immediately above and below. The stark difference implies a spatial difference in sediment source characteristics. The fluvial reworking of the unit is also suggestive of short term sediment exhaustion. The debris flow units also exhibit an apparent pattern in the number of clasts preserved within each unit. The sequential change in clast abundance is illustrated in Figure 5.19a. The pattern is suggestive of a temporal periodicity in the availability of clasts for transport. The debris flow units and their characteristics can be associated with the periodic build up of sediment within the supplying catchment. In phase three periodicity in clast abundance is not evident. The nature of the deposits suggest that the two shallow debris flows lowered the threshold in the supplying catchment, resulting in the large scale of the following event. The thickness of $DCS2_{UN14}$ attests to the continued availability of sediment within the supplying catchment.

The periods of stability in both phase two and phase three are broken by shallow debris flow deposits. The shallow nature of the debris flow units do not suggest their formation in response to an extreme event. It is possible that the onset of activity was caused by the lowering of resistance thresholds within the supplying catchment, either human or climate induced. The subsequent phase of cone aggradation is cyclically controlled by the availability of sediment until the initially eroded area becomes stabilised.

5.6.2 Hermanlaw Burn

Three separate chaotic flood deposits constitute the first phase of fan aggradation in HBS1 (Figure 5.20). The first two units have been separated on the basis of a sharp

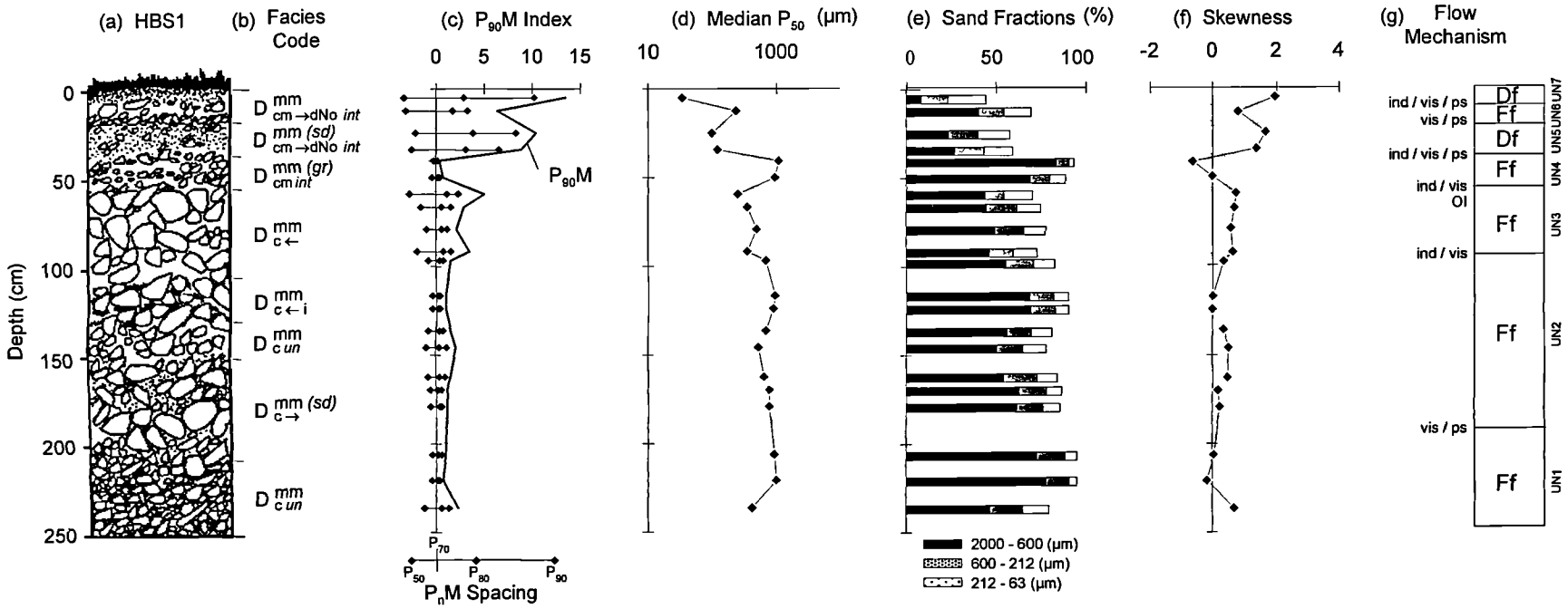


Figure 5.20. The identification of separate flow units and the assignment of flow mechanism for HBS1, Moffat (see Figure 5.13 for key to flow mechanism assignment (g) and Table 4.1 for facies code explanation)

obvious change in the dominant clast size preserved within each unit. The third and last chaotic flood deposit $HBS1_{UN3}$ also exhibits an increase in the dominant clast size but the increase is coincident with a rise in $P_{90}M$ values. Taken together the characteristics are indicative of an increase in flood magnitude. The immature soil (section 4.4.2) is preserved within the upper sediments of $HBS1_{UN3}$. The nature of the contact with the overlying fluvial unit does not indicate an erosive contact. It would take a highly erosive event to strip the large clasts found with the upper sediments of $HBS1_{UN3}$. Therefore, the increase in organic material does not represent the remnants of an eroded soil.

The character of the transported units in the second phase differs significantly from units deposited in phase one. The thickness of the preserved units are shallower, debris flow deposits are present and the dominant clast size has markedly decreased. The shallow nature of the deposits could have resulted from the close proximity of the trunk channel. The shallow debris flow deposits thus represent deposits that have overtopped the banks of the trunk channel. It is clear that the change in clast size either represents a change in the magnitude of the transporting event or is an indicator of a marked change in the character of available sediment between the two phases of fan aggradation.

5.7 Howgill Fells

5.7.1 Burnt Gill

The river terrace origin of the sediments within which the palaeosol in BGS1 and BGS2 has been interpreted to have formed is refuted by the sorting characteristics found in samples taken below both palaeosols. In BGS1 three separate layers have been identified below the soil horizon (Figure 5.21). A well sorted fluvial layer separates two units which have $P_{90}M$ values above 20, indicative of very poor sorting. As the $P_{90}M$ values of $BGS1_{UN1}$ and $BGS1_{UN3}$ are very high, uniform and are separated by an obviously distinct fluvial layer, their high values cannot be attributed to post-depositional alteration. The deposits can be interpreted in two ways. The sediments below the palaeosol represent a discrete earlier phase of cone aggradation completely separate from the influence of the main river. The fluvial layer represents intercalating gully and main river sediments. In both scenarios activity within the supplying gully must have begun before the formation of the palaeosol. In BGS2, only one unit has been identified below its palaeosol (Figure

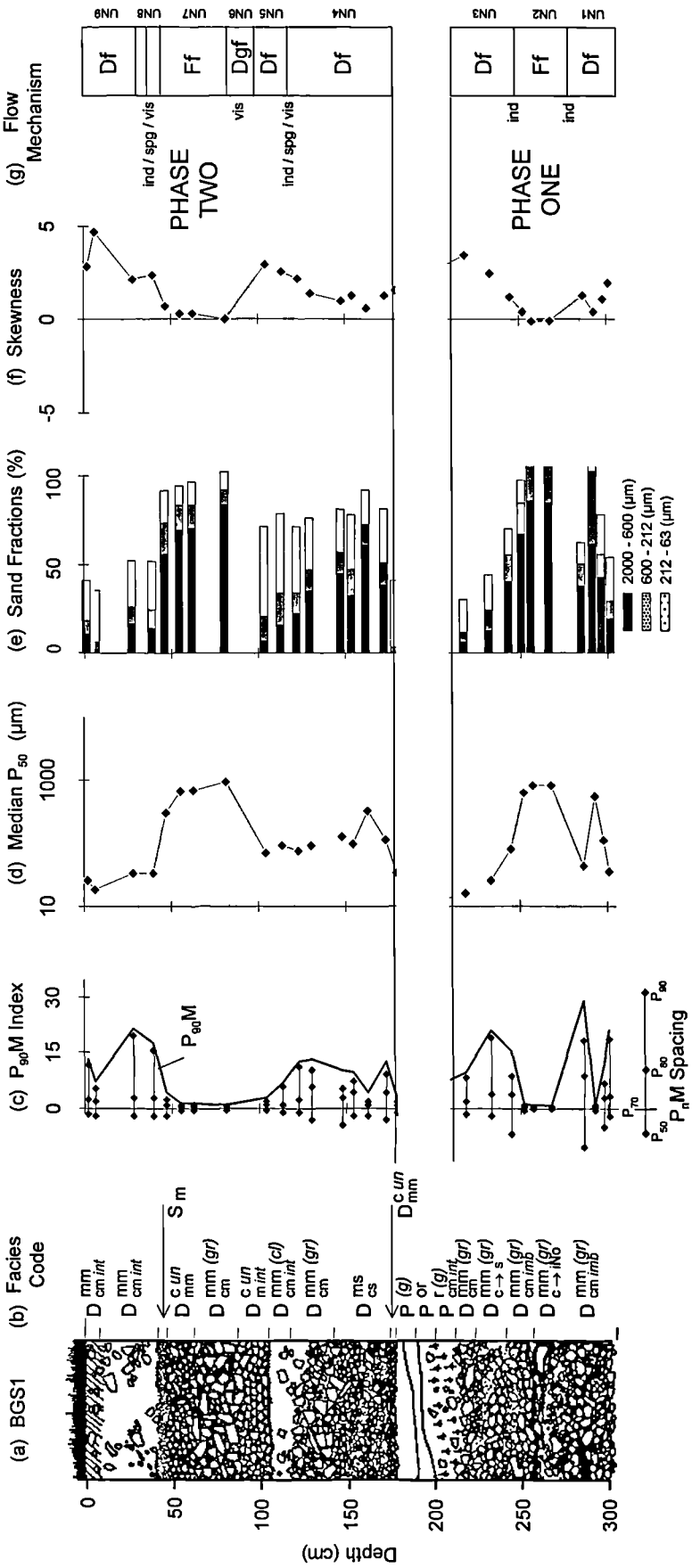


Figure 5.21. The identification of separate flow units and the assignment of flow mechanism for BGS1, the Howgill Fells (see Figure 5.13 for key to flow mechanism assignment (g) and Table 4.1 for facies code explanation)

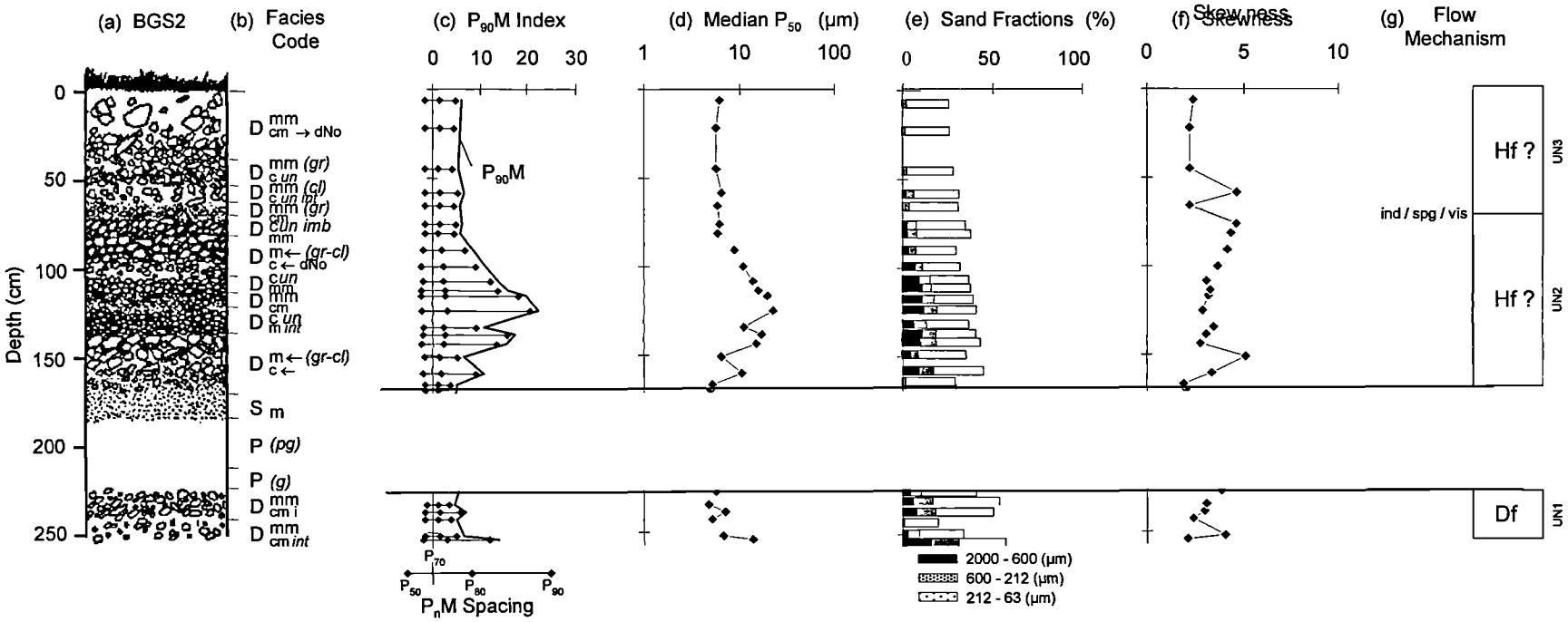


Figure 5.22. The identification of separate flow units and the assignment of flow mechanism for BGS2, the Howgill Fells (see Figure 5.13 for key to flow mechanism assignment (g) and Table 4.1 for facies code explanation)

5.22). Although $P_{90}M$ values are much lower than those found in BGS1, they are still sufficiently high to belie a fluvial origin. The uniformity of the $P_{90}M$ values is also indicative of their concomitant deposition as a discrete debris flow deposit. In both sections, debris cone aggradation began prior to soil formation. The marked difference in $P_{90}M$ values, the number of units, and the sand deficiency in sediments from BGS2 in comparison to BGS1 implies a difference in source of the sediments. The differences found between the two sections are maintained in the sediments which cap the palaeosols.

The aggradation of the cone sediments overlying the palaeosol in BGS1 appears to have occurred in five separate phases. The palaeosol is buried by a debris flow deposit of over half a meter in thickness. The upper sediments of the shallower, matrix dominated debris flow immediately above, may have undergone fluvial reworking before its burial by an open-framework matrix free layer. The complete lack of matrix within unit $BGS1_{UN6}$ and the homogenous size of the clasts is indicative of its deposition as a dry grain flow. Dry grain flows are commonly associated with the build up of clasts within the supplying catchment until a critical angle is reached. The build up of material in sufficient quantity requires an extended period of time, suggesting a period of stability separating the deposition of $BGS1_{UN5}$ and $BGS1_{UN7}$. Clast dominated, normally graded and fluvially transported sediments bury the dry grain flow. The deposits contrast with the sediments of the last event within the section which are debris flow sediments that are matrix dominated and comparable to the characteristics of $BGS1_{UN3}$ below the palaeosol. The sequential order of the layers and the associated change in the abundance of clasts is, as for Dry Cleuch (section 4.7.1), strongly suggestive of the cyclical availability of clasts. When clasts are unavailable within the trunk gully system, slope sediment reserves high in fines are eroded.

In BGS2, within the 2 m of cone sediments that overlie the palaeosol a marked change in the sorting properties, which correlate with a visual change in the properties of the sediment, clearly indicate the aggradation of the sediments by two separate flows (Figure 5.22). Sand contents in both units are low. In $BGS2_{UN3}$ sand contents of around 25% suggest transport by hyperconcentrated flow. Sand contents in all three transported units are low, indicating the sand deficient nature of the source sediment. The uniformity of the $P_{90}M$ values in concert with reverse grading of the clasts within $BGS2_{UN2}$ however are suggestive of their transportation

by debris flow. The abundance of clasts found within both units in BGS2 are not suggestive of cyclical sediment availability as found in BGS1.

A number of differences between the two sections are evident. The difference in the character of aggradation prior to soil formation, the contrast in the thickness and number of flows, the cyclic and non-cyclic nature of sediment aggradation and differences in overall sand content implies a different and discrete origin for flows between the two sections. The difference in the number of events in the aggradation of a similar thickness of sediments signifies that activity within the two gullies is not synchronous despite their close proximity. The timing of palaeosol burial may differ between the two sections. Dating of the palaeosol in BGS2 would determine if there is a difference in timing and thus establish if initiating controls differed.

5.7.2 Nevy Gill

In NGS2, taken from the surviving remnants of the first phase of fan activity, the sequence of flow units preserved attests to temporal changes in the dominant environmental and process controls operating within the fan system. Three separate phases have been identified (Figure 5.23). Initially the fan was built by a substantial phase of aggradation, achieved by both fluvial floods and debris flows, followed by a phase of fluvial erosion and reworking of aggraded sediments. The structural and visual characteristics of two units signify the close proximity of a fan channel. The channel was probably one of many operating on the surface of the fan at the time, drawing from evidence of multiple channels preserved on the surface of the second fan terrace. The return to aggradation is signified by the preservation of fluvial flood and debris flow deposits. Deposition indicates the withdrawal of the influence of the channel. The preservation of debris flow deposits within NGS1 attests to the magnitude of the event required for the preservation of deposits so far from the fan apex, a distance of over 70 m.

The age of the deposits in the section and the nature of the sediments preserved provides limited evidence of sediment exhaustion. The lack of exposures of fan sediments prevent a comparison with younger fan sediments. Evidence of a clear change in the environment of sediment deposition and thus a change in the evolutionary development of the Nevy Gill fan system is however provided.

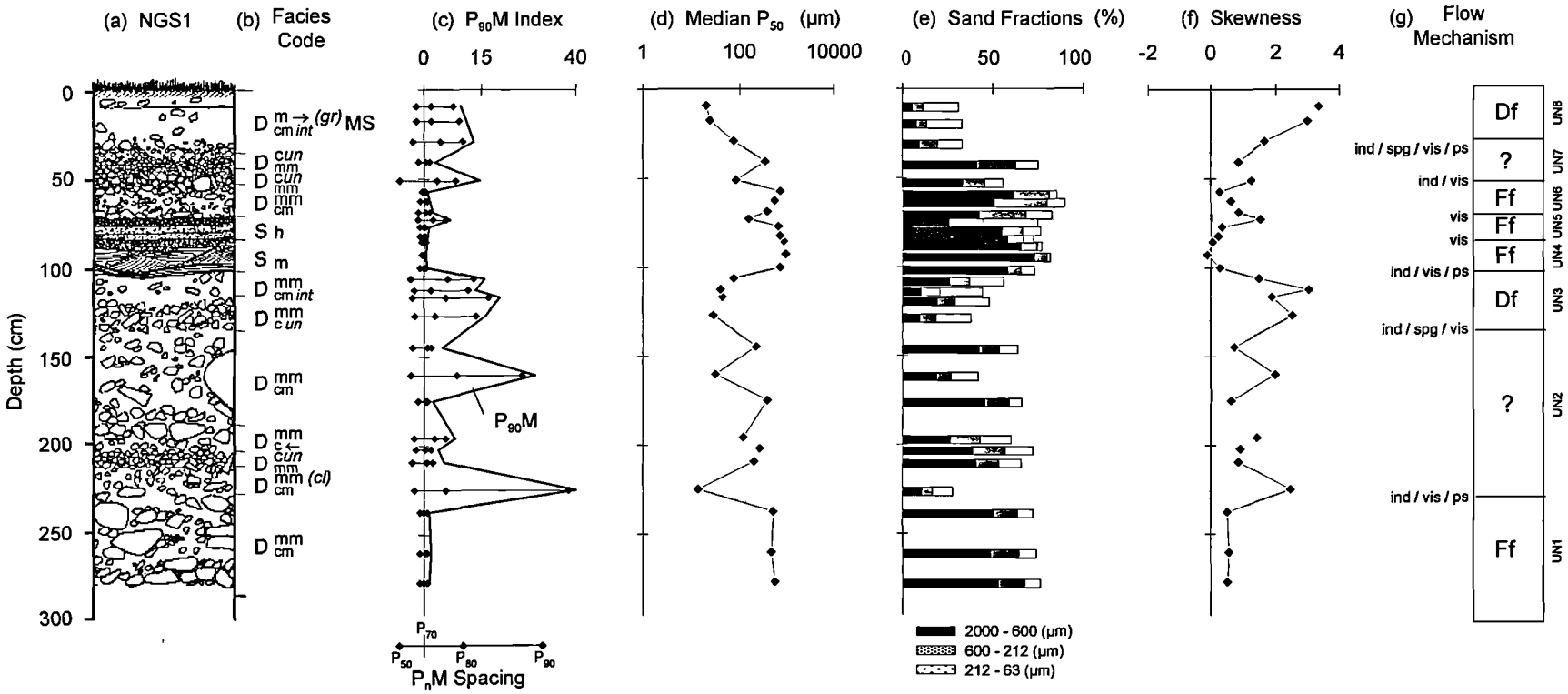


Figure 5.23. The identification of separate flow units and the assignment of flow mechanism for NGS1, the Howgill Fells (see Figure 5.13 for key to flow mechanism assignment (g) and Table 4.1 for facies code explanation)

The last aggradational unit preserved in the section is a debris flow deposit. A debris flow was the last aggradational unit preserved in the section prior to the phase of fluvial incision and formation of an inset fan terrace. The deposition of a debris flow immediately prior to the onset of periods of stability within the section is a characteristic observed in other investigated sections.

5.7.3 Thickcombs Gill

The sorting characteristics indicate that the palaeosol in TGS1 has formed within the deposits of a debris flow, a flow over 1 m in thickness. Overall cone aggradation is characterised by debris flows of substantial thickness, attesting to the availability of sediment through progressive phases of cone aggradation. The general characteristics of the sediments transported in separate units show differences within and between the four phases (Figure 5.24). The sequence of the differences can be attributed to changes in sediment availability within the supplying gully system.

The characteristics of the last debris flow contrast with those of the first two debris flow units. A change in the sediment source of the flow would account for the lack of clasts and the marked difference in the overall particle size distribution found in $TGS1_{UN4}$. On a larger scale a change in sediment source would also account for the difference observed in the sediment characteristics of debris flow deposits in phases three and four. Debris flow deposits in phase three are dominated by clasts which are uniform in size, whist $TGS2_{UN8}$ in phase four has fewer clasts overall and contains large boulders. The uniform size of the clasts preserved in the debris flow deposits of phase three suggests sorting before their transportation.

In both cases the difference in characteristics can be attributed to the cyclic availability of sediment within the trunk gully system. The removal of readily available unconsolidated material leaves only slope sediment reserves which both $TGS2_{UN8}$ and $TGS2_{UN9}$ have tapped. The debris flow units in phase four are buried by fluvial deposits, which signifies the end of activity within the phase. The fluvial unit does not represent the fluvial reworking of the underlying debris flow as clast contents are uniform throughout and lack larger clasts characteristic of the debris flow unit below. The surface of the cone then underwent fluvial incision. The resulting channel has subsequently been infilled by the deposits of a smaller scale debris flow, the upper sediments of which have been reworked by channelled overland flow.

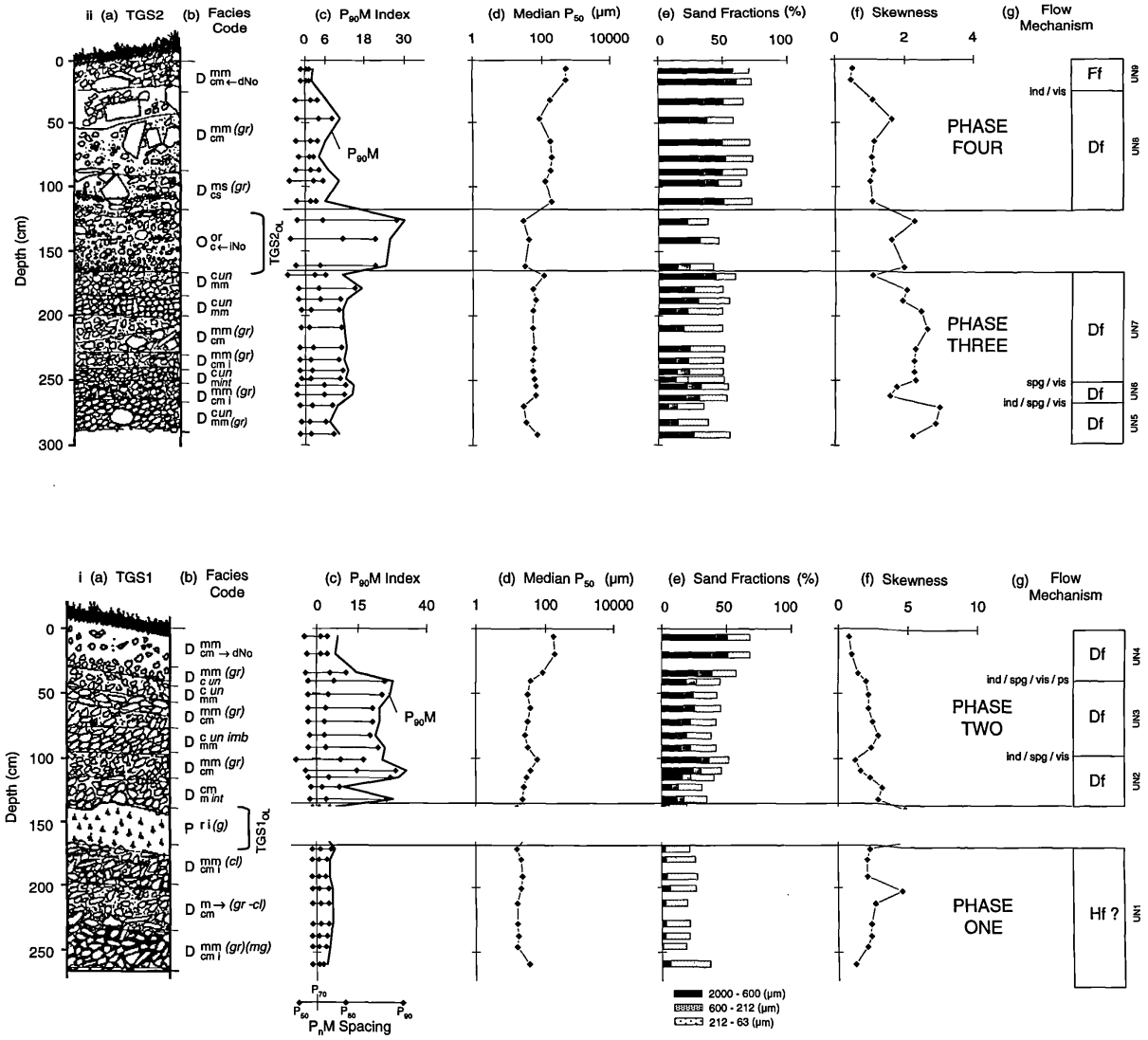


Figure 5.24. The identification of separate flow units and the assignment of flow mechanism for (i) TGS1 and (ii) TGS2, the Howgill Fells (see Figure 5.13 for key to flow mechanism assignment (g) and Table 4.1 for facies code explanation)

Although the last phase of activity within the cone is fluvial it is likely that between the four phases of cone aggradation similar fluvial incisional phases may have occurred. The repeated thickness of debris flow units in all four phases attests to the cyclically controlled build-up and removal of storage within the trunk gully channel. When storage has been removed, higher magnitudes are required in order to tap comparatively less available slope sediment reserves.

5.7.4 Leath Gill

Within LGS1 alternating fluvial and debris flow deposits have been preserved (Figure 5.25). The aggradation of the section has been broken by one period of stability. Between the two separated phases the character of the sediment preserved has changed significantly. LGS1 is located in distal fan deposits. The preservation of flow deposits in the section is as a result sensitive to the proximity of the migrating trunk channel when the flow occurred. A change in the position of the trunk stream may account for the change in the character of the sediment preserved. The sequence found in this section is comparable to that exhibited in HBS1, taken from fan sediments at Hermanlaw Burn, suggesting a similar cause for the change observed.

5.8 Northern Pennines - Langden Beck

5.8.1 Harthope Beck

The apex section HHS1 (Figure 5.26i) and the distal section HHS2 (Figure 5.26ii) do not show a link in transporting mechanism, despite the correlation observed in the onset of activity in the fan. In HHS1 four separate debris flow events can be identified within 1 m of sediment. The four layers, containing characteristic clasts of uniform size, represent the first phase of fan aggradation as the sediments are deposited directly onto glacial material. In HHS2 the comparable layer is limited to one unit, only approximately 20 cm in thickness. The onset of deposition in HHS1 may not be concurrent with the onset of deposition in HHS2. The layer in HHS2 may represent reworked deposits of the earlier phase. It is difficult to assign a transport mechanism to the unit as the formation of the palaeosol will have affected the particle size of the matrix sediment. If $HHS2_{UN2}$ represents the onset of fan aggradation the underlying fluvially transported sediments may be fluvio-glacial deposits as opposed to river terrace sediments exposed downstream. The high

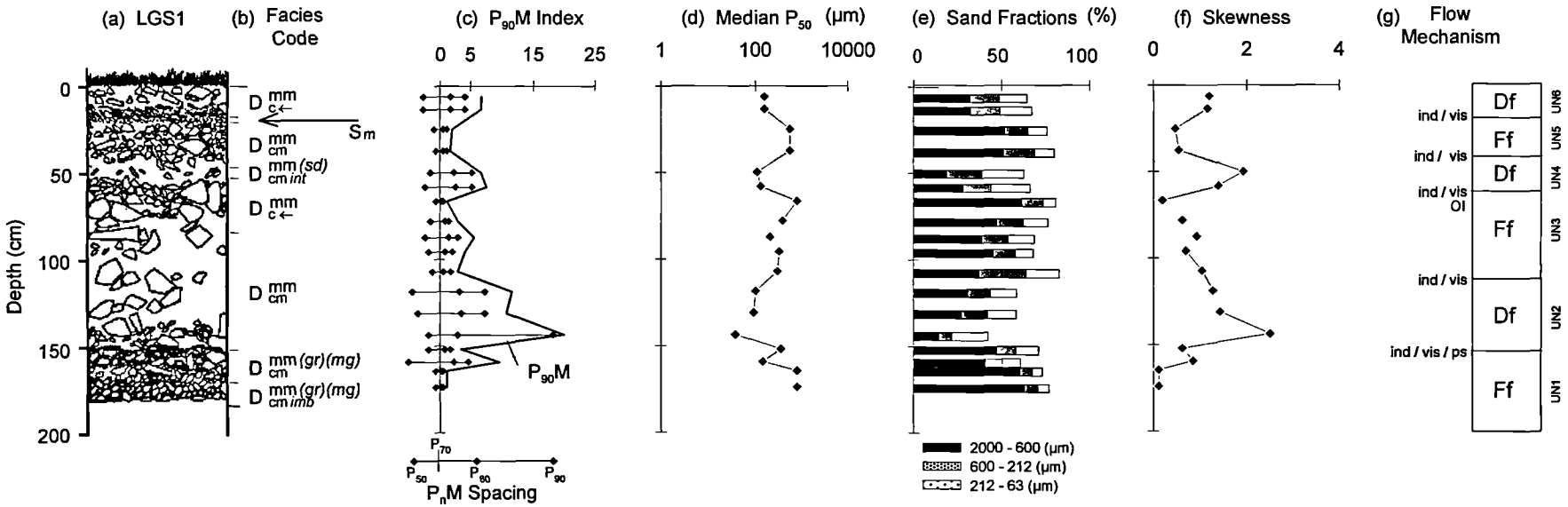


Figure 5.25. The identification of separate flow units and the assignment of flow mechanism for LGS1, the Howgill Fells (see Figure 5.13 for key to flow mechanism assignment (g) and Table 4.1 for facies code explanation)

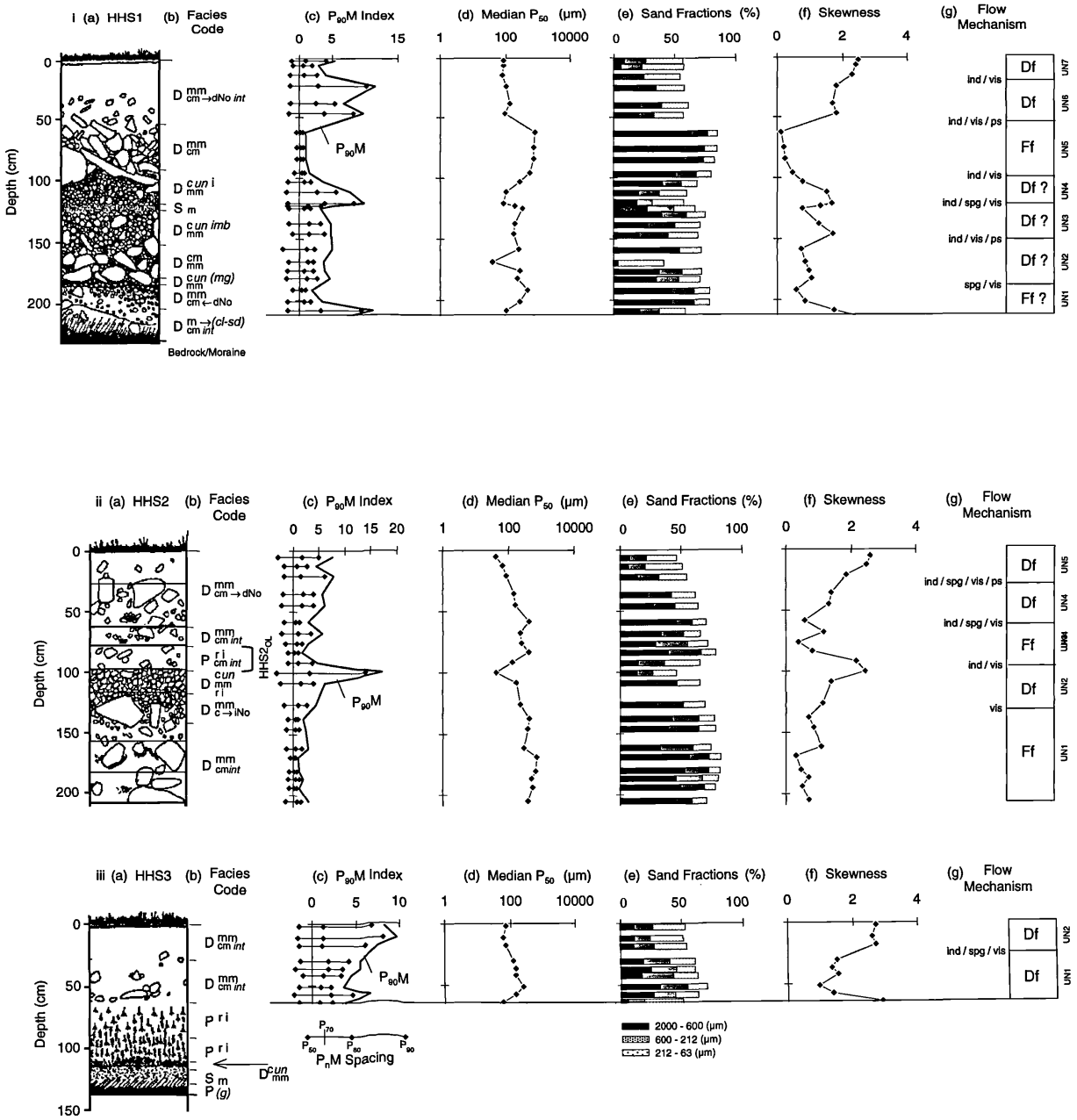


Figure 5.26. The identification of separate flow units and the assignment of flow mechanism for (i) HHS1, (ii) HHS2, and (iii) HHS3, Langden Beck (see Figure 5.13 for key to flow mechanism assignment (g) and Table 4.1 for facies code explanation)

$P_{90}M$ values and large boulders within $HHS2_{UN2}$ may be associated with high magnitude melt-water events that will have deposited the sediment.

Activity after the first aggradational unit appears to have been isolated between the two sections. In HHS2 (Figure 5.26ii) the palaeosol is buried by the deposits of one debris flow event. In HHS1 three separate units have been identified. After initial deposition, sediments of an earlier phase are in abrupt contact with fluvial deposits. The change in transport mechanism is associated with a marked contrast in the physical characteristics of the sediment, suggesting a change in source or complete removal of the previous source from within the supplying catchment. The armoured nature of the contact suggests that the fluvial deposits could have represented former position of the trunk channel. More likely, the unit represents the normally graded deposits of a large flood event. The fluvial deposits are buried by two consecutive debris flow deposits again representing a marked contrast in the characteristics of the sediment. Both layers are matrix supported, the first containing intermittent clasts whilst the uppermost debris flow is clast free. The last two layers $HHS3_{UN1}$ and $HHS3_{UN2}$ are comparable to the two transported units preserved in HHS1, excavated from an exposure of the second fan terrace (Figure 5.26iii). The similarities found between the units in HHS3 and the upper units in HHS1 suggest a link. As the two are separated by a phase of fan incision the units in both sections could not have been transported by the same flow. The link is suggestive of a similar source area within the catchment.

5.8.2 West Beck

The transportation characteristics of both sections have been affected by mining activity but to different degrees. In WBS1, nine separate layers have been identified (Figure 5.27). The characteristics of each layer contrast with those of layers above and below. The thickest layer has been deposited by a fluvial flood, while the others all represent debris flows. The shallow nature of the deposits, in combination with poor sorting, indicate that the layers represent the preservation of debris flow deposits of high magnitude. The debris flow events must have been of sufficient magnitude to have overtopped the banks of the channel and thus be preserved in the section: the section is a substantial distance from the point of origin.

The sediments in WBS2 can be divided in two by the presence of a transported peat layer (Figure 5.27ii). Below the peat layer two separate units have been

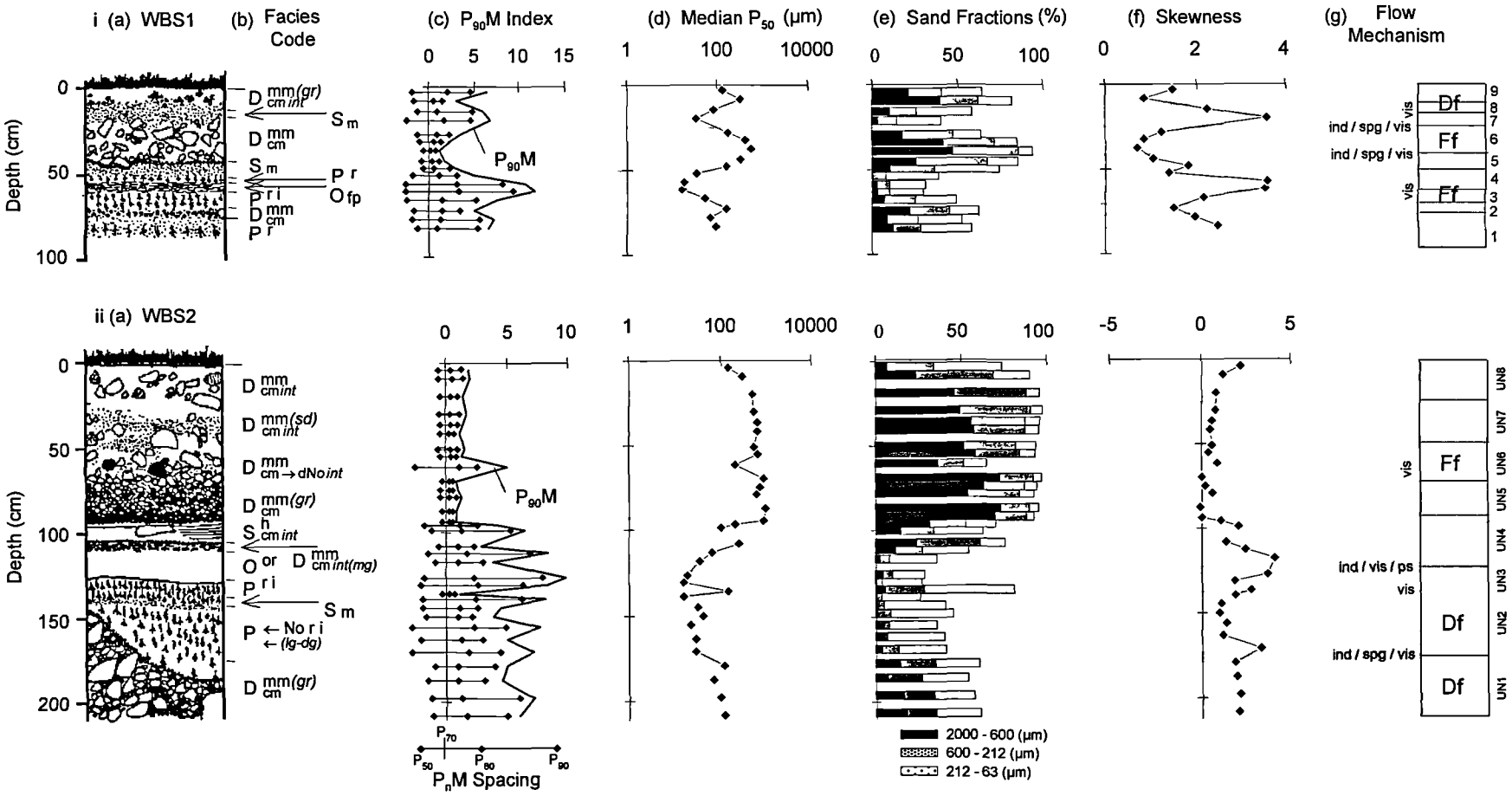


Figure 5.27. The identification of separate flow units and the assignment of flow mechanism for (i) WBS1 and (ii) WBS2, Langden Beck (see Figure 5.13 for key to flow mechanism assignment (g) and Table 4.1 for facies code explanation)

identified. The characteristics of the sediments within the bottom-most unit are comparable to the first phase sediments identified in HHS1 and in sharp irregular contact with a very fine clay layer. The layer contains no rootlets, has limited organic material and was therefore transported. The layer may represent the initial erosion of soliflucted clay material characteristic of the site. It is overlain by a sequence of units which represent the stripping of the soil from the intensely mined side gully. All of the samples taken from sediments which bury the peat have been transported by fluvial activity. The sediment must have been stripped by the action of water, most likely the mining process of hushing. $WBS2_{UN1}$ may therefore be the only deposit in the section that relates to the initial phase of fan aggradation.

The source of deposited sediments in WBS2 is dominated by mining. In Harthope Beck the dramatic change in sediment properties observed between the three separate aggradational phases identified is suggestive of marked temporal or spatial changes in sediment source within the catchment. The deposits of one distinct flow ($HHS1_{UN4}$ and $HHS1_{UN5}$; $HHS3_{UN1}$ and $HHS3_{UN2}$), the youngest identified in the fan, have been preserved in two separate localities. The source of this unit can be tentatively linked with mining within the catchment. If this is the case the phase of fluvial incision that separates the two fan terraces can be linked to the onset of mining within the catchment. An evaluation of the sediment provenance of the three distinct phases in the next chapter will test this hypothesis.

5.9 Evidence for sediment exhaustion

The control exerted by catchment size upon the frequency of debris and fluvial flows is illustrated in Figure 5.28. With increasing catchment size an increasing number of fluvial events account for the aggradation of sediments. Debris flows are the dominant means of sediment aggradation in fans and cones in the four sites, which represent a variety of upland environments in Great Britain. The lack of hyperconcentrated flows identified in the sediment sequences may be because hyperconcentrated flows did not occur. Their absence may have been controlled by the short transport distance between origin and sink, especially within debris cones, and may not have allowed sufficient incorporation of water to result in the transition from debris flow to hyperconcentrated flow. The P_nM measure and facies description do not discriminate hyperconcentrated flow deposits from fluvial flow or debris flow

deposits. The diagnostic properties of hyperconcentrated flows overlap in both cases.

Despite the limited evidence for the reworking of debris flows, the magnitude and type of reworking can be linked to increasing in catchment size and a change in feature morphology. In debris cones, with a smaller surface area and a lack of surface channel, deposits have a higher chance of being reworked following deposition. The hiatuses in the sediment record will not record fluvial reworking of deposits if activity is focused elsewhere on the feature. A change in the focus of activity is more likely on larger features.

Of all the sections only one unit in DCS1 has provided evidence of sediment exhaustion operating on a single event scale. The contacts between separate debris flow deposits are commonly sharp, in keeping with their diagnostic characteristics. The upper sediments of each flow show no evidence of reworking. The lack of reworking of flow deposits following their deposition suggests that the time period separating each flow was not long enough to allow post-depositional alteration. The initiating event was of sufficient magnitude to trigger the flow but not to have reworked the deposit as the rainfall event continued. If threshold conditions within the catchment are lowered, either by human activity or by a previous event, flows will result from lower magnitude rainfall events. The lack of reworking also suggests that the trigger mechanism may not have been a rainfall event but was caused by over-steepening of the deposits within the catchment. Unstable, unconsolidated sediments require limited force to initiate a flow.

Evidence of a temporal switch from debris flow to fluvial flow deposits is lacking. Tentative evidence is found at Thickcombs Gill. The type of flow deposits which represents the end of activity within the feature or within a given phase of activity has been transported by debris flow. Evidence of sediment exhaustion has been found within the sections. The ability to define the upper and lower boundaries of a debris flow deposit has provided valuable information upon the changing characteristics of the sediments available at the time of transport.

Collectively, the evidence suggests that sediment can be exhausted cyclically. Within debris flow deposits a change in sediment availability through consecutive phases of fan aggradation and between separate phases of fan aggradation is

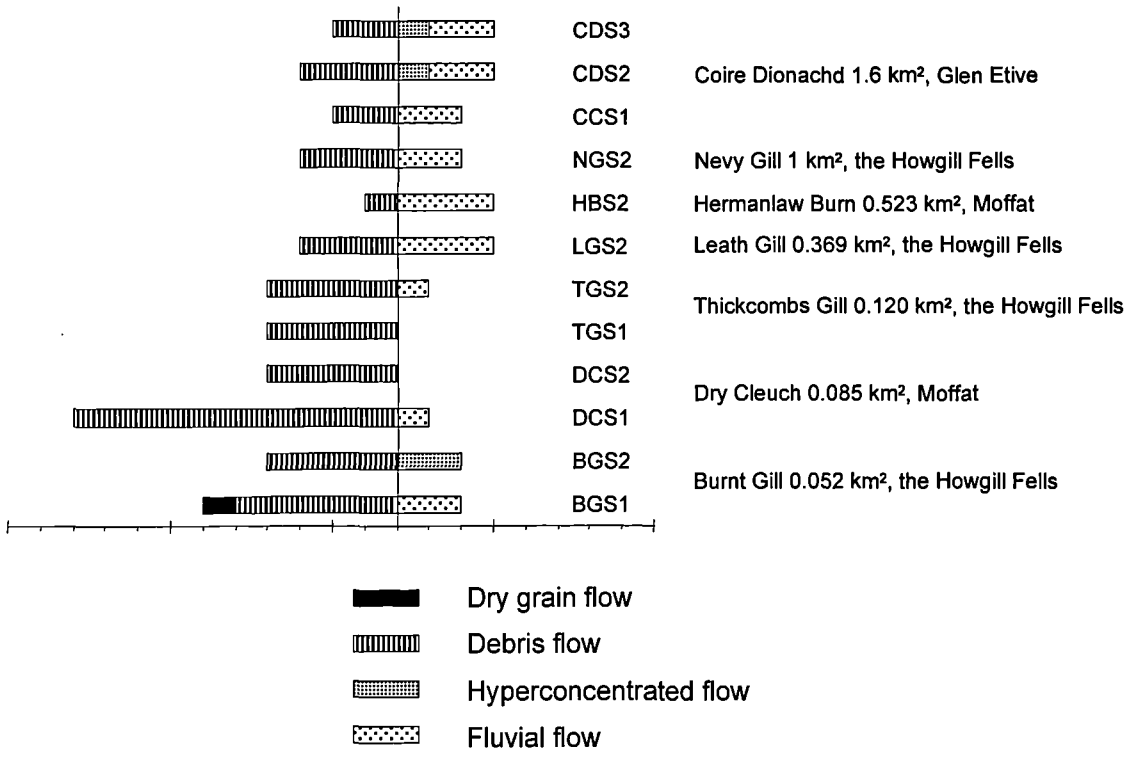


Figure 5.28. Plot of flow mechanisms identified for each feature against catchment size

evident. Phases of aggradation and their continuation are controlled by the temporal availability of unconsolidated, readily transportable sediment reserves, stored within the supplying catchment. The period of stability which separates phases of cone aggradation represents the time period within which sediment reserves are rebuilt. Whilst the readily available sediment supplies are depleted an alternative source is tapped. This may also be associated with an increase in magnitude.

The size of debris cones is conducive for the preservation of the majority of debris flows within the feature. The preservation of consecutive events provides a relatively unbroken recorded of activity within the feature. In larger features, the loci of deposition can change markedly between flow episodes and between phases of fan activity. The active migration of trunk streams on fan surfaces can destroy and remove evidence of earlier phases of activity. Hiatuses within fans can represent marked gaps in development. The presence of a hiatus indicates a broken record of sediment aggradation but its presence is not always clear. Of the three sections studied from the larger features, a period of stability separates marked changes in the characteristics of the sediment transported. The decrease in clasts size found to occur between older and younger phases is difficult to interpret. It is possible that it represents a change in the character of the sediment but it is more likely to reflect material that has been stored within the supplying catchment. A sequential interpretation is useless as consecutive events can erode different sediment reserves preserved within the trunk stream.

The type of sediment exhaustion observed is essentially linked to catchment size. Cyclic periods of sediment exhaustion are readily found within the deposits of debris cones. In the sections investigated from tributary fans no evidence of cyclic availability of sediments was found, principally because the stratigraphic sections do not provide a long record of fan development. The study of change in transport mechanism does provide valuable information upon changes in environmental context within a fan section.

5.10 Summary

The identification of temporal sediment exhaustion is heavily reliant upon the investigation of consecutive phases of cone sediments or fan terraces. The scheme used to delineate flows transported by separate transport mechanisms has defined

clear upper and lower boundaries of individual flows. Additionally, information upon the nature of the contact between units is supplied. Based upon clearly defined diagnostic properties for each flow mechanism identified, using a combination of facies description and measured physical properties, it was possible to assign a transport mechanism to each unit. $P_{90}M$ acts to confirm or clarify transport mechanisms that otherwise would appear to have been transported by debris flow. $P_{90}M$ values have also been proved to be sensitive both to changes in magnitude of fluvial deposits and in identifying changes in parent material supplied to debris flows. It was also possible to determine the rheological properties of individual debris flows. $P_{90}M$, a physically derived technique, is sensitive to the environmental controls. $P_{90}M$ is however not sensitive enough to be used alone. Ancillary methods are required where $P_{90}M$ values overlap.

In applying the combined approach to determine sediment transport modes evidence of a change from debris flow to fluvial flow as an indicator of sediment exhaustion has not been found. The derivation of sediment exhaustion is not directly associated with a change in transport mechanism but with the temporal change in the character of the sediment transported by each separate event. Temporal and spatial changes in the supply of sediment have been found. Temporal changes in sediment reserves can result in a spatial change in sediment source. The study of the sequential change in transport mechanism provides valuable information upon the contextual development history of each feature investigated. The contextual framework for each feature has been modified accordingly. The evidence suggests that of the features investigated no site has yet approached sediment exhaustion.

Chapter Six

Sediment source supply and sediment exhaustion

6.1 Introduction

The main aim of this chapter is to identify changes in source of sediment supplied to the fan and cone since their initiation. In using the mineral magnetic technique to determine changes in the source of sediment within an aggrading profile, as is the case here, or during a storm event, the procedure is the same. The first step is the characterisation of all potential sediment sources. The success of the mineral magnetic technique for assessing erosion within a catchment is dependent on differences in the magnetic properties of the various sources. Without the differences the ability to ascribe a sediment source to samples of unknown origin within fan and cone sections is not feasible. Secondly, if source discrimination is adequate, the source of the samples can be assigned. The success of source assignment is dependent upon sample integrity. Within an alluvial fan or sediment sequence, samples can be subjected to post depositional alteration by soil forming processes and weathering.

6.2 Principle and procedure of magnetic provenancing

6.2.1 Measurement of magnetism and its discrimination

The characterisation of source samples is based upon the measurement of magnetic concentration, grain size or domain state and mineralogy. The types and strengths of magnetisation found in commonly occurring iron-bearing minerals are

Table 6.1. Commonly occuring iron bearing minerals found in natural sediments and soils

Mineral	Formula	Magnetic status	Reported environmental associations
Haematite	αFe_2O_3	Canted antiferromagnetic	Relatively dry, highly oxidised soils, usually in areas of elevated temperature
Goethite	$\alpha FeOOH$	Canted antiferromagnetic	Moister soils, abundant in well-drained temperature areas
Maghemite	γFe_2O_3	Ferrimagnetic	Abundant in highly weathered tropical/ sub-tropical soils
Ferrihydrite	$5Fe_2O_3 \cdot 9H_2O$	Paramagnetic	Poorly drained and podsolised soils
Magnetite	Fe_3O_4	Ferrimagnetic	Restricted occurrence, primarily derived or from soil firing.

Maher (1986)

summarised in Table 6.1. Iron oxides generate almost all of the magnetic properties in rocks and sediments, due to the high net magnetisation or strength and their ability to carry a remanent magnetisation (Thompson *et al.*, 1992). Examples of Iron Oxides include magnetite, maghemite, haematite and the iron hydroxides, which on rehydration revert to haematite. Natural Iron Sulphides and Iron Titanium Oxides also carry a strong remanent magnetisation due to their ferro- and ferri- magnetic behaviour but are commonly a minor component of most sediments. Alumino-silicates, monosulphides and clays can contribute to magnetic susceptibility due to their paramagnetisation (PM) and super-paramagnetisation (SPM) properties but do not retain any induced magnetisation on removal of a magnetising field. The concentration, grain size and mineraology of iron oxides and their derivatives within source materials can be quantified by the combined use of three magnetic measures: magnetic susceptibility (X), isothermal remanent magnetisation (IRM) and anhysteretic remanent magnetisation (ARM). Establishing a signature magnetic characteristic for each source material provides the basis for source discrimination. Magnetic susceptibility is a direct measure of how easily a material can be magnetised and gives a rough indication of the magnetic concentration of all iron-bearing minerals within a sample.

The artificial magnetic saturation of a sample to give the Saturated ARM (SARM) provides a more precise measure of concentration. The strength of the remanent magnetisation retained after a sample has been artificially magnetised is an indicator of magnetic concentration of all magnetic minerals with remanence capability. A stepwise alternating field demagnetisation of the SARM can be used to determine the grain size contribution to the net magnetisation. ARMs are generated by superimposing a small direct magnetic field onto a larger smoothly decreasing magnetic field. The strength of any remanent magnetisation can be measured, giving an indication of concentration.

Exposure of samples to a single, direct or pulsed, magnetic field provides a measure of the degree of remanence retained in response to the applied field strength. Measurements of IRM for a given field strength can give a rough indication of magnetic concentration of minerals that have remanence capabilities. The exposure of samples to successively stronger fields induces progressively higher magnetisations until saturation. Much more information can be obtained by interpreting the variation of IRMs with changing field values, determining coercivity spectra.

Information about magnetic grain size and mineralogy can be obtained by observing the intensity and ease of remanence acquisition.

6.2.2 Source material sampling

A fundamental requirement for sediment provenancing is that all sources must be accounted for in the sampling procedure. Field sampling therefore needs to be systematic with a full understanding of intra- and inter-source variation (Lees, 1994). Tightly constrained differences observed in the magnetic properties of source materials are also a prerequisite. An initial assessment of potential sediment sources for each site was made from field observation both within the supplying catchment and the main valley. It was found at all four sites that a systematic sampling system was hindered by the coarse nature of the material and by the steepness of slopes. The sampling framework was thus restricted to spot sampling of exposures identified within the supplying catchment. Where exposures were limited, samples were taken from exposures within the main valley to supplement source characterisation. Samples which are not from within the supplying catchment are clearly marked as ambiguity in the assignment of sediment source may be introduced.

A number of samples were taken to represent the sediments from each exposure, based on a visual assessment of variation of sediment characteristics. When collecting source samples, care was taken to avoid sampling surficial sediments that were part of the modern soil, to prevent measurement of pedogenetically altered materials rather than the sediment characteristics themselves. Each sample, its location and textural characteristics were logged to aid source categorisation. The amount of differentiation observed between identified sediment sources is restricted by the occurrence of environmental conditions that produce measurable differences between sediment sources.

6.2.3 Sample preparation and laboratory measurement

Catchment samples were sieved to obtain the < 2 mm fraction. A representative sub-sample was taken from the bulk material of both catchment and section samples using a sample splitter. Samples of known weight were then packed and secured with rubber foam into previously magnetically screened 10 ml styrene pots. In provenance studies using magnetics, it is becoming increasingly common to

subdivide material into particular particle size ranges for measurement. Magnetic strength and concentration is associated with the lattice structure and grain size of the iron-bearing compounds. Size-selective transport from the source to the depositional site or point of measurement will affect the retention of source-specific magnetic characteristics. By splitting the samples into a range of particle sizes, source material characterisation is enhanced. Details of the size range retained in the deposited sample can be compared to the given size ranges preserved in each of the source materials sampled.

In comparison to catchment scale investigations in other magnetic provenance studies, the majority of the fan and cone features studied in this research are small. The distance over which the source materials can be mixed or altered is restricted. With decreasing catchment size the transport distance from origin to sink decreases, the amount and residence time of storage material decreases and the severity of reworking and loss of fines from storage material decreases. In addition, with increasing catchment size the ratio of fluvially transported to debris flow events increases. The fluvial events are dominated by chaotic flooding and fines of the original source material are retained within their respective deposits. As the majority of material is transported by debris flows, which rheologically cannot selectively remove sediment of any particle size, the integrity of the source material will be retained. Changes in particle size by selective transport will affect only fluvially transported sediments. As the effects can be accounted for in the interpretation procedure, the time consuming process of sample splitting and subsequent measurement was not used.

The choice of field strengths used for both ARM and IRM measurement is based upon establishing which magnetic fields induce as wide a spread of values as possible. The choice of field strengths was based upon preliminary magnetic susceptibility and remanence readings of six samples. Obtaining the greatest spread possible illustrates the variability in the magnetic properties of the sediments. The six pilot samples were magnetised through a range of field strengths (Figure 6.1). The optimum fields for the samples are 99 mT and 40 mT for ARM and 40 mT, 100 mT, 1000 mT, and 3000 mT for IRM. The field strengths are commonly used because they produce the greatest spread in measurements in comparison to other field strengths. In total eight direct magnetic properties were measured on section and catchment source samples.

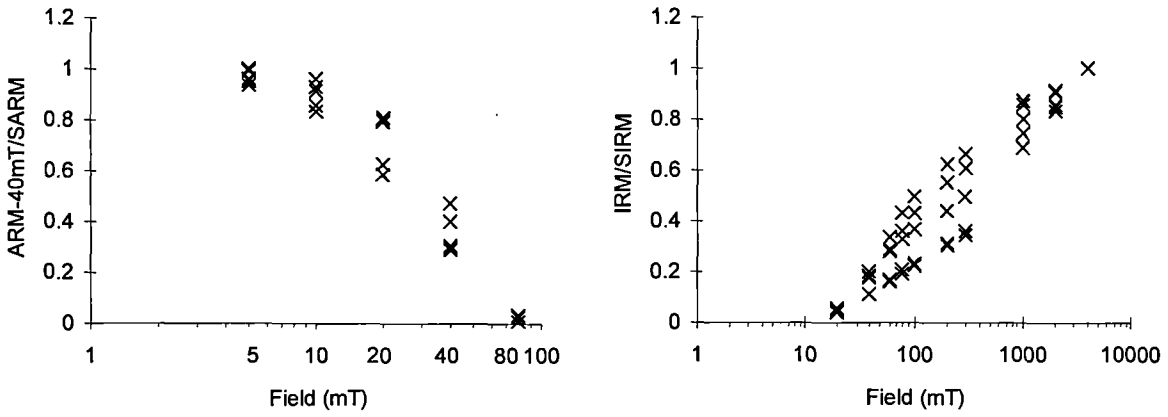


Figure 6.1. Demagnetisation and magnetisation of six pilot samples through a range of field strengths to determine variability in the magnetic properties of the sediments

Initial reversible susceptibility (X) was measured for all samples using a Bartingtons Instruments air-cored Digico susceptibility bridge. Susceptibility calibration was maintained using a sample of the paramagnetic salt $FeSO_4.7H_20$. ARMs were imparted at a mains frequency alternating field of 99 mT (SARM) and 40 mT using a triple variac, while the samples were subjected to a steady field of 0.25 mT. ARMs were measured using a Molspin fluxgate magnetometer. After measuring ARMs, IRMs were successively generated and measured. IRM coercivity was obtained by growing IRMs in successively higher fields. Fields of 40 mT and 100 mT were generated in a Molspin discharge magnetiser. 1T, 2T and 3T fields were produced by a 3240 J Trilec pulsed capacitor discharge unit. Since IRM at 3T field strength gives the highest magnetisation and gives values closest to saturation, the measurement is generally termed the saturation isothermal remanent magnetisation (SIRM). All measurements of ARMs and IRMs were calibrated using a Hall effects probe. The intensity of the magnetisation was calibrated using a high coercivity sliver of magnetic tape of known magnetic moment (see Appendix 1.3 and 1.4).

6.2.4 Discriminating power of magnetic parameters

The magnetic properties and their interpretation used in this study are summarised in Table 6.2. Additional information on other magnetic properties of the sediment can be obtained by calculating ratios of parameters obtained within and between X, ARM and IRM measures. For example, the calculation of the ratios of magnetic IRMs removes the influence of concentration and enables mineralogy and grain size properties to be deduced. The interpretation of the measures in natural sediments is primarily based upon information obtained from laboratory studies of pure minerals of iron oxides. As a result, a number of combined parameters used in biplots and in stratigraphic plots have become the standard for data interpretations. Biplots of different sensitivities are combined in order to emphasise the properties of certain minerals and domain states. Figure 6.2 summarises how the magnetic parameters can be combined and interpreted. In total, fourteen magnetic parameters can be applied in the following source discrimination, including raw magnetic properties and their ratios.

Natural samples are complex mixtures of different magnetic mineralogies (Peters, 1995). Different relative proportions of magnetic minerals provide a useful means of characterising natural materials. The wide range of magnetic properties

Table 6.2. Magnetic parameters, ratios, graphical combinations and their interpretation. After Maher (1986).

Magnetic parameter	Interpretation
X	Magnetisation is reversible. The value is roughly proportional to the concentration of ferrimagnetic minerals. The magnetic signal can be dominated by a large antiferromagnetic component (goethite).
ARM	If a sample is subjected to a decreasing alternating field with a small steady field super-imposed, it acquires an anhysteretic remanence. It is sensitive to both the concentration and grain size (domain states) of ferrimagnetic minerals. It can be used to determine the dominance of SD or MD characteristics within a sample. It is harder to alter the magnetisation of SD and MD grains are easy to magnetise and demagnetise (Walden, 1996; Maher, 1986; Yu and Oldfield, 1993)
ARM40mT/SARM	ARM40 : determines how well a sample is demagnetised SARM : determines the magnetisation characteristics of a sample A high value for the ratio indicates that there is little difference between the concentration of a sample and the strength left after demagnetisation indicative of SD. Low ratios indicate a high concentration but low value for the demagnetisation indicative the ease of loss of magnetisation which is diagnostic of MD.
IRM	Individual IRM values give an indication of the intensity of remanence acquisition or concentration for all remanence carrying minerals within the sample. The strength is related to the mineral assemblage and magnetic grain size variations. SIRM is the highest amount of magnetic remanence that can be induced in a sample by the application of a large magnetic field.
Forward field ratios	More information can be obtained from studying the variation of IRMs with changing field strengths. Calculation of the ratios of magnetic remanence largely removes the influence of concentration and enables other magnetic properties to be investigated. The ease of remanence acquisition can distinguish between mineralogies if more than one is present. At 300mT magnetite is saturated and geothite (anit-ferromagnetic) is present if the sample is not saturated over 800mT (Walden, 1996). If only one mineral type is dominant the information can be used to determine grain size variations for the given dominant mineral within the sample measured.
IRM40mT/SIRM (soft)	Both magnetite and haematite yield higher ratios in their MD states
IRM100mT/SIRM	Haematite continues to magnetise proportionally better than magnetite at higher field strengths
IRM1T/SIRM (hard)	If ratio is low the sample has not been fully saturated indicating the presence of geothite, an imperfect anti-ferromagnetic mineral type.
	(Based upon the assumption that the magnetic component is largely composed of Iron Oxides)
Ratios	**Interpretation**
SIRM/SARM	Values greater that a 100 generally indicate the dominance of MD. Low ratios of less than 30 indicate stable single domain dominance.
SIRM/*X*	Diagnostic of mineral type. Anti-ferromagnetic minerals with have a low *X* but a relatively high SIRM and will therefor produce a relatively high SIRM/*X* ratio. Where samples have a similar mineral types and concentration, the ratio can also indicate the dominant magnetic grain size (Walden et al., 1996). A low ratio indicates the presence of paramagnetic minerals. where samples have similar mineral types and concentrations the dominant magnetic grain size.
SARM/*X*	Reflects magnetic grain size, high values indicating finer grains. If SPM grains are present this relationship breaks down. A ratio of these two parameters indicates the concentration of the finer grain sizes around the single domain and ferrimagnetic minerals in a sample.

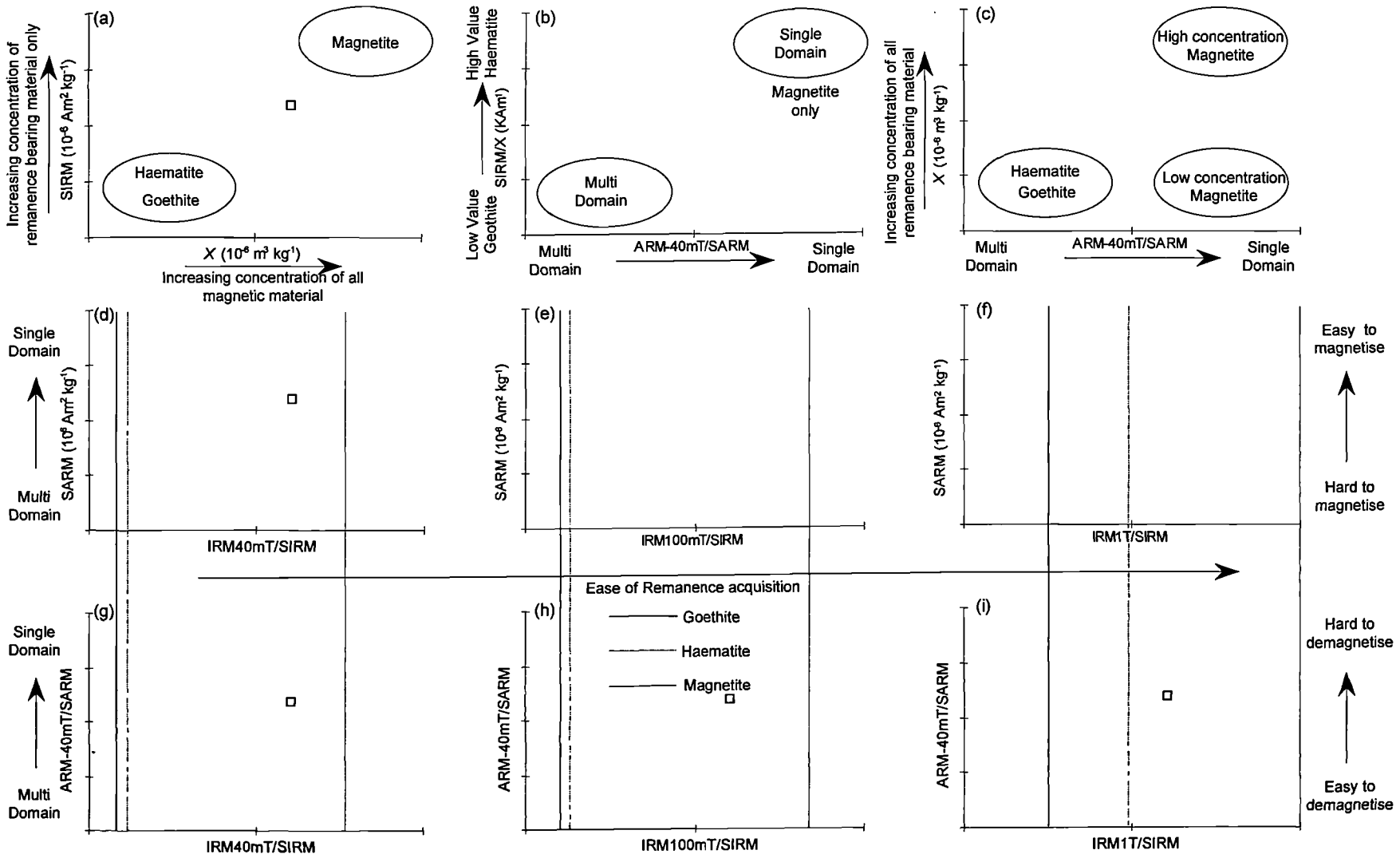


Figure 6.2. A summary of magnetic parameter biplot combinations and their interpretation. Biplots a to c measure magnetic concentration and grain size, biplots d to e and g to i measure ease of acquisition of a magnetic remanence, differentiating mineralogy

that are displayed by natural magnetic minerals show overlapping characteristics. Combinations of properties are therefore more diagnostic.

6.3 Source material characterisation and discrimination

6.3.1 Methodology of source discrimination

A preliminary categorisation of source material types is based upon the initial field interpretation of location and environmental field context. The major source categories identified are glacial material, soliflucted sediments, storage, peat and their underlying sediments, mining waste, and bedrock or parent material (Table 6.3). Two primary sources autochthonous to a supplying catchment are peat and parent material. The remaining source categories are secondary, their sediment characteristics, colour and magnetic properties reflecting a palimpsest of the processes that deposited and / or weathered them. The sediment colour of sediment samples were classified using a Munsell Colour Chart. The objective description of the properties of samples in their stratigraphic context, in combination with field locations and descriptions, were used to link sediments formed by the same secondary source category. The identification of sub-groups, sediments formed by the same process at different intensities or over different time periods, within each secondary source group was also possible. This allows the identification of spatial differences in source within the catchment. The broad primary and secondary categories of source types have been adopted for use between sites. Region-specific characteristics are summarised in Table 6.3 and discussed in more detail for each site in the following sections. The magnetic properties and source classification of all catchment sediments sampled are given in Appendix 1.4).

Using standard combinations of magnetic parameters or ratios in biplots of source materials, an initial and subjective indication of ease of discrimination was obtained. In addition, magnetic parameters which result in the separation between groups were gained for application in multivariate statistics. Nine standard combinations of magnetic parameters have been applied. The parameters used in biplots a to c presented for each site are essentially measures of concentration and grain size variations. Biplots d to f and g to i are plots of concentration and grain size against remanence acquisition. Where little change is observed, other combinations have been used to determine a difference. In the analysis, different combinations were used to obtain the best differentiation.

Table 6.3. Summary of source group classification and region specific characteristics.

	Source Group	Glen Etive	Moffat	Howgill Fells	Langden Beck
PRIMARY	**Parent material / Bedrock :** Taken from exposures of unconsolidated and weathered bedrock	Samples of weathered bedrock taken from a limited number of exposures		Samples of weathered bedrock taken from a limited number of exposures	Unconsolidated layered shales and sandstone
PRIMARY	**Peat :** Autocthonous, formed within catchment		Blanket peat restricted to catchment interfluves		Blanket peat extends to valley floor
SECONDARY	**Peat Substrate :** Sediment directly underlying peat formed *in situ*		Exposures of peat and the underlying substrate restricted to the convex break of slope on valley sides		
SECONDARY	**Glacial Till :** All material transported and generated by glacial processes	Lateral moraine: on catchment slopes Glacial till : deposited in the main valley and in the headwaters of Coire Dionachd	Lateral moraine : on catchment slopes	Lateral moraine : on catchment slopes	
SECONDARY	**Solifluction Deposits :** Stratified slope deposits	Shallow solifluction deposits on valley slopes	Extensive and thick solifluction deposits on valley slopes	Extensive and thick solifluction deposits on valley slopes, two distinct layers	Soliflucted dense grey clay Soliflucted dense grey clay with sandstone blocks
SECONDARY	**Storage**	Deposits of primary and / or secondary source material stored within a catchment's trunk stream system			
SECONDARY	**Mining waste :**				Mining and quarry waste

The use of multivariate statistics, by summarising a larger number of variables, provides an objective interpretation of the data and their grouping. The factors or values reduce the number of dimensions needed to explain all variance within the data set. A number of techniques can be applied, including cluster analysis, principal components analysis and discriminant analysis. Walden *et al.*, (1997) argue the mathematical simplicity of factor analysis using R- and Q-modes. The use of two modes allows a visual interpretation of how a set of samples respond to groups of variables simultaneously. R- and Q-mode factor analysis is performed separately and then combined. The methodology used in this thesis is outlined in detail by Walden and Smith (1995). R-mode provides factor loadings for the magnetic parameters. Those that plot close together are highly correlated with each other. Q-mode attempts to plot samples that have similar properties close together in factor space. Catchment samples plotting in close proximity can be interpreted as being most similar in terms of the values of the original variables.

In combining the two graphs it is possible to determine magnetic parameter controls on source grouping, aiding the detection of patterns in a multivariate data set. Characterisation of the magnetic variation inherent within each source group identified is also obtained. It is possible to determine which magnetic parameters dominate in discriminating between groups or catchment sources. Thus differences in mineralogy, concentration and grain size characteristics associated with a specific source group will provide information upon the environmental controls that resulted in the differences between the magnetic properties of the source groups. The patterns observed for different source groups can only be interpreted in qualitative terms as the technique is not subject to any form of significance testing (Walden and Smith, 1995). In applying both biplot and factor analysis, the interpretation of the source grouping does not rely upon the initial categorisation. Three parameters are employed to determine source grouping and final discrimination : the context of field location, sample colour, and distinctions identified from differences observed in magnetic characteristics of source materials.

6.3.2 Glen Etive - Coire Dionachd

The location of exposures from within the supplying catchment and within close proximity of Coire Dionachd is illustrated in Figure 6.3. A total of 41 samples were taken for source categorisation, the distribution of samples taken between each

exposure is supplied in Figure 6.3. Within the catchment, two main sources of sediment have been identified. A large amount of glacial material is preserved within the supplying catchment. The gently sloping eastern slopes of the catchment are buried by glacial drift deposits or lateral moraine and currently represent the only source of fines within the catchment on a large scale. CD2 and CD3 have been sampled from sediments exposed by a major gully which has dissected the sediments. Large amounts of glacial till deposits are present in the headwaters of the catchment, dumped by the down-wasting of the catchment's Loch Lomond Corrie glacier. Two exposures of glacial till have been sampled, CD5 and CD6 (Figure 6.3a).

The second major sediment source within the catchment has been eroded from sheer, western bedrock slopes and deposited at their base within the trunk stream. In combination with reworked boulders of glacial material, trunk stream storage represents a major source of large clasts and boulders. The storage within the trunk stream is dominated by large boulders and has supplied the most recent phase of activity within the fan. CD1 represents sediment storage samples taken from a lag deposit within the trunk stream. From within the main valley, exposures of glacial till, lateral moraine and shallow soliflucted deposits been sampled to supplement the data analysis (Figure 6.3b) due to lack of exposures available within the supplying catchment. Overall the system is dominated by glacial material formed directly as a result of the Loch Lomond Stadial. Following the short period of glaciation the glacial sediments have undergone limited alteration, apart from the formation of the modern soil and its previous burial by peat during the late Holocene.

Evidence of peat that has been transported by a flow generated within the supplying catchment of Coire Dionachd signifies a catchment peat source . The radiocarbon dates of the peat preserved in the section correlate with a time period of local blanket peat cover development on catchment slopes. In the field, no evidence of a surface or buried peat layer within the catchment was found. A peat source is therefore not represented in the sediment provenance of fan sediments using mineral magnetics.

The magnetic parameter biplots for source samples from Glen Etive are presented in Figure 6.4. The three major sediment sources of glacial till, lateral moraine and soliflucted material cannot be mutually separated. Despite the overlap

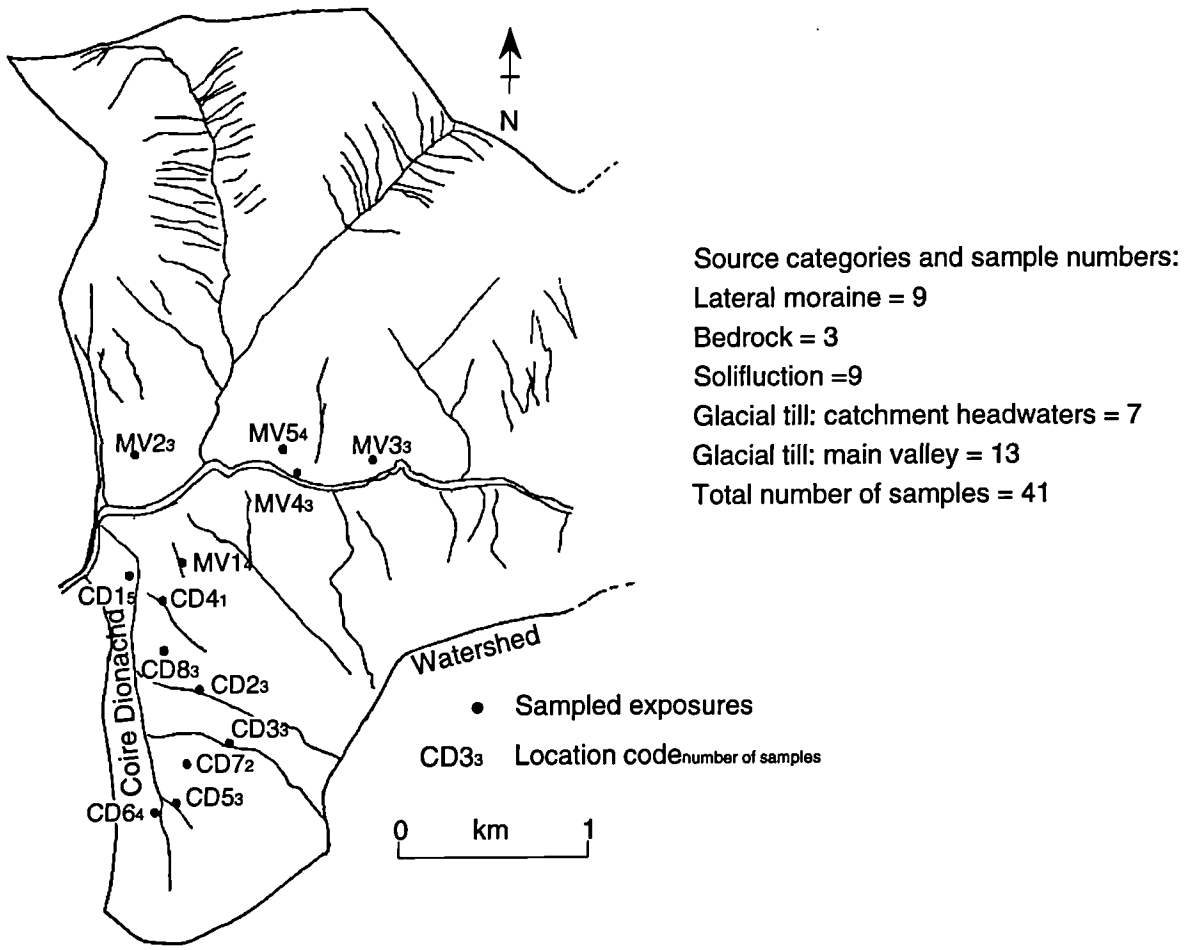


Figure 6.3. Location of catchment sample points, Glen Etive. CD : Coire Dionachd, MV : Glen Etive main valley

observed between the three groups in the bivariate plots, some patterns can be seen. Both solifluction and lateral moraine samples have higher values of both SIRM and *X* (Figure 6.4a), indicating a higher concentration of magnetic minerals relative to glacial till. Concentration values range between two extremes, from very low concentrations with limited magnetic minerals to very high values. The large range can be explained by the presence of pure iron found within the samples. Solifluction values also have higher SIRM/*X* in comparison to both valley and lateral moraine samples. All of the source samples taken have IRM1T/SIRM ratios greater than 0.8. Magnetite is therefore the dominant mineralogy (Thompson and Oldfield, 1986). The relative changes observed for SIRM/*X* ratios are as a result associated with grain size variations (Table 6.2). Relative to lateral and solifluction samples, glacial till samples were harder to magnetise. The samples correlate with those which have the lowest SIRM and *X* values. No additional information is obtained from biplots of the remaining magnetic parameters.

Factor analysis, in combining the variability and thus the patterns found for the eight magnetic parameters used in the bivariate plots, provides a degree of differentiation between the three source groups. The eigenvalues for the analysis indicate that factors 1 and 2 explain 70% of the variation within the raw data set (Table 6.4). Figure 6.5 shows a plot of the R-mode variable (magnetic parameter) and Q-mode source material sample loadings on factors 1 and 2. The differentiation observed between the three groups is essentially controlled by variation of magnetic parameters on factor 2. The separation observed between the source groups is not exclusive, although the mean values for each group are outside of the convex hull or outer limit of each source group (Figure 6.5). The use of all fourteen magnetic parameters in factor analysis does not enhance the differentiation observed between the source groups in Figure 6.6.

The nature of the overlap in combination with the pattern of the differentiation relative to positions of the magnetic parameters has an environmental interpretation. The loadings for each magnetic parameter on factor 1 and 2 are summarised in Figure 6.7. Factor 1 is strongly influenced by *X*, positive factor loading and SIRM/*X*, negative factor loading. SIRM, SARM and IRM1T/SIRM also have large loadings on factor 1 but also have some effect on factor 2. Factor 2 is clearly controlled by the positive loadings of ARM-40mT/SARM and the negative loadings of IRM40mT/SIRM and IRM100mT/SIRM (Table 6.4). The significance of each controlling magnetic

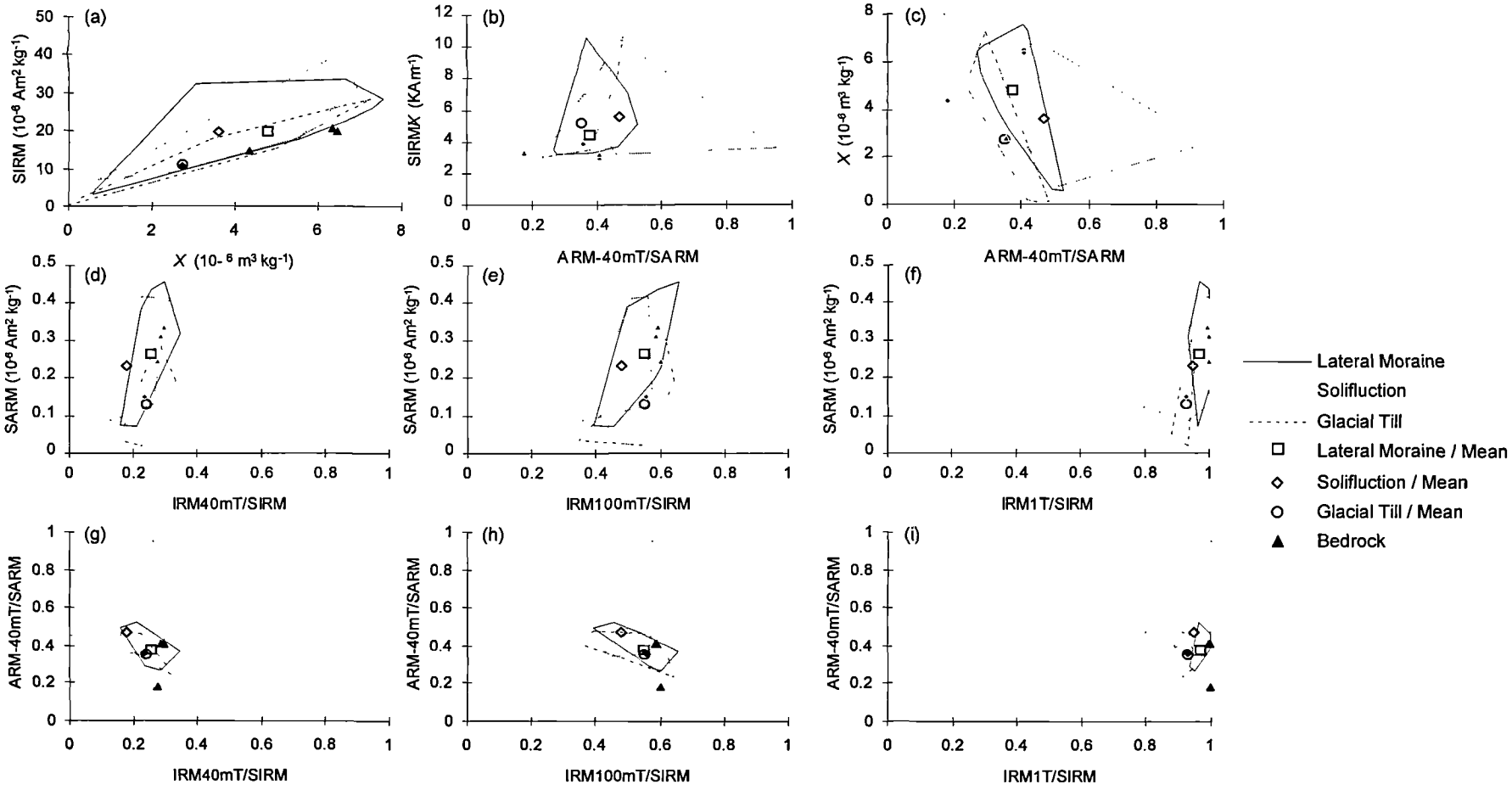


Figure 6.4. Biplots of magnetic parameters showing the variation in magnetic concentration and magnetic remanence acquisition of the catchment source sediments of Glen Etive. A convex hull encloses the outermost samples of the major source groups, lateral moraine, solifluction and glacial till. The plotted position of the respective mean values allows a visual interpretation of source group differentiation (see Figure 6.2 for an explanation of biplot interpretation)

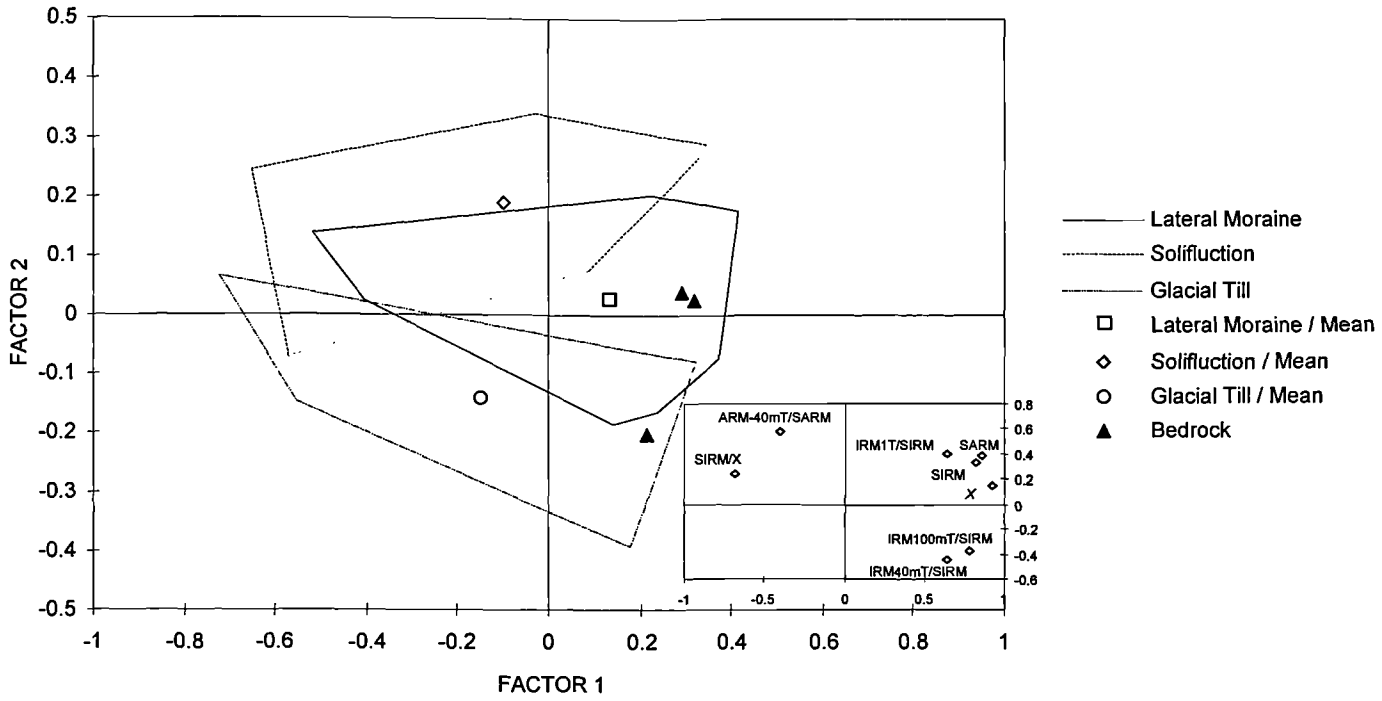


Figure 6.5. Plot of loadings on Factor 1 and Factor 2 obtained for Glen Etive catchment samples based upon the eight magnetic parameters used in the biplot analysis. The position of the catchment samples in relation to their original variables is shown in the inset graph, bottom right.

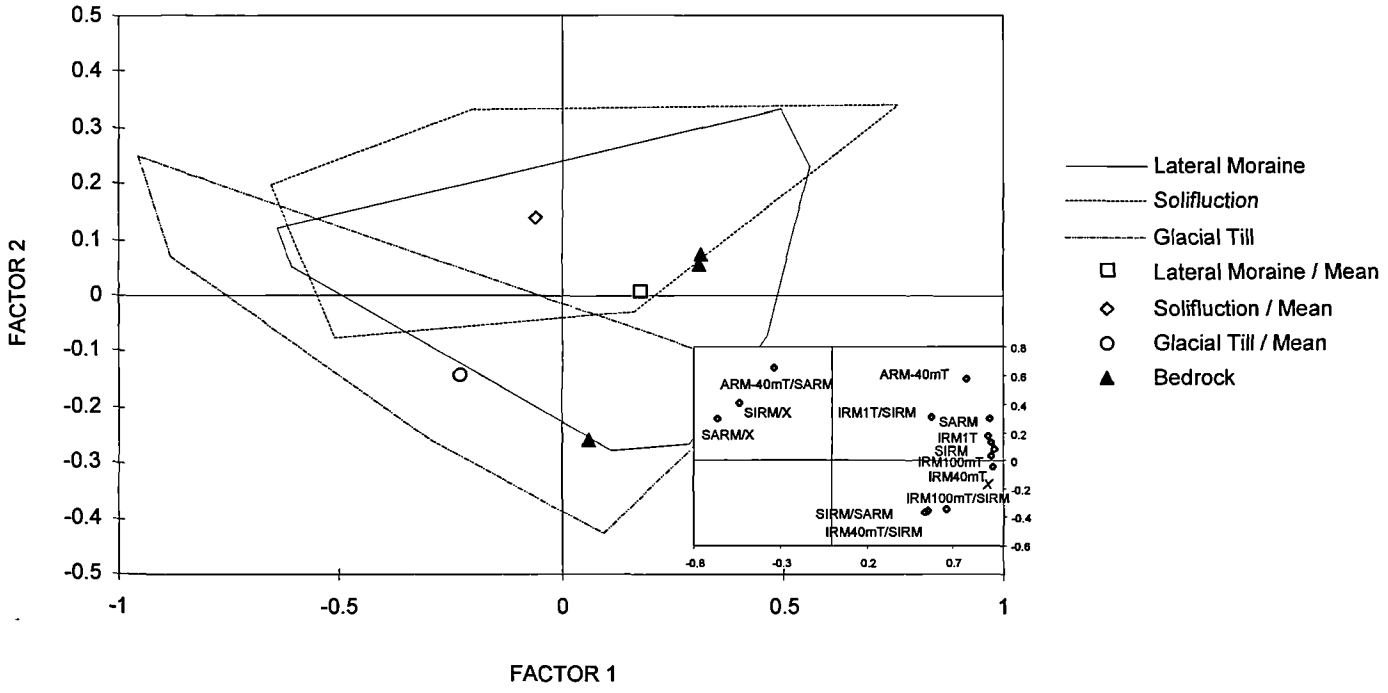


Figure 6.6. Plot of loadings on Factor 1 and Factor 2 for Glen Etive catchment samples using the maximum combination of measured magnetic variables and their ratios. The position of the original variables in relation to the catchment samples is shown in the inset graph, bottom right. The differentiation between the source groups is not enhanced by the use of more magnetic parameters.

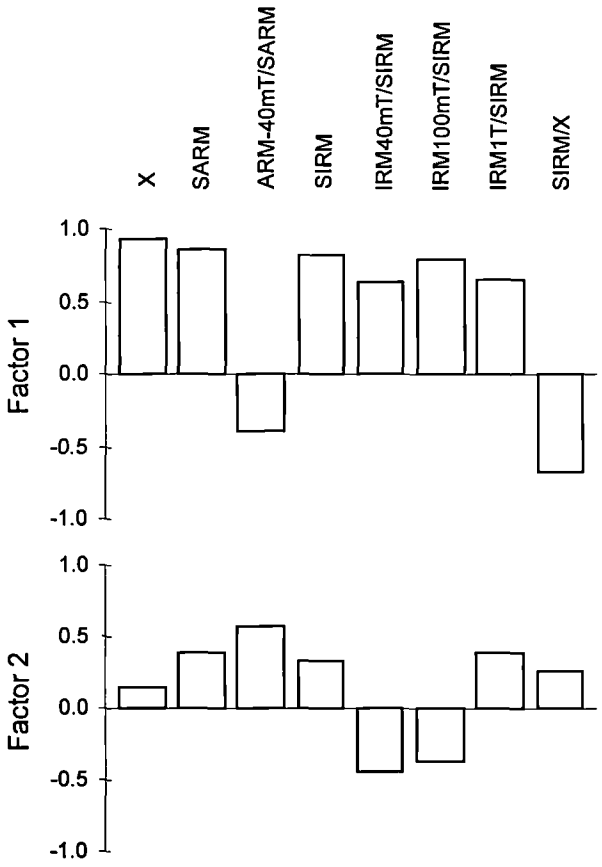


Figure 6.7. Loadings of the magnetic variables on the first two factors of Glen Etive catchment source samples

Table 6.4. Results of Factor analysis for catchment samples of Glen Etive: eigenvalues, eigenvectors and degree of variance

	Eigenvectors			Eigenvalue	Total variance	Total variance
Magnetic Parameter	Factor 1	Factor 2	Factor		(%)	(cumulative %)
X (10^{-6} m^3 kg^{-1})	0.93	0.14	1	4.33	54.12	54.12
SARM (10^{-6} Am^2 kg^{-1})	0.86	0.39	2	1.17	14.57	68.69
ARM-40mT/SARM	-0.40	0.57	3	1.09	13.65	82.34
SIRM (10^{-6} Am^2 kg^{-1})	0.82	0.32	4	0.62	7.72	90.06
IRM40mT/SIRM	0.64	-0.44	5	0.39	4.90	94.96
IRM100mT/SIRM	0.79	-0.37	6	0.28	3.47	98.43
IRMT1/SIRM	0.64	0.39	7	0.08	1.01	99.45
SIRM/*X* (KAm^{-1})	-0.68	0.26	8	0.04	0.55	100.00

parameter is illustrated for factor 1 and factor 2 in Figure 6.8. On factor 1, all three source groups show a wide range in the overall susceptibility or concentration of all magnetic minerals within their samples. The similarity in the loadings of X and SIRM indicates that the magnetic properties of the samples are dominated by the concentration of minerals carrying a magnetic remanence. On factor 2, however relative variations in SIRM/X and SIRM and thus variation in the concentration of remanence-carrying minerals within the samples helps to differentiate between the three source groups. A progressive increase in the concentration of remanence-carrying minerals is evident from glacial till, lateral moraine through to solifluction deposits (Figure 6.8). A change from multi-domain to single-domain dominance is concomitant with a progressive change through the source groups. The three groups can also be separated by differences in the nature of remanence acquisition. Glacial till samples acquire a larger magnetic remanence at 40 mT and 100 mT field strengths, contrasting with solifluction deposits. Solifluction samples are harder to magnetise but are closest to full saturation at IRM1T/SIRM values. As noted from the biplot interpretation, the predominant mineralogy is magnetite. The differences in acquisition are therefore associated with changes in magnetite properties from soft to hard. The nature of the source grouping and the differences in concentration, mineralogy and grain size observed suggest that the process which results in the formation of solifluction deposits has liberated and concentrated magnetite from the lateral moraine which is formed from the parent material. This characteristic accounts for the overlap between the solifluction and lateral moraine source groups.

6.3.3 Moffat - Dry Cleuch and Hermanlaw Burn

The available sediment for transport with the reach studied in Yarrow Water can be split into three main source groups: glacial till deposited as lateral moraine deposits, soliflucted material and interfluve blanket peat. Glacial till and solifluction sources are not independent as soliflucted material has formed within previous lateral moraine deposits which extend to a height of 275 m on valley sides (May, 1981). The formation of extensive solifluction deposits on the valley side has produced two separate sediment sources controlled by the location of the upper surface of the active layer. The temporal association of the two sources, one having been formed subsequently from the other, does not affect the study of a temporal change in sediment source as activity within the fan occurred well after the formation of the soliflucted deposits (Tivy, 1962).

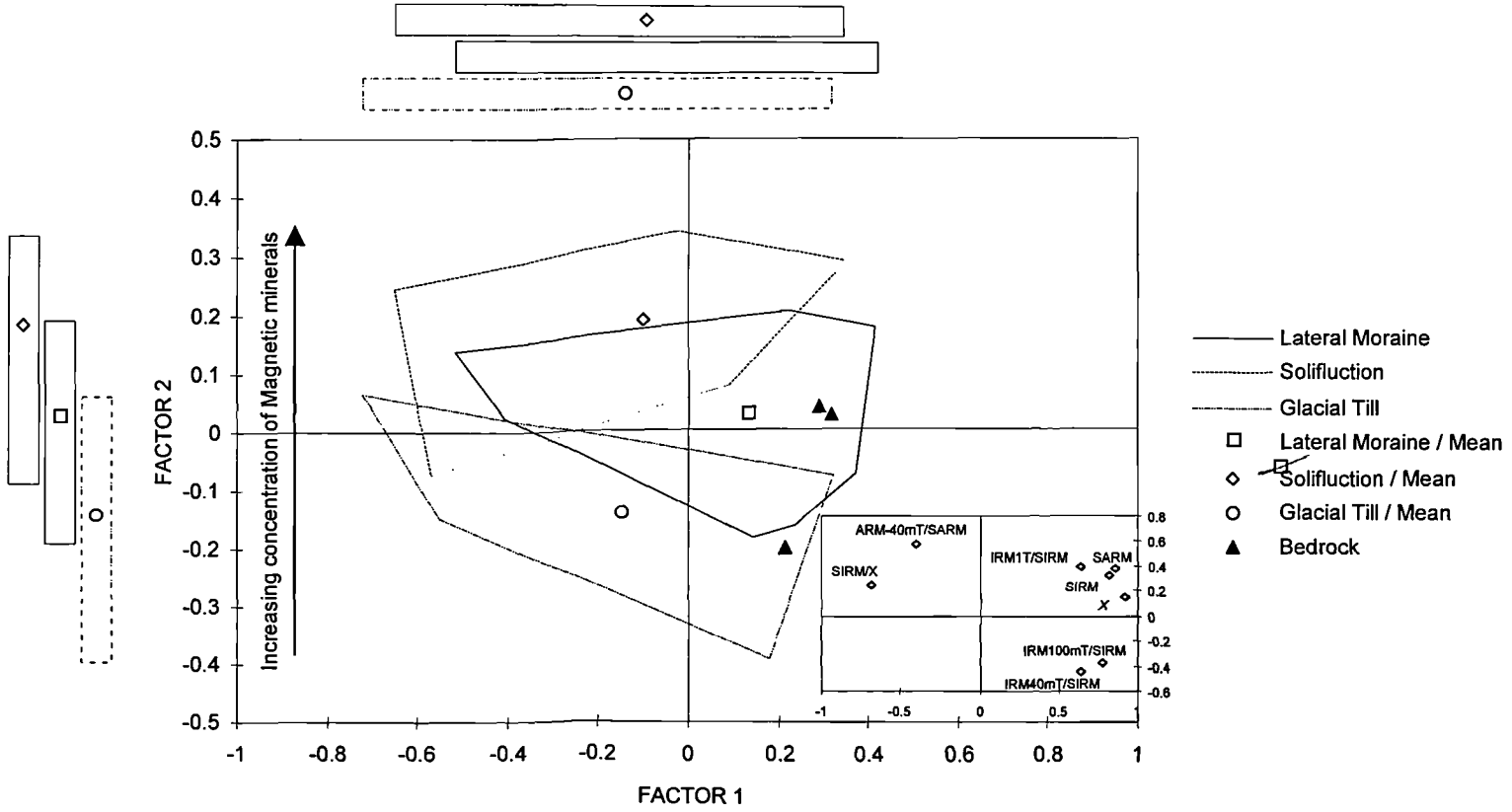
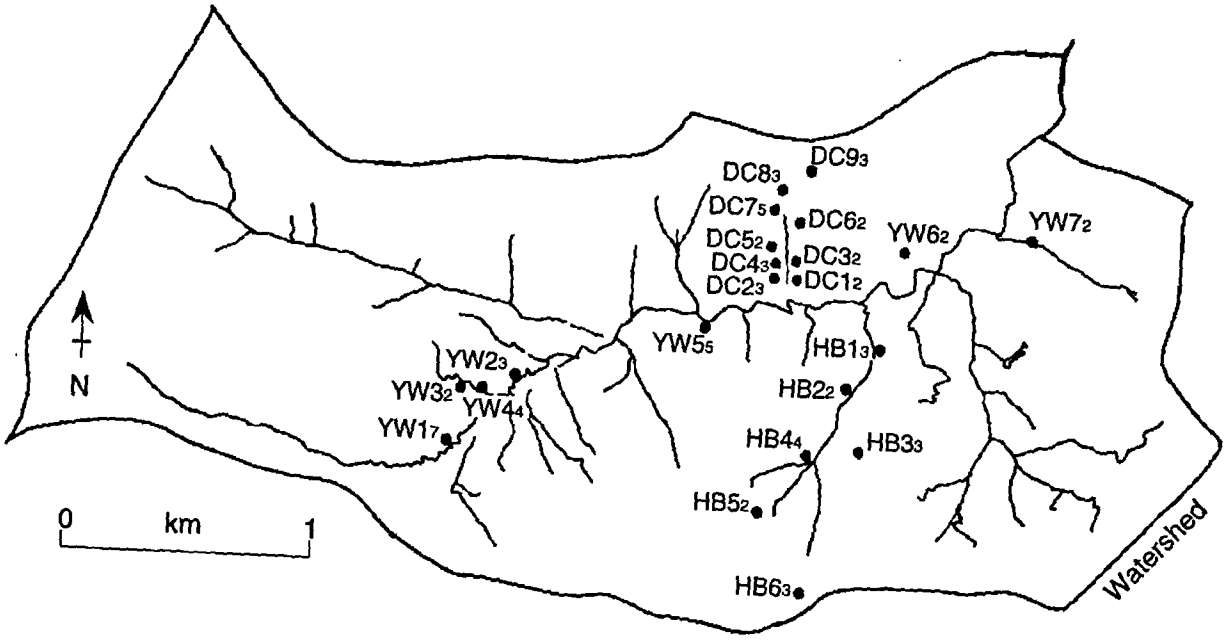


Figure 6.8. A summary of the differentiation observed between the measured magnetic properties of the source groups at Glen Etive using factor analysis. In marking the maximum extent of each source group and the position of its mean on each factor, the degree of differentiation between each source group is readily seen.

The depth of exposures of sediment sources within the catchment of Dry Cleuch have limited sampling to solifluction material only. Samples of peat and the deposits it buries are the only other sediment sources identified within the catchment. Samples have been taken from trunk stream storage (Figure 6.9a). The same source groupings of sediment have been identified within Hermanlaw Burn (Figure 6.9b). The two only differ by catchment configuration. Dry Cleuch is dominated by a linear supplying gully which opens out into a shallow headbowl at the break of slope. Hermanlaw Burn is supplied by an entrenched trunk stream divorced from slope sediment reserves until it opens out within the headwater region. As no exposures of the underlying glacial till were available within both supplying catchments, samples were taken from exposures on valley slopes and at the base of slope eroded by the main river within the study reach to supplement source characterisation (Figure 6.9). In total 25 samples were taken from selected exposures in the main valley, 25 within Dry Cleuch and 17 at Hermanlaw Burn (Figure 6.9).

The biplot of SIRM vs. X (Figure 6.10a) clearly indicates that solifluction samples have a higher concentration of magnetic materials than the glacial material. The greater difference between the two source groups is seen in SIRM values, indicating that solifluction material also has a greater concentration of remanence bearing minerals. This characteristic is confirmed by high SARM values for the solifluction deposits. A marked difference between the solifluction and glacial groups is mirrored in their contrasting ARM-40mT/SARM values (Figure 6.10g). Solifluction deposits have higher SIRM/X values, indicating that solifluction deposits are dominated by a greater concentration of remanence multigrain magnetic minerals (Figure 6.10b).

Higher values of SIRM/X are often associated with presence of haematite and goethite. The nature of remanence acquisition of the two source groups indicates that both groups have similar mixtures of magnetic minerals. The two groups cannot be differentiated using remanence acquisitions. It is evident however that storage samples have relatively lower values of remanence at 1T field for solifluction samples indicates the greater concentration of goethite. The remaining source groups of peat cannot be separated from the other source groups. Peat samples vary in characteristics but commonly have low concentrations of magnetic minerals. The underlying substrate maintains the characteristics of the source substrate, glacial or solifluction.



- Sampled exposures

DC3₂ Location code$_{\text{number of samples}}$

Source categories and sample numbers:
Lateral moraine: main valley = 19
Lateral moraine: catchment slopes = 2
Solifluction = 28
Peat = 6
Peat substrate = 3
Storage = 9
Total number of samples = 67

Figure 6.9. Location of catchment sample points, Yarrow Water. DC : Dry Cleuch, HB : Hermanlaw Burn and YW : Yarrow Water main valley

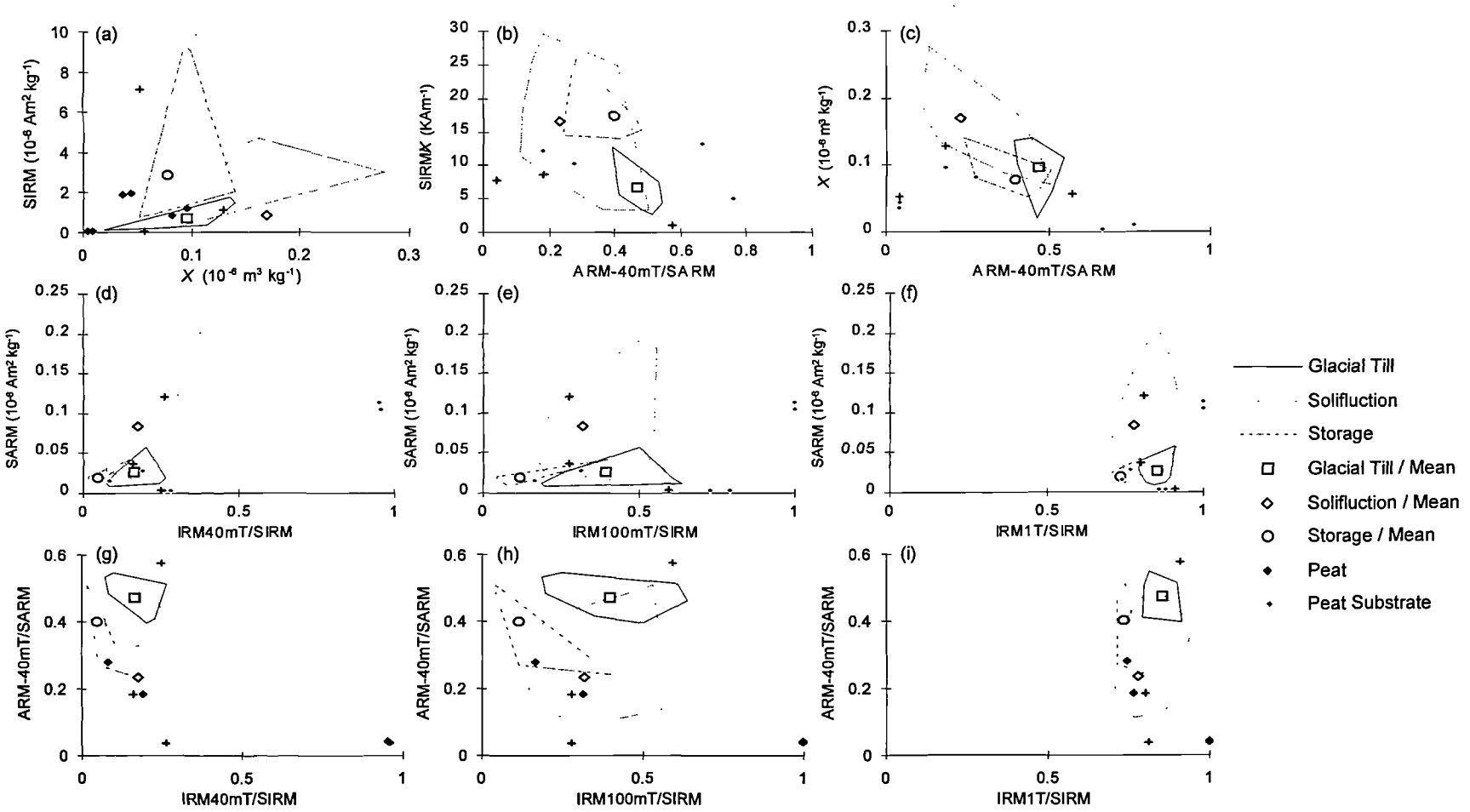


Figure 6.10. Biplots of magnetic parameters showing the variation in magnetic concentration and magnetic remanence acquisition of the catchment source sediments of Moffat. A convex hull encloses the outermost samples of the major source groups glacial till, solifluction deposits and secondary transported material or storage. The plotted position of the respective mean values allows a visual interpretation of source group differentiation (see Figure 6.2 for an explanation of biplot interpretation).

A plot of the variable and sample loadings from the R- and Q-mode factor analysis based upon the eight magnetic parameters used in the biplots for the catchment samples in Figure 6.10 are shown in Figure 6.11. The eigenvalues for the analysis indicate that factors 1 and 2 explain over 70% of the variation in the raw data set (Table 6.5). The interpretation of the biplots and the control exerted by specific magnetic parameters is confirmed from the position of the original variables in relation to source grouping of the catchment samples. Factor 1 is dominated by SIRM, *X* and SIRM/*X*, measures of concentration, and by SARM a measure of the ease of magnetisation of samples (Figure 6.12). The parameters plot close together in factor space as they are fundamentally related. The close proximity of SIRM/*X* and SIRM confirm the importance of remanence concentration of magnetic minerals. Solifluction samples plot close to this indicating higher concentration of magnetic remanence bearing minerals in comparison with the glacial sediments which plot on the opposite end of the axis. High SIRM values of the solifluction samples are indicative of the liberation of magnetic minerals from primary iron oxides (Maher, 1986). The storage source group plots the furthest from IRM1T/SIRM and IRM100mT/SIRM parameters indicative of the greater concentration of goethite/haematite. A plot of ARM-40mT/SARM which dominates factor 2 is plotted against factor 1 and highlights the difference between the source groups (Figure 6.13). The solifluction and glacial deposits form two distinct clusters of samples with overlap of only four solifluction samples within the glacial envelope. The solifluction samples retain the characteristics of parent glacial substrate. The grouping suggests that the source characteristics can be distinguished on the basis of either magnetic parameters, with the greatest difference produced by ARM-40mT/SARM values.

6.3.4 Howgill Fells - Burnt Gill, Nevy Gill, Thickcombs Gill and Leath Gill

A total of 109 samples were taken from exposures within each of the four catchments. The characterisation of source groups is supplemented with 24 samples taken from valley side exposures of both glacial and soliflucted material from Langdale and Bowderdale (Figure 6.14). Source materials available within the Howgill Fells are comparable to that found at Moffat. Valley side slopes are bedecked with a continuous covering of soliflucted material formed within deposits of lateral moraine. At the break of slope solifluction deposits are buried by blanket peat present on valley interfluves. Exposures of glacial till or lateral moraine are limited.

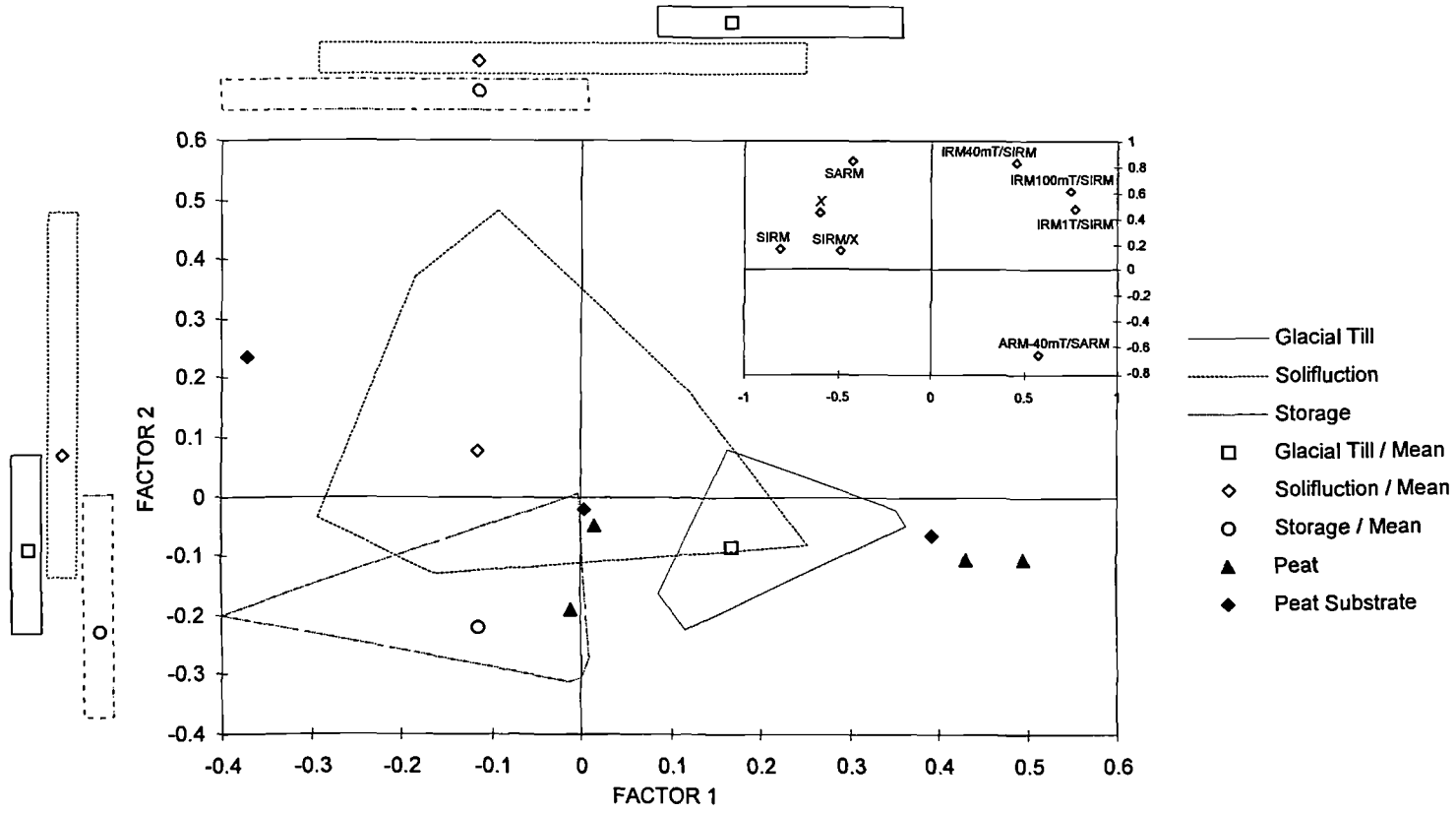


Figure 6.11. Plot of loadings on Factor 1 and Factor 2 obtained for Moffat catchment source samples based upon the eight magnetic parameters used in the biplot analysis. The position of the catchment samples in relation to their original variables is shown in the inset graph, top right. The degree of differentiation observed between the three major source groups on Factor 1 and Factor 2 is also illustrated.

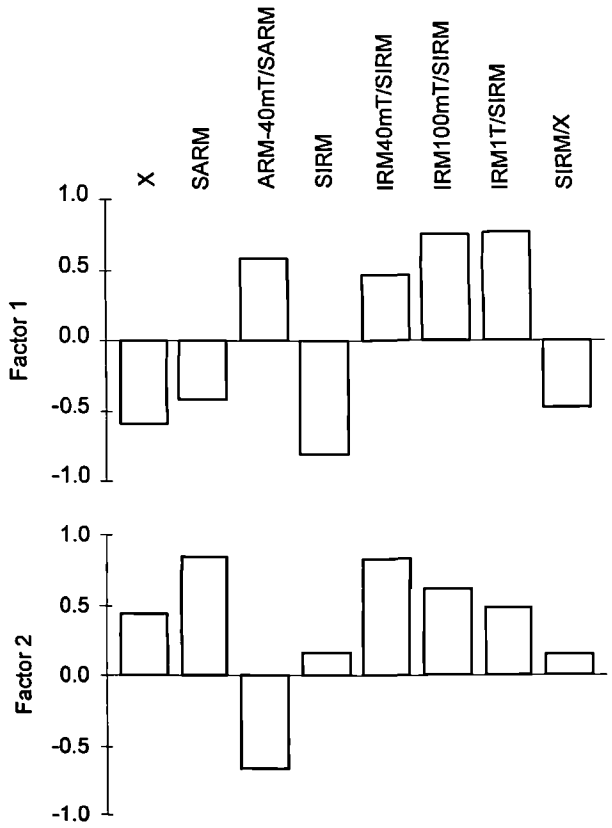


Figure 6.12. Factor Loadings of the eight magnetic parameters used in R- and Q- mode Factor analysis at Moffat

Table 6.5. Results of Factor analysis for catchment samples of Moffat: eigenvalues, eigenvectors and degree of variance

	Eigenvectors			Eigenvalue	Total variance	Total variance
Magnetic Parameter	Factor 1	Factor 2	Factor		(%)	(cumulative %)
X (10^{-6} m^3 kg^{-1})	-0.59	0.44	1	3.12	39.00	39.00
SARM (10^{-6} Am^2 kg^{-1})	-0.42	0.84	2	2.68	33.53	72.53
ARM-40mT/SARM	0.58	-0.67	3	1.44	17.94	90.47
SIRM (10^{-6} Am^2 kg^{-1})	-0.81	0.16	4	0.46	5.79	96.26
IRM40mT/SIRM	0.46	0.82	5	0.14	1.77	98.03
IRM100mT/SIRM	0.75	0.61	6	0.09	1.15	99.18
IRMT1/SIRM	0.77	0.48	7	0.05	0.58	99.76
SIRM/*X* (KAm^{-1})	-0.48	0.14	8	0.02	0.24	100

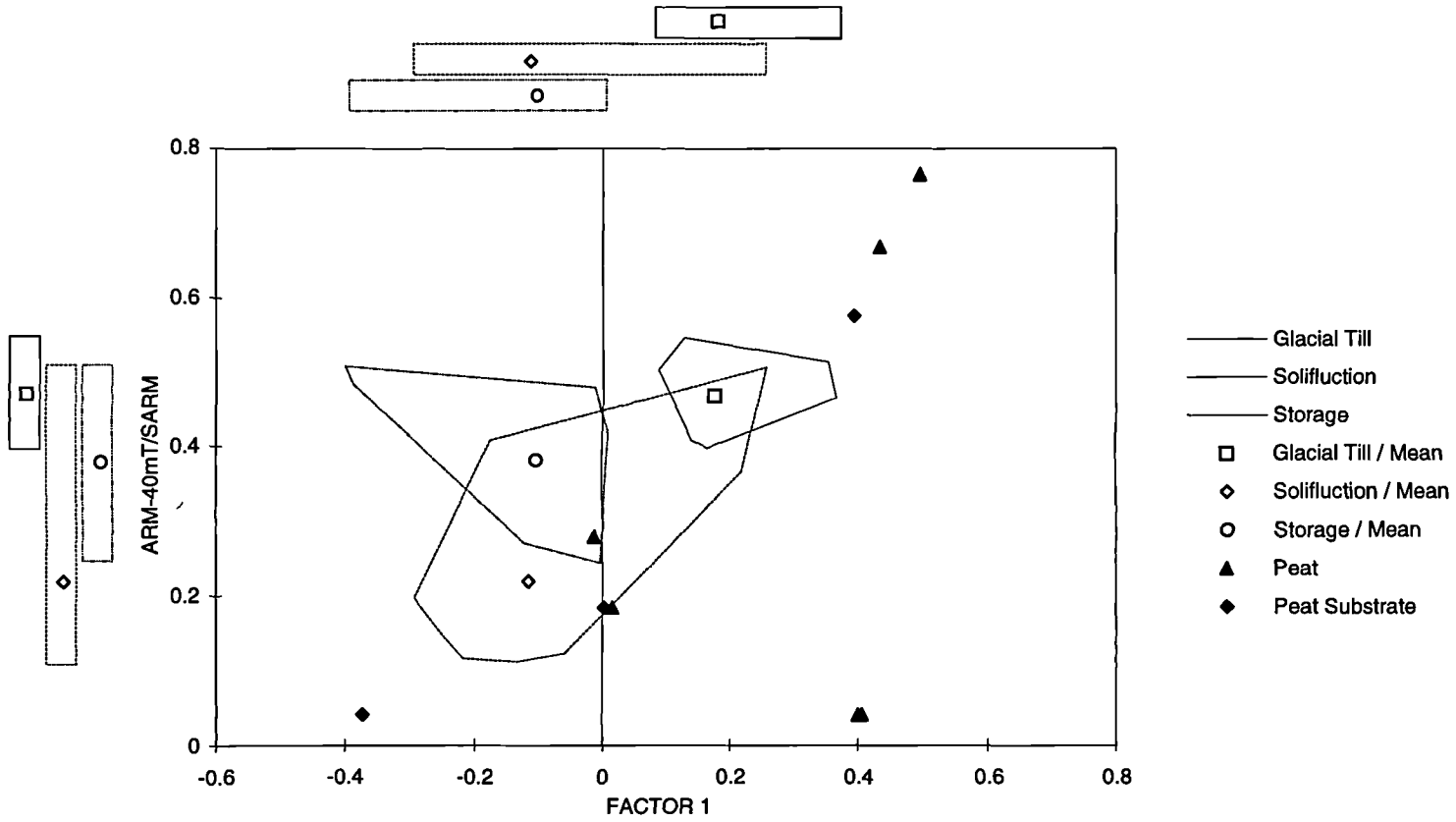
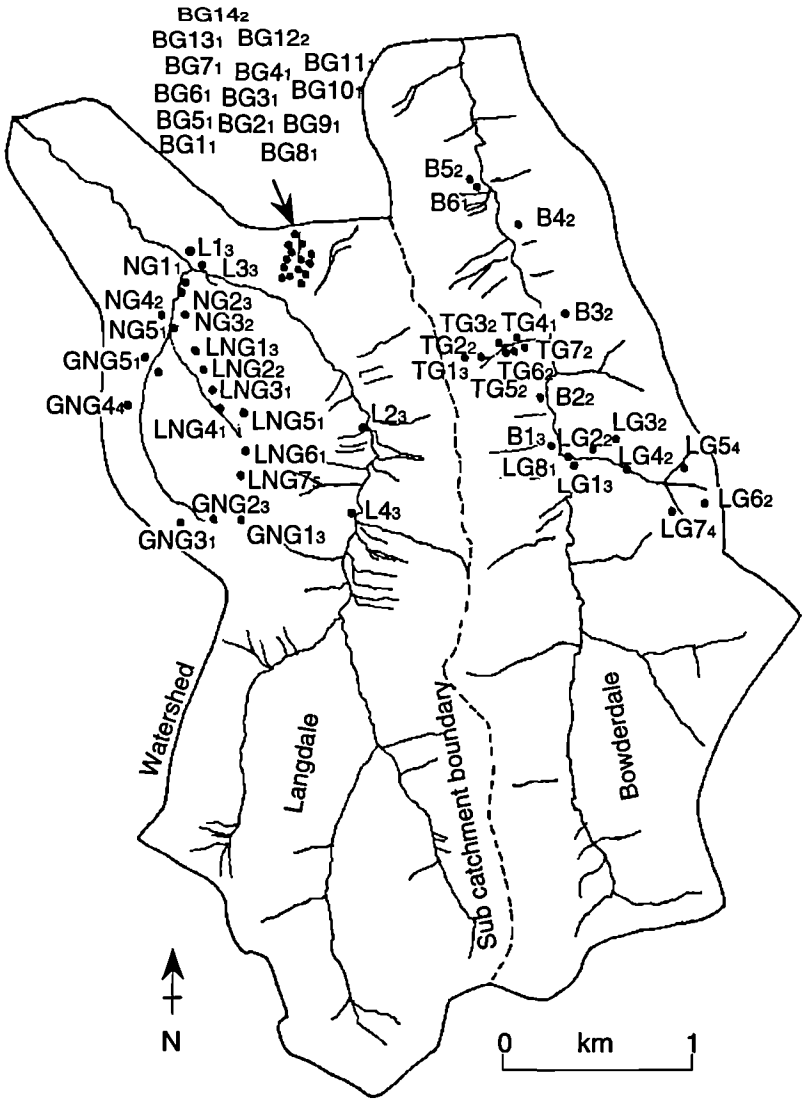


Figure 6.13. Plot of ARM40-mT/SARM against Factor 1 shows the importance of this single magnetic parameter in differentiating between the three major source groups at Moffat.



- Sampled exposures

$TG2_2$ Location code$_{\text{number of samples}}$

Source categories and sample numbers:
Lateral moraine: main valley = 19
Lateral moraine: catchment slopes = 11
Bedrock = 4
Solifluction = 28
Solifluction: lower layer = 10
Solifluction: upper layer = 12
Peat = 11
Peat substrate = 9
Storage = 5
Total number of samples = 109

Figure 6.14. Location of catchment sample points, the Howgill Fells. L : Langdale main valley, B : Bowderdale main valley, BG : Burnt Gill, NG : Nevy Gill, LNG : Little Nevy Gill, GNG : Great Nevy Gill, TG : Thickcombs Gill and LG : Leath Gill

The exposures L1, L2, L3, and L4 are all found within remnants of a former valley side bluff which has been eroded by the migrating river as it has lowered the valley floor to its current position. Within each exposure thick deposits of moraine of over 3m are capped by a solifluction layer which is continuous laterally. The solifluction deposits in the Howgill Fells, in both valleys, are characterised by two separate layers. The contact between each layer is sharp, laterally continuous, at a uniform depth between exposures and coincident with a change in sediment texture. The characteristic suggests two separate phases of solifluction, the contact between the two layers representing the depth of the active layer. The uppermost layer represents a second phase of solifluction activity. The deposits of the initial solifluction phase have been reworked as the layering is found in solifluction deposits near the break of slope.

Bivariate combinations of magnetic parameters identify clear differences in the magnetic properties of the source groups identified within the Howgill Fells. The biplot of SIRM v *X* separates peat and peat substrate from the remaining two groups, due to their very low susceptibility and remanence values. The ease of remanence acquisition illustrated in Figure 6.15 d to f and g to i identify mineralogical differences in the haematite / goethite and magnetite ratios found in glacial and solifluction samples. Glacial moraine samples divide solifluction samples into two groups, with a degree of overlap. The separation of the solifluction samples into two separate groups is confirmed by differences observed in SARM and ARM-40mT/SARM values when plotted against IRM ratios. Essentially, group 1 with high SARM and low ARM-40mT/SARM values is dominated by magnetite whilst group 2 with low SARM and ARM-40mT/SARM values contains a high concentration of haematite/goethite.

The concentration and mineralogical differences are confirmed by the results of the factor analysis, which is based upon the eight magnetic parameters used in the bivariate plots. The plot of factor 1 and factor 2 is presented in Figure 6.16 which accounts of approximately 70% of the variation in the raw data (Table 6.6). Factor 1 and factor 2 loadings of the source samples retain and tightly constrain the differentiation between the source groups identified from the bivariate plots. The dominance of each magnetic parameter on each factor is illustrated in Figure 6.17. A summary of the significance of the dominant magnetic parameter controls on each factor is illustrated in Figure 6.16. Factor 2 influenced by SIRM is a measure of the concentration of the remanence magnetic minerals within the samples. Differences

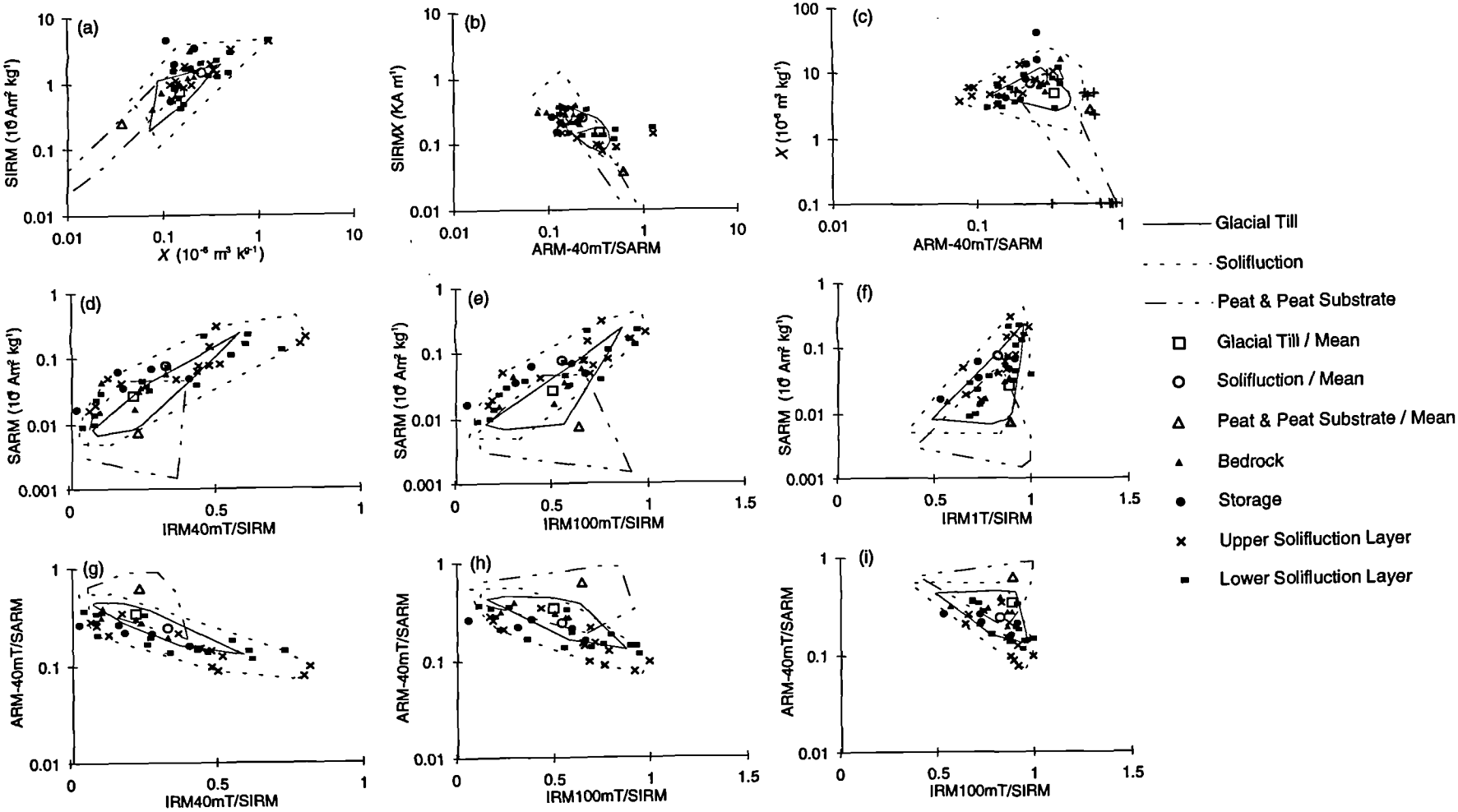


Figure 6.15. Biplots of magnetic parameters showing the variation in magnetic concentration and magnetic remanence acquisition of the catchment source sediments of the Howgill Fells. A convex hull encloses the outermost samples of the major source groups glacial till, solifluction deposits and peat, including the underlying substrate. The plotted position of the respective mean values allows a visual interpretation of source group differentiation (see Figure 6.2 for an explanation of biplot interpretation).

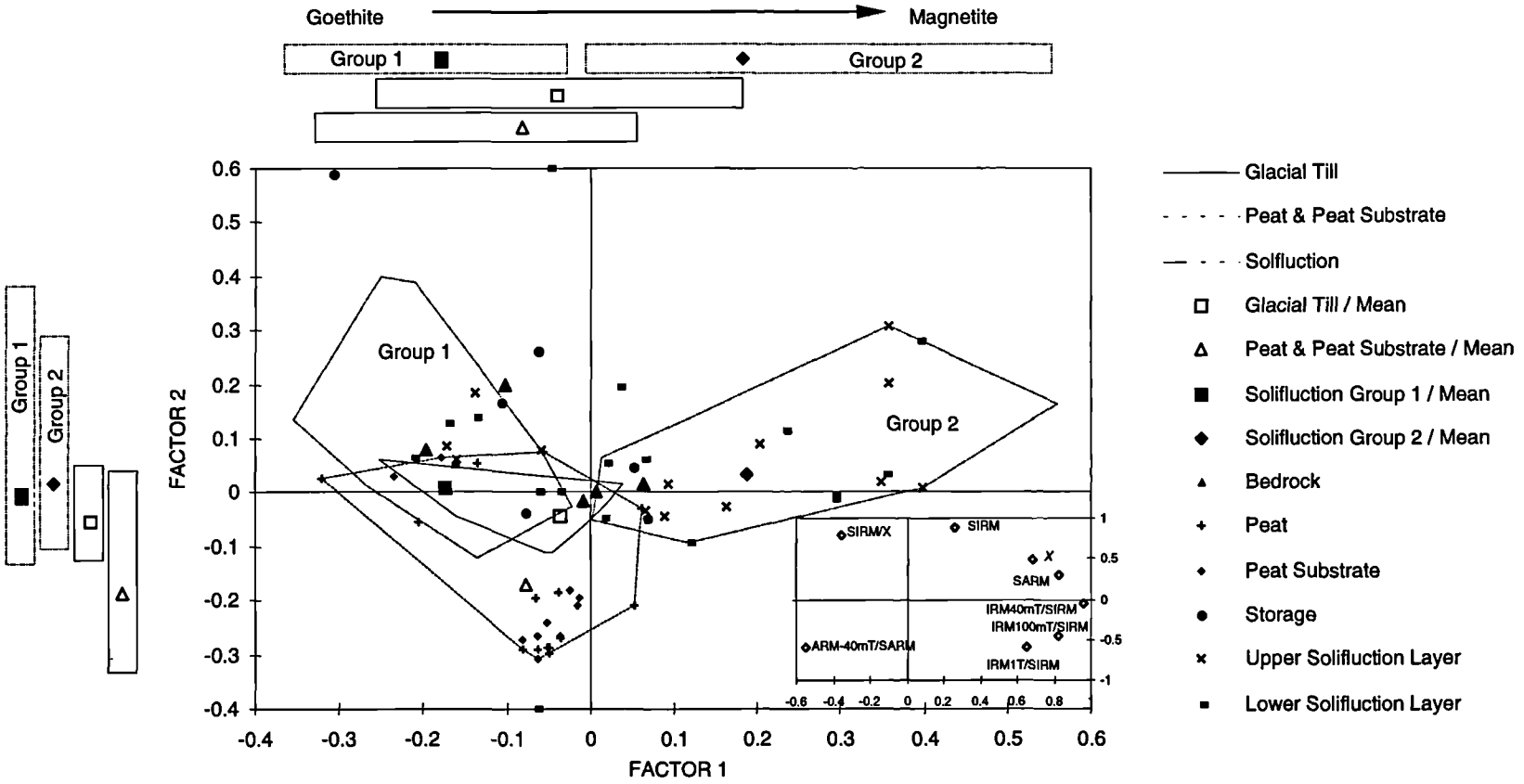


Figure 6.16. Plot of loadings on Factor 1 and Factor 2 obtained for the Howgill Fell catchment source samples based upon the eight magnetic parameters used in the biplot analysis. The position of the catchment samples in relation to their original variables is shown in the inset graph, bottom right. The solifluction source group has been further subdivided based upon mineralogical differences explained by Factor 1. The degree of differentiation observed between the four source groups on Factor 1 and Factor 2 is also illustrated.

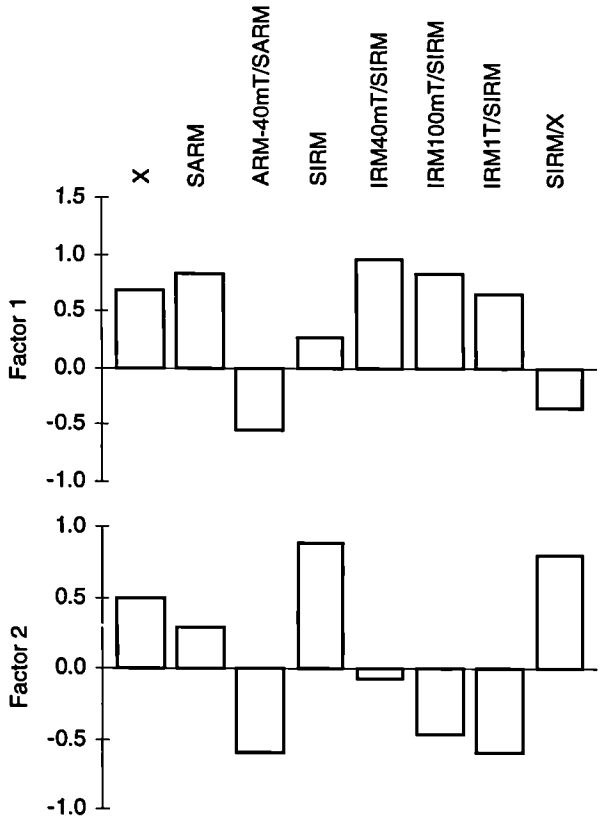


Figure 6.17. Loadings of the magnetic variables on the first two factors of the Howgill Fell catchment source samples

Table 6.6. Results of Factor analysis for catchment samples of the Howgill Fells: eigenvalues, eigenvectors and degree of variance

	Eigenvectors			Eigenvalue	Total variance	Total variance
Magnetic Parameter	Factor 1	Factor 2	Factor		(%)	(cumulative %)
X (10^{-6} m^3 kg^{-1})	0.68	0.49	1	3.68	46.03	46.03
SARM (10^{-6} Am^2 kg^{-1})	0.832	0.29	2	2.68	33.49	79.51
ARM-40mT/SARM	-0.55	-0.60	3	0.59	7.35	86.86
SIRM (10^{-6} Am^2 kg^{-1})	0.26	0.88	4	0.51	6.42	93.28
IRM40mT/SIRM	0.96	-0.07	5	0.33	4.11	97.39
IRM100mT/SIRM	0.83	-0.47	6	0.15	1.85	99.24
IRMT1/SIRM	0.66	-0.60	7	0.04	0.47	99.70
SIRM/*X* (KAm^{-1})	-0.35	0.80	8	0.02	0.30	100

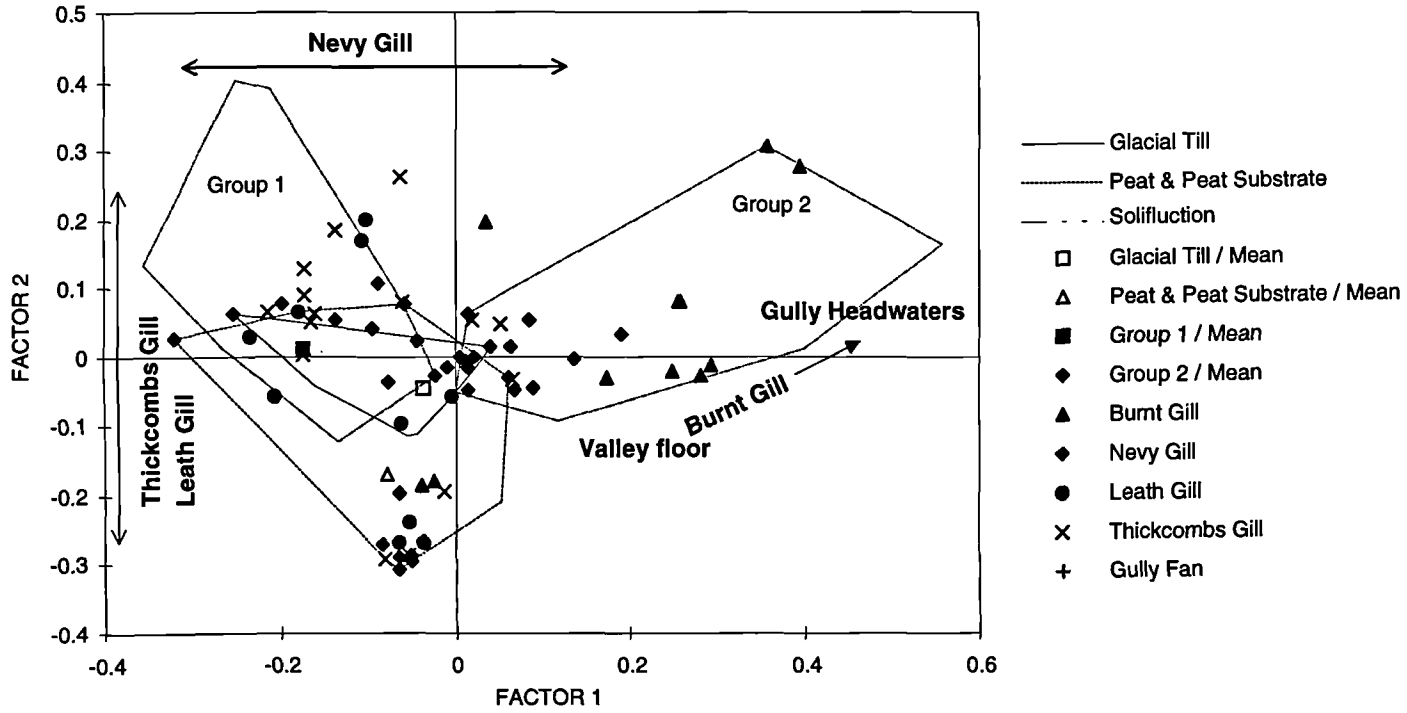


Figure 6.18. An illustration of the within and between catchment variability of the magnetic properties of source samples. Differences observed have environmental and locational explanations (see text for explanation)

on this axis provide the differentiation of the peat samples from glacial and solifluction samples. Concentration of SIRM values for both solifluction groups is variable, whilst values of SIRM for glacial samples are more tightly constrained. The dominance of IRM40mT/SIRM, and IRM100mT/SIRM, IRM1T/SIRM on factor 1 clearly separates the two solifluction groups. Solifluction group 1, which has high positive loadings on factor 1 and therefore high values for the forward field ratios, confirms the dominance of magnetite within the samples. High SARM and *X* values and low ARM-40mT/SARM confirm the presence of magnetite within the solifluction group. The magnetic characteristics of solifluction group 2 are the complete opposite, highlighting the dominance of goethite/ haematite.

A large degree of overlap is observed between solifluction group 1 and the glacial group. A review of the source assignment of the solifluction samples which fall within and in close proximity to the glacial group has shown that some of the samples were previously mis-classified. The majority of the samples which retain their original classification are located low down on the valley side or are sampled at the base of the exposure. Those low down on the valley side have colour comparable to those given for the glacial group. The samples taken from the base of the exposure are likely to retain the characteristics of the glacial substrate. Both can therefore be reclassified. Only three sample show characteristics similar to glacial material which cannot be reclassified, explained by the overlap between the source material and the solifluction deposit which has formed from it. The glacial material is the source substrate for both solifluction groups. The difference between the two solifluction groups cannot be explained by differences in the characteristics between valleys or by differences in the magnetic properties of the two separate solifluction layers. By plotting the catchment identification number it is evident that source group 1 is made up of samples from Gully Fan and Burnt Gill whilst group 2 is dominated by Leath Gill, Thickcombs Gill and Nevy Gill. The differences observed can be attributed to distance from The Calf, the highest point in the Howgill Fells and the location of the Howgill Fells ice cap from which glaciers radiated out and formed both Langdale and Bowderdale valleys.

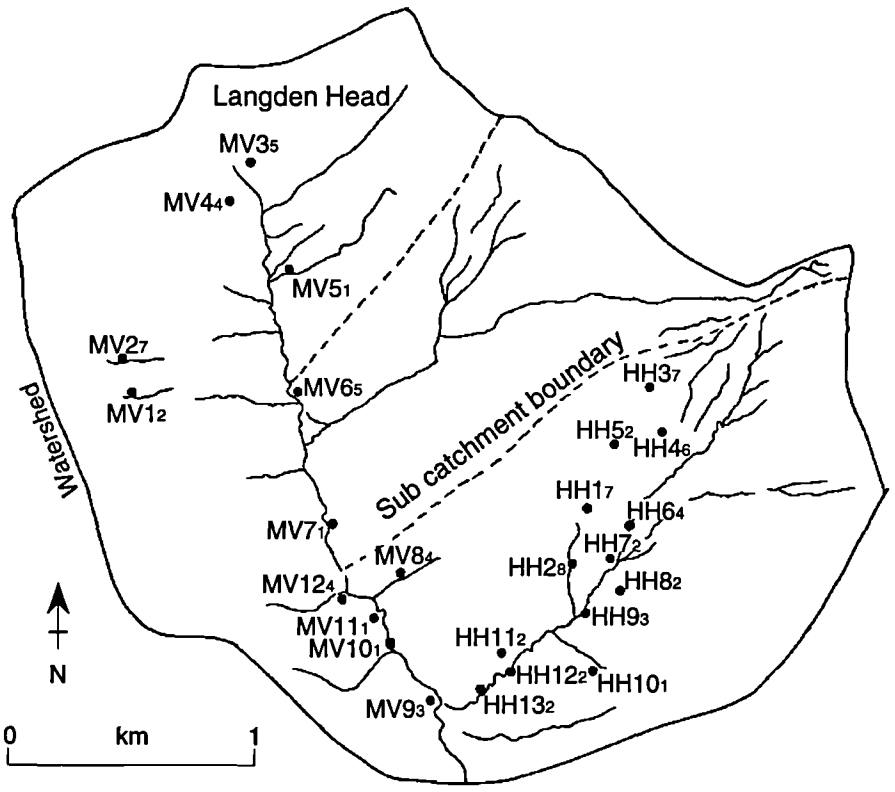
Variation within each individual group is substantial but the positing of the samples within factor space show a gradational relationship with their location within the supplying catchment. The differences observed for each individual catchment are summarised in Figure 6.18. It is evident that for Thickcombs Gill, Leath Gill,

Nevy Gill and Burnt Gill, samples taken from within the headwaters plot the furthest away from the glacial source groups and increasing proximity to the apex of each feature results in samples plotting closer to the glacial group. The restricted number of samples taken from each catchment cannot encompass all of the variation found in solifluction deposits and thus in the interpretation of sediment source some variation is likely to be found.

6.3.5 Northern Pennines - Langden Beck - Harthope Beck

The underlying bedrock and overlying soliflucted till represent the dominant sources of sediment for transport and deposition in the Harthope Beck fan. More recently, mining and quarry waste has been made available within the supplying catchment (Figure 6.19). HH3 has been sampled within the quarry in the headwaters of the Harthope Beck catchment. The exposure presents the full sequence of bedrock found within the catchment and samples have been taken from each stratigraphic layer. Glacial till represented by dense grey clay and solifluction material with intermittent sandstone blocks have been exposed on the side walls of the main trunk stream of Harthope Beck. The thickness of the layers vary, the exposures within the trunk stream are however dominated by bedrock exposures. To fully characterise glacial material, samples exposed within the main catchment have been taken to supplement source characterisation. Samples of bedrock exposed within the main valley have also been taken. The location of sampled exposures within the study reach and the number of samples taken at each site is illustrated in Figure 6.19.

At Langden Beck biplot combinations of magnetic parameters do not separate clearly between the source groups but as at Glen Etive certain patterns in the magnetic parameters are evident (Figure 6.20). A magnetic concentration gradient is evident between solifluction and bedrock samples. Generally, solifluction deposits have the lower SIRM and X values whilst bedrock maintains the highest and thus has the greater magnetic component concentration. The difference between the two source groups is relative as overall concentrations are low. Overlap between the two groups is substantial, indicating a wide range of concentrations for each source group. The gradient between the two groups is maintained in ARM-40mT/SARM, SARM and in remanence acquisition (Figure 6.20 d to f and g to i). Solifluction deposits generally have the lower concentration, but are more readily magnetised. Differentiation between the two groups is hindered by their overlap.



• Sampled exposures

HH5$_2$ Location code$_{\text{number of samples}}$

Source categories and sample numbers:
Bedrock = 27
Solifluction: grey clay = 16
Solifluction: sandstone inclusions = 11
Peat = 10
Peat substrate = 1
Storage = 11
Mining waste = 10
Total number of samples = 86

Figure 6.19. Location of catchment sample points, Langden Beck. HH : Harthope Beck, MV : Langden Beck main valley

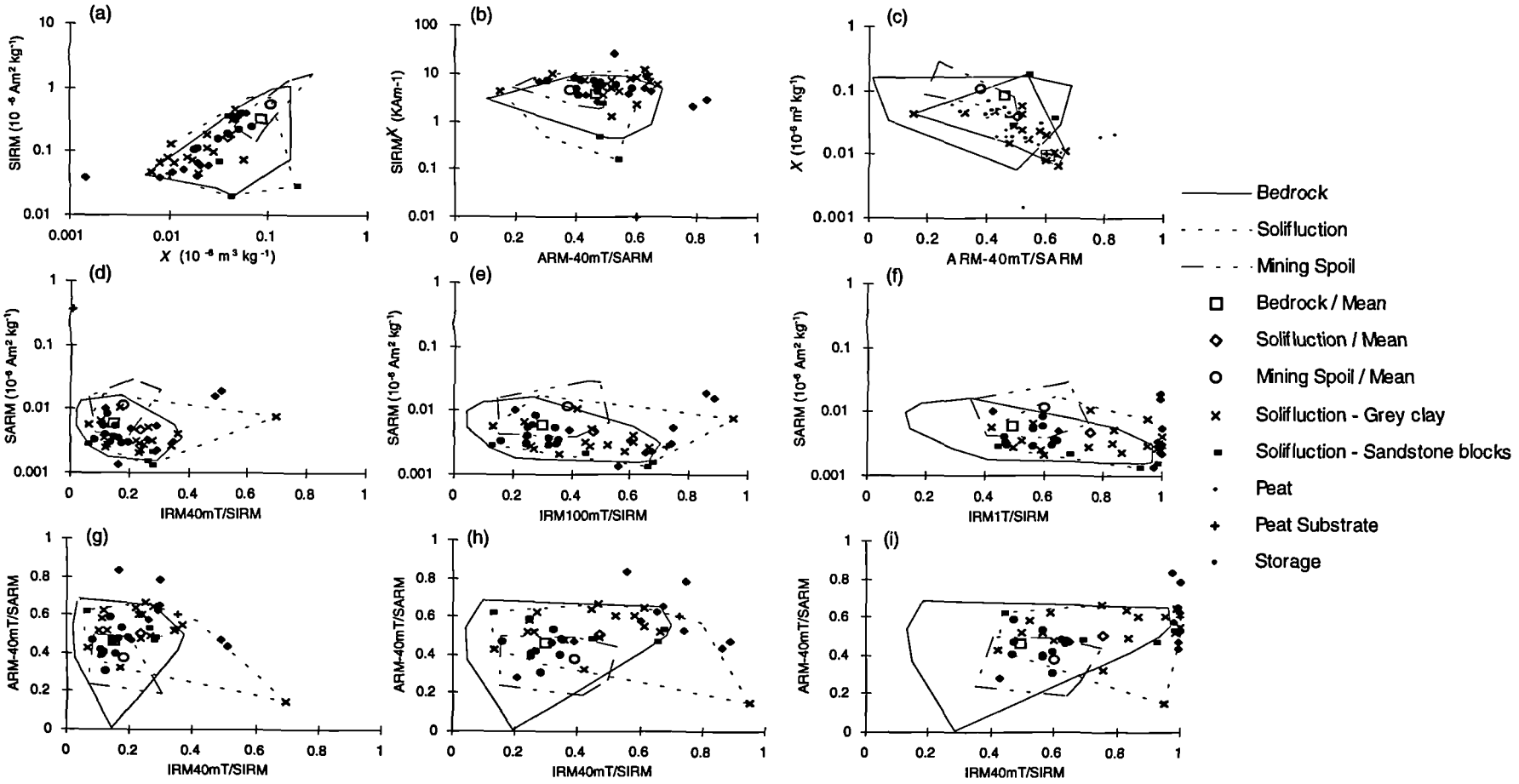


Figure 6.20. Biplots of magnetic parameters showing the variation in magnetic concentration and magnetic remanence acquisition of the catchment source sediments of Langden Beck. A convex hull encloses the outermost samples of the major source groups Bedrock, Solifluction deposits and Mining Spoil. The plotted position of the respective mean values allows a visual interpretation of source group differentiation (see Figure 6.2 for an explanation of biplot interpretation).

Factor analysis based upon the eight biplot variables does not differentiate between the two primary source groups. The trends observed in the biplot analysis are enhanced but the overlap between the two groups is substantial. Separation between the two groups is achieved by a factor analysis based upon all 14 magnetic parameters (Table 6.7). A plot of factor 1 and factor 2, which combined explain approximately 70% of the original variation in the raw data, is shown in Figure 6.21. It is clear from magnetic parameter loadings on the two factors (Figure 6.22) and from their position in factor space (Figure 6.21) that the variation is achieved by the added influence of SIRM/SARM magnetic parameter. The bedrock group is plotted closest to SIRM/SARM variables in factor space and thus has the highest SIRM/SARM values, higher than those found for solifluction group. Bedrock samples are therefore dominated by multi-domain magnetic minerals, with a higher overall magnetic concentration and susceptibility. The solifluction deposits have lower concentrations of single domain magnetic minerals. Due to the close proximity of to forward field ratios solifluction deposits are more readily magnetised, highlighting the presence of magnetite. As the majority of the bedrock samples are not magnetised fully at 1T field strength, haematite / goethite is the dominant mineralogy. As at the other three sites, solifluction deposits are dominated by a magnetite component.

Mining deposits indicate a measurable difference, although three out of the ten samples overlap the bedrock group. Higher SARM values separate the mining deposits from solifluction and bedrock groups. In addition, IRM40mT and IRM100mT values are high, confirming the ease with which samples are magnetised. The three variables plot close together in factor space as the three variables measure the ease with which the magnetic component of a sample is magnetised. Storage samples taken from both the main valley and from within Harthope beck itself plot exclusively within the bedrock convex hull, indicating a bedrock source.

In contrast with the characteristics observed for the other three sites, the solifluction material has a lower concentration of magnetic component than the source substrate. The differences results from the stark contrast in the source substrates for the solifluction material, which is predominantly the soft underlying bedrock. The characteristics of the solifluction material contrast with that found in

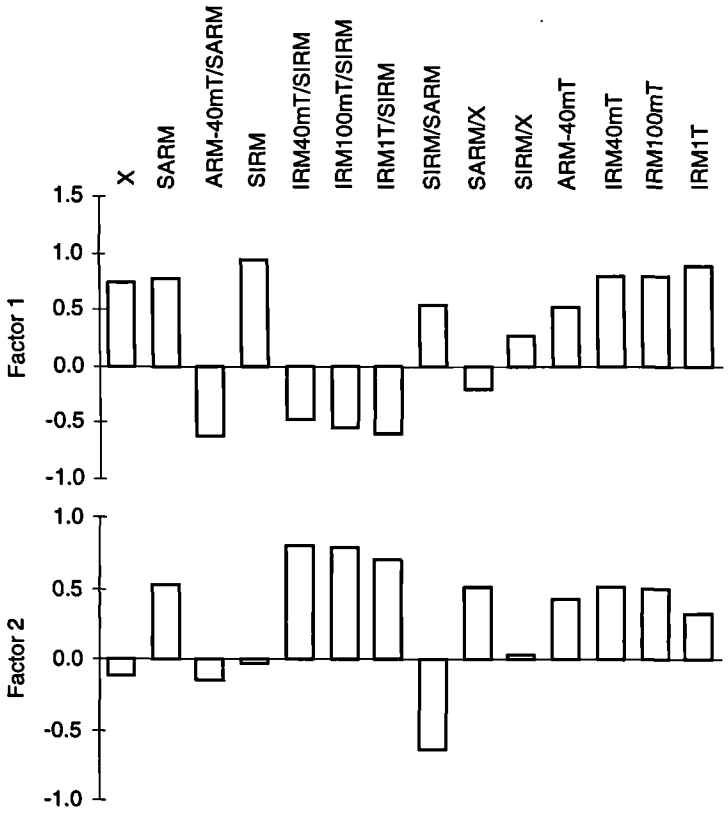


Figure 6.22. Factor Loadings of the fourteen magnetic parameters used in R- and Q- mode Factor analysis at Langden Beck

Table 6.7. Results of Factor analysis for catchment samples of Langden Beck: eigenvalues, eigenvectors and degree of variance

	Eigenvectors			Eigenvalue	Total variance	Total variance
Magnetic Parameter	Factor 1	Factor 2	Factor		(%)	(cumulative %)
X (10^{-6} m^3 kg^{-1})	0.74	-0.12	1	6.05	43.28	43.28
SARM (10^{-6} Am^2 kg^{-1})	0.77	0.53	2	3.49	24.97	68.25
ARM-40mT/SARM	-0.61	-0.14	3	1.68	12.07	80.32
SIRM (10^{-6} Am^2 kg^{-1})	0.94	-0.03	4	0.98	7.03	87.35
IRM40mT/SIRM	-0.48	0.79	5	0.74	5.34	92.69
IRM100mT/SIRM	-0.54	0.79	6	0.44	3.14	95.83
IRMT1/SIRM	-0.60	0.69	7	0.27	2.00	97.83
SIRM/SARM	0.54	-0.64	8	0.12	0.87	98.70
SARM/*X* (KAm^{-1})	-0.20	0.50	9	0.05	0.52	99.22
SIRM/*X* (KAm^{-1})	0.26	0.03	10	0.07	0.35	99.57
ARM-40mT(10^{-6} Am^2 kg^{-1})	0.52	0.42	11	0.03	0.21	99.78
IRM40mT 10^{-6} Am^2 kg^{-1})	0.79	0.51	12	0.02	0.14	99.92
IRM100mT (10^{-6} Am^2 kg^{-1})	0.80	0.49	13	0.01	0.05	99.97
IRMT1 (10^{-6} Am^2 kg^{-1})	0.89	0.31	14	0.003	0.03	100

the other three sites. The nature of the material itself indicates its bedrock source. Within the catchment, large amounts of unconsolidated poorly sorted material usually associated with glaciation are either completely absent or are not visible to the eye.

6.3.6 Source discrimination: separation of source groups

The erosion-deposition system of the fan and cone environment represents an enclosed system. The fan or cone is a sink of sediment that relates in its entirety to sources within the supplying catchment area. It is the variable scale of the system and the nature of the environment of deposition that can introduce restraints upon the feasibility of provenancing using mineral magnetics. Overall source group discrimination has been achieved. Separation is not as clear as in other studies. The overlap between source groups occurs because one source acts as the substrate within which the second group has been formed. The subsequent temporal association between the source groups in all four sites will not affect the interpretation of change in sediment supplied to the fans and cones, as the timescale of aggradation in all of the features investigated occurs after solifluction deposits were formed. Care is taken in the interpretation where the age of the deposits is questionable. The varying success of the separation or the degree of overlap found between source groups will affect the discrimination of the origin of fan and cone sediments. The overlap between the source groups at Glen Etive is substantial and the identification of the source of sediment for samples of unknown origin will, as a result, be difficult and highly subjective. It is worth looking at the position of fan samples relative to the source groups to determine whether a difference is observed due to the marked difference in concentration of values found.

At Moffat the distinct magnetic signatures for both glacial and solifluction deposits has provided the means of identifying a change in sediment source to the cones over time. At Landgen Beck the differentiation between solifluction and the bedrock substrate is poor. Samples of mining spoil deposits however can be differentiated from both solifluction and bedrock samples and can thus be used to determine if sediment deposited with Harthope Beck especially has a mining source. Differentiation at the Howgill Fells, due to the nature of the source grouping, is catchment specific. The patterns and differences can be explained by the formation of solifluction deposits from the upper surface of glacial deposits. The higher concentration of magnetic minerals found within solifluction deposits were produced

by marked changes in temperature and cycles of wetting and drying processes characteristic of solifluction. These processes have liberated paramagnetic and non anti-ferrimagnetic iron from the substrate to form higher concentrations of haematite/goethite (anti-ferromagnetic) and magnetite (ferromagnetic) within the soliflucted sediment.

The type of magnetic mineral which dominates within the solifluction deposits is dependent upon environmental context at the time at which solifluction deposits developed and the character of the underlying bedrock. The two controls must be reconciled. At Glen Etive, magnetite is dominant due to the ready supply from the underlying igneous bedrock. At Moffat the mineralogy of soliflucted material is comparable to that of the glacial substrate. The only difference between the two is the higher concentration of magnetic minerals found within the solifluction material. At the Howgill Fells, locational controls have introduced spatial differences controlled by catchment location within the main valley, changing from haematite / goethite to magnetite down-stream. Individual catchments indicate a concentration gradient in their dominant magnetic mineral from the fan or cone apex to the headwaters. At Langden Beck the concentration of magnetic minerals within the solifluction deposits is lower than the underlying bedrock.

6.4 Source assignment to samples from fan and cone sediments

6.4.1 Sample screening

The application of the provenancing technique rests upon the assumption that the samples of unknown origin retain sediment source magnetic characteristics. Post-depositional alteration of magnetic properties or diagenesis within fan and cone sediments occurs by two main processes: the enhancement of magnetic properties by pedogenesis or soil formation or by their loss caused by dissolution (Singer, 1996). Dissolution is however commonly constrained to the lake depositional environment. Magnetic properties are also susceptible to change during fluvial transport. The original magnetic signature of the source sediment is affected by the removal of fines, dependent on transport distance from the point of origin within the catchment.

The identification of immature palaeosols is supported by high organic contents, organic inversions and details of their magnetic properties (Table 6.8). The

Table 6.8. Summary of the magnetic properties of the palaeosols within the sections investigated

Section (No. of samples)		X (10^{-6} m^3 kg^{-1})	SIRM/X (KAm^{-1})	ARM-40mT/ SARM	SARM (10^{-6} Am^2 kg^{-1})	IRM40mT/ SIRM	IRM100mT/ SIRM	IRM1T/SIRM	Interpretation
DCS1	Max.	0.07	6.59	0.01	0.54	0.23	0.51	0.92	Low magnetic signal compared to sediments above and below - dissolution
(5)	Min.	0.05	2.52	0.01	0.46	0.10	0.24	0.82	
	Mean	0.06	4.05	0.01	0.51	0.19	0.42	0.88	
DCS2	SNo. 4	0.07	5.27	0.02	0.52	0.12	0.30	0.82	Low magnetic signal compared to sediments above dissolution
	SNo. 5	0.06	6.20	0.02	0.48	0.11	0.27	0.80	
BGS1	Max.	0.07	6.56	0.01	0.56	0.42	0.74	0.94	Low magnetic signal compared to sediments above and below - dissolution
(3)	Min.	0.02	1.81	0.01	0.49	0.20	0.34	0.70	
	Mean	0.04	3.44	0.01	0.52	0.28	0.48	0.83	
BGS2	Max.	0.31	4.77	0.06	0.54	0.49	0.72	0.95	Low magnetic signal compared to sediments above and below - dissolution
(12)	Min.	0.05	2.24	0.01	0.48	0.30	0.65	0.91	
	Mean	0.15	3.58	0.03	0.34	0.35	0.61	0.91	
TGS1	Max.	0.07	3.26	0.02	0.64	0.23	0.54	0.92	Low magnetic signal compared to sediments above and below - dissolution
(5)	Min.	0.06	2.52	0.01	0.57	0.18	0.40	0.80	
	Mean	0.06	2.99	0.01	0.61	0.21	0.48	0.85	
TGS2	Max.	0.12	5.89	0.02	0.45	0.14	0.32	0.82	Shows limited dissolution of magnetic minerals
(4)	Min.	0.10	4.19	0.01	0.33	0.09	0.19	0.61	
	Mean	0.11	4.80	0.01	0.39	0.11	0.26	0.72	
GFS1	SNo.5	0.02	10.58	0.05	0.29	0.60	0.87	0.98	Low magnetic concentration as *in situ* peat
	SNo.8	0.02	6.70	0.04	0.38	0.49	0.87	1.00	
HHS2	Max.	0.07	7.49	0.01	0.50	0.18	0.30	0.55	Low magnetic signal compared to sediments above and below - dissolution
(7)	Min.	0.02	4.14	0.00	0.24	0.06	0.11	0.35	
	Mean	0.04	5.86	0.00	0.34	0.09	0.18	0.41	
HHS3	Max.	0.06	11.59	0.02	0.51	0.41	0.59	0.85	Low magnetic signal compared to sediments above - dissolution
(13)	Min.	0.02	3.94	0.00	0.20	0.10	0.23	0.47	
	Mean	0.04	5.52	0.01	0.38	0.20	0.37	0.61	
WBS1	Max.	0.06	40.47	0.01	0.61	0.18	0.74	0.97	Low magnetic signal compared to sediments above - dissolution
(9)	Min.	0.02	4.86	0.01	0.47	0.04	0.20	0.42	
	Mean	0.04	15.08	0.01	0.54	0.11	0.47	0.75	

enhancement of magnetite is associated with pedogenesis. The formation of a soil profile can as a result be recognised by an increase in magnetite concentration (Singer 1996). A review of the magnetic properties of samples associated with the organic inversions in sections, CDS1, CDS2, CDS3, HBS1 and LGS1 reveals the difficulty in identifying an immature palaeosol from their magnetic properties (see Appendix 1.3 and 3.1). The magnetic properties of the organic inversions are comparable to the variability of the magnetic parameters within the profile as a whole.

The identification of section samples affected by diagenesis is more readily achieved by determining the association of their magnetic properties with source sample magnetic properties. The magnetic properties of section samples are converted into factor variables using eigenvectors and can be plotted in the same factor space. Figure 6.23 shows individual biplots for each site of factor 1 against factor 2 for both source and section samples. A small number of section samples have been identified which plot outside catchment sample outer limits. The samples identified with their stratigraphic location and interpretation are presented in Table 6.8. The majority of the fan and cone sediments for each site lie within the range of the properties displayed by their source sediments. It can therefore be assumed that all major source groups were identified for each site.

Samples that have been altered following deposition can be mis-interpreted and thus are removed prior to sediment provenancing. Samples taken from palaeosols within sections and those samples that have been identified from the factor diagram as being affected by diagenesis are removed from subsequent provenancing. As the transport mechanism is assigned to all sediments within the section the potential alteration by fluvial transport can be accounted for in the interpretation procedure (see section 6.2.3).

6.4.2 Provenance: semi-quantitative and quantitative source assignment

The source of samples of unknown origin can be assigned semi-quantitatively using factor analysis or quantitatively using an unmixing model. The application of an unmixing model provides a more objective method of source ascription. Source assignment using factor analysis is based upon the following principle. If tested

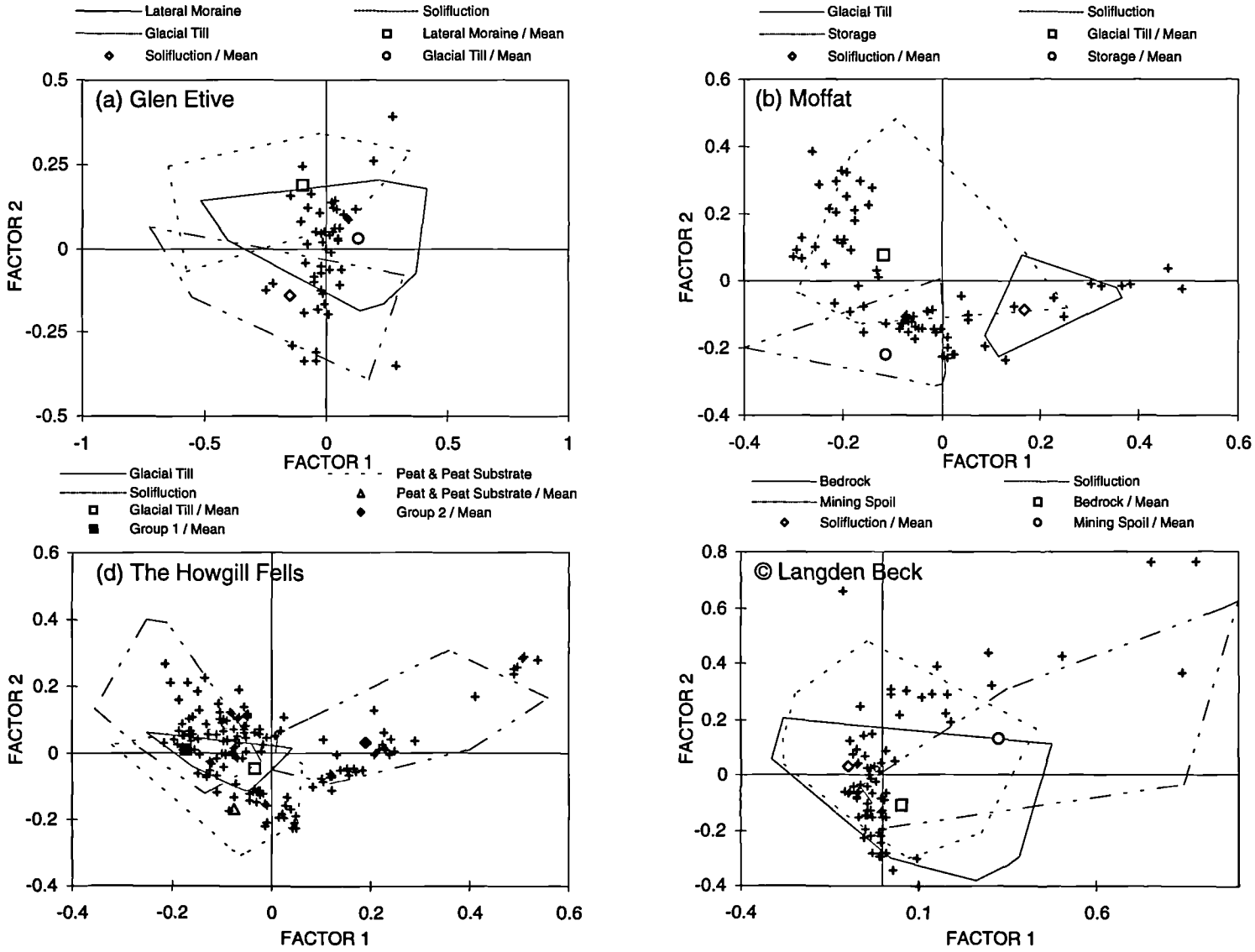


Figure 6.23. Plot of section samples (+) illustrating their position relative to source groupings identified for each of the four sites

samples plot in close proximity to a given source grouping, it can be interpreted as being predominantly formed from the given source material. Source assignment using this method is open to subjectivity in the interpretation. Despite the subjective limitation, the method still provides valuable insight of the dominant source contribution to a sample. Unmixing models are based upon a linear programming algorithm which assigns relative proportions of source material contribution to a sample. The technique compares source and sample magnetic properties (Thompson and Oldfield, 1986; Yu and Oldfield, 1993; Walden *et al.*, 1997). The model adopted in this thesis follows the Simplex algorithm outlined by Thompson and Oldfield (1986) and has been adapted for application within Excel by Walden *et al.* (1997).

The fundamental principle upon which the unmixing model is based can be explained as follows

$$x_r = p_1x_1 + p_2x_2 \qquad \text{(Eq. 6.1)}$$

If the magnetic parameter x of two source materials x_1 and x_2 are mixed in known proportions (p_1 and p_2) the mixture, assuming linear additivity, will equal x_r. All magnetic parameters used in the model should therefore be linearly additive (Thompson and Oldfield, 1986; Lees, 1994; Walden *et al.*, 1997). The choice of which magnetic parameters to use is controlled by site specific environmental controls. Both additional sources and the magnetic parameters chosen to describe them can be added to the above equation by applying linear programming algorithms (Thompson and Oldfield, 1986). A mathematical mixture of the properties of the source materials in relative proportions is placed within an iterative search. The search finds the optimum combination of linearly mixed source material which minimises the difference between the modelled sample and the actual measured properties of the sample that is being tested. Quantitative definition of the relative proportions of source contributions for a sample is the end result. Method choice can be pre-determined by the aims of the study in question. The choice of which method to adopt is restricted by the degree of separation observed between the identified source materials. In addition, certain criteria must be met before the application of unmixing models can be deemed feasible (Lees, 1994). The following criteria must be met for an unmixing model to be feasible. Source groups must be separate and with tightly constrained magnetic parameters with limited variability.

Source groups must show dimensionality and not be numerical multiples of each other. Discriminating magnetic parameters must be linearly additive. Fan and cone samples must display magnetic behaviour which lies within the range of behaviour exhibited by the source groups (Lees, 1994). The criteria can be assessed from an interpretation of source discrimination using factor analysis. It is clear from Figure 6.23 that out of the four sites, the application of an unmixing model will be successful for Moffat only. All four sites exhibit data dimensionality. Fan and cone samples have magnetic parameters which lie within the range of behaviour exhibited by their source material and all discriminating magnetic parameters are linearly additive. For Glen Etive, Langden Beck and the Howgill Fells the degree of overlap between the source groups is substantial and would therefore restrict the derivation of an individual value of the given magnetic parameter used to represent the properties of each source group. An unmixing model will only be applied for sections investigated at Moffat as source groups are tightly constrained and show minimal overlap. For the other three sites sediment provenancing will be based upon an interpretation of samples within factor space.

In applying the unmixing model at Moffat the results of the factor analysis will aid the choice of magnetic parameters used to characterise a particular source within the unmixing model. Walden *et al.* (1997) and Lees (1994) emphasise the importance of the selection of the magnetic parameters as being critical for the successful unmixing of sediment sources. Care must be taken in the interpretation of the results of the unmixing model. Walden *et al.* (1997) emphasise that the model can reliably unmix perfect samples but will not unmix natural samples, with natural levels of variability, without some errors. The multivariate technique can be used to verify the proportions of source material contribution assigned to a sample (Walden *et al.* 1997).

6.4.3 Fan and cone sediment source assignment

The results of the unmixing model provide quantitative values that can be plotted with depth providing the means for identifying change in source contribution. Where the unmixing model has not been applied a temporal change in the source of sediment to fan and cone sediments is achieved by grouping section samples into distinct sediment layers, identified in the previous chapters. To ease interpretation of the magnetic properties and thus the source of each individual unit, a convex hull surrounds all of the samples of the individual unit. The maximum and minimum

values on factor 1 and factor 2 can be more readily seen. Unit hulls have been shaded according to stratigraphic depth.

The variation of the samples or their position relative to each other within the enclosed hull provides valuable information upon the nature of the source material supplied to each unit. The close proximity of samples, a tightly constrained hull, indicates a distinct point source supply of sediment. The inclusion of more than one point source will increase the variation of magnetic properties. This will be reflected in the spread of samples in factor space and thus the proportions of the enclosing hull. A number of source types can be present and thus available for transport at a given point of origin. On valley side slopes solifluction deposits often overly lateral moraine deposits. More than one source type can therefore be mobilised and supplied to an individual flow. Variations in the source types preserved within the deposits of one flow can be introduced by the incorporation of sediment during transport, such as storage within the trunk stream system. For both scenarios the magnetic properties of each will be preserved within one unit. The degree of preservation is dependent upon the transporting mechanism and the transport distance. The combination of two sources within a unit will result in samples from the same unit plotting within its respective source group. A schematic representation of the effect this will have on the characteristics of the enclosing hull is illustrated in Figure 6.24. The enclosing hull is artificially enlarged and instead of representing point source origin indicates the variation of source material available for transport for an individual flow event.

The manner in which the data is displayed allows a direct comparison of the dominant source group contribution to each unit. Those that overlap indicate similarities in source properties (Figure 6.24). The magnetic source properties of units within and between separate phases of fan and cone aggradation can be compared. The interpretation is open to subjectivity but provides an indication of temporal changes in sediment supply for a given feature. An advantage of using the procedure outlined above is the ability to determine if the transporting mechanism of the sediments has altered the magnetic properties of the transported source sediment.

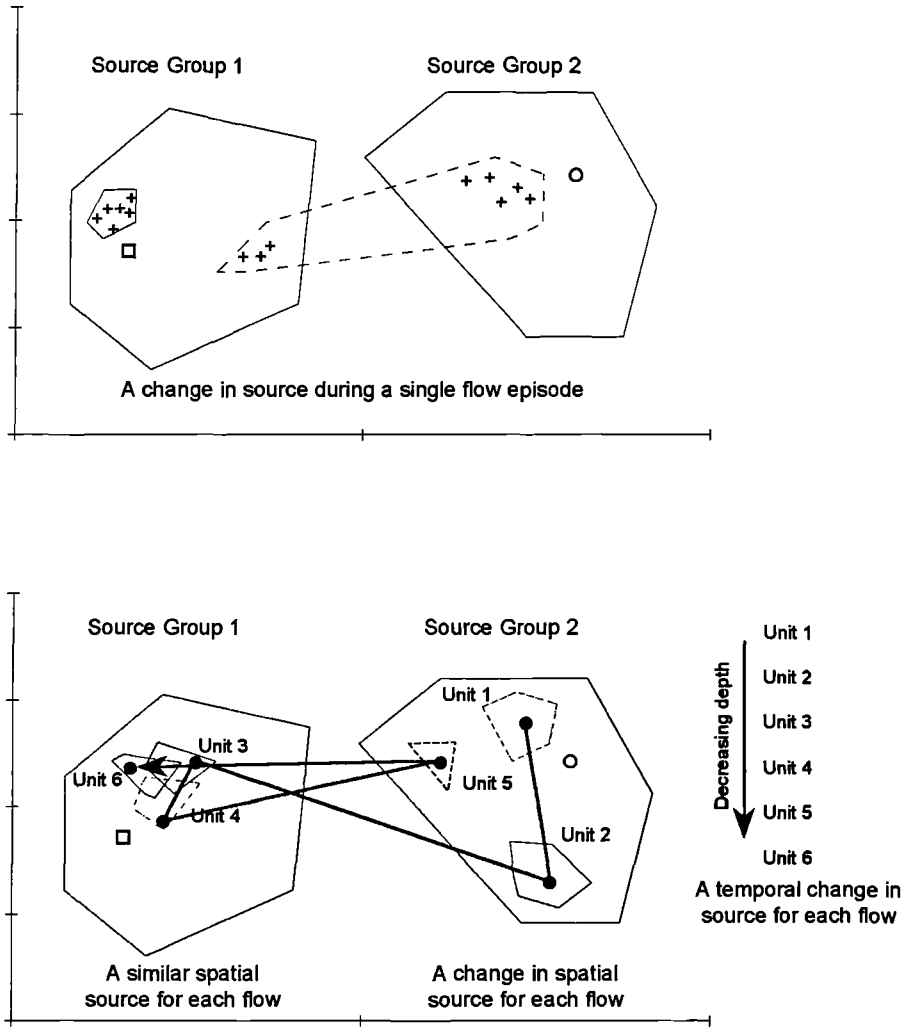


Figure 6.24. A schematic representation of the interpretation and assignment of source to the convex hulls of individual flow units

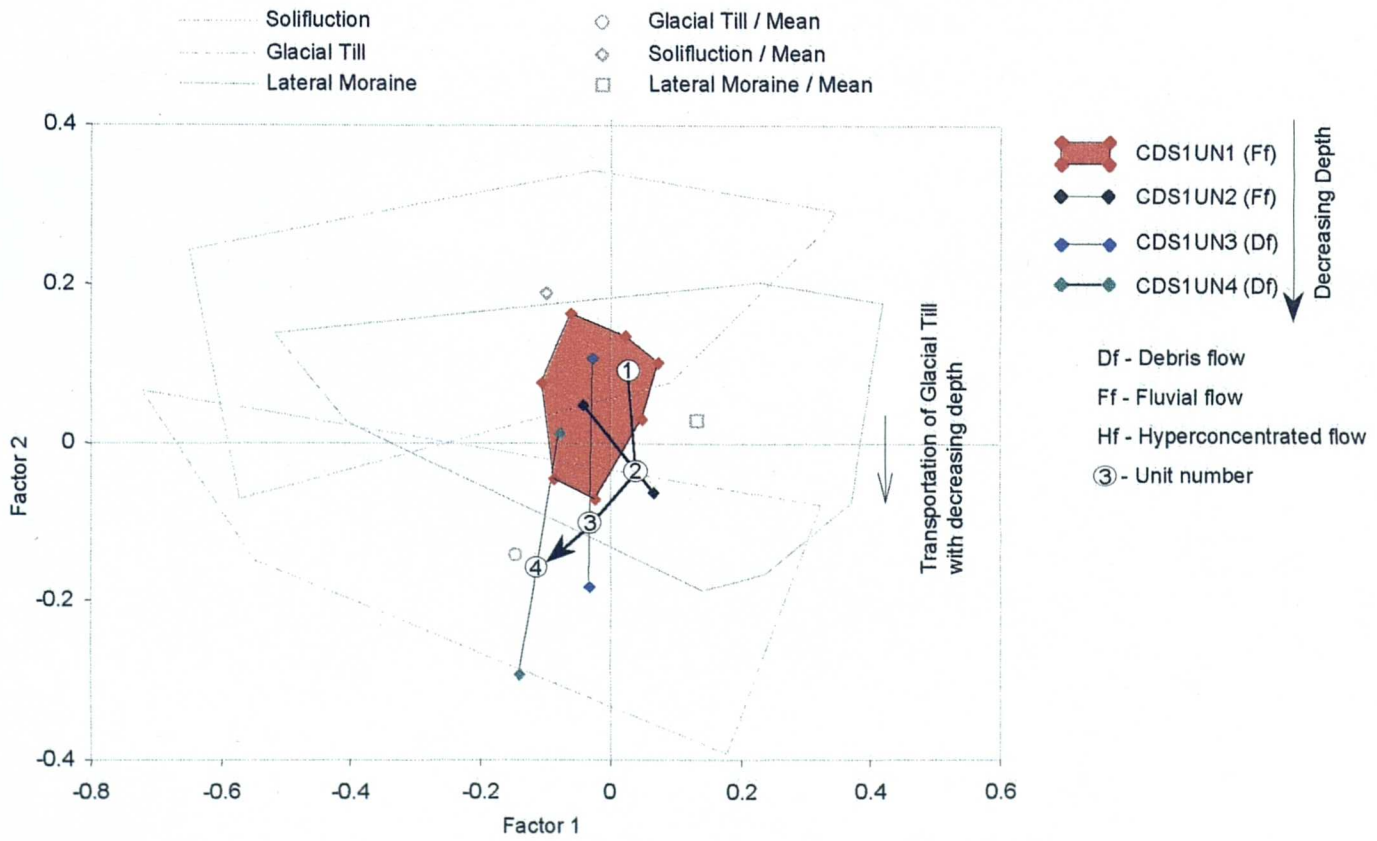


Figure 6.25. Assignment of source for individual flow units identified in CDS1, Glen Etive

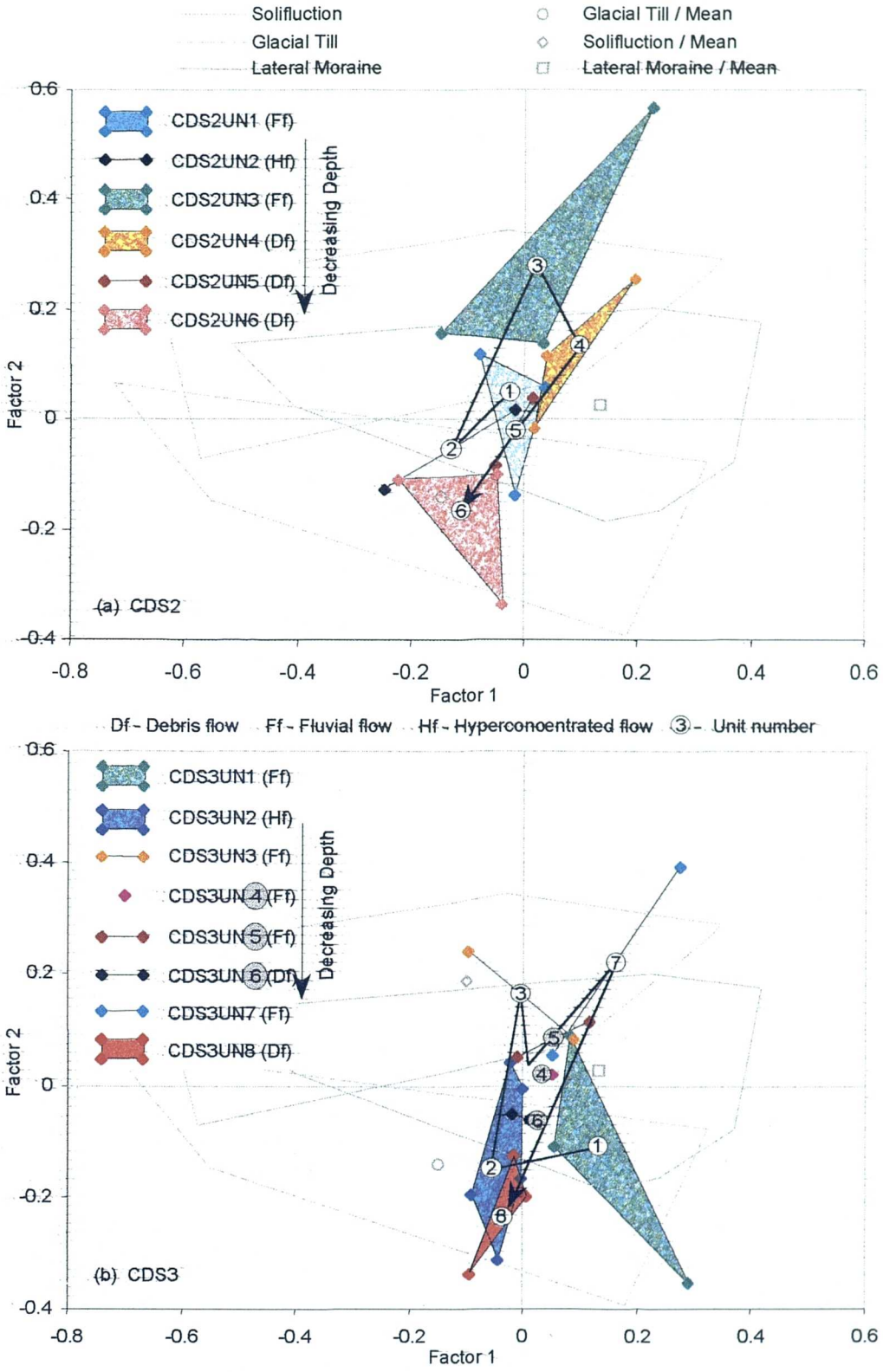


Figure 6.26. Assignment of source for individual flow units identified in (a) CDS2 and (b) CDS3, Glen Etive

6.4.4 Glen Etive - Coire Dionachd

The positions of individual units for CDS1, CDS2 and CDS3 relative to the source groups distinguished in section 6.3.2 are plotted in Figure 6.25 and Figure 6.26. The differentiation between glacial till, lateral moraine and solifluction deposits is restrictive to assigning a source group to the units in each section. The position of an individual unit relative to the means of each source group is used to assign a ratio of the dominant source group contribution. The interpretation is subjective but the magnitude of the differences observed between the positions of the individual units lends some weight to the interpretation of stratigraphic changes in source contribution.

It is evident (Figure 6.25) that the three overlapping bottom-most units of CDS1 were supplied by a mixture of lateral moraine and solifluction sediments. The position of $CDS1_{UN4}$, the last debris flow event deposited in the section, suggests a change in sediment source. The unit lies mainly in the glacial till source envelope. A similar change in sediment source is found in both CDS2 and CDS3 (Figure 6.26). It was previously found (Chapter Five) that the sequential change in transport mechanism was mirrored in the first and third phases of activity/aggradation in the two sections. Similarities are present in the dominant source contribution of the respective units in each phase.

The first phase in each section was formed predominantly from a lateral moraine : solifluction mixture. The source association between the deposits of the hyperconcentrated flow and debris flow in both sections confirm that they have been transported by the same flow event. The association of peat with the hyperconcentrated flow (Section 5.5.1) infers two scenarios for the initiation of the flow. The flow was triggered by a peat slide that occurred within the blanket peat cover in the supplying catchment. The flow originated from the area destabilised by a previous peat slide transporting peat deposits stored within the catchments trunk stream system. Both scenarios highlight the potential importance of the presence of peat in the supplying catchment in initiating activity in fan and cone environments.

The last phase of activity in CDS2 and CDS3, as at CDS1, is deposited by debris flow with a glacial till source. The difference between the two sections is found in the second phase. The five fluvially transported sediments each show a change in

source as the hulls of each unit show limited overlap, thus confirming the alternative main river source of the sediments suggested in the previous chapter.

Glacial till characteristics are typified by the low concentration of magnetic minerals. As the last debris flow event in all three sections comprises, in part, the modern soil horizon, it is possible that the low magnetic properties and thus glacial till assignment might have resulted from the dissolution of magnetic minerals by pedogenesis. A review of the stratigraphic profile indicates that CDS1 may have been affected by soil formation. The magnetic properties of the units in CDS2 and CDS3 show no evidence of a gradual decrease in magnetic concentration to the top of the profile properties which would indicate the translocation of magnetic minerals. The temporal switch in sediment source from predominantly lateral moraine sediments to glacial till suggests a spatial change in sediment supply. The two separate sources within the catchment include eastern valley side lateral moraine deposits and glacial till within the base of the corrie. It is possible that the change in source represents a time-transgressive stripping of overlying sediment, with erosion being concentrated in one area. The bottom-most sediments are the last to be exposed following the removal of the overlying sediments. After the initial removal of lateral moraine : solifluction sediments, the underlying, non-modified substrate till, was exposed and so eroded by the next event. The supply of glacial till in all three sections is associated with a debris flow event. The parallel gully systems on the eastern side of the catchment are narrow and shallow. There is no visual evidence to suggest exposure of the underlying glacial till. The change in source within the section is more likely to represent a spatial change in source.

6.4.5 Moffat - Dry Cleuch and Hermanlaw Burn

A clear gradational succession of changes in the dominant sediment source contribution is seen in the plotted position of separate units in DCS1 and DCS2. The units within the first phase of cone aggradation at the base of DCS1 clearly exhibit a glacial origin for their sediments (Figure 6.27). The hulls of $DCS1_{UN1}$ and $DCS1_{UN2}$ are out of proportion as they contain samples that have been affected by pedogenesis. The second phase, comprising the remaining units in the section, can be separated into two separate but comparable cycles of change in sediment source contribution. $DCS1_{UN4}$, $DCS1_{UN5}$ and $DCS1_{UN6}$ show a gradual change from a glacial : storage mixture to a storage : solifluction mixture. $DCS1_{UN7}$ indicates a reversal back to a glacial sediment supply. The remaining overlying units $DCS1_{UN8}$, $DCS1_{UN9}$,

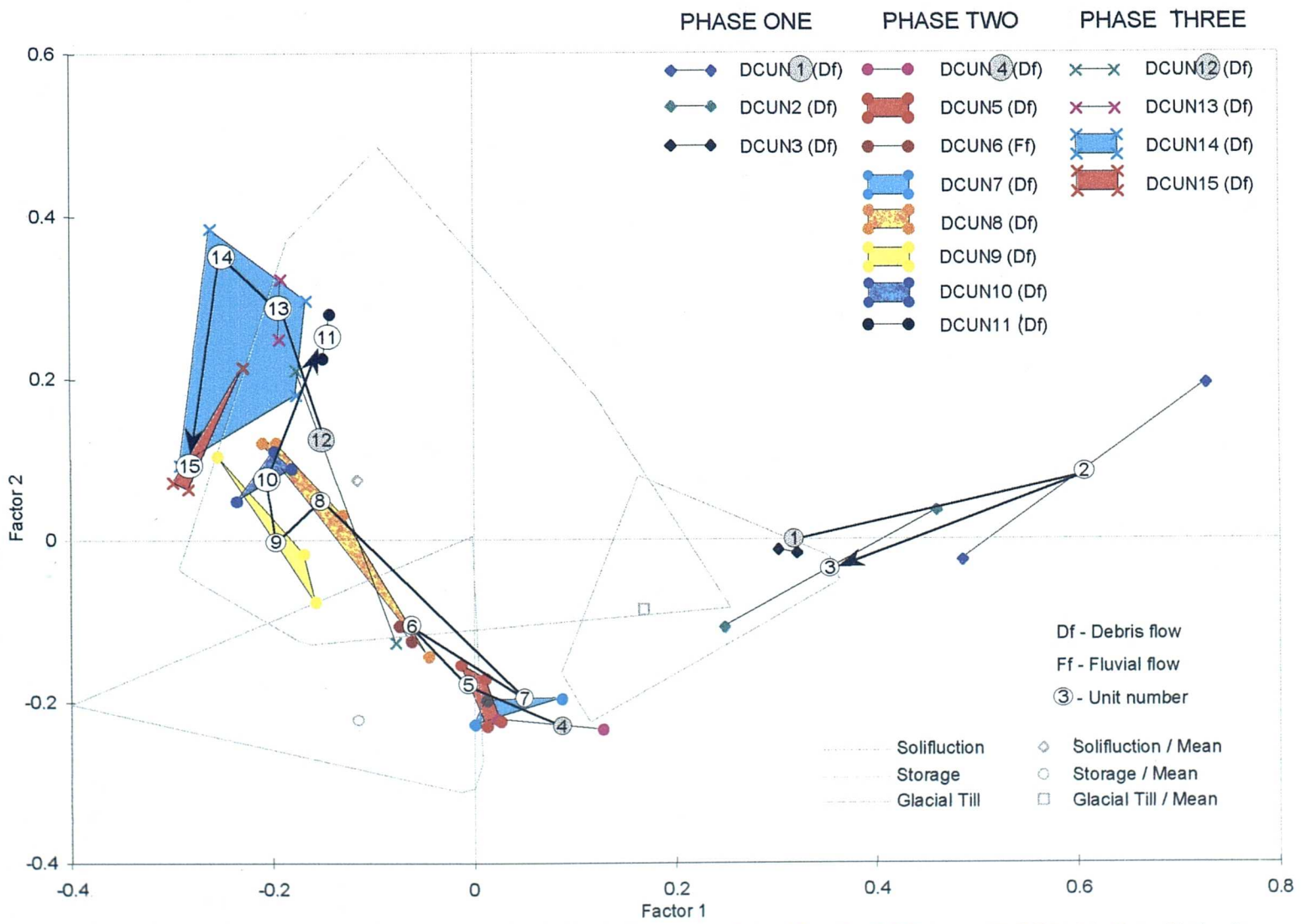


Figure 6.27. Assignment of source for individual flow units identified in DCS1 and DCS2, Moffat. Units in the two sections have been separated according to their phase order.

$DCS1_{UN10}$ and $DCS1_{UN11}$ have a predominately solifluction source. All of the units except $DCS1_{UN11}$ overlap, suggesting a similar point source of the sediments. $DCS1_{UN11}$ is set apart and the magnitude of the separation suggests a complete change in the spatial origin of the sediments within the supplying catchment.

In DCS2, a continuation of the sequence of sediment supplied to the cone, all four units indicate a solifluction origin. The initial debris flow event, $DCS2_{UN12}$, represents a mixture of storage and solifluction sediment. The mixture suggests that the initial debris flow, which represents the reintroduction of activity within the system, incorporates storage material that has built up in the trunk gully between the second and third phase of activity. The overlying unit is a thick deposit but all samples taken from it have magnetic properties that are tightly constrained. The position within factor space is comparable to the position of the last unit deposited in DCS1. It is possible that the previous debris flow destabilised a specific area. The lowered thresholds were subsequently exploited by debris flow, which deposited the remaining three units in this section. All three units overlap indicating similar sediment source signature.

At Hermanlaw Burn the change in the dominant source of sediment within HBS1 is simpler with a switch from a storage to a glacial : solifluction source. The first four units and the thickest identified in HBS1 fall entirely within the storage envelope, overlap and have magnetic properties that are tightly constrained (Figure 6.28). The last three layers indicate the influence of a glacial sediment supply. The switch between sediment supplies is not concurrent with the organic inversion identified in Chapter Four. The interpretation must be taken with caution as the switch identified is also associated with a change in transport event. It is possible that fluvial transport of the first four units in the section may have altered the magnetic properties of the initial sediment supplied. The first three units were transported by chaotic flood events, and fines are dominant within samples. Thus, it can be argued that as a result the overall magnetic signature of the original source is retained. It must be noted that the storage material itself underwent transport to its position within the trunk stream system.

The results of the unmixing model confirm the interpretation of the factor analysis for each section (see Appendix 3.2). To account for the inherent scalar variation in the values of magnetic properties, section and catchment magnetic values were

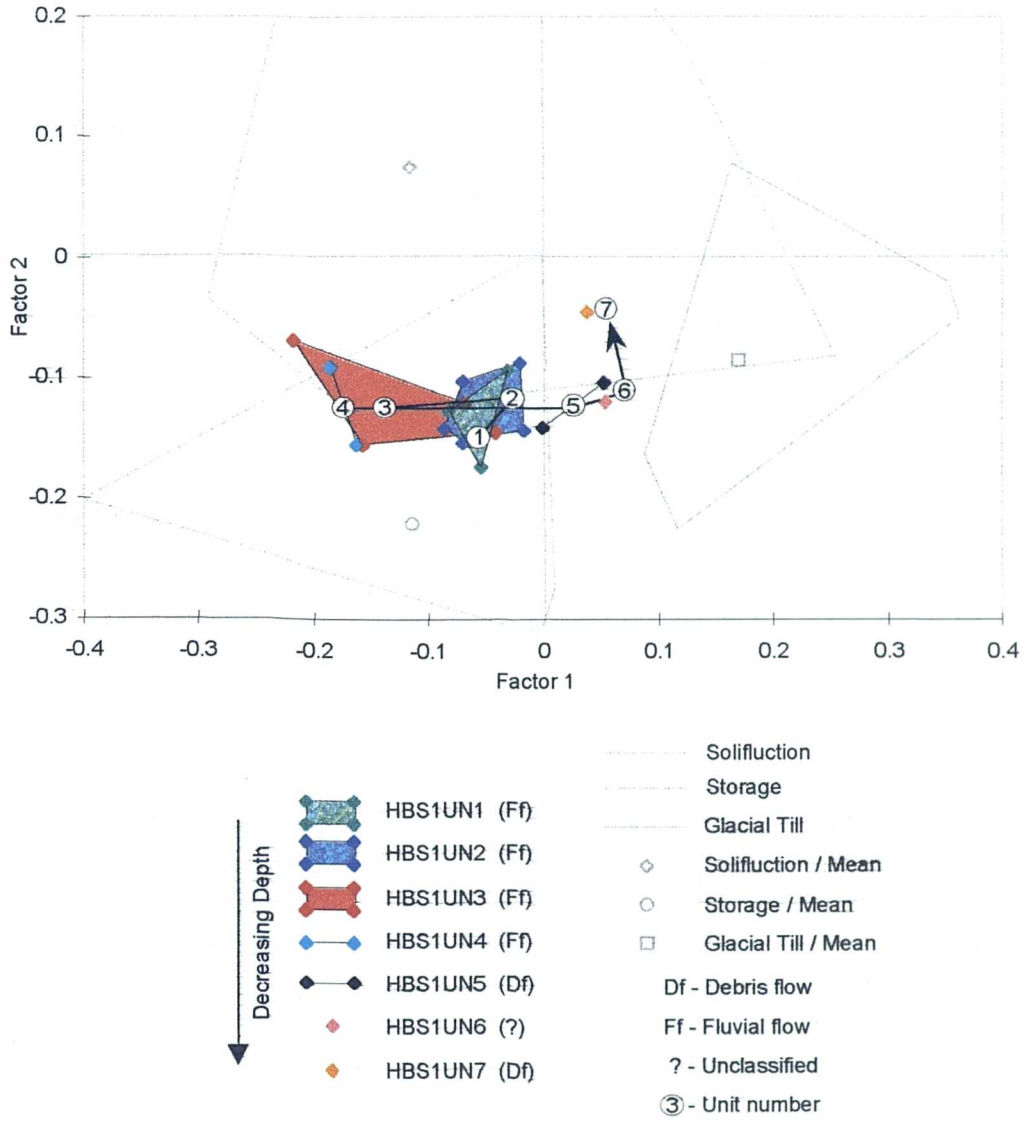


Figure 6.28. Assignment of source for individual flow units identified in HBS1, Moffat

Table 6.9. Magnetic data for glacial, solifluction and storage material source groups

		X (10^{-6} m^3 kg^{-1})	SIRM/X (KAm^{-1})	ARM-40mT/ SARM	SARM (10^{-6} Am^2 kg^{-1})	IRM40mT/ SIRM	IRM100mT/ SIRM	IRM1T/SIRM	IRM1T/SIRM
Glacial Material	Mean	0.10	6.88	0.47	0.03	0.73	0.17	0.41	0.83
	Max.	0.14	12.88	0.55	0.06	1.75	0.26	0.64	0.91
	Min.	0.02	2.71	0.40	0.01	0.12	0.07	0.19	0.79
Solifluction Material	Mean	0.17	16.97	0.22	0.09	2.90	0.18	0.32	0.78
	Max.	0.28	29.60	0.51	0.20	4.66	0.38	0.56	0.95
	Min.	0.07	3.27	0.11	0.01	0.24	0.07	0.15	0.70
Within Channel Storage	Mean	0.08	35.35	0.40	0.02	3.12	0.05	0.12	0.74
	Max.	0.14	100.65	0.51	0.04	9.28	0.15	0.40	0.80
	Min.	0.05	14.01	0.24	0.01	0.80	0.01	0.04	0.71

weighted and standardised prior to unmixing. The eight magnetic parameters used in factor analysis and their mean values used to represent the properties of each source in the unmixing model are given in Table 6.9. The structure of the model constrains how the source contribution is measured, the proportion of each source must lie between 0 and 1 and total 1.

The stratigraphic plot of the relative source contribution of the three major source groups, glacial, solifluction and storage is presented in Figure 6.29. The stratigraphic plot is presented in aggradational phase order, highlighting the sequence of change from glacial, storage and solifluction for each individual phase. Most striking is the sequential change in the contribution of storage material and changes in proportional contribution throughout the two sections. The cyclic change in storage contribution relative to unit boundaries is summarised in Figure 6.29. The four units which immediately overly the palaeosol in DCS1 are dominated by storage sediment. The boundary between $DCS2_{UN7}$ and $DCS2_{UN8}$ marks a decrease in storage contribution concomitant with the first introduction of solifluction sediment. This boundary therefore represents a significant change in source contribution either by the reduction in the availability of storage material within the trunk stream system or from a complete spatial change in sediment supply. The former is more likely to be the case as flows are channelled along the linear gully system at Dry Cleuch and thus will incorporate storage during transit. Solifluction contribution dominates in the flowing events until storage contribution again becomes important in last two events of the final phase of activity DCS2.

Solifluction material makes no contribution to the sediment supplied and stored in HBS1 (Figure 6.30). The source is dominated by storage, with limited glacial sediment contribution. Its characteristics are comparable to $DCS1_{UN4}$, $DCS1_{UN5}$, $DCS1_{UN6}$ and $DCS1_{UN7}$ which bury the palaeosol in DCS1 The increased influence of glacial material in the last two units in the section identified from the factor analysis is confirmed by the increased proportion of glacial material. The transition therefore must represent a spatial or temporal change in the character of sediment supplied between two separate phases of fan aggradation.

6.4.6 Howgill Fells - Burnt Gill, Nevy Gill, Thickcombs Gill and Leath Gill

The different transport history found for the aggradation of sediments between the two sections at Burnt Gill is mirrored in the sequential change in sediment source

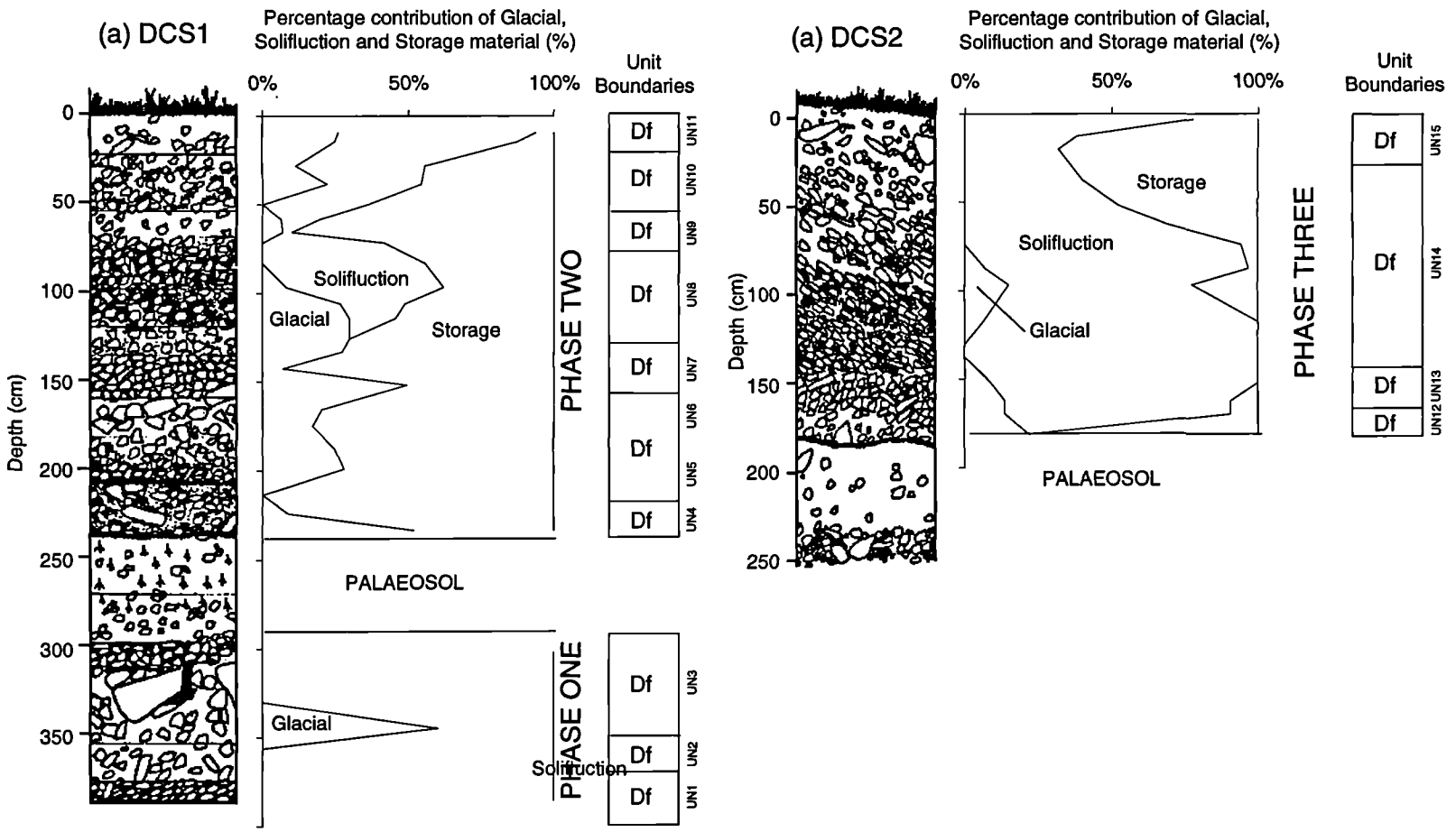


Figure 6.29. Results of the unmixing model for (a) DCS1 and (b) DCS2, Moffat

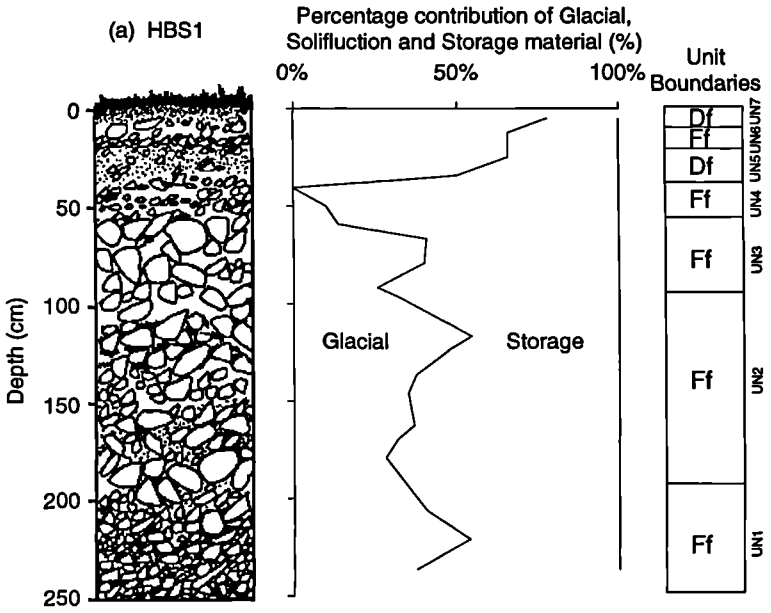


Figure 6.30. Results of the unmixing model for HBS1, Moffat

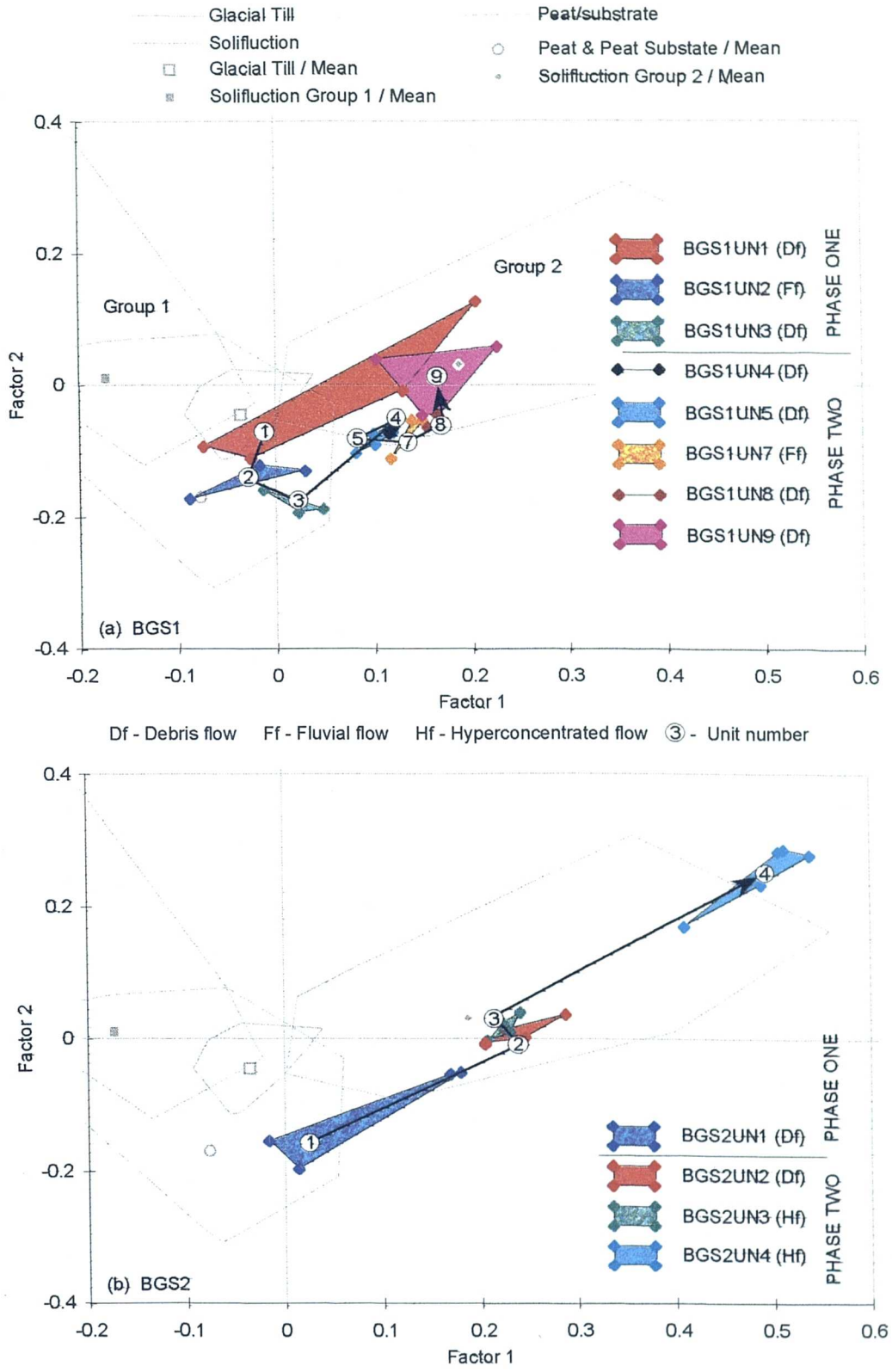


Figure 6.31. Assignment of source for individual flow units identified in (a) BGS1 and (b) BGS2, the Howgill Fells. Phase order is highlighted for each section.

supplied to each event. A similarity shared between the two sections is the source characteristics of the sediment below each respective palaeosol. The units represent the onset of aggradation and the initial formation of the double cone sequence found at the base of Burnt Gill.

From Figure 6.31b its is evident that the majority of the sediments from the initial debris flow $BGS2_{UN1}$ in BGS2, plot within the peat / substrate source group. The samples from the top of the unit plot within the solifluction group. The first five samples are tightly constrained. As the two samples identified as solifluction in origin are located directly at the base of the palaeosol, the samples may have been affected by pedogenesis. The enhancement only has to be slight to produce a marked difference as the initial concentration is extremely low. The three units which mark activity before the formation of the palaeosol in BGS1 also indicate a peat source. $BGS1_{UN1}$, although initially dominated by a solifluction source, indicates a switch in the uppermost samples to a peat / substrate group. The peat/substrate source is maintained in the remaining two units (Figure 6.31a). In BGS1 the subsequent five debris flow events exhibit a gradational change in position from the base of solifluction group 2 to mid-group. The progression in the relative position of the unit groups, taken in association with the valley-side difference in solifluction properties, indicate headwall retreat of the developing gully. The gradational change in position is evident in the positioning of unit groups overlying the palaeosol within group 2. A similar pattern is evident in BGS2. The change in position can also be interpreted as being indicative of headwall retreat of the developing gully.

The two sections differ in magnetic properties exhibited by the unit groups within the solifluction envelope and in the number of units that have aggraded a similar thickness of sediment. It is clear in BGS2 that $BGS2_{UN1}$ and $BGS2_{UN2}$ are both tightly constrained. The degree of overlap taken together with the minimal difference within units is suggestive of their origin from the same point source. In BGS1, although the units plot in close proximity, overlap is minimal. The lack of overlap can be taken to indicate a slight change in source between events which could be spatially or temporally controlled by the availability of sediment within the trunk stream system. The characteristics of the onset of activity for BGS1 and BGS2 is also found for the basal sediments of TGS1. $TGS1_{UN1}$ which comprises the entirety of the basal sediments in TGS1, apart from one sample, is tightly constrained and

positioned in factor space within the peat / substrate envelope near to the mean value (Figure 6.32).

The three debris flow units that overlay the palaeosol have been supplied from solifluction deposits of group 1. The samples within each unit of the second phase of aggradation are tightly constrained and the unit boundaries do not overlap. Both characteristics are consistent with a different source for each event, the difference being introduced by either spatial or temporal controls. The characteristics are maintained in the unit groups of the third and fourth phase in TGS2, although some overlap is found. However, a sequential difference in relative glacial and solifluction contribution is evident in the units in TGS2. The three units below the palaeosol, representing the third phase of aggradation within the section sequence, essentially plot directly between the mean of the solifluction and the glacial source group suggesting a mixture of the two sources. The characteristics of the two units overlying the palaeosol are more dominated by the solifluction source. $TGS2_{UN6}$ and $TGS2_{UN8}$ which have deposited the bulk of the sediments in phase three and four respectively are separate in factor space, indicating their differing solifluction source material characteristics.

The two units in TGS3, which represent the last sediments to be deposited in the cone at Thickcombs Gill, show a reversion back to glacial : solifluction mixture which is overlain by a unit with a predominately solifluction source. The reintroduction of glacial signature within phase three and phase five can be attributed to the exposure of underlying glacial deposits once the solifluction material has been removed. The change of source between units identified between phases does not show a discernible gradation within the solifluction group 1 as found at Burnt Gill. The major source zone has been the supplying linear gully after the initial erosion from the headbowl to form $TGS1_{UN1}$.

A review of all section samples from BGS1, BGS2, TGS1 which have plotted within the peat / substrate source envelope, show that their organic content does not differ significantly in comparison to other samples. The source of sediment is therefore the highly weathered substrate which the peat overlies. If the substrate underlying the peat represents the source of the sediment for the initial formation of the cone aggradation, instability must have originated at the break of slope. The contact between peat and the underlying less permeable substrate represents a

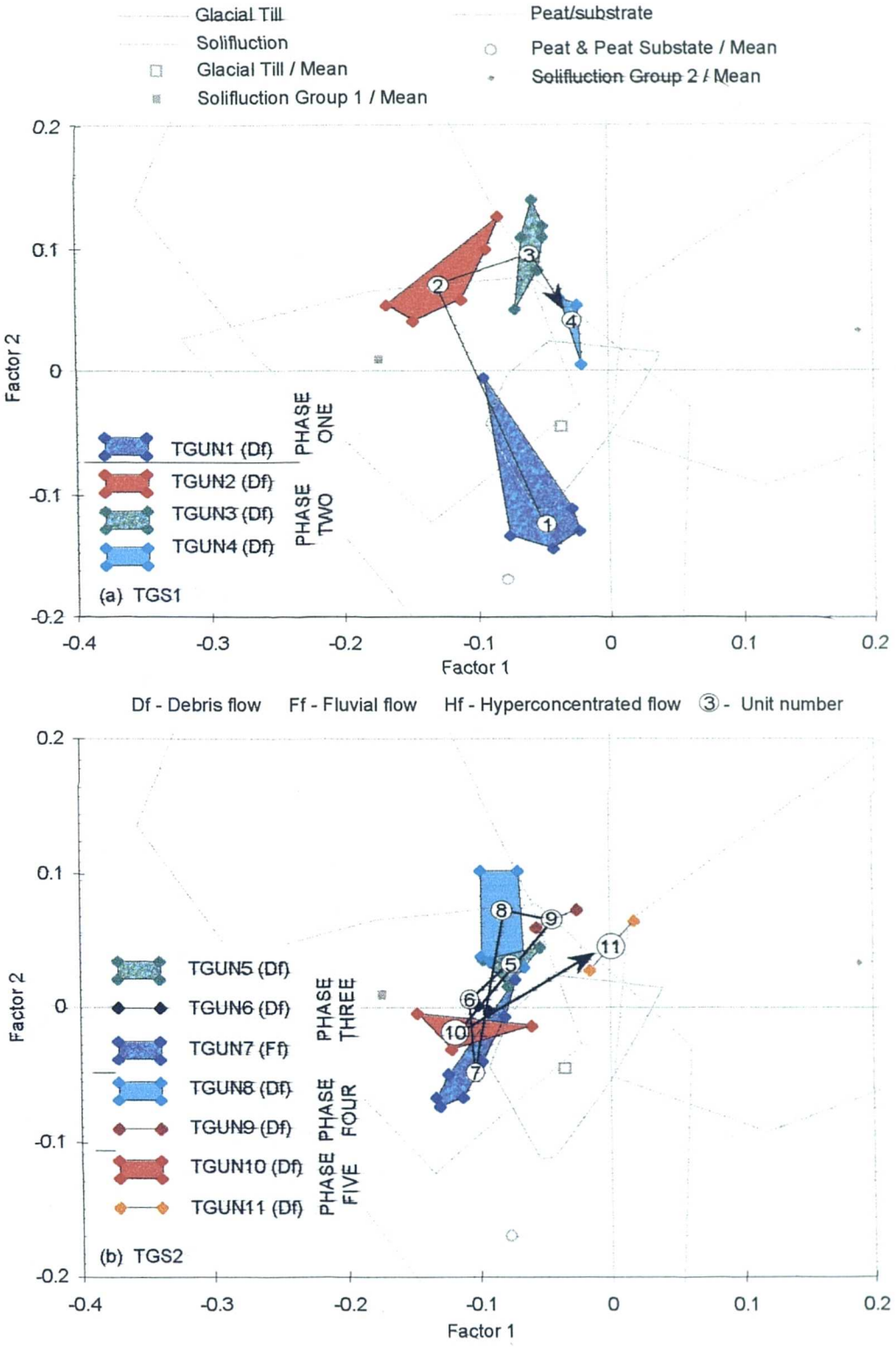


Figure 6.32. Assignment of source for individual flow units identified in (a) TGS1 and (b) TGS2, the Howgill Fells. Phase order is highlighted for each section.

zone of instability. An increase in pore water pressure at this boundary, within blanket peat piping, could be destabilised to initiate cone aggradation. After the initial phase, the destabilised area is laid open for further erosion, tapping into solifluction deposits. The development of cones in this manner contradicts the headwall retreat scenario which in part is validated by the findings for both BGS1 and BGS2. The deposits of the units at BGS1 are separated by a marked period of stability. Harvey *et al.* (1981) have indicated palaeosol formation lasted approximately *c.* 1800 years. This time period separates deposits of the initial cone-building phase from the second phase of aggradation which indicates headwall retreat. The nature of threshold conditions and their interaction within forcing factors which brought about the second phase of cone aggradation could have caused the headward retreat of the two supplying linear gullies.

For NGS1 and LGS1 as the sections only provide a small slice of the overall temporal supply of sediment to each feature, it is not possible to determine the sediment source of the initial phase of activity within each feature. Consideration of the stratigraphic changes in sediment supplied does provide valuable information upon the development history of each section and the phase of activity it represents. For Nevy Gill from the base of the section to the penultimate unit the source of the sediment is dominated by group 1 solifluction material (Figure 6.33). Apart from $NGS1_{UN6}$ the magnetic properties of the unit groups are tightly constrained, including both fluvially reworked sediments and sediments deposited by debris flow. All of the units overlap with each other and, due to their position within group 1, have been supplied from Great Nevy Gill. The last debris flow event within the section is set apart from the other unit groups and plots in close proximity to catchment samples that represent Little Nevy Gill (Figure 6.18). Thus, the last phase of activity within the NGS1 represents a change in the tributary catchment which has supplied sediment to the section.

At Leath Gill the separation of two phases of cone aggradation by an organic inversion is compounded by differences observed in the dominant source supplying the units within each phase. The first phase is made up by three units. From Figure 6.34 it is evident that a distinct source characteristic has supplied each unit. Sequentially the bottom two units are overlain by a solifluction / glacial mixture. The second phase is made up by three units but in this instance the three units overlap within solifluction group 1 and thus were supplied by solifluction sediment from a

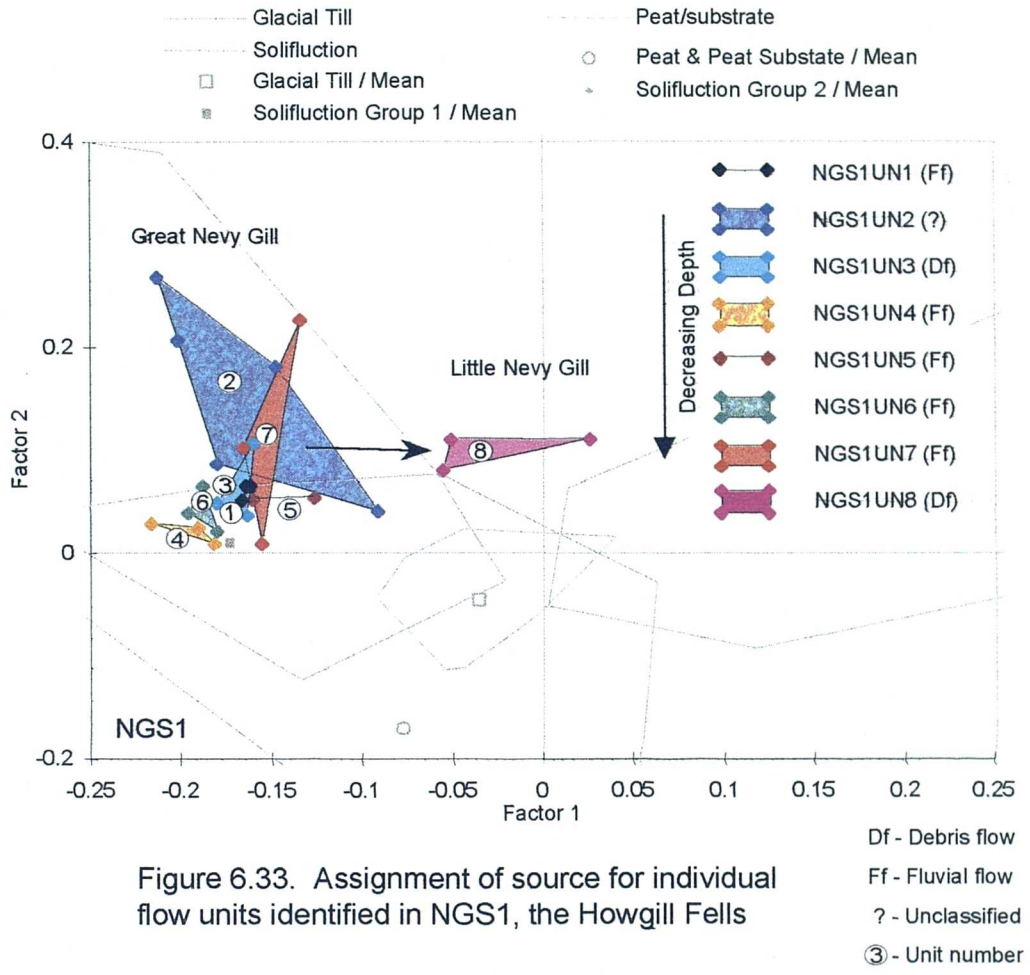


Figure 6.33. Assignment of source for individual flow units identified in NGS1, the Howgill Fells

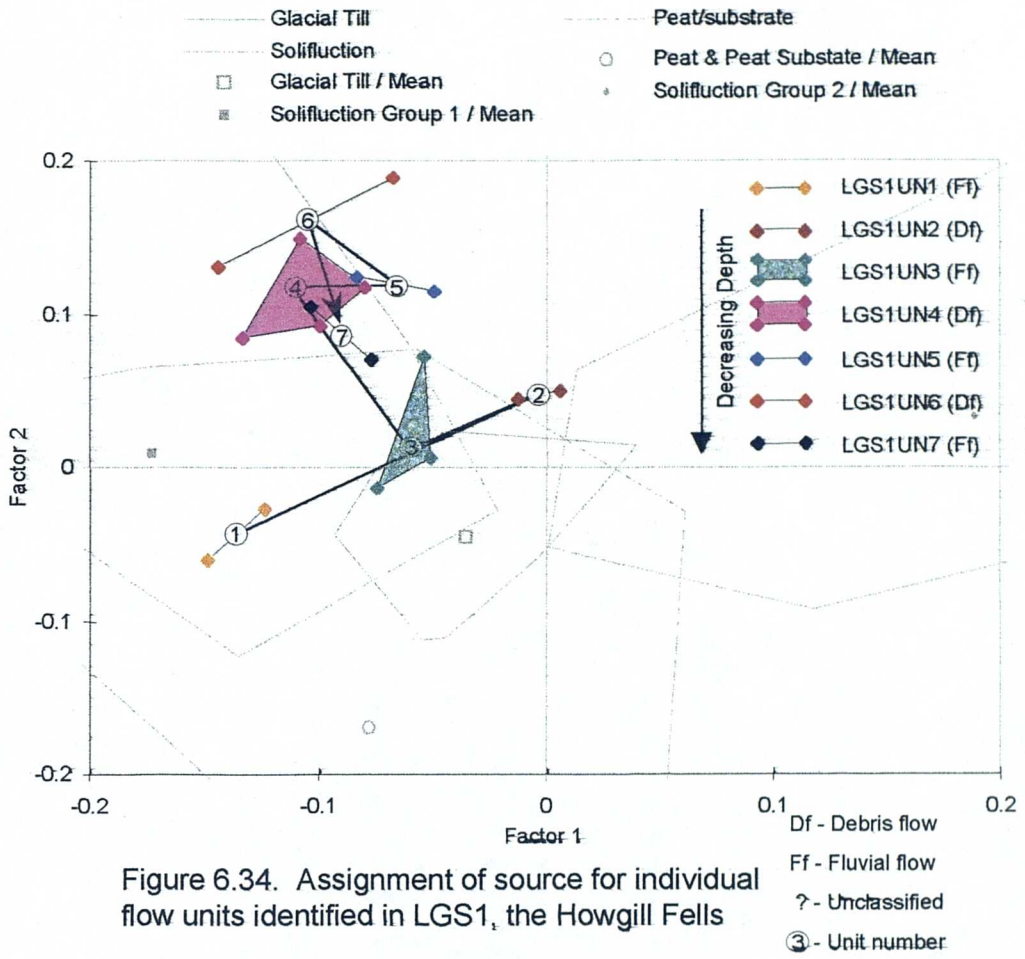


Figure 6.34. Assignment of source for individual flow units identified in LGS1, the Howgill Fells

similar area within the supplying catchment. The sequential change identified within the first phase indicates a switch from solifluction to glacial. Even though the contribution by glacial material is not overriding, the change can be interpreted to represent the removal of overlying solifluction deposits to expose underlying glacial material as found for Thickcombs Gill

6.4.7 Northern Pennines - Langden Beck - Harthope Burn

The degree of overlap between the two primary source groups, bedrock and solifluction deposits is substantial and out of the four sites represents the worst source discrimination. The derivation of change is therefore problematical and open to subjective interpretation. Figure 6.35 presents a plot of the positions of individual units for the three sections taken from Harthope Beck. West Beck sections are also plotted for interpretation. West Beck sections are included even though no samples have been taken from its supplying catchment. As in Figure 6.35 all of the samples plot within the outer limits of the source groups identified from main valley and Harthope Beck catchment. For HHS1 no discernible pattern is evident. Only $HHS1_{UN1}$ and $HHS1_{UN2}$ are tightly constrained. The two units represent sediments for which no representative source material had been sampled or identified in the initial catchment source sampling framework. The hulls plot well within the envelopes of solifluction and bedrock envelope, midway between the two groups mean values. If the sediment source does represent glacial material, on the basis of magnetic signal glacial material must be locally derived.

By contrast, sample viability is tightly constrained in the three units of HHS2. The bottom two units overlap and plot close of the bedrock source group mean. $HHS2_{UN5}$ which buries the palaeosol in HHS2 is separate and plots towards the solifluction mean value. The clearest distinction of the dominant source groups supplying an event in Harthope Beck Fan is achieved in HHS3. The bottom-most unit plots almost entirely within the solifluction envelope, whilst $HHS3_{UN1}$ has magnetic properties that present a mixture of solifluction and mining spoil characteristics. The presence of sediment from mining spoil within this section emphasises its association and formation with mining activity operating within the supplying catchment.

The effect of mining activity is more readily seen in sections taken from West Beck Fan. WBS1 shows characteristics comparable to that found in HHS3, but instead of a solifluction source the bottom-most sediment indicate a solifluction /

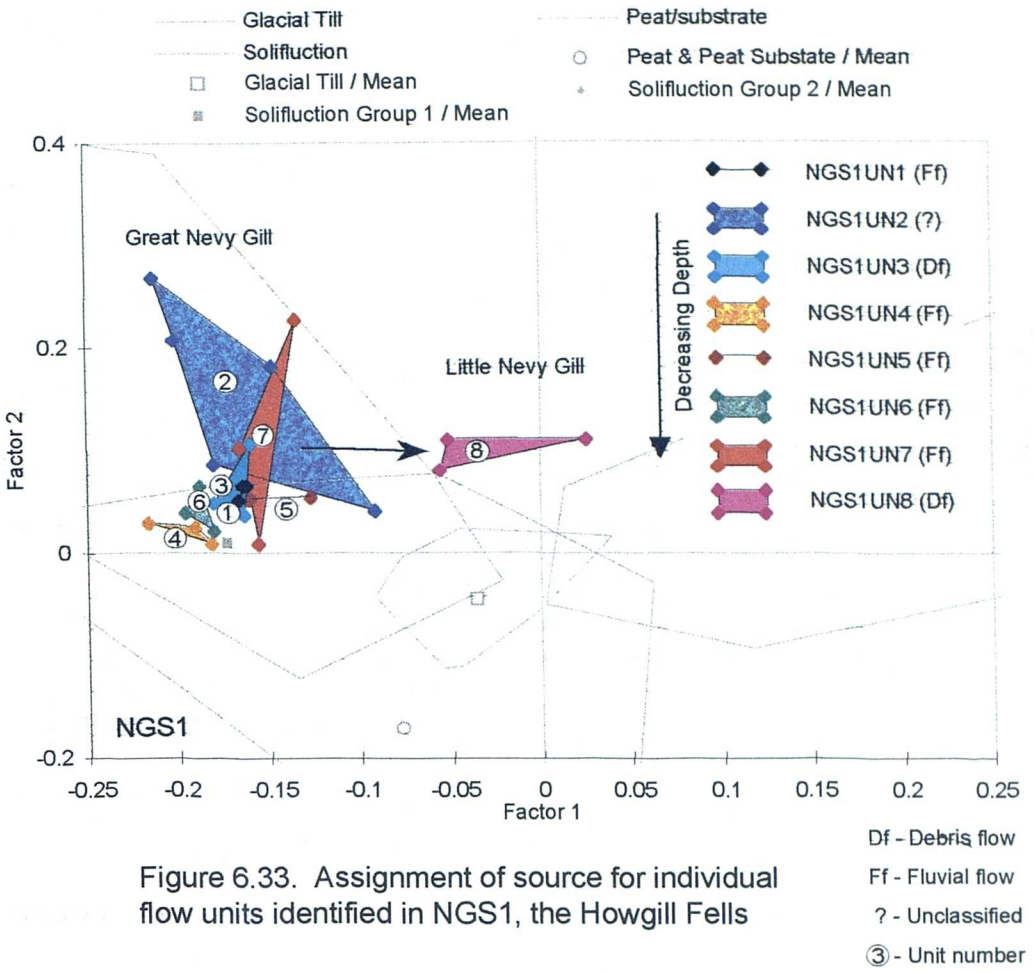


Figure 6.33. Assignment of source for individual flow units identified in NGS1, the Howgill Fells

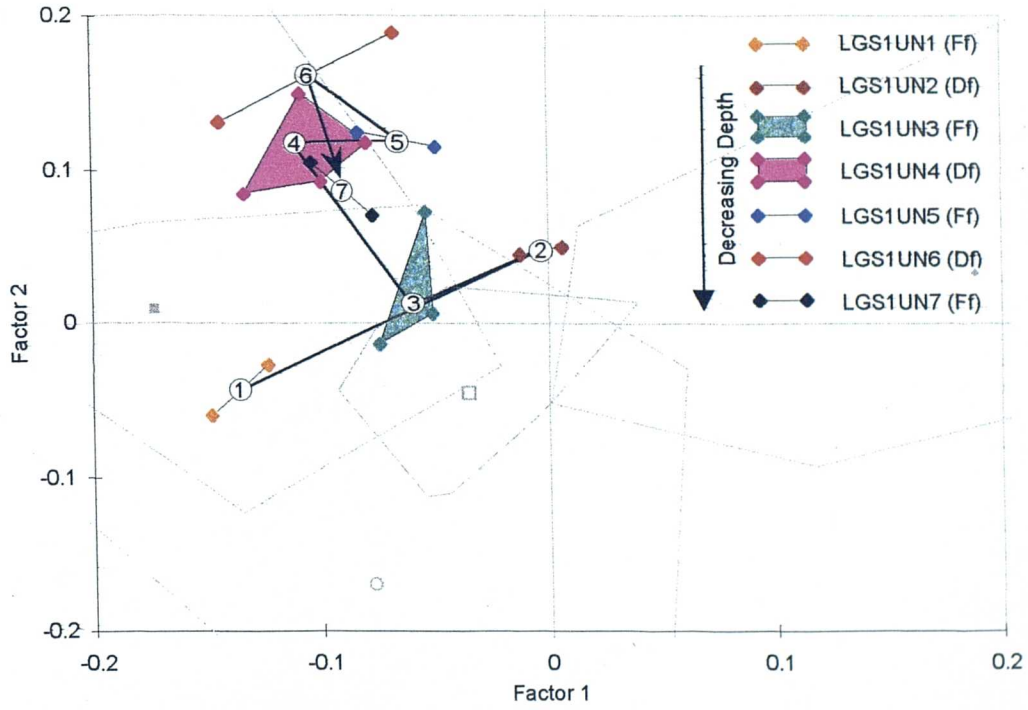


Figure 6.34. Assignment of source for individual flow units identified in LGS1, the Howgill Fells

bedrock mixture. As found at HHS3 the uppermost layer exhibits magnetic properties which are characteristic of and associated with mining spoil. The effects of mining upon temporal changes in sediment supply is clear in the plotted position of separate units identified in WBS2. Units $WBS2_{UN5}$, $WBS2_{UN6}$, $WBS2_{UN7}$, and $WBS2_{UN8}$ which were fluvially transported at high magnitude by hushing processes confirm the bedrock source of the artificially stripped sediment (Figure 6.36).

6.5 Derivation of temporal changes in sediment source

The ability to discern a change in sediment supplied to the fan is highly dependent upon previous environmental processes operating within the supplying catchment, producing measurable and distinguishable differences in the magnetic properties of sediments. In comparison to other environments, the scale of analysis is much smaller and may have affected the ability to measure significant differences between the magnetic properties of the sediment sources identified within the supplying catchment. At Glen Etive, Moffat and the Howgill Fells the major differences have been introduced by the formation of solifluction deposits from the underlying substrate. Solifluction deposits were formed within lateral and valley moraine although the degree of difference observed is related to the timescale over which periglacial conditions operated. The magnitude of the difference observed between the two source groups is of such strength that their traits are still recognisable after size-selective transport and the distance over which the sediments have been transported, which varies with catchment size. The degree of differentiation observed between the source groups is related to the formational link between the groups. The classification procedure of the sediments could be refined to alleviate overlap and if possible, use a systematic sampling procedure. At Langden Beck solifluction deposits are present but the underlying bedrock is the substrate from which solifluction deposits formed. Solifluction deposits do show some magnetic differences from the underlying bedrock but the discrimination is limited when compared with the differentiation evident at the other three sites. Only the marked effect of human activity has resulted in discernible changes in sediment supply to Harthope Beck and West Beck.

The segregation of cone sediments into layers that have been transported individually provides the fundamental basis for determining a temporal change in sediment supply to the fan over time. The interpretative technique adopted also

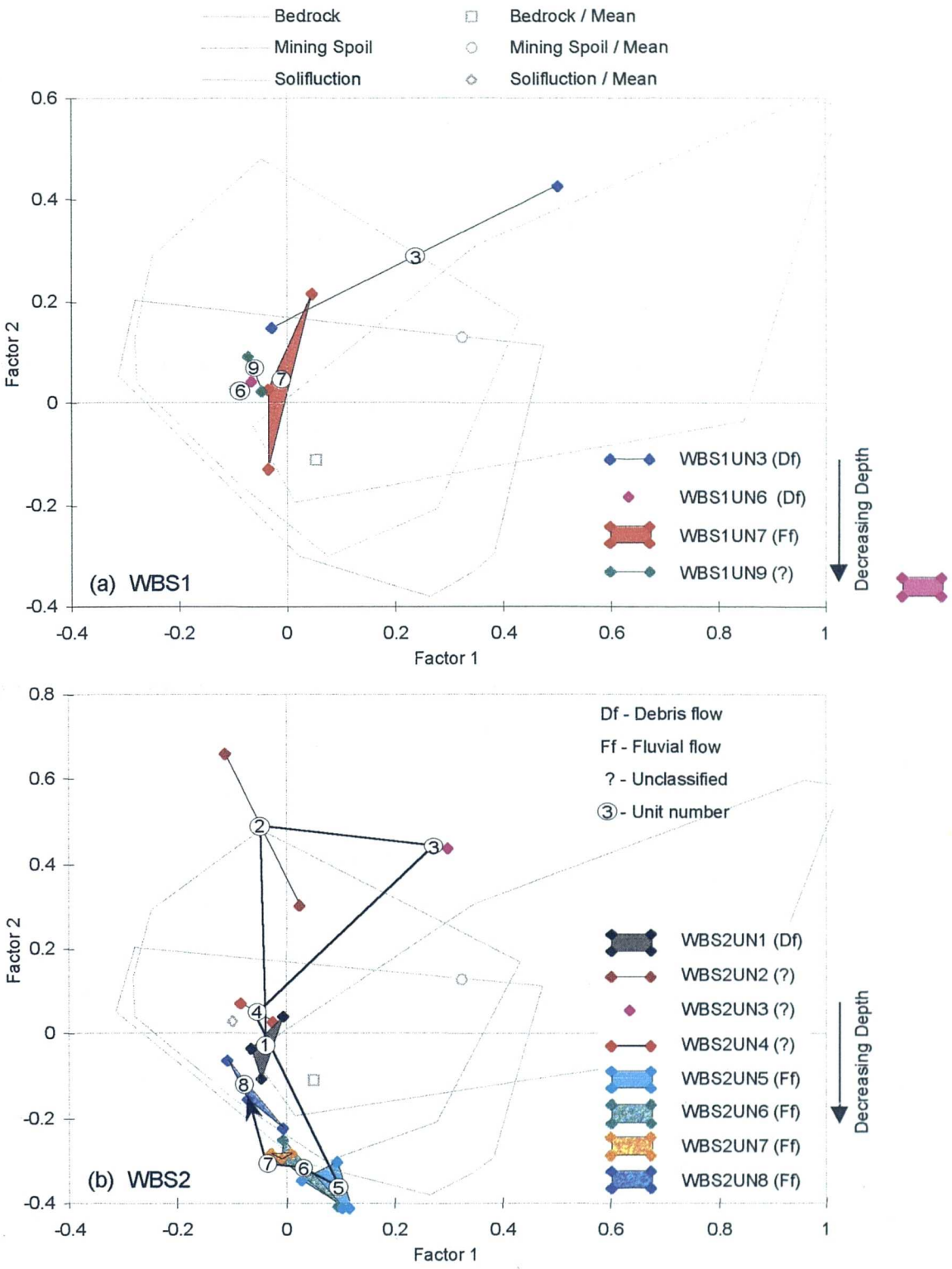


Figure 6.36. Assignment of source for individual flow units identified in (a) WBS1 and (b) WBS2, Langden Beck

allows the identification of changes within an individual source group as well as an interpretation of the dominant supplying source group. It is also possible to determine if sediment sources change as a flow moves from its point of origin to its site of deposition : combined, this data can identify significant changes in the characteristics of the source sediment supplied to the fan or cone and thus confirm breaks in fan and cone activity. In attempting to detect changes in the source of sediment within fan and cone stratigraphy, changes identified can be linked with transport event sequences. Any correlation between the two will help to further constrain the number and indirectly the interrelationship of events that have contributed to alluvial fan or debris cone development. It is possible to recognise when an area with particular source signature, and thus plotted position in factor space, has undergone a prolonged phase of activity or supply as unit groups overlap.

Evidence of a sequential change in the dominant supplying source at Glen Etive, Moffat and the Howgill Fells indicates that the sequence of changes in sediment sources observed represent the initial stripping of the overlying material. This is followed by the incorporation of sediment from the exposed underlying layer. The preservation and signature of the change is catchment-specific but parallels can be drawn between features within and between the regions investigated. At Glen Etive the subsequent change from lateral moraine to valley moraine is found in all three sections. Within the supplying catchment it is evident that valley moraine deposits have been exposed by the erosion of the overlying lateral moraine. As a consequence the sequential change in the character of sediment supplied does not necessarily equate to a spatial change in the origin of the sediment. Activity is concentrated within a supplying gully or an area which has been destabilised as found at Dry Cleuch.

Evidence of the whole sequence of sediment supplied to a feature, from the first flow to the last phase of activity, is preserved at three sites: Dry Cleuch near Moffat, Thickcombs Gill and Burnt Gill from the Howgill Fells. In all three gully systems the onset of cone activity is characterised by the initial stripping of peat and the underlying sediment. The peat has been preserved at Moffat. The eroded area thus has lower thresholds then the surrounding sediments. The destabilised area is as a result more susceptible to subsequent erosive conditions.

After the characteristic initial phase of activity, in all three cases a period of stability ensues and a palaeosol is developed. The time period of stability varies but the sequence of sediment supply which follows shows significant similarities between the three gully catchments. For Dry Cleuch, changes in the relative proportions of storage material supplied provided additional information upon the exhaustion of storage sediment reserves. At Burnt Gill, additional evidence of gully headward retreat is found. As activity progresses glacial and increasingly solifluction sediments are tapped higher up within the catchment.

6.6 Summary

In all of the sections studied there has been no evidence of a difference in source directly attributable to a change in transport mechanism from debris flow to fluvially transported units. At Leath Gill and Nevy Gill a change in transport mechanism is concurrent with a change in the sediment source. The change is also concurrent with a marked change in the development of fan aggradation. In both sections the change is linked with a relative break in fan aggradation. As a result it is difficult to disassociate the two changes and what they signify. It is also difficult to disassociate spatial and temporal changes in sediment supply to individual features. Within-catchment differences in sediment supplies can be observed both spatially and temporally, for example at Coire Dionachd. The interpretation of the change in source is primarily based upon observations of sediment source location within the supplying catchment.

Despite this, the position of the individual transported units in relation to their source groups provides information upon the temporal development of the feature investigated. The ability to discern a temporal change stratigraphically is achieved by the method of data presentation adopted and by the identification of separately deposited sediment layers, from the previous chapter. The degree of success and the resolution of temporal change varies between sites due to the degree of source discrimination achieved. The interpretation of source ascription for both Glen Etive and Langden Beck was subjective but valuable information was obtained upon the inter-relationship of individual unit hulls in relation to source groups. Sequential changes in the sediment supplied to the fan have been identified at all of the sections investigated. Temporal change in sediment source supplied to a fan and cone is constrained by sediment source characteristics and by internal catchment

topographical controls. In accounting for characteristics specific to a given catchment mineral magnetics has discerned a sequential decrease in source supplies in relation to catchment source characteristics. As well as a long-term change in source supplies, short term changes in association with cyclic activity have been identified, resulting in a higher resolution of change than previously anticipated.

Chapter Seven

Sediment supply control: discussion and conclusion

7.1 Introduction

The detailed analysis of the changes in the nature of flow mechanism and catchment sediment source, reported in the two previous chapters, has been undertaken, primarily, to test ideas about the importance of sediment supply in constraining the chronological development of fan and cone features in the British uplands. It has become apparent as the discussion of individual field study areas has progressed that many aspects of fan deposition relate to essentially local controls. The extent to which factors related to the distribution of suitable sediment supplies and the topographic configuration of the field area are important in explaining the nature of landforms in the vicinity, should be considered in relation to the consistent variation in fan and cone characteristics observed between different regions. By considering four somewhat diverse sites in northern Britain some clear variation in the relative importance of scale, dominant sources of sediment supply and the history of deposition and incision in fan and cone development is apparent. However, large variations in the style of fan development have also been observed within individual catchments.

The final chapter of the thesis aims to draw together the evidence for local scale and regional controls on the signature of sediment exhaustion. In so doing, the contribution made by this study to the study of fans and cones in upland Britain can be assessed and ideas for the further pursuance of related studies advanced.

7.2 The signature of sediment exhaustion

The four sites chosen for this study were selected because of differences observed between sites in the relative amount of sediment available and in the regional controls upon sediment transfer from slopes to the fan or cone. These differences will be expressed by evidence of long-term, cyclic and single-event sediment exhaustion observed in the fan and cone sequences investigated. Where sediment supplies are abundant, the sedimentary sequence and form will preserve the signature of short-term, cyclic and single-event sediment exhaustion. This is also applicable if the feature has only recently been initiated.

7.2.1 Sediment exhaustion signatures and local controls

At Langden Beck the rate of sediment supply and its availability has been directly influenced by mining. In the two fans investigated, mining activity has operated at differing intensities. The resulting increase in the volume and rate of sediment supply and change in hydrological regime between the two fans is reflected in their response. The formation of inset terracing in both Harthope Beck and West Beck fans is linked to mining by the fingerprinting of mining sediments in both WBS1 and WBS2. A more comprehensive metallurgical analysis of fan sediments in both features will help to confirm the signature of source change as the source discrimination using mineral magnetics was subjective. The mining process of hushing drastically alters the hydrological regime of the catchment system. Within the catchment areas of both fans, side gullies and tributaries have been mined. It is argued that the concentrated increase in discharge supplied to the fans has resulted in fan terrace formation. In contrast to Harthope Beck, part of the Westbeck fan has been buried by over 2 m of sediment issuing from a mined side gully. In section WBS2 the exposed stratigraphy reveals the sequential stripping of surficial sediments from peat, through to glacial material and bedrock. It is clear from the sorting characteristics of the sediments that they were transported by water, the source of water being either from hushing or from the build-up of water behind a dam and its subsequent release. It is evident that the stripping of surface sediments using water has been applied in the side gullies of both catchments. There is no evidence to suggest that sediments were aggraded on either fans surfaces. This signifies that the stripped and mined sediment was shunted to the main river with some sediments being incorporated as storage within the trunk stream system and within inset terrace sediments.

At Langden Beck highly localised mining activity of differing intensities has resulted in two extreme responses. In WBS2, large volumes of sediment have been aggraded. Changes in the hydrological regime and throughput of water directly into the stream system, bypassing the slope system, have resulted in the incision of the fans and the formation of inset fan terraces. In fan and cone development, aggradation is indicative of sediment abundance whilst incision in combination with changes in discharge is a result of low sediment availability or exhaustion. In this instance incision is a signature of sediment exhaustion within the trunk stream system only. Sediments have aggraded by the artificial erosion of bedrock, glacial till, solifluction material and peat by mining activity. Sediment supply control upon response is exaggerated but clear in both instances.

The spatial differences observed within the response of the two features to localised mining activity at Langden beck is recorded in the chronological development sequence of Dalness Chasm Cone investigated by Brazier *et al.*, (1988), and of Coire Dionachd Fan at Glen Etive. The parallels in form and evidence of "Medieval" lazy bed agriculture on and in close proximity to Coire Dionachd and Dalness chasm cone investigated by Brazier *et al.* (1988) led to the extrapolation of their findings at Dalness Chasm Cone to the development history of Coire Dionachd Fan. Debris cone aggradation is followed by incision of the cone surface. Incision is linked to the disturbance of vegetation cover by burning (Brazier *et al.*, 1988). Burning on the cones surface at Coire Dionachd lowered thresholds to sediment movement on the cone's surface. The incision of cone deposits was then reliant upon the occurrence of a storm event of sufficient intensity to transport destabilised sediments. The long-term effects of sediment exhaustion are thus clear. Although at Coire Dionachd the large volumes of coarse scree within the trunk stream indicate that current activity within the fan is related to cyclic changes in sediment availability. Its transfer is limited by the occurrence of storms of sufficient magnitude that can transport large boulders within the trunk stream.

The investigation of sequences of transport and change in source has highlighted three important controls upon the earlier development of Coire Dionachd. Firstly, the preservation of transported peat attests to the former presence of a blanket peat cover in the supplying catchment. The direct association between the peat and the hyperconcentrated flow that transported it signifies that instability introduced at the contact between a peat cover and the underlying sediments directly or indirectly triggered a phase of activity within the fan. Secondly, the transport mechanism and

source of the sediments in CDS3 highlight the influence of local site of deposition in the sediment sequence and thus the signature preservation. The intercalation of main river sediments between flows issuing from Coire Dionachd in phases prior to known human activity on the fan's surface suggests activity was concurrent in both the main river and in Coire Dionachd. Flooding in the main river system concurrent with heightened activity within the cone highlights the importance of a regional climatic trigger mechanism. Thirdly, the characteristics of the debris flows prior to and following main river intercalation in CDS2 and CDS3 indicate a change in source. A source of lateral moraine and solifluction deposits, characteristic of the gentle eastern slopes changes to glacial till, located in the headwaters of the catchment. The change in source is indicative of a spatial change in source within the catchment. The nature of the spatial change from catchment slope reserves to sediment within the trunk stream system does suggest a change in sediment availability. The excavation of parallel gullies within slope sediments provided the initial source of these sediments to the cone. After their excavation the gullies channelled flow to the stream system subsequently concentrating discharge thus transporting the sediment within the trunk stream system which was predominantly comprised of glacial till.

The sediment sequence of Dry Cleuch at Moffat provides a more comprehensive record of its development history. Although the sequence has been dominated by debris flow deposits since the initiation of the cone, the sediment source has changed from predominantly glacial sediment to solifluction deposits, with a cyclic input from storage within the trunk stream system. Three phases of aggradation have been recognised. An addition phase has been recognised by the sequential change observed in sediment source supplied to each debris flow. The debris flows which comprise each phase are in sharp contact. Only one unit has evidence of being reworked following deposition. The reworking of deposits indicates the magnitude of the event that triggered the flow, rather than a period of stability between debris flows. The source of sediments in the debris flow immediately above indicates the flow is part of the same cyclic removal of sediment. It is the contact of this overlying debris flow with the flow above that represents the introduction of solifluction material as a source of sediment to the cone. On the basis of this evidence the second phase can be split into two. The cyclic change in sediment supply and the contribution of storage material within each phase are clear, as is the overall decrease in the supply of glacial material as the cone ages.

The change in transport mechanism and sediment source within the Hermanlaw Burn sedimentary sequence contrasts markedly with the resolution of the findings obtained from Dry Cleuch. A sedimentary sequence dominated initially by chaotic flood deposits undergoes a period of stability. This is broken by the fluvial aggradation of fine sediments which, due to the thin layering, may represent the lag deposits of large flows. This is then buried by a debris flow deposit. The break in cone activity is accompanied by a change in the relative contribution of glacial : storage material that combined have supplied all of the sediments to the sequence investigated. Below the organic inversion, the relative contribution of storage material increases. Within the last aggraded sediments in the sequence the proportion of glacial material dramatically increases. The change in source is in concert with its transportation by debris flow and represents a spatial change in source within the supplying catchment. A change from within-channel stored sediment to exposed glacial slope sediment reserves occurs. Although the sequence is not representative of the whole depositional history of the fan, it is evident that within the sequence a debris flow event has tapped less readily available sediment directly from slope sediment reserves. Either storage material had been removed and / or a large magnitude event resulted in a debris flow event, which transported sediment over 1 km from the headbowl region along the gorge to the fan. The source must have been within the headbowl region as the main river is isolated from slope sediments by a deep gorge along most of the trunk stream's length.

A similar sequence of events has been recorded in the fan sediments of Nevy Gill at the Howgill Fells. The influence of a migrating channel is suggested by the presence of abandoned channels upon the upper surface of the second fan terrace. The sediment sequence preserved within a section taken from the highest terrace within the fan exhibits a sequence of cross-bedded sediments often associated with channel deposits. This sequence overlays a substantial thickness of sediment. The contact also appears to be erosive and therefore represents an erosional hiatus. The sediment source for both the aggradational phase and for channel deposits all have similar characteristics. It is the last phase of aggradation that has buried the channel deposits and represents a significant change in source. The source of the debris flow contrasts with the source of debris flows earlier in the sequence. Previous flows appear to have originated within the larger tributary catchment.

The other alluvial fan sequence investigated from Leath Gill is comprised of alternating debris flow and fluvial flow deposits. It is clear that similar patterns of

aggradation occur either side of a break in cone activity. The significance of the alternating sequence cannot be readily interpreted in relation to sediment supply control on the long- and short-term.

The short-term control of sediment supply on aggradation of Thickcombs Gill is clear. Four separated phases of cone aggradation are dominated by distinct debris flows of substantial thickness and volume. The sediments of the larger debris flows have a different source signature relative to each other, as do subsequent flows which bury them. Changes in the clast to matrix ratio observed between separated flows are the only evidence of cyclic control upon sediment supply. In each phase the last debris flow suggests a change in supply from predominantly storage material characterised by large numbers of clasts to slope sediment reserves. The last event was transported fluvially. As the fluvial layer follows the thickest debris flow aggraded in the whole sequence, it is probable that the area eroded to give the larger debris flow was the source of the overlying fluvial layer. A rainfall event of a lower magnitude eroded the disturbed sediment from the earlier debris flow.

At Burnt Gill BGS1, the importance of the cyclic build-up of sediment is much clearer. A dry grain flow preserved within the middle of the sediment sequence that buries the palaeosol represents the build-up of storage following the initial onset of activity. After sediment supplies have been depleted, the dry grain flow is followed by a fluvial event. In BGS2, in close proximity to BGS1, the sequence of change within a comparable thickness of sediments contrasts markedly. There is no evidence of cyclic sediment supply control within the four identified debris flows that bury the palaeosol which is also found in BGS1. The sequence of debris flows do however indicate a sequential change in sediment source within the catchment, representing headward retreat of the supplying gully system. The contrast in the development of cones from gullies immediately adjacent to each other highlights the importance of internal controls which operate to control fan and cone development.

7.2.2 A regional comparison of sediment exhaustion signatures

Evidence of both long- and short-term sediment supply control has only been found within the sediment sequence of one feature, Dry Cleuch at Moffat. Thickcombs Gill and Burnt Gill indicate evidence of cyclic sediment supply and short term sediment exhaustion following a larger scale event. Due to the character of sediment supply, namely loose clasts built up within the trunk stream, the initiating event may not have

been a storm event of a large magnitude. Coire Dionachd is the only other feature that indicates long-term evidence of sediment supply control. The comparison of sediment sequences between alluvial fans and debris cones indicates that signatures of sediment exhaustion are affected by catchment size and the pathway of sediment from slopes to the site of deposition. The differences observed are also compounded by the limited sequence of sediments in chronological order found within alluvial fan exposures. Local site controls can also affect the preservation of the signatures of sediment exhaustion. Coire Dionachd, Leath Gill and the two tributaries of Burnt Gill indicate the importance of depositional environment and internal catchment controls.

The scale of sediment exhaustion operating within the sediment sequences found within each feature and the differences observed in comparison to other features are attributable to four controls: regional differences in the rate and relative amount of sediment supply and availability; catchment size; internal process operating within the supplying catchment and local depositional environment controls. The inter-relationship of these controls upon the scale of sediment exhaustion is illustrated in Figure 7.1.

The time period over which sediment exhaustion operates within a feature can be linked to catchment size. The storage of sediment within a trunk stream system may act as a buffer to change in the fan depositional environment. In addition, aggradation of sediments by fluvial flow is more common in features of larger catchment size (Kostaschuk, 1986). It is clear from evidence obtained from the sequences investigated from both Nevy Gill, Hermanlaw Burn and Coire Dionachd that catchment size has an effect on the nature of the sediment source signature. In all three sequences investigated from each feature, a debris flow event represents the last event to be recorded in the sequence. For both Nevy Gill and Hermanlaw Burn the evidence indicates that slope sediment reserves were eroded. Storage within the feature is exhausted. Following a break in cone aggradation, which is recorded in all three sequences, debris flow occurred. The depletion of storage sediment supplies may have resulted in the incision of fan sediments. However, it is difficult to obtain evidence of this. The erosion of slope sediment reserves can therefore be attributable to the destabilisation by human activity or by the occurrence of a storm of high magnitude. The sediment sequences of Burnt Gill, Thickcombs Gill and Dry Cleuch all reveal sediments that represent initial cone building. In all three sections the sediments of the first flow indicate the presence of peat, or are fingerprinted as sediments immediately underlying peat on slope interfluves. From the geomorphological maps of both regions it

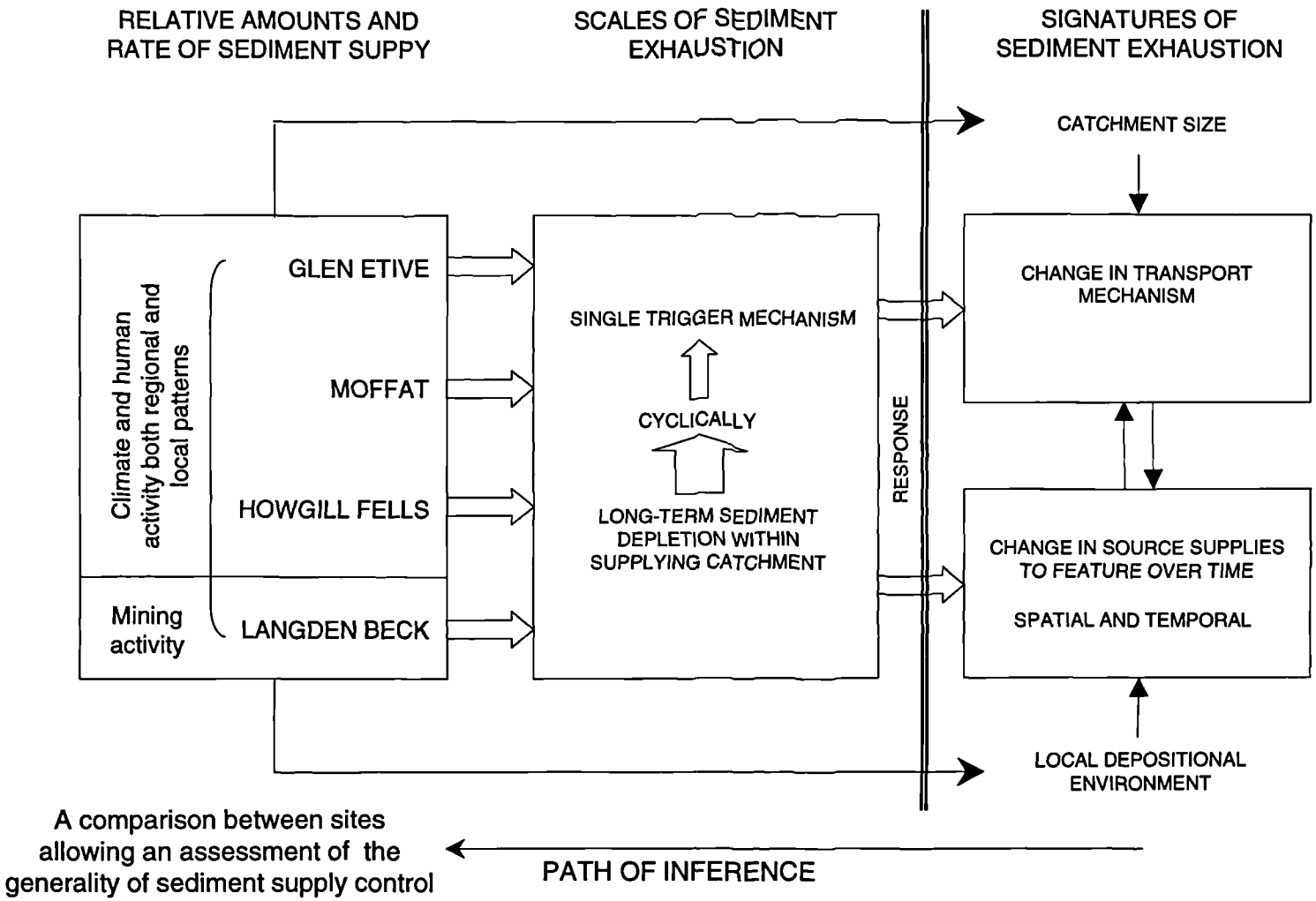


Figure 7.1. A schematic illustration of the interrelationship of supply and availability with sediment exhaustion and the resulting response with the fan or cone

is evident that the contact of peat and solifluction and lateral moraine deposits represents an impermeable unconformity. The contact between peat and an impermeable surface has been cited as the cause of peat flows (Carling, 1986a; Warburton and Higgitt, 1998). It may be that within Nevy Gill and Hermanlaw Burn, a large rainfall event may have triggered a peat slide within the supplying catchments. From the source signature of the two debris flows it is clear that peat is not in evidence. However, a peat slide may have destabilised an area increasing sediment availability and resulting in the debris flow preserved within the cone sequence.

Both the depositional environment and internal characteristics affect the signature of sediment exhaustion preserved within the profile. At Glen Etive the influence of the main river upon the sediment sequence was identifiable because of the identification of source and transport mechanisms and their comparison between two sections investigated from the same exposure. Internal controls upon cone development are less readily identifiable within fan and cone sedimentary sequences. Internal controls may affect the periodicity of sediment removal. The identification of the upper and lower boundaries of individual flows represents an essential stratigraphic marker in establishing the timing of individual flow events.

The link between peat source signature and the onset of aggradation of Burnt Gill, Thickcombs Gill and Dry Cleuch suggests that instability introduced by the impermeability unconformity in concert with a high magnitude storm event was instrumental in their initiation. The similarities between local site characteristics of both Moffat and the Howgill Fells (Chapter Three) include sediment supply, solifluction deposits formed within lateral moraine, and blanket peat developed upon the interfluves. The similarities in regional characteristics are reflected in the similarities observed in the development of both alluvial fans and debris cones between the two sites. Debris cones share the marked control of short -term sediment availability upon their development. In addition, the timing of activity between Burnt Gill and Thickcombs Gill and Dry Cleuch at Moffat at around c. 1000 years BP is also comparative. The onset of activity in the three cones began prior to *c.* 1000 years BP but post-peat formation ≅ *c.* 4000 years BP.

The nature of sediment supply control observed in the Howgill Fells and at Moffat contrasts with the signatures of sediment supply control observed at both Glen Etive and Langden Beck. What is comparable between the four sites is the nature of the response to changes in sediment supply and availability. High sediment availability results in cone

or fan aggradation. Low sediment availability results in a break in aggradation characterised by the formation of a palaeosol or an organic inversion or an erosional hiatus. The sediment supplied to the subsequent phase of activity represents a change in the origin of material within the supplying catchment or the temporal depletion of sediment reserves. The scale at which sediment is exhausted during fan or cone development is reflected by differences in sediment amounts and availability.

7.3 Intra-regional extrapolation of sediment exhaustion

Comparable morphometry between features may reflect similar development history. Variations in fan form can be used to determine geological and tectonic influences upon fan development. The technique is successful when applied to features that were initiated at the same time and thus have experienced a similar development history. The application of basic fan morphometry within the study can be used to establish similarities in the size of features found within the four study regions. The findings for features of a given size may be extrapolated to include features of comparable size found within the local area which are subject to local sediment supply and availability controls.

Scatter plots of catchment area against feature area found within the study areas are presented in Figure 7.2. Study reach areas and the number of features that were measured are also included. The features have been further sub-divided into categories which separate according to local site characteristics. Langden Beck is not considered in the study due to the very small number of features found within the catchment reach. The biplot of catchment and fan and cone morphometry for Glen Etive clearly highlights the disparity in scale between features formed within lateral moraine and those associated with porphyritic gullies (Figure 7.2a). The size grouping is attributable to the disparity in sediment supply and availability. The slope of the regression line for porphyritic debris cones is steeper when compared to debris cones of similar size in the Howgill Fells. This signifies that the catchment sizes of the porphyritic debris cones are much larger relative to the size of the fan. The disparity can be explained by either the removal of sediment from the system completely or by prior removal from a previous phase of erosion that occurred in the interstadial before the Loch Lomond Glaciation. The latter is more likely due to the coarse nature of the sediment supplied and the isolation of features from the main river system.

Parallels have been drawn between the findings at Coire Dionachd and a previous study upon the recent response of Dalness Chasm in association with human controls carried out by Brazier *et al.* (1988). At Coire Dionachd, despite having been influenced by interaction with the main river at the site of deposition, cone development suggests that the first phase of aggradation is associated with the period immediately following deglaciation. The second phase is characterised by the interaction of main river sediments whilst the third phase points towards a change in the origin of sediments within the catchment. A phase of aggradation immediately following deglaciation and in association with climatic change can be extrapolated to the development of the debris cone at Dalness Chasm. The last phase of activity in the cone at Dalness Chasm is dated at c. 4489 ± 300 years BP. Radiocarbon dates of a similar time period have also been obtained from organic material preserved within both CDS2 and CDS3. The origin of the organic material is questionable. It has been associated with transport as debris as part of hyperconcentrated flow and as such the dates are treated with caution. The placement of the organic material within the profile does separate an aggradational phase in the cone from intercalated fan and main river deposits. The heightened phase of activity operating within the fan catchment and within the main river system thus occurred after approximately 4,000 years BP. The extrapolation of data between the two features is limited by depositional controls specific to the local environmental context of Coire Dionachd and by the marked difference in catchment areas.

The correlation in activity and its nature is clear in the comparison of Burnt Gill and Thickcombs Gill, features of comparable size and in close proximity separated only by a watershed boundary between Langdale and Bowderdale catchments. In the scatter plot of fan : area relationships for features in the Howgill Fells, there is a clear distinction in the grouping of features in association within size (figure 7.2b). The variation in the size of debris cones within the main valleys of the Howgill Fells suggests a time progressive development of form, with each group representing a cone at a increasingly older stage in its development. The temporal development of features in a size continuum is advocated by Brazier (1987). If this is the case the similarity in form exhibited by each group suggests that the cones were initiated at the same time in response to similar forcing conditions. With regard to sediment exhaustion, each form is at a different stage in the overall sediment exhaustion cycle. The temporal initiation of debris cones and their subsequent development suggests a cyclic link to forcing conditions.

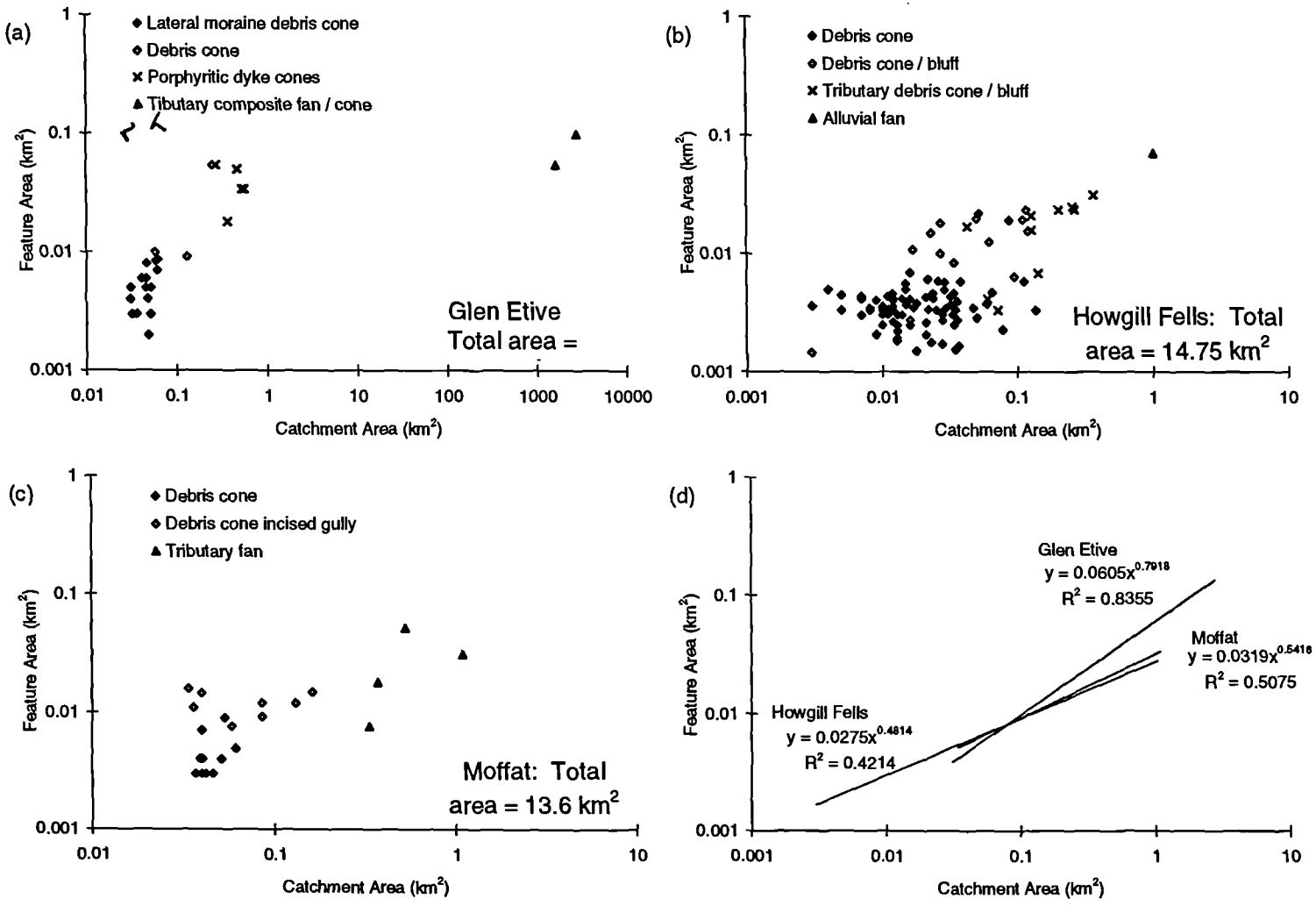


Figure 7.2. Plot of catchment area against fan area for features found within the study reaches of the Howgill Fells, Moffat and Glen Etive.

A similar pattern is observed with the form of debris cones and fans at Moffat (Figure 7.2c) and leads to the suggestion of a similar time frame for their development. If features were formed and initiated at the same time, the dating of one event within any feature could be used to determine the timing of that phase of fan and cone formation. Contemporaneity will be affected by inherent differences within supplying catchments which affect the cycle of development of each feature : their formation in response to the same event is not necessarily a foregone conclusion. The extrapolation of dates between features must be treated with caution. An understanding of local catchment controls upon feature development would aid extrapolation.

Internal thresholds can affect the response of a feature, the stage at which a feature is in the cyclic production or release of sediment to the trunk stream. Internal threshold conditions can explain the differences in the development of features immediately adjacent to each other. Although similar environmental conditions persist, it is possible that the catchments are at different stages in the sediment storage cycle. Thus the response to a similar event can be markedly different. Features may be comparable in size and form but their underlying development within the stratigraphic record could differ in terms of the timing of events. Dating of individual layers to substantiate this statement is problematic.

The comparison of catchment area with fan and cone area supplies limited information on fan and cone development. A more detailed statistical analysis of fan and catchment form is limited by the insufficient number of features found within the area studied in this study. A detailed morphometric study can be used to provide a quantitative means of establishing variation in spatial controls upon fan and cone development.

Morphometric analysis can be used to classify fans as paraglacial (Chapter Two). The debris cones that have developed within lateral moraine slope deposits at Glen Etive can be directly linked with the timescale of formation immediately following deglaciation. Debris cones are likely to have formed immediately following deglaciation whilst unconsolidated, unvegetated sediment was unstable on the oversteepened valley side slopes. At Moffat radiocarbon dates indicate that debris cones were formed during the late Holocene. The Hermanlaw Burn fan could be paraglacial but at present the current exposures do not contain datable material or a comprehensive sediment history of fan development. Thus there is no means of testing the hypothesis. In the Howgill

Fells remnants of aggradational phases preserved on high bluffs could have related to paraglacial activity.

7.4 Original contribution and extension of previous studies

This study includes the following work that makes an original contribution to knowledge.

Sediment supply has tended to be looked at implicitly in studies. What this thesis has done is to seek, explicitly, evidence of the control of sediment supply upon fan and cone development. Changes in the nature of fan stratigraphy indicating periods of fan building, stability or incision can be related to the availability of transportable sediment. A combination of methods including geomorphological mapping, dating, sediment source description and the interpretation of sediment transport processes has permitted this approach. To be aggraded in the depositional environment sediment has to be available for transport. The influence of sediment supply has important implications for the nature of the response of fans and cones to forcing parameters such as climate and human landuse. The sediment supply constrains the response to climate change.

Mineral magnetics have been applied to derive a signature of sediment supply control to fan and cone development for the first time (Chapter Six). The success of the application of mineral magnetics is reliant upon the feasibility of its application within the erosional and depositional environments of alluvial fans and debris cones. In comparison to previous applications of mineral magnetic techniques in sediment provenancing, tracing materials from catchments to fans and cones in upland Britain is conducted on a much smaller scale. The scale affects the recognition of different sediment sources within a catchment. The mixing of separate source materials during transport, the residence time as storage within the trunk stream system and the transport distance from origin within the catchment to site of deposition within the fan or cone all affect the signature of sediment exhaustion. It is likely that catchment size acts as a buffer to the time period over which the effects of sediment exhaustion are expressed within the development of the fan or cone sequence. The successful application of mineral magnetics in a fan and cone context has rested upon differences in environmental weathering producing variation in the iron content of sediment from which sediment source characteristics within the supplying catchment can be distinguished.

An unmixing model has been applied to give a quantitative evaluation of source ascription for alluvial fans for the first time (Chapter Six). The unmixing model requires sufficient discrimination of sediment source types, which is only exhibited in the Moffat field site. At other sites where the magnetic properties of different sediment supply is less clearly separated, a combination of biplots and factor analysis can be used to interpret the relative importance of sediment supply control. The simultaneous application of R- and Q- mode factor analysis has been successful in separating sources to allow an interpretation of sequential changes within a sediment profile. The separation of fan and cone sediments into separate flow units has further aided the assessment of source supply and evidence of its control upon their development.

A key element of the thesis has been the attempt to identify the mode of transport of sediments in fan and cone sequences. The use of quantitative sorting parameters has enabled the identification of debris flow and fluvial flow units. The development of the P90M sorting index has been based upon the success of descriptive interpretation from sorting indices, such as CM plots. The index has applicability in distinguishing properties characteristic to the debris flow : fluvial flow transition. Originally, measures of sorting based on the variation between the coarsest particles and median size were developed for determining differences between major depositional environments such as river, estuarine and marine environments. There has been limited application of sorting indices to identify variation within a single depositional environment but CM plots have been applied successfully to identify debris flow and fluvial flow deposits in arid fan environments. In this thesis the technique has been adapted and shown to be suitable for identifying differences in the sedimentary sequence of small, humid temperate fans.

It was initially expected that fan sequences would display a general transition from debris flow domination towards fluvial flow domination through the Holocene. Field evidence to support this general hypothesis displays a more intricate nature. The transition from debris flow to fluvial flow is supported at Thickcombs Gill. Within identified aggradation phases there is evidence for alternation of debris flow and fluvial flow activity. For example at both Burnt Gill, Thickcombs Gill and Dry Cleuch within the cycle of sediment supply the end of the cycle phases is signified by both the transition to fluvial deposition (a change in the mode of sediment transport) and by a spatial change in sediment source from trunk stream storage to previously untouched slope sediment reserves (a change in the sediment source).

It was expected that fans would display a gradual change from glacially-dominated sediments to solifluction-dominated sediments. Mineral magnetics has permitted this hypothesis to be tested. The signature of change in source is constrained by the character of sediment sources identified within a specific region. At each site the change in sediment source supplied to the fan or cone exhibits a change in source both spatial and temporal. A temporal change is recorded within all debris cones investigated in this study as well as spatial changes within the separate phases of activity identified. Spatial change in source is more commonly observed within the sediment sequences taken from alluvial fans. The difference observed is associated with scale as larger catchments have larger relative amounts of sediment supply in comparison to debris cones and consequently the long-term sediment exhaustion will be manifest within the fan system over a longer time period. The features are therefore at different stages in development in relation to sediment supply.

The evidence for changes in the mode of transport and the origin of the sediment supply point to two main controls. The first is catchment scale and the second the influence of sediment availability. Large catchment areas are more likely to develop fluvial flows whereas smaller catchments with steeper gradients and narrow valley floors are characterised by debris flow deposits. Small, steep catchments limited to one side of a valley are usually characterised by smaller amounts of material overall. The fan sequences therefore indicate a temporal depletion in sediment reserves. The larger catchments, on the other hand, have larger amounts of sediment source material : glacial sediments are also dominant for longer time periods. This has been demonstrated by the sediment provenance of Dry Cleuch cone and Hermanlaw Burn fan at Moffat.

The selection of sites for this research has permitted comparison relative to changes in sediment availability in response to broad climatic changes and human impact. A detailed chronology has been presented for fan and cone activity of four sites in upland Britain. This study has therefore added to understanding of fan and cone initiation, and it supplements previous work done elsewhere in the British Uplands. Phases of renewed aggradation can be correlated with the influence of man whilst the initial onset of the features has been linked to climate in concert with local topographic controls. In the short time period that blanket peat was present on slopes at Coire Dionachd, the resulting instabilities introduced triggered aggradation in the fan system. At Moffat and the Howgill Fells, onset of cone aggradation is linked to instability in blanket peat on

catchment interfluves. After a period of stability at both sites, which allowed the formation of a palaeosol within sediment of the initial cone building phases, renewed activity is correlated to the onset of Viking sheep grazing. Evidence therefore confirms that humid fans in the British Uplands were active around 1,000 years ago. The broad contemporaneity exhibited in the patterns of activity around 1 000 years BP obtained in this thesis and compiled from other studies suggests a common causal factor (Harvey *et al.*, 1981; Tallis, 1985; Harvey and Renwick, 1987; Tipping and Halliday, 1994). As yet there is no evidence of a broad climate change for this time period whilst human settlement patterns exhibit contemporaneity in upland regions.

The study has provided additional information on the timing of fan activity in the British uplands that may contribute to an improved understanding of Holocene sediment dynamics.

7.5 Recommendations for further research

It is possible to make recommendations for further research.

The application of mineral magnetics has provided valuable information upon source supply and its change through fan and cone development. Discrimination of sediment sources using magnetic parameters is sharply defined at the Moffat field site. At the other sites the magnetic parameters point to differences in the sediment supply components, but with overlaps between the convex hulls. Improvements to the provenancing of fan sediments can be generated by incorporating other fingerprinting properties. For example, more detailed information on the geochemistry of source and fan sediments would be helpful in increasing the dimensionality and hence reliability of sediment source separation. Improvements to the reliability of provenancing would result from further attention to causes of enrichment, such as particle size influences, diagenesis and chemical alteration.

Using the methods of this thesis it has been possible to better define the boundaries between individual flow deposits or units within the fan or cone sequence. The physical limits of separate units are quantitatively constrained supplying a reliable framework for the interpretation of the sediment properties of individual flow deposits. The detailed fabric analysis of the defined flow deposits, providing data upon transported clasts sizes, sorting and flow directions, will further the reconstruction of the magnitude of the transporting debris flow or fluvial flow. The P_nM sorting index can be applied to trace the

three-dimensional deposits of a distinct flow in fan and cone sediments. The ability to trace the relict deposits of a flow will allow a more precise quantification of flow volume and magnitude. It may also be possible to retrodict the discharge of relict flood deposits which can then be used to infer the magnitude of the trigger storm event.

Detailed analysis of fans and cones in the British Uplands is largely constrained by the availability of suitable exposures. Most fan interpretations are based on single exposures. The opportunity to incorporate analysis of multiple exposures of the same feature could significantly improve understanding of fan and cone genesis. What would be particularly useful is to study a feature where a three-dimension picture could be developed of the overall feature by a thorough excavation of the feature. The number of locations where this would be undertaken would be limited and might be in association with other purposes, such as archaeological investigations. Nonetheless, such a undertaking would make a potentially significant advance in providing a detailed base-line against which other more limited section analysis and interpretation could be more confidently interpreted.

Within the fan sediment sequences reported in the study identified activity and periods of stability have been constrained by the 14C dating of palaeosols preserved within the section. The preservation of palaeosols within the sediment sequence has two major implications for establishing chronology. First, some of the 14C dates obtained indicate that organic matter may not have been in *situ*. Further attention is required to identify in situ palaeosol development from the occurrence of transported organic matter within the sequence. Second, the sequences commonly exhibit phases of aggradation and hiatuses that occur without organic inclusions. These have been identified using the combined signatures of a change in sediment source and a change in the mode of sediment transport. Techniques to date the sediments between palaeosols would improve the resolution of the fan or cone chronology. Possibilities include the development of thermoluminescence techniques such as OSL, which have not been fully investigated in alluvial fan or debris cone sediments (Nanson and Young, 1985; White *et al.*, 1997). Additional information on the timing of sedimentation may also be available from proxy data, particularly the preservation of pollen and other macrofossils.

Fan morphometric investigation applied within this thesis has provided a tool for the comparison of findings between regions. The application of the technique can be

extended by the inclusion of a more detailed description of fan and cone form combined with quantification of variables describing catchment characteristics. In studying regional characteristics in fan form, specifically their geometric properties more detailed confirmation from site specific controls upon their form and development can be obtained. In particular, the influence of the availability, amount and location of glacially-derived sediment supply might be evaluated. A detailed investigation of morphometric characteristics within a specific region can therefore be established. Comparison of findings between contrasting regions will improve understanding of fan and cone development with regard to changes in sediment supply control. Within the present study, preliminary evidence for the influence of the Loch Lomond readvance on sediment availability for fan development has been advanced.

This thesis has demonstrated the sensitivity of fan and cone development to variations in the nature and availability of sediment supply. A potential application of this understanding is the growing interest in the management and conservation of geological and geomorphological features in upland environments. For example, Scottish Natural Heritage have recently commissioned research to develop a methodology for assessing the stability of Holocene landforms in order to guide sustainable management of those features (Gordon *et al.*, 1998). As some humid temperate fans contain significant archaeological importance or have designations as sites of special scientific interest (SSSIs) the sensitivity of fans to erosional processes and catchment controls is an important influence on the management strategy (Gordon *et al*, 1998). Fans and cones are, as this study shows, dynamic features which are part of an ever-evolving sedimentary landscape. Their effective management must take this into account and be based on a strategy focused on an evolving landform rather than a static feature which requires preservation as a static component of the landscape. By elucidating the dynamics of a fan / cone system as this thesis has attempted to do, a more effective management scheme can be drawn up which is based upon landscape dynamics and sensitivity to change under any given set of controlling environmental conditions.

This thesis is part of a sequence of ongoing research. Its contribution can be assessed both in terms of the details presented for the study areas and also in the conclusions which have wider general application. The results provide a guide to where additional work is required.

APPENDICES

Appendix 1 Raw Data

1.1 Soil profile descriptions of palaeosols

1.2 Section samples, loss on ignition, particle size, P_nM Index

1.3 Section samples, mineral magnetics, parameters, ratios

1.4 Source samples

Appendix 2 Assignment of transport mechanism to sections

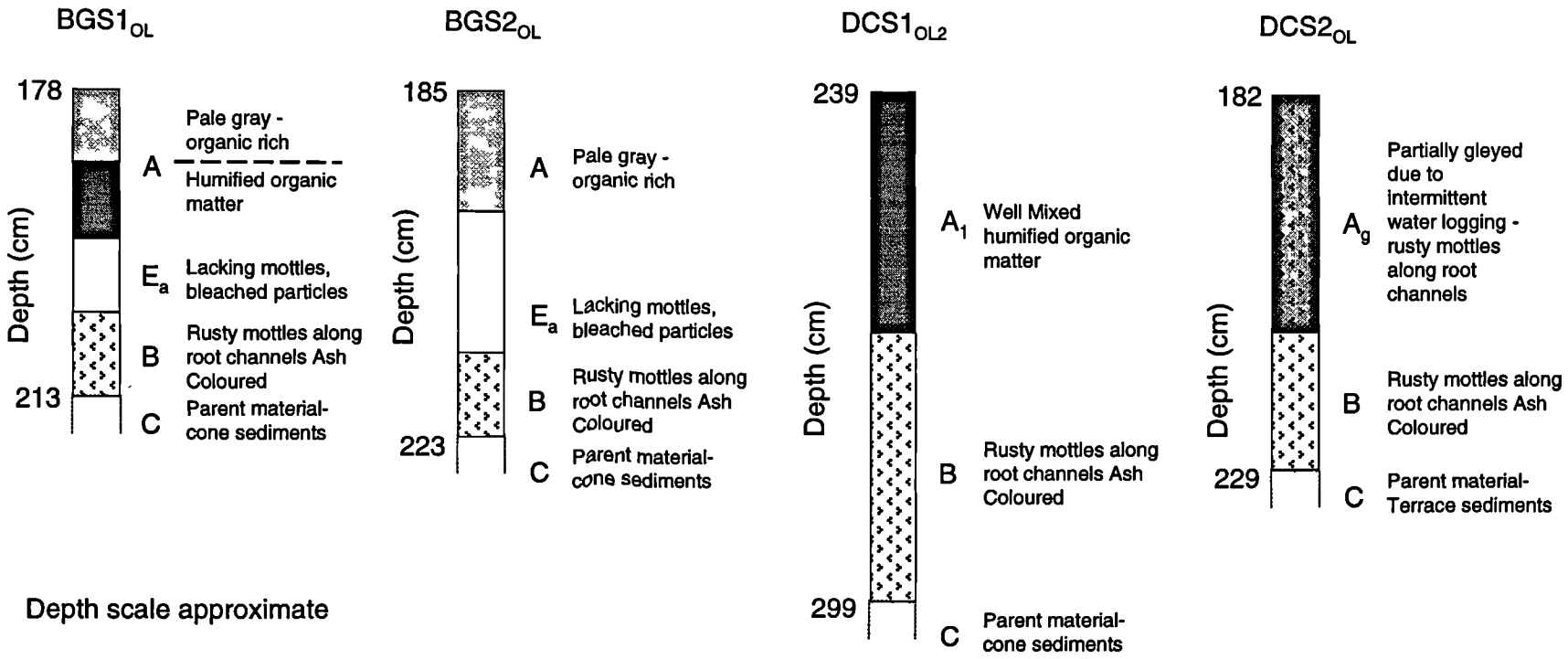
Appendix 3 3.1 Downsection plots of magnetic parameters and ratios

3.2 Unmixing model results

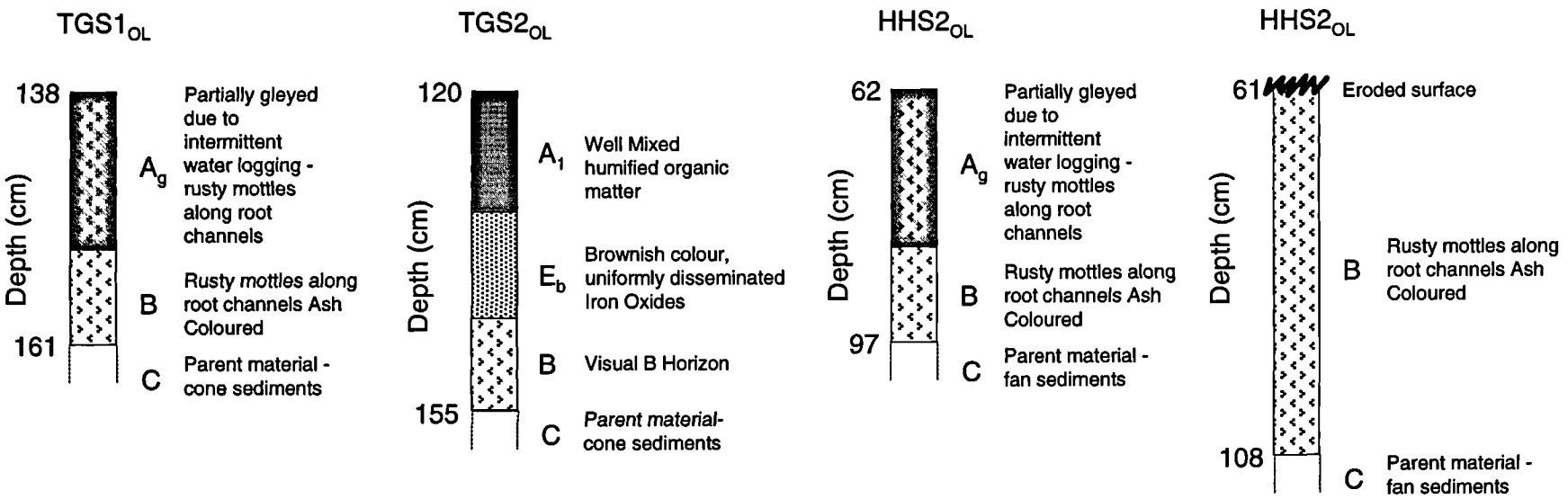
Key to following tables:

Site codes:		Section Codes:			
HF	Howgill Fells	BG	Burnt Gill	HB	Hermanlaw Burn
GE	Glen Etive	CD	Coire Dionachd	LG	Leath Gill
M	Moffat	DC	Dry Cleuch	NG	Nevy Gill
LB	Langden Beck	GF	Gully Fan	TG	Thickcombs Gill
		HH	Harthope Beck	WB	West Beck

Note: The data for sections are presented in tables sorted by alphabetic order.



Appendix 1.1: Soil profile descriptions of palaeosols



Depth scale approximate

HF - BGS1

Depth	%L.O.I	P_n (μm)				%P_nM Index			%Sand	% Size Fraction							Skewness
(cm)		50	70	80	90	50 - 70	50 - 80	50 - 90		2000 - 600	600 - 212	212 - 63	20 - 63	6 - 20	2 - 6	0.04 - 2	
2.5	3.77	25.1	63.9	119.7	353.7	1.55	3.78	13.12	30.27	7.84	5.60	16.83	24.41	20.14	13.38	11.80	2.90
6.5	38.31	17.6	52.4	84.8	143.6	1.97	3.81	7.15	26.23	1.38	3.15	21.70	21.47	22.42	15.87	14.00	4.67
28.5	8.45	32.0	104.1	197.9	730.4	2.25	5.18	21.82	38.56	12.07	7.08	19.41	19.09	17.97	12.90	11.48	2.21
39.5	4.93	33.0	99.0	184.1	612.0	2.00	4.59	17.57	38.40	10.20	8.00	20.20	19.92	17.79	12.63	11.26	2.38
46.5	2.87	293.6	943.9	1246.0	1555.0	2.21	3.24	4.30	67.73	41.12	13.14	13.47	10.57	9.09	6.64	5.96	0.71
55.5	2.33	635.5	1056.0	1265.0	1523.0	0.66	0.99	1.40	69.57	51.22	10.29	8.06	8.92	9.38	6.41	5.72	0.38
62.5	3.43	676.3	1163.0	1384.0	1640.0	0.72	1.05	1.42	71.19	52.06	9.57	9.56	9.02	8.68	5.85	5.25	0.33
81.5	4.07	920.6	1317.0	1515.0	1740.0	0.43	0.65	0.89	75.66	61.82	6.29	7.55	7.95	7.26	4.78	4.35	0.02
104.5	2.46	69.8	126.8	175.4	269.0	0.82	1.51	2.85	53.00	4.74	10.35	37.91	20.48	11.46	8.02	7.05	2.95
113.5	2.90	87.3	174.5	262.9	684.0	1.00	2.01	6.84	58.21	11.41	13.54	33.26	17.10	10.34	7.58	6.78	2.58
122.5	2.70	71.2	162.7	323.8	978.8	1.29	3.55	12.75	52.91	16.30	8.81	27.80	18.85	11.81	8.48	7.96	2.15
130.5	3.69	87.5	346.4	837.5	1257.0	2.96	8.57	13.37	56.46	25.82	8.83	21.81	15.63	10.86	8.64	8.40	1.43
147.5	4.24	122.9	712.3	1035.0	1387.0	4.80	7.42	10.29	60.23	33.13	8.93	18.17	12.06	10.13	8.94	8.64	1.05
154.5	3.34	96.4	319.3	740.4	1024.0	2.31	6.68	9.63	57.69	23.84	11.12	22.73	13.00	11.22	9.26	8.82	1.30
162.5	3.17	315.2	1046.0	1347.0	1664.0	2.32	3.27	4.28	68.00	45.00	8.55	14.45	10.54	8.52	6.72	6.22	0.59
172.5	3.73	107.5	458.9	942.7	1463.0	3.27	7.77	12.61	60.22	28.12	9.40	22.70	14.36	10.55	7.66	7.21	1.32
179.5	4.52	32.5	63.4	85.9	126.6	0.95	1.64	2.89	30.23	0.00	2.20	28.03	30.19	17.64	11.06	10.87	1.61
185.5	16.64	12.4	25.4	39.9	79.8	1.05	2.22	5.44	12.86	0.00	1.16	11.70	23.82	30.71	17.74	14.87	2.93
203.5	6.10	12.6	29.1	47.6	91.3	1.32	2.79	6.27	15.27	0.00	1.37	13.90	23.73	27.50	17.56	15.94	2.68
219	3.35	16.0	41.2	73.2	171.8	1.58	3.59	9.76	22.34	4.27	4.10	13.97	22.85	24.33	16.18	14.30	3.43
233.5	3.64	25.0	74.4	166.7	552.6	1.98	5.67	21.10	32.62	9.07	8.67	14.88	21.76	20.31	13.14	12.17	2.43
244.5	3.54	75.9	596.2	896.1	1251.0	6.85	10.80	15.48	52.07	29.88	11.20	10.99	16.14	14.10	9.06	8.63	1.20
252.5	5.31	595.4	973.1	1189.0	1483.0	0.63	1.00	1.49	72.10	49.78	12.99	9.33	9.38	8.51	5.42	4.60	0.48
257	1.92	783.2	1047.0	1215.0	1400.0	0.34	0.55	0.79	85.92	63.56	17.88	4.48	4.06	4.44	3.00	2.58	-0.05
267.5	5.28	800.7	1107.0	1276.0	1446.0	0.38	0.59	0.81	82.55	62.62	15.01	4.92	5.68	5.41	3.48	2.88	-0.06
286.5	5.18	43.6	512.5	896.5	1312.0	10.75	19.56	29.09	46.39	28.07	9.29	9.03	12.70	15.40	13.62	11.89	1.28
293	2.27	549.4	793.5	940.0	1146.0	0.44	0.71	1.09	83.15	45.70	30.02	7.43	5.02	4.94	3.39	3.49	0.41
297.5	4.83	106.5	661.6	984.9	1373.0	5.21	8.25	11.89	57.92	31.76	9.80	16.36	14.24	11.98	7.98	7.88	1.13
301.5	10.90	36.1	115.7	243.2	793.5	2.21	5.75	21.01	40.22	14.19	7.55	18.48	19.39	18.02	11.60	10.76	2.03

APPENDIX 1.2: Section samples, Loss on Ignition, Particle size and PnM Index

HF - BGS2

Depth	%L.O.I	P_n (µm)				%P_nM Index			%Sand	% Size Fraction							Skewness
(cm)		50	70	80	90	50 - 70	50 - 80	50 - 90		2000 - 600	600 - 212	212 - 63	20 - 63	6 - 20	2 - 6	0.04 - 2	
6	10.34	14.7	37.8	61.7	107.8	1.58	3.21	6.35	19.56	0.00	1.97	17.59	23.94	24.44	16.63	15.43	2.41
22	6.02	15.6	39.2	62.6	106.1	1.51	3.02	5.81	19.86	0.00	1.48	18.38	24.80	24.10	16.26	14.98	2.27
45	5.54	17.1	42.4	66.7	112.8	1.48	2.90	5.59	21.21	0.00	1.91	19.31	25.41	23.47	15.45	14.46	2.19
58	4.18	18.1	46.9	75.8	137.5	1.59	3.19	6.60	23.75	1.74	3.15	18.86	24.18	22.46	15.51	14.10	4.70
66	4.84	18.0	46.7	73.5	126.2	1.60	3.09	6.03	23.34	0.00	3.08	20.27	24.50	21.87	15.71	14.58	2.27
76	6.54	20.7	53.2	84.1	151.8	1.57	3.06	6.33	26.23	2.30	3.81	20.12	24.47	21.52	14.10	13.67	4.69
81	6.39	23.4	59.3	92.9	164.9	1.54	2.98	6.06	28.56	2.08	4.25	22.22	24.54	20.61	13.19	13.10	4.33
91	5.74	14.0	42.3	72.0	136.9	2.02	4.13	8.76	22.48	2.58	3.27	16.63	21.17	21.83	17.79	16.72	4.21
100	5.42	14.2	45.0	81.3	175.4	2.18	4.75	11.40	24.25	5.57	2.86	15.83	19.56	22.72	18.60	14.86	3.69
108	6.09	18.3	55.4	102.8	278.7	2.03	4.63	14.26	27.75	7.27	4.35	16.13	20.49	22.49	16.51	12.76	3.07
114	4.82	18.7	58.1	108.2	316.8	2.11	4.80	15.98	28.61	8.59	3.52	16.50	20.09	22.18	16.38	12.74	3.29
117	4.33	20.2	62.3	119.0	421.3	2.09	4.89	19.87	29.81	8.57	4.86	16.38	20.36	22.63	15.46	11.73	3.24
125	5.31	21.3	67.3	131.5	498.9	2.16	5.17	22.42	31.06	8.92	5.67	16.46	20.15	22.26	15.12	11.41	2.90
134	5.14	18.0	54.7	100.4	216.8	2.03	4.57	11.02	27.57	4.89	5.31	17.37	20.33	23.68	16.16	12.27	3.54
139	4.76	22.7	65.8	127.8	419.8	1.90	4.62	17.47	30.74	8.44	5.68	16.61	21.87	22.04	14.39	10.97	3.13
144	3.60	23.4	72.2	133.1	385.1	2.08	4.69	15.45	32.39	7.87	6.20	18.32	20.59	21.26	14.59	11.17	2.84
151	4.50	20.8	53.8	88.1	160.2	1.58	3.23	6.69	26.68	3.54	3.30	19.85	24.19	22.58	14.74	11.80	5.15
160	3.20	25.9	76.0	132.4	308.4	1.93	4.11	10.90	33.58	7.07	5.96	20.55	21.39	20.68	13.53	10.82	3.35
167	4.04	18.5	44.4	68.8	113.8	1.40	2.71	5.14	21.97	0.00	1.48	20.49	26.31	24.14	15.42	12.17	1.96
170	3.24	18.9	45.5	70.0	113.9	1.41	2.70	5.02	22.43	0.00	1.57	20.86	26.28	24.50	15.44	11.35	2.00
172.5	4.52	18.7	41.9	63.4	104.1	1.25	2.40	4.58	20.16	0.00	1.45	18.71	28.15	24.89	15.05	11.75	2.15
178.5	4.18	17.4	38.1	56.1	88.9	1.19	2.22	4.10	17.11	0.00	0.29	16.82	29.56	25.18	15.69	12.46	1.96
182.5	4.09	14.6	33.8	52.2	90.9	1.32	2.58	5.23	16.10	0.00	1.04	15.05	26.70	25.66	17.14	14.40	2.32
188.5	4.94	10.3	22.1	32.4	53.6	1.14	2.14	4.20	7.66	0.00	0.18	7.48	25.05	30.75	20.61	15.94	3.07
192.5	4.10	11.7	23.0	31.8	47.6	0.97	1.73	3.08	5.38	0.00	0.01	5.37	29.10	31.61	18.23	15.69	2.73
201.5	3.32	19.3	35.8	46.5	62.4	0.85	1.41	2.23	9.68	0.00	0.00	9.68	39.36	23.69	13.92	13.35	1.58
209.5	3.47	15.3	31.2	44.0	66.5	1.04	1.87	3.34	11.09	0.00	0.03	11.06	31.96	26.96	16.01	13.98	2.07
211.5	4.70	10.7	21.1	29.3	44.3	0.98	1.75	3.16	4.79	0.00	0.02	4.78	26.81	33.12	19.26	16.01	3.00
215.5	3.67	13.5	28.5	41.0	62.2	1.11	2.03	3.60	9.72	0.00	0.04	9.68	30.22	28.43	16.85	14.78	2.26
222.5	3.56	14.9	35.0	55.3	94.4	1.36	2.72	5.36	17.24	0.00	1.40	15.84	25.97	25.97	16.41	14.40	2.39
227	3.89	27.5	65.3	102.0	183.1	1.37	2.71	5.66	30.84	3.37	4.72	22.75	25.87	20.51	12.23	10.56	3.86
234	2.59	43.7	93.2	142.9	253.4	1.13	2.27	4.80	40.50	4.65	7.92	27.93	25.26	15.92	9.49	8.83	3.07
239	2.21	37.8	87.3	143.9	305.2	1.31	2.80	7.07	37.72	6.09	7.88	23.76	25.12	16.97	10.36	9.83	3.01
243	3.00	13.6	31.5	49.1	84.3	1.32	2.61	5.20	14.92	0.00	0.87	14.06	26.18	26.61	17.47	14.81	2.46
252	2.70	21.7	51.4	83.2	166.8	1.37	2.84	6.70	25.46	2.46	4.97	18.03	26.25	22.18	13.68	12.43	4.09
254	2.77	45.6	135.1	281.7	685.0	1.96	5.18	14.03	43.22	11.90	11.58	19.75	22.54	15.74	9.44	9.06	2.15

GE - CDS1

Depth	%L.O.I	P_n (µm)				%P_nM Index			%Sand	% Size Fraction							Skewness
(cm)		50	70	80	90	50 - 70	50 - 80	50 - 90		2000 - 600	600 - 212	212 - 63	20 - 63	6 - 20	2 - 6	0.04 - 2	
3	8.72	30.6	88.2	152.3	298.3	1.88	3.98	8.75	35.95	5.97	8.25	21.74	23.08	21.95	10.37	8.65	2.85
11	14.74	50.4	92.2	141.8	334.1	0.83	1.81	5.63	42.03	8.14	5.75	28.13	34.61	14.09	4.58	4.70	3.43
27	12.49	93.1	211.3	556.5	1118.0	1.27	4.98	11.01	61.37	19.29	10.64	31.43	23.62	8.84	3.15	3.02	1.89
44	11.20	133.1	610.0	1004.0	1473.0	3.58	6.54	10.07	68.09	30.23	10.73	27.13	19.24	7.56	2.77	2.34	1.22
56	4.42	305.1	994.6	1296.0	1630.0	2.26	3.25	4.34	72.59	43.31	10.82	18.46	14.98	7.37	2.75	2.31	0.67
75	4.27	788.4	1192.0	1424.0	1688.0	0.51	0.81	1.14	84.42	59.32	16.06	9.04	8.45	4.23	1.77	1.13	0.21
89	5.45	1055.0	1441.0	1627.0	1813.0	0.37	0.54	0.72	88.24	69.76	9.63	8.85	6.64	3.07	1.22	0.83	-0.18
100	4.76	1018.0	1384.0	1579.0	1785.0	0.36	0.55	0.75	89.22	70.84	10.46	7.92	5.93	2.90	1.17	0.77	-0.14
119	2.04	978.1	1370.0	1572.0	1783.0	0.40	0.61	0.82	91.71	67.36	14.49	9.86	4.22	2.25	1.05	0.77	-0.04
128	2.44	634.1	1001.0	1256.0	1589.0	0.58	0.98	1.51	90.71	52.09	26.17	12.44	4.53	2.74	1.17	0.85	0.55
136	3.61	909.9	1278.0	1557.0	1793.0	0.40	0.71	0.97	93.04	68.79	17.41	6.84	2.94	2.20	1.10	0.73	0.10
160	2.29	1174.0	1505.0	1671.0	1831.0	0.28	0.42	0.56	93.86	80.93	9.45	3.47	2.68	1.83	1.04	0.59	-0.40
174	4.25	809.0	1118.0	1312.0	1567.0	0.38	0.62	0.94	89.98	63.35	17.56	9.07	4.85	2.79	1.54	0.84	0.18
190	2.47	992.8	1250.0	1379.0	1546.0	0.26	0.39	0.56	92.57	73.74	12.90	5.93	3.20	2.29	1.20	0.75	-0.29

GE - CDS2

Depth	%L.O.I	P_n (μm)				$\%P_nM$ Index			%Sand	% Size Fraction							Skewness
(cm)		50	70	80	90	50 - 70	50 - 80	50 - 90		2000 - 600	600 - 212	212 - 63	20 - 63	6 - 20	2 - 6	0.04 - 2	
4	14.68	44.6	121.5	193.9	416.2	1.72	3.34	8.33	43.23	7.63	10.73	24.88	22.35	18.92	9.48	6.01	2.700
14	8.73	68.5	179.6	415.8	923.8	1.62	5.07	12.49	51.66	17.50	9.81	24.35	20.73	17.40	8.33	1.89	1.830
18	8.50	35.7	106.3	178.1	405.0	1.98	3.99	10.35	39.59	8.12	8.77	22.70	21.79	21.73	11.82	5.07	2.810
22	8.60	37.2	125.8	249.2	760.1	2.38	5.70	19.45	40.78	13.16	8.85	18.77	21.37	20.27	9.67	7.91	2.520
32	7.87	49.2	176.0	464.1	1015.0	2.58	8.43	19.63	45.42	17.95	9.38	18.09	23.49	17.67	7.32	6.11	2.010
47	11.74	118.5	310.0	661.5	1050.0	1.62	4.58	7.86	67.36	21.77	14.36	31.23	20.64	6.94	2.47	2.60	1.720
57	12.22	185.5	867.7	1179.0	1544.0	3.68	5.36	7.32	72.49	38.50	9.89	24.11	17.89	5.60	1.96	2.07	0.861
70	10.38	350.8	872.0	1027.0	1171.0	1.49	1.93	2.34	75.33	42.74	13.48	19.11	14.84	5.76	2.12	1.95	0.392
99	7.01	1310.0	1695.0	1805.0	1904.0	0.29	0.38	0.45	91.52	73.12	8.61	9.79	5.05	1.89	0.77	0.77	-0.420
110	8.18	699.0	1248.0	1500.0	1750.0	0.79	1.15	1.50	83.96	53.05	12.50	18.41	10.11	3.40	1.27	1.27	0.318
126	4.05	722.5	1196.0	1446.0	1713.0	0.66	1.00	1.37	83.22	54.60	13.20	15.42	10.62	3.68	1.25	1.23	0.312
153	7.65	444.0	1112.0	1402.0	1694.0	1.50	2.16	2.82	76.71	46.38	10.07	20.27	14.85	4.94	1.74	1.75	0.536
168	6.85	167.1	783.0	1117.0	1518.0	3.69	5.68	8.08	70.66	35.75	11.28	23.63	18.64	6.23	2.31	2.15	0.976
179	4.64	749.8	1159.0	1403.0	1681.0	0.55	0.87	1.24	84.79	57.43	15.95	11.42	8.68	3.79	1.50	1.24	0.281
193	5.94	739.9	1094.0	1322.0	1614.0	0.48	0.79	1.18	86.89	57.79	15.12	13.98	7.78	3.04	1.18	1.11	0.316
206	4.17	1096.0	1415.0	1589.0	1782.0	0.29	0.45	0.63	91.15	76.56	8.21	6.38	4.71	2.43	0.90	0.81	-0.310
222	5.80	1252.0	1561.0	1705.0	1848.0	0.25	0.36	0.48	91.91	80.60	5.80	5.50	4.37	2.15	0.85	0.73	-0.564
234	6.61	925.5	1290.0	1486.0	1716.0	0.39	0.61	0.85	88.14	65.71	12.44	10.00	6.15	3.25	1.35	1.12	0.003

GE - CDS3

Depth	%L.O.I	P_n (µm)				%P_nM Index			%Sand	% Size Fraction							Skewness
(cm)		50	70	80	90	50 - 70	50 - 80	50 - 90		2000 - 600	600 - 212	212 - 63	20 - 63	6 - 20	2 - 6	0.04 - 2	
4	11.08	52.5	162.2	314.7	869.9	2.09	4.99	15.56	46.83	14.98	10.34	21.50	20.31	18.42	8.16	6.28	2.25
14	9.28	43.2	133.7	221.2	533.7	2.10	4.13	11.37	43.54	9.04	11.70	22.80	20.27	20.83	9.05	6.31	2.59
20	9.20	162.2	727.9	1021.0	1394.0	3.49	5.29	7.59	61.06	34.10	12.50	14.46	15.61	13.59	5.51	4.23	1.02
31	9.29	639.7	1076.0	1320.0	1613.0	0.68	1.06	1.52	83.59	51.51	14.12	17.96	9.84	3.92	1.48	1.17	0.44
40	12.60	363.3	889.8	1188.0	1554.0	1.45	2.27	3.28	82.29	41.28	17.37	23.64	11.15	3.75	1.47	1.33	0.79
52	9.62	158.1	623.9	900.1	1296.0	2.95	4.69	7.20	65.97	30.86	14.93	20.18	20.76	7.99	2.83	2.44	1.21
59	7.53	181.8	604.8	867.4	1240.0	2.33	3.77	5.82	68.01	30.18	17.31	20.52	19.48	7.13	2.35	3.03	1.22
71	4.53	1122.0	1472.0	1650.0	1822.0	0.31	0.47	0.62	91.37	77.76	7.92	5.69	4.92	2.22	0.80	0.69	-0.33
84	3.29	831.6	1184.0	1399.0	1661.0	0.42	0.68	1.00	88.25	63.16	15.14	9.95	7.05	2.71	1.04	0.95	0.15
96	3.87	732.2	1146.0	1403.0	1689.0	0.57	0.92	1.31	86.19	56.77	17.40	12.01	8.26	3.20	1.20	1.15	0.32
105	3.27	780.9	1175.0	1420.0	1696.0	0.50	0.82	1.17	88.45	60.09	17.03	11.33	6.79	2.69	1.05	1.02	0.25
117	4.03	842.3	1232.0	1456.0	1710.0	0.46	0.73	1.03	87.14	62.22	14.54	10.38	7.66	3.03	1.09	1.09	0.14
128	5.17	116.2	517.4	898.8	1333.0	3.45	6.73	10.47	63.50	28.21	11.53	23.76	22.04	8.73	2.85	2.88	1.32
139	5.84	332.2	1037.0	1331.0	1643.0	2.12	3.01	3.95	74.41	44.22	9.91	20.28	16.50	5.30	1.84	1.95	0.62
146	4.76	98.8	169.7	232.1	407.7	0.72	1.35	3.12	65.73	8.01	14.61	43.12	23.38	6.44	1.97	2.47	3.04
158	7.42	64.7	121.3	175.9	313.1	0.87	1.72	3.84	50.89	6.81	9.12	34.96	30.59	11.30	3.50	3.71	3.61
168	6.86	80.6	159.9	260.2	744.0	0.98	2.23	8.23	58.00	12.46	11.22	34.32	27.04	8.88	2.91	3.17	2.58
209	6.28	696.0	1228.0	1473.0	1728.0	0.76	1.12	1.48	83.53	52.99	12.80	17.74	9.89	3.79	1.39	1.40	0.32
223	5.66	875.0	1288.0	1504.0	1741.0	0.47	0.72	0.99	85.63	61.21	11.30	13.13	8.15	3.62	1.33	1.27	0.11
235	6.09	754.3	1265.0	1503.0	1745.0	0.68	0.99	1.31	78.69	54.82	9.42	14.45	12.64	5.14	1.77	1.76	0.25

M - DCS1

Depth	%L.O.I	P_n (µm)				$\%P_nM$ Index			%Sand	% Size Fraction							Skewness
(cm)		50	70	80	90	50 - 70	50 - 80	50 - 90		2000 - 600	600 - 212	212 - 63	63 - 20	20 - 6	6 - 2	2 - 0.04	
9	10.01	34.9	139.5	190.3	256.1	3.00	4.45	6.34	43.4	3.72	12.35	27.33	13.34	18.55	14.01	10.70	2.74
15	7.77	28.0	135.7	192.3	261.0	3.85	5.87	8.32	41.54	3.92	12.67	24.95	12.58	19.16	15.30	11.43	2.68
28	4.61	77.6	209.5	312.8	753.5	1.70	3.03	8.71	52.3	14.39	15.23	22.68	11.36	14.32	12.19	9.82	1.79
39	4.21	213.5	818.8	1175.0	1549.0	2.84	4.50	6.26	64.55	35.77	14.37	14.41	8.60	10.73	8.89	7.23	0.92
50	4.44	78.6	233.6	364.5	882.3	1.97	3.64	10.22	52.69	16.27	16.45	19.97	13.52	15.01	10.41	8.37	1.69
58	4.68	34.8	122.2	181.2	242.0	2.51	4.20	5.95	41.157	*0.91*	*13.68*	*26.57*	*17.42*	*18.87*	*12.48*	10.07	2.52
66	4.69	32.6	116.0	177.2	235.2	2.56	4.44	6.22	40.07	*0.00*	*13.80*	*26.27*	*17.83*	*19.30*	*12.48*	10.32	1.10
72	4.96	36.6	143.2	195.2	259.9	2.91	4.34	6.10	43.76	4.95	11.90	26.91	13.78	17.66	13.64	11.16	2.67
83	4.81	33.0	149.9	216.6	292.8	3.55	5.57	7.89	42.45	3.53	17.19	21.73	14.18	18.29	13.59	11.48	2.40
97	4.97	36.6	159.3	240.4	357.1	3.35	5.56	8.75	43.19	6.37	17.19	19.63	14.94	17.87	13.13	10.85	2.11
106	4.23	114.6	323.7	808.2	1085.0	1.82	6.05	8.47	58.12	25.54	10.95	21.63	10.98	13.45	9.87	7.57	1.32
115	4.11	86.4	205.0	364.4	863.7	1.37	3.22	8.99	54.51	16.26	12.81	25.44	12.75	14.40	10.48	7.85	1.71
126	3.27	138.6	392.5	843.4	1246.0	1.83	5.09	7.99	60.8	26.53	13.33	20.94	11.54	12.60	8.50	6.56	1.38
133	3.09	37.4	142.1	206.0	288.2	2.80	4.51	6.71	42.62	3.71	15.38	23.53	16.89	18.73	12.44	9.32	2.51
143	3.03	46.2	141.6	199.7	315.7	2.06	3.32	5.83	45.38	6.23	12.02	27.13	17.40	17.65	10.76	8.80	2.39
152	3.50	30.0	106.1	177.1	268.8	2.54	4.91	7.97	38.08	3.83	11.78	*22.47*	*19.04*	*20.48*	*12.25*	10.16	2.70
166	2.74	456.5	1087.0	1387.0	1692.0	1.38	2.04	2.71	73.97	*46.84*	*12.99*	*14.14*	*8.20*	*8.44*	*5.00*	4.39	0.53
175	2.41	419.4	988.0	1247.0	1568.0	1.36	1.97	2.74	73.55	45.61	13.96	13.98	8.73	8.29	5.09	4.34	0.60
188	3.09	195.5	918.4	1391.0	1716.0	3.70	6.12	7.78	66.07	37.06	11.31	17.70	10.91	10.81	6.60	5.61	0.83
199	3.74	158.0	678.1	1026.0	1499.0	3.29	5.49	8.49	63.36	31.82	12.00	19.54	12.43	11.41	6.93	5.88	1.15
209	3.47	155.0	451.5	835.7	1178.0	1.91	4.39	6.60	62.18	27.13	16.12	18.93	12.41	11.72	7.44	6.25	1.32
214	3.21	508.2	1042.0	1312.0	1627.0	1.05	1.58	2.20	73.53	47.56	13.99	11.98	8.08	8.77	5.32	4.30	0.53
224	3.47	97.4	256.4	684.7	1173.0	1.63	6.03	11.05	56.11	21.76	12.18	22.17	15.13	13.87	8.24	6.65	1.71
233	3.44	91.4	258.8	581.7	904.5	1.83	5.37	8.90	56.09	19.54	14.73	21.82	16.19	13.30	7.96	6.47	1.44
253	15.59	58.1	149.0	223.4	407.4	1.56	2.85	6.01	48.44	7.59	13.60	27.25	19.07	16.03	9.22	7.24	2.40
272	6.02	79.2	161.8	215.5	306.0	1.04	1.72	2.87	55.08	5.03	15.52	34.53	19.00	12.49	7.18	6.26	2.58
277	6.78	38.1	110.1	175.9	271.5	1.89	3.61	6.12	40.8	3.91	11.71	25.18	20.34	18.29	11.22	9.36	2.82
287	7.84	78.4	202.7	330.7	1052.0	1.58	3.22	12.41	53.6	17.12	11.66	24.82	16.45	14.21	8.50	7.23	2.07
295	5.15	57.4	152.0	210.2	327.6	1.65	2.66	4.71	48.38	8.31	11.40	28.67	17.94	15.79	9.68	8.20	2.71
302	2.95	51.8	145.9	211.5	288.7	1.82	3.08	4.57	46.54	3.04	16.88	26.62	18.96	16.28	9.90	8.32	2.50
309	2.79	37.9	93.4	133.8	195.2	1.46	2.53	4.14	39.502	0.61	7.52	31.37	22.06	18.02	11.39	9.02	3.15
321	2.55	39.9	117.5	182.7	279.9	1.94	3.58	6.01	41.82	5.21	11.02	25.59	20.14	18.10	11.02	8.92	2.66
330	2.90	43.5	110.6	160.5	220.0	1.55	2.69	4.06	42.496	0.39	10.70	31.41	21.33	17.23	10.17	8.77	2.19
345	5.46	40.3	123.1	185.1	248.5	2.06	3.60	5.17	42.35	0.00	15.51	26.84	19.28	17.90	11.01	9.46	1.12
356	23.48	60.5	169.4	234.0	404.9	1.80	2.87	5.69	49.35	8.77	14.41	26.17	18.39	16.42	8.92	6.92	2.48
364	27.27	38.0	118.5	192.0	284.3	2.12	4.06	6.49	41.17	3.04	14.46	23.67	20.53	19.05	10.74	8.51	2.58
378	1.35	156.6	447.0	894.4	1304.0	1.85	4.71	7.33	65.22	27.50	15.59	22.13	14.96	9.58	5.28	4.96	1.33
385	1.48	75.1	208.7	311.1	682.5	1.78	3.14	8.08	53.09	11.70	17.91	23.48	18.62	13.28	7.72	7.29	1.97

M - DCS2

Depth	%L.O.I	P_n (µm)				%P_nM Index			%Sand	% Size Fraction							Skewness
(cm)		50	70	80	90	50 - 70	50 - 80	50 - 90		2000 - 600	600 - 212	212 - 63	63 - 20	20 - 6	6 - 2	2 - 0.04	
3	6.20	34.7	156.9	246.9	511.20	3.53	6.12	13.75	42.62	8.80	14.83	18.99	14.82	17.69	13.37	11.49	1.95
12	4.30	656.8	1144.0	1394.0	1672.00	0.74	1.12	1.55	71.26	51.66	11.06	8.54	6.64	9.12	7.44	5.55	0.37
20	4.58	56.7	215.1	330.5	639.30	2.79	4.83	10.28	48.82	11.31	19.00	18.51	12.71	16.04	12.76	9.67	1.50
38	5.09	14.5	46.8	87.5	151.00	2.22	5.02	9.39	25.308	0.00	0.75	24.56	18.80	23.84	18.65	13.40	1.43
52	4.38	17.3	65.0	128.7	208.00	2.76	6.45	11.04	30.44	0.00	9.28	21.16	17.04	22.89	17.60	12.04	1.36
62	4.89	20.7	92.6	179.7	824.10	3.49	7.70	38.91	34.45	13.47	4.33	16.65	16.13	23.11	16.02	10.30	2.17
74	5.07	18.1	73.4	137.9	232.60	3.05	6.62	11.85	31.94	5.14	6.31	20.49	16.36	20.89	14.02	16.80	2.97
88	4.25	25.2	116.8	221.6	951.30	3.63	7.79	36.75	37.86	15.68	4.94	17.24	16.01	21.34	14.82	9.96	1.93
97	5.29	19.9	81.7	164.8	238.60	3.11	7.29	11.00	32.91	1.17	12.17	19.57	16.96	23.54	15.68	10.91	2.87
118	4.33	23.6	104.4	178.7	248.50	3.43	6.59	9.55	35.5	1.53	13.35	20.62	17.50	22.07	14.73	10.21	2.77
130	4.72	149.4	243.6	291.0	351.20	0.63	0.95	1.35	63.8	1.19	35.79	26.82	9.96	12.51	7.98	5.75	1.34
138	5.51	16.5	62.6	152.8	406.40	2.80	8.27	23.66	29.93	7.96	7.09	14.88	16.12	25.98	17.08	10.88	2.40
152	5.06	18.4	43.6	87.3	173.70	1.37	3.75	8.46	24.17	2.73	4.30	17.14	23.61	27.57	14.85	9.80	4.00
162	5.24	18.6	53.0	107.7	197.80	1.84	4.78	9.62	27.35	2.28	6.53	18.54	21.09	25.15	15.47	10.92	3.55
170	4.06	40.2	154.0	539.8	995.40	2.83	12.42	23.75	43.33	19.41	6.08	17.84	17.96	18.21	11.52	8.97	1.57
181	3.82	51.1	175.3	542.3	992.20	2.43	9.60	18.40	47.17	19.50	7.03	20.64	15.82	17.22	11.22	8.57	1.57
194	3.24	138.0	279.7	412.7	704.50	1.03	1.99	4.11	64.51	13.34	25.01	26.16	11.56	10.97	7.02	5.94	2.04
213	3.08	179.4	366.9	589.9	856.40	1.05	2.29	3.77	68.45	19.61	25.88	22.96	10.74	9.49	6.05	5.28	1.45
235	1.95	827.9	1263.0	1489.0	1733.00	0.53	0.80	1.09	83.68	59.93	15.23	8.52	5.30	5.12	3.24	2.66	0.15
247	1.99	443.2	858.1	1102.0	1501.00	0.94	1.49	2.39	76.44	43.18	19.77	13.49	7.97	7.21	4.59	3.79	0.77

HF - GFS1

Depth	%L.O.I	P_n (µm)				%P_nM Index			%Sand	% Size Fraction							Skewness
(cm)		50	70	80	90	50 - 70	50 - 80	50 - 90		2000 - 600	600 - 212	212 - 63	20 - 63	6 - 20	2 - 6	0.04 - 2	
17	6.12	12.3	27.3	42.8	81.5	1.21	2.47	5.60	16.56	0.00	1.18	15.38	33.85	23.53	13.22	12.83	2.63
28	72.68	36.3	96.7	159.0	267.8	1.67	3.38	6.38	61.98	9.22	19.49	33.26	19.93	10.83	4.45	2.81	2.07
37	4.98	369.3	1126.0	1384.0	1661.0	2.05	2.75	3.50	27.60	3.66	4.94	19.00	27.05	21.31	12.52	11.52	3.91
44	8.10	35.7	81.2	128.0	234.1	1.27	2.58	5.55	25.10	4.80	3.49	16.81	26.98	21.44	13.47	13.00	3.83
53	60.09	97.3	222.0	350.5	649.7	1.28	2.60	5.67	60.03	11.26	19.80	28.98	20.75	11.71	4.65	2.86	2.36
60	14.71	22.0	50.9	81.3	171.5	1.31	2.69	6.79	36.20	4.88	6.31	25.01	25.99	18.01	10.28	9.53	3.42
66	3.40	24.5	56.6	92.9	184.3	1.31	2.78	6.51	67.65	46.10	8.90	12.65	12.04	9.34	5.70	5.27	0.50
77	7.86	102.3	202.9	303.1	563.7	0.98	1.96	4.51	38.44	3.76	10.28	24.40	24.10	18.42	9.90	9.14	3.05
88	8.03	20.3	39.6	55.4	87.5	0.95	1.72	3.30	13.36	0.00	1.66	11.71	24.60	28.66	18.02	15.36	3.12

M - HBS1

Depth	%L.O.I	P_n (μm)				$\%P_nM$ Index			%Sand	% Size Fraction							Skewness
(cm)		50	70	80	90	50 - **70**	50 - **80**	50 - **90**		2000 - 600	600 - 212	212 - 63	63 - 20	20 - 6	6 - 2	2 - 0.04	
5	6.42	32.5	139.3	234.7	472.6	3.29	6.22	13.54	41.83	7.73	14.27	19.83	14.57	18.88	14.16	10.56	1.99
13	4.46	229.0	941.5	1342.0	1682.0	3.11	4.86	6.34	65.55	38.37	12.98	14.20	8.29	11.28	8.53	6.36	0.79
25	4.40	97.5	309.1	682.8	1113.0	2.17	6.00	10.41	54.8	21.92	15.81	17.07	10.73	14.88	11.25	8.34	1.68
34	4.55	119.9	414.8	788.2	1189.0	2.46	5.57	8.92	56.38	25.33	15.90	15.15	10.36	14.44	10.92	7.91	1.39
41	4.82	1102.0	1324.0	1430.0	1554.0	0.20	0.30	0.41	88.24	78.73	7.25	2.26	2.81	3.94	2.96	2.06	-0.67
50	4.31	941.9	1288.0	1469.0	1687.0	0.37	0.56	0.79	83.59	65.07	10.19	8.33	7.16	4.74	2.45	2.06	-0.04
59	3.87	251.9	925.5	1197.0	1523.0	2.67	3.75	5.05	66.43	41.63	9.83	14.97	20.43	7.28	2.83	3.02	0.73
67	5.36	359.5	894.2	1127.0	1423.0	1.49	2.13	2.96	70.17	42.29	15.69	12.19	7.93	9.82	7.10	4.98	0.68
79	4.90	491.2	994.9	1247.0	1552.0	1.03	1.54	2.16	73.15	46.47	15.16	11.52	8.95	8.35	5.48	4.07	0.56
92	4.11	339.9	996.9	1250.0	1548.0	1.93	2.68	3.55	68.86	43.70	12.83	12.33	7.91	10.21	7.63	5.38	0.62
97	3.53	680.3	1174.0	1417.0	1684.0	0.73	1.08	1.48	77.96	52.76	14.40	10.80	6.56	6.74	4.93	3.81	0.34
117	3.29	954.4	1375.0	1575.0	1781.0	0.44	0.65	0.87	85.17	64.80	12.47	7.90	4.76	4.72	3.38	1.97	-0.03
124	2.59	923.8	1306.0	1505.0	1732.0	0.41	0.63	0.87	85.28	65.26	12.68	7.34	5.00	4.55	2.86	2.31	0.00
136	3.57	691.7	1187.0	1440.0	1707.0	0.72	1.08	1.47	76.5	53.04	12.46	11.00	7.13	7.28	5.14	3.95	0.33
146	3.30	517.1	1018.0	1266.0	1577.0	0.97	1.45	2.05	73.48	47.57	13.83	12.08	7.67	8.29	5.96	4.60	0.53
163	3.07	630.5	1082.0	1345.0	1643.0	0.72	1.13	1.61	79.3	51.32	17.49	10.49	5.87	6.55	4.78	3.49	0.43
170	3.58	805.4	1224.0	1450.0	1704.0	0.52	0.80	1.12	81.64	59.36	14.32	7.96	4.77	6.00	4.42	3.18	0.17
179	3.82	796.2	1233.0	1467.0	1720.0	0.55	0.84	1.16	80.92	58.18	13.79	8.95	5.42	6.09	4.39	3.20	0.20
206	2.58	929.4	1289.0	1526.0	1762.0	0.39	0.64	0.90	89.98	68.56	15.20	6.22	2.54	3.19	2.51	1.78	0.02
221	2.18	1047.0	1403.0	1630.0	1819.0	0.34	0.56	0.74	89.89	73.35	12.39	4.15	2.42	3.25	2.66	1.78	-0.17
236	2.37	439.6	910.9	1152.0	1475.0	1.07	1.62	2.36	75.09	44.10	17.31	13.68	7.01	7.63	5.97	4.30	0.67

LB - HHS2

Depth	%L.O.I	Pn (mm)				%PnM Index			%Sand	% Size Fraction							Skewness
(cm)		50	70	80	90	50 - 70	50 - 80	50 - 90		2000 - 600	600 - 212	212 - 63	20 - 63	6 - 20	2 - 6	0.04 - 2	
5	9.20	39.8	151.7	221.6	347.3	2.81	4.57	7.72	45.05	7.73	13.42	23.90	13.09	17.59	13.48	10.80	2.62
12	4.49	62.0	161.2	213.3	337.8	1.60	2.44	4.45	49.78	6.79	13.41	29.57	13.39	15.44	11.61	9.78	2.49
21	3.86	83.9	223.3	352.0	741.0	1.66	3.20	7.84	53.19	13.86	17.41	21.91	12.28	14.00	10.79	9.75	1.87
35	4.51	136.6	377.2	650.4	924.7	1.76	3.76	5.77	59.64	21.95	19.08	18.61	11.68	11.56	8.86	8.25	1.39
45	3.90	157.3	480.4	781.6	1121.0	2.05	3.97	6.13	62.01	26.40	17.56	18.04	10.50	10.93	8.62	7.95	1.33
58	6.06	404.6	1026.0	1290.0	1583.0	1.54	2.19	2.91	68.30	44.54	12.85	10.92	10.11	8.97	6.56	6.05	0.58
68	4.61	218.2	663.7	914.9	1451.0	2.04	3.19	5.65	63.70	32.67	17.80	13.23	11.29	10.61	7.43	6.96	1.17
76	3.07	245.8	559.7	749.5	1001.0	1.28	2.05	3.07	69.44	27.95	25.69	15.80	10.43	8.92	5.76	5.45	0.38
83	3.27	407.8	736.8	911.5	1160.0	0.81	1.24	1.84	75.91	38.38	26.10	11.43	8.52	6.99	4.40	4.18	0.82
92	2.70	130.4	251.9	388.4	744.6	0.93	1.98	4.71	63.41	14.09	21.36	27.96	12.69	10.31	7.00	6.59	2.18
100	4.27	41.2	167.7	299.1	746.9	3.07	6.25	17.12	44.77	13.30	12.70	18.76	14.68	15.55	12.59	12.40	2.43
108	3.46	164.1	532.8	800.6	1169.0	2.25	3.88	6.12	63.31	27.82	17.30	18.20	10.80	9.69	7.91	8.28	1.39
126	2.83	214.7	581.6	834.3	1159.0	1.71	2.89	4.40	67.23	29.25	20.98	16.99	10.34	8.97	6.65	6.82	1.11
137	3.16	420.5	800.3	997.7	1264.0	0.90	1.37	2.01	74.54	41.13	20.94	12.47	8.90	6.97	4.71	4.87	0.70
146	3.27	373.6	766.1	986.3	1283.0	1.05	1.64	2.43	75.63	38.17	23.95	13.51	8.09	6.76	4.71	4.81	0.84
161	3.28	294.2	637.8	843.0	1152.0	1.17	1.87	2.92	71.90	31.99	25.83	14.08	9.16	7.77	5.40	5.76	1.07
169	3.55	700.6	1052.0	1246.0	1496.0	0.50	0.78	1.14	79.57	54.68	15.78	9.12	7.02	5.76	3.84	3.80	0.30
180	3.86	623.3	963.7	1184.0	1475.0	0.55	0.90	1.37	78.93	51.30	18.66	8.96	6.99	6.02	4.02	4.04	0.47
186	3.97	472.6	874.0	1121.0	1473.0	0.85	1.37	2.12	77.56	44.30	20.84	12.42	7.42	6.28	4.27	4.47	0.70
194	3.66	559.9	906.9	1094.0	1348.0	0.62	0.95	1.41	75.48	48.04	18.87	8.57	7.89	7.10	4.74	4.80	0.50
205	4.16	384.7	925.0	1205.0	1563.0	1.40	2.13	3.06	68.62	43.96	12.77	11.90	11.04	9.14	5.84	5.35	0.68

LB - HHS3

Depth	%L.O.I	P_n (µm)				%P_nM Index			%Sand	% Size Fraction							Skewness
(cm)		50	70	80	90	50 - **70**	50 - **80**	50 - **90**		2000 - 600	600 - 212	212 - 63	20 - 63	6 - 20	2 - 6	0.04 - 2	
2	6.93	72.3	182.8	271.6	672.4	1.53	2.76	8.30	51.91	11.33	14.57	26.02	14.49	14.92	10.06	8.61	2.72
11	5.65	62.7	168.2	248.6	672.7	1.68	2.97	9.74	49.91	11.36	12.42	26.13	16.84	15.60	9.62	8.02	2.61
18	4.73	76.3	189.4	279.6	648.5	1.48	2.67	7.50	52.49	11.06	15.66	25.77	14.95	14.75	9.54	8.27	2.72
30	3.98	130.1	299.3	531.7	851.0	1.30	3.09	5.54	59.02	18.14	20.77	20.11	13.02	12.43	8.05	7.48	1.50
36	3.50	150.1	446.4	713.4	972.8	1.97	3.75	5.48	58.98	24.44	20.06	14.48	13.24	13.27	7.90	6.61	1.35
42	3.13	152.1	322.8	506.2	828.1	1.12	2.33	4.44	61.21	16.91	25.02	19.28	11.98	12.09	7.94	6.79	1.54
51	3.12	250.3	633.2	873.8	1152.0	1.53	2.49	3.60	68.46	31.33	21.88	15.24	11.50	9.50	5.68	4.86	0.97
57	3.39	151.9	460.1	781.1	1165.0	2.03	4.14	6.67	61.51	25.81	17.57	18.13	13.51	11.84	7.08	6.06	1.39
64	3.23	60.9	153.0	204.2	291.9	1.51	2.35	3.79	49.53	5.78	12.93	30.82	14.97	15.15	10.95	9.40	2.91
70	3.96	41.6	116.1	159.9	217.6	1.79	2.84	4.23	43.28	0.00	10.76	32.52	17.93	16.54	11.75	10.51	1.12
77	4.74	24.8	77.2	127.0	196.3	2.11	4.12	6.91	33.60	0.00	8.37	25.22	20.37	19.92	13.99	12.13	1.62
84	4.18	39.9	132.1	193.5	301.2	2.31	3.85	6.55	43.22	4.24	13.33	25.65	17.44	17.15	12.00	10.19	2.90
91	4.47	35.2	112.0	164.4	233.1	2.18	3.67	5.62	40.70	0.00	12.62	28.08	18.43	17.96	12.66	10.24	1.27
97	3.33	104.6	189.7	249.2	397.0	0.81	1.38	2.80	58.96	7.40	18.29	33.28	12.55	11.83	8.86	7.80	3.10
109	3.04	93.5	174.9	224.4	306.4	0.87	1.40	2.28	56.59	4.71	17.44	34.45	13.52	12.42	9.05	8.41	2.40
111	3.98	134.6	254.9	376.4	691.1	0.89	1.80	4.13	62.89	12.46	23.34	27.09	12.92	10.79	7.12	6.28	2.18
119	2.71	103.8	196.0	264.8	608.5	0.89	1.55	4.86	58.05	10.12	17.03	30.91	14.09	12.33	8.49	7.03	2.95
125	2.13	138.4	230.6	293.8	432.2	0.67	1.12	2.12	65.42	5.65	28.01	31.77	12.19	9.89	6.71	5.80	1.69
135	3.12	66.5	164.1	222.4	324.5	1.47	2.35	3.88	50.73	7.00	14.56	29.17	14.77	14.59	10.59	9.32	2.53
139	2.88	79.5	176.2	235.6	354.7	1.22	1.97	3.46	53.30	6.50	17.07	29.73	13.88	13.84	10.20	8.78	3.72

HF - LGS1

Depth	%L.O.I	P_n (µm)				%P_nM Index			%Sand	% Size Fraction							Skewness
(cm)		50	70	80	90	50 - **70**	50 - **80**	50 - **90**		2000 - 600	600 - 212	212 - 63	20 - 63	6 - 20	2 - 6	0.04 - 2	
6	9.76	161.5	605.3	889.5	1257.0	2.75	4.51	6.78	60.89	30.16	15.73	14.99	10.73	11.79	9.17	7.42	1.20
14	4.01	169.1	622.9	913.7	1302.0	2.68	4.40	6.70	63.37	30.74	15.63	17.00	11.93	10.75	7.74	6.21	1.18
25	2.87	564.1	1056.0	1320.0	1624.0	0.87	1.34	1.88	71.79	48.90	12.42	10.47	8.80	8.50	5.97	4.94	0.48
37	2.02	551.9	966.3	1198.0	1508.0	0.75	1.17	1.73	75.70	48.07	16.78	10.86	7.15	7.30	5.34	4.51	0.54
49.5	1.95	112.0	284.8	524.7	858.2	1.54	3.68	6.66	59.22	17.91	18.63	22.68	13.92	11.59	8.35	6.92	1.94
58	1.83	135.5	456.5	805.7	1167.0	2.37	4.95	7.61	62.79	26.50	14.95	21.34	13.44	9.80	7.42	6.55	1.39
67	3.28	791.2	1209.0	1431.0	1688.0	0.53	0.81	1.13	76.41	58.07	11.52	6.82	6.32	7.30	5.41	4.57	0.19
78	3.22	406.6	987.6	1274.0	1603.0	1.43	2.13	2.94	72.18	44.39	14.48	13.31	8.27	8.15	6.18	5.22	0.63
87	3.11	223.2	784.0	1070.0	1446.0	2.51	3.79	5.48	64.80	36.59	14.05	14.16	10.31	10.49	7.79	6.61	0.93
96	3.09	329.8	958.1	1271.0	1611.0	1.91	2.85	3.88	64.37	42.59	11.95	9.83	10.73	10.99	7.51	6.40	0.68
107	2.46	315.9	704.5	917.8	1241.0	1.23	1.91	2.93	78.41	35.10	25.08	18.23	7.55	6.03	4.29	3.72	1.03
119	2.34	101.5	559.6	883.1	1287.0	4.51	7.70	11.68	55.46	28.95	12.36	14.16	13.15	13.55	9.86	7.98	1.27
131	2.89	94.5	438.0	768.2	1117.0	3.64	7.13	10.83	55.15	25.71	13.74	15.70	16.57	14.14	7.84	6.30	1.45
144	4.09	38.6	109.7	221.2	812.8	1.85	4.74	20.08	40.12	13.38	7.07	19.67	22.54	18.40	10.55	8.39	2.52
152	2.69	369.1	1026.0	1317.0	1628.0	1.78	2.57	3.41	67.04	44.38	10.15	12.51	13.37	9.69	5.41	4.49	0.61
159	4.82	146.3	864.2	1183.0	1560.0	4.91	7.09	9.66	57.20	38.49	9.03	9.69	14.76	12.76	7.79	7.49	0.84
165	2.34	843.8	1363.0	1578.0	1789.0	0.62	0.87	1.12	69.13	56.85	6.54	5.74	8.80	9.77	6.48	5.82	0.13
174	1.40	835.3	1299.0	1533.0	1765.0	0.56	0.84	1.11	72.57	59.11	7.49	5.97	7.89	8.54	5.81	5.19	0.13

HF - NGS1

Depth	%L.O.I	P_n (µm)				%P_nM Index			%Sand	% Size Fraction							Skewness
(cm)		50	70	80	90	50 - **70**	50 - **80**	50 - **90**		2000 - 600	600 - 212	212 - 63	20 - 63	6 - 20	2 - 6	0.04 - 2	
9	10.95	21.3	61.3	110.0	230.5	1.88	4.17	9.83	29.49	5.06	5.78	18.65	21.63	20.43	15.11	13.34	3.34
18	5.44	23.9	67.1	120.5	294.2	1.80	4.04	11.30	31.15	7.22	5.44	18.49	22.16	19.76	14.36	12.57	3.03
29	2.27	80.3	287.0	671.4	1132.0	2.57	7.36	13.09	53.49	21.54	13.06	18.89	15.05	12.96	9.78	8.72	1.67
41	2.31	361.2	801.3	1067.0	1460.0	1.22	1.95	3.04	71.16	38.95	20.47	11.74	7.31	8.61	7.20	5.73	0.86
51	2.59	91.4	657.5	989.6	1440.0	6.19	9.83	14.75	52.87	31.69	11.61	9.57	15.32	14.88	8.91	8.02	1.24
57	2.16	733.8	1059.0	1276.0	1578.0	0.44	0.74	1.15	80.66	58.25	18.68	3.73	4.69	6.00	4.67	3.99	0.29
62	1.22	568.1	932.4	1185.0	1557.0	0.64	1.09	1.74	84.97	48.13	27.81	9.03	3.82	4.19	3.70	3.32	0.64
69	1.70	397.3	813.5	1086.0	1534.0	1.05	1.73	2.86	78.41	40.12	24.46	13.83	5.81	5.78	5.14	4.86	0.87
73	2.37	161.0	364.1	776.3	1312.0	1.26	3.82	7.15	70.88	24.53	17.83	28.52	12.61	6.66	4.62	5.23	1.55
78	2.22	673.0	1191.0	1477.0	1747.0	0.77	1.19	1.60	72.42	52.27	10.59	9.55	9.08	8.02	5.38	5.10	0.36
82	2.20	763.0	1268.0	1521.0	1764.0	0.66	0.99	1.31	68.48	55.17	8.31	4.99	7.34	10.82	7.03	6.32	0.23
86	1.30	874.3	1301.0	1532.0	1766.0	0.49	0.75	1.02	73.15	62.19	8.47	2.49	5.05	9.03	6.73	6.04	0.06
93	1.56	987.3	1342.0	1534.0	1752.0	0.36	0.55	0.77	77.68	69.37	6.46	1.85	4.66	7.20	5.54	4.92	-0.16
101	1.19	754.8	1210.0	1443.0	1700.0	0.60	0.91	1.25	69.17	55.23	7.04	6.91	7.92	8.81	7.69	6.41	0.25
106	2.10	78.0	323.3	831.9	1357.0	3.14	9.67	16.40	53.09	24.99	10.42	17.67	15.55	13.11	9.92	8.32	1.47
113	2.74	41.1	123.1	213.0	600.9	2.00	4.19	13.64	42.18	10.01	10.07	22.10	19.82	16.44	11.90	9.66	3.04
117	2.49	47.8	180.7	475.3	1011.0	2.78	8.95	20.16	45.66	18.29	9.52	17.85	17.74	15.28	11.33	9.99	1.88
127	2.89	29.6	91.9	177.9	503.0	2.11	5.02	16.01	36.07	9.00	8.56	18.52	21.51	18.60	12.22	11.60	2.55
145	1.67	240.5	875.8	1116.0	1402.0	2.64	3.64	4.83	60.64	40.31	10.76	9.57	10.10	11.48	9.34	8.45	0.73
160	2.39	31.9	139.6	427.6	961.4	3.37	12.40	29.12	39.78	17.65	7.75	14.38	17.50	16.80	13.47	12.46	2.00
175	2.79	394.0	918.5	1150.0	1431.0	1.33	1.92	2.63	62.63	43.26	12.58	6.80	8.24	11.44	8.94	8.74	0.62
196	2.40	122.3	417.6	773.3	1150.0	2.41	5.32	8.40	56.98	25.18	15.85	15.95	10.86	12.51	10.24	9.42	1.43
202	2.40	272.2	768.7	1016.0	1348.0	1.82	2.73	3.95	68.60	36.80	17.18	14.62	9.89	8.54	6.59	6.38	0.91
209	2.57	222.7	837.3	1113.0	1457.0	2.76	4.00	5.54	62.12	38.57	11.91	11.64	11.26	11.93	7.92	6.77	0.83
225	2.02	15.0	46.2	134.7	615.5	2.08	7.99	40.09	26.52	10.21	5.73	10.58	17.45	24.38	17.46	14.18	2.50
237	2.18	529.5	965.6	1185.0	1469.0	0.82	1.24	1.77	68.54	47.47	12.68	8.39	8.82	10.19	6.79	5.65	0.52
260	1.43	493.7	932.1	1156.0	1446.0	0.89	1.34	1.93	69.96	45.83	14.97	9.15	8.42	9.15	6.63	5.84	0.57
277	1.73	591.9	996.1	1235.0	1544.0	0.68	1.09	1.61	72.24	49.64	14.19	8.41	7.82	8.48	6.10	5.36	0.49

HF - TGS1

Depth	%L.O.I	P_n (µm)				%P_nM Index			%Sand	% Size Fraction							Skewness
(cm)		50	70	80	90	50 - 70	50 - 80	50 - 90		2000 - 600	600 - 212	212 - 63	63 - 20	20 - 6	6 - 2	2 - 0.04	
6	5.35	177.20	900.50	1228.00	1583.00	4.08	5.93	7.93	64.1	38.83	10.19	12.44	16.32	7.15	6.12	8.95	0.82
20	3.37	187.70	783.40	1115.00	1510.00	3.17	4.94	7.04	64.21	35.65	10.45	11.61	15.93	7.53	6.21	12.63	0.95
34	3.31	84.35	396.30	833.80	1312.00	3.70	8.89	14.55	54.09	26.07	13.47	14.78	17.37	9.61	8.05	10.65	1.43
41	3.51	38.60	149.50	397.30	1115.00	2.87	9.29	27.89	42.6	17.85	17.22	17.26	17.34	12.49	10.42	7.41	1.98
51	2.27	33.63	130.30	285.70	930.30	2.87	7.50	26.66	40.54	15.73	18.11	17.57	17.40	13.05	10.74	7.41	2.24
61	2.64	40.74	146.70	294.10	984.10	2.60	6.22	23.16	43.27	15.64	16.93	17.19	19.15	12.08	10.51	8.48	2.20
72	3.68	33.33	118.50	228.20	797.90	2.56	5.85	22.94	39.9	13.14	18.67	18.48	18.96	12.65	10.30	7.80	2.52
82	3.09	28.34	93.86	185.00	643.90	2.31	5.53	21.72	36.27	10.54	20.12	20.28	18.09	12.61	10.73	7.64	2.88
92	2.42	32.98	117.40	229.10	857.70	2.56	5.95	25.01	39.75	13.59	18.81	18.55	18.80	12.72	10.18	7.36	2.45
101	2.00	59.05	469.50	1003.00	1485.00	6.95	15.99	24.15	49.13	28.69	15.59	15.35	14.29	11.02	8.91	6.15	1.27
109	3.30	40.79	190.00	789.10	1374.00	3.66	18.35	32.68	43.72	23.03	17.54	16.92	14.83	12.23	9.59	5.86	1.59
115	2.72	30.32	108.30	242.30	929.20	2.57	6.99	29.65	38.14	14.91	19.26	18.96	16.89	12.84	10.80	6.34	2.31
122	3.66	24.11	60.61	110.80	268.40	1.51	3.60	10.13	29.21	6.81	22.50	24.91	17.14	12.98	10.39	5.26	3.16
131	4.15	23.13	75.69	155.20	667.20	2.27	5.71	27.85	32.86	10.69	21.83	19.89	16.68	13.85	11.57	5.49	2.91
138	13.10	16.63	36.14	57.31	120.50	1.17	2.45	6.25	18.28	2.77	26.44	27.05	12.80	14.96	13.29	2.71	4.76
144	6.07	24.91	51.41	73.75	115.20	1.06	1.96	3.62	24.2	0.00	21.44	31.16	22.58	12.17	11.03	1.62	2.03
149	6.30	30.70	58.80	80.67	118.50	0.92	1.63	2.86	27.72	0.00	18.62	32.77	26.55	10.78	10.11	1.17	1.57
155	7.71	26.59	53.55	76.30	122.70	1.01	1.87	3.61	25.22	0.00	20.16	31.76	22.65	11.62	11.24	2.57	2.06
161	12.55	28.43	61.64	90.93	150.00	1.17	2.20	4.28	29.38	1.27	19.46	28.25	24.48	12.26	10.66	3.63	5.32
170	4.09	15.61	38.57	64.50	121.40	1.47	3.13	6.78	20.4	0.00	24.61	24.18	17.86	16.65	14.16	2.54	2.27
178	2.04	21.08	50.41	77.85	132.60	1.39	2.69	5.29	24.72	0.00	21.34	26.38	21.44	13.89	13.68	3.28	2.14
192	3.04	23.19	53.63	81.53	138.00	1.31	2.52	4.95	25.99	0.00	21.02	27.20	22.27	13.30	12.49	3.72	2.09
201	2.60	21.49	50.52	80.22	150.60	1.35	2.73	6.01	24.96	3.17	21.63	26.58	18.82	13.97	12.86	2.97	4.58
213	2.68	15.34	36.58	58.20	105.60	1.38	2.79	5.88	18.44	0.00	24.76	25.68	16.05	16.60	14.52	2.39	2.68
228	2.94	16.03	39.78	64.20	114.80	1.48	3.00	6.16	20.36	0.00	23.93	24.90	17.58	16.27	14.54	2.78	2.42
237	2.90	17.23	41.07	63.95	110.40	1.38	2.71	5.41	20.31	0.00	23.80	26.39	17.99	15.35	14.15	2.32	2.37
246	2.54	16.04	37.17	57.02	95.76	1.32	2.55	4.97	17.798	0.00	24.50	27.19	17.03	15.86	14.65	0.77	2.09
259	2.31	34.45	76.81	113.00	171.80	1.23	2.28	3.99	35.22	0.00	17.87	25.89	29.44	10.62	10.40	5.78	1.60

HF - TGS2

Depth	%L.O.I	P_n (µm)				%P_nM Index			%Sand	% Size Fraction							Skewness
(cm)		50	70	80	90	50 - **70**	50 - **80**	50 - **90**		2000 - 600	600 - 212	212 - 63	20 - 63	6 - 20	2 - 6	0.04 - 2	
7	6.08	512.60	1096.00	1384.00	1682.00	1.14	1.70	2.28	66.87	47.85	7.03	12.00	10.10	9.61	7.11	6.30	0.50
17	4.21	537.20	1093.00	1371.00	1667.00	1.03	1.55	2.10	68.66	48.30	9.33	11.03	9.07	9.36	6.88	6.03	0.48
32	2.34	180.90	678.40	969.70	1359.00	2.75	4.36	6.51	62.42	32.56	15.20	14.66	11.92	10.68	7.86	7.13	1.09
47	2.34	90.34	302.80	662.40	1032.00	2.35	6.33	10.42	55.21	21.69	14.04	19.49	14.21	12.84	9.38	8.35	1.63
65	2.75	179.80	641.50	924.00	1281.00	2.57	4.14	6.12	67.10	31.31	15.53	20.26	12.40	8.48	6.23	5.78	1.14
77	2.08	202.50	571.50	801.40	1053.00	1.82	2.96	4.20	68.95	28.89	20.16	19.90	10.65	8.32	6.30	5.79	1.05
87	2.71	173.40	684.40	1002.00	1380.00	2.95	4.78	6.96	64.75	32.47	14.18	18.09	11.66	9.41	7.44	6.75	1.07
96	1.84	125.30	736.00	1045.00	1389.00	4.87	7.34	10.09	60.38	33.47	10.25	16.66	14.11	10.72	7.64	7.16	1.02
111	2.87	190.70	672.30	966.20	1328.00	2.53	4.07	5.96	68.72	32.31	16.04	20.37	11.97	7.71	5.99	5.61	1.09
126	8.77	29.65	100.20	252.60	920.80	2.38	7.52	30.06	36.70	14.84	6.72	15.13	21.31	18.94	12.70	10.35	2.29
141	7.40	42.12	228.20	711.00	1122.00	4.42	15.88	25.64	44.41	22.41	8.18	13.83	17.19	16.54	11.95	9.91	1.63
161	2.03	32.57	126.80	270.20	817.90	2.89	7.30	24.11	40.31	14.00	8.81	17.50	16.95	17.11	14.04	11.58	1.97
169	2.78	109.40	695.80	998.80	1356.00	5.36	8.13	11.39	56.33	32.57	9.56	14.20	13.47	12.58	9.64	7.98	1.09
179	2.50	55.05	163.50	395.80	982.80	1.97	6.19	16.85	47.26	17.31	8.89	21.06	19.82	13.77	10.22	8.94	2.05
188	1.58	68.86	201.10	521.00	922.70	1.92	6.57	12.40	51.96	18.19	11.06	22.71	21.99	11.94	7.07	7.04	1.95
196	1.74	56.45	132.50	232.50	705.50	1.35	3.12	11.50	47.18	11.95	9.37	25.86	24.13	12.91	7.91	7.86	2.47
209	1.41	57.02	120.40	192.10	735.90	1.11	2.37	11.91	47.27	11.60	6.85	28.83	24.07	12.59	7.99	8.07	2.69
225	1.85	60.18	144.70	283.50	813.40	1.40	3.71	12.52	48.84	14.31	9.10	25.43	23.21	12.41	7.47	8.07	2.33
234	1.55	56.78	140.10	244.80	724.00	1.47	3.31	11.75	47.61	12.56	9.50	25.56	21.61	13.28	8.69	8.81	2.28
243	2.07	56.99	139.00	262.30	793.50	1.44	3.60	12.92	47.53	13.74	8.91	24.88	23.40	12.98	7.72	8.38	2.29
249	1.42	58.81	137.00	241.40	764.10	1.33	3.10	11.99	48.24	12.94	8.81	26.49	23.46	12.80	7.33	8.18	2.33
254	3.68	65.69	213.70	600.20	1022.00	2.25	8.14	14.56	50.72	20.00	10.12	20.61	17.92	13.52	9.09	8.74	1.80
261	2.11	68.09	230.80	631.30	1045.00	2.39	8.27	14.35	51.19	20.65	10.55	20.00	16.02	13.66	10.12	9.01	1.61
270	1.56	28.86	73.60	132.30	312.90	1.55	3.58	9.84	33.09	6.91	6.39	19.79	24.49	19.11	11.78	11.53	3.02
282	1.01	37.29	82.77	136.30	316.10	1.22	2.66	7.48	36.52	7.37	6.45	22.71	28.08	17.08	8.70	9.61	2.93
292	1.99	70.61	171.10	294.30	776.80	1.42	3.17	10.00	52.48	13.92	11.84	26.72	20.57	12.39	7.12	7.44	2.26

HF - TGS3

Depth	%L.O.I	P_n (µm)				%P_nM Index			%Sand	% Size Fraction							Skewness
(cm)		50	70	80	90	50 - **70**	50 - **80**	50 - **90**		2000 - 600	600 - 212	212 - 63	20 - 63	6 - 20	2 - 6	0.04 - 2	
3	5.79	185.9	1007.0	1344.0	1673.0	4.42	6.23	8.00	59.18	41.83	7.20	10.15	11.37	12.53	9.35	7.57	-1.07
9	3.68	261.5	1050.0	1367.0	1672.0	3.02	4.23	5.39	62.36	42.68	9.03	10.65	10.49	11.20	8.63	7.33	0.63
16	2.17	69.1	369.5	811.3	1335.0	4.34	10.73	18.31	51.30	25.46	9.71	16.13	15.85	14.33	9.55	8.97	1.49
20	1.85	69.0	285.8	751.3	1278.0	3.14	9.89	17.52	51.36	23.26	10.25	17.84	15.98	14.19	9.78	8.70	1.59
25	1.77	91.0	491.5	888.7	1356.0	4.40	8.76	13.89	54.86	27.67	10.94	16.25	14.38	13.25	9.50	8.02	1.34
36	1.62	76.4	626.6	1022.0	1479.0	7.20	12.37	18.35	52.33	30.58	8.17	13.59	14.56	14.48	10.11	8.53	1.18
42	1.79	50.7	118.7	192.8	640.9	1.34	2.80	11.64	44.77	10.59	7.75	26.43	23.67	14.33	8.76	8.47	2.40

LB - WBS1

Depth	%L.O.I	P_n (µm)				%P_nM Index			%Sand	% Size Fraction							Skewness
(cm)		50	70	80	90	50 - 70	50 - 80	50 - 90		2000 - 600	600 - 212	212 - 63	20 - 63	6 - 20	2 - 6	0.04 - 2	
3	10.46	126.7	342.5	623.5	946.1	1.70	3.92	6.47	61.91	20.75	18.47	22.69	15.56	10.57	6.30	5.66	1.48
8	4.26	319.5	794.5	1019.0	1314.0	1.49	2.19	3.11	78.71	38.19	21.49	19.03	7.89	6.13	3.79	3.49	0.85
14.5	6.90	85.5	180.1	271.8	606.8	1.11	2.18	6.10	55.92	10.13	15.27	30.53	17.38	12.62	7.58	6.51	2.25
20	14.55	33.8	108.1	169.9	264.3	2.20	4.03	6.83	38.88	3.68	10.82	24.39	21.13	20.13	11.58	8.29	3.59
28	18.90	172.8	373.4	536.6	800.5	1.16	2.11	3.63	61.33	17.25	28.23	15.85	9.58	11.47	8.25	9.37	1.25
32	5.01	433.6	794.5	1056.0	1427.0	0.83	1.44	2.29	81.83	39.74	28.71	13.08	6.07	5.26	3.70	3.44	0.85
38	3.40	543.7	791.8	956.6	1211.0	0.46	0.76	1.23	89.76	44.99	36.94	7.82	3.26	3.00	2.02	1.96	0.71
44	3.24	322.4	528.0	680.6	898.3	0.64	1.11	1.79	81.68	24.92	39.69	17.07	6.51	5.27	3.31	3.24	1.06
48	3.16	151.8	240.2	328.4	609.9	0.58	1.16	3.02	71.12	10.26	24.89	35.97	11.57	7.77	4.76	4.78	1.83
52.5	5.30	32.6	88.0	129.5	191.9	1.70	2.97	4.88	37.28	0.00	7.69	29.59	22.11	18.60	11.73	10.27	1.40
57.5	12.11	17.9	63.0	118.3	210.8	2.51	5.60	10.76	30.00	2.84	7.07	20.09	18.00	22.32	16.63	13.06	3.58
61.5	5.85	16.7	57.5	113.4	212.7	2.45	5.80	11.75	28.71	3.26	6.79	18.67	17.95	22.74	16.89	13.71	3.52
66.5	3.65	52.2	171.3	252.5	448.7	2.28	3.84	7.59	47.62	7.10	17.42	23.10	14.87	16.35	11.69	9.47	2.19
72.5	4.30	157.7	393.6	646.8	959.1	1.50	3.10	5.08	60.03	21.75	22.20	16.07	10.69	13.24	8.89	7.15	1.50
78.5	4.03	66.8	182.0	274.6	556.2	1.72	3.11	7.33	50.80	9.07	16.94	24.78	15.17	14.91	10.19	8.93	1.98
83.5	4.60	90.7	195.6	288.9	700.4	1.16	2.19	6.73	56.02	11.94	15.70	28.38	14.46	13.00	8.84	7.67	2.48

LB - WBS2

Depth	%L.O.I	P_n (µm)				%P_nM Index			%Sand	% Size Fraction							Skewness
(cm)		50	70	80	90	50 - **70**	50 - **80**	50 - **90**		2000 - 600	600 - 212	212 - 63	20 - 63	6 - 20	2 - 6	0.04 - 2	
4	2.56	143.8	225.7	280.9	398.6	0.57	0.95	1.77	70.89	6.74	26.20	37.95	12.71	7.56	4.42	4.43	2.18
9	2.41	301.1	482.2	656.1	890.1	0.60	1.18	1.96	86.47	22.90	43.34	20.23	4.72	3.73	2.56	2.52	1.17
20	1.88	530.1	813.9	1008.0	1313.0	0.54	0.90	1.48	92.31	44.45	40.08	7.77	2.60	2.13	1.43	1.54	0.84
30	2.39	567.6	865.8	1091.0	1496.0	0.53	0.92	1.64	93.71	47.57	39.51	6.63	2.25	1.77	1.14	1.14	0.85
36	2.78	662.0	971.4	1194.0	1568.0	0.47	0.80	1.37	92.55	53.83	30.51	8.21	2.30	2.25	1.46	1.45	0.60
42	2.94	685.3	994.1	1191.0	1481.0	0.45	0.74	1.16	92.11	55.34	28.76	8.01	2.60	2.34	1.50	1.44	0.49
51	3.05	594.9	953.3	1188.0	1513.0	0.60	1.00	1.54	90.16	49.70	29.30	11.16	3.18	2.65	1.79	2.23	0.61
55	3.85	703.3	1030.0	1262.0	1578.0	0.46	0.79	1.24	89.85	56.33	25.00	8.52	3.29	2.64	1.86	2.36	0.43
61	4.12	208.6	728.3	967.9	1267.0	2.49	3.64	5.07	62.60	35.12	14.67	12.81	9.18	10.73	8.68	8.81	0.95
70	4.75	920.6	1240.0	1434.0	1692.0	0.35	0.56	0.84	93.13	69.87	18.66	4.60	2.12	1.90	1.35	1.49	0.05
75	11.78	757.8	1090.0	1268.0	1512.0	0.44	0.67	1.00	90.60	60.70	22.93	6.97	3.16	2.41	1.62	2.21	0.26
79	4.13	629.1	917.5	1113.0	1413.0	0.46	0.77	1.25	88.79	51.73	28.97	8.08	3.01	2.90	2.57	2.74	0.60
87	4.07	935.2	1261.0	1459.0	1715.0	0.35	0.56	0.83	91.37	70.30	15.98	5.08	2.49	2.29	1.86	2.00	0.00
94	4.21	910.8	1250.0	1452.0	1704.0	0.37	0.59	0.87	88.79	67.19	17.38	4.22	3.42	3.28	2.38	2.13	0.03
96	6.27	220.9	616.9	865.8	1184.0	1.79	2.92	4.36	67.60	30.62	20.10	16.89	12.81	10.07	5.14	4.37	1.15
99	5.08	105.2	237.2	362.5	794.7	1.25	2.45	6.55	60.22	14.24	18.59	27.40	16.77	11.19	6.20	5.61	2.07
108	4.12	265.9	427.8	685.9	1039.0	0.61	1.58	2.91	73.03	22.60	36.14	14.28	9.62	8.70	4.52	4.13	1.44
113	72.44	69.8	174.3	297.5	657.3	1.50	3.27	8.42	52.53	11.24	15.07	26.23	26.22	13.64	4.80	2.81	2.51
118	53.83	37.0	73.3	108.1	182.5	0.98	1.92	3.93	34.29	2.68	5.29	26.32	32.00	19.53	8.61	5.57	4.15
127	23.89	19.1	54.2	97.1	205.9	1.84	4.09	9.80	27.27	4.09	5.63	17.55	21.74	23.26	15.55	12.18	3.73
131	6.78	15.8	48.4	88.9	148.6	2.07	4.64	8.42	25.76	0.00	3.85	21.90	19.67	23.63	16.98	13.97	1.93
136	2.19	146.5	201.1	240.3	310.6	0.37	0.64	1.12	77.72	5.24	21.49	50.99	8.60	5.71	3.84	4.13	2.75
139.5	8.74	15.9	46.4	85.7	145.4	1.91	4.38	8.13	24.97	0.00	3.46	21.51	20.45	24.42	16.88	13.27	1.94
145	5.13	32.5	94.7	131.2	176.0	1.91	3.03	4.41	38.89	0.00	4.88	34.02	18.96	18.61	12.81	10.72	1.12
150	3.88	41.8	112.1	151.1	203.4	1.68	2.62	3.87	43.24	0.00	8.65	34.58	17.90	16.84	11.80	10.22	1.04
156	5.72	22.0	84.4	134.2	191.7	2.83	5.09	7.70	34.49	0.00	7.46	27.04	17.11	20.83	15.20	12.37	1.42
164	4.66	30.7	96.1	136.8	187.0	2.13	3.45	5.09	38.49	0.00	6.48	32.00	18.43	19.20	13.36	10.53	1.19
171	6.11	28.8	110.8	164.9	237.6	2.85	4.72	7.25	39.50	3.63	9.26	26.61	16.10	19.14	13.83	11.42	3.32
179	4.64	121.3	239.3	355.5	733.0	0.97	1.93	5.04	58.21	13.71	20.15	24.35	11.18	13.45	9.62	7.54	1.89
188	5.17	75.0	188.6	256.2	421.8	1.52	2.42	4.63	51.87	6.94	19.13	25.80	13.54	15.22	10.70	8.67	2.01
198	4.42	102.4	232.8	364.5	849.3	1.27	2.56	7.29	55.41	15.68	17.08	22.65	11.77	13.97	10.32	8.52	2.22
208	4.10	120.8	247.4	451.9	849.1	1.05	2.74	6.03	58.86	17.06	16.87	24.92	12.41	12.90	8.75	7.08	2.10

HF - BGS1

Depth (cm)	X (10^{-6} m^3 kg^{-1})	SARM (10^{-6} Am^2 kg^{-1})	ARM40/ SARM	SIRM (10^{-6} Am^2 kg^{-1})	IRM40/ SIRM	IRM100/ SIRM	IRM1T/ SIRM	SIRM/ SARM	SARM/X (kAm^{-1})	SIRM/X (kAm^{-1})	ARM40mT (10^{-6} Am^2 kg^{-1})	IRM40mT (10^{-6} Am^2 kg^{-1})	IRM100mT (10^{-6} Am^2 kg^{-1})	IRM 1T (10^{-6} Am^2 kg^{-1})
2.5	0.23	0.062	0.24	1.81	0.31	0.68	0.98	29.04	0.27	7.85	0.015	0.57	1.22	1.77
6.5	0.16	0.032	0.23	0.82	0.31	0.65	0.94	25.59	0.20	5.13	0.007	0.26	0.53	0.77
28.5	0.11	0.006	0.47	0.24	0.16	0.32	0.73	39.55	0.06	2.24	0.003	0.04	0.08	0.18
39.5	0.11	0.007	0.44	0.22	0.22	0.42	0.79	30.28	0.07	1.98	0.003	0.05	0.10	0.18
46.5	0.11	0.007	0.46	0.22	0.25	0.46	0.80	30.87	0.06	1.94	0.003	0.05	0.10	0.18
55.5	0.11	0.012	0.74	0.19	0.14	0.45	0.77	15.66	0.11	1.73	0.009	0.03	0.09	0.15
62.5	0.11	0.010	0.43	0.26	0.29	0.55	0.87	24.61	0.09	2.25	0.005	0.07	0.14	0.22
81.5	0.10	0.005	0.47	0.09	0.27	0.44	0.84	19.70	0.05	0.94	0.002	0.02	0.04	0.08
104.5	0.09	0.005	0.51	0.06	0.34	0.61	0.85	13.61	0.05	0.73	0.002	0.02	0.04	0.05
113.5	0.08	0.005	0.45	0.07	0.37	0.64	0.87	13.51	0.07	0.89	0.002	0.03	0.04	0.06
122.5	0.04	0.006	0.53	0.07	0.42	0.74	0.94	10.63	0.17	1.81	0.003	0.03	0.05	0.06
130.5	0.02	0.006	0.49	0.13	0.20	0.34	0.70	23.72	0.28	6.56	0.003	0.03	0.05	0.09
147.5	0.07	0.006	0.56	0.14	0.21	0.37	0.85	25.17	0.08	1.94	0.003	0.03	0.05	0.12
154.5	0.09	0.010	0.44	0.18	0.27	0.57	0.92	16.71	0.12	1.98	0.005	0.05	0.10	0.16
162.5	0.11	0.018	0.30	0.30	0.33	0.60	0.91	17.00	0.16	2.67	0.005	0.10	0.18	0.27
172.5	0.11	0.020	0.25	0.32	0.36	0.61	0.92	15.80	0.19	2.93	0.005	0.11	0.19	0.29
179.5	0.12	0.025	0.21	0.38	0.37	0.61	0.92	15.34	0.20	3.13	0.005	0.14	0.23	0.35
185.5	0.12	0.023	0.27	0.40	0.35	0.60	0.91	16.95	0.20	3.40	0.006	0.14	0.24	0.36
203.5	0.14	0.022	0.26	0.53	0.35	0.65	0.93	23.77	0.16	3.89	0.006	0.19	0.34	0.49
219.0	0.13	0.019	0.28	0.53	0.37	0.68	0.95	28.09	0.15	4.13	0.005	0.20	0.36	0.50
233.5	0.14	0.021	0.29	0.59	0.37	0.68	0.95	28.31	0.15	4.36	0.006	0.22	0.40	0.56
244.5	0.17	0.025	0.24	0.60	0.36	0.67	0.94	23.77	0.15	3.57	0.006	0.21	0.41	0.57
252.5	0.17	0.026	0.23	0.61	0.36	0.69	0.95	22.93	0.16	3.56	0.006	0.22	0.42	0.58
257.0	0.14	0.013	0.30	0.33	0.42	0.69	0.90	25.05	0.09	2.27	0.004	0.14	0.23	0.29
267.5	0.17	0.023	0.26	0.61	0.41	0.72	0.95	27.03	0.13	3.56	0.006	0.25	0.44	0.58
286.5	0.18	0.029	0.21	0.64	0.39	0.71	0.94	21.95	0.17	3.63	0.006	0.25	0.45	0.60
293.0	0.17	0.031	0.24	0.63	0.37	0.68	0.93	20.29	0.19	3.79	0.007	0.23	0.43	0.58
297.5	0.12	0.031	0.24	0.99	0.30	0.66	0.94	31.32	0.27	8.31	0.008	0.30	0.65	0.92
301.5	0.31	0.055	0.22	1.30	0.35	0.66	0.94	23.67	0.18	4.23	0.012	0.45	0.87	1.23

APPENDIX 1.3: Section samples, mineral magnetics: parameters and ratios

HF - BGS2

Depth	X	SARM	ARM40/	SIRM	IRM40/	IRM100/	IRM1T/	SIRM/	SARM/X	SIRM/X	ARM40mT	IRM40mT	IRM100mT	IRM 1T
(cm)	(10^{-6} m^3 kg^{-1})	(10^{-6} Am^2 kg^{-1})	SARM	(10^{-6} Am^2 kg^{-1})	SIRM	SIRM	SIRM	SARM	(kAm^{-1})	(kAm^{-1})	(10^{-6} Am^2 kg^{-1})	(10^{-6} Am^2 kg^{-1})	(10^{-6} Am^2 kg^{-1})	(10^{-6} Am^2 kg^{-1})
6	0.59	0.125	0.13	2.87	0.54	0.79	0.96	22.99	0.21	4.84	0.016	1.56	2.27	2.75
22	0.64	0.103	0.12	2.67	0.58	0.80	0.95	25.86	0.16	4.19	0.012	1.54	2.15	2.53
45	0.69	0.114	0.12	2.83	0.61	0.83	0.96	24.92	0.17	4.12	0.014	1.72	2.35	2.72
58	0.69	0.086	0.12	2.49	0.59	0.81	0.96	28.83	0.13	3.62	0.010	1.47	2.03	2.39
66	0.56	0.070	0.14	2.10	0.56	0.79	0.95	29.98	0.13	3.77	0.009	1.17	1.66	2.00
76	0.66	0.098	0.16	2.72	0.57	0.80	0.96	27.66	0.15	4.11	0.016	1.55	2.18	2.63
81	0.69	0.108	0.13	2.90	0.56	0.80	0.95	26.90	0.16	4.22	0.015	1.63	2.31	2.77
91	0.19	0.051	0.16	0.78	0.49	0.72	0.94	15.37	0.27	4.11	0.008	0.38	0.57	0.74
100	0.20	0.055	0.16	0.84	0.48	0.71	0.96	15.18	0.27	4.17	0.009	0.41	0.59	0.81
108	0.26	0.060	0.14	1.07	0.53	0.73	0.95	17.86	0.23	4.04	0.009	0.56	0.78	1.01
114	0.19	0.043	0.16	0.73	0.45	0.68	0.93	16.89	0.23	3.97	0.007	0.33	0.50	0.68
117	0.22	0.049	0.15	0.87	0.45	0.69	0.93	17.83	0.23	4.03	0.007	0.39	0.60	0.81
125	0.19	0.047	0.16	0.74	0.42	0.68	0.93	15.96	0.24	3.87	0.008	0.31	0.50	0.69
134	0.21	0.050	0.18	0.87	0.43	0.68	0.93	17.49	0.23	4.09	0.009	0.38	0.59	0.81
139	0.20	0.044	0.17	0.79	0.43	0.69	0.93	17.91	0.22	3.88	0.007	0.34	0.54	0.73
144	0.24	0.046	0.16	0.89	0.46	0.69	0.93	19.41	0.19	3.72	0.007	0.41	0.61	0.82
151	0.26	0.053	0.18	1.09	0.45	0.68	0.93	20.35	0.20	4.12	0.009	0.48	0.74	1.01
160	0.25	0.044	0.16	0.97	0.44	0.67	0.93	22.16	0.17	3.82	0.007	0.43	0.65	0.90
167	0.28	0.058	0.15	1.15	0.45	0.69	0.93	20.04	0.20	4.09	0.009	0.52	0.79	1.08
170	0.30	0.061	0.15	1.21	0.47	0.71	0.94	20.06	0.20	3.98	0.009	0.57	0.86	1.14
173	0.31	0.060	0.16	1.20	0.47	0.71	0.93	20.11	0.19	3.91	0.010	0.57	0.85	1.12
179	0.25	0.058	0.15	1.01	0.49	0.72	0.94	17.35	0.23	4.04	0.009	0.49	0.72	0.94
183	0.18	0.050	0.18	0.69	0.45	0.70	0.94	13.89	0.28	3.95	0.009	0.31	0.48	0.65
189	0.11	0.021	0.26	0.36	0.38	0.61	0.90	17.30	0.19	3.21	0.006	0.14	0.22	0.32
193	0.09	0.011	0.43	0.35	0.20	0.38	0.85	32.59	0.12	3.86	0.005	0.07	0.13	0.30
202	0.09	0.010	0.48	0.42	0.20	0.40	0.86	44.26	0.11	4.77	0.005	0.08	0.17	0.36
210	0.09	0.011	0.44	0.39	0.22	0.43	0.86	37.32	0.12	4.47	0.005	0.09	0.17	0.34
212	0.07	0.012	0.43	0.17	0.33	0.68	0.94	14.18	0.17	2.39	0.005	0.06	0.12	0.16
216	0.06	0.009	0.48	0.13	0.36	0.72	0.95	14.47	0.15	2.24	0.004	0.05	0.10	0.13
223	0.05	0.009	0.54	0.14	0.30	0.65	0.91	15.25	0.17	2.56	0.005	0.04	0.09	0.13
227	0.20	0.057	0.36	0.68	0.36	0.68	0.94	11.76	0.29	3.37	0.021	0.25	0.46	0.64
234	0.17	0.050	0.35	0.66	0.38	0.70	0.94	13.25	0.29	3.87	0.018	0.25	0.47	0.62
239	0.09	0.010	0.57	0.14	0.27	0.61	0.92	14.79	0.11	1.61	0.005	0.04	0.09	0.13
243	0.09	0.006	0.43	0.13	0.31	0.63	0.89	20.25	0.07	1.45	0.003	0.04	0.08	0.11
252	0.09	0.006	0.51	0.12	0.31	0.60	0.88	21.16	0.06	1.33	0.003	0.04	0.07	0.11
254	0.11	0.005	0.48	0.10	0.26	0.47	0.80	19.43	0.05	0.96	0.003	0.03	0.05	0.08

GE - CDS1

Depth	X	SARM	ARM40/	SIRM	IRM40/	IRM100/	IRM1T/	SIRM/	SARM/X	SIRM/X	ARM40mT	IRM40mT	IRM100mT	IRM 1T
(cm)	(10^{-6} m^3 kg^{-1})	(10^{-6} Am^2 kg^{-1})	SARM	(10^{-6} Am^2 kg^{-1})	SIRM	SIRM	SIRM	SARM	(kAm^{-1})	(kAm^{-1})	(10^{-6} Am^2 kg^{-1})	(10^{-6} Am^2 kg^{-1})	(10^{-6} Am^2 kg^{-1})	(10^{-6} Am^2 kg^{-1})
3	1.03	0.126	0.51	4.15	0.23	0.54	0.98	32.84	0.12	4.03	0.065	0.97	2.26	4.09
11	3.56	0.213	0.45	11.47	0.29	0.61	0.99	53.80	0.06	3.22	0.095	3.31	7.01	11.31
27	6.03	0.321	0.39	19.49	0.27	0.61	0.98	60.78	0.05	3.23	0.123	5.23	11.87	19.09
44	4.39	0.244	0.40	17.70	0.25	0.59	1.00	72.56	0.06	4.03	0.097	4.38	10.39	17.69
56	5.49	0.322	0.39	23.40	0.26	0.60	1.00	72.76	0.06	4.27	0.124	5.98	14.14	23.40
75	5.25	0.305	0.34	18.77	0.31	0.63	0.99	61.50	0.06	3.58	0.103	5.79	11.89	18.57
89	4.84	0.274	0.35	18.85	0.29	0.62	1.00	68.84	0.06	3.90	0.096	5.43	11.75	18.81
100	5.15	0.283	0.33	20.47	0.29	0.61	0.99	72.22	0.06	3.97	0.094	5.93	12.48	20.19
119	5.75	0.338	0.32	22.31	0.30	0.65	1.00	66.09	0.06	3.88	0.108	6.78	14.49	22.31
128	6.39	0.302	0.32	20.53	0.30	0.61	0.98	68.00	0.05	3.21	0.098	6.20	12.59	20.18
136	6.35	0.295	0.35	20.47	0.30	0.64	0.97	69.47	0.05	3.22	0.102	6.07	13.16	19.94
160	5.43	0.334	0.36	19.38	0.31	0.65	0.98	58.05	0.06	3.57	0.120	5.91	12.58	19.09
174	5.43	0.295	0.34	18.50	0.32	0.68	0.99	62.74	0.05	3.41	0.102	5.94	12.50	18.36
190	5.59	0.313	0.35	21.52	0.30	0.68	0.99	68.75	0.06	3.85	0.108	6.50	14.56	21.34

GE - CDS2

Depth	X	SARM	ARM40/	SIRM	IRM40/	IRM100/	IRM1T/	SIRM/	SARM/X	SIRM/X	ARM40mT	IRM40mT	IRM100mT	IRM 1T
(cm)	(10^{-6} m^3 kg^{-1})	(10^{-6} Am^2 kg^{-1})	SARM	(10^{-6} Am^2 kg^{-1})	SIRM	SIRM	SIRM	SARM	(kAm^{-1})	(kAm^{-1})	(10^{-6} Am^2 kg^{-1})	(10^{-6} Am^2 kg^{-1})	(10^{-6} Am^2 kg^{-1})	(10^{-6} Am^2 kg^{-1})
4	3.93	0.249	0.35	17.18	0.23	0.58	0.95	68.94	0.06	4.37	0.087	3.94	9.95	16.29
14	4.53	0.261	0.36	19.06	0.25	0.62	0.98	72.90	0.06	4.21	0.094	4.81	11.79	18.72
18	2.19	0.200	0.44	10.78	0.22	0.56	0.99	53.95	0.09	4.92	0.088	2.37	6.09	10.62
22	1.52	0.175	0.47	5.53	0.23	0.55	0.95	31.67	0.12	3.65	0.082	1.25	3.07	5.27
32	3.08	0.262	0.49	9.16	0.26	0.59	0.99	35.00	0.08	2.97	0.129	2.42	5.41	9.09
47	6.16	0.416	0.45	14.28	0.28	0.63	1.00	34.28	0.07	2.32	0.186	3.93	9.05	14.28
57	6.80	0.347	0.35	20.54	0.28	0.63	0.99	59.15	0.05	3.02	0.122	5.69	13.01	20.39
70	4.75	0.293	0.40	16.87	0.28	0.61	1.00	57.65	0.06	3.55	0.116	4.76	10.37	16.87
99	5.68	0.337	0.38	19.17	0.28	0.64	0.98	56.98	0.06	3.38	0.129	5.45	12.20	18.86
110	5.77	0.310	0.35	19.85	0.28	0.61	0.96	63.94	0.05	3.44	0.107	5.56	12.21	18.96
126	6.79	0.541	0.42	22.32	0.32	0.67	0.96	41.26	0.08	3.29	0.227	7.08	14.85	21.47
153	5.96	0.307	0.38	20.59	0.29	0.61	1.00	67.09	0.05	3.46	0.116	6.01	12.66	20.59
168	4.81	0.296	0.38	19.67	0.25	0.58	0.98	66.36	0.06	4.09	0.113	4.95	11.48	19.36
179	5.54	0.318	0.36	20.56	0.29	0.62	0.99	64.72	0.06	3.71	0.115	5.86	12.81	20.31
193	6.03	0.308	0.36	19.65	0.29	0.61	0.98	63.82	0.05	3.26	0.112	5.69	12.02	19.19
206	5.54	0.324	0.36	19.54	0.30	0.63	1.00	60.27	0.06	3.53	0.117	5.94	12.27	19.54
222	5.15	0.285	0.39	17.93	0.31	0.64	1.00	63.01	0.06	3.48	0.110	5.50	11.55	17.93
234	4.87	0.299	0.37	19.50	0.25	0.59	1.00	65.29	0.06	4.00	0.112	4.85	11.42	19.44

GE - CDS3

Depth	X	SARM	ARM40/	SIRM	IRM40/	IRM100/	IRM1T/	SIRM/	SARM/X	SIRM/X	ARM40mT	IRM40mT	IRM100mT	IRM 1T
(cm)	(10^{-6} m^3 kg^{-1})	(10^{-6} Am^2 kg^{-1})	SARM	(10^{-6} Am^2 kg^{-1})	SIRM	SIRM	SIRM	SARM	(kAm^{-1})	(kAm^{-1})	(10^{-6} Am^2 kg^{-1})	(10^{-6} Am^2 kg^{-1})	(10^{-6} Am^2 kg^{-1})	(10^{-6} Am^2 kg^{-1})
4	2.45	0.202	0.41	11.83	0.23	0.56	0.98	58.68	0.08	4.82	0.083	2.72	6.62	11.64
14	3.69	0.258	0.39	15.92	0.26	0.60	1.00	61.63	0.07	4.32	0.101	4.09	9.57	15.92
20	2.98	0.246	0.42	10.79	0.26	0.61	1.00	43.88	0.08	3.62	0.104	2.85	6.56	10.75
31	6.86	0.447	0.43	18.20	0.32	0.67	1.00	40.72	0.07	2.65	0.193	5.80	12.28	18.20
40	5.43	0.317	0.37	17.18	0.29	0.65	1.00	54.27	0.06	3.16	0.116	4.94	11.12	17.18
52	5.52	0.281	0.39	19.39	0.27	0.60	1.00	68.97	0.05	3.51	0.109	5.22	11.55	19.39
59	5.73	0.324	0.37	20.96	0.26	0.59	1.00	64.72	0.06	3.66	0.120	5.35	12.41	20.96
71	5.52	0.341	0.38	20.04	0.30	0.66	1.00	58.71	0.06	3.63	0.130	6.08	13.16	20.04
84	6.85	0.335	0.35	20.21	0.29	0.60	1.00	60.40	0.05	2.95	0.116	5.79	12.17	20.21
96	5.37	0.343	0.38	19.32	0.28	0.61	1.00	56.33	0.06	3.59	0.131	5.44	11.82	19.32
105	5.37	0.340	0.38	18.66	0.30	0.64	1.00	54.94	0.06	3.48	0.129	5.51	12.03	18.66
117	5.71	0.327	0.38	19.43	0.28	0.62	0.95	59.49	0.06	3.40	0.124	5.54	12.10	18.49
128	5.89	0.378	0.37	25.00	0.24	0.58	0.97	66.17	0.06	4.24	0.139	5.96	14.57	24.25
139	6.24	0.355	0.34	23.34	0.26	0.60	0.99	65.76	0.06	3.74	0.122	6.14	13.96	23.17
146	5.03	0.224	0.37	21.22	0.24	0.59	0.99	94.56	0.04	4.22	0.083	5.05	12.42	21.01
158	4.71	0.317	0.34	24.72	0.21	0.55	0.99	77.90	0.07	5.25	0.108	5.20	13.54	24.48
168	5.07	0.346	0.35	24.63	0.22	0.57	0.99	71.22	0.07	4.86	0.123	5.46	14.07	24.27
209	6.46	0.357	0.37	20.40	0.28	0.63	1.00	57.22	0.06	3.16	0.133	5.62	12.82	20.40
223	6.73	0.361	0.35	21.18	0.00	0.65	1.01	58.71	0.05	3.15	0.128	0.04	13.78	21.35
235	5.64	0.344	0.39	22.47	0.24	0.58	1.00	65.39	0.06	3.99	0.133	5.28	12.99	22.55

M - DCS1

Depth	X	SARM	ARM40/	SIRM	IRM40/	IRM100/	IRM1T/	SIRM/	SARM/X	SIRM/X	ARM40mT	IRM40mT	IRM100mT	IRM 1T
(cm)	(10^{-6} m^3 kg^{-1})	(10^{-6} Am^2 kg^{-1})	SARM	(10^{-6} Am^2 kg^{-1})	SIRM	SIRM	SIRM	SARM	(kAm^{-1})	(kAm^{-1})	(10^{-6} Am^2 kg^{-1})	(10^{-6} Am^2 kg^{-1})	(10^{-6} Am^2 kg^{-1})	(10^{-6} Am^2 kg^{-1})
9	0.15	0.055	0.23	2.25	0.16	0.32	0.82	40.91	14.51	0.35	0.013	0.35	0.72	1.83
15	0.15	0.048	0.21	2.12	0.14	0.29	0.80	43.64	14.39	0.33	0.010	0.29	0.61	1.69
28	0.13	0.041	0.21	2.12	0.10	0.18	0.77	51.84	16.46	0.32	0.008	0.20	0.38	1.64
39	0.13	0.034	0.23	2.17	0.11	0.19	0.77	63.74	17.01	0.27	0.008	0.24	0.40	1.66
50	0.11	0.036	0.19	2.19	0.08	0.14	0.74	61.18	19.15	0.31	0.007	0.17	0.31	1.62
58	0.09	0.030	0.25	1.95	0.06	0.12	0.76	64.58	21.69	0.34	0.007	0.12	0.24	1.49
66	0.09	0.025	0.31	1.92	0.05	0.11	0.75	76.84	22.50	0.29	0.008	0.10	0.21	1.44
72	0.11	0.049	0.19	2.32	0.08	0.14	0.76	47.12	21.53	0.46	0.009	0.19	0.33	1.75
83	0.11	0.048	0.18	2.09	0.10	0.17	0.76	43.05	18.86	0.44	0.009	0.20	0.36	1.59
97	0.12	0.044	0.19	2.05	0.11	0.18	0.76	46.55	17.20	0.37	0.008	0.24	0.38	1.55
106	0.11	0.032	0.21	1.66	0.09	0.16	0.77	52.39	15.45	0.29	0.007	0.14	0.26	1.27
115	0.11	0.031	0.23	1.59	0.08	0.15	0.76	51.39	14.82	0.29	0.007	0.13	0.23	1.20
126	0.09	0.016	0.36	1.23	0.05	0.11	0.74	79.52	13.48	0.17	0.006	0.06	0.14	0.92
133	0.08	0.012	0.44	1.05	0.04	0.10	0.75	87.11	12.44	0.14	0.005	0.04	0.11	0.79
143	0.08	0.011	0.49	1.17	0.03	0.08	0.75	103.45	13.86	0.13	0.006	0.04	0.09	0.88
152	0.08	0.013	0.47	0.84	0.05	0.12	0.78	65.85	11.09	0.17	0.006	0.04	0.10	0.65
166	0.10	0.016	0.39	1.49	0.05	0.11	0.77	90.66	14.56	0.16	0.006	0.07	0.16	1.14
175	0.10	0.018	0.35	1.54	0.05	0.10	0.77	84.37	15.83	0.19	0.006	0.07	0.16	1.19
188	0.09	0.014	0.42	1.29	0.05	0.11	0.77	91.64	13.78	0.15	0.006	0.06	0.14	1.00
199	0.09	0.013	0.45	1.22	0.05	0.11	0.78	97.57	13.43	0.14	0.006	0.06	0.13	0.95
209	0.09	0.011	0.53	1.23	0.03	0.09	0.76	116.28	13.93	0.12	0.006	0.04	0.11	0.94
214	0.10	0.009	0.55	1.31	0.03	0.08	0.80	145.99	13.44	0.09	0.005	0.03	0.10	1.04
224	0.09	0.010	0.52	1.20	0.03	0.09	0.78	117.80	13.12	0.11	0.005	0.04	0.10	0.93
233	0.08	0.011	0.55	0.74	0.04	0.12	0.79	69.62	9.38	0.13	0.006	0.03	0.09	0.59
253	0.05	0.015	0.52	0.26	0.17	0.36	0.86	17.57	5.27	0.30	0.008	0.04	0.09	0.22
272	0.06	0.011	0.54	0.16	0.23	0.50	0.89	13.94	2.52	0.18	0.006	0.04	0.08	0.14
277	0.06	0.013	0.52	0.18	0.21	0.47	0.90	14.14	2.88	0.20	0.007	0.04	0.09	0.16
287	0.06	0.012	0.51	0.19	0.22	0.51	0.92	15.81	2.99	0.19	0.006	0.04	0.10	0.18
295	0.07	0.013	0.46	0.46	0.10	0.24	0.82	34.19	6.59	0.19	0.006	0.04	0.11	0.37
302	0.07	0.016	0.50	0.50	0.10	0.25	0.84	30.24	6.64	0.22	0.008	0.05	0.13	0.42
309	0.07	0.016	0.49	0.33	0.17	0.40	0.87	20.06	4.53	0.23	0.008	0.05	0.13	0.29
321	0.07	0.015	0.47	0.26	0.17	0.42	0.87	17.64	3.73	0.21	0.007	0.04	0.11	0.23
330	0.07	0.014	0.48	0.22	0.19	0.49	0.91	14.87	3.27	0.22	0.007	0.04	0.11	0.20
345	0.09	0.066	0.09	1.10	0.70	0.87	1.00	16.68	12.27	0.74	0.006	0.77	0.96	1.10
356	0.05	0.012	0.56	0.18	0.23	0.45	0.88	14.83	3.84	0.26	0.007	0.04	0.08	0.16
364	0.05	0.012	0.56	0.10	0.34	0.72	1.00	8.21	2.12	0.26	0.007	0.03	0.07	0.10
378	0.09	0.020	0.52	0.31	0.16	0.41	0.83	14.93	3.39	0.23	0.011	0.05	0.12	0.25
385	0.10	0.021	0.54	0.37	0.14	0.38	0.86	17.11	3.55	0.21	0.012	0.05	0.14	0.31

M - DCS2

Depth	X	SARM	ARM40/	SIRM	IRM40/	IRM100/	IRM1T/	SIRM/	SARM/X	SIRM/X	ARM40mT	IRM40mT	IRM100mT	IRM 1T
(cm)	(10^{-6} m^3 kg^{-1})	(10^{-6} Am^2 kg^{-1})	SARM	(10^{-6} Am^2 kg^{-1})	SIRM	SIRM	SIRM	SARM	(kAm^{-1})	(kAm^{-1})	(10^{-6} Am^2 kg^{-1})	(10^{-6} Am^2 kg^{-1})	(10^{-6} Am^2 kg^{-1})	(10^{-6} Am^2 kg^{-1})
3	0.14	0.052	0.16	2.39	0.12	0.23	0.78	45.87	0.38	17.60	0.008	0.29	0.55	1.87
12	0.13	0.037	0.18	2.54	0.08	0.14	0.73	68.09	0.30	20.24	0.007	0.20	0.36	1.85
20	0.12	0.038	0.21	2.62	0.08	0.14	0.74	69.03	0.33	22.69	0.008	0.20	0.37	1.95
38	0.11	0.042	0.17	2.63	0.08	0.14	0.75	63.26	0.38	24.03	0.007	0.22	0.38	1.97
52	0.11	0.048	0.17	2.54	0.10	0.17	0.75	52.32	0.43	22.50	0.008	0.25	0.43	1.89
62	0.13	0.052	0.19	2.43	0.12	0.22	0.80	46.60	0.39	18.18	0.010	0.29	0.53	1.94
74	0.15	0.064	0.15	2.48	0.15	0.25	0.78	38.68	0.44	17.05	0.010	0.36	0.61	1.95
88	0.14	0.065	0.17	2.15	0.16	0.27	0.81	33.26	0.47	15.50	0.011	0.35	0.58	1.73
97	0.13	0.050	0.20	2.07	0.13	0.22	0.78	41.02	0.39	15.81	0.010	0.27	0.46	1.61
118	0.15	0.072	0.18	2.27	0.17	0.28	0.80	31.60	0.48	15.23	0.013	0.38	0.63	1.81
130	0.15	0.082	0.15	2.58	0.17	0.28	0.80	31.55	0.53	16.66	0.012	0.43	0.72	2.06
138	0.15	0.066	0.15	2.23	0.15	0.26	0.79	33.77	0.45	15.29	0.010	0.34	0.58	1.76
152	0.16	0.067	0.18	2.21	0.16	0.29	0.80	32.93	0.42	13.91	0.012	0.36	0.64	1.77
162	0.16	0.052	0.18	2.23	0.15	0.25	0.79	43.23	0.33	14.29	0.009	0.34	0.56	1.77
170	0.14	0.045	0.15	1.99	0.18	0.23	0.76	44.18	0.32	14.08	0.007	0.35	0.47	1.51
181	0.09	0.016	0.35	1.48	0.05	0.11	0.75	92.26	0.17	15.93	0.006	0.08	0.17	1.11
194	0.06	0.016	0.48	0.39	0.11	0.27	0.80	23.70	0.26	6.20	0.008	0.04	0.11	0.31
213	0.07	0.018	0.52	0.38	0.12	0.30	0.82	21.56	0.24	5.27	0.009	0.04	0.11	0.31
235	0.10	0.015	0.45	0.67	0.10	0.22	0.89	45.97	0.15	7.00	0.007	0.06	0.15	0.60
247	0.10	0.015	0.45	0.82	0.09	0.21	0.84	53.51	0.15	8.12	0.007	0.08	0.17	0.69

M - HBS1

Depth	X	SARM	ARM40/	SIRM	IRM40/	IRM100/	IRM1T/	SIRM/	SARM/X	SIRM/X	ARM40mT	IRM40mT	IRM100mT	IRM 1T
(cm)	(10^{-6} m^3 kg^{-1})	(10^{-6} Am^2 kg^{-1})	SARM	(10^{-6} Am^2 kg^{-1})	SIRM	SIRM	SIRM	SARM	(kAm^{-1})	(kAm^{-1})	(10^{-6} Am^2 kg^{-1})	(10^{-6} Am^2 kg^{-1})	(10^{-6} Am^2 kg^{-1})	(10^{-6} Am^2 kg^{-1})
5	0.08	0.020	0.27	0.89	0.11	0.20	0.76	44.25	0.24	10.70	0.005	0.10	0.17	0.67
13	0.08	0.014	0.34	0.87	0.08	0.15	0.77	61.82	0.17	10.58	0.005	0.07	0.13	0.67
25	0.08	0.014	0.32	0.90	0.09	0.16	0.77	62.32	0.19	11.82	0.005	0.08	0.15	0.70
34	0.08	0.013	0.33	1.02	0.07	0.13	0.74	77.02	0.17	12.90	0.004	0.07	0.14	0.76
41	0.11	0.012	0.32	1.68	0.03	0.07	0.72	140.05	0.11	15.79	0.004	0.05	0.11	1.21
50	0.11	0.016	0.29	2.01	0.05	0.10	0.73	125.28	0.15	18.84	0.005	0.10	0.21	1.47
59	0.11	0.016	0.33	2.50	0.06	0.14	0.73	157.42	0.15	23.01	0.005	0.15	0.35	1.83
67	0.09	0.015	0.32	1.27	0.07	0.13	0.72	85.07	0.16	13.50	0.005	0.09	0.17	0.92
79	0.09	0.014	0.34	1.17	0.06	0.12	0.73	83.12	0.16	13.27	0.005	0.07	0.15	0.86
92	0.10	0.014	0.31	1.52	0.06	0.12	0.71	108.34	0.15	15.77	0.004	0.09	0.18	1.08
97	0.10	0.013	0.33	1.45	0.07	0.13	0.74	112.89	0.13	14.80	0.004	0.10	0.19	1.08
117	0.10	0.012	0.33	1.25	0.10	0.16	0.75	108.39	0.11	12.00	0.004	0.12	0.20	0.94
124	0.11	0.012	0.43	1.24	0.08	0.13	0.74	102.63	0.11	11.73	0.005	0.10	0.16	0.93
136	0.10	0.014	0.33	1.40	0.07	0.14	0.75	99.15	0.14	14.14	0.005	0.09	0.19	1.05
146	0.10	0.014	0.32	1.42	0.07	0.13	0.75	99.45	0.14	14.31	0.005	0.09	0.19	1.07
163	0.10	0.011	0.36	1.34	0.07	0.13	0.73	121.21	0.11	13.34	0.004	0.09	0.17	0.98
170	0.10	0.012	0.35	1.43	0.07	0.12	0.72	122.55	0.11	14.03	0.004	0.09	0.18	1.02
179	0.10	0.012	0.36	1.35	0.06	0.11	0.73	117.08	0.12	13.63	0.004	0.08	0.15	0.98
206	0.10	0.009	0.39	1.20	0.07	0.12	0.70	132.14	0.09	11.58	0.004	0.08	0.15	0.84
221	0.11	0.013	0.34	1.26	0.08	0.16	0.75	99.88	0.11	11.43	0.004	0.10	0.20	0.95
236	0.10	0.013	0.35	1.43	0.07	0.14	0.72	110.18	0.13	13.93	0.005	0.10	0.20	1.03

LB - HHS1

Depth	X	SARM	ARM40/	SIRM	IRM40/	IRM100/	IRM1T/	SIRM/	SARM/X	SIRM/X	ARM40mT	IRM40mT	IRM100mT	IRM 1T
(cm)	(10^{-6} m^3 kg^{-1})	(10^{-6} Am^2 kg^{-1})	SARM	(10^{-6} Am^2 kg^{-1})	SIRM	SIRM	SIRM	SARM	(kAm^{-1})	(kAm^{-1})	(10^{-6} Am^2 kg^{-1})	(10^{-6} Am^2 kg^{-1})	(10^{-6} Am^2 kg^{-1})	(10^{-6} Am^2 kg^{-1})
2	0.12	0.026	0.23	1.10	0.26	0.63	0.89	41.62	0.23	9.40	0.006	0.28	0.69	0.98
6	0.10	0.028	0.21	0.94	0.26	0.61	0.90	33.53	0.29	9.62	0.006	0.24	0.58	0.85
15	0.05	0.011	0.23	0.33	0.22	0.40	0.64	28.57	0.21	6.14	0.003	0.07	0.13	0.21
24	0.05	0.009	0.24	0.24	0.21	0.39	0.59	26.26	0.19	5.00	0.002	0.05	0.10	0.14
39	0.06	0.009	0.25	0.31	0.15	0.29	0.56	32.30	0.16	5.30	0.002	0.05	0.09	0.17
47	0.15	0.022	0.14	0.95	0.51	0.86	0.84	43.15	0.15	6.38	0.003	0.49	0.81	0.80
63	0.08	0.011	0.13	0.54	0.28	0.34	0.57	49.16	0.14	6.78	0.001	0.15	0.18	0.31
75	0.20	0.052	0.09	3.36	0.42	0.94	0.93	64.56	0.26	16.75	0.005	1.40	3.16	3.13
84	0.07	0.006	0.23	0.47	0.18	0.27	0.49	83.12	0.08	6.74	0.001	0.09	0.12	0.23
96	0.10	0.010	0.17	0.44	0.33	0.43	0.63	42.58	0.10	4.33	0.002	0.15	0.19	0.28
103	0.10	0.014	0.21	0.88	0.48	0.72	0.82	64.34	0.14	9.22	0.003	0.42	0.63	0.72
111	0.05	0.006	0.49	0.27	0.14	0.26	0.46	46.57	0.11	5.14	0.003	0.04	0.07	0.12
121	0.04	0.004	0.44	0.23	0.14	0.30	0.54	51.93	0.11	5.60	0.002	0.03	0.07	0.12
123	0.04	0.004	0.28	0.21	0.16	0.27	0.50	52.15	0.09	4.77	0.001	0.03	0.06	0.11
125	0.07	0.006	0.34	0.36	0.26	0.35	0.53	56.43	0.09	4.99	0.002	0.09	0.13	0.19
137	0.05	0.006	0.45	0.29	0.15	0.26	0.50	46.88	0.12	5.51	0.003	0.04	0.07	0.14
146	0.05	0.004	0.38	0.22	0.14	0.26	0.47	49.70	0.08	4.15	0.002	0.03	0.06	0.10
158	0.06	0.005	0.29	0.40	0.10	0.17	0.37	85.39	0.07	6.38	0.001	0.04	0.07	0.15
169	0.07	0.004	0.44	0.25	0.10	0.16	0.42	60.38	0.06	3.55	0.002	0.02	0.04	0.10
176	0.05	0.004	0.41	0.26	0.10	0.15	0.39	66.27	0.08	5.07	0.002	0.03	0.04	0.10
182	0.07	0.004	0.43	0.29	0.10	0.17	0.42	77.40	0.05	3.87	0.002	0.03	0.05	0.12
192	0.05	0.003	0.39	0.35	0.06	0.09	0.42	128.24	0.05	6.77	0.001	0.02	0.03	0.15
201	0.15	0.035	0.10	3.05	0.60	0.88	0.88	86.97	0.24	20.47	0.003	1.83	2.70	2.68
208	0.07	0.006	0.41	0.41	0.13	0.28	0.59	73.59	0.07	5.50	0.002	0.05	0.11	0.24
219	0.06	0.006	0.46	0.52	0.06	0.16	0.53	93.77	0.09	8.65	0.003	0.03	0.08	0.28
231	0.07	0.008	0.49	0.58	0.06	0.18	0.59	75.19	0.12	8.70	0.004	0.04	0.11	0.35

LB - HHS2

Depth	X	SARM	ARM40/	SIRM	IRM40/	IRM100/	IRM1T/	SIRM/	SARM/X	SIRM/X	ARM40mT	IRM40mT	IRM100mT	IRM 1T
(cm)	(10^{-6} m^3 kg^{-1})	(10^{-6} Am^2 kg^{-1})	SARM	(10^{-6} Am^2 kg^{-1})	SIRM	SIRM	SIRM	SARM	(kAm^{-1})	(kAm^{-1})	(10^{-6} Am^2 kg^{-1})	(10^{-6} Am^2 kg^{-1})	(10^{-6} Am^2 kg^{-1})	(10^{-6} Am^2 kg^{-1})
5	0.04	0.009	0.21	0.32	0.22	0.55	0.83	35.18	0.22	7.72	0.002	0.07	0.18	0.27
12	0.04	0.005	0.27	0.20	0.15	0.32	0.54	40.02	0.12	4.75	0.001	0.03	0.06	0.11
21	0.03	0.004	0.26	0.15	0.13	0.29	0.54	40.21	0.11	4.61	0.001	0.02	0.05	0.08
35	0.04	0.004	0.24	0.19	0.12	0.27	0.49	50.86	0.09	4.71	0.001	0.02	0.05	0.09
45	0.04	0.004	0.24	0.18	0.12	0.26	0.49	48.89	0.11	5.16	0.001	0.02	0.05	0.09
58	0.05	0.004	0.29	0.22	0.11	0.18	0.43	57.39	0.07	4.19	0.001	0.02	0.04	0.09
68	0.07	0.004	0.24	0.28	0.08	0.17	0.38	75.11	0.06	4.14	0.001	0.02	0.05	0.11
76	0.05	0.003	0.29	0.27	0.06	0.11	0.39	99.71	0.06	5.94	0.001	0.02	0.03	0.11
83	0.04	0.002	0.30	0.22	0.06	0.13	0.35	96.67	0.06	6.07	0.001	0.01	0.03	0.07
92	0.02	0.002	0.33	0.14	0.10	0.23	0.46	61.00	0.12	7.49	0.001	0.01	0.03	0.07
100	0.04	0.006	0.33	0.24	0.18	0.30	0.55	41.19	0.13	5.56	0.002	0.04	0.07	0.13
108	0.05	0.003	0.42	0.28	0.09	0.16	0.38	84.39	0.07	5.52	0.001	0.03	0.04	0.10
126	0.04	0.002	0.50	0.25	0.06	0.13	0.38	115.83	0.05	6.32	0.001	0.01	0.03	0.10
137	0.04	0.002	0.59	0.31	0.05	0.09	0.38	129.59	0.06	7.78	0.001	0.01	0.03	0.12
146	0.05	0.003	0.57	0.35	0.06	0.12	0.45	128.23	0.06	7.54	0.002	0.02	0.04	0.16
161	0.04	0.002	0.46	0.29	0.05	0.11	0.40	133.33	0.05	6.67	0.001	0.01	0.03	0.11
169	0.07	0.006	0.33	0.34	0.07	0.13	0.37	61.03	0.08	5.14	0.002	0.03	0.05	0.13
180	0.06	0.005	0.24	0.35	0.10	0.17	0.41	67.94	0.09	5.78	0.001	0.04	0.06	0.14
186	0.05	0.002	0.29	0.33	0.06	0.13	0.44	136.00	0.05	6.45	0.001	0.02	0.04	0.14
194	0.06	0.007	0.29	0.38	0.11	0.19	0.49	53.29	0.11	5.91	0.002	0.04	0.07	0.19
205	0.06	0.007	0.26	0.41	0.18	0.36	0.52	61.83	0.10	6.35	0.002	0.07	0.15	0.22

LB - HHS3

Depth	X	SARM	ARM40/	SIRM	IRM40/	IRM100/	IRM1T/	SIRM/	SARM/X	SIRM/X	ARM40mT	IRM40mT	IRM100mT	IRM 1T
(cm)	(10^{-6} m^3 kg^{-1})	(10^{-6} Am^2 kg^{-1})	SARM	(10^{-6} Am^2 kg^{-1})	SIRM	SIRM	SIRM	SARM	(kAm^{-1})	(kAm^{-1})	(10^{-6} Am^2 kg^{-1})	(10^{-6} Am^2 kg^{-1})	(10^{-6} Am^2 kg^{-1})	(10^{-6} Am^2 kg^{-1})
2	0.05	0.014	0.18	0.45	0.38	0.68	0.82	32.39	0.26	8.37	0.002	0.17	0.31	0.37
11	0.05	0.016	0.20	0.30	0.27	0.49	0.67	18.84	0.30	5.62	0.003	0.08	0.15	0.20
18	0.10	0.021	0.18	0.57	0.43	0.67	0.85	27.48	0.20	5.55	0.004	0.24	0.38	0.48
30	0.11	0.021	0.20	0.90	0.33	0.68	0.86	43.45	0.19	8.43	0.004	0.29	0.62	0.78
36	0.10	0.018	0.31	1.35	0.21	0.53	0.79	73.29	0.19	14.09	0.006	0.28	0.71	1.07
42	0.09	0.025	0.24	1.80	0.23	0.57	0.95	73.37	0.26	19.05	0.006	0.42	1.03	1.71
51	0.17	0.030	0.31	4.33	0.14	0.44	0.96	145.71	0.17	24.94	0.009	0.60	1.92	4.16
57	0.09	0.021	0.33	1.27	0.20	0.53	0.85	61.03	0.23	13.92	0.007	0.25	0.67	1.08
64	0.04	0.012	0.30	0.49	0.24	0.56	0.85	40.73	0.28	11.59	0.004	0.12	0.27	0.41
70	0.06	0.021	0.20	0.36	0.41	0.59	0.75	17.33	0.33	5.71	0.004	0.15	0.21	0.27
77	0.06	0.016	0.25	0.31	0.30	0.50	0.66	19.80	0.27	5.31	0.004	0.09	0.15	0.20
84	0.05	0.012	0.24	0.27	0.26	0.45	0.63	23.19	0.24	5.48	0.003	0.07	0.12	0.17
91	0.05	0.007	0.32	0.19	0.19	0.37	0.60	27.33	0.14	3.94	0.002	0.04	0.07	0.12
97	0.03	0.005	0.45	0.16	0.13	0.25	0.51	34.46	0.15	5.22	0.002	0.02	0.04	0.08
109	0.03	0.004	0.45	0.16	0.14	0.24	0.51	37.05	0.13	4.97	0.002	0.02	0.04	0.08
111	0.04	0.005	0.37	0.19	0.16	0.27	0.51	38.00	0.12	4.56	0.002	0.03	0.05	0.10
119	0.04	0.004	0.43	0.16	0.12	0.23	0.47	39.60	0.10	4.05	0.002	0.02	0.04	0.07
125	0.02	0.003	0.51	0.10	0.10	0.25	0.50	36.57	0.15	5.57	0.001	0.01	0.03	0.05
135	0.02	0.003	0.47	0.09	0.17	0.35	0.64	29.50	0.15	4.43	0.001	0.02	0.03	0.06
139	0.02	0.003	0.50	0.09	0.20	0.39	0.69	27.26	0.20	5.45	0.002	0.02	0.03	0.06

HF - LGS1

Depth	X	SARM	ARM40/	SIRM	IRM40/	IRM100/	IRM1T/	SIRM/	SARM/X	SIRM/X	ARM40mT	IRM40mT	IRM100mT	IRM 1T
(cm)	(10^{-6} m^3 kg^{-1})	(10^{-6} Am^2 kg^{-1})	SARM	(10^{-6} Am^2 kg^{-1})	SIRM	SIRM	SIRM	SARM	(kAm^{-1})	(kAm^{-1})	(10^{-6} Am^2 kg^{-1})	(10^{-6} Am^2 kg^{-1})	(10^{-6} Am^2 kg^{-1})	(10^{-6} Am^2 kg^{-1})
6	0.11	0.014	0.32	0.86	0.11	0.23	0.79	60.89	0.13	8.06	0.005	0.09	0.19	0.68
14	0.12	0.013	0.37	1.01	0.10	0.21	0.68	75.96	0.11	8.53	0.005	0.10	0.21	0.68
25	0.13	0.017	0.22	1.33	0.14	0.23	0.64	79.33	0.13	10.01	0.004	0.19	0.30	0.85
37	0.12	0.009	0.38	1.11	0.05	0.13	0.66	120.78	0.08	9.56	0.004	0.06	0.14	0.73
50	0.12	0.016	0.33	1.15	0.10	0.23	0.75	73.62	0.13	9.70	0.005	0.12	0.26	0.86
58	0.12	0.014	0.28	1.12	0.16	0.29	0.77	79.64	0.12	9.23	0.004	0.18	0.32	0.85
67	0.11	0.008	0.38	0.90	0.06	0.12	0.70	115.15	0.07	7.95	0.003	0.06	0.11	0.63
78	0.12	0.013	0.29	1.01	0.08	0.16	0.70	79.14	0.11	8.65	0.004	0.08	0.16	0.71
87	0.12	0.012	0.35	0.98	0.09	0.18	0.75	83.84	0.10	8.44	0.004	0.09	0.18	0.73
96	0.12	0.015	0.30	1.09	0.11	0.21	0.75	73.83	0.12	9.05	0.004	0.11	0.23	0.82
107	0.12	0.015	0.32	1.19	0.08	0.15	0.73	79.28	0.13	10.29	0.005	0.09	0.18	0.86
119	0.12	0.016	0.32	0.95	0.13	0.28	0.80	58.28	0.14	7.93	0.005	0.12	0.26	0.75
131	0.11	0.014	0.36	0.68	0.13	0.27	0.85	49.69	0.12	6.20	0.005	0.09	0.18	0.58
144	0.09	0.013	0.40	0.55	0.12	0.26	0.82	42.36	0.14	5.93	0.005	0.07	0.15	0.45
152	0.15	0.015	0.27	0.83	0.19	0.31	0.78	53.32	0.11	5.63	0.004	0.16	0.26	0.65
159	0.17	0.019	0.23	0.76	0.22	0.33	0.71	39.78	0.12	4.58	0.004	0.17	0.25	0.53
165	0.12	0.007	0.48	0.52	0.06	0.15	0.75	79.11	0.05	4.26	0.003	0.03	0.08	0.39
174	0.11	0.004	0.53	0.27	0.09	0.17	0.60	61.15	0.04	2.34	0.002	0.02	0.05	0.16

HF - NGS1

Depth	X	SARM	ARM40/	SIRM	IRM40/	IRM100/	IRM1T/	SIRM/	SARM/X	SIRM/X	ARM40mT	IRM40mT	IRM100mT	IRM 1T
(cm)	(10^{-6} m^3 kg^{-1})	(10^{-6} Am^2 kg^{-1})	SARM	(10^{-6} Am^2 kg^{-1})	SIRM	SIRM	SIRM	SARM	(kAm^{-1})	(kAm^{-1})	(10^{-6} Am^2 kg^{-1})	(10^{-6} Am^2 kg^{-1})	(10^{-6} Am^2 kg^{-1})	(10^{-6} Am^2 kg^{-1})
9	0.12	0.036	0.25	1.09	0.20	0.46	0.77	30.36	0.29	8.92	0.009	0.22	0.51	0.84
18	0.10	0.021	0.28	0.77	0.15	0.32	0.67	36.93	0.20	7.51	0.006	0.12	0.25	0.51
29	0.12	0.014	0.29	1.03	0.20	0.36	0.64	74.36	0.11	8.45	0.004	0.20	0.37	0.66
41	0.11	0.007	0.43	0.64	0.07	0.16	0.52	89.78	0.07	5.91	0.003	0.05	0.11	0.34
51	0.11	0.009	0.40	0.70	0.09	0.22	0.59	75.28	0.08	6.39	0.004	0.07	0.16	0.41
57	0.11	0.005	0.48	0.53	0.05	0.11	0.45	110.14	0.04	4.91	0.002	0.03	0.06	0.24
62	0.11	0.006	0.51	0.53	0.06	0.14	0.51	87.61	0.06	5.00	0.003	0.03	0.08	0.27
69	0.11	0.006	0.46	0.67	0.05	0.12	0.47	117.39	0.05	6.18	0.003	0.03	0.08	0.32
73	0.10	0.008	0.43	0.86	0.08	0.18	0.51	112.79	0.07	8.27	0.003	0.07	0.16	0.44
78	0.12	0.014	0.24	1.31	0.09	0.16	0.46	95.30	0.11	10.61	0.003	0.12	0.21	0.60
82	0.11	0.006	0.47	0.51	0.07	0.17	0.55	85.75	0.05	4.42	0.003	0.04	0.09	0.28
86	0.12	0.005	0.54	0.59	0.04	0.10	0.52	114.61	0.04	5.15	0.003	0.03	0.06	0.31
93	0.11	0.005	0.57	0.56	0.04	0.08	0.44	122.54	0.04	4.92	0.003	0.02	0.04	0.25
101	0.11	0.006	0.49	0.43	0.07	0.14	0.47	74.81	0.05	4.06	0.003	0.03	0.06	0.20
106	0.09	0.008	0.44	0.54	0.07	0.16	0.54	66.03	0.09	5.89	0.004	0.04	0.09	0.29
113	0.08	0.009	0.47	0.56	0.07	0.16	0.51	60.05	0.11	6.82	0.004	0.04	0.09	0.29
117	0.09	0.007	0.47	0.56	0.07	0.15	0.50	74.87	0.08	6.31	0.003	0.04	0.08	0.28
127	0.09	0.010	0.41	0.82	0.08	0.17	0.55	81.18	0.11	8.74	0.004	0.07	0.14	0.45
145	0.12	0.011	0.32	1.25	0.06	0.12	0.46	110.36	0.10	10.53	0.004	0.08	0.15	0.57
160	0.11	0.014	0.33	1.13	0.08	0.16	0.52	80.07	0.13	10.53	0.005	0.09	0.18	0.59
175	0.11	0.008	0.37	1.51	0.03	0.08	0.41	178.64	0.07	13.31	0.003	0.05	0.11	0.61
196	0.11	0.009	0.40	1.05	0.05	0.11	0.46	119.17	0.08	9.42	0.004	0.05	0.12	0.48
202	0.11	0.007	0.39	1.25	0.04	0.10	0.45	168.38	0.07	11.66	0.003	0.05	0.12	0.57
209	0.11	0.006	0.42	0.75	0.06	0.11	0.49	135.58	0.05	6.69	0.002	0.04	0.09	0.37
225	0.12	0.014	0.36	0.66	0.12	0.23	0.64	46.91	0.12	5.56	0.005	0.08	0.16	0.43
237	0.11	0.008	0.44	0.60	0.07	0.14	0.50	78.06	0.07	5.48	0.003	0.04	0.09	0.29
260	0.12	0.006	0.46	0.78	0.07	0.14	0.56	126.16	0.05	6.68	0.003	0.05	0.11	0.44
277	0.13	0.005	0.52	0.90	0.07	0.16	0.56	178.94	0.04	6.86	0.003	0.07	0.15	0.50

HF - TGS1

Depth	X	SARM	ARM40/	SIRM	IRM40/	IRM100/	IRM1T/	SIRM/	SARM/X	SIRM/X	ARM40mT	IRM40mT	IRM100mT	IRM 1T
(cm)	(10^{-6} m^3 kg^{-1})	(10^{-6} Am^2 kg^{-1})	SARM	(10^{-6} Am^2 kg^{-1})	SIRM	SIRM	SIRM	SARM	(kAm^{-1})	(kAm^{-1})	(10^{-6} Am^2 kg^{-1})	(10^{-6} Am^2 kg^{-1})	(10^{-6} Am^2 kg^{-1})	(10^{-6} Am^2 kg^{-1})
6	0.13	0.021	0.30	0.86	0.16	0.37	0.77	41.90	0.16	6.80	0.006	0.14	0.31	0.66
20	0.12	0.017	0.33	0.68	0.16	0.36	0.83	40.51	0.14	5.71	0.006	0.11	0.25	0.57
34	0.12	0.019	0.30	0.84	0.15	0.34	0.75	44.53	0.16	6.96	0.006	0.12	0.28	0.64
41	0.12	0.024	0.27	0.97	0.14	0.28	0.71	41.06	0.20	8.27	0.007	0.14	0.28	0.69
51	0.12	0.025	0.34	1.00	0.14	0.27	0.68	39.52	0.22	8.53	0.009	0.14	0.27	0.68
61	0.11	0.026	0.35	0.90	0.15	0.30	0.71	34.23	0.23	7.95	0.009	0.14	0.27	0.64
72	0.12	0.046	0.63	0.97	0.14	0.28	0.71	20.96	0.40	8.37	0.029	0.14	0.28	0.69
82	0.12	0.027	0.28	0.98	0.15	0.28	0.68	36.00	0.23	8.40	0.008	0.15	0.28	0.66
92	0.11	0.020	0.21	1.01	0.14	0.26	0.67	49.82	0.18	8.91	0.004	0.14	0.26	0.67
101	0.11	0.014	0.68	1.00	0.10	0.20	0.62	73.11	0.12	8.78	0.009	0.10	0.20	0.62
109	0.11	0.024	0.32	1.00	0.12	0.23	0.64	41.85	0.21	8.80	0.008	0.12	0.23	0.64
115	0.10	0.027	0.41	0.94	0.12	0.23	0.68	35.12	0.26	9.12	0.011	0.11	0.22	0.64
122	0.09	0.016	0.49	0.64	0.07	0.18	0.63	38.89	0.19	7.25	0.008	0.05	0.12	0.40
131	0.09	0.017	0.40	0.72	0.10	0.21	0.70	41.13	0.19	7.84	0.007	0.07	0.15	0.50
138	0.07	0.018	0.63	0.21	0.19	0.45	0.81	11.65	0.27	3.17	0.011	0.04	0.09	0.17
144	0.07	0.009	0.59	0.22	0.18	0.40	0.80	26.19	0.12	3.26	0.005	0.04	0.09	0.18
149	0.06	0.008	0.64	0.16	0.23	0.54	0.92	19.86	0.13	2.52	0.005	0.04	0.09	0.15
155	0.06	0.009	0.62	0.18	0.23	0.54	0.90	20.27	0.14	2.86	0.005	0.04	0.10	0.16
161	0.06	0.010	0.57	0.19	0.21	0.49	0.83	18.63	0.17	3.12	0.006	0.04	0.09	0.16
170	0.07	0.008	0.56	0.17	0.19	0.37	0.78	22.93	0.10	2.39	0.004	0.03	0.07	0.14
178	0.08	0.010	0.47	0.24	0.21	0.46	0.82	23.81	0.12	2.85	0.005	0.05	0.11	0.19
192	0.08	0.010	0.43	0.22	0.20	0.43	0.83	21.12	0.13	2.73	0.004	0.04	0.09	0.18
201	0.09	0.013	0.47	0.25	0.19	0.41	0.83	18.82	0.16	2.95	0.006	0.05	0.10	0.21
213	0.08	0.012	0.41	0.45	0.15	0.26	0.69	36.84	0.15	5.62	0.005	0.07	0.12	0.31
228	0.08	0.011	0.48	0.21	0.21	0.47	0.86	20.24	0.14	2.76	0.005	0.05	0.10	0.18
237	0.08	0.007	0.51	0.18	0.19	0.45	0.85	25.87	0.09	2.31	0.003	0.03	0.08	0.15
246	0.08	0.010	0.47	0.23	0.19	0.42	0.85	23.75	0.13	3.03	0.005	0.04	0.10	0.20
259	0.09	0.010	0.56	0.31	0.21	0.42	0.85	29.49	0.12	3.49	0.006	0.07	0.13	0.26

HF - TGS2

Depth	X	SARM	ARM40/	SIRM	IRM40/	IRM100/	IRM1T/	SIRM/	SARM/X	SIRM/X	ARM40mT	IRM40mT	IRM100mT	IRM 1T
(cm)	(10^{-6} m^3 kg^{-1})	(10^{-6} Am^2 kg^{-1})	SARM	(10^{-6} Am^2 kg^{-1})	SIRM	SIRM	SIRM	SARM	(kAm^{-1})	(kAm^{-1})	(10^{-6} Am^2 kg^{-1})	(10^{-6} Am^2 kg^{-1})	(10^{-6} Am^2 kg^{-1})	(10^{-6} Am^2 kg^{-1})
7	0.13	0.027	0.29	0.89	0.15	0.32	0.74	33.50	0.21	6.92	0.008	0.13	0.29	0.66
17	0.12	0.024	0.33	0.79	0.12	0.26	0.72	32.26	0.20	6.49	0.008	0.09	0.21	0.57
32	0.11	0.020	0.36	0.95	0.09	0.21	0.68	47.83	0.17	8.33	0.007	0.09	0.20	0.64
47	0.11	0.024	0.35	0.99	0.11	0.26	0.74	40.73	0.22	9.06	0.008	0.11	0.26	0.73
65	0.11	0.016	0.38	0.84	0.10	0.23	0.69	53.74	0.14	7.44	0.006	0.08	0.20	0.58
77	0.11	0.014	0.41	0.74	0.11	0.24	0.70	53.75	0.12	6.50	0.006	0.08	0.18	0.51
87	0.12	0.014	0.35	0.72	0.12	0.30	0.74	52.48	0.12	6.08	0.005	0.09	0.21	0.53
96	0.12	0.013	0.36	0.76	0.12	0.29	0.71	59.11	0.11	6.47	0.005	0.09	0.22	0.54
111	0.12	0.013	0.36	0.68	0.10	0.24	0.69	51.86	0.11	5.78	0.005	0.07	0.16	0.47
126	0.12	0.017	0.33	0.72	0.12	0.30	0.76	43.61	0.14	5.89	0.005	0.09	0.22	0.55
141	0.11	0.013	0.36	0.54	0.14	0.32	0.82	41.79	0.11	4.72	0.005	0.07	0.17	0.44
161	0.11	0.010	0.43	0.47	0.10	0.22	0.68	47.18	0.09	4.39	0.004	0.05	0.10	0.32
169	0.10	0.008	0.45	0.42	0.09	0.19	0.61	55.59	0.08	4.19	0.003	0.04	0.08	0.26
179	0.10	0.006	0.49	0.31	0.11	0.24	0.72	48.87	0.07	3.23	0.003	0.03	0.07	0.23
188	0.09	0.006	0.56	0.33	0.10	0.24	0.71	52.78	0.07	3.72	0.003	0.03	0.08	0.23
196	0.09	0.007	0.49	0.37	0.10	0.23	0.71	54.35	0.08	4.21	0.003	0.04	0.08	0.26
209	0.08	0.005	0.55	0.34	0.10	0.24	0.72	63.65	0.07	4.22	0.003	0.03	0.08	0.25
225	0.09	0.008	0.47	0.46	0.12	0.29	0.76	55.49	0.09	5.01	0.004	0.06	0.13	0.35
234	0.10	0.010	0.42	0.61	0.12	0.31	0.77	61.91	0.10	5.96	0.004	0.08	0.19	0.47
243	0.10	0.010	0.42	0.65	0.13	0.33	0.76	68.25	0.09	6.34	0.004	0.08	0.21	0.49
249	0.11	0.011	0.43	0.80	0.13	0.35	0.77	70.29	0.10	7.26	0.005	0.11	0.28	0.61
254	0.11	0.009	0.43	0.60	0.12	0.27	0.74	65.52	0.09	5.65	0.004	0.07	0.17	0.44
261	0.11	0.008	0.41	0.58	0.10	0.24	0.73	68.14	0.08	5.41	0.003	0.06	0.14	0.42
270	0.11	0.012	0.43	0.74	0.13	0.32	0.77	62.92	0.11	6.90	0.005	0.09	0.24	0.57
282	0.11	0.014	0.39	0.89	0.14	0.37	0.80	63.13	0.13	8.11	0.005	0.13	0.33	0.71
292	0.10	0.010	0.42	0.76	0.11	0.29	0.74	77.80	0.10	7.65	0.004	0.09	0.22	0.56

HF - TGS3

Depth	X	SARM	ARM40/	SIRM	IRM40/	IRM100/	IRM1T/	SIRM/	SARM/X	SIRM/X	ARM40mT	IRM40mT	IRM100mT	IRM 1T
(cm)	(10^{-6} m^3 kg^{-1})	(10^{-6} Am^2 kg^{-1})	SARM	(10^{-6} Am^2 kg^{-1})	SIRM	SIRM	SIRM	SARM	(kAm^{-1})	(kAm^{-1})	(10^{-6} Am^2 kg^{-1})	(10^{-6} Am^2 kg^{-1})	(10^{-6} Am^2 kg^{-1})	(10^{-6} Am^2 kg^{-1})
3	0.14	0.028	0.26	0.97	0.17	0.43	0.82	34.64	0.21	7.10	0.007	0.17	0.41	0.79
9	0.13	0.020	0.32	0.78	0.17	0.38	0.80	38.58	0.16	6.22	0.006	0.13	0.29	0.62
16	0.11	0.010	0.41	0.61	0.13	0.31	0.80	62.43	0.09	5.57	0.004	0.08	0.19	0.49
20	0.10	0.008	0.47	0.55	0.10	0.23	0.73	66.60	0.08	5.32	0.004	0.05	0.13	0.40
25	0.10	0.007	0.47	0.45	0.09	0.21	0.71	66.57	0.07	4.42	0.003	0.04	0.09	0.32
36	0.10	0.007	0.48	0.50	0.07	0.16	0.65	72.31	0.07	4.97	0.003	0.03	0.08	0.32
42	0.11	0.011	0.43	0.66	0.14	0.36	0.82	62.41	0.10	6.20	0.005	0.09	0.24	0.54

LB - WBS1

Depth	X	SARM	ARM40/	SIRM	IRM40/	IRM100/	IRM1T/	SIRM/	SARM/X	SIRM/X	ARM40mT	IRM40mT	IRM100mT	IRM 1T
(cm)	(10^{-6} m^3 kg^{-1})	(10^{-6} Am^2 kg^{-1})	SARM	(10^{-6} Am^2 kg^{-1})	SIRM	SIRM	SIRM	SARM	(kAm^{-1})	(kAm^{-1})	(10^{-6} Am^2 kg^{-1})	(10^{-6} Am^2 kg^{-1})	(10^{-6} Am^2 kg^{-1})	(10^{-6} Am^2 kg^{-1})
3	0.06	0.010	0.33	0.36	0.22	0.51	0.73	36.43	0.18	6.51	0.003	0.08	0.18	0.26
8	0.05	0.006	0.30	0.43	0.22	0.44	0.61	66.60	0.12	7.82	0.002	0.09	0.19	0.26
15	0.06	0.014	0.30	0.50	0.24	0.55	0.79	36.18	0.21	7.66	0.004	0.12	0.27	0.39
20	0.18	0.055	0.25	1.91	0.19	0.57	0.89	34.90	0.31	10.78	0.013	0.36	1.09	1.70
28	0.08	0.021	0.27	0.68	0.25	0.55	0.81	31.69	0.28	8.90	0.006	0.17	0.37	0.55
32	0.06	0.008	0.26	0.51	0.15	0.34	0.71	61.34	0.15	9.10	0.002	0.08	0.17	0.37
38	0.05	0.004	0.42	0.37	0.10	0.21	0.48	91.48	0.08	7.00	0.002	0.04	0.08	0.18
44	0.06	0.009	0.31	0.41	0.19	0.40	0.60	45.39	0.15	6.78	0.003	0.08	0.16	0.25
48	0.04	0.010	0.32	0.30	0.20	0.39	0.55	29.74	0.23	6.88	0.003	0.06	0.12	0.17
53	0.03	0.016	0.26	0.33	0.38	0.67	0.83	20.52	0.52	10.68	0.004	0.13	0.22	0.27
58	0.02	0.009	0.41	0.09	0.36	0.68	0.90	9.84	0.38	3.69	0.004	0.03	0.06	0.08
62	0.04	0.005	0.44	0.14	0.16	0.32	0.55	29.60	0.11	3.25	0.002	0.02	0.04	0.08
67	0.03	0.003	0.56	0.20	0.08	0.17	0.34	61.65	0.11	6.55	0.002	0.02	0.03	0.07
73	0.05	0.003	0.49	0.38	0.05	0.10	0.27	111.76	0.07	8.27	0.002	0.02	0.04	0.10
79	0.03	0.004	0.48	0.20	0.12	0.23	0.42	45.93	0.14	6.22	0.002	0.02	0.04	0.08
84	0.03	0.004	0.54	0.18	0.12	0.23	0.46	44.46	0.13	5.59	0.002	0.02	0.04	0.08

LB - WBS2

Depth	X	SARM	ARM40/	SIRM	IRM40/	IRM100/	IRM1T/	SIRM/	SARM/X	SIRM/X	ARM40mT	IRM40mT	IRM100mT	IRM 1T
(cm)	(10^{-6} m^3 kg^{-1})	(10^{-6} Am^2 kg^{-1})	SARM	(10^{-6} Am^2 kg^{-1})	SIRM	SIRM	SIRM	SARM	(kAm^{-1})	(kAm^{-1})	(10^{-6} Am^2 kg^{-1})	(10^{-6} Am^2 kg^{-1})	(10^{-6} Am^2 kg^{-1})	(10^{-6} Am^2 kg^{-1})
4	0.04	0.004	0.45	0.21	0.13	0.33	0.55	49.83	0.10	4.86	0.002	0.03	0.07	0.11
9	0.04	0.002	0.37	0.18	0.09	0.19	0.40	75.50	0.07	4.92	0.001	0.02	0.03	0.07
20	0.05	0.002	0.27	0.24	0.06	0.10	0.28	107.93	0.05	5.06	0.001	0.01	0.02	0.07
30	0.04	0.001	0.47	0.26	0.04	0.09	0.24	193.05	0.03	6.11	0.001	0.01	0.02	0.06
36	0.06	0.002	0.48	0.35	0.04	0.10	0.31	196.52	0.03	5.72	0.001	0.02	0.03	0.11
42	0.05	0.002	0.57	0.27	0.04	0.09	0.29	178.29	0.03	5.27	0.001	0.01	0.02	0.08
51	0.05	0.001	0.55	0.30	0.04	0.10	0.24	205.05	0.03	5.78	0.001	0.01	0.03	0.07
55	0.05	0.002	0.54	0.33	0.04	0.09	0.26	181.42	0.03	6.13	0.001	0.01	0.03	0.09
61	0.07	0.003	0.61	0.42	0.04	0.11	0.30	142.06	0.04	5.88	0.002	0.02	0.05	0.13
70	0.08	0.002	0.53	0.57	0.02	0.04	0.20	373.53	0.02	7.17	0.001	0.01	0.02	0.11
75	0.07	0.001	0.50	0.54	0.02	0.04	0.23	369.91	0.02	7.68	0.001	0.01	0.02	0.12
79	0.07	0.002	0.63	0.43	0.02	0.05	0.24	251.54	0.03	6.29	0.001	0.01	0.02	0.10
87	0.09	0.002	0.48	0.58	0.02	0.03	0.20	355.70	0.02	6.54	0.001	0.01	0.02	0.11
94	0.09	0.003	0.30	0.48	0.02	0.05	0.20	183.16	0.03	5.17	0.001	0.01	0.03	0.10
96	0.06	0.012	0.48	0.50	0.09	0.39	0.68	42.59	0.19	7.98	0.006	0.05	0.20	0.34
99	0.05	0.011	0.42	0.28	0.18	0.47	0.67	25.05	0.22	5.39	0.005	0.05	0.13	0.19
108	0.05	0.034	0.63	1.71	0.10	0.59	0.93	50.23	0.68	34.36	0.021	0.18	1.01	1.59
113	0.03	0.044	0.35	0.18	0.43	0.89	0.98	4.08	1.51	6.15	0.015	0.08	0.16	0.17
118	0.06	0.028	0.52	0.59	0.12	0.63	0.96	21.33	0.49	10.49	0.014	0.07	0.37	0.56
127	0.05	0.014	0.47	0.26	0.16	0.65	0.96	18.78	0.29	5.49	0.007	0.04	0.17	0.25
131	0.04	0.013	0.49	0.43	0.18	0.74	0.97	33.30	0.34	11.19	0.006	0.08	0.32	0.41
136	0.02	0.009	0.61	0.70	0.07	0.38	0.61	76.36	0.53	40.47	0.006	0.05	0.26	0.42
140	0.05	0.015	0.60	0.67	0.13	0.66	0.94	45.28	0.32	14.55	0.009	0.09	0.44	0.63
145	0.05	0.011	0.56	1.45	0.04	0.20	0.42	128.80	0.21	27.40	0.006	0.06	0.29	0.61
150	0.04	0.009	0.57	0.59	0.08	0.34	0.64	64.01	0.23	14.63	0.005	0.05	0.20	0.38
156	0.04	0.008	0.53	0.29	0.12	0.47	0.77	35.54	0.20	7.20	0.004	0.03	0.14	0.23
164	0.04	0.010	0.55	0.43	0.12	0.49	0.82	44.18	0.22	9.89	0.005	0.05	0.21	0.36
171	0.06	0.007	0.50	0.31	0.09	0.30	0.61	45.86	0.11	4.86	0.003	0.03	0.09	0.19
179	0.08	0.008	0.44	0.30	0.09	0.33	0.60	38.10	0.10	3.95	0.004	0.03	0.10	0.18
188	0.07	0.007	0.41	0.24	0.12	0.34	0.60	32.23	0.10	3.27	0.003	0.03	0.08	0.14
198	0.06	0.006	0.44	0.32	0.07	0.23	0.48	53.49	0.11	5.81	0.003	0.02	0.07	0.15
208	0.05	0.012	0.59	0.68	0.07	0.40	0.70	57.87	0.24	13.77	0.007	0.05	0.27	0.48

GLEN ETIVE

Sample Code	Source Category	Munsell Colour	X (10^{-6} m^3 kg^{-1})	SARM (10^{-6} Am^2 kg^{-1})	ARM40/ SARM	SIRM (10^{-6} Am^2 kg^{-1})	IRM40/ SIRM	IRM100/ SIRM	IRM1T/ SIRM	SIRM/ SARM	SARM/X (kAm^{-1})	SIRM/X (kAm^{-1})	ARM40mT (10^{-6} Am^2 kg^{-1})	IRM40mT (10^{-6} Am^2 kg^{-1})	IRM100mT (10^{-6} Am^2 kg^{-1})	IRM 1T (10^{-6} Am^2 kg^{-1})
CD 1/1	2	10YR 2/2	5.13	0.28	0.38	16.92	0.29	0.58	1.00	61.12	0.05	3.30	0.106	4.99	9.75	16.92
CD 1/2	2	10YR 2/3	5.01	0.31	0.39	18.30	0.29	0.57	1.00	59.16	0.06	3.65	0.121	5.30	10.47	18.30
CD 1/3	2	10YR 3/2	3.05	0.17	0.46	11.33	0.26	0.54	1.00	66.32	0.06	3.72	0.079	2.93	6.17	11.33
CD 1/4	2	10YR 3/2	6.24	0.31	0.40	21.44	0.31	0.61	1.00	68.88	0.05	3.43	0.126	6.54	13.10	21.44
CD 1/5	2	2.5Y 3/2	6.67	0.32	0.37	22.56	0.35	0.61	0.98	70.94	0.05	3.38	0.117	7.88	13.78	22.18
CD 2/1	3	10YR 2/1	6.49	0.34	0.41	19.59	0.30	0.59	1.00	58.23	0.05	3.02	0.137	5.79	11.64	19.53
CD 2/2	3	10YR 2/3	6.35	0.31	0.41	20.47	0.29	0.59	1.00	65.64	0.05	3.22	0.127	5.88	11.99	20.47
CD 2/3	3	10YR 2/3	4.36	0.24	0.18	14.44	0.28	0.60	1.00	59.28	0.06	3.31	0.043	4.00	8.67	14.44
CD 3/1	4	10YR 2/3	2.58	0.13	0.95	9.20	0.26	0.58	1.00	71.83	0.05	3.57	0.122	2.41	5.31	9.20
CD 3/2	4	10YR 2/1	5.53	0.32	0.46	17.93	0.00	0.55	0.98	56.37	0.06	3.24	0.145	0.07	9.95	17.55
CD 3/3	4	10YR 2/3	6.96	0.42	0.44	31.47	0.22	0.56	1.00	75.27	0.06	4.52	0.182	7.02	17.74	31.33
CD 4	4	2.5Y 4/4	6.47	0.41	0.45	39.59	0.31	0.51	1.00	95.62	0.06	6.12	0.185	12.27	20.11	39.55
CD 5/1	5#1	2.5Y 4/4	0.59	0.07	0.52	2.98	0.21	0.45	0.96	42.80	0.12	5.09	0.036	0.63	1.35	2.88
CD 5/2	5#1	7.5YR 2.5/2	0.64	0.08	0.49	4.47	0.16	0.39	0.96	59.26	0.12	7.04	0.037	0.72	1.76	4.30
CD 5/3	5#1	10YR 3/6	3.91	0.22	0.33	19.94	0.23	0.56	0.95	89.16	0.06	5.10	0.074	4.68	11.19	18.99
CD 6/1	5#1	10YR 3/4	7.31	0.39	0.42	26.00	0.22	0.50	0.96	66.88	0.05	3.56	0.163	5.84	12.88	25.07
CD 6/2	5#1	10YR 2/2	6.74	0.37	0.41	24.26	0.25	0.57	0.99	64.70	0.06	3.60	0.155	5.96	13.85	23.91
CD 6/3	5#1	7.5YR 2.5/2	7.56	0.44	0.40	28.27	0.26	0.59	1.00	64.87	0.06	3.74	0.175	7.27	16.79	28.27
CD 6/4	5#1	10YR 3/6	3.06	0.46	0.37	32.37	0.30	0.66	0.97	70.98	0.15	10.56	0.167	9.57	21.26	32.37
CD 7/1	4	2.5Y 3.5/3	3.96	0.21	0.34	26.20	0.19	0.44	0.98	125.36	0.05	6.62	0.071	5.04	11.64	11.64
CD 7/2	4	10YR 4/6	4.63	0.28	0.35	28.85	0.22	0.57	0.95	102.18	0.06	6.23	0.099	6.28	16.43	2.86
CD 8/1	4	2.5Y 4/4	1.64	0.12	0.47	11.31	0.16	0.43	0.80	91.99	0.08	6.92	0.058	1.85	4.88	9.04
CD 8/2	4	7.5YR 2.5/2	0.73	0.09	0.51	7.12	0.13	0.36	0.94	82.30	0.12	9.81	0.044	0.90	2.54	6.66
CD 8/3	4	10YR 3/4	2.99	0.25	0.38	16.39	0.18	0.46	0.93	66.55	0.08	5.49	0.094	3.03	7.47	15.29
MV 1/1	2	10YR 3/4	5.54	0.20	0.27	17.59	0.27	0.58	0.95	88.94	0.04	3.17	0.054	4.73	10.27	16.67
MV 1/2	2	7.5YR 2.5/2	6.66	0.31	0.29	33.28	0.23	0.57	0.93	107.15	0.05	4.99	0.089	7.75	18.84	31.09
MV 1/3	2	2.5Y 4/3	6.38	0.28	0.34	30.43	0.22	0.55	0.94	107.65	0.04	4.77	0.097	6.63	16.61	28.74
MV 1/4	2	2.5Y 3.5/3	6.42	0.23	0.27	22.43	0.28	0.60	0.95	98.09	0.04	3.50	0.061	6.38	13.48	21.31
MV 2/1	5#2	2.5Y 3/3	4.57	0.20	0.34	16.62	0.25	0.56	0.94	81.69	0.04	3.64	0.070	4.16	9.25	15.54
MV 2/2	5#2	10YR 1.5/1	7.25	0.30	0.29	28.39	0.28	0.62	0.94	93.81	0.04	3.92	0.089	7.83	17.52	26.80
MV 2/3	5#2	10YR 2/2	5.02	0.19	0.23	15.25	0.33	0.64	0.91	79.42	0.04	3.03	0.045	5.05	9.83	13.93
MV 3/1	5#2	10YR 3/4	2.50	0.10	0.38	8.82	0.24	0.52	0.92	85.09	0.04	3.53	0.039	2.13	4.62	8.09
MV 3/2	5#2	2.5Y 4/4	4.33	0.19	0.28	16.35	0.29	0.59	0.94	84.99	0.04	3.78	0.055	4.68	9.70	15.31
MV 3/3	5#2	10YR 2/2	3.43	0.19	0.34	17.91	0.23	0.58	0.95	92.37	0.06	5.22	0.066	4.14	10.41	17.04
MV 4/1	5#2	10YR 4/4	0.04	0.02	0.46	0.30	0.23	0.56	0.94	15.23	0.51	7.81	0.009	0.07	0.17	0.28
MV 4/2	5#2	2.5Y 4/4	0.22	0.04	0.42	1.90	0.15	0.35	0.90	51.83	0.17	8.84	0.015	0.29	0.66	1.72
MV 4/3	5#2	10YR 2/1	5.57	0.22	0.30	22.99	0.26	0.63	0.95	102.41	0.04	4.12	0.067	5.98	14.40	21.88
MV 5/1	5#2	10YR 3/3	0.13	0.05	0.44	0.96	0.20	0.49	0.88	18.87	0.40	7.49	0.022	0.19	0.47	0.85
MV 5/2	5#2	2.5Y 4/4	0.15	0.06	0.48	1.62	0.17	0.39	0.89	27.97	0.38	10.61	0.028	0.27	0.63	1.44
MV 5/3	5#2	2.5Y 4.5/4	2.17	0.13	0.36	9.27	0.27	0.59	0.94	70.02	0.06	4.28	0.048	2.48	5.49	8.72
MV 5/4	5#2	2.5Y 4.5/4	2.77	0.18	0.35	11.99	0.27	0.62	0.95	67.83	0.06	4.33	0.062	3.23	7.44	11.33

Key to source categories:

- 2 Lateral moraine
- 3 Bedrock
- 4 Solifluction
- 5#1 Glacial till: catchment headwaters
- 5#2 Glacial till: main valley

APPENDIX 1.4: Source samples, mineral magnetics: parameters and ratios.

HOWGILL FELLS

Sample	Code	Source Category	Munsell Colour	X (10^{-8} m^3 kg^{-1})	SARM (10^{-6} Am^2 kg^{-1})	ARM40/ SARM	SIRM (10^{-4} Am^2 kg^{-1})	IRM40/ SIRM	IRM100/ SIRM	IRM1T/ SIRM	SIRM/ SARM	SARM/X (kAm^{-1})	SIRM/X (kAm^{-1})	ARM40mT (10^{-6} Am^2 kg^{-1})	IRM40mT (10^{-4} Am^2 kg^{-1})	IRM100mT (10^{-4} Am^2 kg^{-1})	IRM 1T (10^{-4} Am^2 kg^{-1})
HF - L	L 1/1	4	2.5Y 3/3	0.14	0.01	0.38	0.39	0.22	0.53	0.87	43.62	0.06	2.828	0.003	0.09	0.21	0.34
HF - L	L 1/2	2#2	2.5Y 3/3	0.15	0.01	0.38	0.64	0.22	0.53	0.87	56.68	0.07	4.194	0.004	0.14	0.34	0.56
HF - L	L 1/3	2#2	2.5Y 4/2	0.16	0.01	0.41	0.48	0.22	0.57	0.88	59.68	0.05	2.901	0.003	0.11	0.27	0.42
HF - L	L 2/1	4	10YR 3/3	0.41	0.23	0.13	1.93	0.59	0.88	0.97	8.22	0.57	4.675	0.030	1.14	1.70	1.88
HF - L	L 2/2	2#2	2.5Y 4/3	0.16	0.02	0.32	0.83	0.19	0.45	0.78	50.54	0.10	5.178	0.005	0.16	0.37	0.64
HF - L	L 2/3	2#2	2.5Y 4/3	0.15	0.01	0.41	0.72	0.20	0.49	0.83	66.69	0.07	4.689	0.005	0.14	0.36	0.60
HF - L	L 3/1	4	2.5Y 4/4	0.15	0.02	0.40	0.75	0.22	0.54	0.87	49.39	0.10	5.050	0.006	0.16	0.40	0.65
HF - L	L 3/2	2#2	2.5Y 4/3	0.21	0.02	0.37	1.15	0.27	0.64	0.89	50.25	0.11	5.480	0.009	0.31	0.74	1.03
HF - L	L 3/3	2#2	2.5Y 3.5/3	0.24	0.02	0.34	1.36	0.27	0.63	0.91	58.33	0.10	5.687	0.008	0.36	0.86	1.23
HF - L	L 4/1	4	10YR 3/4	0.17	0.02	0.30	3.95	0.09	0.17	0.53	180.17	0.13	22.903	0.007	0.36	0.67	2.11
HF - L	L 4/2	2#2	10YR 3/4	0.14	0.02	0.31	3.65	0.06	0.13	0.51	216.94	0.12	25.649	0.005	0.22	0.47	1.86
HF - L	L 4/3	2#2	2.5Y 3.5/4	0.45	0.03	0.36	2.95	0.27	0.61	0.89	93.75	0.07	6.542	0.011	0.81	1.80	2.62
HF - B	B 1/1	4	2.5Y 4/4	0.11	0.01	0.43	0.43	0.10	0.26	0.79	60.87	0.07	4.058	0.003	0.04	0.11	0.35
HF - B	B 1/2	2#2	2.5Y 3.5/3	0.11	0.01	0.45	0.44	0.10	0.26	0.79	63.96	0.06	4.133	0.003	0.04	0.11	0.35
HF - B	B 1/3	2#2	2.5Y 3.5/4	0.10	0.01	0.43	0.53	0.08	0.22	0.77	64.37	0.08	5.313	0.004	0.04	0.12	0.40
HF - B	B 2/1	2#2	5Y 4/2	0.09	0.00	0.54	0.11	0.15	0.34	0.85	22.56	0.05	1.199	0.003	0.02	0.04	0.09
HF - B	B 2/2	2#2	2.5Y 3.5/2	0.10	0.01	0.47	0.18	0.11	0.25	0.80	31.05	0.06	1.843	0.003	0.02	0.05	0.14
HF - B	B 3/1	2#2	2.5Y 3/2	0.16	0.08	0.17	0.91	0.37	0.68	0.94	11.79	0.47	5.517	0.013	0.34	0.62	0.85
HF - B	B 3/2	2#2	2.5Y 3/3	0.15	0.04	0.26	0.78	0.26	0.59	0.94	21.21	0.24	5.175	0.009	0.20	0.46	0.73
HF - B	B 4/1	2#2	2.5Y 3/1	0.10	0.02	0.27	0.50	0.27	0.62	0.87	22.26	0.24	5.244	0.006	0.14	0.31	0.44
HF - B	B 4/2	2#2	2.5Y 4/3	0.12	0.01	0.36	0.47	0.19	0.48	0.77	46.37	0.09	4.061	0.004	0.09	0.23	0.37
HF - B	B 5/1	2#2	2.5Y 4/4	0.07	0.01	0.36	0.19	0.25	0.57	0.87	19.25	0.14	2.688	0.004	0.05	0.11	0.17
HF - B	B 5/2	2#2	2.5Y 4/3	0.07	0.01	0.36	0.19	0.22	0.54	0.88	19.72	0.13	2.660	0.004	0.04	0.10	0.17
HF - B	B 6	2#2	2.5Y 4/2	0.06	0.00	0.57	0.05	0.30	0.67	0.89	10.86	0.08	0.844	0.003	0.01	0.03	0.04
HF - L	BG L1	4	10YR 4/4	0.17	0.04	0.16	0.57	0.32	0.53	0.87	13.03	0.26	3.326	0.007	0.18	0.30	0.50
HF - L	BG L2	4	2.5Y 3/3	0.13	0.03	0.27	0.71	0.26	0.59	0.92	24.35	0.22	5.327	0.008	0.18	0.41	0.65
HF - L	BG L3	4	10YR 3/3	0.16	0.04	0.19	0.80	0.31	0.61	0.90	18.87	0.27	5.060	0.008	0.25	0.48	0.72
HF - L	BG L4	4	2.5Y 3/3	0.12	0.02	0.25	0.49	0.23	0.51	0.90	22.60	0.19	4.221	0.006	0.11	0.25	0.45
HF - L	BG L5	4	10YR 3/4	0.55	0.44	0.07	2.60	0.78	0.96	0.96	5.87	0.80	4.721	0.031	2.02	2.50	2.49
HF - L	BG L6	4	10YR 3/3	0.30	0.12	0.10	0.94	0.61	0.85	0.92	7.76	0.40	3.088	0.012	0.57	0.80	0.86
HF - L	BG L7	4#2	10YR 2/2	0.29	0.13	0.14	1.30	0.73	0.92	0.94	9.85	0.46	4.527	0.018	0.95	1.20	1.23
HF - L	BG L8	4	10YR 4/6	0.30	0.15	0.12	1.00	0.65	0.89	0.95	6.86	0.49	3.345	0.017	0.65	0.89	0.95
HF - L	BG R9	4	10YR 3.5/6	0.62	0.08	0.13	2.11	0.53	0.79	0.92	26.03	0.13	3.410	0.010	1.12	1.67	1.94
HF - L	BG R10	4	10YR 3/4	0.53	0.10	0.11	2.06	0.55	0.77	0.91	19.75	0.20	3.857	0.012	1.14	1.59	1.86
HF - L	BG R11	4#2	10YR 3/3	1.18	0.11	0.18	4.44	0.55	0.79	0.92	39.87	0.09	3.752	0.020	2.43	3.48	4.06
HF - L	BG R12/1	4#1	10YR 3/4	1.31	0.08	0.14	4.29	0.48	0.67	0.88	56.26	0.06	3.285	0.011	2.07	2.86	3.79
HF - L	BG R12/2	4#2	10YR 3/3	0.49	0.04	0.17	2.96	0.26	0.35	0.77	80.54	0.08	6.058	0.006	0.77	1.04	2.29
HF - L	BG R13	4	10YR 2/2	0.22	0.10	0.15	0.91	0.50	0.80	0.92	9.10	0.46	4.216	0.015	0.46	0.73	0.84
HF - L	BG R14/1	7	10YR 2/1	0.01	0.00	0.60	0.06	0.32	0.76	0.91	13.51	0.34	4.533	0.002	0.02	0.04	0.05
HF - L	BG R14/2	8	10YR 3/2	0.02	0.00	0.55	0.07	0.37	0.71	0.91	14.21	0.24	3.375	0.003	0.02	0.05	0.06
HF - L	NG 1	9	10YR 3/3	0.12	0.05	0.16	0.53	0.41	0.66	0.88	10.48	0.42	4.398	0.008	0.21	0.35	0.47
HF - L	NG 2/1	2#1	10YR 3/4	0.22	0.09	0.14	1.01	0.46	0.72	0.88	11.20	0.41	4.582	0.012	0.46	0.72	0.88
HF - L	NG 2/2	2#1	10YR 3/3	0.17	0.06	0.16	0.85	0.37	0.58	0.78	14.65	0.34	5.042	0.009	0.32	0.50	0.67
HF - L	NG 2/3	2#1	2.5Y 3.5/4	0.09	0.01	0.42	0.51	0.08	0.16	0.49	62.99	0.09	5.726	0.003	0.04	0.08	0.25
HF - L	NG 3/1	3	10YR 2/2	0.21	0.06	0.19	1.24	0.33	0.65	0.86	21.42	0.27	5.771	0.011	0.41	0.80	1.07
HF - L	NG 3/2	4	10YR 2.5/3	0.25	0.08	0.18	1.71	0.32	0.65	0.89	22.63	0.31	6.965	0.014	0.55	1.11	1.52
HF - L	NG 4/1	4#1	10YR 3/3	0.12	0.06	0.15	0.56	0.44	0.72	0.87	8.97	0.51	4.595	0.009	0.25	0.40	0.49
HF - L	NG 4/2	4#2	10YR 3/4	0.14	0.03	0.19	0.59	0.27	0.59	0.90	18.45	0.23	4.165	0.006	0.16	0.34	0.53
HF - L	NG 5	9	7.5YR 2.5/1	0.08	0.02	0.30	0.40	0.23	0.51	0.77	23.92	0.22	5.281	0.005	0.09	0.21	0.31
HF - L	LNG 1/1	4	10YR 3/4	0.21	0.06	0.29	1.91	0.24	0.56	0.89	34.15	0.27	9.239	0.016	0.45	1.06	1.69
HF - L	LNG 1/2	2#1	2.5Y 3/3	0.18	0.04	0.25	1.21	0.27	0.60	0.90	29.49	0.23	6.793	0.010	0.33	0.73	1.09
HF - L	LNG 1/3	3	2.5Y 3/3	0.19	0.04	0.27	1.21	0.25	0.57	0.89	33.30	0.20	6.512	0.010	0.30	0.68	1.07

Key to source categories:

- 2#1 Lateral moraine: main valley
- 3 Bedrock
- 4 Solifluction
- 7 Peat
- 8 Peat Substrate
- 9 Storage

HOWGILL FELLS - con't.....

Sample	Code	Source	Munsell	X	SARM	ARM40/	SIRM	IRM40/	IRM100/	IRM1T/	SIRM/	SARM/X	SIRM/X	ARM40mT	IRM40mT	IRM100mT	IRM 1T
		Category	Colour	(10^{-8} m^3 kg^{-1})	(10^{-4} Am^2 kg^{-1})	SARM	(10^{-4} Am^2 kg^{-1})	SIRM	SIRM	SIRM	SARM	(kAm^{-1})	(kAm^{-1})	(10^{-4} Am^2 kg^{-1})	(10^{-4} Am^2 kg^{-1})	(10^{-4} Am^2 kg^{-1})	(10^{-4} Am^2 kg^{-1})
HF - L	LNG 2/1	4	10YR 2/2	0.10	0.04	0.22	0.84	0.30	0.64	0.88	21.22	0.38	8.068	0.009	0.26	0.54	0.74
HF - L	LNG 2/2	4	10YR 2/2	0.11	0.04	0.21	0.87	0.29	0.64	0.87	20.41	0.40	8.193	0.009	0.26	0.56	0.76
HF - L	LNG 3	3	2.5Y 3/3	0.10	0.02	0.31	0.72	0.11	0.23	0.57	46.67	0.16	7.315	0.005	0.08	0.17	0.41
HF - L	LNG 4	3	2.5Y 3/2	0.15	0.03	0.27	0.96	0.24	0.58	0.87	31.59	0.20	6.204	0.008	0.23	0.56	0.83
HF - L	LNG 5	4	10YR 3/2	0.13	0.02	0.27	0.75	0.25	0.58	0.85	32.29	0.18	5.904	0.006	0.19	0.44	0.63
HF - L	LNG 6	4	10YR 4/4	0.19	0.03	0.38	2.05	0.17	0.41	0.76	68.40	0.15	10.518	0.011	0.35	0.84	1.55
HF - L	LNG 7/1	7	10YR 2/2	0.02	0.00	0.67	0.06	0.28	0.70	0.88	13.56	0.17	2.324	0.003	0.02	0.04	0.05
HF - L	LNG 7/2	7	10YR 2/1	0.00	0.00	0.82	0.02	0.24	0.80	1.00	9.27	0.00	0.000	0.002	0.00	0.02	0.02
HF - L	LNG 7/3	8	10YR 2/1	0.00	0.00	0.92	0.02	0.20	0.85	1.00	7.38	0.00	0.000	0.003	0.00	0.02	0.02
HF - L	LNG 7/4	8	10YR 2/1	0.00	0.00	0.72	0.04	0.25	0.77	1.00	12.00	0.00	0.000	0.002	0.01	0.03	0.04
HF - L	LNG 7/5	8	10YR 3/2	0.00	0.00	0.83	0.05	0.20	0.66	1.00	21.33	0.00	0.000	0.002	0.01	0.03	0.05
HF - L	RNG 1/1	7	10YR 2/1	0.05	0.00	0.65	0.27	0.06	0.14	0.41	90.23	0.06	4.995	0.002	0.02	0.04	0.11
HF - L	RNG 1/2	7	10YR 2/1	0.00	0.00	0.90	0.04	0.30	0.77	1.00	15.80	0.00	0.000	0.002	0.01	0.03	0.04
HF - L	RNG 1/3	7	10YR 3/2	0.00	0.00	0.86	0.03	0.20	0.80	1.00	15.43	0.00	0.000	0.002	0.01	0.03	0.03
HF - L	RNG 2/1	4	10YR 2/2	0.04	0.00	0.54	0.56	0.03	0.07	0.37	112.15	0.11	12.497	0.003	0.02	0.04	0.20
HF - L	RNG 2/2	2#1	10YR 2/2	0.09	0.02	0.28	1.09	0.23	0.58	0.87	45.34	0.27	12.089	0.007	0.25	0.64	0.95
HF - L	RNG 2/3	2#1	10YR 2/2	0.09	0.02	0.27	0.92	0.19	0.47	0.77	50.62	0.21	10.381	0.005	0.17	0.43	0.70
HF - L	RNG 3	4	10YR 3/6	0.14	0.02	0.40	2.67	0.06	0.15	0.51	162.93	0.12	19.315	0.007	0.15	0.39	1.37
HF - L	RNG 4/1	7	10YR 3/4	0.07	0.01	0.55	0.31	0.09	0.19	0.50	58.36	0.08	4.649	0.003	0.03	0.06	0.15
HF - L	RNG 4/2	2#1	10YR 3/4	0.17	0.04	0.31	1.65	0.18	0.45	0.81	37.33	0.26	9.784	0.013	0.30	0.74	1.33
HF - L	RNG 4/3	2#1	10YR 2/2	0.14	0.02	0.36	1.12	0.13	0.35	0.72	59.89	0.14	8.180	0.007	0.15	0.39	0.80
HF - L	RNG 4/4	7	2.5Y 3/3	0.14	0.02	0.38	1.56	0.13	0.22	0.68	79.41	0.14	10.799	0.007	0.20	0.34	1.06
HF - L	RNG 5	2#1	10YR 3/2	0.14	0.05	0.19	0.76	0.40	0.68	0.86	16.57	0.32	5.295	0.009	0.30	0.51	0.65
HF - B	LG 1/1	4	2.5Y 3/3	0.19	0.02	0.35	0.80	0.24	0.54	0.87	43.31	0.10	4.124	0.006	0.19	0.43	0.70
HF - B	LG 1/2	2#1	2.5Y 4/3	0.15	0.01	0.44	0.47	0.19	0.49	0.90	46.18	0.07	3.245	0.004	0.09	0.23	0.43
HF - B	LG 1/3	2#1	2.5Y 3/3	0.21	0.02	0.36	0.87	0.23	0.59	0.92	42.46	0.10	4.172	0.007	0.20	0.51	0.80
HF - B	LG 2/1	4#1	7.5YR 2.5/3	0.51	0.30	0.09	3.14	0.51	0.76	0.89	10.42	0.59	6.139	0.027	1.59	2.39	2.81
HF - B	LG 2/2	4#2	10YR 3/4	0.17	0.02	0.20	1.63	0.09	0.22	0.71	69.41	0.14	9.732	0.005	0.14	0.36	1.16
HF - B	LG 3/1	4#1	10YR 2/2	0.14	0.08	0.15	1.09	0.45	0.66	0.88	14.11	0.56	7.833	0.012	0.49	0.72	0.96
HF - B	LG 3/2	4#2	7.5YR 2.5/3	0.35	0.21	0.14	2.16	0.46	0.68	0.88	10.07	0.62	6.239	0.029	1.00	1.48	1.90
HF - B	LG 4/1	9	10YR 3/3	0.11	0.02	0.26	4.58	0.03	0.06	0.53	274.34	0.16	43.305	0.004	0.13	0.30	2.43
HF - B	LG 4/2	9	10YR 3/2	0.13	0.03	0.22	1.93	0.19	0.31	0.73	55.43	0.26	14.429	0.008	0.36	0.61	1.40
HF - B	LG 5/1	4	7.5YR 2.5/2	0.06	0.01	0.57	0.30	0.08	0.19	0.78	47.28	0.11	5.012	0.004	0.02	0.06	0.24
HF - B	LG 5/2	4	10YR 2/2	0.09	0.01	0.38	1.07	0.09	0.23	0.77	90.58	0.13	11.556	0.004	0.09	0.24	0.83
HF - B	LG 5/3	4	10YR 2/2	0.08	0.01	0.38	0.88	0.10	0.27	0.77	68.58	0.17	11.669	0.005	0.09	0.23	0.68
HF - B	LG 5/4	4	10YR 4/4	0.13	0.02	0.40	2.62	0.08	0.23	0.78	128.54	0.16	20.794	0.008	0.22	0.59	2.05
HF - B	LG 6/1	4#1	10YR 3/6	0.32	0.15	0.10	1.92	0.49	0.69	0.88	12.90	0.46	5.958	0.014	0.93	1.32	1.70
HF - B	LG 6/2	4#2	10YR 3/4	0.22	0.07	0.13	1.54	0.33	0.55	0.87	21.57	0.33	7.090	0.010	0.52	0.85	1.33
HF - B	LG 7/1	7	10YR 2/1	0.00	0.00	0.71	0.03	0.23	0.81	1.00	14.86	0.00	0.000	0.001	0.01	0.02	0.03
HF - B	LG 7/2	8	10YR 2/1	0.00	0.00	0.67	0.04	0.25	0.73	0.95	17.00	0.00	0.000	0.002	0.01	0.03	0.04
HF - B	LG 7/3	8	10YR 2/1	0.00	0.00	0.80	0.04	0.24	0.72	0.98	18.80	0.00	0.000	0.002	0.01	0.03	0.04
HF - B	LG 7/4	8	10YR 2/2	0.08	0.01	0.38	0.38	0.07	0.13	0.60	57.95	0.08	4.892	0.002	0.02	0.05	0.23
HF - B	LG 8	8	10YR 4/4	0.19	0.04	0.38	3.08	0.11	0.30	0.82	71.35	0.23	16.078	0.016	0.35	0.92	2.54
HF - B	TG 1/1	7	10YR 2/1	0.00	0.00	0.83	0.03	0.24	0.80	1.00	17.50	0.00	0.000	0.002	0.01	0.03	0.03
HF - B	TG 1/2	7	10YR 2/1	0.00	0.00	0.90	0.03	0.19	0.75	1.00	13.00	0.00	0.000	0.002	0.01	0.02	0.03
HF - B	TG 1/3	8	10YR 3/1	0.02	0.01	0.52	0.05	0.32	0.73	0.98	10.29	0.32	3.293	0.003	0.02	0.04	0.05
HF - B	TG 2/1	4#1	10YR 2/2	0.17	0.05	0.21	0.85	0.37	0.70	0.88	17.73	0.28	5.020	0.010	0.31	0.60	0.75
HF - B	TG 2/2	4#2	10YR 3/4	0.24	0.05	0.32	2.00	0.25	0.56	0.90	44.20	0.19	8.316	0.015	0.49	1.12	1.80
HF - B	TG 3/1	4#1	10YR 3/4	0.17	0.04	0.34	1.81	0.18	0.44	0.83	44.49	0.24	10.656	0.014	0.33	0.80	1.51
HF - B	TG 3/2	4#2	10YR 3/6	0.12	0.03	0.36	1.53	0.10	0.26	0.67	52.48	0.23	12.259	0.010	0.16	0.40	1.02
HF - B	TG 4	9	10YR 2/2	0.22	0.06	0.26	3.45	0.17	0.39	0.72	54.59	0.29	15.983	0.016	0.57	1.34	2.48
HF - B	TG 5/1	4#1	10YR 3/4	0.13	0.05	0.20	1.75	0.13	0.25	0.65	35.36	0.38	13.320	0.010	0.23	0.43	1.14
HF - B	TG 5/2	4#2	2.5Y 3/3	0.15	0.01	0.34	0.43	0.08	0.17	0.70	43.70	0.07	2.922	0.003	0.03	0.07	0.30
HF - B	TG 6/1	4#1	10YR 3/4	0.14	0.02	0.28	0.98	0.07	0.18	0.74	62.40	0.11	6.790	0.004	0.07	0.17	0.72
HF - B	TG 6/2	4#2	10YR 3/4	0.13	0.01	0.36	0.88	0.04	0.11	0.67	97.17	0.07	6.788	0.003	0.04	0.10	0.59
HF - B	TG 7/1	4#1	10YR 3/4	0.12	0.02	0.26	0.95	0.09	0.20	0.67	50.22	0.16	8.025	0.005	0.09	0.19	0.63
HF - B	TG 7/2	4#2	10YR 3/3	0.12	0.01	0.28	0.81	0.08	0.19	0.73	58.29	0.11	6.585	0.004	0.07	0.16	0.59

LANGDEN BECK

Sample Code	Source Category	Munsell Colour	X (10^{-6} m^3 kg^{-1})	SARM (10^{-6} Am^2 kg^{-1})	ARM40/ SARM	SIRM (10^{-6} Am^2 kg^{-1})	IRM40/ SIRM	IRM100/ SIRM	IRM1T/ SIRM	SIRM/ SARM	SARM/X (kAm^{-1})	SIRM/X (kAm^{-1})	ARM40mT (10^{-6} Am^2 kg^{-1})	IRM40mT (10^{-6} Am^2 kg^{-1})	IRM100mT (10^{-6} Am^2 kg^{-1})	IRM 1T (10^{-6} Am^2 kg^{-1})
HH 1/1	7	10YR 2/2	0.06	0.01	0.28	0.40	0.12	0.21	0.43	40.18	0.16	6.48	0.003	0.05	0.08	0.17
HH 1/2	3	10YR 2/2	0.08	0.01	0.36	0.40	0.07	0.11	0.27	60.81	0.09	5.26	0.002	0.03	0.04	0.11
HH 1/3	3	10YR 2/2	0.10	0.01	0.32	0.39	0.05	0.09	0.20	56.36	0.07	3.94	0.002	0.02	0.04	0.08
HH 1/4	3	10YR 3/2	0.13	0.01	0.37	0.70	0.02	0.04	0.15	129.55	0.04	5.42	0.002	0.02	0.03	0.10
HH 1/5	3	10YR 3/4	0.16	0.01	0.54	1.08	0.02	0.04	0.13	109.54	0.06	6.57	0.005	0.02	0.05	0.14
HH 1/6	3	10YR 3/3	0.12	0.01	0.69	0.57	0.04	0.10	0.18	41.87	0.11	4.71	0.009	0.02	0.06	0.10
HH 1/7	3	10YR 3/3	0.10	0.01	0.65	0.24	0.11	0.27	0.37	18.59	0.13	2.34	0.009	0.03	0.07	0.09
HH 2/1	7	10YR 1.5/1	0.02	0.01	0.47	0.10	0.21	0.39	0.65	20.86	0.27	5.61	0.002	0.02	0.04	0.07
HH 2/2	3	10YR 2.5/2	0.11	0.01	0.38	0.93	0.03	0.05	0.25	141.05	0.06	8.70	0.002	0.03	0.05	0.23
HH 2/3	3	10YR 1.5/1	0.07	0.00	0.51	0.13	0.15	0.26	0.44	36.64	0.05	1.83	0.002	0.02	0.03	0.06
HH 2/4	3	2.5Y 3/2	0.16	0.01	0.01	0.45	0.14	0.20	0.29	40.91	0.07	2.83	0.000	0.06	0.09	0.13
HH 2/5	3	2.5Y 3/3	0.12	0.01	0.24	0.62	0.11	0.17	0.26	57.54	0.09	5.06	0.003	0.07	0.10	0.16
HH 2/6	3	10YR 3/2	0.16	0.02	0.27	0.76	0.17	0.27	0.35	45.09	0.11	4.84	0.005	0.13	0.21	0.27
HH 2/7	3	10YR 2/2	0.11	0.01	0.37	0.25	0.11	0.16	0.26	43.04	0.05	2.23	0.002	0.03	0.04	0.06
HH 2/8	3	10YR 3/3	0.10	0.01	0.50	0.13	0.16	0.29	0.43	19.79	0.07	1.33	0.003	0.02	0.04	0.06
HH 3/1	7	10YR 2/1	0.02	0.02	0.43	0.07	0.51	0.86	1.00	3.57	0.97	3.46	0.008	0.03	0.06	0.07
HH 3/2	7	10YR 2/1	0.02	0.02	0.47	0.06	0.49	0.89	0.99	3.87	0.64	2.48	0.007	0.03	0.05	0.06
HH 3/3	7	10YR 2/1	0.02	0.01	0.79	0.04	0.30	0.75	1.00	7.61	0.28	2.13	0.004	0.01	0.03	0.04
HH 3/4	4#2	10YR 2/1	0.02	0.01	0.57	0.06	0.41	0.79	0.96	7.73	0.46	3.58	0.004	0.02	0.04	0.05
HH 3/5	4#2	10YR 2/1	0.03	0.01	0.42	0.08	0.34	0.56	0.79	11.32	0.26	2.90	0.003	0.03	0.04	0.06
HH 3/6	4#2	10YR 3/1	0.04	0.01	0.33	0.10	0.31	0.56	0.76	10.53	0.22	2.28	0.003	0.03	0.06	0.08
HH 3/7	3	2.5Y 3/1	0.05	0.01	0.41	0.06	0.35	0.61	0.84	10.64	0.11	1.16	0.002	0.02	0.04	0.05
HH 4/1	7	2.5Y 3/1	0.00	0.00	0.52	0.04	0.35	0.74	1.00	12.24	2.10	25.70	0.002	0.01	0.03	0.04
HH 4/2	8	10YR 2/2	0.00	0.00	0.60	0.04	0.35	0.72	1.00	15.92	0.00	0.00	0.002	0.02	0.03	0.04
HH 4/3	4#2	10YR 2.5/1	0.05	0.00	0.50	0.03	0.31	0.75	1.00	13.23	0.05	0.71	0.001	0.01	0.03	0.03
HH 4/4	3	10YR 2.5/1	0.06	0.00	0.55	0.04	0.31	0.70	0.97	12.76	0.05	0.63	0.002	0.01	0.03	0.04
HH 4/5	3	10YR 2.5/1	0.17	0.00	0.50	0.07	0.14	0.31	0.47	33.00	0.01	0.45	0.001	0.01	0.02	0.03
HH 4/6	3	2.5Y 3/2	0.10	0.00	0.41	0.30	0.12	0.33	0.52	88.71	0.03	2.87	0.001	0.03	0.10	0.16
HH 5/1	10	2.5Y 3/2	0.16	0.03	0.26	1.29	0.21	0.46	0.68	44.32	0.18	7.96	0.008	0.27	0.59	0.88
HH 5/2	10	2.5Y 3/2	0.15	0.03	0.26	1.20	0.20	0.49	0.66	42.60	0.19	8.11	0.007	0.25	0.60	0.80
HH 6/1	10	2.5Y 3/3	0.08	0.00	0.41	0.16	0.16	0.40	0.58	35.80	0.06	2.11	0.002	0.03	0.06	0.09
HH 6/2	10	2.5Y 3/2	0.08	0.00	0.47	0.14	0.20	0.41	0.61	35.92	0.05	1.87	0.002	0.03	0.06	0.09
HH 6/3	10	2.5Y 3/2	0.09	0.01	0.41	0.23	0.16	0.43	0.68	31.78	0.08	2.54	0.003	0.04	0.10	0.16
HH 6/4	10	2.5Y 3/2	0.08	0.00	0.49	0.16	0.16	0.39	0.60	34.19	0.06	2.01	0.002	0.03	0.06	0.10
HH 7/1	4#2	2.5Y 3/2	0.03	0.00	0.48	0.08	0.16	0.34	0.55	27.55	0.10	2.76	0.001	0.01	0.03	0.05
HH 7/2	3	10YR 3/2	0.01	0.00	0.50	0.04	0.37	0.69	0.93	12.10	0.60	7.26	0.002	0.02	0.03	0.04
HH 8/1	4#2	7.5YR 2.5/1	0.06	0.01	0.44	0.69	0.06	0.15	0.44	121.39	0.09	10.64	0.002	0.04	0.10	0.31
HH 8/2	3	2.5Y 3/3	0.07	0.00	0.62	0.28	0.07	0.13	0.31	83.51	0.05	3.81	0.002	0.02	0.04	0.09
HH 9/1	4#2	2.5Y 3/2	0.11	0.02	0.35	0.72	0.12	0.29	0.64	41.76	0.16	6.79	0.006	0.08	0.21	0.46
HH 9/2	3	10YR 3/4	0.03	0.00	0.40	0.16	0.13	0.21	0.41	85.75	0.05	4.64	0.001	0.02	0.03	0.06
HH 9/3	3	10YR 4/6	0.06	0.00	0.52	0.03	0.29	0.62	0.89	15.00	0.03	0.52	0.001	0.01	0.02	0.03

Key to source categories:

3	Bedrock
4#1	Solifluction: grey clay
4#1	Solifluction: sandstone inclusions
7	Peat
8	Peat Substrate
9	Storage
9	Mining waste

LANGDEN BECK - con't....

Sample Code	Source Category	Munsell Colour	X (10^{-8} m^3 kg^{-1})	SARM (10^{-6} Am^2 kg^{-1})	ARM40/ SARM	SIRM (10^{-3} Am^2 kg^{-1})	IRM40/ SIRM	IRM100/ SIRM	IRM1T/ SIRM	SIRM/ SARM	SARM/X (kAm^{-1})	SIRM/X (kAm^{-1})	ARM40mT (10^{-6} Am^2 kg^{-1})	IRM40mT (10^{-6} Am^2 kg^{-1})	IRM100mT (10^{-3} Am^2 kg^{-1})	IRM 1T (10^{-3} Am^2 kg^{-1})
HH 10	9	10YR 1.5/1	0.07	0.00	0.40	0.24	0.12	0.25	0.47	59.87	0.06	3.47	0.002	0.03	0.06	0.11
HH 11/1	9	10YR 2.5/2	0.05	0.01	0.42	0.36	0.11	0.27	0.59	59.90	0.12	7.19	0.003	0.04	0.10	0.22
HH 11/2	9	10YR 2/2	0.05	0.01	0.31	0.33	0.12	0.28	0.60	38.91	0.18	6.99	0.003	0.04	0.09	0.20
HH 12/1	9	2.5Y 2.5/1	0.04	0.01	0.40	0.19	0.15	0.34	0.56	35.80	0.14	4.88	0.002	0.03	0.07	0.11
HH 12/2	9	10YR 2/2	0.03	0.00	0.59	0.16	0.14	0.25	0.47	51.48	0.10	4.98	0.002	0.02	0.04	0.07
HH 13/1	9	10YR 2/2	0.02	0.00	0.48	0.11	0.20	0.35	0.63	37.42	0.16	5.88	0.001	0.02	0.04	0.07
HH 13/2	9	2.5Y 3/2	0.02	0.00	0.53	0.11	0.17	0.32	0.56	37.41	0.16	6.06	0.002	0.02	0.04	0.06
MV 1/1	10	2.5Y 3/2	0.09	0.02	0.19	0.48	0.30	0.41	0.64	24.45	0.22	5.32	0.004	0.15	0.20	0.31
MV 1/2	10	10YR 3/2	0.04	0.00	0.50	0.25	0.08	0.15	0.41	56.28	0.10	5.49	0.002	0.02	0.04	0.10
MV 2/1	4#1	10YR 3/2	0.03	0.01	0.49	0.10	0.27	0.47	0.84	18.60	0.19	3.50	0.003	0.03	0.05	0.08
MV 2/2	4#1	10YR 3/2	0.02	0.00	0.54	0.07	0.36	0.61	1.00	18.40	0.23	4.29	0.002	0.03	0.04	0.07
MV 2/3	4#1	5YR 2.5/1	0.05	0.01	0.32	0.46	0.17	0.42	0.76	43.48	0.23	10.01	0.003	0.08	0.19	0.35
MV 2/4	4#1	10YR 3/2	0.01	0.00	0.60	0.06	0.23	0.52	0.95	22.32	0.36	7.97	0.002	0.02	0.03	0.06
MV 2/5	4#1	10YR 2/2	0.02	0.00	0.58	0.18	0.11	0.25	0.52	52.68	0.15	7.78	0.002	0.02	0.05	0.10
MV 2/6	4#1	10YR 2/2	0.04	0.01	0.52	0.32	0.10	0.24	0.56	48.87	0.15	7.33	0.003	0.03	0.08	0.18
MV 2/7	9	2.5Y 3/3	0.04	0.01	0.39	0.36	0.11	0.25	0.56	65.18	0.12	8.11	0.002	0.04	0.09	0.20
MV 3/1	7	2.5Y 2.5/1	0.01	0.00	0.57	0.05	0.26	0.60	0.98	15.79	0.23	3.68	0.002	0.01	0.03	0.05
MV 3/2	4#1	10YR 2/1	0.01	0.00	0.64	0.05	0.28	0.61	0.99	14.75	0.47	6.88	0.002	0.01	0.03	0.05
MV 3/3	4#2	10YR 2/1	0.04	0.00	0.47	0.02	0.27	0.65	0.92	14.27	0.03	0.48	0.001	0.01	0.01	0.02
MV 3/4	4#2	10YR 2/1	0.18	0.00	0.53	0.03	0.25	0.67	0.98	19.20	0.01	0.16	0.001	0.01	0.02	0.03
MV 3/5	3	10YR 2/1	0.04	0.00	0.56	0.02	0.29	0.63	0.94	12.56	0.03	0.43	0.001	0.01	0.01	0.02
MV 4/1	4#1	10YR 1.5/1	0.01	0.00	0.63	0.13	0.12	0.27	0.59	50.83	0.24	12.20	0.002	0.02	0.03	0.07
MV 4/2	4#2	2.5Y 3/3	0.04	0.00	0.62	0.35	0.06	0.12	0.44	123.55	0.08	9.43	0.002	0.02	0.04	0.15
MV 4/3	3	2.5Y 3/3	0.03	0.00	0.65	0.03	0.28	0.66	0.97	16.00	0.05	0.88	0.001	0.01	0.02	0.03
MV 4/4	4#1	10YR 1.5/1	0.05	0.01	0.43	0.34	0.07	0.13	0.42	58.91	0.12	7.28	0.002	0.02	0.05	0.14
MV 5	4#1	10YR 3/3	0.06	0.00	0.52	0.07	0.34	0.66	0.98	26.90	0.05	1.24	0.001	0.02	0.05	0.07
MV 6/1	10	5Y 3/1	0.28	0.02	0.24	1.70	0.07	0.15	0.35	110.84	0.06	6.13	0.004	0.11	0.25	0.60
MV 6/2	10	10YR 3/6	0.06	0.01	0.44	0.38	0.21	0.53	0.75	57.42	0.12	6.87	0.003	0.08	0.20	0.29
MV 6/3	7	2.5Y 3/2	0.02	0.00	0.83	0.06	0.16	0.56	0.97	43.00	0.07	2.87	0.001	0.01	0.03	0.06
MV 6/4	7	10YR 2/1	0.01	0.00	0.65	0.05	0.29	0.67	1.00	20.41	0.21	4.34	0.001	0.01	0.03	0.05
MV 6/5	7	10YR 1.5/1	0.01	0.00	0.63	0.04	0.29	0.65	1.00	18.06	0.27	4.82	0.001	0.01	0.03	0.04
MV 7	9	10YR 1.5/1	0.05	0.00	0.48	0.30	0.16	0.35	0.64	86.70	0.08	6.54	0.002	0.05	0.11	0.19
MV 8/1	4#1	2.5Y 3/2	0.04	0.01	0.15	0.18	0.69	0.95	0.95	23.27	0.18	4.21	0.001	0.12	0.17	0.17
MV 8/2	4#1	10YR 3/1	0.02	0.00	0.48	0.08	0.23	0.36	0.60	39.61	0.14	5.36	0.001	0.02	0.03	0.05
MV 8/3	4#2	10YR 3/3	0.03	0.00	0.48	0.07	0.27	0.44	0.68	31.92	0.07	2.35	0.001	0.02	0.03	0.05
MV 8/4	3	10YR 3/1	0.04	0.00	0.46	0.15	0.13	0.25	0.51	45.71	0.08	3.56	0.002	0.02	0.04	0.08
MV 9/1	4#1	10YR 3/2	0.01	0.00	0.67	0.07	0.25	0.46	0.75	23.44	0.25	5.75	0.002	0.02	0.03	0.05
MV 9/2	4#1	10YR 3/2	0.02	0.00	0.52	0.11	0.13	0.26	0.49	41.10	0.12	4.77	0.001	0.01	0.03	0.06
MV 9/3	3	2.5Y 3/2	0.05	0.01	0.46	0.49	0.06	0.14	0.49	55.40	0.17	9.37	0.004	0.03	0.07	0.24
MV 10	9	2.5Y 2.5/1	0.05	0.00	0.47	0.22	0.08	0.16	0.47	65.77	0.06	4.20	0.002	0.02	0.03	0.10
MV 11	9	10YR 3/2	0.05	0.00	0.46	0.40	0.15	0.32	0.63	105.21	0.07	7.32	0.002	0.06	0.13	0.25
MV 12/1	4#1	2.5Y 2.5/1	0.02	0.00	0.60	0.05	0.24	0.58	0.87	19.50	0.12	2.25	0.001	0.01	0.03	0.04
MV 12/2	4#1	10YR 2/2	0.01	0.00	0.64	0.08	0.22	0.44	0.83	25.52	0.33	8.42	0.002	0.02	0.04	0.07
MV 12/3	3	2.5Y 3/3	0.03	0.00	0.57	0.26	0.07	0.12	0.29	96.36	0.09	8.43	0.002	0.02	0.03	0.07
MV 12/4	3	2.5Y 2.5/1	0.06	0.00	0.54	0.31	0.08	0.22	0.70	74.52	0.07	5.04	0.002	0.02	0.07	0.22

MOFFAT

Sample Code	Source Category	Munsell Colour	X (10^{-8} m^3 kg^{-1})	SARM (10^{-5} Am^2 kg^{-1})	ARM40/ SARM	SIRM (10^{-5} Am^2 kg^{-1})	IRM40/ SIRM	IRM100/ SIRM	IRM1T/ SIRM	SIRM/ SARM	SARM/X (kAm^{-1})	SIRM/X (kAm^{-1})	ARM40mT (10^{-5} Am^2 kg^{-1})	IRM40mT (10^{-5} Am^2 kg^{-1})	IRM100mT (10^{-5} Am^2 kg^{-1})	IRM 1T (10^{-5} Am^2 kg^{-1})
DC 1/1	4	10YR 2.5/2	0.13	0.08	0.17	1.71	0.21	0.32	0.78	21.15	0.61	12.94	0.014	0.36	0.55	1.33
DC 1/2	4	10YR 3/3	0.27	0.20	0.14	2.95	0.38	0.56	0.87	14.63	0.75	10.94	0.028	1.11	1.65	2.56
DC 2/1	4	7.5YR 3/3	0.15	0.08	0.15	3.03	0.14	0.24	0.72	36.15	0.54	19.58	0.013	0.44	0.72	2.19
DC 2/2	4	7.5YR 3/3	0.15	0.08	0.17	3.60	0.12	0.19	0.71	47.83	0.51	24.40	0.013	0.43	0.67	2.56
DC 2/3	4	7.5YR 3/3	0.15	0.08	0.15	3.52	0.12	0.19	0.70	46.69	0.52	24.09	0.011	0.43	0.67	2.47
DC 3/1	4	7.5YR 3/4	0.27	0.18	0.13	2.94	0.29	0.45	0.80	16.44	0.66	10.85	0.024	0.85	1.32	2.36
DC 3/2	4	7.5YR 3/3	0.22	0.10	0.16	2.86	0.18	0.31	0.79	28.79	0.44	12.79	0.016	0.51	0.89	2.26
DC 4/1	4	7.5YR 3/4	0.21	0.15	0.11	2.45	0.31	0.44	0.78	15.83	0.73	11.50	0.017	0.75	1.08	1.90
DC 4/2	4	10YR 3.5/3	0.16	0.03	0.38	4.08	0.07	0.19	0.74	150.42	0.17	25.09	0.010	0.30	0.78	3.04
DC 4/3	4	7.5YR 3/3	0.18	0.07	0.19	3.59	0.13	0.25	0.76	49.16	0.41	19.97	0.014	0.46	0.89	2.73
DC 5/1	4	7.5YR 3/3	0.18	0.14	0.12	2.02	0.30	0.44	0.81	14.35	0.77	11.10	0.017	0.61	0.88	1.65
DC 5/2	4	7.5YR 3/4	0.18	0.11	0.13	3.19	0.20	0.31	0.76	28.01	0.65	18.22	0.015	0.63	0.98	2.43
DC 6/1	4	7.5YR 3/3	0.16	0.08	0.18	4.09	0.11	0.19	0.73	49.96	0.52	25.86	0.014	0.45	0.79	2.98
DC 6/2	4	7.5YR 3/3	0.15	0.07	0.18	4.50	0.08	0.15	0.71	65.34	0.45	29.60	0.013	0.36	0.66	3.18
DC 7/1	9	10YR 3/3	0.06	0.01	0.46	0.97	0.03	0.08	0.73	87.05	0.20	17.41	0.005	0.03	0.08	0.70
DC 7/2	9	10YR 3/2	0.05	0.01	0.44	0.80	0.03	0.08	0.72	87.21	0.18	15.50	0.004	0.03	0.06	0.58
DC 7/3	9	7.5YR 2.5/3	0.08	0.02	0.28	2.04	0.05	0.11	0.72	87.66	0.30	25.90	0.007	0.10	0.23	1.47
DC 7/4	9	5YR 3/4	0.10	0.02	0.48	9.01	0.01	0.04	0.74	433.06	0.21	91.47	0.010	0.13	0.39	6.65
DC 7/5	9	10YR 3/3	0.14	0.04	0.24	2.02	0.15	0.40	0.80	47.32	0.31	14.46	0.010	0.30	0.81	1.61
DC 8/1	7	10YR 3/3	0.10	0.03	0.18	1.15	0.19	0.31	0.77	42.03	0.29	12.07	0.005	0.22	0.36	0.88
DC 8/2	7	10YR 3/3	0.08	0.02	0.28	0.85	0.08	0.17	0.74	56.15	0.18	10.29	0.004	0.07	0.14	0.63
DC 8/3	8	10YR 2/2	0.13	0.04	0.18	1.11	0.16	0.28	0.80	29.84	0.29	8.57	0.007	0.17	0.31	0.88
DC 9/1	7	10YR 2/1	0.04	0.11	0.04	1.97	0.95	1.00	1.00	17.39	2.60	45.22	0.005	1.88	1.97	1.97
DC 9/2	7	10YR 2/1	0.00	0.00	0.67	0.05	0.26	0.73	0.86	14.61	0.90	13.15	0.002	0.01	0.04	0.04
DC 9/3	8	10YR 3/1	0.06	0.00	0.58	0.06	0.25	0.59	0.91	13.53	0.08	1.02	0.002	0.01	0.03	0.05
HB 1/1	4	7.5YR 3/3	0.17	0.10	0.12	2.99	0.14	0.24	0.73	31.44	0.54	17.12	0.011	0.43	0.72	2.17
HB 1/2	4	7.5YR 3/3	0.15	0.08	0.16	3.52	0.12	0.19	0.71	46.52	0.50	23.13	0.012	0.41	0.67	2.50
HB 1/3	4	10YR 3/3	0.15	0.08	0.15	3.69	0.12	0.19	0.70	46.67	0.54	25.30	0.012	0.46	0.70	2.59
HB 2/1	4	7.5YR 3/4	0.28	0.18	0.13	2.98	0.29	0.45	0.80	16.33	0.66	10.74	0.025	0.86	1.35	2.39
HB 2/2	4	7.5YR 3/3	0.23	0.10	0.15	2.87	0.18	0.31	0.79	27.94	0.45	12.58	0.015	0.51	0.89	2.26
HB 3/1	4	7.5YR 3/3	0.20	0.15	0.12	2.40	0.31	0.44	0.77	16.10	0.73	11.79	0.017	0.74	1.05	1.85
HB 3/2	4	10YR 3/4	0.18	0.03	0.41	4.40	0.07	0.19	0.74	150.21	0.17	24.90	0.012	0.33	0.84	3.28
HB 3/3	4	7.5YR 3/3	0.18	0.08	0.20	3.77	0.13	0.25	0.76	48.75	0.43	20.87	0.015	0.48	0.94	2.86

Key to source categories:

2#1	Lateral moraine: main valley
2#2	Lateral moraine: catchment slopes
3	Bedrock
4	Solifluction
7	Peat
8	Peat Substrate
9	Storage

MOFFAT - con't....

Sample	Source	Munsell	X	SARM	ARM40/	SIRM	IRM40/	IRM100/	IRM1T/	SIRM/	SARM/X	SIRM/X	ARM40mT	IRM40mT	IRM100mT	IRM 1T
Code	Category	Colour	(10^{-6} m^3 kg^{-1})	(10^{-6} Am^2 kg^{-1})	SARM	(10^{-6} Am^2 kg^{-1})	SIRM	SIRM	SIRM	SARM	(kAm^{-1})	(kAm^{-1})	(10^{-6} Am^2 kg^{-1})	(10^{-6} Am^2 kg^{-1})	(10^{-6} Am^2 kg^{-1})	(10^{-6} Am^2 kg^{-1})
HB 4/1	9	10YR 3/3	0.06	0.01	0.42	0.90	0.03	0.10	0.75	77.67	0.18	14.01	0.005	0.03	0.09	0.67
HB 4/2	9	10YR 3/2	0.09	0.02	0.27	2.02	0.05	0.11	0.71	81.69	0.29	23.42	0.007	0.11	0.23	1.44
HB 4/3	9	5YR 3/4	0.09	0.02	0.51	9.28	0.01	0.04	0.74	464.16	0.22	100.65	0.010	0.13	0.40	6.87
HB 4/4	9	10YR 3/3	0.07	0.01	0.48	1.00	0.04	0.08	0.72	91.09	0.17	15.29	0.005	0.04	0.08	0.72
HB 5/1	4	7.5YR 3/4	0.16	0.08	0.18	4.09	0.11	0.19	0.73	49.96	0.52	25.86	0.014	0.45	0.79	2.98
HB 5/2	4	10YR 3.5/3	0.16	0.07	0.20	4.66	0.08	0.15	0.71	63.54	0.45	28.78	0.015	0.38	0.68	3.30
HB 6/1	7	10YR 2/1	0.01	0.00	0.76	0.05	0.28	0.79	0.88	14.94	0.34	5.08	0.003	0.01	0.04	0.04
HB 6/2	7	10YR 2/1	0.04	0.11	0.04	1.87	0.96	1.00	1.00	17.72	2.88	51.05	0.004	1.79	1.87	1.87
HB 6/3	8	10YR 3/1	0.05	0.12	0.04	7.14	0.26	0.28	0.81	59.34	2.29	135.91	0.005	1.86	1.97	5.78
YW 1/1	4	10YR 2/2	0.11	0.03	0.46	1.04	0.19	0.45	0.82	29.86	0.32	9.66	0.016	0.19	0.47	0.85
YW 1/2	4	10YR 3.5/4	0.12	0.03	0.47	1.11	0.18	0.43	0.81	31.67	0.28	8.89	0.016	0.20	0.48	0.90
YW 1/3	2#2	10YR 3.5/4	0.14	0.04	0.45	1.48	0.20	0.47	0.86	36.38	0.29	10.59	0.018	0.30	0.70	1.27
YW 1/4	2#2	10YR 4/4	0.10	0.03	0.49	0.76	0.18	0.43	0.79	22.56	0.33	7.41	0.016	0.14	0.33	0.61
YW 1/5	2#2	10YR 3/3	0.11	0.03	0.45	0.71	0.20	0.48	0.80	22.67	0.29	6.67	0.014	0.14	0.34	0.57
YW 1/6	2#2	10YR 3/3	0.10	0.03	0.44	0.69	0.20	0.47	0.81	21.18	0.31	6.58	0.014	0.14	0.32	0.56
YW 1/7	2#2	10YR 3/3	0.02	0.01	0.46	0.12	0.24	0.64	0.88	9.45	0.60	5.67	0.006	0.03	0.07	0.10
YW 2/1	2#2	2.5Y 3.5/2	0.07	0.02	0.51	0.24	0.22	0.53	0.82	10.14	0.32	3.27	0.012	0.05	0.13	0.19
YW 2/2	2#2	2.5Y 3/3	0.06	0.02	0.51	0.26	0.21	0.50	0.84	11.20	0.38	4.30	0.012	0.05	0.13	0.22
YW 2/3	2#2	2.5Y 4/3	0.07	0.02	0.51	0.18	0.26	0.61	0.90	9.23	0.29	2.71	0.010	0.05	0.11	0.16
YW 3/1	2#2	2.5Y 3.5/3	0.18	0.08	0.32	1.93	0.23	0.49	0.89	24.87	0.43	10.82	0.025	0.44	0.95	1.72
YW 3/2	2#2	10YR 2/1	0.10	0.04	0.41	0.73	0.22	0.45	0.79	19.21	0.37	7.19	0.015	0.16	0.33	0.58
YW 4/1	2#2	7.5YR 2.5/3	0.18	0.08	0.38	2.93	0.22	0.55	0.95	37.14	0.44	16.34	0.030	0.64	1.60	2.78
YW 4/2	2#2	2.5Y 3/3	0.14	0.06	0.40	1.75	0.20	0.50	0.91	29.99	0.43	12.88	0.023	0.35	0.87	1.59
YW 4/3	2#2	7.5YR 2.5/3	0.12	0.04	0.43	1.09	0.19	0.46	0.84	27.82	0.33	9.05	0.017	0.21	0.50	0.92
YW 4/4	2#2	10YR 3/4	0.10	0.03	0.47	0.87	0.16	0.37	0.82	27.94	0.32	8.98	0.015	0.14	0.33	0.72
YW 5/1	2#2	2.5Y 3/3	0.09	0.01	0.37	0.29	0.20	0.46	0.85	20.45	0.16	3.30	0.005	0.06	0.13	0.25
YW 5/2	2#2	2.5Y 3/3	0.11	0.01	0.49	0.38	0.08	0.19	0.84	41.02	0.08	3.34	0.005	0.03	0.07	0.32
YW 5/3	2#2	10YR 4/4	0.09	0.01	0.53	0.69	0.07	0.19	0.82	55.33	0.14	7.64	0.007	0.05	0.13	0.57
YW 5/4	2#2	2.5Y 3/2	0.12	0.03	0.50	0.73	0.11	0.26	0.79	28.24	0.21	5.96	0.013	0.08	0.19	0.58
YW 5/5	2#2	10YR 2/2	0.11	0.02	0.51	0.91	0.12	0.29	0.85	40.93	0.20	8.10	0.011	0.11	0.26	0.77
YW 6/1	4	10YR 2/2	0.18	0.06	0.21	2.93	0.14	0.25	0.79	45.18	0.37	16.60	0.013	0.40	0.73	2.32

APPENDIX 2.1: Assignment of transport mechanism to sections.

HF - BGS1

UNIT 1 (4)	$P_{90}M$ fluctuates dramatically, 3 out of 4 above 10, greatest →29.09, lowest 1.08. Compact, clast dominated layer, stones appear rounded, not especially angular, no structure evident.	Df
CONTACT:	↓ in $P_{90}M$ from 29.09 to 0.80, ↓ in gap between median :$P_{70}M$. ↑ in total sand content : greater than 613 μm	
UNIT 2 (3)	Uniform low $P_{90}M$- ↑ slightly to top of layer. Normal grading, decrease in no. of clasts to top of layer and ↓ in size. Correspondingly low $P_{90}m$-high median.	Ff
CONTACT:	Visual contact. Iron pan layer, iron staining continues horizontally. Change to stony layer continuous ↑ in $P_{90}M$ from 1.49 to 15.48. ↑ in gap median:$P_{70}M$	
UNIT 3 (3)	$P_{90}M$ high but fluctuating 9.76-15.48, spacing fluctuating also. Clast supported layer, no obvious structure. Low sand content, decrease from 52 to 22%	Df
CONTACT:	PALAEOSOL	
UNIT 4 (6)	$P_{90}M$ fluctuating but predominantly high (all but 1 ≈10), general decrease to the top of the section. Change in spacing also : no discernible pattern. Total sand content ≈52-68%, shows a ↓ in 613 μm fraction towards top of the unit → replaced by smaller sand fraction, becoming finer towards the top? Clast supported layer- reverse grading, larger clasts to top of the layer.	Df
CONTACT:	Visual- loss of clasts- matrix supported, visual only, slight decrease in $P_{90}M$.	
UNIT 5 (2)	Matrix supported layer- clasts intermittent. $P_{90}M$ 6.835 to 2.85. Fine content high.	Capping layer Df
CONTACT:	Sharp visual change → stony layer- no matrix material and air gaps.	
UNIT 6 No samples	No matrix support, clasts –open framework homogenous in size, no obvious grading. Not a sieve deposit- base layers →fine material acting as a plug.	Dry grain flow
CONTACT:	Visual increase in clast size, re inclusion of matrix material.	
UNIT 7 (3)	Low $P_{90}M$ 0.89-1.39, sand content high, dominated by greater than 613 μm fraction Normal grading in clast supported layer.	Ff
CONTACT:	Change to sandy layer-sharp contact, ↑ in $P_{90}M$, small relative to below. greatest distance gap between median :$P_{70}M$.	
UNIT 8 (1)	Sand layer continuous laterally, $P_{90}M$ 4.29, depositional	Df. very shallow relative to above and below.
CONTACT:	Dramatic↑ in $P_{90}M$ from 4.29 to 17.56. Stark visual change from horizontal sandy layer – matrix dominated layer intermittent clasts Significant ↓ in sand content greater loss in greater than 613 μm fraction.	
UNIT 9 (4)	$P_{90}M$ high, decreasing from 17 to 13 towards top of the section. Spacing uniformly left skewed, sand content decreases from 38% to ≈30%. Low sand content, clasts intermittent, indicate slight reverse grading.	Df/Hf.

HF - BGS2

UNIT 1 (6)	$P_{90}M$ values spacing, median:$P_{70}M$ fairly uniform, $P_{90}M \approx 6$. Sand content fluctuates also, dominated by smallest sand fraction. Fine sand content fluctuates between 14 and 40 at both extremes.	Df.
CONTACT:	PALAEOSOL- samples 7-18 (11 samples)	
UNIT 2a (5)	$P_{90}M$ fluctuates between 6.68 and 17.49 whilst $P_{70}M$:$P_{80}M$ stays relatively constant as does median :$P_{70}M$. Clast supported layer, increase in clast size : reverse grading , sand content ≈30%.	Hf?
CONTACT:	Visual change in size of clasts, decreases significantly. $P_{90}M$ increase from 11.01 to 22.	
UNIT 2b (6)	$P_{90}M$ suddenly decreases to top of the unit from 22 to 8.57, median :$P_{70}M$, $P_{70}M$:$P_{80}M$ constant. Clast size uniform appears to be layered slight change in size. Clast supported, sand content ≈30%, ↓ in 613 μm to top of the section. Gravel lenses.	Hf?
CONTACT:	$P_{90}M$ values become uniform Change in dominance of clasts, increase in matrix support	
UNIT 4 (7)	Sorting values $P_{90}M$, spacing between all percentiles uniform in all 7 samples. No discernible structure, generally larger clasts found at the top :gravel lenses present. Sand content between 19 to 28&, very low.	Hf.

GE - CDS1

UNIT 1 (8)	$P_{90}M$ values 0.56-1.51 Normal grading PS distribution dominated by <613 μm. low P90M, high median value.	Ff fluvial flood aggrading. over a meter of sediment, 1 event.
CONTACT:	Visual change → contact → change in clast:matrix ratio and inclusion of larger clasts. NB. Visual only. still related to unit 2.	
UNIT 2 (2)	$P_{90}M$ values 0.72 and 1.14 No discernible structure, inclusion of clasts Over 15cm → slight normal grading. Low $P_{90}M$ correlates with high median value.	Ff fluvial flood (higher magnitude larger clasts) Shallow deposits.
CONTACT:	Visual change Sharp increase in P_90M 1.14 to 4.34-10.1. Increase in gap median: $P_{70}M$. correlation with sharp increase in organic content.	
UNIT 3 (2)	$P_{90}M$ high 11 and 10.1 uniform. Clast supported, no structure. Sand content greater 60%.	Df Clast supported channel source?
CONTACT:	Obvious visual change and sharp contact. Distinct decrease in clasts Marked increase in fines in PS distribution over all. Change in spacing of percentiles even to left skewed.	
UNIT 4 (2)	$P_{90}M$ high 8.75 and 5.63 Matrix supported, very high fine content, sand total still very high. Sand content greater than 35%	Df Matrix supported Different source.

GE - CDS2

UNIT 1 (5)	$P_{90}M$ 0.48-1.24, increases generally to top of the unit. Normal grading-megaclasts 20+ at base Gravel lenses in lee of larger clasts <613 μm (high median vlaue correlates with low P90m).	Ff flood deposits aggrading
CONTACT:	Increase in gap between median:$P_{70}M$, associated increase in $P_{90}M$ → re-Introduction of large clasts.	
UNIT 2 (2)	$P_{90}M$ 8.08 and 2.82 fluctuating. Organic layers at top of the unit. Contains very large clasts 10cm+, sand content over 70%.	HF?
CONTACT:	Decrease in gap between median:$P_{70}M$, decrease in $P_{90}M$, very sharp. Correlate potential organic inversion → organic layers at top of unit 2.	
UNIT 3 (3)	$P_{90}M$ 0.45-1.37 fluctuating Inclusion of very larger clasts, not over 18cm: largest 25 cm, no structure.	Ff chaotic
CONTACT:	Overlying sandy layer/fine layer (sharp contact layer above and below) – Continuous laterally – unit above, significant change in PS fractionations. Decrease in total sand content , increase in median:$P_{70}M$, increase in $P_{90}M$, Change in size of megaclasts smaller in comparison, sharp contact.	
UNIT 4 (3)	$P_{90}M$ 2.34-7.32 increasing (two uniform) No structure, smaller clasts, sand content greater 65%.	Df
CONTACT:	Visual change (including structural) $P_{90}M$ values sharply increase, doubled. Correlates with organic inversion. Significant change in fine content ↑, Decrease in dominance of sand fractionations.	
UNIT 5 (2)	$P_{90}M$ uniform and very high 19.6 and 19.4. Matrix supported, clasts intermittent and sand content greater than 40%.	Ff
CONTACT:	$P_{90}M$ significantly decreased- halved (only). No obvious visual change.	
UNIT 6 (3)	$P_{90}M$ values uniform – 10 , left percentiles. Matrix supported, clasts intermittent. Sand content greater than 40%.	Df.

GE - CDS3

UNIT 1 (3)	P90m low 0.99-1.48 uniform characteristics median:P70m . inclusion of larger clasts in clast-supported unit. Tend to be rounded – no obvious structure, (clasts 15cm+, 4 visible in section) low P90m correlates –high median.	Ff Flood- highish magnitude
CONTACT:	Visual→ contact with broken/ intermittent layered organic material. Significant change in PS fractionation → P90m values increase significantly and increase in gap between median:P70m Change from clast supported to matrix support- sharp visual change.	
UNIT 2 (5)	P90m generally high but fluctuating, no discernible pattern with depth, 3.12-10.5. Increase in gap between median:P70m to top of layer, intermittent inclusion of larger clasts, contact to top of unit. Layered organic material → parallel beds towards top of layer. Sand content greater than 60%.	HF? organic material floating on surface?
CONTACT:	Sharp visual change → linear/horizontal- organic layer uniform thickness. Significant decrease in P90m and decrease in gap between median:P70m.Change in PS distribution- increase dominance of >613 μm	
UNIT 3 (2)	P90m 1.03 and 1.17 uniform, clast supported layer.	Ff
CONTACT:	Sharp visual contact (complete loss of clasts)	
UNIT 4 (1)	P90m 1.31 → sandy/fine. Lack of clasts.	Ff
CONTACT:	Sharp visual change ie inclusion of clasts.	
UNIT 5 (2)	P90m 1 and 0.62 Matrix supported, clasts intermittent No obvious structure.	Ff
CONTACT:	Sharp visual change. Significant increase in P90m values 0.62 to 5.82 and increase in gap between median:P70m. significant change, decrease in local sand fraction. Decrease mainly in greater 613 m μfraction.	
UNIT 6 (2)	Layer, clast free, sharp contact with layers above and below. Sand content > 65%.	Df
CONTACT:	Visual change ie inclusion of clasts , decrease in P90m (halved). Decrease in Gap between median:P70m, increase in sand content.	
UNIT 7 (2)	Matrix supported, intermittent clasts. P90m, 3.28 and 1.59 decreasing towards top of unit (only 2 samples). Sand content greater than 60%.	Ff?
CONTACT:	Sharp visual change, decrease in clast content P90m increases significantly, greatest difference increase in gap between Median:P70m. ↓ in total sand content correlates with organic inversion.	
UNIT 8 (3)	P90m ↑ towards top of the layer Larger intermittent clasts found at top of the layer Inverse grading. Total sand >than 40%.	Df

M - DCS1

UNIT 1 (2)	$P_{90}M$ high 8.08 7.33 Clast supported: appears imbricated. Limited depth visible. ≈40% sand content.	Df
CONTACT:	Visual change only – inclusion of matrix material → organic peaty material	
UNIT 2 (2)	Matrix supported → high organic content. $P_{90}M$ high 6.49-5.69. Sand content 52 to 64%.	Df inclusion of organic material
CONTACT:	Loss of organic matrix material	
UNIT 3 (5)	Matrix supported → large clasts at the top, slight revise grading. Organic material embedded throughout. $P_{90}M$ fairly uniform between 4.14-6.01 fluctuating, spacing fluctuates also. Sand content between 40 & 52%	Df organic material
CONTACT:	Base of Palaeosol	
UNIT 4 (2)	$P_{90}M$ highest in section 8.90 to 11.05 Chaotic, matrix supported not structured. Sand content 38 to 45%.	Df Shallow
CONTACT:	Visual change in properties many layer immediately above. Marked change in Particle Size distribution → increase in total sand content	
UNIT 5 (4)	Initial sample low $P_{90}M$, rest uniform → high, between 6.60, 8.49, 7.78. High sand content between 63 to 74%.	Df
CONTACT:	↓ in $P_{90}M$	
UNIT 6 (2)	Low, uniform $P_{90}M$ between 2.74 and 2.71. Sand content 62-73%	Ff - reworking
CONTACT:	Sharp contact visual → stony/clast dominated layer Sharp ↑ in $P_{90}M$.	
UNIT 7 (3)	$P_{90}M$ uniform and high between 5.83-7.97, spacing left skewed. Clast supported, stony layer, no structure evident. Sand content 48-56%.	Df
CONTACT:	↑ in $P_{90}M$ relative and change in spacing- even spacing and visual change-lots of clasts.	
UNIT 8 (5)	$P_{90}M$ high but decreases to the top of the section. Sand content between 40 and 55%. Spacing fluctuating, becoming even towards the top.	Df
CONTACT:	$P_{90}M$ decreases slightly but becomes even and uniform. Visual correspondence with change in physical properties Loss of clasts – become intermittent.	
UNIT 9 (3)	$P_{90}M$ uniform ≈ 6.0 Spacing even, median : $P_{70}M$ uniform. Matrix supported, clasts intermittent, no structure. Sand content ≈ 40%	Df
CONTACT:	↑ in $P_{90}M$, median $P_{70}M$ fluctuating. Loss of uniformity.	
UNIT 10 (3)	$P_{90}M$ fluctuates Matrix suported, clasts intermittent, greater than in unit 9. No structure. Sand content 41-49%.	Df
CONTACT:	Visual loss of clasts, ↓ in clast numbers. Change in Particle Size distribution – sharp ↑ in total sand content.	
UNIT 11 (2)	$P_{90}M$ decreasing 8.32-6.34 Clasts intermittent, similar to unit 9.	Df

M - DCS2

Not Cone sediments (2)	$P_{90}M$ very low, 1.09-2.39 Gravel lenses→ no structure evident, base of layer not visible. Contains large clasts between 5-10cm. Sand content high 76-83%, dominated by greater than 613 μm. Low $P_{90}M$ correlation, high median value.	Ff Terrace sediments
CONTACT:	PALAEOSOL	
UNIT 12 (2)	$P_{90}M$ very high relative to unit 1. 18 to 23, spacing even. Matrix supported, clasts intermittent No structure. Sand ≈ 45%.	Df Shallow debris flow
CONTACT:	$P_{90}M$ ↓ and change in spacing to left skewed Visual change, increase in clast:matrix ratio. Significant decrease in sand Content greater loss in those greater than 613 μm	
UNIT 13 (2)	$P_{90}M$ uniform ≈ 8, left skewed. Clast content high. Not structured. Approx. 25% sand content.	Df shallow
CONTACT:	Significant visual change → orientation → clasts obtain an incline, slipping down from left to right. P90m increases but fluctuates.	
UNIT 14 (9)	$P_{90}M$ fluctuates from 1.35 to 38.91, no discernible pattern, average around 10. Gap between $P_{90}M$ and $P_{80}M$ stays uniform, - $P_{90}M$ indicates fluctuation. Inclined maintained in whole of unit gravel lenses. Decrease in no of clasts to top of the unit but increase in size. Sand content 25-37%, loss of > 613 μm fraction.	Df
CONTACT:	Significant change in Particle Size distribution, total sand content and Fractionation ONLY.	
UNIT 15 (3)	$P_{90}M$ fluctuation significant Clast:matrix ratio low, matrix supported, inclusion of large clasts, inclination not as strong in this unit. Sand content between 41-71%.	?Df

HF - GFS1

UNIT 1 (4)	P90m low between 3.3 and 6.79, 3 uniform, 1 gravel lense, clasts intermittent at the base of the layer, normal grading, sand content variable.	Hf.
CONTACT:	Peat layer (1) 6	
UNIT 2 (2)	P90m low but uniform ≈ 5.5, uniform fractionation, matrix supported, intermittent clasts. Sand content 27 and 25%.	Hf
CONTACT:	Peat layer (1) 8.	
UNIT 3 (1)	P90m 5.6, sand content 16.5%, matrix-clasts very intermittent.	Hf.

M - HBS1

UNIT 1 (3)	$P_{90}M$ low, 2.3, 0.73 and 0.89, Greater than 613 μm dominates, Uniform size of clasts in clast supported layer, no structure evident,	Ff smaller magnitude event
CONTACT:	↑ in clast size, sharp contact visually, slight ↓ in sand content, ↓ in greater than 613 μm fraction	
UNIT 2 (8)	$P_{90}M$ low, between 0.86 and 2.04 Normal grading in clasts, ↓ in size to top of unit. Large clasts in base over 10cm.	Ff greater magnitude event
CONTACT:	Visual change, ↑ overall in clast size, sharp contact. $P_{90}M$↑ relative in comparison to unit below, ↓ in total sand content (greater than 613 μm only). Significant ↑in median: $P_{70}M$ gap.	
UNIT 3 (5)	2.1-5.04 $P_{90}M$↑ to top of unit, spacing even and uniform, clast dominated→ very large size majority above or = to 10 cm, no structure evident. sand fractionation fairly uniform in all samples.	Ff Large magnitude flood event
CONTACT:	Sharp visual contact→ ↓ in clast size, →loss of larger clasts. Significant decrease in $P_{90}M$, plus ↓ in gap between median:$P_{70}M$, Corresponds to organic incursion.	
UNIT 4 (2)	Low $P_{90}M$ = 0.50, very high sand content 83-88% dominated by greater than 613 μm- 78 and 65% of total sand content. Small clasts → intermittent→in matrix- no structure	Ff small shallow deposit, aggraded, erosive?
CONTACT:	↑ in $P_{90}M$ sharp from 0.41 to 8.91. Sharp visual contact, loss of clasts→ become intermittent Significant ↓ in sand content , especially greater than 613 μm fraction.	
UNIT 5 (2)	$P_{90}M$ uniform and high 8.91-10.4 Clasts intermittent , no structure, sand content ≈55%.	Df very shallow deposit
CONTACT:	Visual change →shallow lense, continuous horizontally.	
UNIT 6 (1)	Shallow layer continued horizontally, $P_{90}M$ significantly low in comparison to layers bove and below, 6.345.	Ff
CONTACT:	↑ $P_{90}M$ → change in visual properties, ↓ in clast numbers, ↑ in size.	
UNIT 7 (1)	Characteristics similar to unit 5, higher $P_{90}M$, highest in section, 13.54.	Df very shallow deposit

LB - HHS1

UNIT 1 (2)	$P_{90}M$ values low, 2.44 and 1.37. matrix supported, no structure-in homogenous rounded clasts, few larger clasts.	Ff flood
CONTACT:	Sharp visual change → presence of larger clasts, ↑ in number of clasts also slight relative increase in $P_{90}M$.	
UNIT 2 (4)	$P_{90}M$ uniform- 4, even spacing. Large clasts throughout, clast supported layer, no obvious grading. 10 cm+	Df
CONTACT:	Loss of large clasts, clast size becomes uniform, relative ↑ in $P_{90}M$.	
UNIT 3 (4)	$P_{90}M$ uniform ≈5 even spacing, clast supported, homogenous stony layer, no obvious grading.	Df?
CONTACT:	Thin horizontal fine layer visually separates two units. ↑ in $P_{90}M$ values also change in homogenous clast size.	
UNIT 4 (3)	$P_{90}M$ decreases from 9 to 3.57, spacing remains even. Small homogenous clast, clasts appear rounded.	Df
CONTACT:	Obvious change between layers → very large boulders act as a shield/ bedding layer. → change to large angular clasts, marked ↓ in $P_{90}M$ values and in gap between median:$P_{70}M$.	
UNIT 5 (4)	$P_{90}M$ approx 1. Total sand content high = 80% dominated by greater than 613 μm fraction. Clast supported layer → armour between layers, normal grading.	Ff channel?
CONTACT:	Change in clast number, becomes matrix dominated. Substantial ↑ in $P_{90}M$ values 0.99 to 9.84, ↓ in total sand content , greatest loss in greater than 613 μm fraction.	
UNIT 6 (3)	$P_{90}M$ values high and fluctuate between 6.79 and 11.5. gap between median : $P_{70}M$ remains comparatively uniform. Matrix supported layer, clasts intermittent, appear normal grading.	Df.
CONTACT:	loss of clasts, $P_{90}M$ values halved.	
UNIT 7 (3)	$P_{90}M$ values fluctuate between 2.91 and 5.29. Median:$P_{70}M$ gap remains uniform.	Df.

LB - HHS2

UNIT 1 (8)	$P_{90}M$ values low but fluctuating between 1.14 and 3.06. Total sand content high between 68-76%, coarse sand fraction dominates. Matrix supported, heterogenous clast sizes, no structure, largest 30-40cm.	Ff chaotic
CONTACT:	Becomes clast supported, change in clast size becoming uniform.	
UNIT 2 (3)	Clast supported , uniform clast size- rounded. $P_{90}M$ increases from 4 to to 17. Matrix weathered at top of unit.	Df.
CONTACT:	Complete change – removal of small rounded pebbles ↓ in $P_{90}M$, main part of palaeosol.	
UNIT 3 (4)	Low $P_{90}M$ → matrix supported, intermittent clasts. Matrix- soil development in lens weathering, left skewed.	Ff? Affected by palaeosol
CONTACT:	↑ in $P_{90}M$, change in dominant clast size, increasing change in spacing.	
UNIT 4 (3)	$P_{90}M$ becomes uniform ↑ to ≈ 5, even spacing.	Df
CONTACT:	Loss of clasts, change in skew and relative increase in $P_{90}M$.	
UNIT 5 (3)	Uniform characteristics measured properties. $P_{90}M$ = ≈ 7, → left skewed, uniform sand content ≈ 50%.	Df.

HF - HHS3

CONTACT:	PALAEOSOL	
UNIT 1 (5)	P90M fluctuates from 6.67 to 3.36, ≈5. Spacing changes from even to left skewed Gap between median:P70M remains uniform c.f. fractionation and total sand content =60% matrix supported layer, clasts intermittent, no structure.	Df
CONTACT:	Loss of clasts completely. Significant increase in P90M, change in spacing, becomes more left skewed ↓ in sand content to become uniform.	
UNIT 2 (3)	P90M uniform ≈ 8, change in P90M value ????? spacing remains uniform. Sand content uniform ≈ 50%, no clasts.	Df

HF - LGS1

UNIT 1 (4)	$P_{90}M$ values low ≈ 1. Particle size fractionation uniform, clast supported unit, no structure evident, - uniform size, closely packed.	Ff aggrading?
CONTACT:	↑ $P_{90}M$ dramatic 3.41 to 20.1. Visual change, ↑ matrix, ↑ in clast size, loss of sand greater than 613 μm.	
UNIT 2 (3)	$P_{90}M$ values highest in section, 20.1 decreasing to ≈10, even distribution, fractionation relative, sand content greater 40-55% Chaotic structure, matrix dominated, very large clasts intermittent.	Df
CONTACT:	↓ in $P_{90}M$ 11.7 to 2.93, ↓ in gap between median and $P_{70}M$. ↑ in greater than 613 μm and total sand (no visual change).	
UNIT 3 (5)	$P_{90}M$ values low 2.93-5 – not uniform, PS: fractionation uniform relatively. 64-76%. Greatest contribution to greater than 613 μm compared to above and below. Matrix supported, large clasts- heterogenous intermittent- normal grading, smaller clasts at top of the unit.	Ff aggrading
CONTACT:	↑ $P_{90}M$ from 1.13 to 7.61, decrease in total sand content. Visual change in clast size, removal of large clasts, increase in the number of smaller clasts, correlates with organic inversion.	
UNIT 4 (2)	$P_{90}M$ values uniform ≈ 7, even spacing, Fractionation in sand uniform, content ≈ 60%, Small clasts ≈2cm, uniform size, clast supported.	Df
CONTACT:	↓ in $P_{90}M$ 6.66 to 1.73, ↑ in total sand – greater than 613 μm , clasts not as compact, increase in matrix.	
UNIT 5 (2)	Low $P_{90}M$ 1.34 and 1.17, high total sand content 71 and 75%, greater than 613 μm fraction dominates. Clast supported but clasts similar in size, no structure evident, few anomalously large clasts <10cm.	Ff aggrading
CONTACT:	↑ in $P_{90}M$ from 1.34 to 4.4 Visually separated by sandy horizon (no sample) Change in clast size.	
UNIT 6 (2)	$P_{90}M$ uniform ≈ 4 , uniform PS fractionation ≈60%, clast structure, reverse grading, larger clasts at top, ≈ 5 cm.	Df.

HF - NGS1

UNIT 1 (3)	$P_{90}M$ uniform and average? ≈1.7, Particle Size distribution uniform, Clast supported, no structure, large clasts. 15-20 cm → large range in size.	Ff
CONTACT:	Dramatic increase in $P_{90}M$ from 1.77-40.09 Significant decrease in total sand content greatest loss in the greater than 613 μm fraction.	
UNIT 2 (7)	$P_{90}M$ fluctuates dramatically, spacing and median:$P_{70}M$ and $P_{70}M$:$P_{80}M$. No discernible structure-clast supported, contains megaclasts over 30cm, Particle size distribution also fluctuates.	Fluctuating values not deposited by one flow
CONTACT:	$P_{90}M$ remains fairly uniform. Visually layer appears horizontally uniform.	
UNIT 3 (4)	P_90M = ≈20, change in spacing in uppermost sample only. Clast supported layer appears normally graded with clasts becoming intermittent towards the top of the unit.	Df.
CONTACT:	Very sharp. $P_{90}M$ dramatic ↓, ↓ in median:$P_{70}M$. Visual change → to structured deposits, loss of clasts, ↑ in total sand content (greater than 613 μm).	
UNIT 4 (3)	Unit cross bedded, structures indicative of an erosive contact P90M low ≈ 1.	Ff erosive
CONTACT:	Visual only change from cross bedded to laminar beds	
UNIT 5 (3)	3 horizontally laminated layers, $P_{90}M$ low in each layer.	Ff
CONTACT:	Visual change from structured fluvial deposits to fluvial aggraded clast support.	
UNIT 6 (3)	$P_{90}M$ low, but high relative to units 5 and 4 ≈ 2. Clast supported layer, no structure evident.	Ff aggrading
CONTACT:	Increasing $P_{90}M$, Visual change in layer, ↓ in clast size ↓ in particle size distribution total sand content.	
UNIT 7 (2)	$P_{90}M$ high but fluctuating in comparison to layer above and below, clast supported layer, uniform clast size, no clear structure, sand content 52-71%.	?
CONTACT:	Sharp visual change, loss of clasts. Significant increase in $P_{90}M$ from 3.04-13.09. Significant loss of sand content (greater than 613 μm only).	
UNIT 8 (3)	$P_{90}M$ fairly uniform (≈10)- sorting also and particle size total sand fractionation Clasts intermittent in matrix dominated layer.	Df.

HF - TGS1

UNIT 1 (9)	$P_{90}M$, medain:$P_{70}M$ and $P_{70}M$:$P_{80}M$ all approx uniform. Total sand content ≈20-25% and fractionation. Clast supported layer, no structure. No obviously large clasts.	Hf?
CONTACT:	PALAEOSOL (5)	
UNIT 2 (5)	$P_{90}M$ very high, fluctuates, spacing fluctuates. Increase in sand content to top of unit, ↑ in greater 613 μm, clast supported layer, normally graded, ↓ in size to top of the unit.	Df
CONTACT:	Sorting values-measured properties become uniform, → to sharp visual change →stony horizontal layer.	
UNIT 3 (6)	$P_{90}M$, median:$P_{70}M$, $P_{70}M$:$P_{80}M$ all uniform. Total sand content ≈40% and fractionation uniform.	Df
CONTACT:	↓ in $P_{90}M$ significant from ↑ in total sand content in greater than 613 μm. Change in clast no. and change in clast size - visual change.	
UNIT 4 (3)	$P_{90}M$ lower, uniform, gap between median :$P_{70}M$ stays the same. Clasts intermittent but concentrated at the base of the layer normal grading.	Df

HF - TGS2

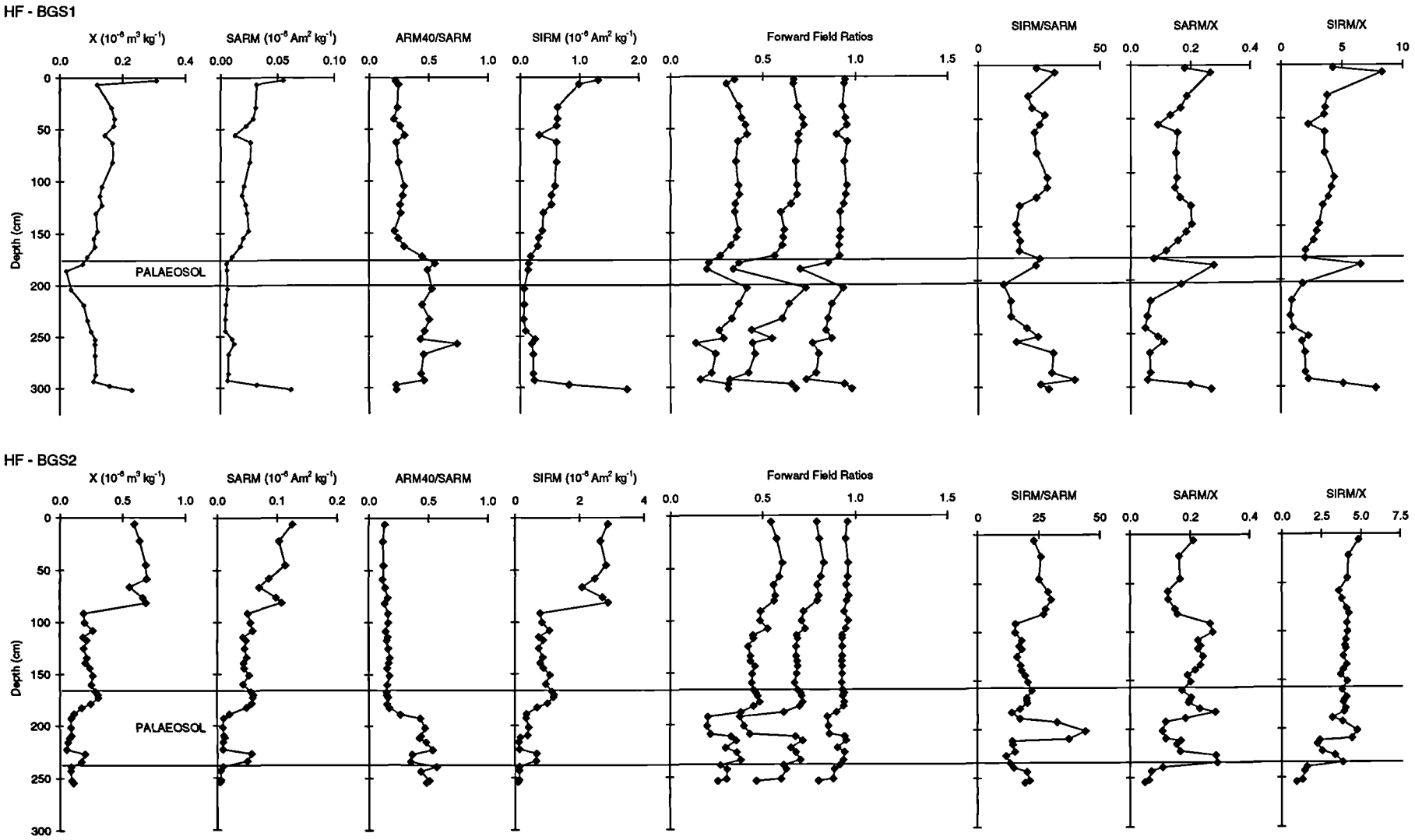
UNIT 5 (3)	$P_{90}M$ spacing values uniform ≈ 8. Clast supported unit, closely packed, uniform sizes, no structure evident . sand content greater than 33-52%.	Df.
CONTACT:	Visual change in clast matrix ratio, relative increase in $P_{90}M$ and the gap between median:$P_{70}M$.	
UNIT 6 (2)	Uniform $P_{90}M$ ≈ 14, and spacing even between percentiles. Uniform sand content approx. 50%.	Df shallow deposit
CONTACT:	↓ in $P_{90}M$, ↓ in median:$P_{70}M$, change in visual clast matrix ratio-clast Dominant- values become uniform. Organic inversion.	
UNIT 7 (8)	$P_{90}M$ uniform ≈11 and 12. Spacing heavily left skewed, uniform. Particle size distribution and total sand content are uniform (≈47%). Becomes ???? towards the top of the layer. Larger clasts/boulders intermittent.	Df
CONTACT:	Base of palaeosol-: ↑ in $P_{90}M$, greater clasts:matrix ratio.	
PALAEOSOL (4)	Formed in a Dflow deposit, $P_{90}M$ values highest in section 25-30, change in spacing , clasts small in size ≈5cm, no structures evident/slight reverse grading.	
CONTACT:	$P_{90}M$ values ↓ dramatically from 30 to 6, only visual change, top of organic layer.	
UNIT 8 (7)	$P_{90}M$ values fluctuate between 4 and 10, all even spacing between percentiles but no discernible pattern. Particle size sand fractionation more uniform, varies sand content 60-70%. Matrix supported, clasts intermittent → variation in size from 5cm to more than 10 cm and dispersed intermittently.	Df
CONTACT:	↓ in $P_{90}M$ from 4.36 to 1.55, greater than 613 μm content, visual change, Clast numbers increase and becomes more homogenous.	
UNIT 9 (2)	$P_{90}M$ low and uniform, 2.1 and 2.28, clast supported, uniform clast size, no apparent structure.	Ff reworking?

LB - WBS1

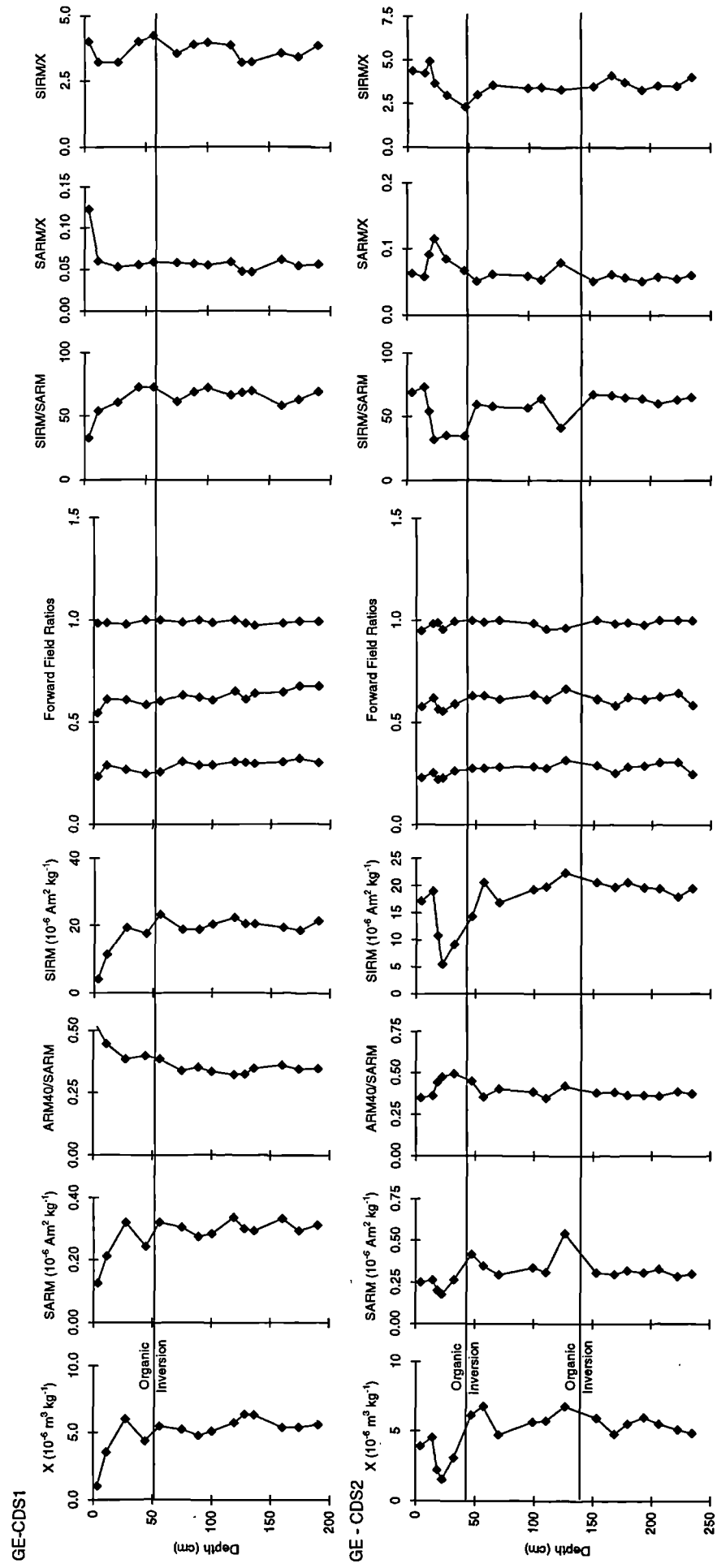
CONTACT:	PALAEOSOL	
UNIT 1 (2)	$P_{90}M$ 3.02 and 4.88 Sandy layer, total sand content variable 37 and 71%.	Df
CONTACT:	Sharp horizontal contact→ inclusion of clasts. Change in colour and ↓ in $P_{90}M$.	
UNIT 2(4)	Low $P_{90}M$ 1-79-2.29 Matrix supported, clasts intermittent, heterogenous, no structure.	Ff flood
CONTACT:	↑ $P_{90}M$, loss of clasts.	
UNIT 3 (2)	$P_{90}M$ uniform high ≈ 6, no clasts compared to unit 1 Sand content 38% and 55%.	Df
CONTACT:	Change from fine to gravely sandier layer. Sharp increase in sand content.	
UNIT 4 (2)	$P_{90}M$ fluctuates, 3.11 and 6.47 but sand content high in bottom 78-61%.	?

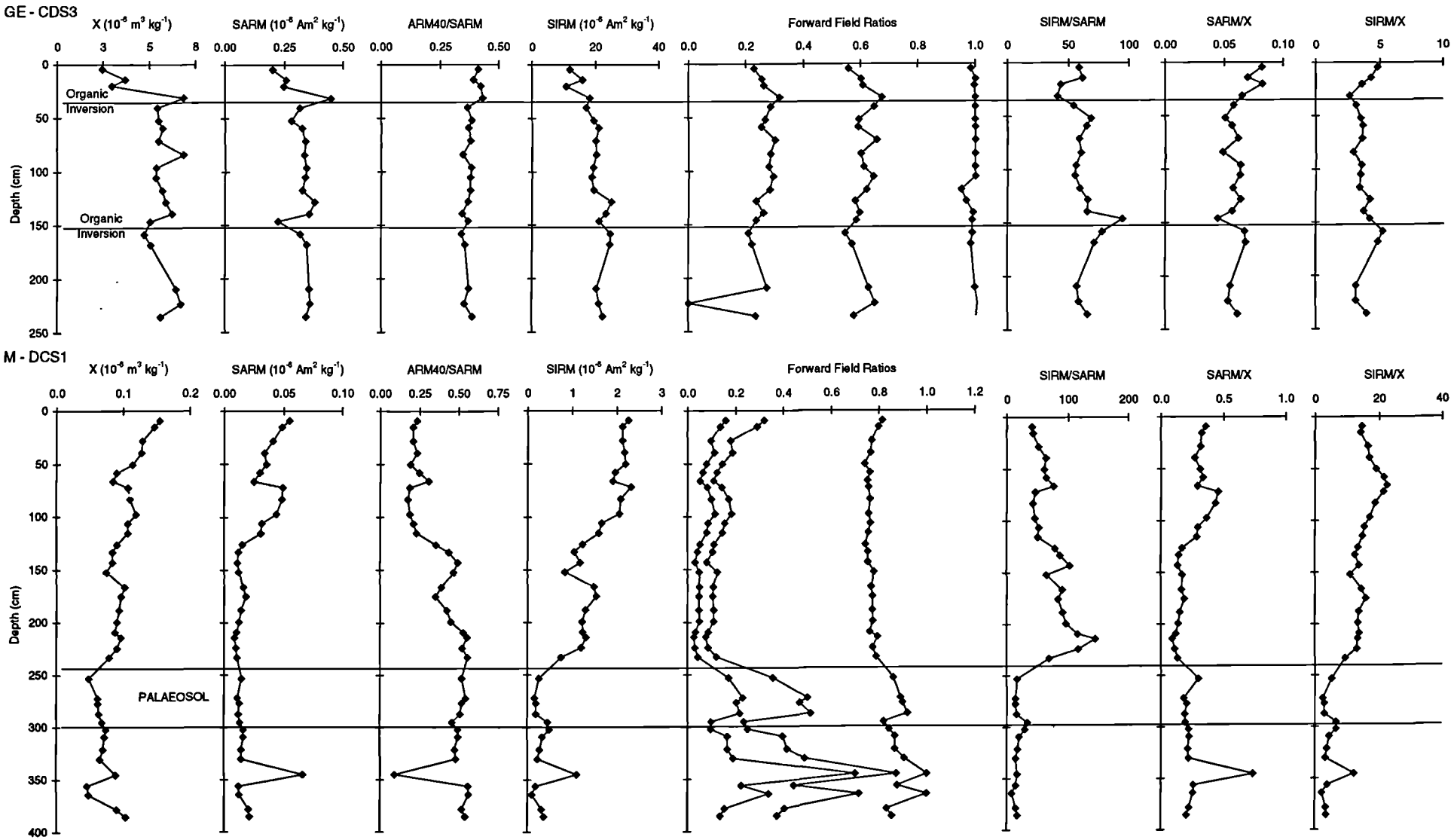
LB - WBS2

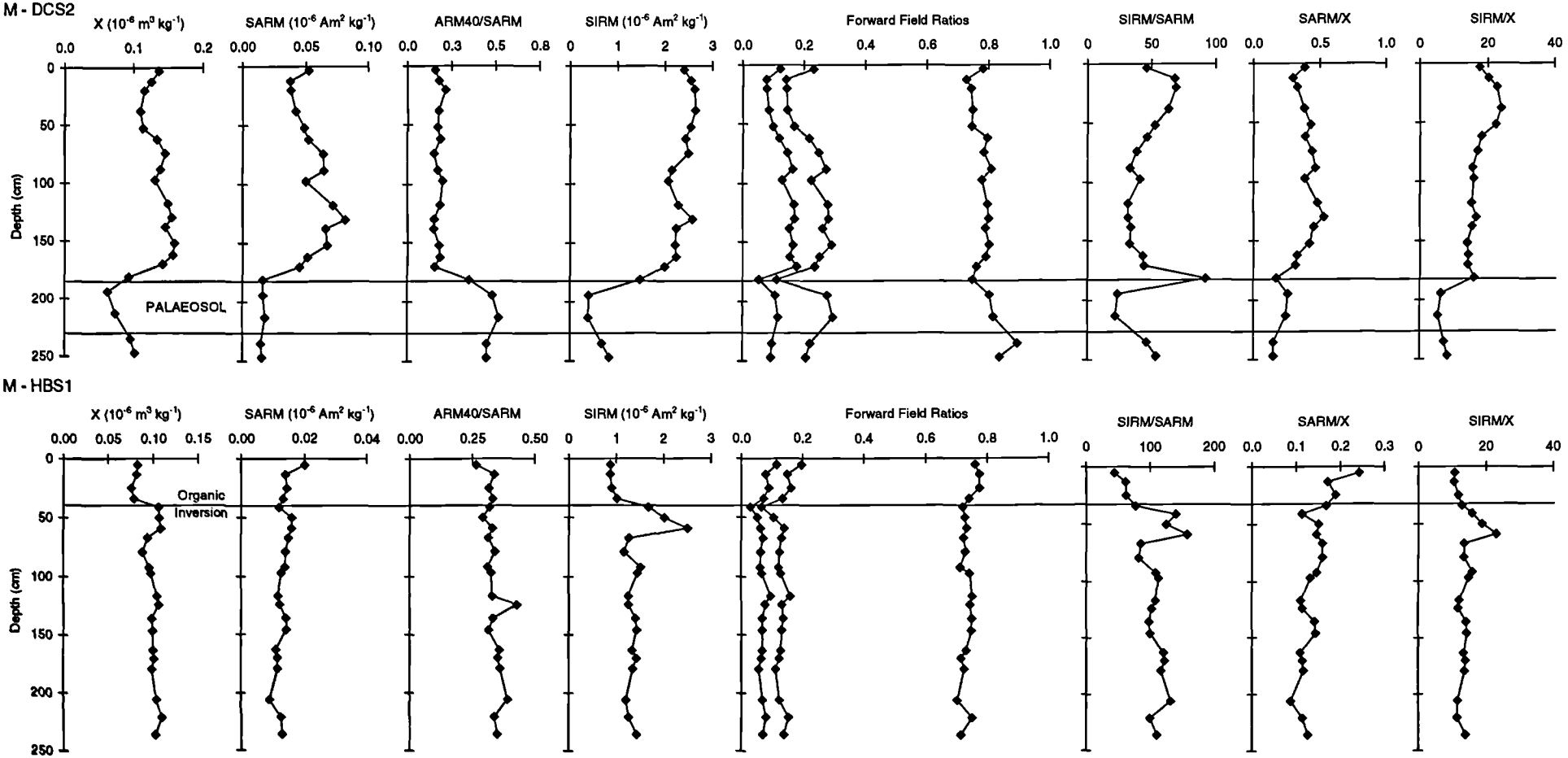
UNIT 1 (4)	$P_{90}M$ fluctuates between 4.63 and 7.29 but median:$P_{70}M$ and $P_{70}M$:$P_{80}M$ remain uniform. Sand fractionation comparable. Clast supported layer, heterogenous clast size, largest ≈ 10cm+, no structure, sand fraction between 39-55%.	Df
CONTACT:	PALAEOSOL	
UNIT 2 (8)		
CONTACT:		
UNIT 3 (2)	Transported peat layer. $P_{90}M$ values fluctuate between 2.91 and 8.42.	Ff
CONTACT:	Sharp contact change from peaty layer to sandy/gravel layer.	
UNIT 4 (1)	Shallow gravel lense. $P_{90}M$ value 2.91, sand content 73.03%	Ff
CONTACT:	Change to clast free layer.	
UNIT 5 (2)	$P_{90}M$ values 6.5 and 4.3, sand content 60-70%, no clasts, appears laminated.	Ff
CONTACT:	Sharp visual contact, horizontal re-introduction of gravel/large clasts $P_{90}M$ also ↓ dramatically.	
UNIT 6 (4)	$P_{90}M$ values low 0.57 to 1. Increase to top of the unit. Comprises small rounded clasts closely packed , clast supported, no structure. Sand content ≈ *90%, greater than* 613 μm.	Ff
CONTACT:	Visual change, loss of small clasts, ↑ in clast size, inclusion of clumps of debris.	
UNIT 7 (4)	$P_{90}M$ values low 0.85-1.54 Normal grading in clasts , ↓ in no towards top of unit. Inclusion of clumps of peat, sand content between 62-93%, greater than 613 μm dominates.	Ff
CONTACT:	Decrease in clast numbers, becoming intermittent.	
UNIT 8 (3)	Low $P_{90}M$ 1.16 increasing to 1.64 at top of the unit. Matrix supported, clasts intermittent, no structure, sand content approx 92%, greater than 613 μm dominates.	Ff.
CONTACT:	Relative increase in clast content, inclusion of clumps of *in situ* bedrock shale.	
UNIT 9 (3)	$P_{90}M$ low 1.48-1.96 fluctuating. Clast supported, inclusion of clumps of *in situ* bedrock material. Sand content 70-92%, even distribution in sand fractions.	Ff.

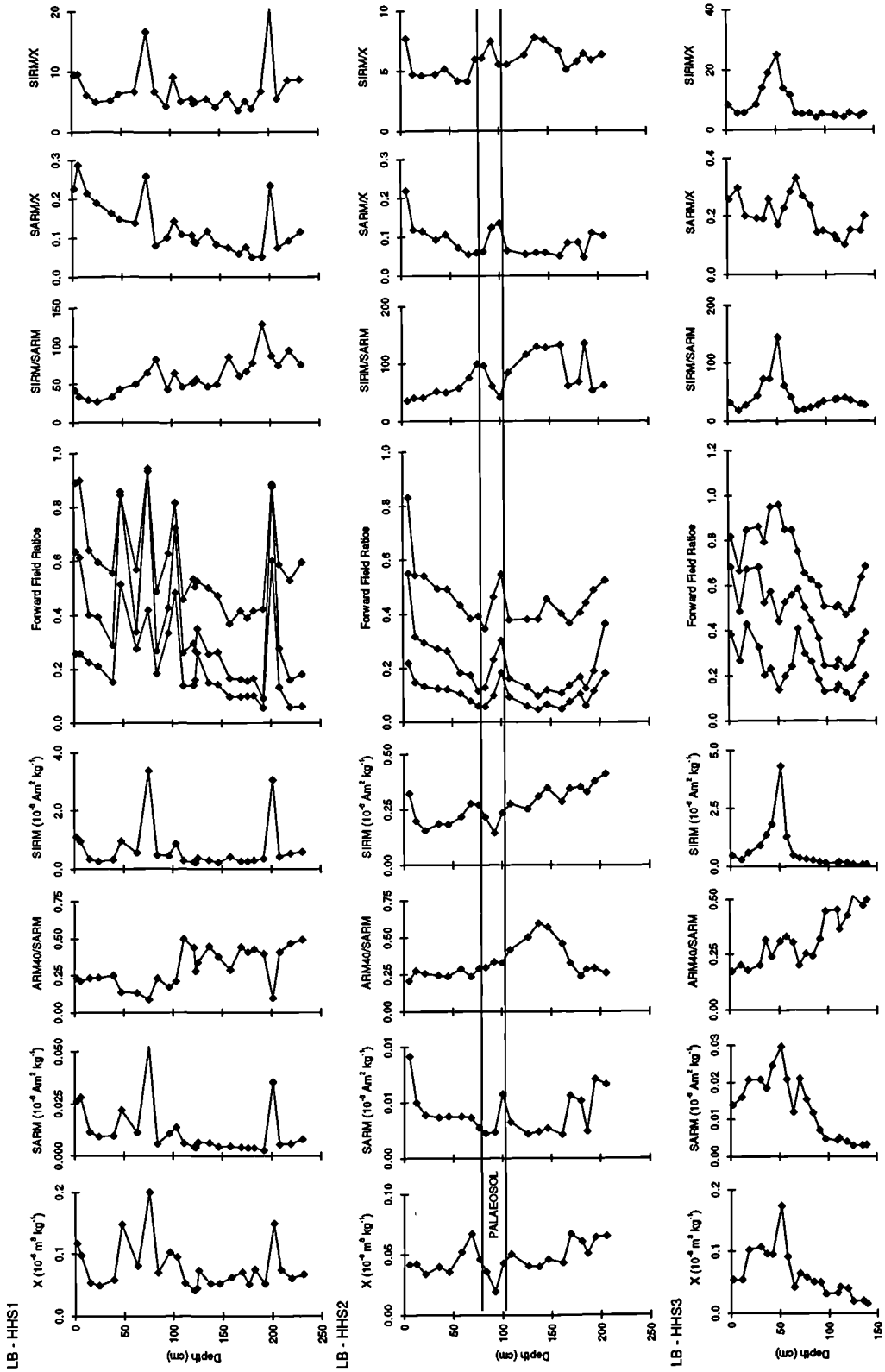


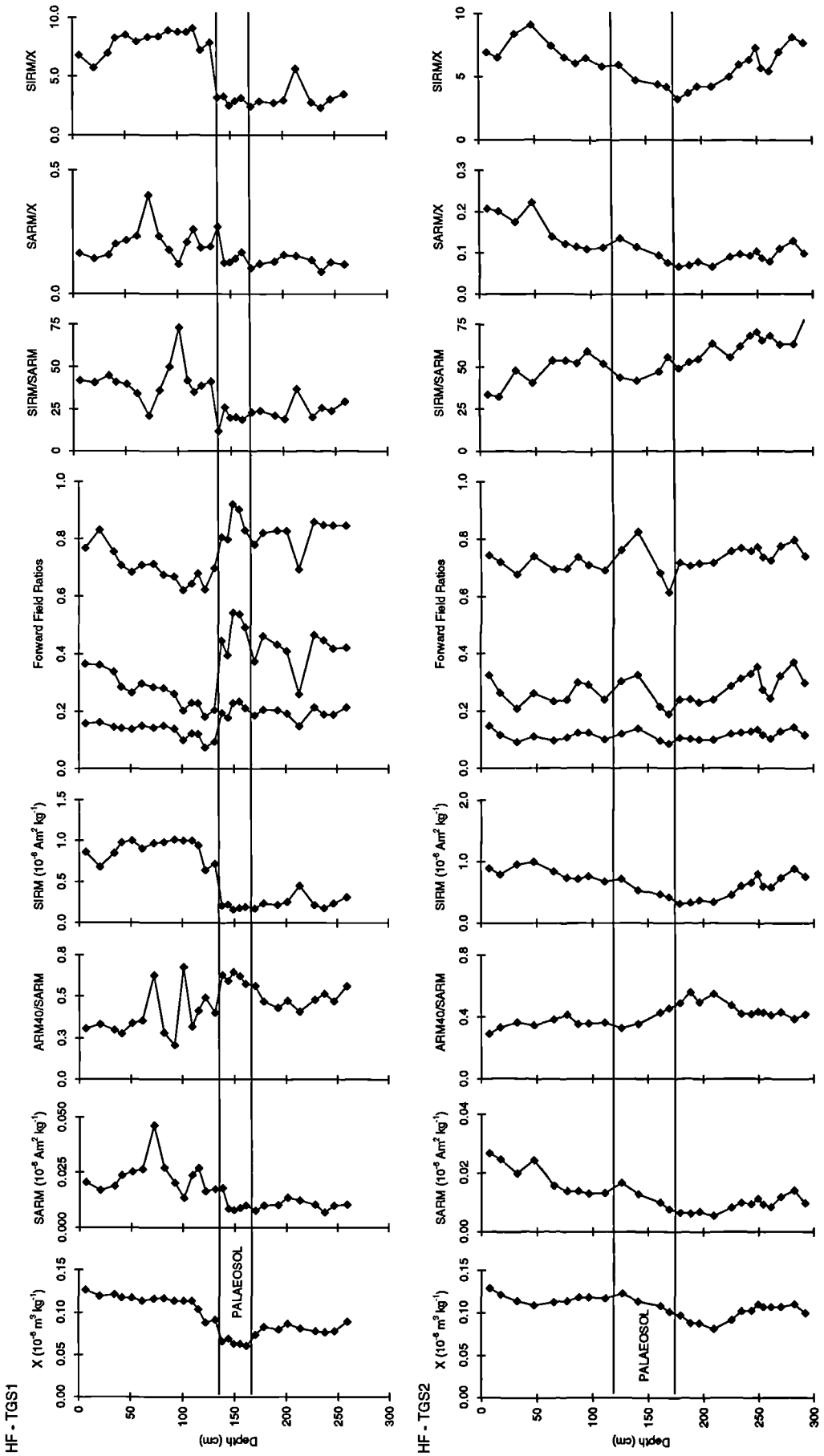
APPENDIX 3.1: Downsection plots of magnetic parameters and ratios

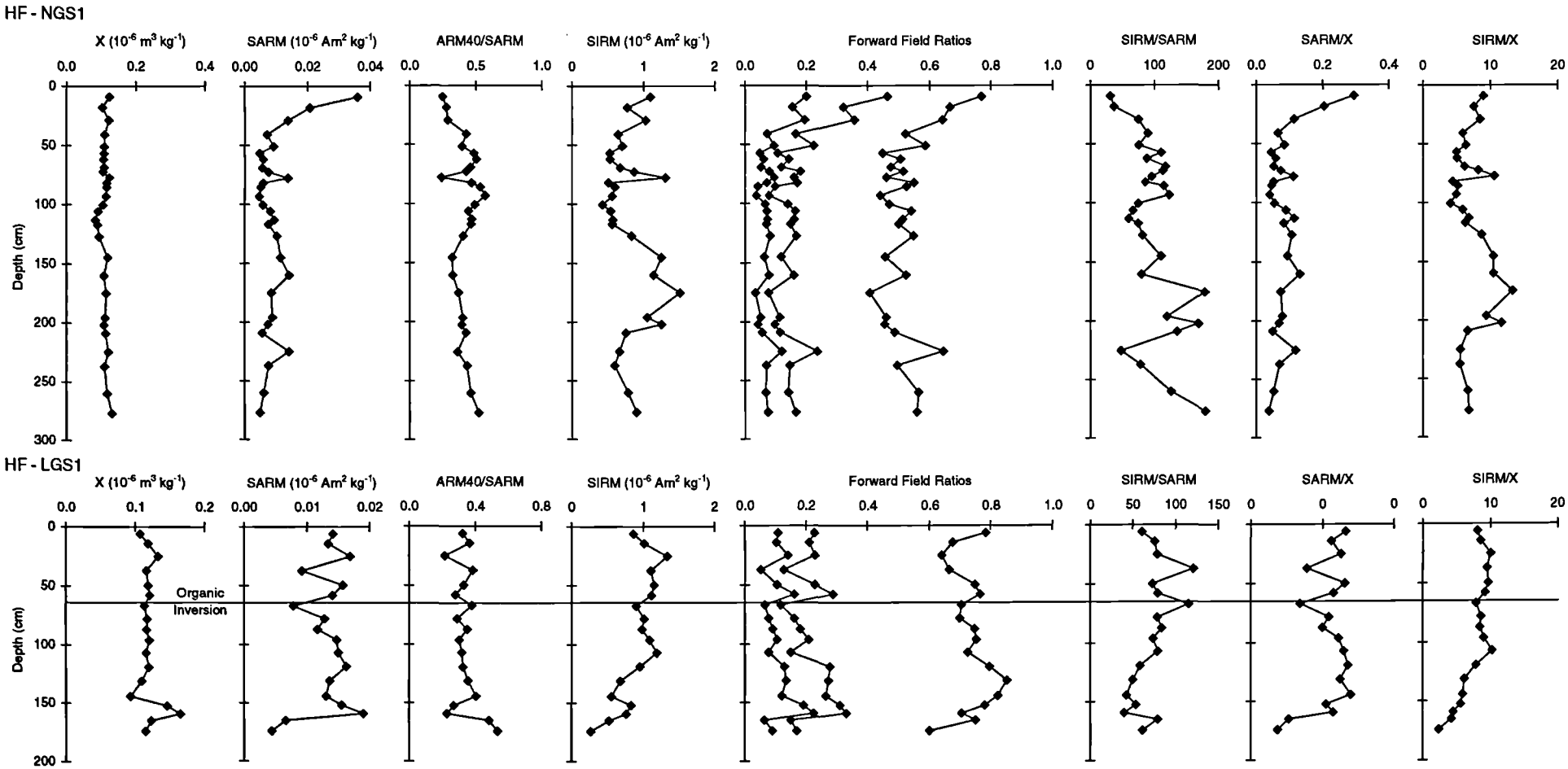

GE-CDS1
GE - CDS2
X (10⁻⁶ m³ kg⁻¹)
SARM (10⁻⁶ Am² kg⁻¹)
ARM40/SARM
SIRM (10⁻⁶ Am² kg⁻¹)
Forward Field Ratios
SIRM/SARM
SARM/X
SIRM/X
Organic
Inversion
Depth (cm)


GE - CDS3
X (10⁻⁶ m³ kg⁻¹)
SARM (10⁻⁶ Am² kg⁻¹)
ARM40/SARM
SIRM (10⁻⁶ Am² kg⁻¹)
Forward Field Ratios
SIRM/SARM
SARM/X
SIRM/X
Depth (cm)
Organic Inversion
Organic Inversion
M - DCS1
PALAEOSOL

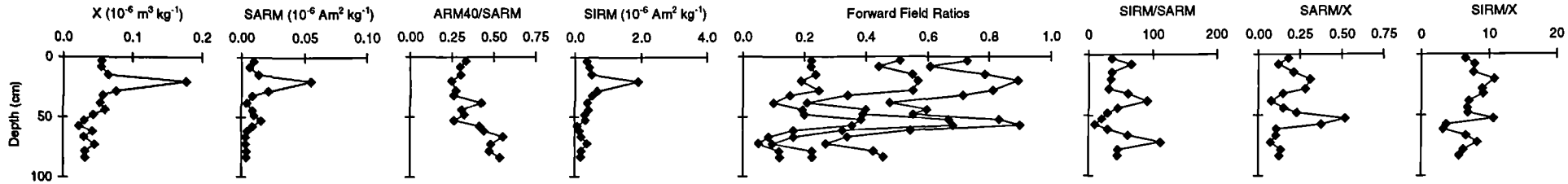

M - DCS2
X (10⁻⁶ m³ kg⁻¹)
SARM (10⁻⁶ Am² kg⁻¹)
ARM40/SARM
SIRM (10⁻⁶ Am² kg⁻¹)
Forward Field Ratios
SIRM/SARM
SARM/X
SIRM/X
Depth (cm)
PALAEOSOL
M - HBS1
Organic
Inversion


LB - HHS1
LB - HHS2
LB - HHS3
Depth (cm)
X (10⁻⁸ m³ kg⁻¹)
SARM (10⁻⁴ Am² kg⁻¹)
ARM40/SARM
SIRM (10⁻⁴ Am² kg⁻¹)
Forward Field Ratios
SIRM/SARM
SARM/X
SIRM/X
PALAEOSOL

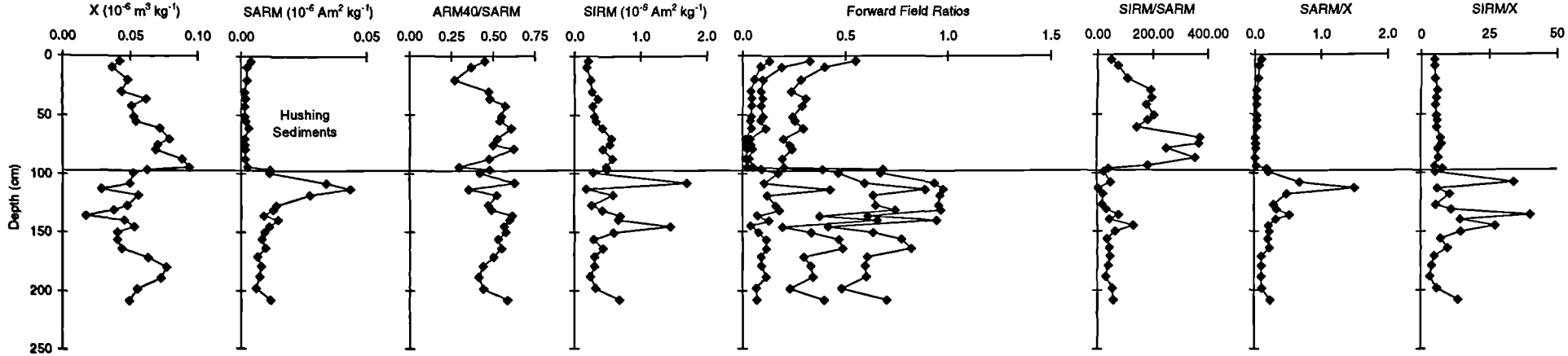

HF - TGS1
HF - TGS2
X (10⁻⁶ m³ kg⁻¹)
SARM (10⁻⁶ Am² kg⁻¹)
ARM40/SARM
SIRM (10⁻⁶ Am² kg⁻¹)
Forward Field Ratios
SIRM/SARM
SARM/X
SIRM/X
Depth (cm)
PALAEOSOL


HF - NGS1
X (10⁻⁶ m³ kg⁻¹)
SARM (10⁻⁶ Am² kg⁻¹)
ARM40/SARM
SIRM (10⁻⁶ Am² kg⁻¹)
Forward Field Ratios
SIRM/SARM
SARM/X
SIRM/X
Depth (cm)
HF - LGS1
Organic
Inversion

LB - WBS1



LB - WBS2



DCS1	Glacial Till	Solifluction	Storage	Sum difference
9	0.26	0.68	0.06	1452.76
15	0.25	0.62	0.13	4192.39
28	0.12	0.44	0.44	8643.98
39	0.23	0.32	0.46	6409.42
50	0.00	0.36	0.69	11437.33
58	0.06	0.14	0.80	8471.24
66	0.07	0.03	0.90	7243.9
72	0.00	0.42	0.58	9286.34
83	0.00	0.56	0.44	10271.02
97	0.08	0.54	0.38	8943.09
106	0.26	0.22	0.51	15056.88
115	0.30	0.16	0.55	16106.67
126	0.30	0.00	0.70	31924.7
133	0.27	0.00	0.73	56286.3
143	0.07	0.00	0.93	59476.62
152	0.50	0.00	0.50	58865.56
166	0.21	0.00	0.79	24445.35
175	0.17	0.00	0.80	20489.21
188	0.25	0.00	0.75	32436.92
199	0.28	0.00	0.72	37201.97
209	0.08	0.00	0.92	5507.87
214	0.00	0.00	1.00	69361.81
224	0.09	4.00	0.91	63756.7
233	0.52	0.00	0.48	93251.27
302	1.00	4.00	0.00	17856.44
309	1.00	0.00	0.00	23752.64
321	1.00	0.00	0.00	48557.74
330	1.00	1.00	0.00	81162
345	0.06	0.94	0.00	67468.27
356	1.00	0.00	0.00	132667.45
364	1.00	0.00	0.00	459385.49
378	1.00	0.00	0.00	31777.11
385	1.00	0.00	0.00	20326.08

DCS2	Glacial Till	Solifluction	Storage	Sum difference
3	0.00	0.78	0.22	7714.47
12	0.00	0.38	0.62	11631.83
20	0.00	0.32	0.68	5701.46
38	0.00	0.40	0.60	10248.23
52	0.00	0.53	0.47	8653.54
62	0.00	0.69	0.31	4679.39
74	0.00	0.94	0.06	5290.39
88	0.07	0.90	0.03	4043.32
97	0.15	0.62	0.23	5563.76
118	0.06	0.94	0.00	2111.04
130	0.00	1.00	0.00	2849.77
138	0.00	0.98	0.00	5642.5
152	0.09	0.91	0.00	2835.95
162	0.14	0.77	0.09	5526.75
170	0.14	0.77	0.09	12263.95
181	0.22	0.00	0.78	19199.71
194	0.93	0.00	0.07	19534.12
213	0.85	0.00	0.15	17323.62

HBS1	Glacial Till	Solifluction	Storage	Sum difference
5	0.78	0.00	0.22	14733.72
13	0.66	0.00	0.34	31436.31
25	0.66	0.00	0.34	24016.18
34	0.50	0.00	0.50	30908.38
41	0.00	0.00	1.00	37278.45
50	0.10	0.00	0.90	11546.43
59	0.14	0.00	0.86	3560.12
67	0.41	0.00	0.59	22317.82
79	0.40	0.00	0.60	28202.1
92	0.26	0.00	0.74	18383.7
97	0.33	0.00	0.67	20398.18
117	0.55	0.00	0.45	24310.55
124	0.48	0.00	0.52	29403.63
136	0.38	0.00	0.62	19292.33
146	0.35	0.00	0.65	19772.48
163	0.37	0.00	0.63	29666.32
170	0.32	0.00	0.68	26163.99
179	0.28	0.00	0.72	32665
0.41	0.00	0.60	49836	49835.91
0.54	0.00	0.46	24195	24195.48
236	0.38	0.00	0.62	19850.25

APPENDIX 3.2: Unmixing model results

BIBLIOGRAPHY

Addison, K. 1987. Debris flow during intense rainfall in Snowdonia, North Wales: A preliminary survey, *Earth Surface Processes and Landforms*, 12, pp. 561-566.

Allen, P. A. 1981. Sediments and processes on a small stream-flow dominated, Devonian alluvial fan, Shetland Islands, *Sedimentary Geology*, 29, pp. 31-66.

Andersson, S. P. & Hussey, K. M. 1962. Alluvial fan development at Franklin Bluffs, Alaska, *Science*, 69, pp. 310-322.

Atherden, M. 1992. *Upland Britain - A natural history.* Manchester University Press, Manchester.

Atkinson, T. C., Briffa, K. R., Coope, G. R. 1987. Seasonal temperatures in Britain during the last 22,000 years, reconstructed using beetle remains, *Nature*, 325, pp. 587-592.

Bagnold, R. A. 1954. Experiments on a gravity-free dispersion of large solid spheres in a Newtonian fluid under shear, *Proceedings of the Royal Society of London*, A225, pp. 49-63.

Ball, D. F. 1964. Loss-on-ignition as an estimate of organic matter and organic carbon in non-calcareous soils, *Journal of Soil Science*, 15, pp. 84-92.

Ballantyne, C. K. 1990. The Late Quaternary glacial history of the Trotternish Escarpment, Isle of Skye, Scotland, and its implications for ice-sheet reconstruction, *Proceedings of the Geological Association*, 101, pp. 171-186.

Ballantyne, C. K. 1991. Late Holocene erosion in upland Britain: climatic deterioration or human influence, *The Holocene*, 1, pp. 81-85.

Ballantyne, C. K. 1991, Periglacial features on the mountains of Skye, in Ballantyne, C. K., Benn, D. I., Lowe, J. J., Walker, M. J. C. (Eds.), *The Quaternary of Skye*, Quaternary Research Association, Cambridge, pp. 68-81.

Ballantyne, C. K. 1995. Paraglacial debris-cone formation on recently deglaciated terrain, western Norway, *The Holocene*, 5, pp. 25-33.

Ballantyne, C. K. & Benn, D. I. 1994. Paraglacial slope adjustment and resedimentation following glacier retreat, Faberstolsdalen, Norway, *Arctic and Alpine Research*, 26, pp. 255-269.

Ballantyne, C. K. & Harris, C. 1994. *The periglaciation of Great Britain.* Cambridge University Press, Cambridge.

Beaty, B. C. 1963. Origin of alluvial fans, White Mountains, California and Nevada, *Annals of the Association of American Geographers*, 53, pp. 516-535.

Beaudoin, A. B. & King, R. H. 1994. Holocene palaeoenvironmental record preserved in a paraglacial alluvial fan, Sunwapta Pass, Jasper National Park, Alberta, Canada, *Catena*, 22, pp. 227-248.

Beaumont, P. 1968. A history of glacial research in Northern England from 1860 to the present day, *Department of Geography, University of Durham, Occasional Paper Series* No. 9

Benn, D. I. 1990. Scottish Lateglacial moraines: Debris supply, genesis and significance, Unpublished Ph.D. Thesis, University of St Andrews.

Benn, D. I., Lowe, J. J., Walker, M. J. C. 1992. Glacier response to climate change during the Loch Lomond Stadial and early Flandrian: Geomorphological and palynological evidence from the Isle of Skye, Scotland, *Journal of Quaternary Science*, 7, pp. 125-144.

Bertran, P., Hetu, B., Texier, J. P., Van Steijn, H. 1997. Fabric characteristics of subaerial slope deposits, *Sedimentology*, 44, pp. 1-16.

Bertran, P. & Texier, J. P. 1994. Sedimentary structures in a debris flow cone (Vars, southern French Alps, *Permafrost and Periglacial Processes*, 5, pp. 155-170.

Birks, H. H. 1975. Studies in the vegetational history of Scotland IV. Pine stumps in Scottish Blanket Peat, *Philosophical Transactions of the Royal Society of London*, 3270, pp. 181-226.

Blair, T. C. & McPherson, J. G. 1993. The Trollhiem alluvial fan and facies model revisited: Reply to R.L. Hooke, *Geological Society of America Bulletin*, 105, pp. 564-567.

Blair, T. C. & McPherson, J. G. 1994. Alluvial fans and their natural distinction from rivers based on morphology, hydraulic processes, sedimentary processes and facies assemblages, *Journal of Sedimentary Research A: Sedimentary Petrology & Processes*, 4, pp. 450-489.

Blair, T. C. and McPherson, J.G. 1992. The Trollheim alluvial fan and facies model revisited, *Geological Society of America Bulletin*, 104, pp. 762-769.

Blissenbach, E. 1954. Geology of alluvial fans in semi-arid regions, *Geological Society of America Bulletin*, 65, pp. 175-190.

Boardman, J. 1985. *Field Guide to the periglacial landforms of Northern England*. Quaternary Research Association, Cambridge.

Bowen, D. Q., Rose, J., McCabe, A. M., Sutherland, D. G. 1986. Correlation of Quaternary glaciations in England, Ireland, Scotland and Wales, *Quaternary Science Reviews*, 5, pp. 299-340.

Bradley, R. S. & Jones, P. D. 1993. 'Little Ice Age' summer temperature variations : their nature and relevance to recent global warming trends, *The Holocene*, 3, pp. 367-376.

Brazier, V. 1987. Late Quaternary alluvial fans, debris cones and talus cones in the Grampian Highlands, Unpublished Ph.D. Thesis, University of St Andrews.

Brazier, V. & Ballantyne, C. K. 1989. Late Holocene debris cone evolution in Glen Feshie, western Cairngorm Mountains, Scotland, *Transactions of the Royal Society of Edinburgh: Earth Sciences*, 80, pp. 17-24.

Brazier, V., Whittington, G., Ballantyne, C. K. 1988. Holocene debris cone evolution in Glen Etive, western Grampian Highlands, Scotland, *Earth Surface Processes and Landforms*, 13, pp. 525-531.

Brierley, G. J., Liu, K., Crook, K. A. W. 1993. Sedimentology of coarse-grained alluvial fans in the Markham Valley, Papua New Guinea, *Sedimentary Geology*, 86, pp. 297-324.

Bridge, M.C., Haggart, B.A. & Lowe, J.J. 1990. The history and palaeoclimatic significance of subfossil remains of *Pinus silvestris* in blanket peats from Scotland. *Journal of Ecology,* 78, 77-99.

Briffa, K. & Atkinson, T. 1997, Reconstructing Late-glacial and Holocene climates, in Hulme, M. & Barrow, E. (Eds.), *Climates of the British Isles*, Routledge, London, pp. 84-101.

Brunsden, D. 1990. Tablets of Stone: toward the Ten Commandments of Geomorphology, *Zeitschrift fur Geomorphologie, Supplement Band* 79, pp. 1-37.

Brunsden, D. & Thornes, J. B. 1979. Landscape sensitivity and change, *Transactions of the Institute of British Geographers*, 4, pp. 463-484.

Bull, W. B. 1962a. Relationship of alluvial fan size and slope to drainage basin size and lithology in Western Fresno County, California, USA, *Credo Survey Paper (Prof),* 430B, pp. 51-53.

Bull, W. B. 1962b. Relation of textural (CM) patterns to depositional environments of alluvial-fan deposits, *Journal of Sedimentary Petrology*, 32, pp. 211-216.

Bull, W. B. 1977. The alluvial fan environment, *Progress in Physical Geography*, 1, pp. 222-270.

Buller, A. T. & MacManus, J. 1972. Simple metric sedimentary statistics used to recognize different environments, *Sedimentology*, 18, pp. 1-21.

Buller, A. T. & McManus, J. 1973. The quartile-deviation / median diameter relationship of glacial deposits, *Sedimentary Geology*, 10, pp. 135-146.

Caitcheon, G. G. 1993. Sediment source tracing using environmental magnetism: a new approach with examples from Australia, *Hydrological Processes*, 7, pp. 349-358.

Caitcheon, G. G. 1998. The significance of various sediment magnetic mineral fractions for tracing sediment sources in Killimicat Creek, *Catena*, 32, pp. 131-142.

Campbell, D. & McAndrews, J. H. 1993. Forest disequilibrium caused by rapid Little Ice Age cooling, *Nature*, 366, pp. 336-338.

Carling, P. A. 1986. Peat slides in Teesdale and Weardale, Northern Pennines, July 1983: Description and failure mechanisms, *Earth Surface Processes and Landforms*, 11, pp. 193-206.

Carling, P. A. 1986, A terminal debris-flow lobe in the Northern Pennines, United Kingdom, in Macklin, M. G. & Rose, T. (Eds.), *Quaternary River Landforms and Sediments in the Northern Pennines*, Quaternary Research Association, Cambridge, pp. 47-67.

Carryer, S. J. 1966. A note on the formation of alluvial fans, New Zealand, *Journal of Geology and Geophysics*, 9, pp. 91-94.

Catto, N. R. 1993. Morphology and development of an alluvial fan in a permafrost region, Aklavik range, Canada, *Geografiska Annaler Series A - Physical Geography*, 75, pp. 83-93.

Church, M. & Ryder, J. M. 1972. Paraglacial Sedimentation: A consideration of Fluvial Processes conditioned by glaciation, *Geological Society of America Bulletin*, 83, pp. 3059-3072.

Clarke, M. L. 1994. Infrared stimulated luminescence ages from aeolian sand and alluvial fan deposits from the eastern Mojave Desert, California, *Quaternary Science Reviews*, 5-7, pp. 533-538.

Collins, A. L., Walling, D. E., Leeks, G. J. L. 1998. Use of composite fingerprints to determine the provenance of the contemporary suspended sediment load transported by rivers, *Earth Surface Processes and Landforms*, 23, pp. 31-52.

Costa, J. E. 1984, The physical geomorphology of debris flows, in Costa, J. E. & Fleisher, P. J. (Eds.), *Developments and applications of geomorphology*, Springer Verlag, Berlin, pp. 268-317.

Costa, J. E. 1988, Rheologic, geomorphic, and sedimentologic differentiation of water floods, hyperconcentrated flows, and debris flows, in Baker, V. R., Kochel, R. C., Patten, C. P. (Eds.), *Flood Geomorphology*, Wiley Interscience, New York, pp. 113-122.

Costa, J. E. 1991. Nature, mechanics, and mitigation of the Val Pola landslide, Valtellina, Italy, 1987-1988, *Zeitschrift fur Geomorphologie*, 35, pp. 15-38.

Coussot, P. & Meunier, M. 1996. Recognition, classification and mechanical description of debris flows, *Earth-Science Reviews*, 40, pp. 209-227.

Cundill, P. R. 1976. Late Flandrian vegetation and soils in Carlingill Valley, Howgill Fells, *Transactions of the Institute of British Geographers*, 1, pp. 301-317.

Dearing, J. A. 1992. Sediment yields and sources in a welsh upland lake-catchment during the past 800 years, *Earth Surface Processes and Landforms*, 17, pp. 1-22.

Deboer, D. H. & Crosby, G. 1995. Evaluating the potential of SEM/EDS analysis for fingerprinting suspended sediment derived from 2 contrasting topsoils, *Catena,* 24, pp. 243-258.

Dejong, C. 1992. Thresholds for channel change on 2 contrasting pro-glacial river fans, west Greenland, *Geografiska Annaler Series A - Physical Geography*, 74, pp. 1-12.

Denny, C. S. 1965. Alluvial fans in Death Valley region, California and Nevada, *U.S. Geological Survey Professional Paper*, 466, pp. 1-62.

Derbyshire, E. & Owen, L. A. 1990, Quaternary alluvial fans in the Karakoram Mountains, in Rachocki, A. H. & Church, M. (Eds.), *Alluvial fans: A field approach*, John Wiley, Chichester, pp. 27-54.

East, T. J. 1987. A multivariate analysis of the particle size characteristics of regolith in a catchment on the Darling Downs, Australia, *Catena*, 4, pp. 101-118.

Eckis, R. 1928. Alluvial fans of the Cucamunga district, southern California, *The Journal of Geology*, 36, pp. 225-247.

Engelen, G. B. & Venneker, R. G. W. 1988, ETA (Erosion Transport Accumulation) systems, their classification, mapping and management, in Bordas, M. P. & Walling, D. E. (Eds.), *Sediment budgets*, IAHS 174,, pp. 397-412.

Evans, J. E. 1991. Facies relationships, alluvial architecture and palaeohydrology of a paleogene, humid-tropical alluvial fan system - Chumstick formation, Washington State, USA, *Journal of Sedimentary Petrology*, 61, pp. 732-755.

Eyles, N., Eyles, C. H., McCabe, A. M. 1988. Late Pleistocene subaerial debris-flow facies of the Bow Valley, near Banff, Canadian Rocky Mountains, *Sedimentology*, 35, pp. 465-480.

Eyles, N., Eyles, C. H., Miall, A. D. 1983. Lithofacies types and vertical profile models; an alternative approach to the description and environmental interpretation of glacial diamict and diamictite sequences, *Sedimentology*, 30, pp. 393-410.

Eyles, N. & Kocsis, S. 1988. Sedimentology and clast fabric of subaerial debris flow facies in a glacially-influenced alluvial fan, *Sedimentary Geology*, 59, pp. 15-28.

Faegri, k & Inverson, J. (Eds.) 1975. *Textbook of pollen analysis*, 3rd, Oxford Press, Oxford.

Fisher, R. V. 1971. Features of coarse-grained, high-concentration fluids and their deposits, *Journal of Sedimentary Petrology*, 41, pp. 916-927.

Fitzimons, S. J. 1996. Paraglacial redistribution of glacial sediments in the Vestfold Hills, East Antarctica, *Geomorphology*, 15, pp. 93-108.

Flower, R. J., Dearing, J. A., Nawas, R. 1984. Sediment supply and accumulation in a small Moroccan lake: An historical perspective, *Hydrobiologia*, 112, pp. 81-92.

Folk, R. L. & Ward, W. C. 1957. Brazoz River bar, a study in the significance of grain size parameters, *Journal of Sedimentary Petrology*, 62, pp. 394-416.

French, R. H. 1995. Estimating the depth and length of sediment deposition at slope transition on alluvial fans during flood events, *Journal of Soil and Water Conservation*, 50, pp. 521-522.

French, R. H., Fuller, J. E., Waters, S. 1993. Alluvial fan - Proposed new process-oriented definitions for arid southwest, *Journal of water resources planning and management-ASCE*, 1993, pp. 588-598.

Friend, P. F. 1983. Towards the field classification of alluvial architecture or sequence, *International Association of Sedimentologists*, 6, pp. 345-354.

Gascoyne, M., Schwarcz, H. P., Ford, D. C. 1983. Uranium series ages of speleothems from northwest England: correlation with Quaternary climate, *Philosophical Transactions of the Royal Society of London*, B301, pp. 143-164.

Gordon, J.E., Thompson, D.B.N., Haynes, V.M., Brazier, V. and Macdonald, R. 1998 Environmental sensitivity and conservation management in the Cairngorm Mountains, Scotland. *Ambio*, 27, pp. 335-344

Gottesfeld, S. A., Mathewes, R. W., Gottesfeld, L. M. J. 1991. Holocene debris flows and environmental history, Hazelton area, British Columbia, *Canadian Journal of Earth Sciences*, 28, pp. 1583-1593.

Gregory, K. J. & Maizels, J. K. 1991, Morphology and Sediments:, in Starkel, L., Gregory, K. J., Thornes, B. (Eds.), *Typological characteristics of fluvial forms and deposits*, John Wiley and Sons Ltd, Chichester, pp. 31-59.

Guzzetti, F., Marchelli, M., Reichenbach, P. 1997. Large alluvial fans in the north-central Po Plain (Northern Italy), *Geomorphology*, 18, pp. 119-136.

Harris, S. A. & Gustafson, C. A. 1993. Debris flow characteristics in an area of continuous permafrost, St-Elias Range, Yukon-Territory, *Zeitschrift fur Geomorphologie*, 37, pp. 41-56.

Harvey, A. M. 1984. Aggradation and dissection sequences of Spanish alluvial fans: influence on morphological development, *Catena*, 11, pp. 289-304.

Harvey, A. M. 1984, Debris flow and fluvial deposits in Spanish Quaternary alluvial fans: implications for fan morphology, in Koster, E. H. & Steel, R. (Eds.), Sedimentology of gravels and conglomerates, *Canadian Society for Petroleum Geology Memoir* 10,, pp. 123-132.

Harvey, A. M. 1986. Geomorphic effects of a 100 year storm in the Howgill Fells, Northwest England, *Zeitschrift fur Geomorphologie*, 30, pp. 71-91.

Harvey, A. M. 1987, Sediment supply to upland streams: influence on channel adjustment, in Thorne, C. R., Bathurst, J. C., Hey, R. D. (Eds.), *Sediment transport in gravel-bed rivers*, John Wiley and Sons Ltd, Chichester, pp. 121-150.

Harvey, A. M. 1988. Controls of alluvial fan development: the alluvial fans of Sierra de Carrascoy, Murcia, Spain, *Catena, Supplement* 13, pp. 123-137.

Harvey, A. M. 1989, The occurrence and the role of arid zone alluvial fans, in Thomas, D. S. G. (Ed.), *Arid zone geomorphology*, Wiley, New York, pp. 136-158.

Harvey, A. M. 1990, Factors influencing Quaternary alluvial fan development in southeast Spain, in Rachocki, A. & Church, M. (Eds.), *Alluvial fans: A field approach*, John Wiley, Chichester, pp. 247-269.

Harvey, A. M. 1996. The role of alluvial fans in the mountain fluvial systems of Southeast Spain: Implications of climatic change, *Earth Surface Processes and Landforms*, 21, pp. 543-553.

Harvey, A. M., Oldfield, F., Baron, A. F., Pearson, G. W. 1981. Dating of post glacial landforms in the Central Howgills, *Earth Surface Processes and Landforms*, 6, pp. 401-412.

Harvey, A. M. & Renwick, W. H. 1987. Holocene alluvial fan and terrace formation in the Bowland Fells, northwest England, *Earth Surface Processes and Landforms*, 12, pp. 249-257.

Hooke, R. L. 1967. Processes on arid region alluvial fans, *The Journal of Geology*, 75, pp. 438-460.

Hooke, R. L. 1968. Steady-state relationships of arid-region alluvial fans in closed basins, *American Journal of Science*, 266, pp. 609-629.

Hoppe, G. & Eckman, S. 1964. A note on the alluvial fans of Lattjovagge, Swedish Lapland, *Geografiska Annaler Series A - Physical Geography*, 46, pp. 338-342.

Hubert, J. F. & Filipov, A. J. 1989. Debris-flow deposits in alluvial fans on the west flank of the White Mountains, Owens Valley, California, U.S.A, *Sedimentary Geology*, 61, pp. 177-205.

Hutchinson, S. M. 1995. Erosion and sedimentation in an Upland Catchment, *Earth Surface Processes and Landforms*, 20, pp. 293-314.

Ingham, J. K. 1966. The Ordovician rocks in the Cautley and dent districts of Westmorland and Yorkshire, *Proceedings of the Yorkshire Geological Society*, 35, pp. 455-505.

Inman, D. L. 1952. Sorting of sediments in the light of fluid mechanics, *Journal of Sedimentary Petrology*, 19, pp. 51-70.

Innes, J. L. 1983. Lichenometric dating of debris flow deposits in the Scottish Highlands, *Earth Surface Processes and Landforms*, 8, pp. 579-588.

Jenkins, A., Ashworth, R. J., Ferguson, R. I., Grieve, I. C., Rowling, P., Stott, T. A. 1988. Slope failures in the Ochill Hills, Scotland, November 1984, *Earth Surface Processes and Landforms*, 13, pp. 69-76.

Johnson, A. M. 1970. *Physical processes in geology.* Freeman & Cooper, San Francisco.

Johnson, A. M. & Rodine, J. R. 1984, Debris flow, in Brunsden, D. & Prior, D. B. (Eds.), *Slope instability*, John Wiley, New York, p. Ch. 8.

Johnson, G. A. L. & Hickling, G. 1970. Geology of Durham County, *Transactions of the Natural History Society of Northumberland, Durham and Newcastle upon Tyne* 41, 1

Johnson, P. G. 1984. Paraglacial conditions of instability and mass movement: A discussion, *Zeitschrift fur Geomorphologie*, 28, pp. 235-250.

Kodama, Y. 1994. Downstream changes in the lithology and grain size of fluvial gravels, the Watarase River, Japan: Evidence of the role of abrasion in downstream fining, *Journal of Sedimentary Research A: Sedimentary Petrology & Processes*, 64, pp. 68-75.

Kostaschuk, R. A., Macdonald, G. M., Putnam, P. E. 1986. Depositional process and alluvial fan-drainage basin morphometric relationships near Banff, Alberta, Canada, *Earth Surface Processes and Landforms*, 11, pp. 471-484.

Krumbein, W. C. 1934. Size frequency distribution of sediments, *Journal of Sedimentary Petrology*, 4, pp. 65-77.

Lamb, H. H. 1977. *Climate: Past, present and future,, Volume 2: Climatic history and the future,* Methuen, London.

Lamb, H. H. 1984, Some studies of the Little Ice Age of recent centuries and its great storms, in Morner, N. A. & Karlin, W. (Eds.), *Climatic change on a yearly to millennium basis*, Reidel, Dordrecht, .

Landim, P. M. B. & Frakes, L. A. 1968. Distinction between tills and other diamicts based upon textural characteristics, *Journal of Sedimentary Petrology*, 38, pp. 1213-1223.

Lecce, S. A. 1991. Influence of lithologic erodibility on alluvial fan area, Western White Mountains, California and Nevada, *Earth Surface Processes and Landforms*, 16, pp. 11-18.

Lees, J. A. 1994. Modelling the magnetic properties of natural and environmental materials, Unpublished Ph.D. Thesis, University of Coventry.

Leggett, R. F., Brown, R. J. E., Johnson, G. H. 1966. Alluvial fan formation near Aklavik, Northwest Territories, Canada, *Geological Society of America Bulletin*, 77, pp. 15-30.

Lewin, J., Bradley, S. B., Macklin, M. G. 1983. Historical valley alluviation in mid-Wales, *Geological Journal*, 18, pp. 331-350.

Lowe, D. R. 1986. Grain flow or grain-flow deposits, *Journal of Sedimentary Petrology*, 46, pp. 188-199.

Macklin, M. G. 1996. *Holocene fluvial geomorphology of Northeast England.* (in Press)

Macklin, M. G. & Lewin, J. 1993. Holocene river alluviation in Britain, *Zeitschrift fur Geomorphologie*, 88, pp. 109-122.

Macklin, M. G. & Needham, S. 1992, Studies in British alluvial archaeology : potential and prospect, in Needham, S. & Macklin, M. G. (Eds.), *Alluvial archaeology in Britain*, Oxbow Press, Oxford, pp. 9-23.

Macklin, M. G., Passmore, D. G., Rumsby, B. T. 1992, Climate and cultural signals in Holocene alluvial sequences : the Tyne Basin, northern England, in Needham, S. & Macklin, M. G. (Eds.), *Alluvial archaeology in Britain*, Oxbow Press, Oxford, pp. 123-139.

Magilligan, F. J. 1992. Sedimentology of a fine grained aggrading floodplain, *Geomorphology*, 4, pp. 393-408.

Maher, B. A. 1986. Characterisation of soils by mineral magnetic measurements, *Physics of the Earth and Planetary interiors*, 42, pp. 76-92.

Maizels, J & Aitken, J. 1991. Palaeohydrological change during deglaciation in Upland Britain : A case study from Northeast Scotland, in Starkel, L., Gregory, K.J. & Thornes, J.B. (Eds.), *Temperate Palaeohydrology*, John Wiley & Sons Ltd, Chichester, pp. 105 - 145.

Marchi, L. & Tecca, R. R. 1995. Alluvial fans of the eastern Italian Alps - morphometry and depositional processes, *Geodinamic*a, 18, pp. 20-27.

Marr, J. E. & Fearnsides, W. G. 1909. The Howgill Fells and their topography, *Quarterly Journal of the Geological Society London*, 65, pp. 587-610.

Martin, C. W. & Johnson, W. C. 1995. Variation in radiocarbon ages of soil organic matter fractions from Late Quaternary buried soils., *Quaternary Research*, 43, pp. 232-237.

Mathewson, C. C., Keaton, J. R., Santi, P. M. 1990. Role of bedrock ground water in the initiation of debris flows and sustained post-flow stream discharge, *Association of engineering Geologists Bulletin*, 27, pp. 73-83.

May, J. A. 1981. The glaciation and deglaciation of Upper Nithsdale and Annandale, Unpublished Ph.D. Thesis, University of Glasgow.

McBride, E. F. 1971, Mathematical treatment of size distribution data, in Carver, R. E. (Ed.), *Procedures in Sedimentary petrology*. pp. 109-127.

McCammon, R. B. 1962. Efficiencies of percentile measures for describing the mean size and sorting of sedimentary particles, *The Journal of Geology*, 70, pp. 453-465.

Melton, M. A. 1965. The geomorphic and palaeoclimatic significance of alluvial deposits in southern Arizona, *The Journal of Geology*, 73, pp. 1-38.

Meunier, M. 1994. Process in knowledge and methods for studying torrential phenomena, *Houille Blanche*, 3, pp. 25-31.

Miall, A. 1977. A review of the braided river deposition environment, *Earth-Science Reviews*, 13, pp. 1-62.

Miall, A. D. 1985. Architectural element analysis: a new method of facies analysis applied to fluvial deposits, *Earth-Science Reviews*, 22, pp. 261-308.

Miall, A. D. 1988. Architectural elements and bounding surfaces in fluvial deposits - anatomy of the Kayenta formation (lower Jurrasic), southwest Colorado, *Sedimentary Geology*, 55, pp. 232-262.

Mitchell, W. A. 1991, Loch Lomond Stadial glacial landforms and palaeoglaciological reconstruction, in Mitchell, W. A. (Ed.), *Western Pennines: Field Guide*, Quaternary Research Association, London, pp. 43-53.

Mitchell, W. A. 1996. Significance of snowblow in the generation of Loch Lomond Stadial (Younger Dryas) glaciers in the western Pennines, northern England, *Journal of Quaternary Science,* 11, pp. 233-248.

Nanson, G. C. & Young, R. W. 1986. Comparison of thermoluminescence and radiocarbon age- determinations from Late Pleistocene alluvial deposits near Sydney, Australia, *Quaternary Research*, 27, pp. 263-269.

Oguchi, T. & Tokyo, H. O. 1994. Analysis of relationships among alluvial fan area, source basin area, basin slope, and sediment yield, *Zeitschrift fur Geomorphologie*, 38, pp. 405-420.

Oldfield, F., Maher, B. A., Donaghue, J., Pierce, J. 1985. Particle-size related, mineral magnetic source sediment linkages in the Rhode River catchment, Maryland, USA, *Journal of the Geological Society,* 142, pp. 1035-1046.

Oldfield, F., Rummery, T. A., Thompson, R., Walling, D. E. 1979. Identification of suspended sediment sources by means of magnetic measurements, *Water Resources Research*, 15, pp. 211-218.

Otto, G. H. 1939. A modified logarithmic probability graph for the interpretation of mechanical analyses of sediments, *Journal of Sedimentary Petrology*, 9, pp. 62-76.

Owen, L. A. 1991. Mass movement deposits in the Karakoram Mountains : their sedimentary characteristics, recognition and role in Karakoram landform evolution, *Zeitschrift fur Geomorphologie*, 8, pp. 475-491.

Parker, K. C. 1995. Effects of complex geomorphic history on soil and vegetation patterns on alluvial fans, *Journal of Arid Environments*, 30, pp. 19-39.

Passega, R. 1957. Texture as a characteristic of clastic deposition, *American Association of Petroleum Geologists Bulletin*, 41, pp. 1952-1984.

Passega, R. 1964. Grain size representation by CM patterns as a geological tool, Journal of *Sedimentary Petrology*, 34, pp. 830-847.

Passega, R. 1977. Significance of CM diagrams of sediments deposited by suspension, *Sedimentology*, 24, pp. 723-733.

Patten, C. P. 1970. *Physical Geography*. Wandsworth, Belmont.

Pe, G.G. and Piper, D.J.W. 1975. Textual recognition of mudflow deposits, *Sedimentary Geology*, 13, pp. 303-306.

Pennington, W. 1974. *The history of British vegetation*, 2nd Edition,, English Universities Press, London.

Penny, L. F., Coope, G. R., Catt, J. A. 1969. Age and insect fauna of the Dimlington Silts, East Yorkshire, *Nature*, 224, pp. 65-67.

Peters, C. 1995. Unravelling magnetic mixtures in sediments, soils and rocks, Unpublished Ph.D. Thesis, University of Edinburgh.

Phillips, C. J. & Davies, T. R. H. 1991. Determining rheological parameters of debris flow material, *Geomorphology*, 4, pp. 101-110.

Pierson, T. C. 1985, Effects of slurry composition on debris flow dynamics, Rudd Canyon, Utah, in Bowles, D. S. (Ed.), *Delineation of landslide, flash-flood and debris flow hazards in Utah*, Utah Water Research Laboratory, Logan, pp. 132-152.

Pierson, T. C. & Scott, K. M. 1985. Downstream dilution of a lahar : transition from debris flow to hyperconcentrated flow, *Water Resources Research*, 21, pp. 1511-1524.

Porat, N., Amit, R., Ziverman, E., Enzel, y 1997. Luminescence dating of fault-related alluvial fan sediments in the southern Arava valley, Israel, *Quaternary Science Reviews*, 16, pp. 397-402.

Prior, D. B., Stephens, N., Douglas, G. R. 1970. Some examples of modern debris flows in north-east Ireland, *Zeitschrift fur Geomorphologie*, 14, pp. 275-288.

Rickenmann, D. 1990. Debris flows 1987 in Switzerland: modelling and fluvial sediment transport, *International Association of Hydrological Sciences Publication*, 194, pp. 371-378.

Rickson, R. J. & Morgan, R. P. C. 1988. Erosion in the Howgill Fells, Unpublished Soil Erosion on agricultural land Thesis, Silsoe College.

Roed, M. A. & Wasylyk, D. G. 1973. Age of inactive alluvial fans - Bow River Valley, Alberta, *Canadian Journal of Earth Sciences*, 8, pp. 279-298.

Royse, C. F. 1968. Recognition of fluvial environments by particle-size characteristics, *Journal of Sedimentary Petrology*, 38, pp. 1171-1178.

Ruddiman, W. F. & McIntyre, A. 1981. The North Atlantic during the last deglaciation, *Palaeogeography, Palaeoclimatology, Palaeoecology*, 35, pp. 145-214.

Ryder, J. M. 1971. Some aspects of the morphometry of paraglacial alluvial fans in South-central British Columbia, *Canadian Journal of Earth Sciences*, 8, pp. 1252-1264.

Ryder, J. M. 1971. The stratigraphy and morphology of paraglacial alluvial fans in South-central British Columbia, *Canadian Journal of Earth Sciences*, 8, pp. 279-298.

Sahu, B. K. 1952. Depositional mechanisms from the analysis of clastic sediments, *Journal of Sedimentary Petrology*, 34, pp. 73-83.

Schumm, A., Mosley, M. P., Weaver, W. 1987. *Experimental fluvial geomorphology.* John Wiley, New York.

Schumm, S. A. 1979. Geomorphic thresholds: The concept and its applications, *Institute of British Geographers*, 4, pp. 485-515.

Scott, K. M. 1985. Lahars and lahar-runout flows in the Toutle-Cowlitz river system, Mount St Helens, Washington - origins, behaviour and sedimentology, *Geological Survey Open-File Report (U.S.)* 85-500, pp. 1-202

Scott, P. F. & Erskine, W. D. 1994. Geomorphic effects of a large flood on fluvial fans, *Earth Surface Processes and Landforms*, 19, pp. 95-108.

Sharma, M. C. & Owen, L. A. 1996. Quaternary glacial history of NW Garhwal, central Himalayas, *Quaternary Science Reviews*, 15, pp. 335-365.

Silva, P. G., Harvey, A. M., Zazo, C., Goy, J. L. 1992. Geomorphology, depositional style and morphometric relationships of Quaternary alluvial fans in the Guadalentin Depression (Murcia, Southeast Spain), *Zeitschrift fur Geomorphologie*, 36, pp. 325-341.

Singer, M. J., Verosub, K. L., Fine, P., TenPas, J. 1996. A conceptual model for the enhancement of magnetic susceptibility in soils, *Quaternary International*, 34-36, pp. 243-248.

Sissons, J. B. 1976. *The geomorphology of the British Isles*: Scotland. Methuen, London.

Sissons, J. B. 1979. The Loch Lomond Stadial in the British Isles, *Nature*, 280, pp. 199-203.

Sissons, J. B. 1979. The Loch Lomond advance in the Cairngorm Mountains, *Scottish Geographical Magazine*, 95, pp. 66-82.

Souch, C. 1994. A methodology to interpret down valley lake-sediments as records of neoglacial activity - Coast Mountains, British Columbia, Cananda, *Geografiska Annaler Series A - Physical Geography*, 76, pp. 169-185.

Squires, R. 1978. Conservation in Upper Teesdale: Contributions from the palaeoecological record, *Transactions of the Institute of British Geographers*, 3, pp. 129-150.

Starkel, L. 1972. The role of the catastrophic rainfall in the shaping of the relief of the lower Himalaya (Darjeeling Hills), *Geogr. Pol.*, 21, pp. 103-147.

Statham, I. 1976. Debris flows on vegetated screes in the Black Mountain, Camarthenshire, *Earth Surface Processes and Landforms*, 1, pp. 173-180.

Stokes, S., Campbell, S. N., Healy, T. R. 1989. Textural procedures for the environmental discrimination of Late Neogene coastal sand deposits, southwest Auckland, New Zealand, *Sedimentary Geology*, 61, pp. 135-150.

Stott, A. P. 1986. Sediment tracing in a reservoir-catchment system using a magnetic mixing model, *Physics of the Earth and Planetary interiors*, 42, pp. 105-112.

Sutherland, D. G. 1984. The Quaternary deposits and landforms of Scotland and the adjacent shelves, *Quaternary Science Reviews*, 3, pp. 157-254.

Sutherland, D. G. 1991, Late Devensian glacial deposits and glaciation in Scotland and the adjacent offshore region, in Ehlers, J., Gibbard, P. L., Rose, J. (Eds.), *Glacial deposits in Great Britain and Ireland*, Balkema, Rotterdam, pp. 53-60.

Takahashi, T. 1980. Debris flow on a prismatic open channel, *Journal of the Hydraulics Division, American Society of Civil Engineers*, 106, pp. 381-396.

Tallis, J. H. 1985. Mass movement and erosion of a Southern Pennine blanket peat, Journal of *Ecology*, 73, pp. 283-315.

Thompson, R., Cameron, T. D. J., Schwarz, C., Jensen, K. A., van Lemberge, V. M., Sha, L. P. 1992. the magnetic properties of Quaternary and tertiary sediments in the southern North Sea, *Journal of Quaternary Science*, 7, pp. 319-334.

Thompson, R. & Oldfield, F. 1986. *Environmental magnetism*. Allen and Unwin, London.

Thorp, P. 1991, The glaciation and glacial deposits of the western Grampians, in Ehlers, J., Gibbard, P. L., Rose, J. (Eds.), *Glacial deposits in Great Britain and Ireland*, Balkema, Rotterdam, pp. 137-150.

Thorp, P. W. 1981. A trimline method for defining the upper limit of the Loch Lomond Advance glaciers: examples from the Loch Leven and Glen Coe areas, *Scottish Journal of Geology*, 17, pp. 49-64.

Tipping, R. 1994. Fluvial chronology and valley floor evolution of the upper Bowmont Valley, Borders region, Scotland, *Earth Surface Processes and Landforms*, 19, pp. 641-657.

Tipping, R. 1995. Holocene evolution of a lowland Scottish landscape - Kirkpatrick-Fleming. 3. Fluvial history, *The Holocene*, 5, pp. 184-195.

Tipping, R. & Halliday, S. P. 1994. The age of alluvial fan deposition at a site in the southern uplands of Scotland, *Earth Surface Processes and Landforms*, 19, pp. 333-348.

Tivy, J. 1962. An investigation of certain slope deposits in the Lowther Hills, Southern uplands of Scotland, *Transactions of the Institute of British Geographers*, 30, pp. 59-73.

Trask, P. D. 1939. Mechanical analysis of sediments by centrifuge, *Economic Geology*, 25, pp. 581-599.

Turner, J. & Hodgson, J. 1979. Studies in the vegetational history of the northern Pennines: 1. Variations in the composition of the early Flandrian forests, *Journal of Ecology*, 67, pp. 629-646.

Vandenbergtie, N. 1975. An evaluation of CM patterns for grain size studies of fine-grained sediments, *Sedimentology*, 22, pp. 615-622.

Van Steijn, H., Bertran, P., Francou, B., Hetu, B., Texier, J. P. 1995. Models for genetic and environmental interpretation of stratified slope deposits: A review, *Permafrost and Periglacial Processes*, 6, pp. 125-146.

Van Steijn, H. & Coutard, J. P. 1989. Laboratory experiments with small debris flows: Physical properties related to sedimentary characteristics, *Earth Surface Processes and Landforms*, 14, pp. 587-596.

Varnes, D. J. 1978, Slope movement types and processes, in Schuster, R. L. & Krizek, R. J. (Eds.), *Landslides analysis and control*, Transport Research board Special Report 176, National Academy of Science, Washington, pp. 11-33.

Viseras, C. & Fernandez, J. 1994. Channel migration patterns and related sequences in some alluvial fan systems, *Sedimentary Geology*, 88, pp. 201-217.

Viseras, C. & Fernandez, J. 1995. The role of erosion and deposition in the construction of alluvial fan sequences in the Guadix formation (SE Spain), *Geologie en Mijnbouw*, 74, pp. 21-33.

Walden, J., Slattery, M. C., Burt, T. P. 1997. Use of mineral magnetic measurements to fingerprint suspended sediment sources: Approaches and techniques for data analysis, *Journal of Hydrology*, 202, pp. 353-372.

Walden, J. & Smith, J. P. 1995, Factor analysis: A practical application, in Maddy, D. & Brew, J. S. (Eds.), *Statistical modelling of Quaternary Science data: A practical manual*, Technical Guide Series, Quaternary Research Association, pp. 39-63.

Walker, M. J. C. & Lowe, J. J. 1977. Postglacial environmental history of Rannoch Moor, Scotland. I. Three pollen diagrams from the Kingshouse area, *Journal of Biogeography*, 4, pp. 333-351.

Walker, M. J. C. & Lowe, J. J. 1981. Postglacial environmental history of Rannoch Moor, Scotland III. Early- and mid- Flandrian pollen stratigraphic data from sites on western Rannoch moor and near Fort William, *Journal of Biogeography*, 8, pp. 475-491.

Walling, D. E., Peart, M. R., Oldfield, F., Thompson, R. 1979. Suspended sediment sources identified by magnetic measurements, *Nature*, 281, pp. 110-113.

Warburton, J. (Ed.) 1998. *Geomorphological studies in the North Pennines: Field Guide.* British Geomorphological Research Group, Durham.

Warburton, J. & Higgitt, D. L. 1998, Harthope Burn peat slide: an example of slope channel coupling, in Warburton, J. (Ed.), *Geomorphological studies in the North Pennines*, British Geomorphological Research Group, Durham, pp. 92-104.

Wasson, R. J. 1979. Sediment history of the Mundi alluvial fans, western New South Wales, *Sedimentary Geology*, 22, pp. 21-51.

Weir, J. A. 1979. Tectonic contrasts in the Southern Uplands, *Scottish Journal of Geology*, 15, pp. 169-186.

Wells, S. G. & Harvey, A. M. 1987. Sedimentologic and geomorphic variations in storm-generated alluvial fans, Howgill Fells, northwest England, *Geological Society of America Bulletin*, 98, pp. 182-198.

Whintle, A. G. & Catt, J. A. 1985. Thermoluminescence dating of soils developed in Late Devensian loess at Pegwell Bay, Kent, *Journal of Soil Science*, 36, pp. 293-298.

White, K., Drake, N., Millington, A., Stokes, S. 1996. Constraining the timing of alluvial fan response to Late Quaternary climatic changes, southern Tunisia, *Geomorphology*, 17, pp. 295-304.

White, K. & Walden, J. 1997. The iron oxide enrichment of arid zone alluvial fan soils, Tunisian Southern Atlas, measured by mineral magnetic techniques, *Catena*, 30, pp. 215-227.

Whitehouse, I. E. & McSaveney, M. J. 1990, Geomorphic appraisal for development on two steep, active alluvial fans, Mt. Cook, New Zealand, in Rachocki, A. H. & Church, M. (Eds.), *Alluvial fans - A field approach*, Wiley, New York, pp. 369-384.

Whol, E. E. & Pearthree, P. P. 1991. Debris flows as geomorphic agents in the Huachuca Mountains of Southeastern Arizona, *Geomorphology*, 4, pp. 273-292.

Wolfe, K. J. 1996. Discussion: Application of the QDa-Md method of environmental discrimination to particle size analysis of fine sediments, *Earth Surface Processes and Landforms*, 21, pp. 477-478.

Woodward, J. C., Lewin, J., Macklin, M. G. 1992. Alluvial sediment sources in a glaciated catchment: The Voidomatis Basin, Northwest Greece, *Earth Surface Processes and Landforms*, 17, pp. 205-216.

Wright, V. P. 1992, Paleopedology: Stratigraphic relationships and empirical models, in Marnn, I. P. & Chesworm (Eds.), *Weathering, soils and palaeosols*, Elsevier, Amsterdam, pp. 475-500.

Yu, L. & Oldfield, F. 1989. A multivariate mixing model for identifying sediment source from magnetic measurements, *Quaternary Research*, 32, pp. 168-181.

Yu, L. & Oldfield, F. 1993. Quantitative sediment source ascription using magnetic measurements in a reservoir-catchment system near Nijar, S.E. Spain, *Earth Surface Processes and Landforms*, 18, pp. 141-454.

